

UC Irvine

UC Irvine Electronic Theses and Dissertations

Title

Investigation into the Dyotropic Rearrangement of Arene-Allene Cycloadducts, Studies Toward the Synthesis of Isonitrile-Containing Diterpene Natural Products, and Synthesis of Indolines via Cobalt(III)-Carbene Radical Catalysis

Permalink

<https://escholarship.org/uc/item/9p27v6kw>

Author

Karns, Alexander

Publication Date

2018

Peer reviewed|Thesis/dissertation

UNIVERSITY OF CALIFORNIA,
IRVINE

Investigation into the Dyotropic Rearrangement of Arene-Allene Cycloadducts,
Studies Toward the Synthesis of Isonitrile-Containing Diterpene Natural Products, and
Synthesis of Indolines via Cobalt(III)-Carbene Radical Catalysis

DISSERTATION

submitted in partial satisfaction of the requirements for the degree of

DOCTOR OF PHILOSOPHY

In Chemistry

By

Alexander Sager Karns

Dissertation Committee:
Professor Christopher D. Vanderwal, Chair
Professor Larry E. Overman
Professor Sergey V. Pronin

2018

Portions of Chapter 3 have been adapted with permission from: Pham, H. V.; Karns, A. S.; Vanderwal, C. D.; Houk, K. N. *J. Am. Chem. Soc.* **2015**, *137*, 6956–6964. © 2015 American Chemical Society

Portions of Chapter 9 have been adapted from: Karns, A. S.; Goswami, M.; de Bruin, B. *Chem. Eur. J.* **2017**, Early View.

DEDICATION

To my family for their unwavering, unconditional support

TABLE OF CONTENTS

LIST OF FIGURES	viii
LIST OF TABLES	x
LIST OF SCHEMES	xi
LIST OF ACRONYMS AND ABBREVIATIONS	xiv
ACKNOWLEDGMENTS	xvii
CURRICULUM VITAE	xx
ABSTRACT OF THE DISSERTATION	xxii
CHAPTER 1: BACKGROUND TO DYOTROPIC REARRANGEMENTS	1
1.1 Introduction and Definition of Terms	1
1.2 Type I Dyotropic Rearrangements	2
1.2.1 Dyotropic Rearrangements of Dihalides	2
1.2.2 Dyotropic Rearrangements of Lactones	4
1.2.3 Dyotropic Rearrangements of Chlorolactones	8
1.2.4 Dyotropic Rearrangements of Nitroso Acetals	9
1.3 Type II Dyotropic Rearrangements	10
1.3.1 Hydrogen Transfer to Form π -Bonds	10
1.4 Stepwise Dyotropic Rearrangements	11
1.5 Conclusions	12
1.6 Notes and References	13
CHAPTER 2: BACKGROUND TO THE ARENE-ALLENE CYCLOADDITION	15
2.1 Introduction to Cycloadditions	15
2.2 Gerhard Himbert's Arene-Allene Dearomatizing Cycloaddition	17
2.2.1 Discovery of the Cycloaddition	17
2.2.2 Scope of the Arene-Allene Cycloaddition	19
2.2.3 Mechanism of the Arene-Allene Cycloaddition	21
2.3 Further Reactivity of Arene-Allene Cycloadditions	23
2.3.1 Vanderwal's RCM/ROM Cascade	23
2.3.2 Additional Vanderwal Ring-Closing Reactions on Cycloaddition Products	25
2.3.3 Himbert's Observed Dyotropic Shift	26
2.4 Conclusions	27
2.5 Notes and References	27
CHAPTER 3: INVESTIGATION INTO THE DYOTROPIC REARRANGEMENT OF ARENE-ALLENE CYCLOADDUCTS	29
3.1 Introduction and Inspiration	29
3.2 Lewis Acid Catalyzed Dyotropic Rearrangement	30
3.2.1 Computational Data Supporting the Lewis Acid Catalyzed Dyotropic Rearrangement	31
3.2.2 Experimental Validation of the Lewis Acid Catalyzed Dyotropic Rearrangement	32
3.3 Dyotropic Rearrangement via Electron Withdrawing Group Stabilization	34
3.3.1 Computational Data Supporting the Electron Withdrawing Group Stabilized Dyotropic Shift	34

3.3.2 Attempted Installation of an α -Electron Withdrawing Group via Direct Nucleophilic Attack	35
3.3.3 Attempted Installation of an α -Electron Withdrawing Group via Ketene Wittig Strategy	36
3.3.4 Attempted Installation of an α -Electron Withdrawing Group via Retrocycloaddition Strategy	37
3.3.5 Attempted Installation of an α -Electron Withdrawing Group via the Bromide Precursor	38
3.3.6 Successful Synthesis of the α -Electron Withdrawing Group Substituted Cycloadduct via Elimination	39
3.3.7 Experimental Validation of the Lower Activation Energy for Anion Stabilizing Cycloadducts	40
3.4 Attempted Dyotropic Shift via Cation Stabilization and Isolation of a Trapped Intermediate	40
3.4.1 Computational Data Supporting the Electron Donating Group Stabilized Dyotropic Shift	40
3.4.2 Synthesis of the Cation-Stabilizing Cycloadduct Precursor	41
3.4.3 Isolation of a Trapped Intermediate	42
3.5 Attempted Application to (\pm)-Securinine	43
3.5.1 Securinega Alkaloids Introduction	43
3.5.2 Attempted Synthesis of Securinine	44
3.6 Conclusions	47
3.7 Experimental Procedures	47
3.8 Notes and References	63
CHAPTER 4: BACKGROUND TO ISOCYANOTERPENE NATURAL PRODUCTS	66
4.1 Introduction	66
4.1.1 Natural Product Families	66
4.2 Isocyanoterpene Genesis	68
4.2.1 Biosynthesis of the Core	68
4.2.2 Biosynthesis of the Isonitrile and Related Functional Groups	71
4.2.3 Biological Function	72
4.3 Malaria and the Antiplasmodial Activity of the Isocyanoterpenes	73
4.3.1 Malaria	73
4.3.2 Antimalarial Drugs	74
4.3.3 Antiplasmodial Activity of Isocyanoterpenes	75
4.3.4 Mechanism of Action for Antiplasmodial Isocyanoterpenes	82
4.4 Other Bioactivities of the Isocyanoterpenes	83
4.5 General Considerations for Isocyanoterpene Natural Product Synthesis	84
4.5.1 A Divergent Approach to All Isocyanoterpene Natural Products	84
4.5.2 Isonitrile Installation	86
4.6 Conclusions	90
4.7 Notes and References	91

CHAPTER 5: BACKGROUND TO KALIHINOL A AND RELATED NATURAL PRODUCTS	97
5.1 Introduction	97
5.2 Isolation and Characterization of the Kalihinanes	97
5.3 Syntheses of the Kalihinanes and Related Natural Products	100
5.3.1 Yamada's Synthesis of Kalihinene X	100
5.3.2 Wood's Synthesis of (\pm)-Kalihinol C	103
5.3.3 Miyaoka's Synthesis of Kalihinol A	106
5.3.4 Vanderwal's Synthesis of Kalihinol B	108
5.3.5 Shenvi's Synthesis of Kalihinol C	111
5.4 Conclusions	114
5.5 Notes and References	115
CHAPTER 6: STUDIES TOWARD THE SYNTHESIS OF THP-CONTAINING KALIHINANES	117
6.2 Original Cascade for the Formation of Two Rings	119
6.2.1 Proposed Core Formation	119
6.2.2 Synthesis of Carbon Framework via Allyl Halide Displacement	122
6.2.3 Early Cascade Attempts	125
6.3 Revised Cascade for the Formation of Three Rings	126
6.3.1 Revised Cascade Strategy	126
6.3.2 Mechanistic Considerations	128
6.4 Linear Route toward the Cascade Precursor	129
6.4.1 Early Installation of the Tertiary Alcohol	129
6.4.2 Diels-Alder with Danishefsky's Diene	130
6.4.3 Elaboration to the Precursor	132
6.4.4 Route Summary	132
6.5 Convergent Synthesis via Enolate Allylation	133
6.5.1 Motivation	133
6.5.2 Enolate Allylation Attempts	134
6.6 Convergent Synthesis via Epoxide Opening	138
6.6.1 Motivation	138
6.6.2 Synthesis of Allylic Nucleophile	139
6.6.3 Synthesis of Epoxide Precursor	140
6.6.4 Successful Epoxide Opening	143
6.6.5 Route Summary	144
6.7 Ring-Closing Efforts via Heck Cascade	144
6.7.1 Initial Stepwise Strategy	144
6.7.2 Oxymercuration and 1,4-Addition Attempts	145
6.8 Ring-Closing Efforts via Single-Electron Processes	147
6.8.1 Rationale for Single-Electron Strategy	147
6.8.2 Initial Radical Precursor Formation	147
6.8.3 Attempts to Increase the Rate of 1,4-Radical Additions	148
6.9 Ring-Closing Efforts via Michael Cascade	152
6.9.1 Motivation for Michael Cascade	152
6.9.2 Attempted Synthesis of Michael Cascade Precursor	152
6.9.3 Use of Vinyl Sulfides as Nucleophiles for Ring-Closure	155

6.10 Conclusions and Future Work	156
6.11 Experimental Procedures	157
6.12 Notes and References	191
CHAPTER 7: ISOLATION AND SYNTHETIC STRATEGIES TOWARD 7,20-DIISOCYANOADOCIANE	194
7.1 Introduction	194
7.2 Isolation and Characterization of DICA	194
7.3 Previous Syntheses of 7,20-Diisocyanoadociane	195
7.2.1 Corey's Total Synthesis of (+)-DICA	195
7.2.2 Mander's Synthesis of (±)-DICA	198
7.2.3 Miyaoka's Synthesis of (+)-DICA	201
7.2.4 Vanderwal's Formal Synthesis of (+)-DICA	202
7.2.5 Shenvi's Synthesis of (+)-DICA	205
7.2.6 Thomson's Formal Synthesis of DICA	208
7.3 Conclusions	210
7.4 Notes and References	211
CHAPTER 8: A SECOND-GENERATION SYNTHESIS OF (+)-7,20-DIISOCYANOADOCIANE	212
8.1 Introduction and Motivation	212
8.1.1 Original Strategy and Room for Improvement	212
8.1.2 Proposed Revised Route	213
8.2 Initial Des-Methyl Strategy toward (+)-DICA	215
8.2.1 Early Work and C-7 Stereocenter Installation	215
8.2.2 Des-Methyl Birch Reduction	216
8.2.3 Completion of the Formal Synthesis	220
8.2.4 Route Summary	221
8.3 Early Installation of Methyl Group	222
8.3.1 Effects of Early Methyl Incorporation	222
8.3.2 Revised Birch Reduction	223
8.3.3 Completion of the Formal Synthesis	224
8.3.4 Route Summary	226
8.4 Improved Endgame	227
8.5 Conclusions and Future Work	228
8.6 Experimental Procedures	229
8.7 Notes and References	250
CHAPTER 9: CATALYTIC SYNTHESIS OF INDOLINES BY HYDROGEN ATOM TRANSFER TO COBALT(III)-CARBENE RADICALS	252
9.1 Introduction, Motivation, and Relevant Background	252
9.1.1 Introduction to Radical Carbenes	252
9.1.2 Typical Reactions of Radical Carbenes	253
9.1.3 Application to Indoline Synthesis	254
9.2 Optimization of Conditions	256
9.3 Substrate Synthesis	258

9.4 Scope Analysis	260
9.5 Reaction Mechanism	261
9.6 Conclusions	263
9.7 Acknowledgments	263
9.8 Experimental Procedures	264
9.9 Notes and References	277
Appendix	282

LIST OF FIGURES

Figure 1.1 Reetz's Classification of Dyotropic Rearrangements	1
Figure 1.2 Orbital Requirements for the Type I Dyotropic Rearrangement	3
Figure 1.3 Reetz's Initially Proposed Type II Dyotropic Rearrangements	10
Figure 2.1 Effect of Allene γ -Substitution on the Yield of the Cycloaddition	20
Figure 2.2 Houk's Computational Data Supporting Equilibrium Formation of Radical Species	22
Figure 3.1 The Houk Group's Calculated Mechanism for the Dyotropic Shift	29
Figure 3.2 The Strain Energy of Bicyclooctadiene Scaffolds	30
Figure 3.3 Effect of α -Functionality on the Energy Landscape of the Dyotropic Rearrangement	31
Figure 3.4 Effect of Several α -Electron Withdrawing Substituents on the Dyotropic Rearrangement	34
Figure 3.5 Computational Support for the Cation-Stabilized Dyotropic Rearrangement	41
Figure 3.6 Completed and Proposed Syntheses of Securinine	43
Figure 4.1 Scaffolds of the Isocyanoterpene Natural Products	67
Figure 4.2 General Overview of the Biosynthesis of Isonitrile-containing Diterpenes	68
Figure 4.3 In-Depth Proposed Biosynthesis of Relevant Families of Isocyanoterpenes	70
Figure 4.4 Vanderwal's Strategy Toward Kalihinol B and its Attempted Application to Kalihinol A	85
Figure 4.5 Isonitrile Installation via Nucleophilic Attack	89
Figure 5.1 Kalihinanes and Related Diterpenes	98
Figure 6.1 Successful Oxy-Mannich Cyclization and Attempted Application to Kalihinol A	118
Figure 6.2 Matched Polarity of Cascade Precursor 6.9 and the Proposed Wacker/Heck/Saegusa Cascade	119
Figure 6.3 Chloride-Directed Stereoselectivity in THP Formation	121
Figure 6.4 Proposed Formation of Tentatively-Assigned Bis-Enone 6.32	126
Figure 6.5 Revised Strategy toward Kalihinol A	127
Figure 6.6 Mechanistic Considerations for Stereocenter Formation	128
Figure 6.7 Linear vs. Convergent Strategies in Total Synthesis	134
Figure 6.8 Selective Deprotonation of Ketone 6.60	136
Figure 6.9 Reversal of Polarity of Fragment Coupling	139

Figure 6.10 Potential Substrates for α -Chloroenone Formation	149
Figure 6.11 Oxy-Michael/Michael Strategy Toward the Kalihinane Core	152
Figure 7.1 Corey's Strategy toward (+)-DICA	195
Figure 7.2 Mander's Curtius Rearrangement Approach to (\pm)-DICA	198
Figure 7.3 Robinson and Thomson's Oxidative Enone Coupling	208
Figure 8.1 Reported Endgames to (+)-DICA	213
Figure 8.2 Proposed Revised Strategy Toward (+)-DICA	214
Figure 8.3 Proposed Mechanism Toward Cyclohexene Byproduct 8.22	219
Figure 8.4 Impact of Initial Introduction of Methyl Group on the Arene Ring	222
Figure 8.5 Summary of our Syntheses of (+)-DICA	228
Figure 9.1 Unlocking Radical Reactivity from Carbene Precursors	252
Figure 9.2 Formation of Cobalt(III)-Carbene Radical Intermediates	253
Figure 9.3 Commonly Observed Reactions of Carbene Radicals	254
Figure 9.4 Conventional Methods for Indoline Formation	255
Figure 9.5 Cobalt(III)-Carbene Radical Catalysis Applied to Indoline Formation	256
Figure 9.6 Strategies toward the N-Derivatized Substrates	259
Figure 9.7 Computational Data for Indoline Formation	262

LIST OF TABLES

Table 1.1 Substituent Effects on the Activation Energy and Symmetry of Type I Dyotropic Rearrangements	3
Table 2.1 Pericyclic Reactions and Enthalpic Considerations	15
Table 3.1 Lewis Acid Promoted Dyotropic Rearrangement of Unactivated Cycloadducts	33
Table 4.1 IC ₅₀ Values of Common Antimalarial Drugs and Early Isocyanoterpenes against <i>P. falciparum</i>	76
Table 4.2 IC ₅₀ Values of the Amphilectanes and (Iso)cycloamphilectanes against <i>P. falciparum</i>	77
Table 4.3 IC ₅₀ Values of Several Kalihinanes against Drug-Resistant <i>P. falciparum</i>	79
Table 4.4 Wood's IC ₅₀ Values of Simplified Kalihinane Analogues against <i>P. falciparum</i>	80
Table 4.5 Vanderwal's IC ₅₀ Values of Simplified Isocyanoterpenes against <i>P. falciparum</i>	81
Table 4.6 Shenvi's Liver-stage Active ICTs and 9-isocyanopupukeanane	83
Table 8.1 Birch Reduction Conditions on the Des-Methyl Substrate	217
Table 8.2 Enamine-Mediated Aldol Condensation	225
Table 9.1 Optimization of Conditions for Indoline Formation	257
Table 9.2 Substrate Scope for Indoline Formation	260

LIST OF SCHEMES

Scheme 1.1 The Type I Dyotropic Rearrangement of Vicinal Dihalides	2
Scheme 1.2 Mulzer's Observed Lactone-Expanding Dyotropic Rearrangement	4
Scheme 1.3 Romo's Lactone-Expanding Dyotropic Rearrangement	5
Scheme 1.4 Romo's Dyotropic Rearrangement Applied to Spirolactone Natural Product Synthesis	6
Scheme 1.5 Tang's Synthesis of the Xanthanolides via Dyotropic Rearrangement	7
Scheme 1.6 Fuchs's Ring-Contracting Dyotropic Rearrangement Toward Deoxycephalostatin 1 Analogues	7
Scheme 1.7 Formation of Anti-Baldwin α -Halolactones via Dyotropic Rearrangement	8
Scheme 1.8 Denmark's Observed Nitroso Acetal Dyotropic Rearrangement	9
Scheme 1.9 Type II Dyotropic Rearrangements Involving Hydrogen Transfer	11
Scheme 1.10 Monti's Observed Stepwise Dyotropic Rearrangement	12
Scheme 2.1 Hoye's Dearomatizing Cycloaddition from Benzyne Intermediates	16
Scheme 2.2 Himbert's Cycloaddition and Rate-Increasing Substituent Patterns	18
Scheme 2.3 Effect of Aromatic Stabilization Energy on the Cycloaddition and Representative Cycloadducts	19
Scheme 2.4 Orahovats's Observed Degradation of Enantioselectivity and Proposed Mechanism	21
Scheme 2.5 Vanderwal's RCM/ROM Cascade on Arene-Allene Cycloaddition Products	24
Scheme 2.6 Vanderwal's Ring-Closing Reactions on Arene-Allene Cycloadducts	25
Scheme 2.7 Himbert's Observed Dyotropic Shift of Arene-Allene Cycloadducts	26
Scheme 3.1 Preparation of the Unsubstituted Dyotropic Rearrangement Precursor	32
Scheme 3.2 Attempted Direct Substitution of α -Nitro Functionality	35
Scheme 3.3 Attempted Ketene Wittig Route Toward the α -EWG Substituted Cycloadduct	36
Scheme 3.4 Attempted Retrocycloaddition Strategy Toward the α -EWG Substituted Cycloadduct	37
Scheme 3.5 Attempted Formation as a Bromide Precursor to the α -EWG Substituted Cycloadduct	38
Scheme 3.6 Synthesis of the α -EWG Substituted Cycloadduct via Vinyl Halide Elimination	39
Scheme 3.7 Experimental Observation of the Effect of α -EWG on the Rate of the Dyotropic Rearrangement	40
Scheme 3.8 Synthesis of the EDG-Substituted Dyotropic Rearrangement Precursor	41
Scheme 3.9 Isolation of a "Trapped Intermediate" of the Dyotropic Rearrangement	42

Scheme 3.10 Studies Toward Ester Formation from Acid Chloride Precursors	44
Scheme 3.11 Studies Toward Ester Formation from Carboxylic Acid Precursors	45
Scheme 3.12 Attempted Isomerization of the Internal Alkyne to the Allene	46
Scheme 3.13 Attempted Alkyne Silylation to Prevent Decomposition	46
Scheme 4.1 Isonitrile Syntheses from Amine Precursors	87
Scheme 4.6 Vanderwal's One-pot Bis-isonitrile Installation on Route to Kalihinol B	90
Scheme 5.1 Yamada's Synthesis of the Kalihinene X Core	101
Scheme 5.2 Yamada's Completion of Kalihinene X	102
Scheme 5.3 Wood's Model Study Toward the Kalihinanes	104
Scheme 5.4 Wood's Total Synthesis of Kalihinol C	105
Scheme 5.5 Miyaoka's Contributions to the Synthesis of Kalihinanes	107
Scheme 5.6 Vanderwal's Synthesis of Kalihinol B	109
Scheme 5.7 Shenvi's Early Work Toward Kalihinol C	112
Scheme 5.8 Shenvi's Completion of Kalihinol C	114
Scheme 6.1 Initial Methods Investigated for α -Carbonyl Allylation	123
Scheme 6.2 Formation of the Chlorohydrin Cascade Precursor	124
Scheme 6.3 Synthesis of Silylated Geranylacetone Derivative 6.48	130
Scheme 6.4 Dienophile Synthesis and Europium-Catalyzed Diels-Alder	131
Scheme 6.5 Completion of the Cascade Precursor	132
Scheme 6.6 Synthesis of Coupling Partners for the Enolate Allylation Strategy	135
Scheme 6.7 Fragment Coupling via Enolate Allylation	137
Scheme 6.8 Formation of Allyl Grignard Nucleophile 6.74	140
Scheme 6.9 Synthesis of a Mixture of Epoxide Diastereomers	141
Scheme 6.10 Methods for Synthesis of Stereodefined Epoxide 6.83	142
Scheme 6.11 Completion of the Acyclic Precursor 6.86 via Epoxide-Opening Strategy	143
Scheme 6.12 Oxymercuration Precedent	146
Scheme 6.13 Iodoetherification and 1,5-Hydrogen Atom Abstraction	148
Scheme 6.14 Synthesis and Testing of α -Chloroenone 6.107	150
Scheme 6.15 Synthesis and Testing of the Michael Cascade Precursor	154
Scheme 6.16 Disulfide Analogue Synthesis and Attempted Ring Closure	155
Scheme 6.17 A Potential π -Cyclization to form the Kalihinane Core	156
Scheme 7.1 Corey's Synthesis of (+)-DICA	196
Scheme 7.2 Mander's Formal Synthesis of (\pm)-DICA	199
Scheme 7.3 Mander's Completion of the Formal Synthesis of (\pm)-DICA	200

Scheme 7.4 Miyaoka's Formation of the C-3 - C-4 Stereocenter Motif Toward (+)-DICA	202
Scheme 7.5 Vanderwal's Formal Synthesis of (+)-DICA	203
Scheme 7.6 Synthesis of the Diels-Alder Components	205
Scheme 7.7 Shenvi's Synthesis of (+)-DICA	207
Scheme 7.8 Thomson's Formal Synthesis of (+)-DICA	209
Scheme 8.1 Formation of the Des-Methyl Lactone-Containing Birch Precursor	216
Scheme 8.2 Completion of the Des-Methyl Formal Synthesis	220
Scheme 8.3 Early Work and Birch Reduction with the Methyl-Containing Substrate	223
Scheme 8.4 Attempted Application of the Base-Catalyzed Aldol Condensation	224
Scheme 8.5 Improved Completion of the Formal Synthesis	226
Scheme 8.6 Completed Route Toward Formal Synthesis Product 8.4	227

LIST OF ACRONYMS AND ABBREVIATIONS

λ	wavelength
μ	micro
ν	frequency
$[\alpha]_D$	specific rotation at wavelength of sodium D line
$^{\circ}\text{C}$	degrees Celsius
Ac	acetyl
AIBN	azobisisobutyronitrile
app	apparent
BHT	butylated hydroxytoluene
Bn	benzyl
bp	boiling point
br	broad
<i>n</i> Bu	<i>n</i> -butyl
<i>t</i> Bu	<i>tert</i> -butyl
<i>ca.</i>	about (Latin <i>circa</i>)
CAN	ceric ammonium nitrate
calcd	calculated
cat.	catalytic
CI	chemical ionization
cm^{-1}	wavenumber(s)
d	doublet
DCB	dichlorobenzene
DCC	<i>N,N</i> -Dicyclohexylcarbodiimide
DCM	dichloromethane
DMAP	4-dimethylaminopyridine
DME	1,2-dimethoxyethane
DMF	dimethylformamide
DMM	dimethoxymethane
DMP	Dess-Martin periodinane
DMPU	1,2-dimethyl-3,4,5,6-tetrahydro-2(1H)-pyrimidinone
DMSO	dimethylsulfoxide
DPPA	diphenylphosphoryl azide
DTBP	2,6-di- <i>tert</i> -butylpyridine
dr	diastereomeric ratio
EC ₅₀	half maximal effective concentration
EDC	<i>N</i> -(3-dimethylaminopropyl)- <i>N</i> -ethylcarbodiimide
EDG	electron-donating group
EWG	electron-withdrawing group
EI	electron impact
equiv	equivalent
ee	enantiomeric excess
er	enantiomeric ratio
ESI	electrospray ionization
Et	ethyl
EtOAc	ethyl acetate
FI	flame ionization
g	gram(s)

GABA	gamma-amino butyric acid
GC	gas chromatography
h	hour(s)
HAT	hydrogen atom transfer
HOMO	highest occupied molecular orbital
HMDS	hexamethyldisilazide
HPLC	high-performance liquid chromatography
HRMS	high-resolution mass spectrometry
Hz	Hertz
IBX	<i>o</i> -iodoxybenzoic acid
ICT	isocyanoterpene
IMDA	intramolecular Diels–Alder
IPA	isopropanol, 2-propanol
<i>i</i> Pr	isopropyl
IC ₅₀	half maximal inhibitory concentration
IR	infrared
<i>J</i>	coupling constant
K	Kelvin (absolute temperature)
kcal	kilocalorie
L	liter
LDA	lithium diisopropylamide
LD ₅₀	half lethal dose
lit.	literature value
LLS	longest linear sequence
LUMO	lowest unoccupied molecular orbital
m	multiplet; milli
M	molar; molecular ion
<i>m/z</i>	mass to charge ratio
<i>m</i> CPBA	<i>meta</i> -chloroperoxybenzoic acid
Me	methyl
MHz	megahertz
min	minute(s)
mol	mole(s)
mp	melting point
Ms	methanesulfonyl (mesyl)
MTBE	methyl <i>tert</i> -butyl ether
MVK	methyl vinyl ketone
n	nano
n.d.	not determined; non detected
NBS	<i>N</i> -bromosuccinimide
NCS	<i>N</i> -chlorosuccinimide
NIS	<i>N</i> -iodosuccinimide
NMR	nuclear magnetic resonance
NOE	nuclear Overhauser effect
NOESY	nuclear Overhauser enhancement spectroscopy
PBQ	<i>para</i> -benzoquinone
PCC	pyridinium chlorochromate
PDC	pyridinium dichromate
Ph	phenyl
PhMe	toluene
ppm	parts per million

Pr	propyl
py	pyridine
q	quartet
quant.	quantitative
rt	room temperature
RCM	ring closing metathesis
ROM	ring opening metathesis
s	singlet
SAR	structure-activity relationships
SI	selectivity index
t	triplet
TBAF	tetrabutylammonium fluoride
TBDPS	<i>tert</i> -butyldiphenylsilyl
TBHP	<i>tert</i> -butylhydroperoxide
TBS	<i>tert</i> -butyldimethylsilyl
TCA	trichloroacetoxy; trichloroacetic acid
TCAA	trichloroacetic anhydride
TES	triethylsilyl
TEMPO	2,2,6,6-tetramethylpiperidin-1-oxyl
Teoc	2-trimethylsilylethyl carbamate
Tf	trifluoromethanesulfonyl
TFA	trifluoroacetoxy
TFAA	trifluoroacetic anhydride
THF	tetrahydrofuran
THP	tetrahydropyran
TIPS	triisopropylsilyl
TLC	thin-layer chromatography
TMEDA	<i>N,N,N',N'</i> -tetramethylethylenediamine
TMP	2,2,6,6-tetramethylpiperidine
TMS	trimethylsilyl
TMSCN	trimethylsilyl cyanide
TOF	time-of-flight
Trt	trityl
Ts	<i>p</i> -toluenesulfonyl (tosyl)
UV	ultraviolet

ACKNOWLEDGMENTS

I would like to first thank Professor Chris Vanderwal for accepting me into his research group and for allowing me to learn under his supervision. I distinctly remember our first conversation during my visitation weekend when we exchanged our opinions on the current state of total synthesis, and I remember you genuinely expressing interest in my opinion despite my lack of true experience at the time. Since then, you've continued to consider my personal growth above all, giving me the freedom to feel the excitement of trying my own ideas, while allowing me to learn from making my own senseless mistakes. Your acceptance of my desire to conduct research abroad is perhaps the greatest example of your selfless support for my personal success. Thank you for your trust, which has allowed me to develop confidence in myself as an independent scientist.

Thank you, Professor Larry Overman, for continuously providing valuable feedback on my research through my graduate studies. It is not often that a distinguished professor can be found with such modest and selfless character, and it is this unique combination that I will seek to emulate in my future. I appreciate your feedback and guidance following my group meeting presentations, and I thank you for not embarrassing me during my second year oral examination. To Professor Sergey Pronin, your relentless drive and determination have been an inspiration to me since you joined the UCI community. Your interest in my progress provided motivation to help me get through my third and fourth years, a time of without deadlines or an end to graduate school in sight. Thank you for being an endless source of enthusiasm, knowledge, and sarcastic banter. I would also like to thank Professor Zhibin Guan, Professor Aaron Esser-Kahn, and Professor Vy Dong for sitting on my oral examination committee, and Professor Scott Rychnovsky for providing feedback from my second year report. Thank you to Professor Ken Houk and Professor Hung Pham for collaborating with me on my first-year project.

My early years in the Vanderwal group were pivotal in converting me from an immature, inexperienced student to the immature, experienced scientist I am today. Although my overlapping time with Dr. Evan Horn, Dr. Peter Mai, Prof. Won-Jin Chung, Prof. Sam Tartakoff, Dr. Jon Lam, Dr. Allen Hong and Dr. Diane Lim was short, their willingness and enthusiasm for teaching the younger lab members was, and continues to be, inspirational. Thank you for introducing me to dry ice bowling, all-you-can-eat Korean barbecue, long nights in lab, and quick trips to Baja Fish Tacos. I will always remember my early days in lab fondly.

I would like to thank Dr. Joey Carlson, Dr. Gregg Schwarzwald, and Dr. Carl Vogel (honorary member) for welcoming me into Bro Bay, and for playing a key role in my early education. Joey taught me to fully investigate each reaction, to stain every TLC plate, to find the positives in an undesired result. Learning from you was worth putting up with the abundance of repurposed socks and toenail clippings in our bay. Thank you, Gregg, for instilling in me a love for reaction mechanisms and for being a fan of New York sports teams so I could enjoy your suffering. My lengthy conversations with Carl over a glass of whiskey at the end of a difficult day were of immeasurable importance to both my education and my sanity throughout my second year.

Dr. Zef Könst and Prof. Mary-Beth Daub were the first members of the Vanderwal group I met, and they ended up being two of my best friends in graduate school. I would like to thank Zef for being an amazing friend and role model to me over the last several years, and for showing me that it is possible to excel both in chemistry and in life. I would also like to thank Mary-Beth for the open, honest conversations that one can only have with true friends, and for the abundant advice in support of my battle with the kalihinanes. Following my transfer over to (+)-7.20-diisocyanoadociane as a synthetic target, Philipp Roosen became an incredible source of knowledge and motivation. Although only one slide in each presentation I give on DICA is dedicated to the wonderful work performed by Philipp, his advice and encouragement are the backbone for the rest.

I would like to thank Dr. Alex White, Brian Atwood, and Bryan Ellis for their friendship and support. Our trips to the Side Door and Java City will remain some of my best memories from graduate school, and I appreciate you all reminding me of life outside of lab from time to time. To Alex and Brian, I realize my independent nature might not make me the most enjoyable of desk neighbors, and I appreciate you putting up with my occasional grumpiness. Thank you, Sharon Michalak, for your unbreakably positive attitude toward chemistry and life, and for cheering me up in difficult times. Thank you, Dr. Dmitriy Uchenik, for teaching me the basics of DFT calculations and for playing an active role in preparing me for my second year oral examination.

To the rest of the Vanderwal lab who I only overlapped with for a short amount of time, including Dr. Florian de Nanteuil, Dr. Matthias Gohl, Dr. Vini Ramella, Michael Freidberg, Glynis Coyne, Ryan Kozlowski, Darius Vrubliauskas, Riley Mills, and Natalie Dwulet, it has been a pleasure working with each of you, and I look forward to hearing about your future successes. To the undergraduates Sean Feng, Kathy Dao, Susanna Liang, and Sierra Nguyen, thank you for instilling life and enthusiasm into the everyday life of our lab. I would like to especially thank Guillaume Masson, Reo Sato, and Thomas Chung who conducted research under my supervision and consequently taught me a significant amount about myself as an instructor and role model.

My time conducting research in the Netherlands was a truly incredible experience. I would like to thank Professor Bas de Bruin for reading an email from a random graduate student and agreeing to co-write a grant application with him. Bas's passion for all types of research was inspiring, and his interest in the everyday progress of my research were crucial to the success of my project. I would like to thank Dr. Linda Jongbloed for introducing me to Dutch culture and for the truly wonderful experiences we had together. Thank you to Dr. Monalisa Goswami for being an excellent friend and researcher, and thank you for teaching me necessary lessons about myself as a collaborator. Dr. Vincent Vreeken and Dr. Sofia Derossi, thank you for welcoming me into your friend group and for putting up with my Americanisms. Thank you to the NSF GROW program for funding my international research experience.

Although the time spent outside of the laboratory in graduate school is short, my friend group has helped me make the most of it. Thank you to David George for being a great scientific role model, roommate, and friend. Your intensity and enthusiasm for chemistry has without a doubt pushed me to be a better scientist than I would have otherwise been, and your companionship throughout graduate school as a roommate and friend has been nothing but enjoyable. Thank you, Valentina Barrera, for joining us to make our house a home, and for forcing us to expand our conversation topics outside of chemistry every once in a while. Although it would be impossible to name everyone whose friendship I appreciate from the UCI community, I would like to specifically thank Tom Endean, Sammie Endean, Gunther Endean, David Fabian, Kelly Rotstan, Hanna Neal, James Neal, and Ellie Neal for being such great friends for the past several years. Whether our weekends involved game nights, escape rooms, or 2AM milk jugs, my experiences with you have been enjoyable throughout.

I can't thank my friends from Massachusetts enough for supporting me despite the long distance separating us. To my high school friends Kurt Sabacinski, Matt Ball, Mark Pappas, Corey Steadman, Vinny Palmerino, and Seamus McGrath, thank you for checking in with me frequently and for welcoming me back during my visits. To my Boston College friends Matt Johnson, Josie Scheunemann, Adam Rohde, Joe LaCorte, Ben Goldberg, Casey Corcoran, and Tiia Groden, thank you for your continued friendship.

I would like to thank the GAANN fellowship for funding my first two years of graduate study, and the National Science Foundation for funding the remaining three. The facilities at UCI are excellent and one of the first things I mention to prospective students on visitation weekends. Thank you to Dr. Philip Demison, Dr. John Greaves, and Dr. Felix Grun for excelling in your respective specialties. I would like to especially acknowledge Tenley Dunn for her exceptional contributions to the UCI chemistry department. I hope to one day be as irreplaceable in my future career as she is to the UCI community.

I must end by thanking my family, without whose support and understanding I would never be in a position to earn a PhD. My father, Kenneth Karns, taught me the importance of hard work and dedication to one's craft. My mother, Theresa Karns, taught me the importance of compassion and has never failed to remind me of what is truly important in life. To my brother, Adam Karns, thank you for providing a consistently positive example of how life should be lived, and to my sister, Jillian Karns, thank you for willing speaking with me about anything, and for your boundless understanding and encouragement. To my recently gained family members, Nicole Karns, Paloma Karns, Len Zannotti, and Anne Scales, thank you for making my family happy while I've been away, and I can't wait to spend time with you all.

CURRICULUM VITAE

ALEXANDER S. KARNS

UNIVERSITY OF CALIFORNIA, IRVINE
PHONE : (774) 696-9870 · EMAIL : AKARNS@UCI.EDU

EDUCATION

University of California, Irvine · Irvine, CA September 2013 – April 2018

- Program · Doctor of Philosophy in Organic Synthesis · GPA – 3.99/4.00
- Relevant Courses · Organic Reaction Mechanisms, Organic Spectroscopy, Organometallic Chemistry, Organic Reaction Mechanisms I and II, Organic Synthesis I and II, Industrial Chemistry

Boston College · Chestnut Hill, MA September 2009 – May 2013

- Program · Bachelor of Science in Chemistry · GPA – 3.57/4.00
- Relevant Courses · Honors General Chemistry, Honors Organic Chemistry, Honors Biochemistry, Analytical Chemistry, Inorganic Chemistry, Physical Chemistry I and II, Advanced Methods in Chemistry, NMR Spectroscopy
- Graduate Courses · Modern Methods in Organic Synthesis, Organometallic Chemistry

RESEARCH EXPERIENCE

Christopher D. Vanderwal Laboratory · University of California, Irvine December 2013 – April 2018

- Total Synthesis of 7,20-Diisocyanoadociane, a Potent Antimalarial Terpenoid
 - Investigation into a Birch reduction/aldol sequence for the total synthesis of antiplasmodial natural products
- Studies Toward the Core of Tetrahydropyran-Containing Kalihinanes with Potent Antiplasmodial Activity
 - Examination of a cyclization cascade to form the tricyclic core from a simple acyclic precursor
- Experimental Investigation of the Formal Dyotropic Rearrangement of Himbert Arene/Allene Cycloadducts
 - Exploration of substituent influence on the formal dyotropic rearrangement of Himbert bicyclo[2.2.2]octadiene precursors to bicyclo[3.2.1]octadiene products.
 - Development of Lewis acid conditions to promote the rearrangement of nonactivated bicycles

Bas de Bruin Laboratory · University of Amsterdam September 2016 – December 2016

- Synthesis of Substituted Indolines via Cobalt(III)-Carbene Radical Catalysis
 - Complete development and optimization of a methodology utilizing unprecedented cobalt-radical reactivity
 - Synthesis of a broad library of substrates for scope analysis

James P. Morken Laboratory · Boston College January 2011 – May 2013

- Stereoselective Amination of Alkyl and Aryl Pinacol Boronates

- Molecular Linker Synthesis for Drug-Polymer Conjugation
 - Development and testing of a variety of molecular linkers for stability and efficacy
- Efficient Preparation of Ellman Imines from Electron-Deficient Trifluoromethyl Ketones
 - Complete optimization of reaction conditions to produce significantly improved yields of Ellman imines

PUBLICATIONS

- **Karns, A. S.**; Goswami, M.; de Bruin, B. “Catalytic Synthesis of Indolines via Hydrogen Atom Transfer to Cobalt (III)-Radical Carbenes” *Chem. Eur. J.* **2017**, *24*, 5253–5258.
- **Karns, A. S.**; Pham, H. V.; Vanderwal, C. D.; Houk, K. N. “Computational and Experimental Investigations of the Formal Dyotropic Shift of Himbert Arene/Allene Cycloadducts” *J. Am. Chem. Soc.* **2015**, *137*, 6956–6964.
- Kawanami, T.; **Karns, A.S.**; Adams, C. M.; Serrano-Wu, M. “Efficient Preparation of Ellman Imines from Trifluoromethyl Ketones Promoted by Zirconium *tert*-Butoxide” *Tetrahedron Letters*, **2013**, *54*, 7202–7205.
- Mlynarski, S. N.; **Karns, A. S.**; Morken, J. P. “Direct Stereospecific Amination of Alkyl and Aryl Pinacol Boronates” *J. Am. Chem. Soc.* **2012**, *134*, 16449–16451.

POSTERS and PRESENTATIONS

- **Karns, A. S.**; Vanderwal, C. D. (2017, July). *Progress Toward the Total Synthesis of Kalihinol A*. Poster presented at the ACS Graduate Research Symposium (GRS) in Portland, OR.
- **Karns, A. S.**; Vanderwal, C. D. (2017, June). *Progress Toward the Total Synthesis of Kalihinol A*. Poster presented at the ACS National Organic Chemistry Symposium (NOS) in Davis, CA.
- **Karns, A. S.**; Vanderwal, C. D. (2017, March). *Progress Toward the Total Synthesis of Kalihinol A*. Oral Presentation at the University of California Chemical Symposium (UCCS) at Lake Arrowhead, CA.
- **Karns, A. S.**; Pham, H. V.; Houk, K. N.; Vanderwal, C. D. (2016, March). *Investigation into the Formal Dyotropic Shift of Arene-Allene Intramolecular Cycloadducts*. Poster presented at the RSC ISACS19 conference at the University of California, Irvine. **Awarded the Chemical Science poster prize.**
- **Karns, A. S.**; Kawanami, T.; Adams, C. M.; Serrano-Wu, M. (2012, August). *Molecular Linker Synthesis for Drug-Polymer Conjugation and Zirconium *tert*-Butoxide Promoted Ellman Imine Synthesis*. Poster presented at the annual intern poster session at the Novartis Institutes for Biomedical Research, Cambridge, MA.

FELLOWSHIPS, AWARDS, and ACHIEVEMENTS

- 2015-2018 NSF GRFP Fellow
- 2016 NSF GROW Fellow • University of Amsterdam
- 2016 *Chemical Science* Poster Prize • ISACS19 Conference
- 2013-2014 and 2014-2015 GAANN Fellow • University of California, Irvine
- 2014 NSF GRFP Honorable Mention
- The *Journal of Organic Chemistry* Undergraduate Research Award • Boston College

ABSTRACT OF THE DISSERTATION

Investigation into the Dyotropic Rearrangement of Arene-Allene Cycloadducts,
Studies Toward the Synthesis of Isonitrile-Containing Diterpene Natural Products, and
Synthesis of Indolines via Cobalt(III)-Carbene Radical Catalysis

By

Alexander Sager Karns

Doctor of Philosophy in Chemistry

University of California, Irvine, 2018

Professor Christopher D. Vanderwal, Chair

Described herein is a compilation of studies in both methodology development and total synthesis in organic chemistry. Chapter 1 describes in detail notable discoveries in the field of dyotropic rearrangements, highlighting computational investigations, methodological analyses, and application to the total synthesis of natural products. Chapter 2 summarizes the formal dyotropic rearrangement observed initially by Gerhard Himbert, and discusses the scope, limitations, and applications of this unique bicyclic rearrangement. Chapter 3 discusses our collaborative computational and experimental investigation into the formal dyotropic shift of arene-allene cycloadducts. Notable contributions include the discovery of Lewis acid-promoted dyotropic rearrangement conditions and isolation of a “trapped intermediate”, strongly supporting a proposed two-step polar mechanism.

Chapter 4 discusses in detail the isocyanoterpene natural products, including their proposed biogenesis, their observed bioactivity, and synthetic strategies by which they can be obtained in a laboratory setting. Chapter 5 elaborates specifically on the kalihinane family of natural products, highlighting their isolation, and summarizing total syntheses targeting their complex structures. Chapter 6 summarizes our progress toward the synthesis of kalihinanes that contain a tetrahydropyran ring. Notable contributions include a convergent sequence that procures an acyclic precursor to the kalihinane core and several methods by which this acyclic precursor can be cyclized to form the tetrahydropyran ring.

Chapter 7 describes in detail the isolation of (+)-7,20-diisocyanoadociane and summarizes the total synthesis efforts toward the completed natural product. Chapter 8 highlights our improvements to our previously published formal synthesis of DICA, which lowers the step count from 24 steps to 17 steps, increases the overall yield significantly, and targets an intermediate from which the natural product can be obtained with high diastereoselectivity.

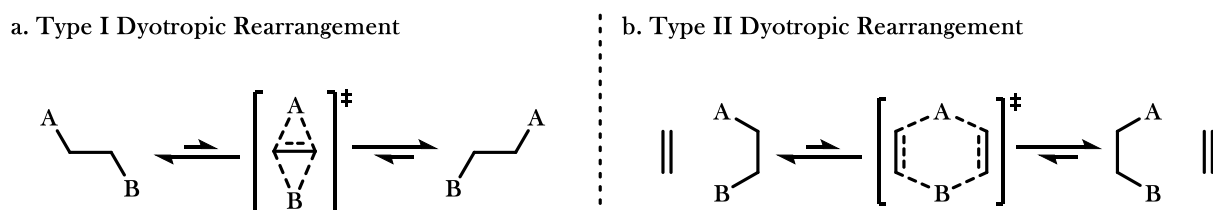
Chapter 9 provides a short summary of the field of cobalt(III)-carbene radical catalysis, including both mechanistic studies and applications to small molecule synthesis. Chapter 10 details our application of this unique reactivity to a rapid and efficient synthesis of indolines. The discovery and optimization of this methodology is described in detail, accompanied by an investigation into both scope and mechanism.

CHAPTER 1: BACKGROUND TO DYOTROPIC REARRANGEMENTS

1.1 Introduction and Definition of Terms

The dyotropic rearrangement is a seldom observed transformation in organic chemistry with interesting features from both synthetic and physical chemistry perspectives. First defined by Reetz in 1972, the dyotropic rearrangement is described as “an uncatalyzed process by which two σ -bonds simultaneously migrate intramolecularly”.¹ Due to the high energetic barrier of these rearrangements, they are typically observed only from highly-strained or sterically-congested precursors to form energetically-favored products, although exceptions exist. If the precursor is easily procured, the dyotropic shift can be a powerful tool for the synthesis of difficult-to-access molecular scaffolds.

Figure 1.1 Reetz’s Classification of Dyotropic Rearrangements



Reetz defined Type I dyotropic rearrangements as an *interchange* of two vicinal bonds in a concerted manner (Figure 1.1a). Although originally inspired by a thermal rearrangement, this definition has been expanded over time to include Lewis-acid catalyzed processes as well. This process almost exclusively proceeds via the exchange of bonds in an *anti* manner, in which the participants are separated by the axis of their movement. The exchange of bonds in a *syn* manner has been observed in cases where a shift participant has a low-energy unoccupied p- or d-orbital,² but this process is otherwise orbital disallowed.

The Type II dyotropic rearrangement is defined as “an intramolecular process in which two σ -bonds migrate in such a way as not to interchange positions” (Figure 1.1b).³ Although this definition could theoretically include a variety of processes, it is generally used to describe a simultaneous intramolecular

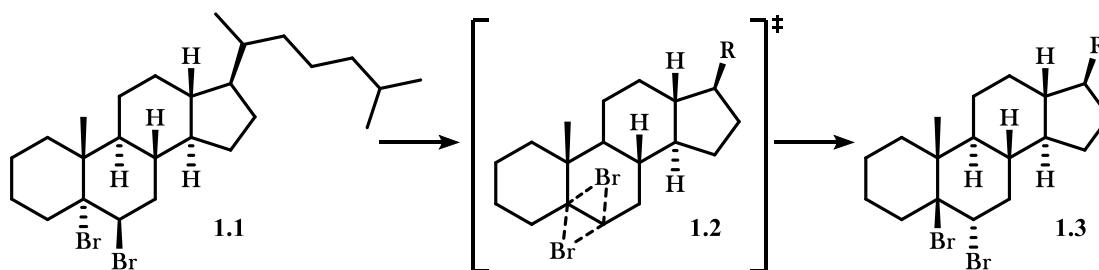
transfer of two vicinal bonds through space to a pendant point of unsaturation. The driving force for this transfer of unsaturation often involves the generation of aromatic or otherwise highly stabilized π -systems.

1.2 Type I Dyotropic Rearrangements

1.2.1 Dyotropic Rearrangement of Dihalides

Among the earliest examples of dyotropic shifts involve vicinal dihalide rearrangements, wherein two C-X bonds simultaneously exchange positions to result in a formal double inversion of stereochemistry (Scheme 1.1). Originally investigated by Grob and Winstein, this rearrangement is typically observed as the double inversion of diaxial dihalides (**1.1**) to the energetically-preferred diequatorial products (**1.3**).⁴ Although significantly higher reaction rates in polar solvents were observed, the rate of the reaction was unaffected by the addition of exogenous hydrogen bromide, suggesting a purely intramolecular transformation. Furthermore, a transition state of entropy $S^\ddagger = -5.1$ cal/(K • mol) was calculated, indicating a highly ordered transition state relative to the ground state conformations. It was proposed that the degree of charge separation in the transition state is directly correlated with the polarity of the solvent, with negligible charge separation in nonpolar solvents.^{4,5} This suggests a mechanism involving a highly concerted exchange of bonds, indicated by **1.2**.⁶

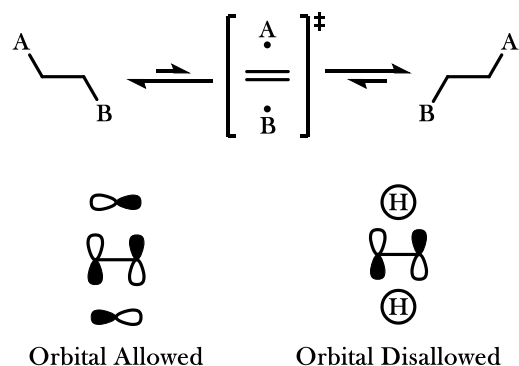
Scheme 1.1 The Type I Dyotropic Rearrangement of Vicinal Dihalides



Concerted Type I dyotropic rearrangements are only possible when at least one migrating group possesses low-energy orbitals that allow for proper orbital overlap in the transition state. In computational studies, it was proposed that the transition state for a dihalide dyotropic rearrangement could be considered

as a diradical interacting with a π -system (Figure 1.2).⁷ Using this model, the molecular orbitals of the bromide atoms in a dihalide rearrangement allow for interaction with the LUMO of an ethylene moiety. Atoms lacking the proper orbitals to interact with the ethylene LUMO in the transition state, such as hydrogen atoms, are unable to participate in the dyotropic rearrangement. This inability of hydrogen atoms to participate in Type I dyotropic rearrangements is crucial to the thermal stability of stereocenters in organic molecules.

Figure 1.2 *Orbital Requirements for the Type I Dyotropic Rearrangement*



Fernandez and co-workers also propose that the activation energy for a Type I dyotropic rearrangement of vicinal dihalides is dependent on the stabilization of the π -system in the transition state. To provide evidence for their point, they measured the activation energy for the dyotropic rearrangement of a variety of dihalide precursors and found that the calculated activation energy correlates with the electron-donating character of the alkene substituent (Table 1.1). Additionally, electron donating-groups stabilize one side of the ethylene moiety, leading to more unsymmetrical transition states indicated by S_y values.

Table 1.1 *Substituent Effect on the Activation Energy and Symmetry of Type I Dyotropic Rearrangements*

Entry	R	E (kcal/mol)	S_y^*
1	H	28.2	0.87
2	Me	25.5	0.78
3	OH	22.0	0.75
4	NH ₂	14.1	0.72
5	NO ₂	33.6	0.80

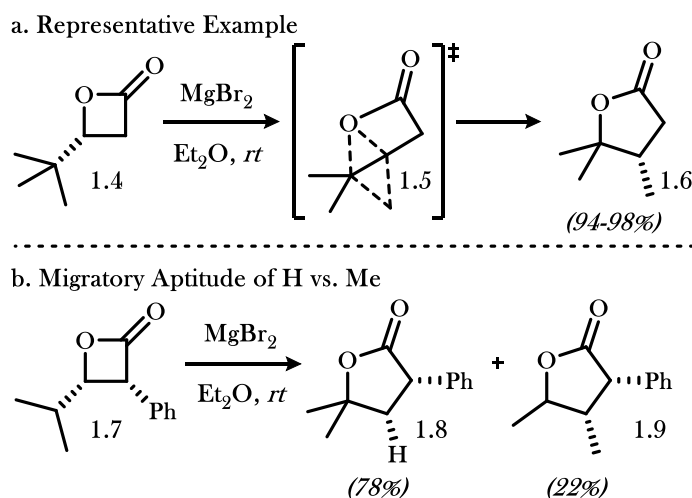
* Higher S_y values indicate a more symmetrical transition state

Although synthetic chemists have found few applications of vicinal dihalide dyotropic rearrangements, their discovery has led to new insight in thinking about molecular rearrangements. Initial studies into these transformations has eventually led to the discovery and synthetic application of a variety of other types of dyotropic rearrangements as well.

1.2.2 Dyotropic Rearrangement of Lactones

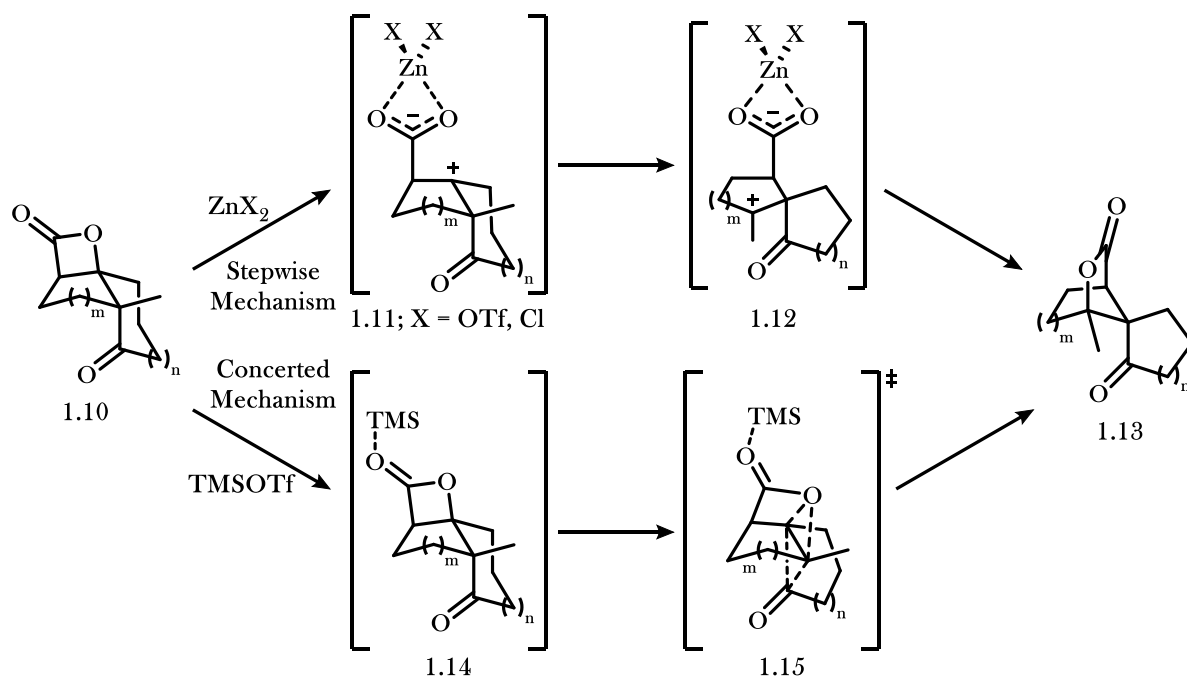
Another commonly observed dyotropic rearrangement involves the ring-expansion of strained lactones to energetically favored products. In 1979, the Mulzer group reported the expansion of substituted β -lactones (**1.4**) to γ -lactones (**1.6**) in high yields via Lewis acid catalysis (Scheme 1.2). These reactions involve the 1,2-shift of a C-O σ -bond within a lactone resulting in a less-strained cyclic product. At the same time, an exocyclic substituent will undergo an opposite 1,2-shift to maintain proper bond order, as indicated in **1.5**.

Scheme 1.2 Mulzer's Observed Lactone-Expanding Dyotropic Rearrangement



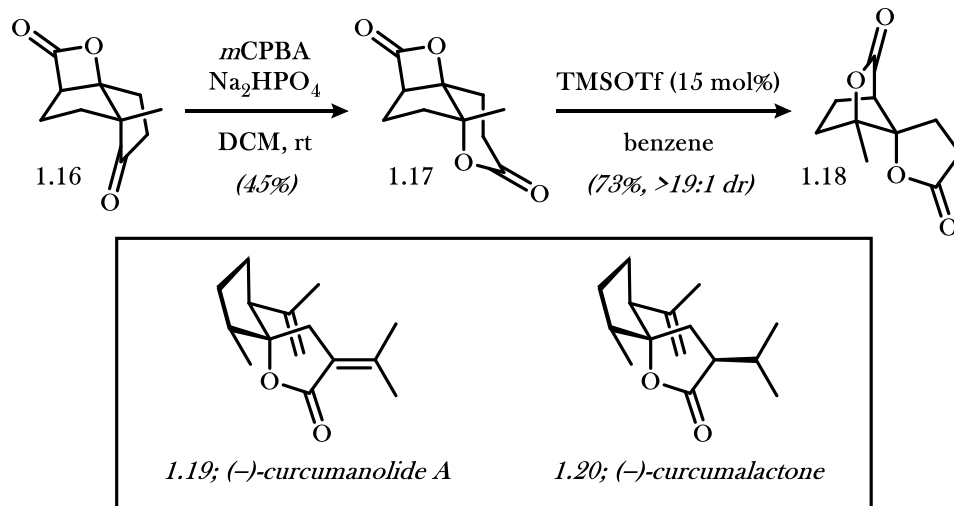
When performed on stereodefined precursors, such as **1.4**, they found the reactions proceeded with complete retention of stereochemistry, supporting a concerted mechanism rather than the formation of a discrete carbocation. Hydrogen atoms are also reported to have a higher migratory aptitude compared to the methyl group under these conditions (Scheme 1.2b), except in cases where a hydrogen atom is unable to adopt an *anti*-configuration to the migrating C-O bond.⁸

Scheme 1.3 Romo's Lactone-Expanding Dyotropic Rearrangement



The Romo group has studied a similar ring-expanding dyotropic rearrangement of β -lactones to form spirocyclic, bridged γ -butyrolactone products (**1.13**; Scheme 1.3). Although originally proposed to proceed stepwise via zwitterionic intermediates,⁹ a collaboration with the Tantillo group provided insight into the effect of varying Lewis acids on the mechanistic pathway.¹⁰ Calculations by the Tantillo group suggest that the use of $Zn(OTf)_2$ indeed leads to full heterolytic cleavage of the lactone C-O bond to form **1.11**, and a subsequent 1,2-shift and charge recombination provides the ring-expanded spirocyclic γ -lactone product **1.13**. However, in the presence of $TMSOTf$ as a Lewis acid, calculations instead supported a concerted dyotropic rearrangement mechanism involving the simultaneous interchange of bonds (indicated by **1.15**) to directly form the γ -lactone products. The authors suggest the mechanistic differences can be attributed to zinc's ability to bind with both oxygens on the lactone, thereby better stabilizing the zwitterionic intermediate and increasing its equilibrium presence. Since the trimethylsilyl Lewis acid is unable to coordinate in a bidentate fashion, the concerted dyotropic shift is the more favorable mechanistic pathway.

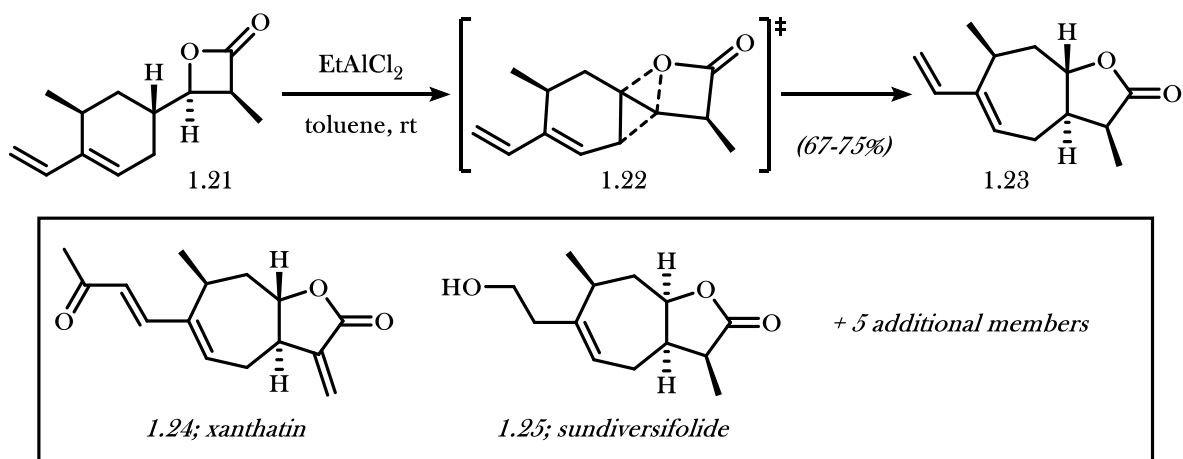
Scheme 1.4 Romo's Dyotropic Rearrangement Applied to Spirolactone Natural Product Synthesis



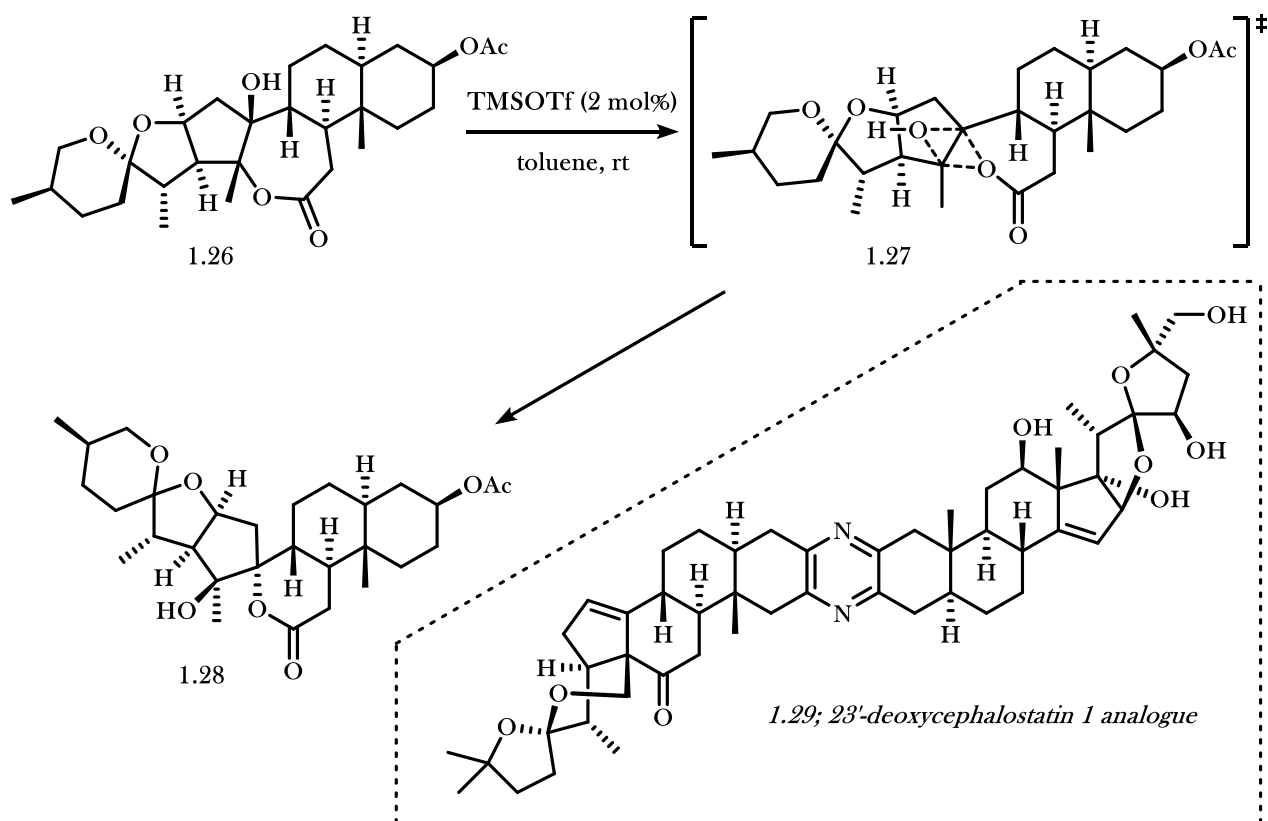
The Romo group then applied their dyotropic rearrangement methodology to total syntheses of (-)-curcumanolide A (**1.19**) and (-)-curcumalactone (**1.20**; Scheme 1.4).¹¹ Prior to the dyotropic rearrangement, the β -lactone precursor was converted to the bis-lactone rearrangement precursor **1.17**. Subsequent TMSOTf catalyzed dyotropic rearrangement proceeds via a concerted mechanistic pathway analogous to that of **1.10**. The product of this skeletal rearrangement was then elaborated to both (-)-curcumanolide A and (-)-curcumalactone.

In 2012, Yang, Leo, and Tang reported the use of a ring-expanding dyotropic rearrangement of β -lactones to form the core of the xanthanolide family of nature products (**1.23**; Scheme 1.5).¹² Using EtAlCl_2 as a Lewis acid, they observed a simultaneous ring-expanding/ring-contracting transformation of precursor **1.21** to form the 5,7-ring system of the xanthanolides. The high diastereoselectivity of this transformation (>19:1 dr) can be attributed to the preferred conformation of the starting material which orients the two migrating bonds in an *anti* fashion to minimize steric interactions. The authors did not propose a mechanism for this transformation, but the high diastereoselectivity of this transformation suggest a concerted interchange of bonds. The product of the dyotropic rearrangement was then elaborated to complete the syntheses of various members of the xanthanolide family.

Scheme 1.5 Tang's Syntheses of the Xanthanolides via Dyotropic Rearrangement



Scheme 1.6 Fuchs's Ring-Contracting Dyotropic Rearrangement Toward Deoxycephalostatin 1 Analogues

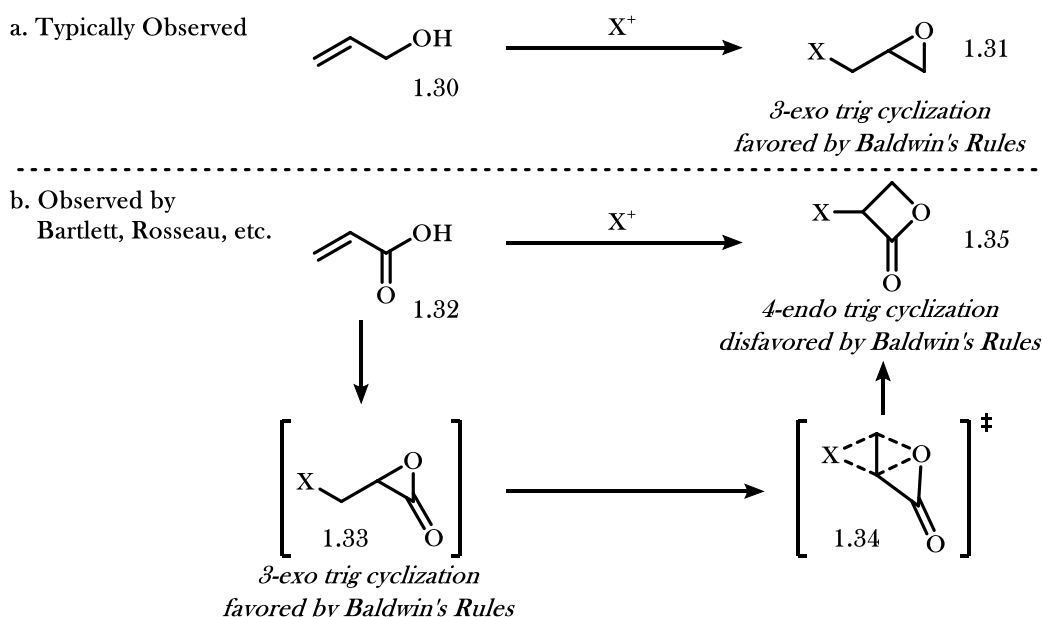


In 2002, the Fuchs group applied a ring-*contracting* dyotropic rearrangement of 7-membered lactones in their total syntheses of 23'-deoxycephalostatin 1 analogues (**1.29**; Scheme 1.6).¹³ Using catalytic TMSOTf as a Lewis acid, they observed an interchange of two C-O bonds of a fused 5,7-ring system to give the corresponding spirocyclic 6,5-fused ring system. The authors did not propose a stepwise or concerted mechanism for this transformation, and the driving force for the ring contraction was not investigated.

1.2.3 Dyotropic Rearrangement of Chlorolactones

In 2008, the Williams group reported a computational investigation into the formation of α -halo, β -lactones by addition of a cationic halide source to acrylates. Typically, activation of an allylic heteroatom with an electrophilic halide source, as in the case of an allylic alcohol **1.30**, will lead selectively to the three-membered ring via the preferred *exo* cyclization (**1.31**; Scheme 1.7). However, as originally reported by Bartlett¹⁴ and subsequently studied by Rosseau,¹⁵ the electrophilic halide activation of acrylates leads instead to the four-membered *endo* cyclization product **1.35**. Rosseau originally described the formation of β -lactones as a direct 4-endo trig cyclization, which is disfavored by Baldwin's rules.¹⁶ They find that increased β -substitution leads to higher yields of four-membered rings, attributed to an increased rate of *endo* cyclization.

Scheme 1.7 Formation of Anti-Baldwin α -Halolactones via Dyotropic Rearrangement

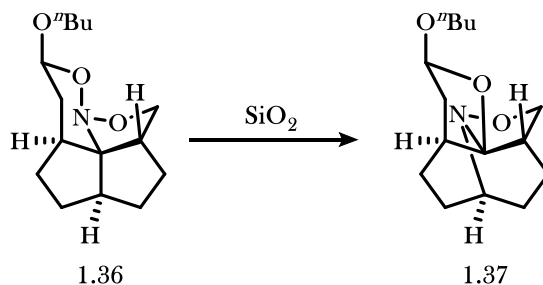


However, a publication by the Williams group reported that the energetic barrier to α -lactone formation via *exo* cyclization from the halonium intermediate is negligible, suggesting that the α -lactone **1.33** is first formed as a kinetic product.¹⁷ To determine the cause of the discrepancy in the literature, the Williams group later showed that a Type I dyotropic rearrangement occurs between the C-O and C-X bonds to form the β -lactone **1.35**.¹⁸ The rate of the dyotropic shift is found to increase depending on β -substitution, providing a rationale for the higher yields of four-membered rings in substituted substrates.

1.2.4 Dyotropic Rearrangement of Nitroso Acetals

In 2005, the Denmark group reported an undesired dyotropic shift of nitrosoacetal **1.36** to the rearranged product (**1.37**; Scheme 1.8).¹⁹ Nitrosoacetal **1.36** was formed via a 1,3-dipolar cycloaddition of a nitronate precursor and pendant olefin. Following attempted purification on silica gel, they observed an interchange of the C-C and N-O bonds of the strained polycyclic core to give rearranged product **1.37**. Although not discussed, the rearrangement likely proceeds in a concerted manner, supported by the preservation of the butoxide acetal which would likely decompose over the course of a stepwise mechanism passing through a zwitterionic intermediate.

Scheme 1.8 Denmark's Observed Nitroso Acetal Dyotropic Rearrangement



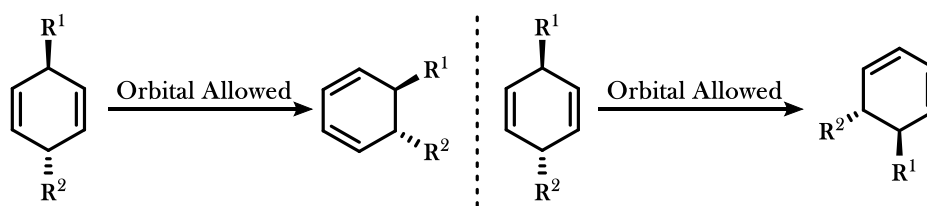
To prevent the dyotropic shift from occurring, the Denmark group exchanged the *n*-butoxy group of **1.36** with a *t*-butoxy derivative, which changed the conformation of the intermediate and prevented the C-C and N-O bonds from adopting an *anti* conformation. In combination with the use of neutral alumina as a

stationary phase during purification, the Denmark group was able to completely prevent the undesired dyotropic rearrangement.

1.3 Type II Dyotropic Rearrangements

Type II dyotropic rearrangements are a less well-defined category of transformations, encompassing all simultaneous transfers of two bonds to another portion of the molecule. Since this reaction by definition brings two parts of a molecule in close proximity, these dyotropic rearrangements are not often observed except in tailormade scaffolds.

Figure 1.3 Reetz's Initially Proposed Type II Dyotropic Rearrangements



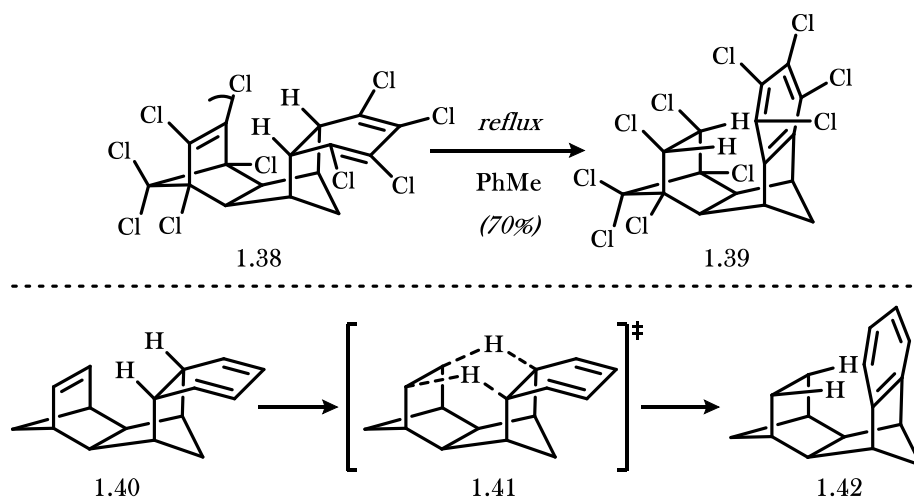
Reetz originally defined these rearrangements based on orbital calculations supporting the proposed rearrangement of substituted cyclohexadiene substrates,³ this predicted reactivity has not yet been validated experimentally (Figure 1.3). Instead, hydrogen transfer mechanisms dominate the literature for Type II dyotropic rearrangements.

1.3.1 Hydrogen Transfer to Form π -bonds

Although early experiments involved hydrogen transfer to form simple alkenes,²⁰ a large majority of Type II dyotropic rearrangements involve the concerted transfer of two C-H bonds to generate aromatic rings (Scheme 1.9). First discovered by MacKenzie in 1965,²¹ and studied extensively with deuterium effect measurements and rate studies,²² these transformations³ are proposed to pass through a concerted, cyclic transition state such as **1.41**.²³ To access this cyclic transition state, the hydrogen atoms and the reactive carbon must be in close proximity prior to the reaction. In a particularly interesting study, the Fernández group also

found that the aromatic stabilization energy of the formed aromatic ring is inversely proportional to the energy of activation for the hydrogen transfer.²⁷ In all cases, they found the synchronicity values (S_0) to indicate a highly concerted mechanism.

Scheme 1.9 Type II Dyotropic Rearrangement Involving Hydrogen Transfer



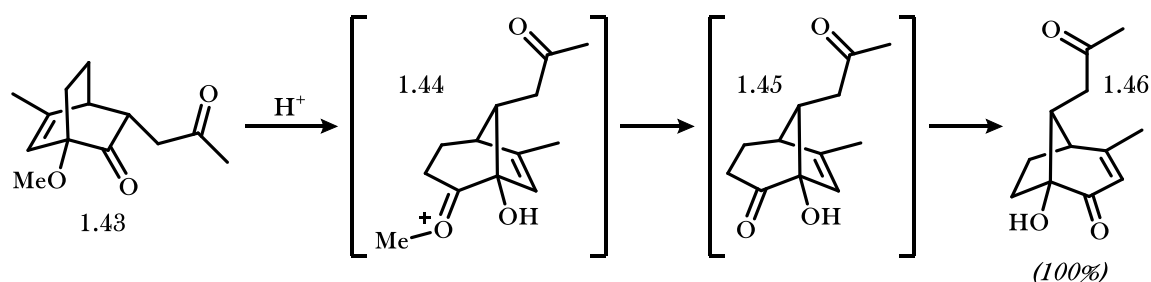
Entry	Aromatic Ring	ASE*	E_a^*
1	Cyclobutadiene	-31.9	62.2
2	Furan	16.2	36.2
3	Thiophene	21.9	35.3
4	Benzene	42.5	29.2

* Values given in kcal/mol

1.4 Stepwise Dyotropic Rearrangements

Although dyotropic rearrangements are concerted by definition, there are a number of reactions that accomplish the same powerful transformation in a formal stepwise manner. Of note is the Monti group's reported rearrangement of [2.2.2]bicycloctene (**1.43**) to the energetically favored [3.2.1]cyclooctene product (**1.46**; Scheme 1.10).²⁴

Scheme 1.10 Monti's Observed Stepwise Dyotropic Rearrangement



Although not discussed by the authors, this rearrangement likely proceeds via a stepwise mechanism involving a charged intermediate **1.44**, as supported by two main observations. First, the two C-C bonds of the precursor that interchange positions are unable to adopt an *anti*-conformation owing to the strained scaffold of the bicyclic core. Additionally, the methyl ether of the starting material undergoes demethylation over the course of the dyotropic rearrangement. This demethylation is unlikely to occur directly from a methyl ether and is more likely occurring via hydrolysis of the oxocarbenium in the proposed intermediate **1.44**.

As described above, dyotropic rearrangements can often switch between concerted and stepwise mechanisms based on the solvent or catalyst system. The individual steps of a formal dyotropic rearrangement might resemble more commonly observed transformations in organic chemistry and therefore might seem less fascinating to the computational or physical chemist. However, to the organic chemist, the overall transformation can be quite useful.

1.5 Conclusions

The dyotropic rearrangement is a unique reaction type by which molecular scaffolds can be procured by unconventional means. The value of dyotropic rearrangements is fully realized when the precursor to the transformation is easily accessed and when the product is difficult to obtain by more conventional methodologies. To make the dyotropic rearrangement a common consideration for an organic chemist when designing a strategy toward a synthetic target, we first must improve our understanding of the favorability and reliability of these transformations. In Chapter 3, our research designed to gain understanding the dyotropic rearrangement of arene-allene cycloadducts is discussed.

1.6 Notes and References

- (1) Reetz, M. T. *Angew. Chem. Int. Ed.* **1972**, *11*, 129–130.
- (2) (a) Köster, R.; Seidel, G.; Boese, R.; Wrackmeyer, B. *Chem. Ber.* **1990**, *123*, 1013–1028. (b) Hupe, E.; Denisenko, D.; Knochel, P. *Tetrahedron* **2003**, *59*, 9187–9198.
- (3) Reetz, M. T. *Angew. Chem. Int. Ed.* **1972**, *11*, 130–131.
- (4) Grob, C. A.; Winstein, S. *Helv. Chim. Acta* **1952**, *35*, 782–802.
- (5) Barton, D. H. R.; Head, A. J. *J. Chem. Soc.* **1956**, *0*, 932–937.
- (6) (a) Christopher Braddock, D.; Roy, D.; Lenoir, D.; Moore, E.; Rzepa, H. S.; Wu, J. I.-C.; von Ragué Schleyer, P. *Chem. Commun.* **2012**, *48*, 8943–8945. (b) Zou, J.-W.; Yu, C.-H. *J. Phys. Chem. A.* **2004**, *108*, 5649–5654. (c) Frontera, A.; Suner, G. A.; Deya, P. M. *J. Org. Chem.* **1992**, *57*, 6731–6735.
- (7) (a) Fernández, I.; Sierra, M. A.; Cossío, F. P. *Chem. Eur. J.* **2006**, *12*, 6323–6330. (b) Reetz, M. T. *Tetrahedron* **1973**, *29*, 2189–2194.
- (8) (a) Mulzer, J.; Brütrup, G. *Angew. Chem. Int. Ed.* **1979**, *18*, 793–794. (b) Black, T. H.; J. DuBay, W. *Tetrahedron Lett.* **1988**, *29*, 1747–1750.
- (9) Purohit, V. C.; Matla, A. S.; Romo, D. *J. Am. Chem. Soc.* **2008**, *130*, 10478–10479.
- (10) Davis, R. L.; Leverett, C. A.; Romo, D.; Tantillo, D. J. *J. Org. Chem.* **2011**, *76*, 7167–7174.
- (11) Leverett, C. A.; Purohit, V. C.; Johnson, A. G.; Davis, R. L.; Tantillo, D. J.; Romo, D. *J. Am. Chem. Soc.* **2012**, *134*, 13348–13356.
- (12) Ren, W.; Bian, Y.; Zhang, Z.; Shang, H.; Zhang, P.; Chen, Y.; Yang, Z.; Luo, T.; Tang, Y. *Angew. Chem. Int. Ed.* **2012**, *51*, 6984–6988.
- (13) Li, W.; LaCour, T. G.; Fuchs, P. L. *J. Am. Chem. Soc.* **2002**, *124*, 4548–4549.

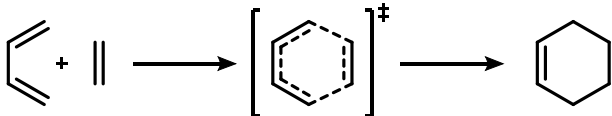


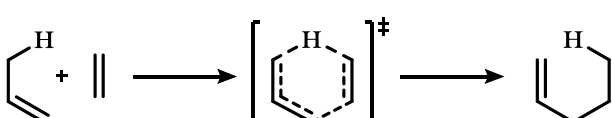
- (14) Tarbell, D. S.; Bartlett, P. D. *J. Am. Chem. Soc.* **1937**, *59*, 407–410.
- (15) Homsí, F.; Rousseau, G. *J. Org. Chem.* **1999**, *64*, 81–85.
- (16) Baldwin, J. E. *J. Chem. Soc. Chem. Commun.* **1976**, *0*, 734–736.
- (17) Ruggiero, G. D.; Williams, I. H. *Chem. Commun.* **2002**, *0*, 732–733.
- (18) Buchanan, J. G.; Ruggiero, G. D.; Williams, I. H. *Org. Biomol. Chem.* **2008**, *6*, 66–72.
- (19) (a) Denmark, S. E.; Montgomery, J. I.; Kramps, L. A. *J. Am. Chem. Soc.* **2006**, *128*, 11620–11630.
(b) Denmark, S. E.; Montgomery, J. I. *Angew. Chem. Int. Ed.* **2005**, *44*, 3732–3736. (c) Davis, R. L.; Tantillo, D. J. *J. Org. Chem.* **2010**, *75*, 1693–1700.
- (20) Grimme, W.; Pohl, K.; Wortmann, J.; Frowein, D. *Liebigs Ann.* **1996**, *1996*, 1905–1916.
- (21) (a) Mackenzie, K. *J. Chem. Soc.* **1965**, *0*, 4646–4653. (b) Mackenzie, K. *J. Chem. Soc. C* **1969**, *0*, 1784–1787.
- (22) (a) Frenking, G.; Cossío, F. P.; Sierra, M. A.; Fernández, I. *Eur. J. Org. Chem.* **2007**, *2007*, 5410–5415. (b) Mackenzie, K.; Howard, J. A. K.; Siedlecka, R.; Astin, K. B.; Gravett, E. C.; Wilson, C.; Cole, J.; Gregory, R. G.; Tomlins, A. S. *J. Chem. Soc., Perkin Trans. 2* **1996**, *0*, 1749–1760. (c) Mackenzie, K.; Howard, J. A. K.; Mason, S.; Gravett, E. C.; Astin, K. B.; Shi-Xiong, L.; Batsanov, A. S.; Vlaovic, D.; Maher, J. P.; Murray, M.; Kendrew, D.; Wilson, C.; Johnson, R. E.; Preiß, T.; Gregory, R. J. *J. Chem. Soc., Perkin Trans. 2* **1993**, *0*, 1211–1228. (d) Mackenzie, K.; Proctor, G.; Woodnutt, D. J. *Tetrahedron* **1987**, *43*, 5981–5993. (e) Houk, K. N.; Li, Y.; McAllister, M. A.; O’Doherty, G.; Paquette, L. A.; Siebrand, W.; Smedarchina, Z. K. *J. Am. Chem. Soc.* **1994**, *116*, 10895–10913.
- (23) Fernández, I.; Sierra, M. A.; Cossío, F. P. *J. Org. Chem.* **2007**, *72*, 1488–1491.
- (24) Monti, S. A.; Dean, T. R. *J. Org. Chem.* **1982**, *47*, 2679–2681.

CHAPTER 2: BACKGROUND TO THE ARENE-ALLENE CYCLOADDITION

2.1 Introduction to Cycloadditions

A pericyclic reaction is any concerted transformation that passes through a cyclic transition state.²⁵ Although this general definition could include a wide variety of reaction types, this category is typically represented by four main types of molecular transformations: cycloadditions, electrocyclizations, sigmatropic rearrangements, and ene reactions (Table 2.1). Although each type of pericyclic reaction has found utility in the synthesis of complex molecular scaffolds, the cycloaddition arguably stands alone as the most important complexity-building pericyclic reaction.

Table 2.1 Pericyclic Reactions and Enthalpic Considerations

Reaction Type	Representative Scheme	Enthalpic Change
Cycloaddition		$2\pi \rightarrow 2\sigma$
Electrocyclization		$1\pi \rightarrow 1\sigma$
Sigmatropic Rearrangement		<i>no change</i>
Ene		$1\pi \rightarrow 1\sigma$

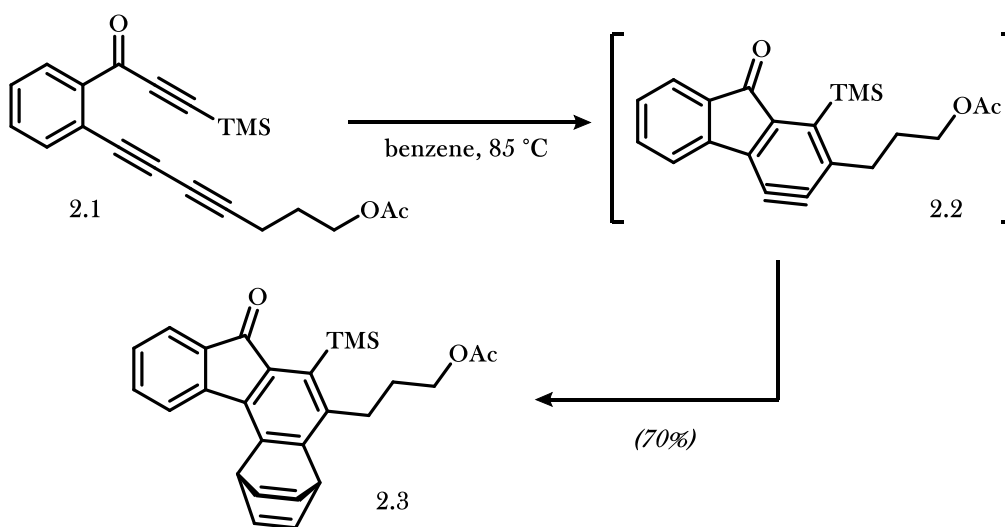
Cycloadditions involve the formation of a cyclic product via the reaction of two π -systems, resulting in a formal exchange of two π -bonds for energetically favored σ -bonds. Due to both steric and electronic impact on the reactive conformation, the rings can be formed with both high regio- and stereoselectivity. The energetic bias of the two components, most often introduced by electron-donating or electron-withdrawing functional groups, promotes electronic “matching” in the transition state between atoms of high and low electron density, which can lead to highly regioselective transformations. Additionally, because the reactive

conformation of the two participants can often be influenced by remote stereocenters or chiral catalysts, the new stereocenters can be formed with high selectivity. The advanced level at which we understand cycloaddition reactions has allowed for their utility in a variety of highly valuable complexity-building transformations.

The Diels–Alder reaction is a $[4\pi + 2\pi]$ cycloaddition involving the formation of a ring from a conjugated diene and an energetically-matched alkene referred to as a dienophile. This reaction is highly energetically favorable owing to the formal exchange of two C–C π -bonds (*ca.* 61 kcal/mol) for two C–C σ -bonds (*ca.* 85 kcal/mol). The large enthalpic benefit from this transformation can therefore overcome the entropic cost of combining two molecules to form a single product. As a result, intermolecular Diels–Alder reactions are quite ubiquitous in the literature.

Diels–Alder reactions involving aromatic rings as diene components are less developed owing to the additional energetic penalty of dearomatization (Table 2.2). Aromaticity is a highly-stabilizing effect of cyclic compounds with alternating single and double bonds that allows for electron density to be distributed throughout the π -network. For benzene, the value of aromatization is *ca.* 36 kcal/mol; the total enthalpy contained within its bonds is 36 kcal/mol greater than that of hypothetical 1,3,5-cyclohexatriene.

Scheme 2.1 Hoye's Dearomatizing Cycloaddition from Benzyne Intermediates



To compensate for the energetic disadvantage and promote the dearomatizing Diels–Alder, several strategies have been utilized. Systems involving highly-reactive cycloaddition participants, such as substrates containing π -bonds with decreased bond dissociation energies, will increase the enthalpic benefit of σ -bond formation and promote ring-formation. Additionally, *intramolecular* cycloadditions, which minimize the entropic cost of ring formation, have been found useful in making complex polycyclic frameworks. The Hoye group has demonstrated the ability of benzyne intermediate **2.2**, which possesses a drastically low bond dissociation energy, to participate in a dearomatizing Diels–Alder reaction as a dienophile (Scheme 2.1).²⁶ In this case, the energy gain for the formation of two the σ -bonds of **2.3** from a high-energy aryne precursor outweighs the aromatic stabilization energy of benzene.

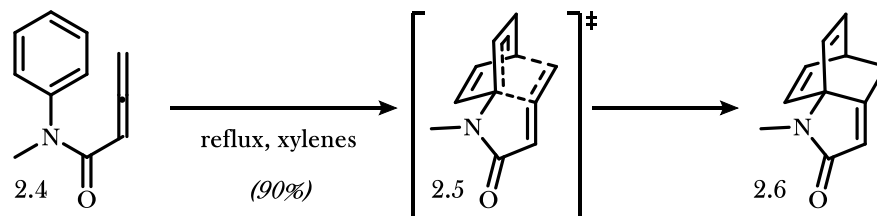
2.2 Himbert’s Arene-Allene Dearomatizing Cycloaddition

2.2.1 Discovery of the Arene-Allene Cycloaddition

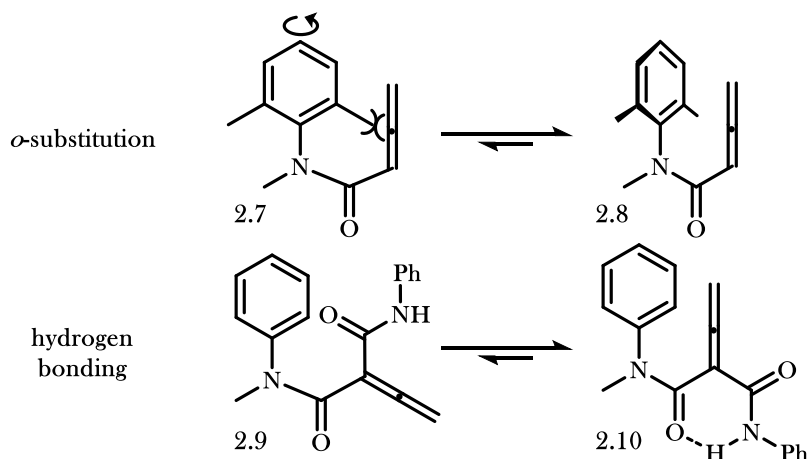
In 1982, Himbert observed an intramolecular dearomatizing Diels–Alder reaction between the aromatic ring and appended allene of precursor **2.4** to form tricyclic cycloadduct (**2.6**; Scheme 2.2a).²⁷ The decreased bond dissociation energy of the allene and the low entropic cost of the intramolecular cycloaddition allow the energetic benefit of σ -bond formation to surpass the stabilization energy of the aromatic ring. Over the course of *ca.* 20 years, Himbert reported a thorough investigation of the scope of this transformation by describing both successful and unsuccessful cycloaddition reactions.²⁸

Scheme 2.2 Himbert's Cycloaddition and Rate-Increasing Substitution Patterns

a. Himbert's Observed Dearomatizing [4+2] Cycloaddition



b. Substituents that Promote the Dearomatizing Cycloaddition

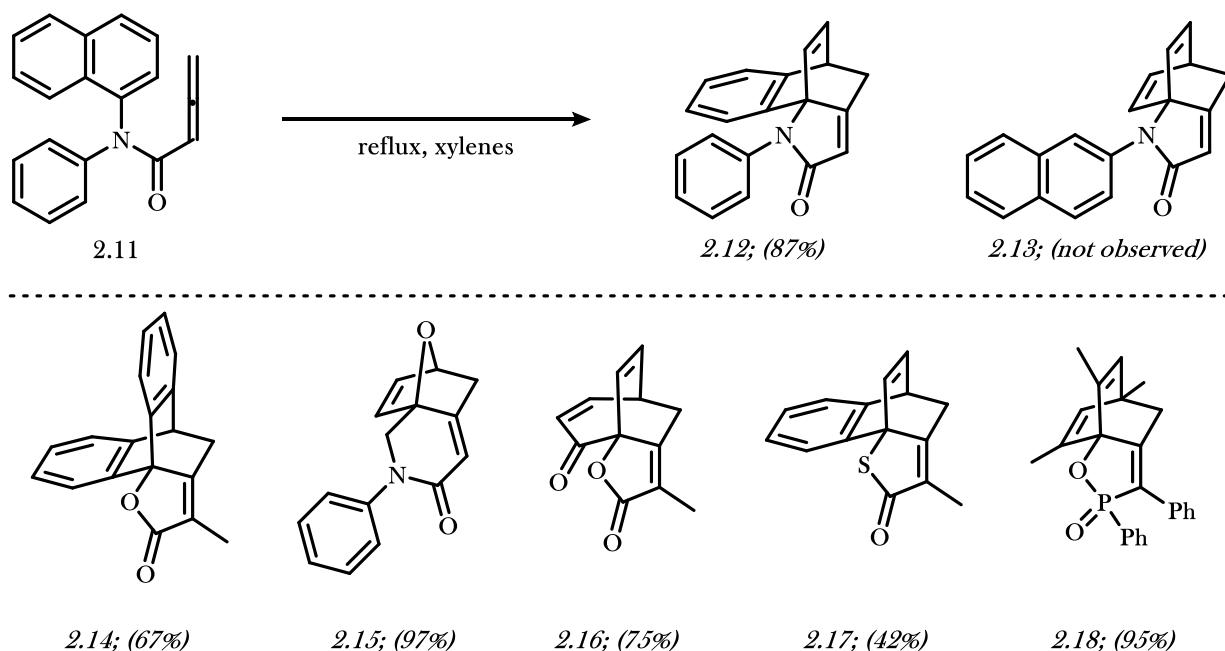


Himbert found that although the degree of electron density has a minute effect on the rate of the transformation, the installation of substituents that promote overlap of the two π -systems results in a significant rate increase. Precursors with substituents in each ortho position of the aromatic ring, such as **2.7**, are unable to adopt a planar confirmation with respect to the allene and the aromatic ring rotates out of plane as a result (Scheme 2.2b).^{4c} The π -system of the rotated aromatic ring then aligns with the π -bond of the allene dienophile, which increases the rate of the transformation. Additionally, α -amide substituted precursors such as **2.9** undergo the cycloaddition at decreased temperatures, likely due to the preferred adoption of a hydrogen-bonding conformation which puts the allene in close proximity to the aromatic ring.^{4a} In a similar manner, α -substitution on the allene increases preference for the reactive conformation and can allow for cycloadditions to occur^{4s} on substrates where lack of substitution results in decomposition under cycloaddition conditions.^{4t}

2.2.2 Scope of the Arene-Allene Cycloaddition

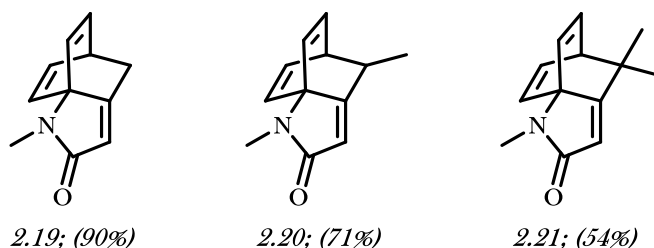
This transformation tolerates significant variability in both the identity and substitution of the aromatic ring and linker, while also allowing for substitution on the allene moiety. In addition to simple benzene rings, naphthalene^{4c,g,l,o,p,r,s} and anthracene^{4j,p} rings can also be dearomatized to form cycloaddition products (**2.12** and **2.14**; Scheme 2.3). In the case of **2.11** where both benzene and naphthalene substituents could both participate in the cycloaddition, naphthalene dearomatized products are observed in high yields.^{4g} This likely corresponds to the decreased dearomatization energy of naphthalene (*ca.* 25 kcal/mol) compared to benzene (*ca.* 36 kcal/mol). A variety of electron-rich and electron-poor substituents at various positions throughout the aromatic ring are also tolerated by the cycloaddition. In addition to simple aniline-derived precursors, the cycloaddition has been observed from furans,^{4m,o,t} thiophenes,⁴ⁿ and tropolones (**2.16**).^{4p}

Scheme 2.3 Effect of Aromatic Stabilization on the Cycloaddition and Representative Cycloadducts



The amide linker has also been replaced with different connecting functional groups with varying results. The linker is not required to be directly bonded to the aromatic ring; *N*-acyl benzylic amine linkers also afford cycloaddition products.^{4j,m,o} In the case of cycloadditions to form [2.2.1]bicyclic systems, such as **2.15**, these expanded linker systems are necessary. In addition to tertiary amides, substrates with ester linkers have also provided cycloaddition products albeit at consistently lower yields; compared to the *N*-methyl amide linker which provides cycloadduct **2.6** in 90% isolated yield,³ the analogous ester linker results in a 63% yield of product.^{4c} Thioester linkers also provide access to cycloaddition products (**2.17**), but are restricted to the dearomatization of naphthalene and anthracene rings.^{4q,r} Furthermore, phosphoryl linkers have also been explored, forming phosphinate (**2.18**) and phosphinamide containing cycloadducts in high yields.^{4w} In a recent publication, our group has also expanded the scope the cycloaddition to include all-carbon linkers.²⁹

Figure 2.1 Effect of Allene γ -Substitution on the Yield of the Cycloaddition

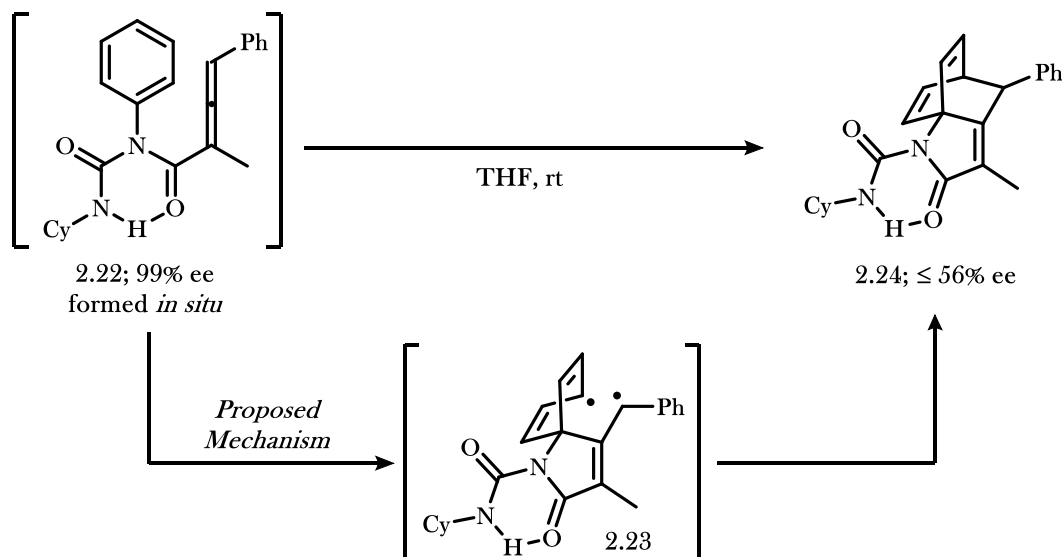


There has been very little exploration of the allene portion of the cycloaddition precursor owing to both the relative lack of sites for derivatization compared to aromatic rings as well as the relative instability of allenes with heteroatom substituents. The α -position of the acyl allene has been substituted with alkyl, aryl,^{4p} silyl,^{3,4d} and secondary amide substituents^{4a,h} to provide cycloadducts with σ -functionalization on the heterocyclic ring. Furthermore, the cycloaddition tolerated allenes with σ -germanium- and σ -arsenic-based substituents.^{4d} On the allenyl γ -position, alkyl,^{4c,l,m} aryl,^{4l,m,r} and silyl³ substituents have been installed, but they typically have a negative impact on the yield of the cycloaddition due to the increased steric hindrance of the reactive dienophile (Figure 2.1).

2.2.3 Mechanism of the Arene-Allene Cycloaddition

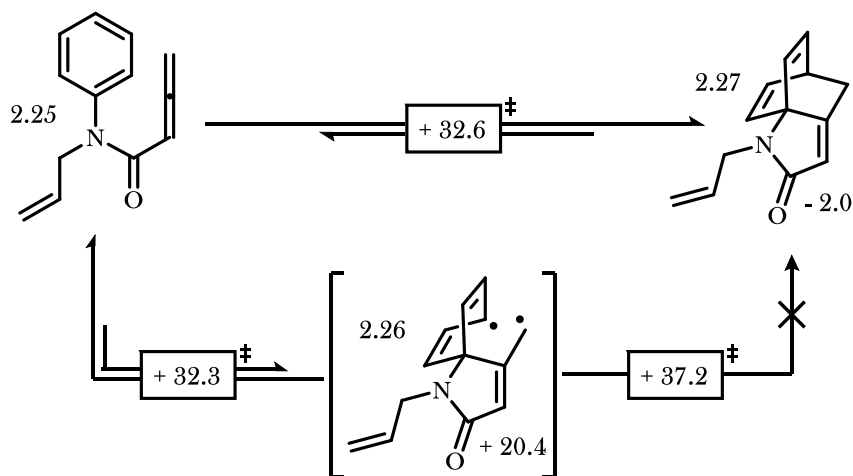
There have been a several mechanistic studies on the dearomatizing arene-allene cycloaddition. Himbert first determined the reversibility of the cycloaddition by resubjecting an isolated cycloaddition product to cycloaddition conditions and observing the regeneration of the aromatic precursor.³ Additionally, Himbert's work measuring substituent effects on cycloaddition rates led him to propose a concerted cycloaddition mechanism; a stepwise mechanism involving transient formation of charged intermediates would likely be impacted more significantly by the electronic influence of substituents. However, in a future study, the Orahovats group observed epimerization of the stereocenter formed from enantioenriched, axially chiral γ -substituted allene **2.22**, which would not occur via a purely concerted mechanism (Scheme 2.4).³⁰ Considering Himbert's elimination of a polar stepwise mechanism, Orahovats proposed a radical mechanism involving intermediate formation of spirocycle **2.23** and subsequent radical recombination of the allylic and pentadienyl radicals to form **2.24**. Aside from these contributions, very little insight into the mechanism had been developed prior to our group's interest in this powerful transformation.

Scheme 2.4 Orahovats's Observed Degradation of Enantioselectivity and Proposed Mechanism



With this in mind, we entered into a collaborative experimental and computational investigation with the Houk group at UCLA to provide insight into the mechanism of this transformation. The Houk group's computational results show that both radical and concerted pathways contribute to the overall reaction landscape (Figure 2.2). The concerted mechanism passes through a transition state energy of 32.6 kcal/mol to form cycloaddition product **2.27**, which is calculated to be 2.0 kcal/mol more stable than the aromatic precursor **2.25**.⁵ However, an initial *ipso* bond formation to give spirocycle **2.26**, which contains an allylic and non-conjugated pentadienyl radical pair, passes through a transition state 32.3 kcal/mol in energy. The almost identical transition state energies for these two mechanistic steps mean they proceed with similar rates, and therefore both can impact reaction outcome. However, the radical recombination of diradical species **2.26** proceeds through a transition state *ca.* 37.2 kcal/mol in energy, significantly higher than the transition state for the concerted cycloaddition. As a result, it can be concluded that although the diradical spirocycle **2.26** is likely formed under the reaction conditions, this intermediate is not productive toward the formation of cycloaddition product **2.27**; cycloadduct **2.27** is instead formed via a concerted cycloaddition. When the precursor contains γ -substitution, sampling of a radical intermediate like **2.26** would result in epimerization.

Figure 2.2 Houk's Computational Data Supporting Equilibrium Formation of Radical Species



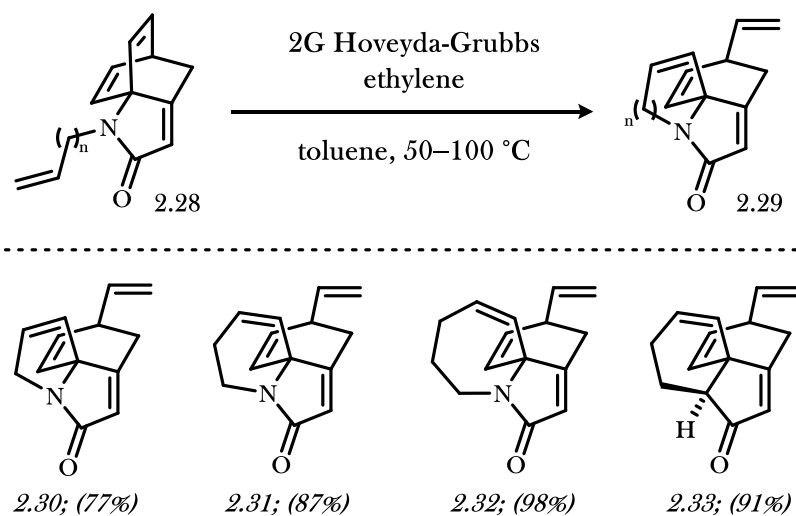
2.3 Further Reactivity of Arene-Allene Cycloadducts

There have been several efforts to expand the complexity of molecular scaffolds that the dearomatizing cycloaddition can provide access to beyond the simple bicyclo[2.2.2]octadiene core. The cycloaddition product contains five sp^2 hybridized carbon atoms which introduce a great deal of strain to the tricyclic system. As a result, reactions that alleviate this strain often proceed via surprisingly low energetic barriers to provide strain-relieved products. Sequences involving a dearomatizing cycloaddition and subsequent rearrangement can be a strategic way by which complex molecular scaffolds can be procured from simple, aromatic precursors.

2.3.1 *Vanderwal's RCM/ROM Cascade*

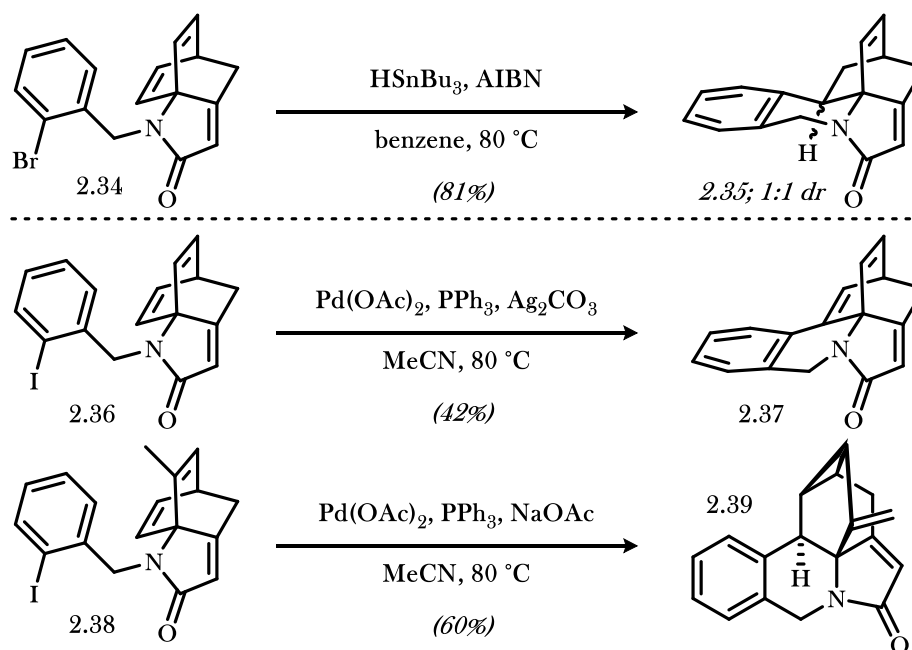
The discovery of alkene metathesis marks one of the most important developments in organic chemistry to date, and this powerful complexity-building tool has been used in the formation of a number of natural product scaffolds. Although ring-closing metathesis (**RCM**) has found more utility in natural product synthesis,³¹ ring-opening metathesis (**ROM**) also enables the formation acyclic alkenes from cyclic precursors. In the case of highly-strained cyclic alkene precursors, ring-opening metathesis often leads to high yields of products due to the unfavorability of the reverse ring-closing reaction to reform the strained ring. The alkenes of arene-allene cycloaddition products, therefore, are excellent candidates for ring-opening metathesis reactions due to their strain.

Scheme 2.5 Vanderwal's RCM/ROM Cascade on Arene-Allene Cycloaddition Products



The Vanderwal group developed a RCM/ROM cascade to form novel, stereodefined polycyclic scaffolds from cycloadduct products (Scheme 2.5).³² The cascade typically initiates from an *N*-tethered alkene substituent, such as that of **2.28**, and a subsequent RCM/ROM cascade releases the strain of the bicyclo[2.2.2]octadiene core. Under a pressure of ethylene gas, the resulting ruthenium carbenoid will then undergo an additional alkene metathesis to regenerate the catalyst and release products **2.29**. In the case of short *N*-tethers, such as *N*-allyl derivatives, initial metalcarbenoid formation from the terminal olefin is unproductive toward product formation, and the reaction must first undergo ring-opening metathesis prior to ring-closure to form products such as **2.30**. This metathesis cascade tolerates a variety of functional groups to form substituted polycyclic products. Although the product scaffolds resemble those of *Erythrina* alkaloids,³³ no efforts have so far been made in the application of this strategy toward their total synthesis.

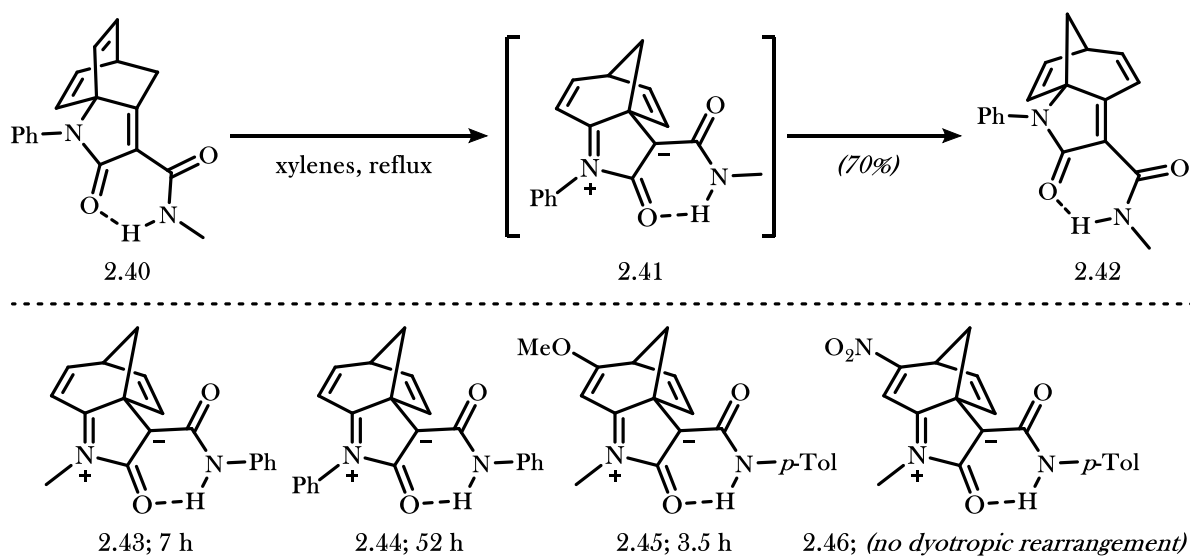
Scheme 2.6 Vanderwal's Ring-Closing Reactions of Arene-Allene Cycloadducts



2.3.2 Additional Vanderwal Ring-Closing Reactions of Cycloaddition Products³⁴

The Vanderwal group extended their interest in functionalization of the ring alkenes of the bicyclo[2.2.2]octadiene core to include new radical and organometallic ring-closing reactions (Scheme 2.6). It was discovered that *N*-functionalization with proper substituents allow ring-closure across the olefins. Single-electron reduction of aryl bromide **2.34** results in 6-exo-trig radical cyclization and hydrogen atom transfer to the resulting secondary radical to form ring-closed product **2.35**. Additionally, two-electron reduction of the analogous aryl iodide **2.36** via palladium catalysis promotes a Heck cyclization to form either **2.37** or **2.39**, depending on substitution and conditions. Although these transformations have yet to find utility, these examples show the great potential for complexity-building elaborations on the products of arene-allene cycloadditions.

Scheme 2.7 Himbert's Observed Dyotropic Shift of Arene-Allene Cycloadducts



2.3.3 Himbert's Formal Dyotropic Shift

As previously discussed, Himbert observed that cycloaddition precursors with α -amide substituents undergo the dearomatizing Diels-Alder reaction to form **2.40** at decreased temperatures, likely owing to hydrogen bonding effects which place the reactive π -systems in close proximity.^{4a} However, at elevated temperatures, Himbert also observed that the bicyclo[2.2.2]octadiene core of this cycloadduct **2.40** undergoes a thermal rearrangement to product **2.42** containing a bicyclo[3.2.1]octadiene core.^{4a,v}

This formal dyotropic shift product is proposed to proceed via a two-step, polar mechanism involving a zwitterionic intermediate **2.41**, based on several observations by the Himbert group. First, an *N*-phenyl substituent greatly extends the reaction time of the transformation to form **2.44** compared to **2.43**; the half-life increases from 7 hours to 52 hours.^{4v} This is likely due to the electron-withdrawing effects of a phenyl ring which would destabilize the partial positive character of the nitrogen component of the zwitterionic intermediate **2.41**. Additionally, they found electron-donating substituents on the non-migrating alkene to increase the rate of the transformation, as in **2.45**, while cycloadducts with analogous electron withdrawing groups (**2.46**) hamper the reactivity. These observations correlate with the ability of substituents to stabilize

the cationic character of the zwitterionic intermediate, since the non-migrating alkene moves into conjugation with the cationic lactam nitrogen.

2.4 Conclusions

Himbert's arene-allene cycloaddition is a rare example of a dearomatizing [4 + 2] cycloaddition that is both high-yielding and tolerant of a wide range of substituents. Although several strategies exist that increase the precursor's preference to sit in the reactive conformation and thereby increase the reaction rate, the dearomatizing cycloaddition can also provide high yields of simple cycloaddition product, albeit at slower rates. The cycloaddition products have been elaborated to form ring-appended or ring-opened products using a variety of strategies. Additionally, Himbert's cycloaddition provides clean conversion to a rearranged [3.2.1] bicyclic scaffold that welcomes analysis from both a synthetic and computational perspective. In our opinion, Himbert's discovery of the dyotropic rearrangement of arene-allene cycloadducts warranted further analysis, and our contributions to the study of this formal dyotropic shift are highlighted in Chapter 3.

2.5 Notes and References

- (1) E. A. Anslyn, D. A. Dougherty, in *Modern Physical Organic Chemistry*, Chapt. 15, **2006**.
- (2) Hoye, T. R.; Baire, B.; Niu, D.; Willoughby, P. H.; Woods, B. P. *Nature* **2012**, *490*, 208-212.
- (3) Himbert, G.; Henn, L. *Angew. Chem. Int. Ed.* **1982**, *21*, 620.
- (4) (a) Himbert, G.; Diehl, K.; Maas, G. *J. Chem. Soc., Chem. Commun.* **1984**, 900-901. (b) Himbert, G.; Henn, L. *Liebigs. Ann.* **1984**, 1358-1366. (c) Himbert, G.; Fink, D. *Tetrahedron Lett.* **1985**, *26*, 4363-4366. (d) Henn, L.; Himbert, G.; Diehl, K.; Kaftory M. *Chem. Ber.* **1986**, *119*, 1953-1963. (e) Diehl, K.; Himbert, G.; Henn, L. *Chem. Ber.* **1986**, *119*, 2430-2443. (f) Diehl, K.; Himbert, G. *Chem. Ber.* **1986**, *119*, 2874-2888. (g) Himbert, G.; Diehl, K.; Schlindwein, H. J. *Chem Ber.* **1986**, *119*, 3227-3235. (h) Diehl, K.; Himbert, G. *Chem. Ber.* **1986**, *119*, 3812-3825. (i) Himbert, G.; Fink, D.; Diehl, K. *Chem. Ber.* **1988**, *121*, 431-441. (j) Schlindwein, H. J.; Diehl, K.; Himbert, G.

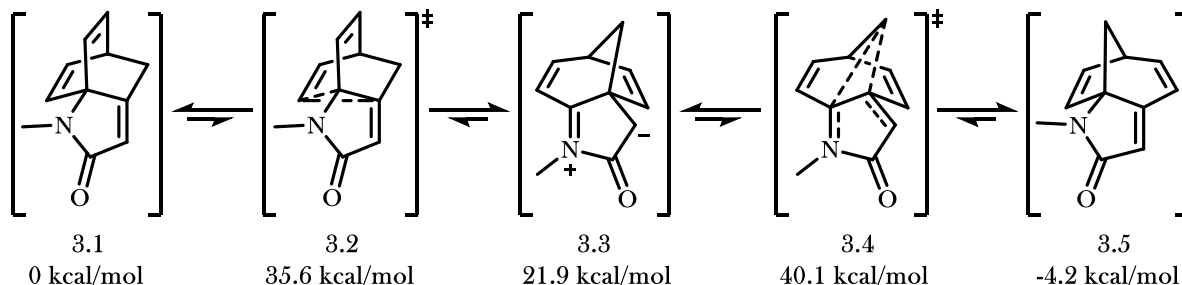
- Chem. Ber.* **1989**, *122*, 577-584. (k) Himbert, G.; Fink, D.; Diehl, K.; Rademacher, P.; Bittner, A. *J. Chem. Ber.* **1989**, *122*, 1161-1173. (l) Himbert, G.; Diehl, K.; Schlindwein, H. J. *Chem. Ber.* **1989**, *122*, 1691-1699. (m) Schlindwein, H. J.; Himbert, G. *Chem. Ber.* **1989**, *122*, 2331-2339. (n) Himbert, G.; Schlindwein, H. J.; Maas, G. *J. Chem. Soc., Chem. Commun.* **1990**, 405-406. (o) Himbert, G.; Schlindwein, H. J. *Z. Naturforsch. B; Chem. Sci.* **1992**, *47*, 1785-1793. (p) Himbert, G.; Fink, D.; Stuermer, M. *Z. Naturforsch. B; Chem. Sci.* **1994**, *49*, 63-75. (q) Himbert, G.; Fink, D. *Z. Naturforsch. B; Chem. Sci.* **1994**, *49*, 542-550. (r) Himbert, G.; Fink, D. *J. Prakt. Chem.* **1994**, *336*, 654-657. (s) Himbert, G.; Fink, D. *J. Prakt. Chem.* **1996**, *338*, 355-362. (t) Himbert, G.; Schlindwein H. J. *Liebigs Ann.* **1997**, 435-439. (u) Himbert, G.; Fink, D. *J. Prakt. Chem.* **1997**, *339*, 233-242. (v) Himbert, G.; Diehl, K. *Liebigs Ann.* **1997**, 1255-1260. (w) Himbert, G.; Ruppnich, M.; Knoring, K. *J. Chin. Chem. Soc.* **2003**, *50*, 143-151.
- (5) Schmidt, Y.; Lam, J. K.; Pham, H. V.; Houk, K. N.; Vanderwal, C. D. *J. Am. Chem. Soc.* **2013**, *135*, 7339-7348.
- (6) Trifoniv, L. S.; Orahovats, A. S. *Helv. Chim. Acta* **1989**, *72*, 59-64.
- (7) Atwood, B. A.; Vanderwal, C. D. *Aldrichimica Acta* **2017**, *50*, 17-27.
- (8) Lam, J. K.; Schmidt, Y.; Vanderwal, C. D. *Org. Lett.* **2012**, *14*, 5566-5569.
- (9) Parsons, A. F.; Palfreman, M. J. *Alkaloids* **2010**, *68*, 39-81.
- (10) Data obtained by Dr. Diane Lim.

CHAPTER 3: INVESTIGATION INTO THE FORMAL DYOTROPIC REARRANGEMENT OF ARENE-ALLENE CYCLOADDUCTS

3.1 Introduction and Inspiration

Himbert's formal dyotropic shift of arene-allene cycloadducts marked the discovery of an interesting and potentially useful transformation, and therefore prompted further investigation from both computational and synthetic perspectives. To probe the mechanism, scope, and limitations of this transformation, we entered into an experimental and computational collaboration with the Houk group at UCLA.¹ The goal of the collaboration was to identify a plausible mechanism for the dyotropic rearrangement, and to support the proposed mechanism by measuring the effect of substituents on the rate of the reaction.

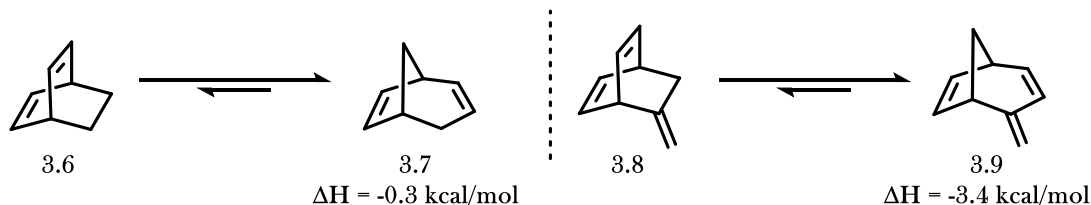
Figure 3.1 The Houk Group's Calculated Mechanism for the Formal Dyotropic Shift



It was first determined that the dyotropic shift proceeds via a polar, stepwise mechanism passing through a zwitterionic intermediate (Figure 3.1). As first proposed by Himbert,² but not yet supported by computational data, a thermal 1,2-vinyl shift promoted by the lactam nitrogen initiates the rearrangement away from the bicyclo[2.2.2]octadiene core. For precursor **3.1**, the activation energy for the initial 1,2-vinyl shift is 35.6 kcal/mol, and the resulting zwitterionic intermediate **3.3** 21.9 kcal/mol higher in energy than the neutral starting material. The anionic component of the zwitterionic intermediate **3.3** can then promote a 1,2-methylene shift, passing through a transition state at 40.1 kcal/mol in energy (**3.4**), to form the terminal bicyclo[3.2.1]octadiene product **3.5**. The higher energy necessary to accomplish the 1,2-methylene shift can be attributed to the lack of a π -orbital on the migrating group to participate in the shift, which is a contributing

factor for the initial 1,2-vinyl shift. Each step in this transformation is reversible; the anion of the zwitterionic intermediate can also promote a retro 1,2-vinyl shift to regenerate the starting material. However, under equilibrating conditions, the bicyclic scaffold strongly prefers to rest as the bicyclo[3.2.1]octadiene **3.5**, which is energetically preferred by 4.2 kcal/mol.

Figure 3.2 *The Strain Energy of Bicyclooctadiene Scaffolds*



The product of the dyotropic shift is energetically preferred for two reasons. First, an alkene of the bicyclic core of **3.5** falls into conjugation with the alkene on the lactam ring, resulting in an $\alpha,\beta,\gamma,\delta$ -unsaturated lactam. This increase in stabilization energy can be attributed to the dissociation of the alkene electron density throughout the π -network. Secondly, the Houk group showed that bicyclo[3.2.1]octadiene **3.7** is more stable than the analogous bicyclo[2.2.2]octadiene isomer **3.6** due to the decreased mechanical strain (Figure 3.2). Although the rearrangement of simple bicyclo[2.2.2]octadiene bicycles only results in a modest release of energy, the introduction of an additional sp^2 carbon center, a feature of arene-allene cycloadducts, significantly increases the energetic favorability of the rearranged bicyclo[3.2.1]octadiene core (**3.9**).

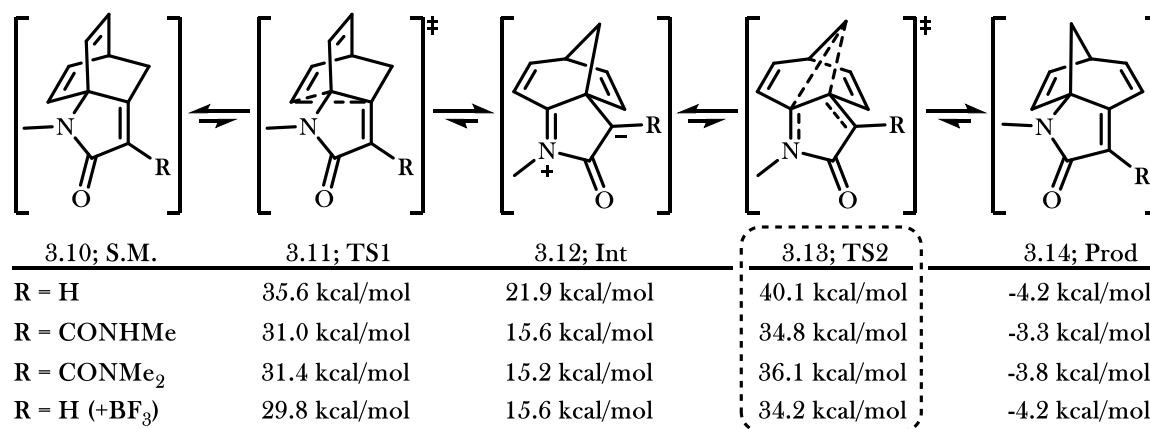
3.2 Lewis Acid Catalyzed Dyotropic Rearrangement

The Himbert group first observed the dyotropic rearrangement on substrates that possessed an amide in the α -position of the lactam.^{2,3} It was postulated that the anionic component of the zwitterionic intermediate was resonance-stabilized by the π -system of the amide, thereby lowering the energy of the zwitterion and allowing the shift to occur at a lower temperature. We began our efforts by computationally investigating the impact of alternative α -substitution on the energy landscape of the dyotropic rearrangement, which would provide insight into whether an α -substituent was necessary to promote the rearrangement.

3.2.1 Computational Data Supporting the Lewis Acid Catalyzed Dyotropic Rearrangement

Compared to the unsubstituted cycloadduct, arene-allene cycloadducts with an amide in the α -position of the lactam benefit from significantly decreased energies of both the zwitterionic intermediate and transition states throughout the mechanistic pathway (Figure 3.3). The anion-stabilizing effect of the amide in the zwitterionic intermediate leads to an overall decrease in energy of 6.3 kcal/mol. As a result, the amide also stabilizes the charged character in each transition state, stabilizing TS1 by 4.6 kcal/mol and TS2 by 5.3 kcal/mol. The significant decrease in the energy of TS2 leads to an overall decreased energy of activation for the entire transformation, allowing the dyotropic shift to occur at lower temperatures in activated substrates.

Figure 3.3 Effect of α -Functionality on the Energy Landscape of the Dyotropic Rearrangement

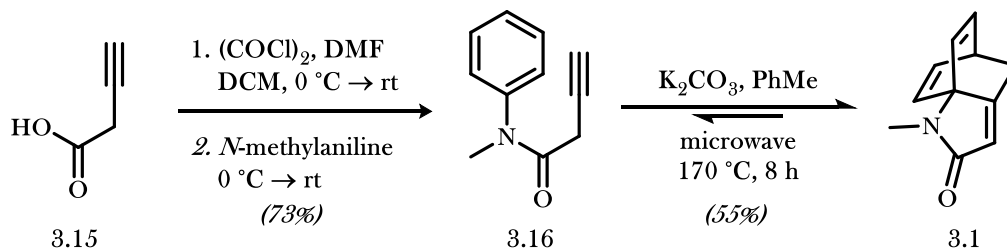


This result led us to consider whether the dyotropic shift could occur on unsubstituted substrates via intermolecular stabilization of the anion. Lewis acids have previously been used to accomplish formal dyotropic shifts that proceed through a zwitterionic intermediate.⁴ If the addition of a Lewis acid could sufficiently stabilize the anionic character of TS2, then the need for α -functionality to stabilize the anionic charge could be rendered unnecessary. To this end, the Houk group found that the addition of BF₃ as a Lewis acid to the unsubstituted cycloadduct would decrease the energy of TS2 to 34.2 kcal/mol, theoretically permitting the dyotropic shift to occur at a similar rate to cycloadducts with α -amide substituents.

3.2.2 Experimental Validation of the Lewis Acid Catalyzed Dyotropic Rearrangement

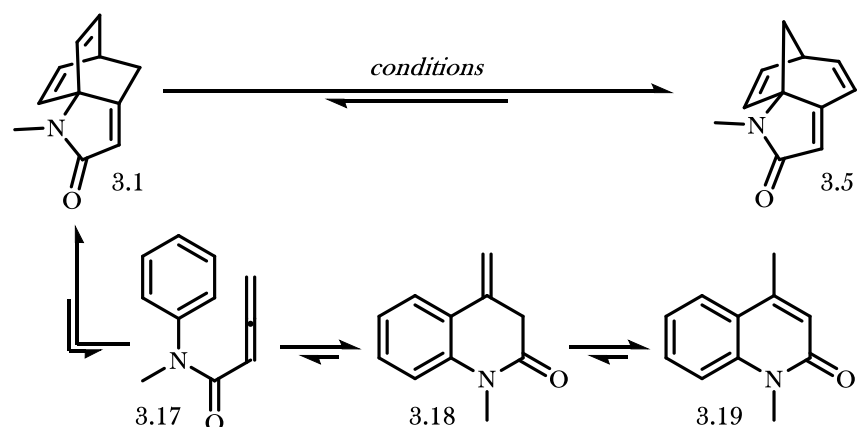
We began our efforts toward experimental validation of the Houk group's computations by first procuring the unsubstituted rearrangement precursor **3.1** (Scheme 3.1). We first prepared substrate **3.16** via formation of the corresponding acid chloride of 3-butynoic acid and subsequent amide coupling with *N*-methylaniline. Of note, other methods for the formation of amide bonds from carboxylic acid precursors, including carbodiimide activated amide couplings, resulted in product mixtures formed via alkyne isomerization. By instead activating 3-butynoic acid as the acid chloride, we found we could eliminate the formation of isomerized products. The dearomatizing [4+2] cycloaddition of amide **3.16** at elevated temperatures affords cycloadduct **3.1** in moderate but reproducible yields.

Scheme 3.1 Preparation of the Unsubstituted Dyotropic Rearrangement Precursor



With **3.1** in hand, we began our investigation on Lewis acid activation to accomplish the dyotropic rearrangement. We first found that, in the *absence* of Lewis acid, quinolone **3.19** is formed as a major product when the reaction was run at temperatures necessary to afford conversion (Table 3.1).⁵ The quinolone product is presumably formed via a [4+2]-cycloreversion and subsequent electrocyclicization to form the unconjugated lactam **3.18**. From there, a simple alkene migration into conjugation with the lactam affords quinolone **3.19**.

Table 3.1 Lewis Acid Promoted Dyotropic Rearrangement of Unactivated Cycloadducts



Entry	Reagents	Solvent	Conditions	Yield of 3.5 ^Ψ
1	(None)	<i>o</i> -DCB	250 °C*, 3h	12%
2	BF ₃ ·Et ₂ O (0.5 equiv.)	<i>o</i> -DCB	200 °C*, 3h	31%
3	TMSOTf (0.5 equiv.)	<i>o</i> -DCB	200 °C*, 3h	74%
4	TMSOTf (0.5 equiv.) DTBP (0.1 equiv.)	<i>o</i> -DCB	200 °C*, 3h	99%
5	TMSOTf (0.5 equiv.) DTBP (0.1 equiv.)	toluene	100 °C, 3h	92%

o-DCB = *o*-dichlorobenzene; DTBP = 2,6-di-*tert*-butylpyridine; * = microwave heating
TMSOTf = trimethylsilyl trifluoromethylsulfonate; Ψ = isolated yield

We were excited to initially observe the formation of the dyotropic shift product **3.5** in 31% yield at decreased temperatures in the presence of BF₃·Et₂O as a Lewis acid using microwave irradiation as a heating source. However, we also observed significant uncharacterizable decomposition. We suspected that a milder Lewis acid might reduce the amount of decomposition, and soon identified TMSOTf as an efficient Lewis acid for this transformation. To further reduce the amount of decomposition, which we suspect resulted from trace acid present in prepared dilute solutions of TMSOTf, we added 10 mol% of the non-nucleophilic base 2,6-di-*tert*-butylpyridine (DTBP) to neutralize any trace acid in the reaction mixture.⁶ Under these conditions, we observed quantitative yields of desired dyotropic shift product **3.5**. In a search for milder reaction conditions, we found that nearly quantitative yields of the rearranged product could be formed thermally at just 100 °C using toluene as a solvent. These simple, relatively mild conditions greatly expand the substrate scope for the dyotropic rearrangement of arene-allene cycloadducts.

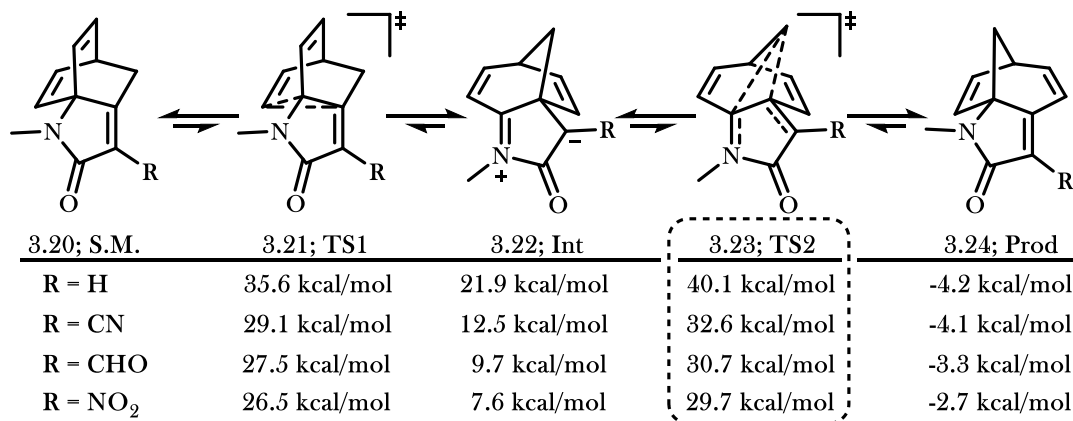
3.3 Dyotropic Rearrangement via Electron Withdrawing Group Stabilization

In each of Himbert's reported examples of the dyotropic rearrangement, the α -amide substituent necessary to accomplish the transformation was a secondary amide. The free N-H bond present in a secondary amide introduces ambiguity as to whether anion stabilization or hydrogen bonding with the amide N-H is the key factor in promoting the dyotropic rearrangement. To disprove hydrogen bonding as a necessary factor, and instead identify resonance stabilization as the principal promotor of the dyotropic rearrangement, we investigated the impact of non-hydrogen bonding α -electron withdrawing substituents on the reaction mechanism.

3.3.1 Computational Data Supporting the Electron Withdrawing Group Stabilized Dyotropic Shift

The Houk group found that a lack of hydrogen bonding has very little effect on the energy landscape of the dyotropic rearrangement; a tertiary amide also decreases the activation energy for the transformation by 4.0 kcal/mol (Figure 3.3). Although the tertiary amide does not stabilize the transition state as effectively as the secondary amide, which decreases the activation energy by 5.3 kcal/mol, the discrepancy could be due to the increased electron density of the tertiary amide π -system and the resulting decrease in its ability to stabilize anions.

Figure 3.4 Effect of Several α -Electron Withdrawing Substituents on the Dyotropic Rearrangement

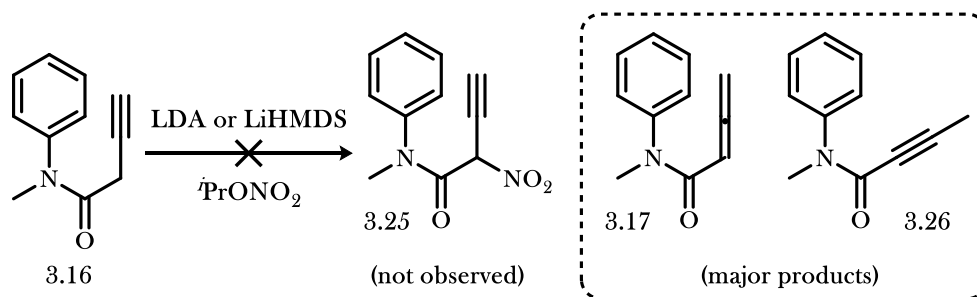


To further prove that hydrogen bonding is not necessary for the dyotropic rearrangement, the Houk group found that a variety of resonance stabilizing groups, including nitriles, aldehydes, and nitro substituents, are able to sufficiently stabilize the zwitterionic intermediate and promote the dyotropic rearrangement (Figure 3.4). Because cycloadducts with these substituents in the α -position had not previously been synthesized, we explored different approaches to procure these cycloadducts and validate the computational results.

3.3.2 Attempted Installation of an α -Electron Withdrawing Group via Direct Nucleophilic Attack

Inspired by the work of the Zajac group,⁷ we first attempted to directly substitute the cycloaddition precursor **3.16** via enolate attack of an electrophilic nitro source. On this system, we expected to encounter difficulties in installing the nitro substituent with high regioselectivity; similar work toward methylation at this position by the Vanderwal group resulted in a 27% yield of the α -methylated product, with significant alkyne methylation due to preferred deprotonation of the more acidic sp-hybridized position.⁸

Scheme 3.2 Attempted Direct Substitution of α -Nitro Functionality



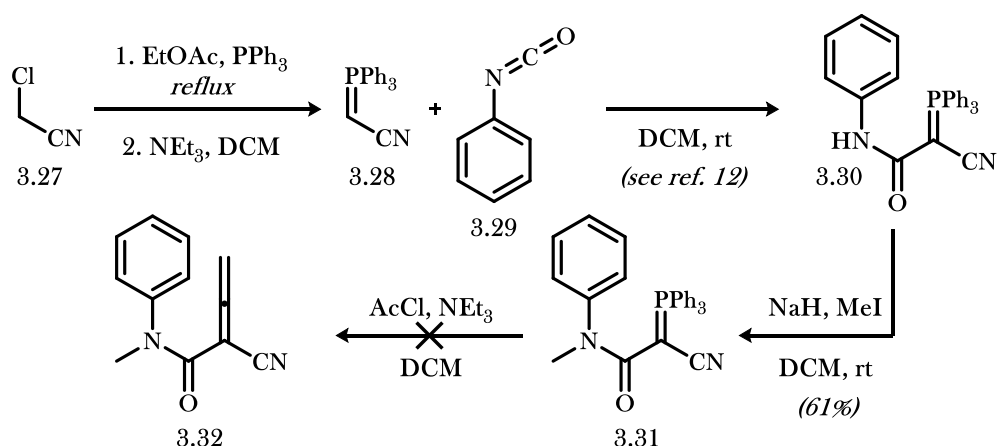
Attempts to install a nitro group at the α -position to form amide **3.25** resulted predominantly in isomerization to allene **3.17** and internal alkyne **3.26**, accompanied by a significant degree of decomposition (Scheme 3.2). The rapid isomerization of **3.16** to **3.17** suggests that, if α -nitro installation were successful, rapid isomerization would likely produce a doubly-activated conjugate acceptor allene product. We speculated that transient formation of the highly-electrophilic species could be a contributing pathway toward decomposition. For this reason, we turned our attention to allenyl nitrile **3.32**, as the more moderate electron-

withdrawing properties of the nitrile might improve the stability of the allene.

3.3.3 Attempted Installation of an α -Electron Withdrawing Group via Ketene Wittig Strategy

We hypothesized that allene **3.32** could be formed via a ketene Wittig reaction, as used by both the Himbert⁹ and the Vanderwal¹⁰ groups in the synthesis of several cycloaddition precursors. This reaction involves nucleophilic attack of an ylide precursor into the highly reactive carbonyl of ketene, and subsequent [2+2]-cycloreversion to release triphenylphosphine oxide and generate an allene product. Ketene can either be prepared by a ketene generator, which takes advantage of the thermal Type I Norrish fragmentation of acetone,¹¹ or it can be generated *in situ* through the base-catalyzed elimination of acetyl chloride. Typically, *in situ* generation of ketene is sufficient for the purpose of ketene Wittig-type transformations.

Scheme 3.3 Attempted Ketene Wittig Route Toward the α -EWG Substituted Cycloadduct

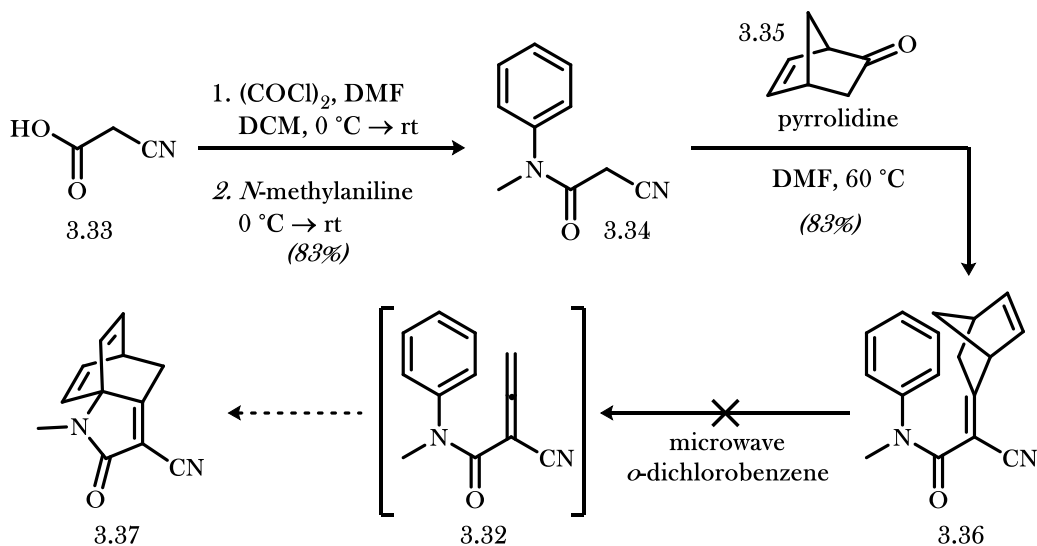


Ylide **3.28** was first prepared in two steps from chloroacetonitrile and then treated with phenyl isocyanate as shown by the Kumar group (Scheme 3.3).¹² The secondary amide **3.31** was subsequently methylated to afford ylide **3.32**. Unfortunately, various attempts to accomplish the ketene Wittig transformation were unsuccessful, resulting in recovery of starting material and observation of diketene. We reasoned that the highly stabilized nature of ylide **3.32** renders it non-nucleophilic and unable to participate in the Wittig reaction.

3.3.4 Attempted Installation of an α -Electron Withdrawing Group via Cycloreversion Strategy

At this point, we identified the instability of the doubly-activated allene as the most important factor preventing the formation of the α -electron withdrawing group substituted cycloadduct. We therefore changed our strategy to seek methods that circumvented the need to isolate this unstable species. Inspired by the Tielens group's method for quinone formation via retrocycloaddition,¹³ we attempted to form **3.32** via a [4+2]-cycloreversion of bicyclo[2.2.1]heptene adduct **3.36** to liberate cyclopentadiene. Although this reaction is typically used to unveil conjugated alkenes, we had hoped that we could accomplish a one-pot retrocycloaddition/cycloaddition at elevated temperatures to directly afford the arene-allene cycloadduct **3.37** without having to isolate the highly electrophilic allene intermediate **3.32**.

Scheme 3.4 Attempted Retrocycloaddition Strategy Toward the α -EWG Substituted Cycloadduct



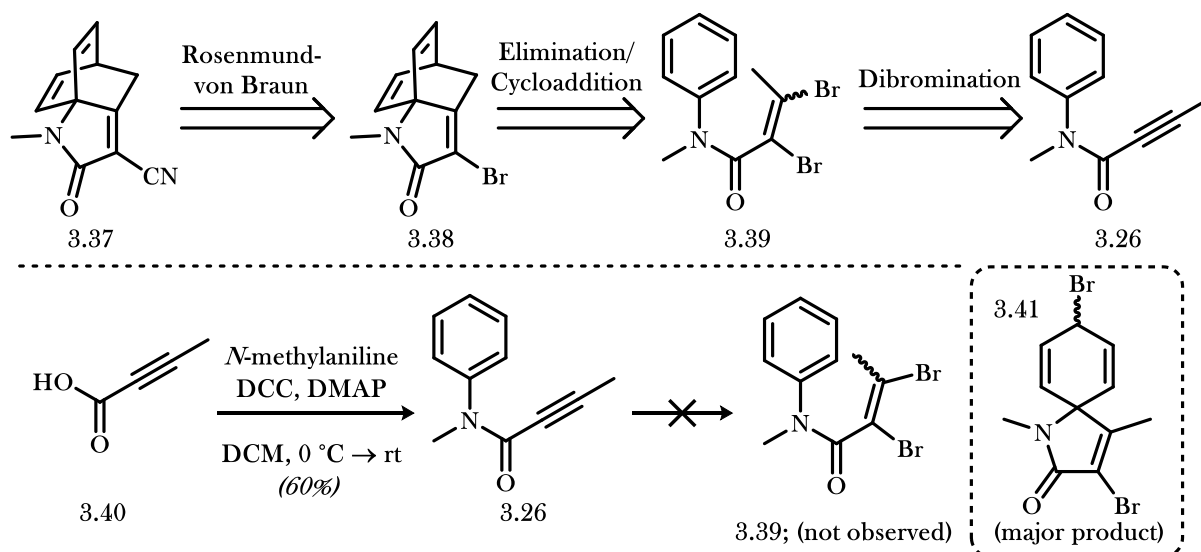
Our synthesis of bicycle **3.36** began with an amide coupling of *N*-methylaniline and cyanoacetic acid (**3.33**) yielding **3.34** in 83% yield (Scheme 3.4). Knoevenagel condensation of bicyclo[2.2.1]hept-5-en-2-one (**3.35**) and amide **3.34** using pyrrolidine as a catalyst produced **3.36** in 83% yield as a mixture of E/Z isomers. Despite the subjection of bicycle **3.36** to temperatures as high as 250 °C, cycloreversion to form allene **3.32** was not observed. Although the cycloreversion may have been successful at higher temperatures, we suspected that the subsequently formed cycloadduct would rapidly undergo the dyotropic shift at those temperatures,

and decided to pursue other strategies.

3.3.5 Attempted Installation of an α -Electron Withdrawing Group via the Bromide Precursor

We considered preparing an allene with a substituent that could be converted to a nitrile following the cycloaddition. We reasoned that an allenyl bromide might be more stable than an allenyl nitrile, and therefore isolable prior to the Himbert cycloaddition. Following the cycloaddition with the allenyl bromide, the resulting vinyl bromide could be converted to the nitrile via a Rosenmund von Braun type transformation. We planned to access the allenyl bromide via elimination of vinyl bromide **3.39**, which might be prepared via dibromination of internal alkyne **3.26** (Scheme 3.5).

Scheme 3.5 Attempted Formation as a Bromide Precursor to the α -EWG Substituted Cycloadduct

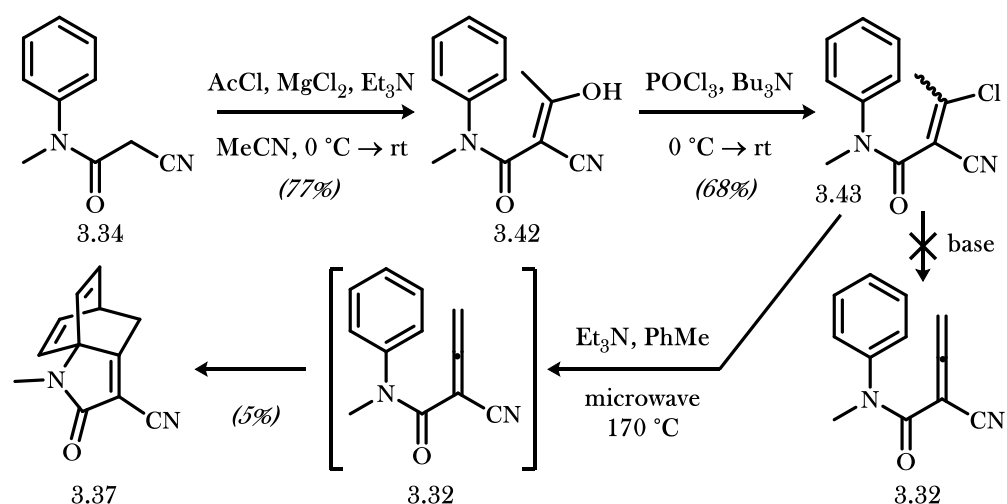


DCC promoted amide coupling of *N*-methylaniline with 2-butynoic acid (**3.40**) produced the conjugated amide **3.26** in 60% yield. Bromination using Li's conditions¹⁴ was found to be unsuccessful, instead leading to formation of spirocyclic product **3.41**. We believe this product is formed via initial bromonium formation from the alkyne of **3.26** and intramolecular *ipso* attack from the electron-rich aromatic ring. Although bromination using alternative conditions may have been successful,¹⁵ favorable results in a pathway we were concurrently investigating led us to set this route aside.

3.3.6 Successful Synthesis of the α -Electron Withdrawing Group Substituted Cycloadduct via Elimination

Because various groups have reported allene formation from vinyl halide precursors via elimination,¹⁶ we reasoned that elimination of vinyl halide **3.43** might successfully form allene **3.32**. Acylation of amide **3.34** using acetyl chloride and magnesium chloride as a Lewis acid afforded vinyl chloride precursor **3.42** in 77% yield (Scheme 3.6). Dehydrative chlorination using phosphorus oxychloride and tributylamine yielded vinyl chloride **3.43** in 68% yield. As expected, attempts to isolate the allene **3.32** via elimination of the chloride were unsuccessful, resulting in either decomposition or hydration to β -ketoamide **3.42** upon workup.

Scheme 3.6 Synthesis of the α -EWG Substituted Cycloadduct via Vinyl Halide Elimination

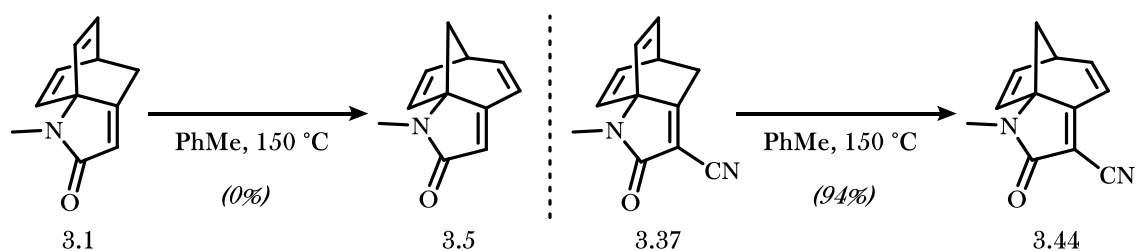


We suspected the highly electrophilic nature of doubly-activated allene **3.32** likely precludes isolation, and therefore considered a one-pot elimination/cycloaddition to avoid isolation of reactive allene **3.32**. Indeed, we observed formation of cycloadduct **3.37** in 5% yield upon heating **3.43** to 170 °C in the presence of triethylamine. Despite attempts to optimize formation of **3.37** with different bases and conditions, the cycloadduct could not be procured in higher yield.

3.3.7 Experimental Validation of the Lower Activation Energy for Anion Stabilizing Cycloadducts

With **3.37** in hand, we tested its propensity to undergo the dyotropic rearrangement. We predicted that the dyotropic rearrangement for the substituted cycloadduct could be performed at a lower temperature than the rearrangement of the analogous unsubstituted substrate. Indeed, we found that cycloadduct **3.37** rearranged to the dyotropic shift product in 94% yield upon heating at 150 °C in toluene, whereas the unsubstituted cycloadduct **3.1** failed to convert under identical conditions (Scheme 3.7).

Scheme 3.7 Experimental Observation of the Effect of α -EWG on the Rate of the Dyotropic Rearrangement



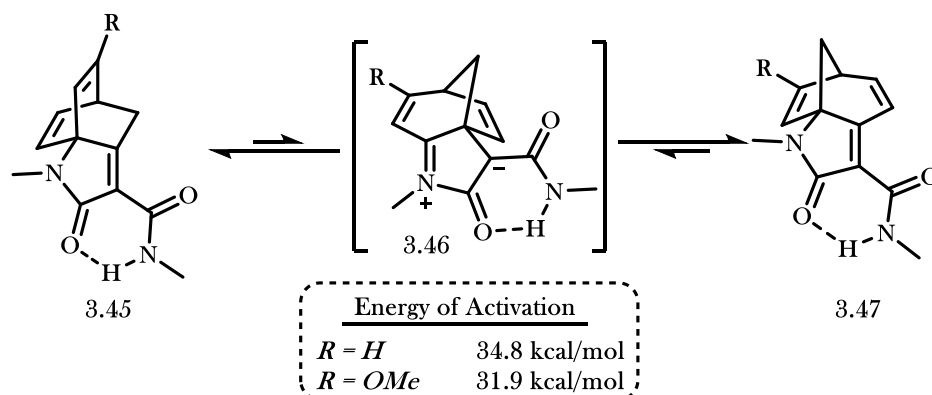
The experimentally observed rate increase for cycloadducts containing electron-withdrawing, non-hydrogen bonding α -substituents supports our theory that resonance stabilization of the zwitterionic intermediate is key to the success of the dyotropic rearrangement.

3.4 Attempted Dyotropic Shift via Cation Stabilization and Isolation of a Trapped Intermediate

3.4.1 Computational Data Supporting the Electron Donating Group Stabilized Dyotropic Shift

To complement our experimental confirmation that stabilization of the anionic component of the zwitterionic intermediate will increase the rate of the dyotropic rearrangement, we decided to also measure the effect of cation stabilization. The Houk group's computations indicated that the installation of a methyl ether on one alkene of the cycloadduct allows for resonance stabilization of the zwitterionic intermediate, and will subsequently lower the activation energy for the rate-limiting methylene shift by 2.9 kcal/mol (Figure 3.5). We believed we could support these computational results using a similar strategy to that in section 3.3.7.

Figure 3.5 Computational Support for the Cation-Stabilized Dyotropic Rearrangement

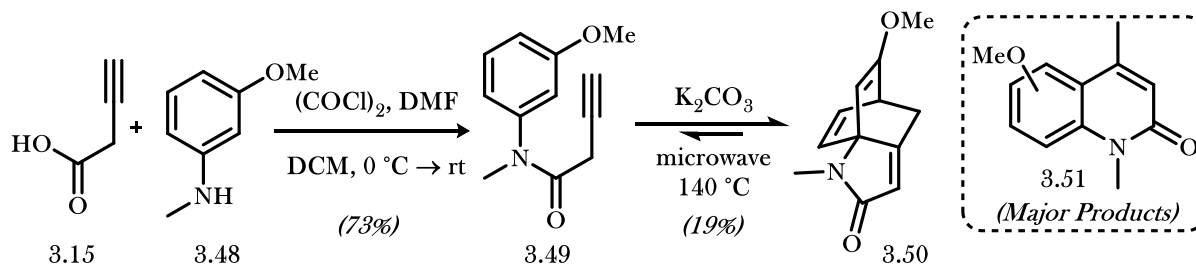


Interestingly, the incorporation of a methyl ether on one alkene of the [2.2.2] bicyclic core will initially promote 1,2-vinyl migration of the *substituted* alkene due to an increase in π -density that can participate in the shift. However, the resulting unstabilized zwitterionic intermediate must then proceed via a higher transition state for the subsequent methylene shift, making this mechanism no longer the overall lowest-energy pathway for the dyotropic shift. Instead, the more electron-poor alkene will undergo the 1,2-vinyl shift to form a more highly stabilized zwitterionic intermediate **3.46**, which will then proceed to the dyotropic rearrangement product **3.47** via a subsequent 1,2-methylene shift.

3.4.2 Synthesis of the Cation-Stabilizing Cycloadduct Precursor

To provide experimental evidence for the Houk group's findings, we began efforts to synthesize **3.50**, previously made by Himbert,¹⁷ and measure the difference in the rate of the dyotropic rearrangement.

Scheme 3.8 Synthesis of the EDG-Substituted Dyotropic Rearrangement Precursor

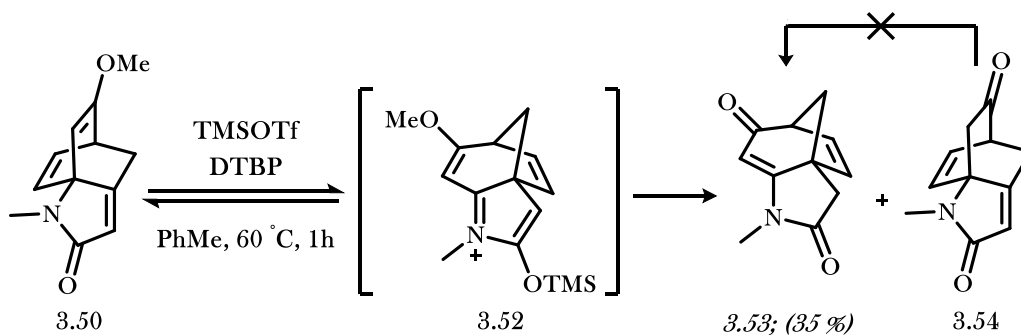


Amide coupling of *N*-methylanisidine **3.48** with 1-butynoic acid (**3.15**) yielded cycloaddition precursor **3.49** in 73% yield (Scheme 3.8). As reported by Himbert, the attempted cycloaddition resulted predominantly in formation of quinolone byproducts. The presence of an electron-donating substituent in the meta-position of the aromatic ring increases partial negative charge in the ortho positions, significantly increasing the rate of electrocyclization. As a result, cycloadduct **3.50** was obtained in only 19% yield.

3.4.3 Isolation of a Trapped Intermediate

We expected cycloadduct **3.50** to fully rearrange to the dyotropic shift product upon heating. However, when **3.50** was subjected to mild heating with TMSOTf, we instead found that the formed zwitterionic intermediate **3.52** undergoes a demethylation and isomerization to polycycle **3.53** in 35% yield (Scheme 3.9). Although calculations have not been run for this exact substrate, there are two possible mechanisms by which this product can be formed. One possibility involves demethylation of the zwitterionic intermediate **3.52** within the reaction mixture resulting in the observed product. Alternatively, the highly stabilized zwitterionic intermediate could remain in the reaction mixture until workup, upon which the addition of water will hydrolyze the charged intermediate to the neutral product. Although the mechanism could be investigated via NMR analysis of the reaction mixture, these experiments were not performed.

Scheme 3.9 Isolation of a “Trapped Intermediate” of the Dyotropic Rearrangement



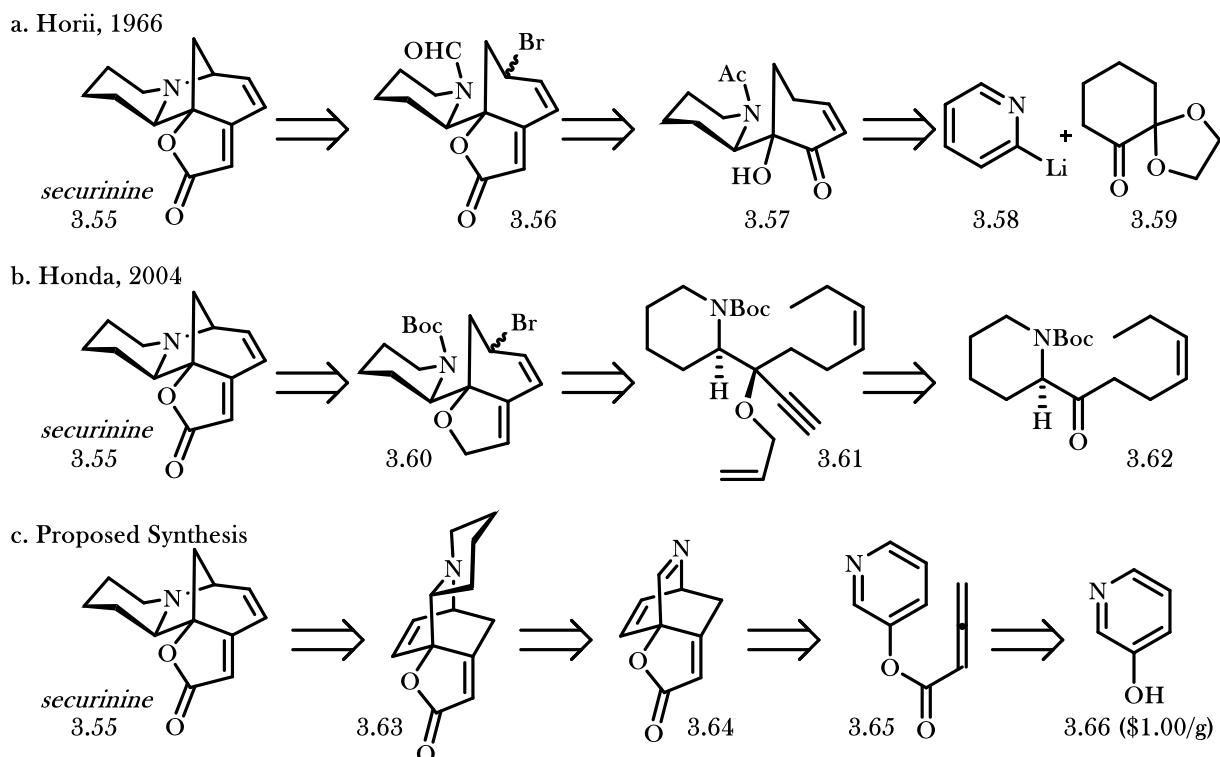
The “trapping” of intermediate **3.53** is potentially our strongest experimental contribution to the collaborative investigation of the mechanism of the dyotropic rearrangement. By isolating this unanticipated product, we provide strong circumstantial experimental evidence for the proposed mechanism.

3.5 Attempted Application to (±)-Securinine

3.5.1 *Securinega* Alkaloids Introduction

Following our investigation into the dyotropic rearrangement of arene-allene cycloadducts, we hoped to apply our gained knowledge to the total synthesis of securinine (**3.55**), a member of the *Securinega* family of natural products. The *Securinega* alkaloids are a class of complex polycyclic alkaloids that contain an azabicyclic core and possess a wide range of bioactivity.¹⁸ Securinine stands out among the *Securinega* alkaloids, exhibiting bioactivity as a potent GABA receptor antagonist,¹⁹ and possessing antimalarial²⁰ and antibacterial properties.²¹

Figure 3.6 Completed and Proposed Syntheses of Securinine

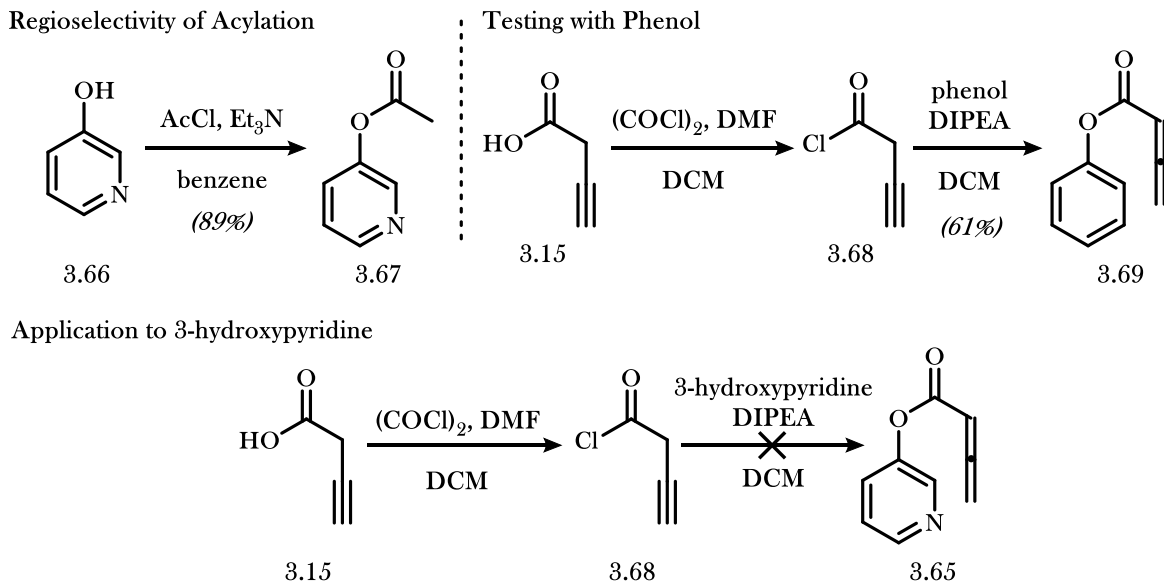


The first synthesis of racemic securinine was reported by the Horii group in 1966 (Scheme 3.6a).²² Using a radical allylic bromination and intramolecular amine alkylation as key steps, they procured securinine (**3.55**) in 11 steps in a 0.6% overall yield. In 2004, an impressive synthesis by the Honda group used a ring-closing metathesis cascade as a key step, affording (-)-securinine in 8 steps in 17% overall yield.²³

3.5.2 Attempted Synthesis of Securinine

Because the framework of the dyotropic rearrangement product closely resembles the structure of securinine, we began attempts to use the dyotropic shift as a key step in a total synthesis. Our proposed synthesis of racemic securinine would require only five steps, utilizing the inexpensive and commercially available 3-hydroxypyridine (**3.66**) as a starting material (Scheme 3.6c). An ester coupling with 3-butynoic acid (**3.15**) followed by isomerization would form cycloaddition precursor **3.65**. Upon heating, the allene would undergo a dearomatizing [4+2] cycloaddition to afford tricyclic product **3.64**. A two-step ring annulation to form **3.63** followed by the Lewis acid promoted dyotropic rearrangement would form securinine (**3.55**) in just five steps. Although this strategy resembled that of Magnus and co-workers in their synthesis of norsecurinine,²⁴ the [4+2] cycloaddition was performed on a nonaromatic diene, and we believed a dearomatizing cycloaddition would provide a significant contribution to the field.

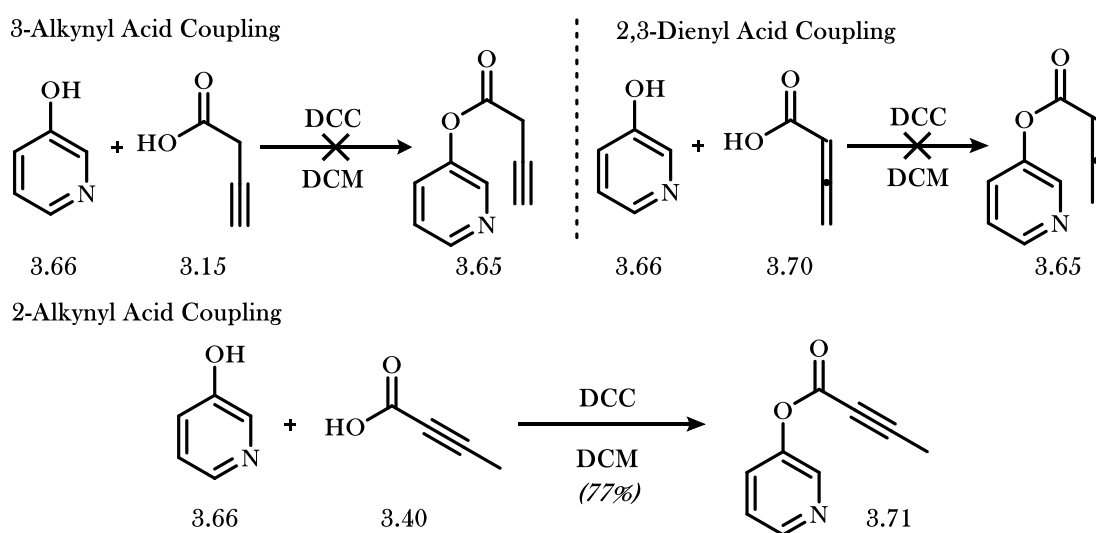
Scheme 3.10 Studies Toward Ester Formation from Acid Chloride Precursors



Initial control experiments were designed to test the plausibility of ester formation from 3-hydroxypyridine. By introducing 3-hydroxypyridine (**3.66**) to acetyl chloride and triethylamine, the chemoselectivity of acylation was determined to be predominantly O-selective (Scheme 3.10). Additionally,

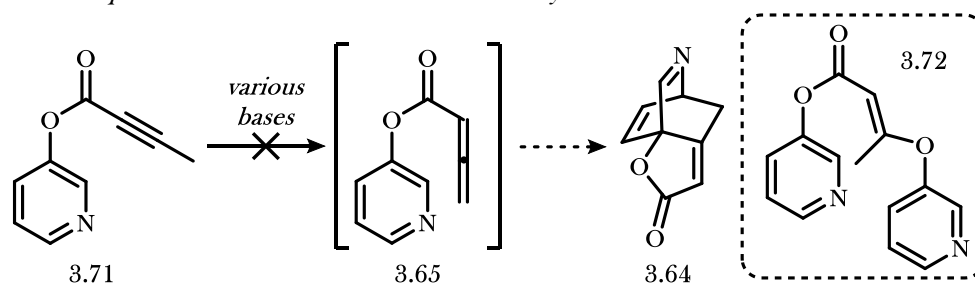
formation of the acid chloride of 3-butynoic acid (**3.68**) and exposure to phenol in the presence of Hünig's base formed allenyl ester product **3.69** in acceptable yields. However, when the optimized conditions were applied to the functionalization of 3-hydroxypyridine, rapid and exclusive decomposition resulted. Attempts to form ester **3.65** with a variety of bases proved unsuccessful, and no identifiable products could be isolated from the resulting tar. Notably, the addition of radical inhibitors somewhat reduced the rate of decomposition, providing evidence for possible radical decomposition pathways.

Scheme 3.11 Studies Toward Ester Formation from Carboxylic Acid Precursors



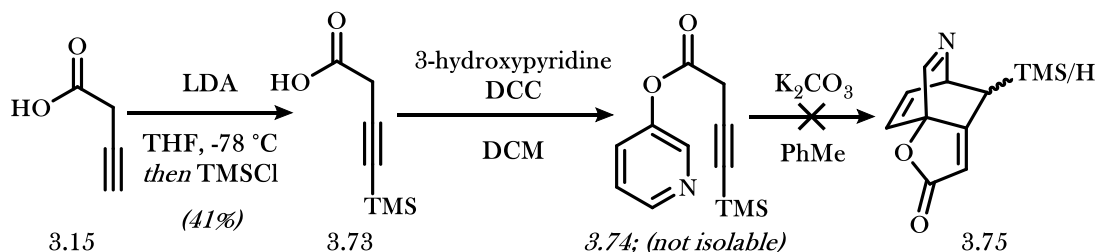
At this point, we considered forming the ester using DCC as a coupling agent. Introduction of either 3-butynoic acid (**3.15**) or 2,3-butadienoic acid (**3.70**) to 3-hydroxypyridine in the presence of DCC again resulted in rapid decomposition to a tar. Interestingly, the ester formed from the DCC-promoted coupling of 2-butynoic acid (**3.40**) and 3-hydroxypyridine could be isolated in 77% yield (Scheme 3.11). We predicted that strong base-promoted isomerization of the conjugated alkynyl ester **3.71** to the corresponding allene **3.65** might be a reasonable method to procure the cycloaddition precursor.

Scheme 3.12 Attempted Isomerization of the Internal Alkyne to the Allene



A range of bases were tested in the isomerization of alkynyl ester **3.71** (Scheme 3.12). Potassium carbonate, cesium carbonate, and potassium *tert*-butoxide as additives resulted only in recovery of starting material, while the addition of triethylamine or Hünig's base resulted in decomposition. Interestingly, the addition of *tert*-butanol and potassium *tert*-butoxide to the reaction mixture and heating at 200 °C, in an attempt to accomplish a one-pot isomerization/cycloaddition, resulted in formation of **3.72** as a major product. We hypothesized that the enolate intermediate formed by γ -deprotonation of ester **3.71** might expel 3-hydroxypyridine, which would then attack an additional molecule of **3.71** or **3.65**.

Scheme 3.13 Attempted Alkyne Silylation to Prevent Decomposition



We hoped that the installation of a silyl group at the γ -position might prevent decomposition through stabilization of the ester intermediate. Following formation of silylated 3-butynoic acid **3.73**, we then formed intermediate **3.74** via DCC coupling (Scheme 3.13). Although ester **3.74** could not be concentrated *in vacuo*, it could be purified by column chromatography and stored in a solution of toluene at low temperatures. All attempts to isomerize the silylated alkyne **3.74** to the allene, including a one-pot isomerization/cycloaddition, resulted in decomposition. For the time being, we have set the synthesis of securinine aside owing to issues with intermediate stability.

3.6 Conclusions

Our work on the mechanism of the dyotropic rearrangement of arene-allene cycloadducts represents the most complete investigation of this interesting transformation to date. We have provided computational support for a proposed stepwise mechanism passing through a zwitterionic intermediate. Additionally, we have shown that lowering the energy of the second transition state, corresponding to the Wagner–Meerwein-type 1,2-methylene shift, increases the rate of the transformation. The incorporation of substituents that stabilize the charged character of the zwitterionic intermediate has been shown to lower the energy of this transition state both computationally and experimentally. We hope that our research will contribute toward a deeper understanding of the dyotropic rearrangement and its more general use in synthetic organic chemistry.

3.7 Experimental Procedures

Unless otherwise noted, all reactions were performed under an atmosphere of argon using flame-dried or oven-dried glassware and Teflon® coated stir bars. Anhydrous solvents were prepared by passage through columns of activated alumina. All amine bases were distilled from calcium hydride prior to use. All reagents were used as received or prepared according to literature procedures, unless otherwise noted. TMSOTf was distilled from calcium hydride prior to use. Microwave reactions were performed in a CEM Discover or Anton-Parr Monowave 300 microwave, as indicated. Reactions were monitored by thin-layer chromatography (TLC) using 250 μm EMD Millipore glass-backed TLC plates impregnated with a fluorescent dye, using UV (254 nm), KMnO_4 /heat, or *para*-anisaldehyde/heat as developing agents. Flash column chromatography was performed on EMD Millipore 60 Å (0.040–0.063 mm) mesh silica gel, and flash column chromatography eluent mixtures are reported as %v/v. ^1H NMR spectra were recorded at 500 MHz on a Bruker 500 MHz (CRYO500 probe) instrument or at 600 MHz on a Bruker 600 MHz (AVANCE600 probe) instrument at 298 K. ^{13}C NMR spectra were recorded at 125 MHz on a Bruker 500 MHz (CRYO500 probe) at 298 K. Chemical shifts are reported in parts per million (ppm), referenced using residual undeuterated solvent (CHCl_3) at 7.26 ppm for ^1H and 77.16 ppm for ^{13}C spectroscopy. Chemical splitting is reported with the

following designated peak multiplicities: app = apparent, s = singlet, d = doublet, t = triplet, q = quartet, m = multiplet, br = broad. Coupling constants are reported in Hertz (Hz). IR spectra were recorded on a Varian 640-IR spectrometer using NaCl plates. High resolution mass spectra (HRMS) were recorded on a Waters LCT Premier spectrometer (using ESI-TOF) or Waters GCT Premier spectrometer (GC-CI), as indicated.

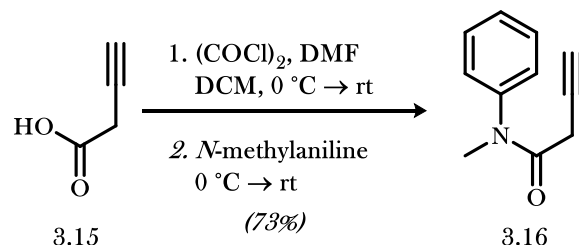
General Procedure A: Freeze-drying solids

To a small vial charged with substrate was added a minimum amount of benzene in order to fully dissolve the solid. The vial was then covered with a septum that had been pierced with a needle, and the needle was attached to a hi-vac. The solution was then submerged in a $-78\text{ }^{\circ}\text{C}$ dry ice/acetone bath for 10 minutes, and then exposed to vacuum. After 2 minutes at $-78\text{ }^{\circ}\text{C}$, the vial was removed from the bath and allowed to slowly warm to room temperature over 1-2 hours under vacuum to afford a dry powder.

General Procedure B: Fusing metal-halide salts

To a small round bottom flask charged with the hydrated metal halide was added a stir bar. The round bottom flask was attached to a hi-vac and opened to vacuum, while stirring. The flask was then flame dried with a butane torch, moving from the top of the flask downward, until the metal halide salt melted into a liquid. The flask was allowed to naturally cool to room temperature under vacuum. The flame drying/cooling process was repeated two times to afford a dry metal halide salt.

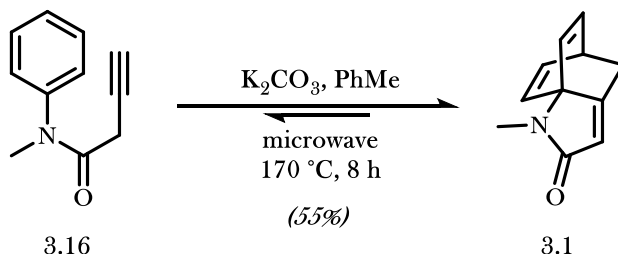
N-methyl-*N*-phenylbut-3-ynamide (**3.16**)



To a flame dried round bottom flask with stir bar was added but-3-ynoic acid (**3.15**)²⁵ (1.00 g, 11.9 mmol, 1.0 equiv.), CH₂Cl₂ (24.0 mL), and catalytic DMF (0.10 mL, 1.3 mmol) under argon. The reaction mixture was then cooled to 0 °C in an ice/water bath and oxalyl chloride (1.3 mL, 16 mmol, 1.3 equiv.) was added dropwise over 2 minutes down the side of the flask. The reaction mixture was left in the ice/water bath and was allowed to naturally warm to room temperature. After two hours, off gassing ceased, and a balloon with an attached needle was then used to bubble argon through the dark red solution for 10 minutes to expel HCl gas through a vent needle. The reaction mixture was cooled to 0 °C in an ice/water bath and the aniline (3.2 mL, 28 mmol, 2.4 equiv.) was added dropwise down the side of the flask over 2 minutes. The reaction mixture was left in the ice/water bath and allowed to naturally warm to room temperature. After 2.5 hours, the reaction mixture was added to saturated aqueous NaHCO₃ (25 mL), and the aqueous layer was extracted with CH₂Cl₂ (3 x 25 mL). The organic layers were combined, dried over MgSO₄, filtered through cotton, and concentrated *in vacuo*. The crude product mixture was purified by silica gel chromatography (25–33% EtOAc in hexanes) to afford a white solid. The white solid was then dissolved in a minimum amount of EtOAc (1.0 mL), diluted to 15 mL with hexanes, and cooled to -20 °C overnight. The formed crystals were filtered, washed with cold hexanes, and collected. Freeze-drying (see **General Procedure A**) afforded *N*-methyl-*N*-phenylbut-3-ynamide (**3.16**) as a white solid (1.51 g, 73%); mp: 109–116 °C; ¹H NMR (500 MHz, CDCl₃) δ 7.43 (ap t, *J* = 7.6 Hz, 2H), 7.37 (t, *J* = 7.3 Hz, 1H), 7.23 (d, *J* = 7.3 Hz, 2H), 3.29 (s, 3H), 3.05 (d, *J* = 2.5 Hz, 2H), 2.10 (t, *J* = 2.5 Hz, 1H); ¹³C NMR (126 MHz, CDCl₃) δ 166.9, 143.5, 130.1, 128.4, 127.3, 71.4,

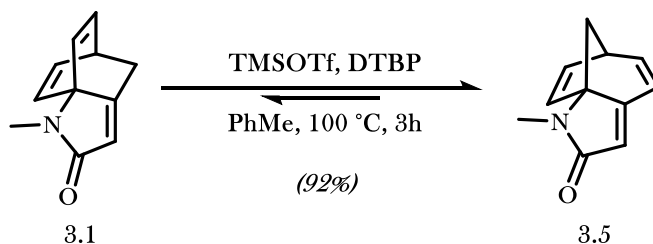
37.9, 26.2; IR (film) 3293, 3245, 2124, 1666, 1595, 1496, 1384, 1122 cm^{-1} ; HRMS (GC-ESI) m/z calcd for $\text{C}_{11}\text{H}_{11}\text{NO}$ $[\text{M} + \text{H}]^+$ 174.0919, found 174.0912.

Cycloadduct 3.1



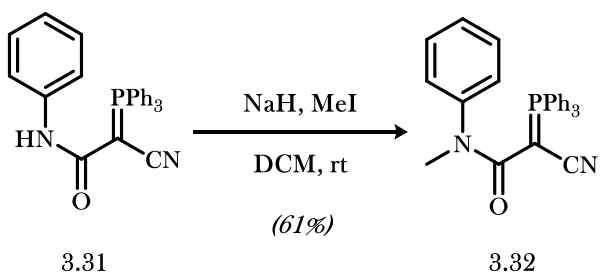
To a flame dried CEM microwave vial with stir bar was added *N*-methyl-*N*-phenylbut-3-ynamide (**3.16**) (173 mg, 1.0 mmol, 1.0 equiv.) and toluene (5.0 mL) under argon. K_2CO_3 (70.0 mg, 0.50 mmol, 0.5 equiv.) was then added in a single portion, and the vial was sealed. The reaction mixture was heated at 170 °C for 8 hours. The dark red reaction mixture was then filtered through Celite, and CH_2Cl_2 (5 mL) was used to wash the reaction flask and filtered through Celite. The combined filtrates were concentrated *in vacuo* to afford a red solid. The crude product mixture was purified by silica gel chromatography (50% EtOAc in hexanes) to afford a white solid. The white solid was then dissolved in a minimum amount of CH_2Cl_2 (1.0 mL), diluted to 15 mL with Et_2O , and cooled to -20 °C overnight. The formed crystals were filtered, washed with cold Et_2O , and collected. Freeze-drying (see **General Procedure A**) afforded cycloadduct **3.1** as a white solid (95 mg, 55%): ^1H NMR (500 MHz, CDCl_3) δ 6.48 (ap t, J = 6.6 Hz, 2H), 6.25 (d, J = 7.1 Hz, 2H), 5.76 (ap t, J = 1.7 Hz, 1H), 4.09-4.06 (m, 1H), 3.20 (s, 3H), 2.29 (ap t, J = 2.0 Hz, 2H); ^{13}C NMR (126 MHz, CDCl_3) δ 173.9, 160.4, 134.7, 130.4, 114.9, 75.3, 39.6, 30.5, 26.9; IR (film) 3048, 2917, 2943, 1672, 1418, 1375 cm^{-1} ; HRMS (GC-ESI) m/z calcd for $\text{C}_{11}\text{H}_{11}\text{NO}$ $[\text{M} + \text{H}]^+$ 174.0919, found 174.0926.

Dyotropic Shift Product 3.5

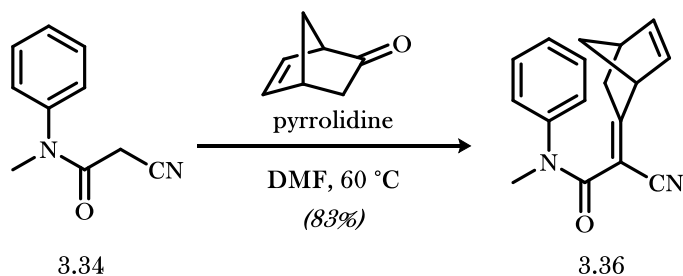


To a flame-dried one-dram vial with stir bar was added cycloadduct **3.1** (30.0 mg, 0.17 mmol, 1.0 equiv.) and toluene (1.3 mL) under argon. A solution of TMSOTf (16.0 μ L, 0.087 mmol, 0.5 equiv.) and 2,6-di-*tert*-butylpyridine (4 μ L, 0.017 mmol, 0.1 equiv.) in toluene (84 μ L) was added dropwise over one minute. The reaction mixture was then added to an oil bath preheated at 100 °C for 3 hours, and slowly turned pink over time. After 3 hours, EtOAc (1 mL) and saturated aqueous NaHCO₃ (2 mL) were added. The layers were separated, and the aqueous layer was extracted with CH₂Cl₂ (3 x 2 mL). The combined organic layers were dried over MgSO₄, filtered through cotton, and concentrated *in vacuo* to a pink oil. The crude product mixture was purified by silica gel chromatography (33–100% EtOAc in hexanes) to afford dyotropic shift product **3.5** as a colorless oil (28 mg, 92%): ¹H NMR (500 MHz, CDCl₃) δ 6.52 (dd, *J* = 9.2, 6.3 Hz, 1H), 6.33 (dd, *J* = 5.3, 3.3 Hz, 1H), 6.21 (d, *J* = 9.2 Hz, 1H), 5.77 (d, *J* = 5.3 Hz, 1H), 5.75 (s, 1H), 3.41–3.39 (m, 1H), 2.97 (s, 3H), 2.50 (dd, *J* = 8.9, 4.5 Hz, 1H), 1.75 (d, *J* = 8.9 Hz, 1H); ¹³C NMR (126 MHz, CDCl₃) δ 171.7, 154.5, 139.7, 138.6, 134.1, 119.3, 115.9, 75.7, 52.6, 42.5, 25.0 cm⁻¹; IR (film) 3064, 3040, 2963, 1681, 1379, 1363 cm⁻¹; HRMS (GC-CI) *m/z* calcd for C₁₁H₁₁NO [M + H]⁺ 174.0919, found 174.0922.

Ylide 3.32

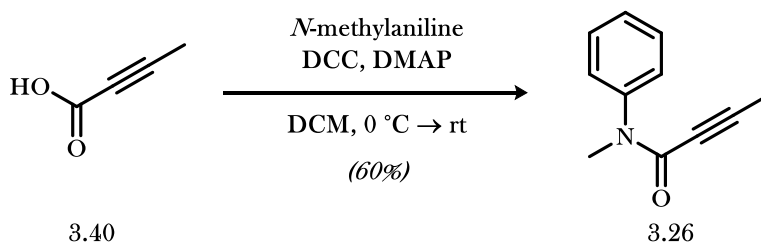


To a flame dried round bottom flask with stir bar was added ylide **3.31**²⁶ (200.0 mg, 0.48 mmol, 1.0 equiv.) followed by THF (4.3 mL) and CH₂Cl₂ (4.3 mL) under argon. Sodium hydride (190 mg, 60% in mineral oil, 4.8 mmol, 10 equiv.) was then added in several portions, followed by methyl iodide (0.30 mL, 4.8 mmol, 10 equiv.) dropwise over the course of 2 minutes. The reaction mixture was stirred at room temperature for 5 hours. The crude product mixture was then concentrated *in vacuo* to a solid wax and dissolved in CH₂Cl₂. The combined organic layers were filtered through cotton and concentrated *in vacuo*. The crude product mixture was purified by silica gel chromatography (50% EtOAc in hexanes) to afford ylide **3.32** as a white solid (125 mg, 61%): ¹H NMR (500 MHz, CDCl₃) δ 7.68-7.63 (m, 6H), 7.57-7.56 (m, 3H), 7.48 (ddd, *J* = 7.7, 7.7, 3.2 Hz, 6H), 7.39-7.36 (m, 4H), 7.27-7.23 (m, 1H), 3.29 (s, 3H); ¹³C NMR (126 MHz, CDCl₃) δ 170.0 (d, *J* = 8.8 Hz), 145.5, 133.8 (d, *J* = 9.9 Hz), 133.6 (d, *J* = 3.0 Hz), 129.34, 129.0 (d, *J* = 9.8 Hz), 127.6, 126.8, 125.3 (d, *J* = 94.7 Hz), 121.3 (d, *J* = 15.5 Hz), 38.8, (d, *J* = 1.5 Hz), 34.6 (d, *J* = 142.4 Hz, C7); IR (film) 2167, 1559, 1437, 1356, 1150, 1106 cm⁻¹; HRMS (ESI) *m/z* calcd for C₂₈H₂₃N₂OP [M + Na]⁺ 457.1446, found 457.1426; Mp: 122–129 °C.

Bicycle 3.36²⁷

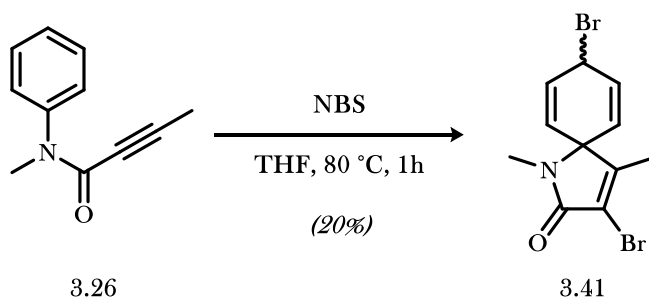
To a flame dried vial with stir bar was added bicyclo[2.2.1]hept-5-en-2-one²⁸ (929 mg, 8.6 mmol, 5.0 equiv.) and DMF (3.5 mL) under argon. 2-cyano-*N*-methyl-*N*-phenylacetamide (**3.34**)²⁹ (300 mg, 1.7 mmol, 1.0 equiv.) was then added in a single portion. Pyrrolidine (1.4 mL, 17 mmol, 10 equiv.) was added dropwise over 2 minutes, and the reaction mixture was added to an oil bath preheated at 60 °C. After 12 hours of stirring at 60 °C, the reaction mixture was cooled to room temperature and diluted with Et₂O (3 mL) and H₂O (10 mL). The layers were separated, and the organic layer was washed with H₂O (10 x 10 mL). The organic layer was dried over MgSO₄, filtered through cotton, and concentrated *in vacuo*. The crude product mixture was purified by silica gel chromatography (20% EtOAc in hexanes) to give a 1:1 mixture of E/Z isomers of bicycle **3.36** as a slightly yellow oil (375 mg, 83%): ¹H NMR (500 MHz, CDCl₃) δ 7.39 (ap q, *J* = 7.2 Hz, 4H), 7.35-7.31 (m, 2H), 7.17 (d, *J* = 7.7 Hz, 2H), 7.12 (d, *J* = 7.6 Hz, 2H), 6.35 (ap td, *J* = 5.9, 2.8 Hz, 2H), 5.98 (ap t, *J* = 4.2 Hz, 1H), 5.90 (ap t, *J* = 4.2 Hz, 1H), 4.00 (s, 1H), 3.67 (s, 1H), 3.41 (s, 3H), 3.35 (s, 3H), 3.12 (s, 1H), 3.05 (s, 1H), 2.63 (dd, *J* = 17.6, 3.2 Hz, 1H), 2.35 (d, *J* = 16.8 Hz, 1H), 2.24 (dd, *J* = 17.6, 3.9 Hz, 1H), 2.05 (dd, *J* = 17.0, 3.0 Hz, 1H), 1.81 (dt, *J* = 8.9, 1.8 Hz, 1H), 1.76 (dt, *J* = 8.7, 1.8 Hz, 1H), 1.50 (d, *J* = 8.9 Hz, 1H), 1.45 (d, *J* = 8.8 Hz, 1H); ¹³C NMR (126 MHz, CDCl₃) δ 175.08, 175.01, 163.1, 162.7, 142.9, 142.7, 141.2, 141.1, 129.6, 128.1, 128.0, 126.9, 126.8, 115.4, 115.1, 51.8, 51.0, 50.8, 50.1, 42.1, 41.0, 37.7, 37.0; IR (film) 3064, 2988, 2941, 2214, 1659, 1595, 1496, 1371 cm⁻¹; HRMS (GC-CD) *m/z* calcd for C₁₇H₁₆N₂O [M + H]⁺ 265.1341, found 265.1332.

N-methyl-*N*-phenylbut-2-ynamide (**3.26**)³⁰



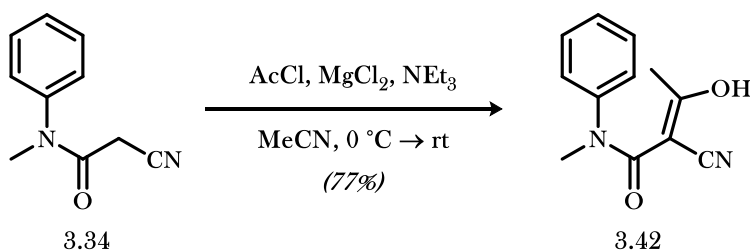
To a flame dried round bottom flask with stir bar was added acid but-2-ynoic acid (**3.40**) (200 mg, 2.4 mmol, 1.0 equiv.) and CH₂Cl₂ (5 mL) under argon. The solution was then cooled to 0 °C, and DCC (540 mg, 2.6 mmol, 1.1 equiv.) and DMAP (30 mg, 0.24 mmol, 0.1 equiv.) were added. *N*-methylaniline (260 μL, 2.4 mmol, 1.0 equiv.) was then added drop wise down the side of the flask over two minutes, and the reaction mixture was left in the ice/water bath and allowed to naturally warm to room temperature. After 12 hours, the deep orange reaction mixture was filtered through Celite. The reaction flask was rinsed with CH₂Cl₂ (3 x 5 mL) and filtered through the Celite. To the filtrate was added H₂O (10 mL) and HCl (1.0 M in H₂O, 10 mL). The layers were separated, and the organic layer was dried over MgSO₄, filtered through cotton, and concentrated. The crude product mixture was purified by silica gel chromatography (33% EtOAc in hexanes) to give *N*-methyl-*N*-phenylbut-2-ynamide (**3.26**) as a colorless oil (247 mg, 60%): ¹H NMR (500 MHz, CDCl₃) δ 7.40 (ap t, *J* = 7.6 Hz, 2H), 7.32 (t, *J* = 7.3 Hz, 1H), 7.27 (d, *J* = 8.3 Hz, 2H), 3.31 (s, 3H), 1.73 (s, 3H); ¹³C NMR (126 MHz, CDCl₃) δ 154.5, 143.4, 129.2, 127.8, 127.2, 125.6, 90.0, 74.2, 36.5, 4.0; IR (film) 2918, 2360, 2340, 2226, 1633, 1593, 1363 cm⁻¹; HRMS (GC-Cl) *m/z* calcd for C₁₁H₁₁NO [M + H]⁺ 174.0919, found 174.0914.

Spirocycle **3.41**³¹



To a flame dried round bottom flask was added *N*-methyl-*N*-phenylbut-2-ynamide (**3.26**) (40 mg, 0.23 mmol, 1.0 equiv.) and THF (0.92 mL) under argon. NBS (123 mg, 0.69 mmol, 3.0 equiv.) was then added in one portion to form a dark orange solution. The reaction mixture was warmed to 80 °C in an oil bath, which caused the solution to turn a pale yellow. The reaction mixture was stirred at 80 °C for 1 hour and was then cooled to room temperature and concentrated *in vacuo*. The product mixture was purified by silica gel chromatography (20–33% EtOAc in hexanes) to afford a 1:0.3 mixture of diastereomers of spirocycle **3.41** as a thin film (15 mg, 20%): ¹H NMR (500 MHz, CDCl₃) δ 6.49 (dd, *J* = 9.9, 3.8 Hz, 1H), 5.41 (d, *J* = 10.0 Hz, 1H), 5.22 (ap td, *J* = 4.0, 0.8 Hz, 1H), 2.81 (s, 3H), 1.95 (s, 3H); ¹³C NMR (126 MHz, CDCl₃) δ 166.1, 154.4, 133.3, 132.8, 129.2, 117.2, 66.8, 38.9, 26.5; IR (film) 2916, 1708, 1366, 1008 cm⁻¹; HRMS (ESI) *m/z* calcd for C₁₁H₁₁NO⁷⁹Br₂ [M + H]⁺ 353.9105, found 353.9122.

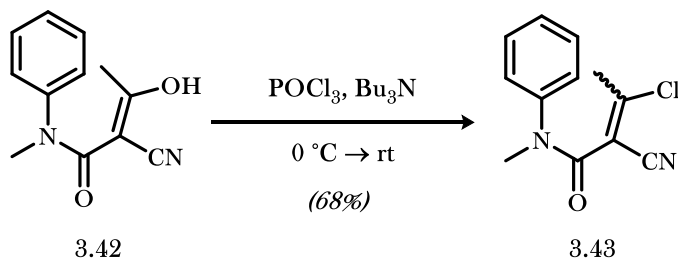
2-cyano-3-hydroxy-*N*-methyl-*N*-phenylbut-2-enamide (**3.42**)³²



To a flame-dried vial with stir bar was added freshly fused (see **General Procedure B**) MgCl₂ (1.84 g, 19.3 mmol, 1.0 equiv.), MeCN (19.3 mL), and 2-cyano-*N*-methyl-*N*-phenylacetamide (**3.34**)³³ (3.42 g, 19.3

mmol, 1.0 equiv.) under argon. The reaction mixture was cooled to 0 °C in an ice/water bath, and Et₃N (5.4 mL, 39 mmol, 2.0 equiv.) was added dropwise down the side of the flask over 2 minutes. The solution was stirred for 15 minutes at 0 °C, and AcCl (1.4 mL, 19 mmol, 1.0 equiv.) was added dropwise down the side of the flask over 3 minutes. The reaction mixture was left in the ice/water bath and allowed to naturally warm to room temperature. After 4 hours, HCl (4.0 M in H₂O, 20 mL) was added followed by Et₂O (40 mL). The layers were separated, and the aqueous layer was extracted with Et₂O (3 x 40 mL). The combined organic layers were dried over MgSO₄, filtered through cotton, and concentrated *in vacuo*. The crude product mixture was purified by silica gel chromatography (20–33% EtOAc in hexanes) to afford 2-cyano-3-hydroxy-*N*-methyl-*N*-phenylbut-2-enamide (**3.42**) as a white solid (3.2 g, 77%): mp: 89–92 °C; ¹H NMR (500 MHz, CDCl₃) δ 7.46 (m, 3H), 7.26 (m, 1H), 3.37 (s, 3H), 2.24 (s, 3H); ¹³C NMR (126 MHz CDCl₃) δ 191.2, 169.6, 141.9, 130.0, 129.4, 127.8, 115.4, 79.2, 39.2, 22.4; IR (film) 2209, 1580, 1472, 1454 cm⁻¹; HRMS (ESI) *m/z* calcd for C₁₂H₁₂N₂O₂ [M + Na]⁺ 239.0797, found 239.0788.

3-chloro-2-cyano-*N*-methyl-*N*-phenylbut-2-enamide (**3.43**)³⁴



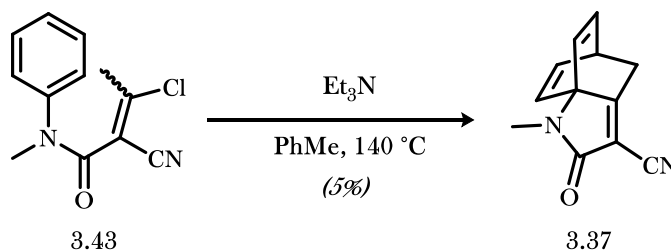
To a flame-dried vial with stir bar was added 2-cyano-3-hydroxy-*N*-methyl-*N*-phenylbut-2-enamide (**3.42**) (3.2 g, 14.8 mmol, 1.0 equiv.) followed by POCl₃ (3.7 mL, 40 mmol, 2.7 equiv.) at 0 °C under argon. After stirring at 0 °C for 10 minutes, Bu₃N (3.5 mL, 15 mmol, 1.0 equiv.) was added dropwise over 10 minutes, and the reaction was allowed to warm to room temperature naturally in the bath. After stirring for 1 hour, the reaction mixture was heated to 55 °C and stirred for 135 minutes. Upon completion, the reaction mixture was concentrated *in vacuo* to remove residual POCl₃, and CH₂Cl₂ (10 mL) was added. Saturated

aqueous NH_4Cl (10 mL) was added, and the layers were separated. The aqueous layer was extracted with CH_2Cl_2 (3 x 10 mL), and the combined organic layers were dried over MgSO_4 , filtered through cotton, and concentrated *in vacuo*. The crude product mixture was purified by silica gel chromatography (10–33% EtOAc in hexanes) to afford each E/Z isomer of 3-chloro-2-cyano-N-methyl-N-phenylbut-2-enamide (**3.43**).

Isomer **3.43a**: (1.29 g, 37%): ^1H NMR (500 MHz, CDCl_3) δ 7.45-7.39 (m, 3H), 7.28-7.27 (m, 2H), 3.38 (s, 3H), 2.25 (s, 3H); ^{13}C NMR (126 MHz, CDCl_3) δ 160.2, 153.1, 141.7, 129.8, 128.9, 126.7, 113.7, 110.9, 37.5, 25.6; IR (film) 3063, 2925, 2219, 1668, 1616, 1595, 1495, 1383 cm^{-1} ; HRMS (GC-Cl) *m/z* calcd for $\text{C}_{12}\text{H}_{11}\text{N}_2\text{OCINH}_4$ ($\text{M} + \text{NH}_4$) $^+$ 252.0904, found 252.0894; $\text{Mp} = 75\text{--}78$ $^\circ\text{C}$.

Isomer **3.43b**: (1.08 g, 31%): ^1H NMR (500 MHz, CDCl_3) δ 7.46-7.42 (m, 2H), 7.38 (t, $J = 7.3$ Hz, 1H), 7.17 (d, $J = 7.5$ Hz, 2H), 3.39 (s, 3H), 2.38 (s, 3H); ^{13}C NMR (126 MHz, CDCl_3) δ 162.5, 155.1, 141.8, 130.0, 128.8, 126.7, 113.3, 38.0, 24.9; IR (film) 3063, 2937, 2222, 1663, 1595, 1495, 1377 cm^{-1} ; HRMS (GC-Cl) *m/z* calcd for $\text{C}_{12}\text{H}_{11}\text{N}_2\text{OCl}$ [$\text{M} + \text{H}$] $^+$ 235.0638, found 235.0639; $\text{Mp} = 49\text{--}50$ $^\circ\text{C}$.

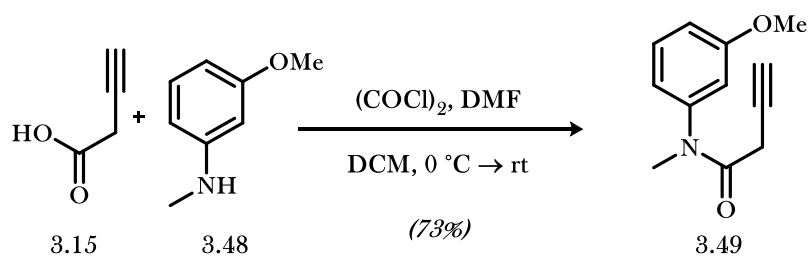
Cycloadduct **3.37**



To a flame-dried Anton-Parr G30 glass vial with stir bar was added a mixture of E/Z isomers of 3-chloro-2-cyano-N-methyl-N-phenylbut-2-enamide (**3.43**) (600 mg, 2.6 mmol, 1.0 equiv.) followed by toluene (20 mL). Et_3N (1.8 mL, 13 mmol, 5.0 equiv.) was then added in one portion, and the vial was sealed and quickly transferred to the microwave, where the reaction mixture was heated at 140 $^\circ\text{C}$ for 2 hours. Upon completion, the crude product mixture was diluted with EtOAc (20 mL) and washed with 1M aqueous HCl (2 x 20 mL) and water (20 mL). The organic layer was dried over MgSO_4 , filtered through cotton, and concentrated *in vacuo* to afford a black oil. The crude mixture was first purified by column chromatography (33–100% EtOAc

in hexanes), then separated from the quinolone byproduct with AgNO₃-doped silica gel chromatography³⁵ (1:1:0-1:0:0-9:0:1 EtOAc:hexanes:methanol). The remaining product mixture was then separated by column chromatography (0-10% EtOAc in DCM) to afford cycloadduct **3.37** as a white solid (24.5 mg, 5%): ¹H NMR (500 MHz, CDCl₃) δ 6.62 (ap t, *J* = 6.7 Hz, 2H), 6.23 (d, *J* = 7.2 Hz, 2H), 4.20-4.28 (m, 1H), 3.21 (s, 3H), 2.51 (d, *J* = 2.3 Hz); ¹³C NMR (126 MHz, CDCl₃) δ 172.6, 167.0, 136.7, 128.7, 112.6, 103.1, 74.6, 39.5, 32.3, 27.4; IR (film) 3065, 2918, 2850, 2361, 2340, 2230, 1700, 1376 cm⁻¹; HRMS (GC-CI) *m/z* calcd for C₁₂H₁₀N₂O [M + NH₄]⁺ 216.1137, found 216.1134; Mp = 152-153 °C.

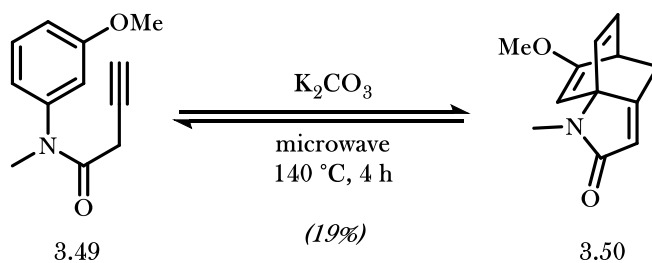
N-(3-methoxyphenyl)-*N*-methylbut-3-ynamide (**3.49**)



To a flame-dried vial with stir bar was added but-3-ynoic acid¹² (35 mg, 0.42 mmol, 1.0 equiv.), CH₂Cl₂ (0.84 mL), and DMF (50 μL, 0.70 mmol, 1.7 equiv.) under argon. The reaction mixture was then cooled to 0 °C in an ice/water bath and oxalyl chloride (50 μL, 0.50 mmol, 1.2 equiv.) was added dropwise over 2 minutes down the side of the flask. The reaction mixture was left in the ice/water bath, allowed to naturally warm to room temperature, and stirred for 2 hours until off gassing ceased. A balloon with attached needle was then used to bubble argon through the dark red solution for 10 minutes to expel HCl gas through a vent needle. The reaction mixture was cooled to 0 °C in an ice/water bath and 3-methoxy-*N*-methylaniline (**3.48**)³⁶ (143 mg, 1.0 mmol, 2.4 equiv.) was added dropwise down the side of the flask over 2 minutes. The reaction mixture was left in the ice/water bath and allowed to naturally warm to room temperature, and was then stirred for 2.5 hours. The reaction mixture was then added to saturated aqueous NaHCO₃ (1 mL), and the aqueous layer was extracted with CH₂Cl₂ (3 x 1 mL). The organic layers were combined, dried over MgSO₄, filtered through cotton, and concentrated *in vacuo*. The crude product mixture was purified by silica gel

chromatography (10%–33% EtOAc in hexanes) to afford a white solid. The white solid was then dissolved in a minimum amount of EtOAc (1.0 mL), diluted to 15 mL with hexanes, and cooled to $-20\text{ }^{\circ}\text{C}$ overnight. The formed crystals were filtered, washed with cold hexanes, and collected. Freeze-drying (see **General Procedure A**) afforded *N*-(3-methoxyphenyl)-*N*-methylbut-3-ynamide (**3.49**) as a white solid (47 mg, 55%): ^1H NMR (500 MHz, CDCl_3) δ 7.32 (t, J = 8.1 Hz, 1H), 6.89 (dd, J = 8.3, 1.9 Hz, 1H), 6.80 (d, J = 7.8 Hz, 1H), 6.77 (ap t, J = 2.1 Hz, 1H), 3.81 (s, 3H), 3.27 (s, 3H), 3.07 (d, J = 2.4 Hz, 2H), 2.11 (t, J = 2.4 Hz, 1H); ^{13}C NMR (126 MHz, CDCl_3) δ 166.8, 160.7, 144.6, 130.8, 119.3, 113.9, 113.0, 77.6, 71.3, 55.6, 37.8, 26.1; IR (film) 3292, 2942, 2125, 1668, 1601, 1489, 1383, 1231, 1117, 1040 cm^{-1} ; HRMS [GC-ESI] m/z calcd for $\text{C}_{12}\text{H}_{13}\text{NO}_2$ ($\text{M} + \text{H}$) $^+$ 204.1024, found 204.1017; Mp = $72\text{--}76\text{ }^{\circ}\text{C}$.

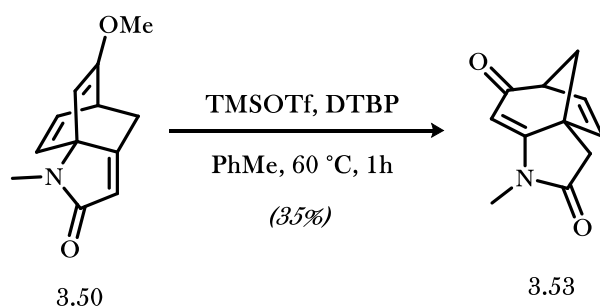
Cycloadduct **3.50**



To an Anton-Parr G30 microwave vial with stir bar was added *N*-(3-methoxyphenyl)-*N*-methylbut-3-ynamide (**3.49**) (325 mg, 1.60 mmol, 1.0 equiv.) and toluene (8.0 mL) under argon. K_2CO_3 (111 mg, 0.80 mmol, 0.5 equiv.) was added in one portion. The reaction mixture was heated in the Anton-Parr microwave (maximum heating rate, cooling to $55\text{ }^{\circ}\text{C}$ upon completion) for 4 hours at $140\text{ }^{\circ}\text{C}$. The resulting dark red solution was then filtered through Celite. CH_2Cl_2 (8 mL) was then used to wash the reaction vial and Celite. The combined filtrates were concentrated *in vacuo*. The crude product mixture was first purified by silica gel chromatography (50–75% EtOAc in hexanes) to produce a mixture of product **3.50** and a quinolone byproduct. The mixture was then separated using AgNO_3 -doped silica gel chromatography (100% EtOAc). In order to remove residual AgNO_3 , the compound was quickly filtered through a small pad of silica (75% EtOAc in hexanes). The purified product was then freeze-dried (see **General Procedure A**) to afford

cycloadduct **3.50** as a white solid (62 mg, 19%): ^1H NMR (499 MHz CDCl_3) δ 6.46 (t, J = 6.8 Hz, 1H), 6.30 (dd, J = 7.4, 0.6 Hz, 1H), 5.73 (ap t, J = 1.6 Hz, 1H), 4.79 (d, J = 2.5 Hz, 1H), 3.74-3.72 (m, 1H), 3.51 (s, 3H), 3.15 (s, 3H), 2.53 (ap dt, J = 16.7, 2.1 Hz, 1H), 2.31 (ap dt, J = 16.6, 2.0 Hz, 1H); ^{13}C NMR (126 MHz, CDCl_3) δ 173.8, 165.6, 162.3, 133.5, 133.2, 113.9, 92.7, 73.8, 56.4, 42.7, 30.4, 26.7; IR (film) 2933, 1682, 1629, 1421, 1374, 1386, 1215 cm^{-1} ; HRMS (GC-ESI) m/z calcd for $\text{C}_{12}\text{H}_{13}\text{NO}_2$ [$\text{M} + \text{H}$] $^+$ 204.1024, found 204.1022.

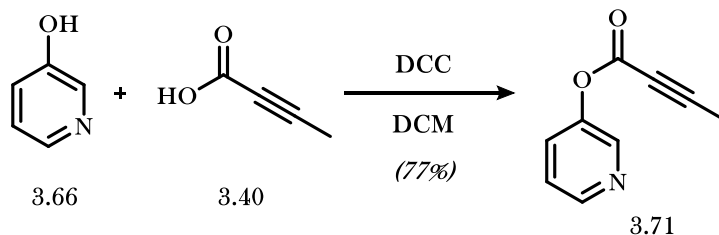
Cycloadduct 3.53



To a flame-dried 1-dram vial with stir bar was added cycloadduct **3.50** (7.0 mg, 0.04 mmol) and toluene (0.13 mL) under argon. A solution of TMSOTf (2.4 μL , 0.013 mmol, 0.3 equiv.) and 2,6-di-*tert*-butylpyridine (0.5 μL , 0.002 mmol, 0.05 equiv.) in toluene (0.083 mL) was then added dropwise over one minute. The reaction mixture was added to an oil bath preheated to 60 $^\circ\text{C}$ and stirred for 60 minutes, slowly turning yellow over time. After 60 minutes, the reaction mixture was cooled to room temperature, and 10 μL of H_2O was added to halt the reaction. After stirring for 10 minutes, EtOAc (1 mL) and saturated aqueous NaHCO_3 (1 mL) were added. The layers were separated, and the aqueous layer was extracted with CH_2Cl_2 (3 x 1 mL). The combined organic layers were dried over MgSO_4 , filtered through cotton, and concentrated *in vacuo* to give a yellow oil. The crude product mixture was purified by silica gel chromatography (50–75% EtOAc in hexanes) to afford cycloadduct **3.53** as a thin film (2.4 mg, 35%): ^1H NMR (500 MHz, CDCl_3) δ 6.39 (dd, J = 5.1, 3.6 Hz, 1H), 6.29, (d, J = 5.2 Hz, 1H), 4.88 (d, 1.4 Hz, 1H), 3.43-3.40 (m, 1H), 3.01 (s,

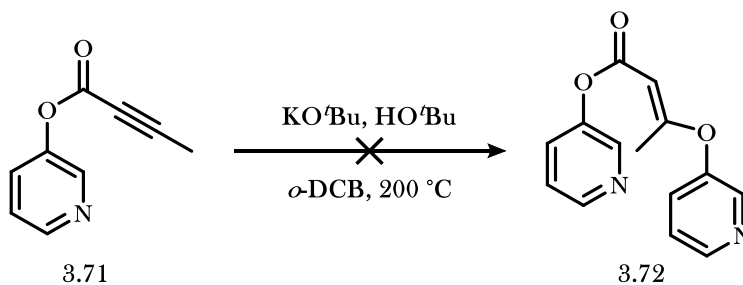
3H) 2.84 (d, $J=18.3$ Hz, 1H), 2.65 (d, $J=18.6$ Hz, 1H), 2.63 (dd, $J=9.9, 4.2$ Hz, 1H), 2.55 (d, $J=9.7$ Hz); ^{13}C NMR (126 MHz, CDCl_3) δ 196.9, 175.3, 169.9, 143.1, 136.6, 93.8, 57.4, 54.1, 50.0, 36.5, 26.7; IR (film) 2920, 1739, 1609, 1581 cm^{-1} ; HRMS (ESI) m/z calcd for $\text{C}_{11}\text{H}_{11}\text{NO}_2$ $[\text{M} + \text{Na}]^+$ 212.0687, found 212.0678.

Ester 58



To a flame dried round bottom flask with stir bar was added 3-hydroxypyridine (**3.66**) (200 mg, 2.1 mmol, 1.0 equiv.) and CH_2Cl_2 (12.5 mL) under argon. DCC (434 mg, 2.1 mmol, 1.0 equiv.) was added as a solution in CH_2Cl_2 (5.6 mL). A solution of 2-butynoic acid (**28**; 177 mg, 2.1 mmol, 1.0 equiv.) in CH_2Cl_2 (5.6 mL) was added in one portion. After 60 minutes, CH_2Cl_2 (25 mL) and saturated aqueous NaHCO_3 (50 mL) were added sequentially, and the layers were separated. The aqueous layer was extracted with CHCl_3 (2 x 50 mL). The organic layers were combined, dried, filtered, and concentrated *in vacuo*. The crude product mixture was purified by silica gel chromatography (33–50% EtOAc in hexanes) to afford **3.71** as a slightly yellow oil (260 mg, 77%): ^1H NMR (500 MHz, CDCl_3) δ 8.49 (dd, $J=4.8, 1.0$ Hz, 1H), 8.45 (d, $J=2.7$ Hz, 1H), 7.50 (ddd, $J=8.4, 2.6, 1.3$ Hz, 1H), 7.33 (dd, $J=8.4, 4.8$ Hz, 1H), 2.06 (t, 3H); ^{13}C NMR (126 MHz, CDCl_3) δ 151.1, 146.8, 143.1, 129.0, 123.9, 89.3, 71.2, 4.0; IR (film) 2265, 2231, 1732, 1462, 1243, 1203; HRMS (GC-ESI) m/z calcd for $\text{C}_9\text{H}_7\text{NO}_2$ $[\text{M} + \text{H}]^+$ 162.0555, found 162.0559.

Ester 3.72



To a flame-dried Anton-Parr G10 glass microwave vial with stir bar was added ester **3.71** (5.0 mg, 0.031 mmol, 1.0 equiv.) and *ortho*-dichlorobenzene (2 mL). Potassium *tert*-butoxide (3.5 mg, 0.031 mmol, 1.0 equiv.) and *tert*-butanol (*ca.* 10 μ L) were then added. The reaction mixture was heated at 200 °C for 60 minutes. Upon completion, saturated aqueous NaHCO₃ (2 mL) was added, and the layers were separated. The aqueous layer was extracted with CH₂Cl₂ (2 x 2 mL) and the combined layers were dried, filtered, and concentrated *in vacuo*. The remaining *o*-DCB was distilled off via simple distillation. The resulting oil was purified via silica gel chromatography (50–75% EtOAc in hexanes) to afford ester **3.72** as a slightly yellow oil: ¹H NMR (500 MHz, CDCl₃) δ 8.57 (d, *J* = 4.5 Hz, 1H), 8.44–8.46 (m, 2H), 8.38 (d, *J* = 2.3 Hz, 1H), 7.41–7.47 (m, 3H), 7.30 (dd, *J* = 8.3, 4.7 Hz, 1H), 5.05 (s, 1H), 2.57 (s, 3H); ¹³C NMR (126 MHz, CDCl₃) δ 175.3, 165.0, 149.6, 147.4, 147.2, 146.6, 143.8, 143.6, 129.4, 129.2, 124.6, 123.7, 95.3, 18.7; IR (film) 1730, 1575, 1426, 1242, 1205; HRMS (GC-CI) *m/z* calcd for C₁₄H₁₂N₂O₃ [M + H]⁺ 257.0926, found 257.0916.

3.8 Notes and References

- (1) Pham, H. V.; Karns, A. S.; Vanderwal, C. D.; Houk, K. N. *J. Am. Chem. Soc.* **2015**, *137*, 6956–6964.
- (2) Himbert, G.; Diehl, K.; Maas, G. *J. Chem. Soc., Chem. Commun.* **1984**, 900–901.
- (3) Himbert, G.; Diehl, K. *Liebigs Ann.* **1997**, 1255–1260.
- (4) (a) Davis, R. L.; Leverett, C. A.; Romo, D.; Tantillo, D. J. *J. Org. Chem.* **2011**, *76*, 7167–7174. (b) Leverett, C. A.; Purohit, V. C.; Johnson, A. G.; Davis, R. L.; Tantillo, D. J.; Romo, D. *J. Am. Chem. Soc.* **2012**, *134*, 13348–13356. (c) Mulzer, J.; Brütrup, G. *Angew. Chem. Int. Ed.* **1979**, *18*, 793–794.
- (5) Himbert, G.; Diehl, K.; Schlindwein, H.-J. *Chem. Ber.* **1989**, *122*, 1691–1699.
- (6) Brown, H. C.; Kanner, B. *J. Am. Chem. Soc.* **1966**, *88*, 986–992.
- (7) (a) Schaub, R. E.; Fulmor, W.; Weiss, M. J. *Tetrahedron* **1964**, *20*, 373–385. (b) Elfehail, F. E.; Zajac, W. W. *J. Org. Chem.* **1981**, *46*, 5151–5155.
- (8) Lam, J. K.; Schmidt, Y.; Vanderwal, C. D. *Org. Lett.* **2012**, *14*, 5566–5569.
- (9) Himbert, G.; Fink, D. *Tetrahedron Lett.* **1985**, *26*, 4363–4366.
- (10) Schmidt, Y.; Lam, J. K.; Pham, H. V.; Houk, K. N.; Vanderwal, C. D. *J. Am. Chem. Soc.* **2013**, *135*, 7339–7348.
- (11) (a) Ott, E.; Schröter, R.; Packendorff, K. *J. Prakt. Chem.* **1931**, *130*, 177–179. (b) Hurd, C. D. *Org. Synth.* **1925**, *4*, 39.
- (12) Aitken, R. A.; Al-Awadi, N. A.; El-Dusouqui, O. M. E.; Farrell, D. M. M.; Kumar, A. *Int. J. Chem. Kinet.* **2006**, *38*, 496–502.
- (13) Van der Klei, A.; de Jong, R. L. P.; Lugtenburg, J.; Tielens, A. G. M. *Eur. J. Org. Chem.* **2002**, *2002*, 3015–3023.
- (14) Liu, J.; Li, W.; Wang, C.; Li, Y.; Li, Z. *Tetrahedron Lett.* **2011**, *52*, 4320–4323.

- (15) Rossi, R.; Bellina, F.; Carpita, A.; Mazzarella, F. *Tetrahedron* **1996**, *52*, 4095–4110.
- (16) Danion-Bougot, R.; Danion, D.; Carrié, R. *Tetrahedron* **1985**, *41*, 1953–1958.
- (17) Himbert, G.; Fink, D.; Diehl, K.; Rademacher, P.; Bittner, A. J. *Chem. Ber.* **1989**, *122*, 1161–1173.
- (18) Weinreb, S. M. *Nat. Prod. Rep.* **2009**, *26*, 758.
- (19) Rognan, D.; Boulanger, T.; Hoffmann, R.; Vercauteren, D. P.; Andre, J. M.; Durant, F.; Wermuth, C. G. *J. Med. Chem.* **1992**, *35*, 1969–1977.
- (20) Weenen, H.; Nkunya, M.; Bray, D.; Mwasumbi, L.; Kinabo, L.; Kilimali, V.; Wijnberg, J. *Planta Med.* **1990**, *56*, 371–373.
- (21) Mensah, J. L.; Lagarde, I.; Ceschin, C.; Michelb, G.; Gleye, J.; Fouraste, I. *J. Ethnopharmacol.* **1990**, *28*, 129–133.
- (22) (a) Saito, S.; Yoshikawa, H.; Sato, Y.; Nakai, H.; Sugimoto, N.; Horii, Z.; Hanaoka, M.; Tamura, Y. *Chem. Pharm. Bull. (Tokyo)*. **1966**, *14*, 313–314. (b) Horii, Z.; Hanaoka, M.; Yamawaki, Y.; Tamura, Y.; Saito, S.; Shigematsu, N.; Kotera, K.; Yoshikawa, H.; Sato, Y.; Nakai, H.; Sugimoto, N. *Tetrahedron* **1967**, *23*, 1165–1174.
- (23) Honda, T.; Namiki, H.; Kaneda, K.; Mizutani, H. *Org. Lett.* **2004**, *6*, 87–89.
- (24) Magnus, P.; Rodriguez-Lopez, J.; Mulholland, K.; Matthews, I. *Tetrahedron Lett.* **1993**, *49*, 8059–8072.
- (25) But-3-ynoic acid was prepared from 3-butyn-1-ol according to: Wipf, P.; Coish, D. G. *Tetrahedron Lett.* **1997**, *38*, 5073–5076.
- (26) Prepared according to: Aitken, R. A.; Al-Awadi, N. A.; El-Dusouqui, O. M. E.; Farrell, D. M. M.; Kumar, A. *Int. J. Chem. Kinet.* **2006**, *38*, 496–502.
- (27) Procedure modified from: Fioravanti, S.; Pellacani, L.; Tardella, P. A.; Vergari, M. C. *Org. Lett.* **2008**, *10*, 1449–1451.

- (28) Bicyclo[2.2.1]hept-5-en-2-one was prepared from cyclopentadiene according to: Freerksen, R. W.; Selikson, S. J.; Wroble, R. R.; Kyler, K. S.; Watt, D. S. *J. Org. Chem.* **1983**, *48*, 4087-4096.
- (29) Procedure modified from: Kobayashi, Y.; Harayama, T. *Tetrahedron Lett.* **2009**, 6665-6667.
- (30) Procedure modified from: Qian, D.; Zhang, J. *Chem. Commun.* **2012**, *48*, 7082-7084.
- (31) Procedure modified from: Liu, J.; Li, W.; Wang, C.; Li, Y.; Li, Z. *Tetrahedron Lett.* **2011**, *52*, 4320-4323.
- (32) Procedure modified from: Rathke, M. W.; Cowan, P. J. *J. Org. Chem.* **1985**, *50*, 2622-2624.
- (33) 2-cyano-*N*-methyl-*N*-phenylacetamide was prepared according to: Kobayashi, Y.; Harayama, T. *Tetrahedron Lett.* **2009**, *50*, 6665-6667.
- (34) Procedure modified from: Boger, D. L.; Brotherton, C. E.; Georg, G. I. *Org. Synth.* **1987**, *65*, 32.
- (35) AgNO₃-doped TLC plates and silica gel prepared according to: Li, T.-S.; Li, J.-T.; Li, H.-Z. *J. Chromatogr. A* **1995**, *715*, 372-375.
- (36) 3-methoxy-*N*-methylaniline was prepared according to: Kamino, S.; Murakami, M.; Tanioka, M.; Shirasaki, Y.; Watanabe, K.; Horigome, J.; Ooyama, Y.; Enomoto, S. *Org. Lett.* **2014**, *16*, 258-261.

CHAPTER 4: BACKGROUND TO ISOCYANOTERPENE NATURAL PRODUCTS

4.1 Introduction

The isocyanoterpene classification of natural products includes a diverse set of terpenoid carbon frameworks that each contain one or more isonitrile or closely related substituents. First reported in 1973, this class has expanded to include both sesqui- and diterpenes that distinguish themselves by both scaffold and substitution. Over time, interest in these marine metabolites has amplified significantly owing to the discovery of potent and significant biological activity, and this increased attention has in turn led to the isolation and characterization of over 130 structures. The number of interesting discoveries reported from isocyanoterpene natural product research merits a thorough summary of the field.

4.1.1 Natural Product Families

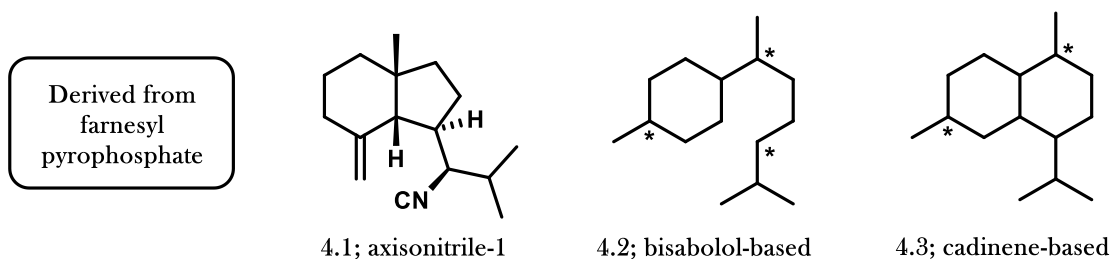
In 1973, axisonitrile-1 (**4.1**) was reported as the first marine isocyanoterpene natural product characterized, isolated from the marine sponge *Axinella cannabina* (Figure 4.1).¹ Since then, several other members of the family have been discovered that vary widely based on scaffold and substitution pattern. Compared to the 6,5-fused ring system of the parent compound, axisonitrile-2 contains a 5,7,3-fused tricyclic ring system,² and axisonitrile-3 can be identified by a spirocyclic 5,6-ring system.³ In each case, these derivatives were isolated as part of a triad with the corresponding isothiocyanate and formamide derivatives, but the isonitrile was observed predominantly as the major analogue in each case. It was later discovered that the isocyanate is observed alongside this triad as well, completing the collection of isocyanoterpene analogues commonly referred to as a ‘tetrad’.⁴

Since the discovery of the axisonitrile family of natural products, several other families have been described in the literature.⁴⁻⁵ The acanthellin-⁶ and cadinene-based (**4.3**)⁷ isocyanoterpenes can be identified by the fused 6,6-fused ring system. The bisabolenes (**4.2**) are easily recognized by their monocyclic core and their extensive and highly variable side chain.⁸ The diterpene amphilectane isocyanoterpenes (**4.7**) introduce a third fused ring to the cadinene-based core,⁹ while the cycloamphilectane/isocycloamphilectane (**4.8/4.9**)

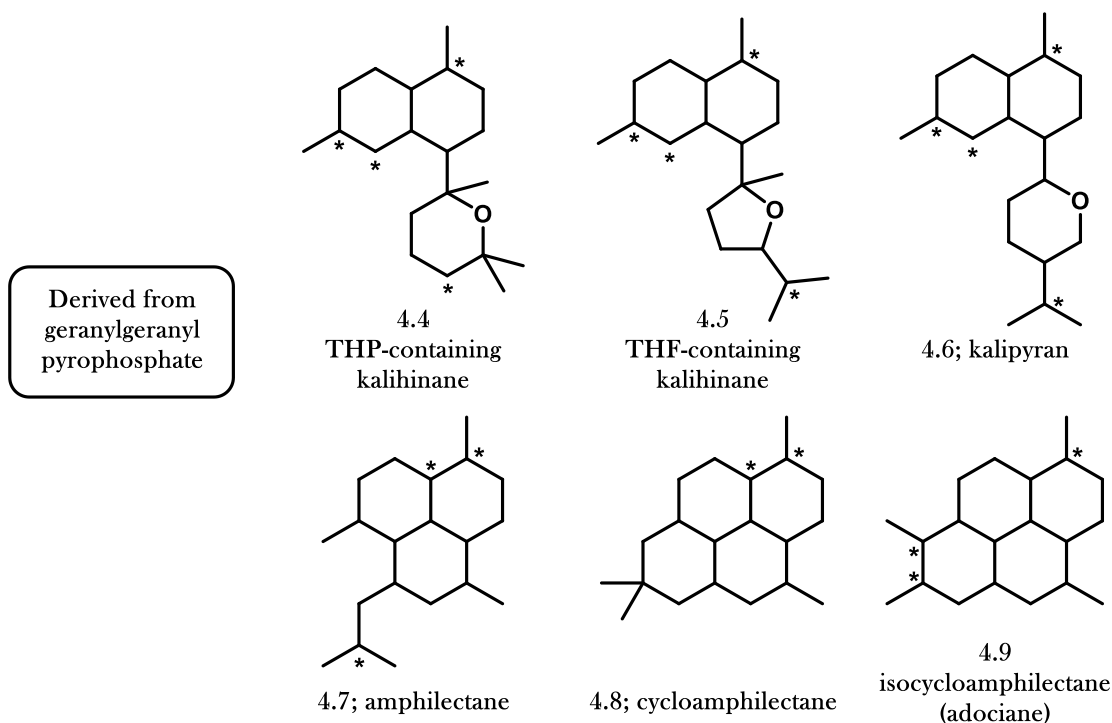
structures introduce a fourth.¹⁰ The kalihinane (**4.4/4.5**) and kalipyran (**4.6**) families of isocyanoterpenes resemble the cadinene-based natural products but introduce a heterocyclic ring substituent.¹¹ Although these natural product families include a majority of isocyanoterpene compounds of interest, there are several other isolated species in smaller families that remain outside the scope of this thesis.

Figure 4.1 Scaffolds of the Isocyanoterpene Natural Products

a. Representative Sesquiterpene Isonitriles



b. Representative Diterpene Isonitriles



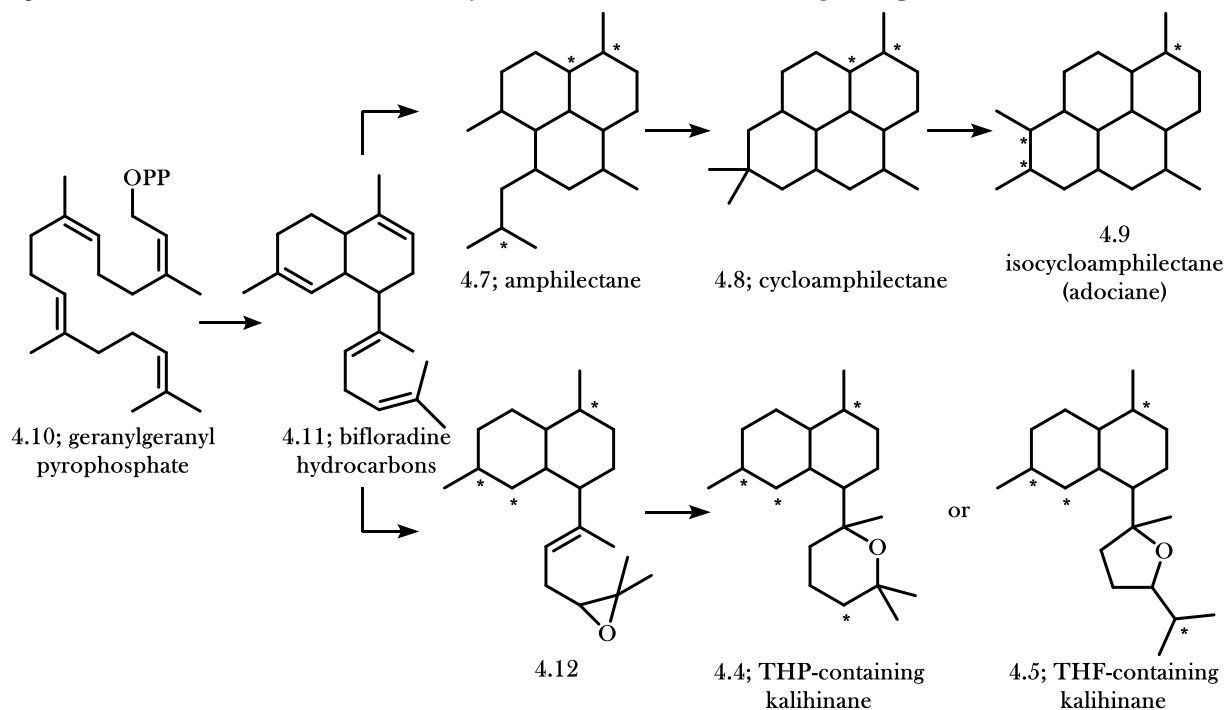
* = indicates functionality (isonitrile, isocyanate, isothiocyanate, formamide, amine, halide, or alkene)

4.2 Isocyanoterpene Genesis

4.2.1 Biosynthesis of the Core

Although the biosynthesis of sesquiterpene cores is rather unambiguous, the method by which complex isonitrile-containing diterpene natural products are formed from acyclic precursors is not as easily ascertained. The frequently observed kalihinane, amphilectane, and (iso)cycloamphilectane scaffolds are proposed to originate from the common bifloradine precursor **4.11**, derived from an oxidation and cyclization of geranylgeranyl pyrophosphate (**4.10**; Figure 4.2). Substitution on the carbon core, which diversifies each family into its different members, is often introduced at positions that are susceptible to nucleophilic attack; substituents are most often added via nucleophilic epoxide opening or attack of carbocations generated from trisubstituted olefins. Considering the content reported in Chapters 5–8, only the biosyntheses relevant to kalihinol A (**4.15**; Figure 4.3) and 7,20-diisocyanoadociane (**4.24**; DICA; Figure 4.3) will be discussed.

Figure 4.2 General Overview of the Biosynthesis of Isonitrile-containing Diterpenes



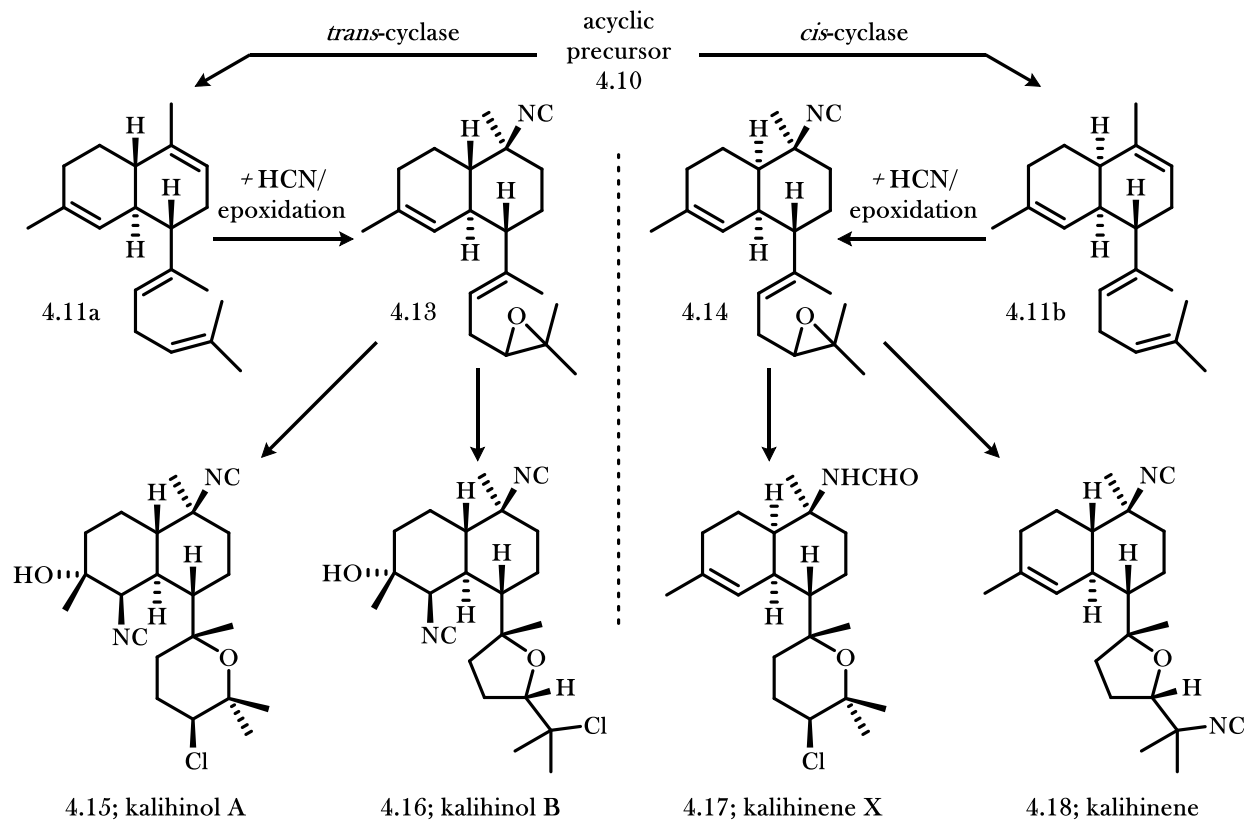
* = indicates functionality (isonitrile, isocyanate, isothiocyanate, formamide, amine, halide, or alkene)

The specific biosynthesis of the kalihinane family of natural products has been thoroughly studied by Clardy, Chang, and Scheuer (Figure 4.3a).¹² The process begins with enzymatic cyclization of geranylgeranyl pyrophosphate precursor **4.10** to the bifloradine product with either a *trans*- (**4.11a**) or *cis*-decalin (**4.11b**) junction. This initial step is supported by the isolation of reduced bifloradine precursors **4.19** and **4.20**, (Figure 4.3b). Intermediates **4.11a** and **4.11b** then undergo hydroisocyanation and enzymatic epoxidation of corresponding trisubstituted olefins to generate **4.13** and **4.14**, respectively. Again, this step in the biosynthesis is supported by the isolation of **4.21**, resulting from an identical hydroisocyanation but with epoxidation of the other remaining olefin (Figure 4.3b). The regioselectivity of the subsequent epoxide opening then determines the nature of the heterocycle of the kalihinane natural product; attack of the less substituted position of **4.13** or **4.14** will eventually form THP-containing kalihinanes, whereas attack of the more substituted position will form THF-containing kalihinanes. The heterocyclic rings are formed via protonation and cation-quenching of the remaining acyclic trisubstituted olefin. Interestingly, only kalihinanes containing a *trans*-decalin core will undergo an additional epoxidation and nucleophilic epoxide opening. Intermediates possessing a *cis*-decalin are instead isolated with the cyclic trisubstituted olefin intact. Information on the isolation, characterization, and synthesis of the kalihinane natural products is presented in Chapter 5.

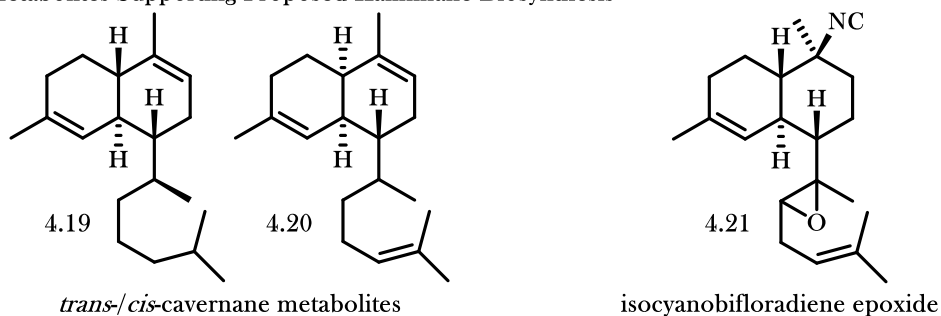
The method by which the amphilectanes and (iso)cycloamphilectanes are biosynthesized again begins with the formation of *trans*-fused bifloradine hydrocarbon skeleton **4.11a** (Figure 4.3c). However, instead of the epoxidation step which leads to the kalihinanes, amphilectane isonitrile products are formed via cyclization and hydroisocyanation. These elementary transformations are supported by the isolation of amphilectane isonitrile **4.22**. An additional cyclization will form the tetracyclic framework of the cycloamphilectanes (**4.23**), which then undergo a rearrangement involving 1,2-methyl shift to form the commonly observed isocycloamphilectane class of natural products, of which DICA (**4.24**) is a member. Although speculation exists as to the mechanism for isocycloamphilectane formation, the exact mechanism by which the structure is formed has not been confirmed. Further information on the isolation, characterization, and synthesis of 7,20-diisocyanoadociane can be found in Chapter 7.

Figure 4.3 In-Depth Proposed Biosynthesis of Relevant Families of Isocyanoterpenes

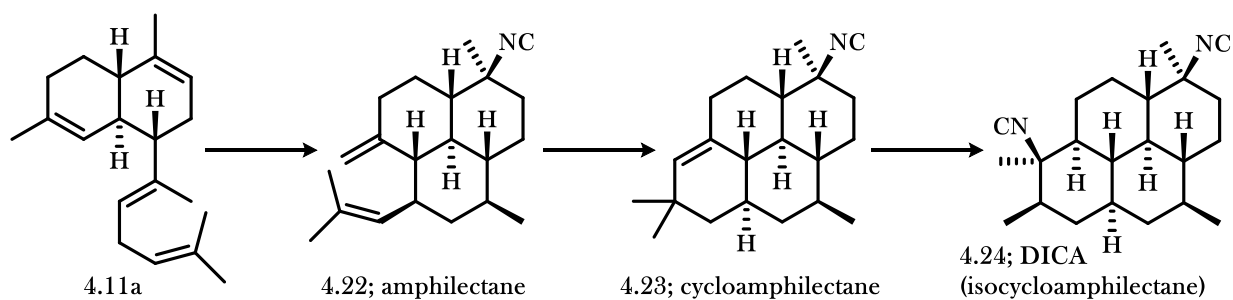
a. Proposed Biosynthesis of Kalihinane Derivatives



b. Isolated Metabolites Supporting Proposed Kalihinane Biosynthesis



c. Proposed Biosynthesis of Amphilectane/(Iso)cycloamphilectane Derivatives



Further research is required to determine the source of the geranylgeranyl pyrophosphate (**4.10**) precursor to the isocyanoterpenes. Typical carbon sources for terpene synthesis including sodium acetate, alanine, arginine, glycine, and leucine, were radiolabeled and fed to DICA-producing sponges but were not incorporated into the DICA skeleton.^{13,14} It has been proposed that the terpene starting materials are likely formed from more complex fragments or obtained from symbionts. The source of the carbon framework is an area that warrants further investigation.

4.2.2 Biosynthesis of the Isonitrile and Related Functional Groups

Although the biogenesis of the carbon framework for ICTs is not well understood, the installation and interconversion of the isonitrile ‘tetrad’ has been heavily studied. A crucial initial study by Garson showed that radiolabeled DICA can be isolated by feeding sodium [¹⁴C]cyanide to *Amphimedon terpenesis*,¹⁴ and Karuso and Scheuer found that radiolabeled kalihinol F is observed upon feeding sodium [¹⁴C]cyanide to *Acanthella* sp.¹⁵ Furthermore, Karuso and Scheuer also revealed that sodium [¹⁴C][¹⁵N]cyanide incorporated both radiolabeled nuclei into the ICT 9-isocyanoneopupukeanane.¹⁵ Degradation studies then confirmed that the radiolabeling is introduced exclusively in the isonitrile functional group; hydrolysis of a single isonitrile of DICA to the corresponding amine results in a 51% loss of radioactivity, and further hydrolysis of the remaining isonitrile results in loss of all unnatural radioactivity.¹⁴ These efforts prove that, independent of the biogenesis of the carbon skeleton, the polar functionality is introduced by the sponge. The source of the inorganic cyanide is proposed to be symbionts such as cyanobacteria.¹⁶

There are several mechanisms by which isonitriles can be introduced by incorporation of inorganic cyanide. In all cases involving inorganic cyanide as a nucleophile, the process is likely enzymatic; in addition to the fact that free inorganic cyanide is nucleophilic at the carbon atom, Karuso and Scheuer also found that attempted radiolabeling of ICT precursors with sodium [¹⁴C]cyanide in the absence of *Ciocalypta* sp. did not produce radiolabeled ICT natural products.¹⁵ Hydroisocyanation, the proposed method by which isonitriles are incorporated, likely proceeds via a mechanism involving protonation of an electron-rich alkene and

trapping of the resulting carbocation.¹⁷ Alternatively, isonitriles with α -oxidation patterns are likely introduced via epoxide opening.

The interesting observation that ICTs are often isolated along with fellow ‘tetrad’ derivatives also prompted further investigation. Early reports hypothesized that the isonitrile was formed via formylation and dehydration of a precursor alkaloid. However, radiolabeling experiments indicate that the isonitrile is instead the precursor to the formamide and amine via hydrolysis; radiolabeled axamide-1 was fed to *Axinella cannabina* and no transfer of radioactivity to isolated axisonitrile-1 was observed.¹⁸ The Garson group also showed that sodium [¹⁴C]-cyanide is incorporated into both axisonitrile-3 and axisothiocyante-3 suggesting that the isonitrile-containing natural product is the precursor to the isothiocyante-containing analogue.¹⁹ However, radiolabeled sodium [¹⁴C]-thiocyanate is also incorporated into both axisonitrile-3 and axisothiocyante-3 as well. It was later determined from radiolabeling experiments that both enzymatic interconversion between inorganic cyanide and isothiocyante *and* interconversion between the isonitrile and isothiocyante functional groups of ICTs occur. Radiolabel exchange between mixtures of isonitrile- and isothiocyante-containing natural products does not occur in the absence of the sponge, again indicating an enzymatic process.^{20,21}

4.2.3 Biological Function

The evolutionary benefit to the sponge’s development of isocyanoterpenes is not well understood. These natural products can be observed in high abundance throughout the cell; DICA is isolated in 2% yield from the dry weight of the producing sponge¹⁰ independent of geography or season.²² This likely indicates that isonitrile natural products hold a structural role in the cell, rather than a signaling role.²³ To further support this point, it was discovered that DICA is present in both the mesohyl and the pinacodermal tissues of the isocyanoterpene-containing sponge of genus *Amphimedon*.²⁴ Since cyanobacteria symbionts, believed to be the source of inorganic cyanide for the sponge’s biosynthesis of isocyanoterpenes, are only present only in the pinacodermal tissue of this sponge, it is believed that the sponge’s distribution of DICA throughout the organism indicates a structural role within the cell membrane. However, the exact purpose of DICA remains

unclear, as DICA was found to be not integral when lipid bilayers were prepared synthetically using more conventional phospholipids.²³

It is also proposed that ICTs have antifeeding and antifouling properties, which play a role in warding off predators from the sponges that produce these interesting natural products. A mixture of isocyanoterpenes at low concentrations (10 µg/mL) was found to prevent the feeding of goldfish upon the sponge.²⁵ At higher concentrations (100 µg/mL), both in the above case and in the case of sponge predators *Chromis chromis* and *Carassius carassius*,²⁶ isocyanoterpenes were found to be toxic to predators. In addition to preventing attack, a process which has obvious benefits to the health of the sponge, isocyanoterpenes have also demonstrated antifouling properties, which prevent the nearby growth of non-symbiotic species. Diterpenes such as kalihinol A (**4.15**; LD₅₀ = ca. 0.1 µg/mL) and kalihinenes X, Y, and Z (EC₅₀ = ca. 0.5-1.1 µg/mL) have shown potent antifouling activity.²⁷ The purpose of isocyanoterpene natural products in the sponge is yet to be fully elucidated.

4.3 Malaria and the Antiplasmodial Activity of the Isocyanoterpenes

4.3.1 Malaria

Plasmodium is a genus of parasite that is responsible for causing malaria. Most commonly transmitted by the saliva of the female *Anopheles* mosquito,²⁸ *Plasmodium* parasites are estimated to be responsible for over one million deaths per year.^{29,34a} The highest number of deaths from malaria occurs in sub-Saharan Africa, due to the combination of a high concentration of infected *Anopheles* mosquitos, the presence of the deadlier *Plasmodium falciparum* species, and the lack of advanced health care resources to provide rapid treatment. Since complete removal of the vector of transmission, the *Anopheles* mosquito, is unlikely, efforts have instead turned toward pharmaceutical therapies to reduce the death rate of malaria. Although there are treatments available for this disease, the cost of their acquirement leaves underdeveloped areas particularly prone to high mortality rates.

There are several types of *Plasmodium* that lead to human malaria. *P. falciparum* is a particularly dangerous species of *Plasmodium* that is responsible for approximately 75% percent of cases in sub-Saharan

Africa and virtually all malaria-related deaths.³⁰ *P. vivax* and *P. ovale*, although less deadly, possess a dormant liver stage that can cause reoccurring symptoms until the parasite is fully evacuated from the body.³¹ *P. milariae* is a far less common and less dangerous species of parasite that rarely leads to fatal symptoms.³²

The immune system alone is unable to eradicate *Plasmodium* from the body for several reasons. First, *Plasmodium* reside within human red blood cells and human liver cells and reproduce within, limiting contact with human immune cells within the body. Following initial infection, parasitic cells infect the liver and multiply within the cells of the liver.³³ They then migrate back into the bloodstream by concealing themselves within the cell membrane of liver cells,³⁴ and proceed to infect red blood cells, within which they are also hidden from the body's immune system.³⁵ In order to prevent processing of infected cells by the spleen, *Plasmodium* cells will promote protein expression on the cell membrane of their infected host which cause adhesion to blood vessels.³⁶ Following further replication within red blood cells, the multiplied parasitic cells will reinitiate the life cycle. To counter the highly-advanced mechanisms by which *Plasmodium* cells evade the immune system, the human body often requires the use of medicine.

4.3.2 Antimalarial Drugs

A large majority of antimalarial treatments are effective by taking advantage of the toxicity of heme to the parasitic cell. Blood stage *Plasmodium* feed on the hemoglobin of red blood cells to fuel replication. A byproduct of this digestion is free heme, which is toxic to *Plasmodium* in higher concentrations and therefore must be removed from the cell.³⁷ *Plasmodium* eradicates heme through a biocrystallization process in which free heme is oligomerized to form hemozoin, which can then be cleared from the cell.³⁸ Antimalarial therapies with known mechanisms of action almost exclusively act to prevent hemozoin formation, which increases the concentration of heme within *Plasmodium falciparum* resulting in parasitic cell death.³⁹

Quinoline-based drugs (quinine, chloroquine, amodiaquine, mefloquine, primaquine) have found use as treatments against malaria since the early discovery of the therapeutic effects of cinchona tree bark, which contains the quinoline-containing cinchona alkaloid quinine. Chloroquine (**4.26**; Table 4.1), a synthetic derivative, is significantly more active and can be produced at a lower cost, making it more affordable to

underdeveloped countries. *P. falciparum* eventually developed resistance to chloroquine, prompting the development of a series of synthetic derivatives which aimed to restore efficacy with mixed results. Despite known resistance, chloroquine is still effective when used in combination therapies for the treatment of less-deadly forms of malaria (*P. vivax*).

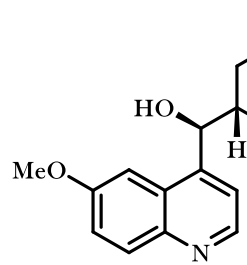
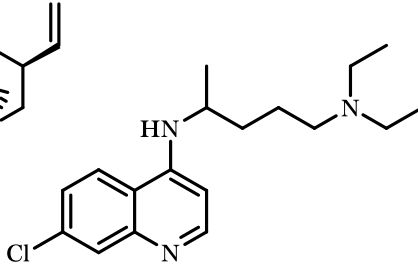
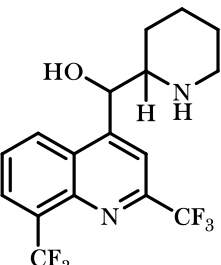
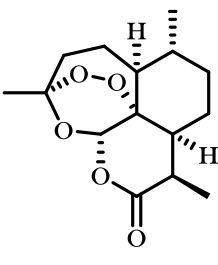
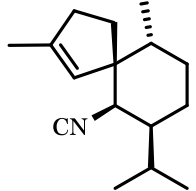
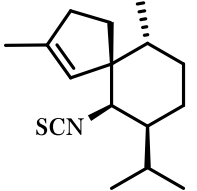
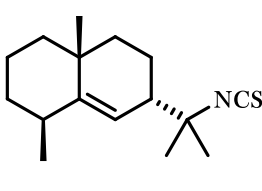
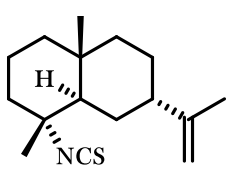
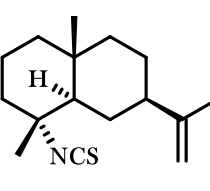
Artemisinin (**4.28**; Table 4.1) has emerged as a solution to the problem of chloroquine-resistance observed from *Plasmodium*. Artemisinin is a sesquiterpene recognized by a unique endoperoxide bridge as part of the polycyclic core. The peroxide bridge demonstrates a useful combination of stability and activity; the O-O bond remains intact throughout penetration of the parasitic cell but is then believed to directly contribute to the mechanism of action by which artemisinin demonstrates its antimalarial activity. It is believed that artemisinin acts to prevent hemozoin formation by parasitic cells, but controversy as to the exact mechanism of action exists. Since resistance to artemisinin develops rapidly when utilized as a lone therapy, the use of artemisinin-based combination therapies, which include aminoquinoline additives, is highly recommended.

Although there are several other drug scaffolds that function via different or unknown mechanisms of action, such as the tetracycline⁴⁰ or pyrimethamine/sulfadoxine⁴¹ combination therapies, artemisinin-based combination therapies remain the most utilized for the treatment of malaria. However, as is the case with many antimalarial treatments, it has been discovered that resistance to artemisinin is developing.⁴² For this reason, it is important that new molecular scaffolds with novel mechanisms of action be discovered to restore efficacy against malaria once resistance inevitably spreads.⁴³

4.3.3 Antiplasmodial Activity of Isocyanoterpenes

In 1992, a collaboration between the Angerhofer and König groups led to the initial discovery that isonitrile-containing terpene natural products are active against chloroquine-resistant *Plasmodium falciparum*.^{44,45} The natural products **4.29–4.33** were isolated from the sponge *Acanthella klethra* from Pelorus Island off the coast of Queensland, Australia, and **4.29** displayed highly potent activity against both chloroquine-sensitive (D6) and chloroquine-resistant (W2) strains of *Plasmodium falciparum* (Table 4.1).

Table 4.1 IC_{50} Values of Common Antimalarial Drugs and Early Isocyanoterpenes against *P. falciparum*

				
4.25; Quinine KB = > 60,000 nM D6 = 31 nM W2 = 73 nM	4.26; Chloroquine KB = ca. 54,400 nM D6 = 6.1 nM W2 = 71 nM	4.27; Mefloquine* KB = ca. 9,300 nM D6 = 22 nM W2 = 1.3 nM	4.28; Artemisinin KB = > 70,000 nM D6 = 15 nM W2 = 2.5 nM	
				
4.29; axisonitrile-3 KB = > 86,000 nM D6 = 610 nM W2 = 71 nM	4.30 KB = > 75,000 nM D6 = 47,000 nM W2 = 12,000 nM	4.31 KB = > 75,000 nM D6 = 8,500 nM W2 = 2,300 nM	4.32 KB = > 75,000 nM D6 = 15,000 nM W2 = 2,100 nM	4.33 KB = > 75,000 nM D6 = > 38,000 nM W2 = > 38,000 nM

KB cells are human cells

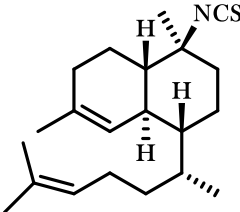
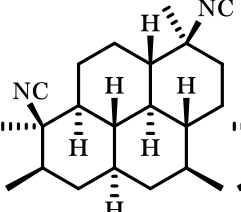
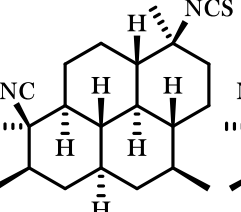
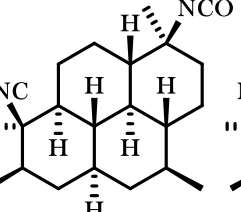
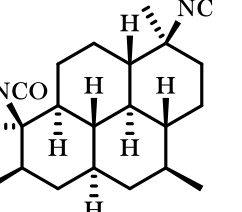
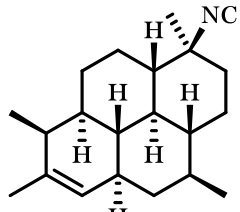
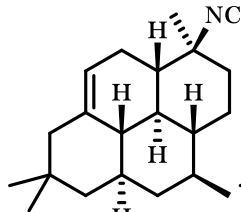
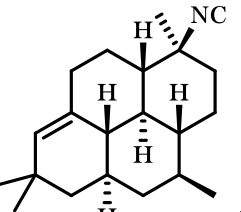
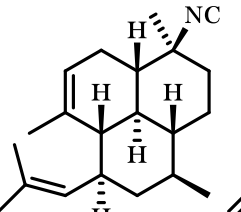
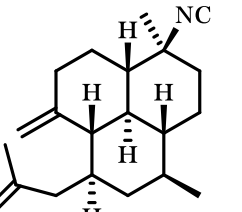
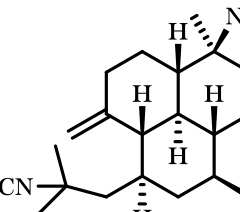
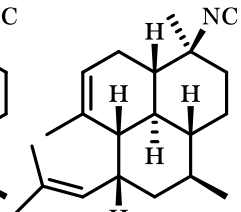
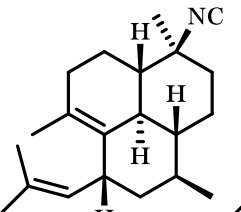
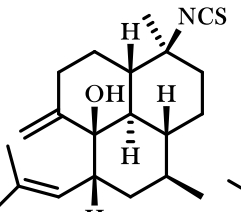
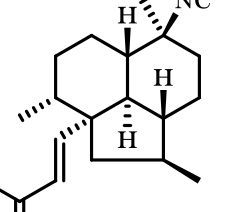
D6 is a chloroquine-sensitive strain of *Plasmodium falciparum*

W2 is a chloroquine-resistant strain of *Plasmodium falciparum*

* Mefloquine is produced a mixture of (R,S) and (S,R) enantiomers

Despite the limited number of derivatives tested in the initial study, a few observations can be made. In the case of axane-based structures **4.29** and **4.30**, the isonitrile exhibits significantly higher activity (71 nM against W2) compared to that of isothiocyanate-substituted terpene **4.30** (12,000 nM). Furthermore, the configuration of the hydrophobic portion of the molecule can have a significant impact on the antiparasitic activity; the configuration of the isopropylidene substituent on ICTs **4.32** and **4.33** results in more than an order of magnitude difference in activity for chloroquine-resistant *Plasmodium falciparum*. Importantly, each compound isolated exhibited no toxicity toward human KB-3 cells. The high selectivity index of these compounds for parasitic cells as opposed to mammalian cells, in combination with their potent activity against *Plasmodium falciparum*, initiated a still-ongoing investigation into the potential utility of isocyanoterpenes natural products as drugs to treat malaria.

Table 4.2 IC_{50} Values of the Amphilectanes and (Iso)cycloamphilectanes against *P. falciparum*

				
4.34	4.24	4.35	4.36	4.37
KB = > 60,000 nM D6 = > 30,000 nM W2 = > 30,000 nM	KB = 14,483 nM D6 = 14 nM W2 = 13 nM	KB = 4,487 nM D6 = 126 nM W2 = 80 nM	KB = 5,847 nM D6 = 220 nM W2 = 265 nM	KB = 12,628 nM D6 = 9 nM W2 = 7 nM
				
4.38	4.39	4.23	4.40	4.22
KB = 61,179 nM D6 = 210 nM W2 = 66 nM	KB = > 67,000 nM D6 = 285 nM W2 = 95 nM	KB = 48,741 nM D6 = 249 nM W2 = 80 nM	KB = > 67,000 nM D6 = 1015 nM W2 = 447 nM	KB = > 67,000 nM D6 = 1,748 nM W2 = 813 nM
				
4.41	4.42	4.43	4.44	4.45
KB = > 56,000 nM D6 = 1,318 nM W2 = 306 nM	KB = 10,757 nM D6 = 47 nM W2 = 31 nM	KB = 51,094 nM D6 = 197 nM W2 = 86 nM	KB = 15,338 nM D6 = 2,307 nM W2 = 1,224 nM	KB = 64,139 nM D6 = 303 nM W2 = 100 nM

KB cells are human cells

D6 is a chloroquine-sensistive strain of *Plasmodium falciparum*

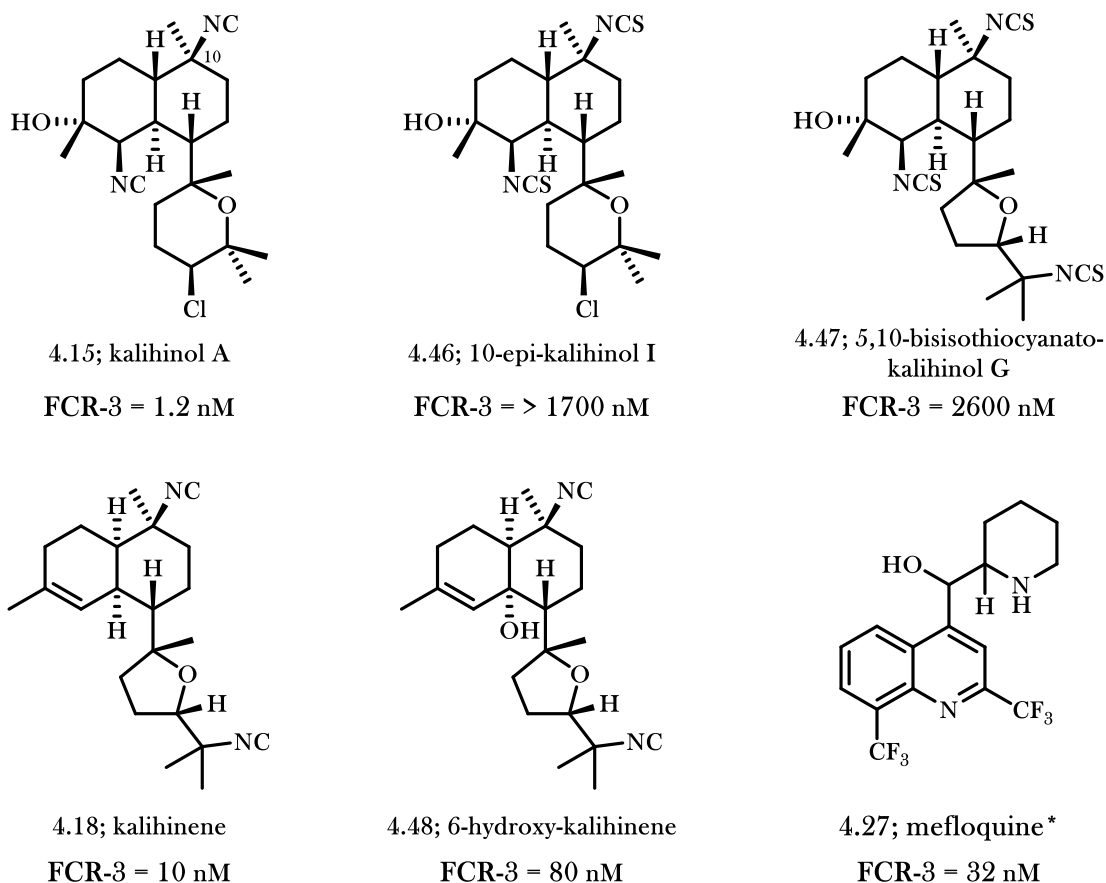
W2 is a chloroquine-resistant strain of *Plasmodium falciparum*

Following the initial discovery that isonitrile-containing terpenes express potent activity against *Plasmodium falciparum*, a more in-depth screen of known ICT natural products was undertaken by the König and Angerhofer groups in 1996 (Table 4.2). In this study, (+)-7,20-diisocyanoadociane (**4.24**; DICA) was identified as a highly potent, low-nanomolar inhibitor of both chloroquine-sensitive (D6) and chloroquine-resistant (W2) strains of *Plasmodium falciparum*, while displaying limited toxicity toward mammalian cells (KB). A screen of several other known ICT natural products was also reported which includes both isocycloamphilectanes (**4.24–4.38**) and amphilectanes (**4.22, 4.34, 4.40–4.45**). Although the efficacy of each compound screened varies slightly based on substitution and configuration, the ICTs generally maintain a high selectivity index for parasitic cells over those of humans.

The range of activities expressed by the several ICT derivatives again clearly indicates that isonitriles are the most active of the four commonly observed functional group derivatives. Compared to (+)-DICA, analogues with an isocyanate (**4.36**) and isothiocyanate (**4.35**) in the C-7 position suffer from significantly decreased activity. Interestingly, replacement of the C-20 isonitrile of DICA with an isocyanate (**4.37**), results in an increased potency against both D6 and W2 *Plasmodium falciparum* strains. Although the reason for this observation requires further investigation, these data suggest that the C-7 isonitrile may be the functional group mainly responsible for (+)-DICA's activity since the isocyanate had previously been proven less active in monofunctionalized compounds. To further support this hypothesis, monofunctionalized DICA-derivative **4.38** and cycloamphilectanes **4.39** and **4.23** retain nanomolar activity despite the lack of C-20 functionality.

In the amphilectane class of ICTs, the effects of small changes in configuration can again be clearly observed. For ICTs **4.40** and **4.42**, which possess the same 2-methylpropenyl substituent with opposing stereochemistry, the difference in antiplasmodial activity is more than an order of magnitude. This amphilectane-based **4.42** represents the only member of the amphilectane class tested that possesses comparable antiplasmodial activity to that of (+)-DICA. Similar isomers to **4.42**, including those with transposed olefins or additional functionality, suffer from drastically decreased activity. Further studies are necessary to fully determine the structure-activity relationship of the DICA-related compounds.

Table 4.3 IC_{50} Values of Several Kalihinanes against Drug-Resistant *P. falciparum*

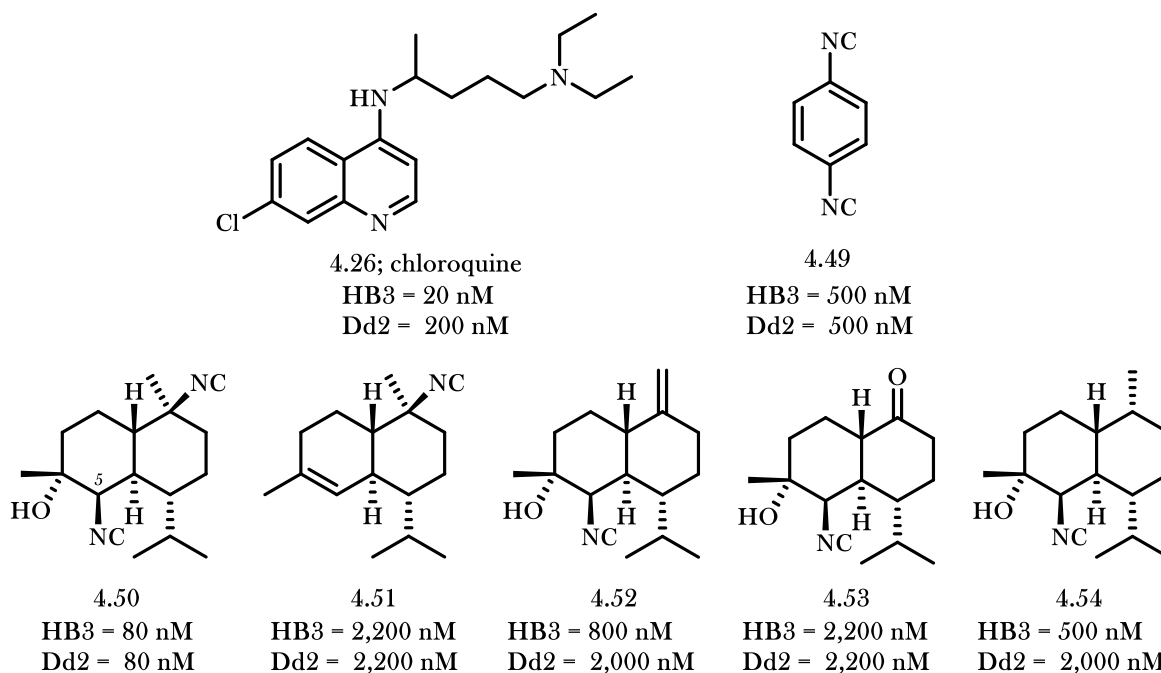


FCR-3 is a drug-resistant strain of *P. falciparum*

* Mefloquine is produced a mixture of (R,S) and (S,R) enantiomers

In 1998, the study of ICT activity against *Plasmodium falciparum* was extended to the related kalihinane family of natural products by Miyaoka and co-workers (Table 4.3). Kalihinol A (**4.15**), described in detail in Chapter 5, was found to have highly potent antimalarial activity against the drug-resistant parasitic strain FCR-3. The corresponding *bis*-isothiocyanate **4.46** possessed significantly dampened activity, again highlighting the antimalarial potency of the isonitrile. Also of note is the retained activity of kalihinene (**4.18**) and 6-hydroxy-kalihinene (**4.48**) despite loss of an isonitrile. This again indicates the importance of the axial C-10 (analogous to the DICA C-7) isonitrile, although the retained activity of **4.18** and **4.48** could be due to the additional acyclic isonitrile in these substrates. Importantly, a few of the originally tested kalihinanes express similar or better activity than the chloroquine-derivative mefloquine (**4.27**).

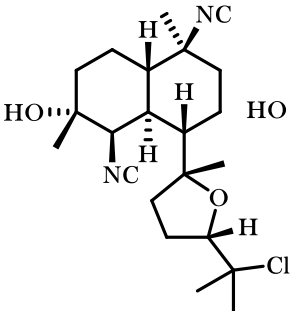
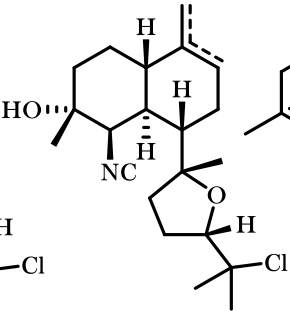
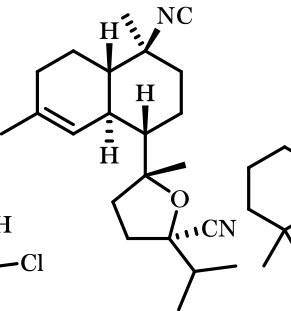
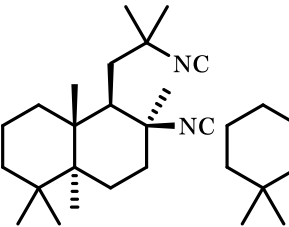
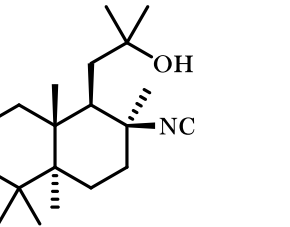
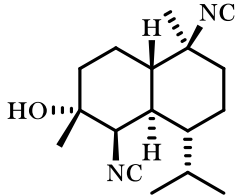
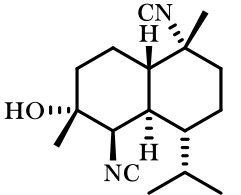
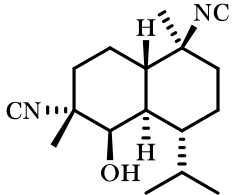
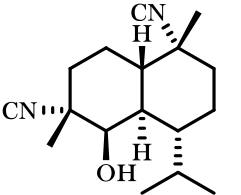
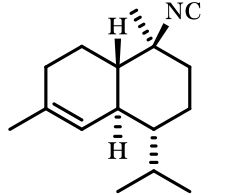
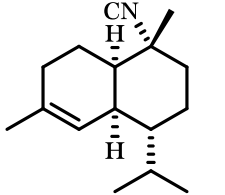
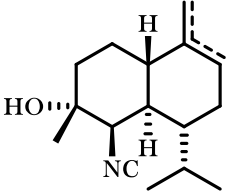
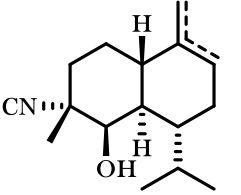
Table 4.4 Wood's IC_{50} Values of Simplified Kalihinane Analogues against *P. falciparum*



 HB3 is a chloroquine-sensitive strain of *Plasmodium falciparum*
 Dd2 is a chloroquine-resistant strain of *Plasmodium falciparum*

To further investigate the structure-activity relationship of these compounds, the Wood group has expanded the bioactivity studies of the kalihinanes to include simplified analogues **4.49–4.54** (Table 4.4). They found that analogue **4.50**, which resembles kalihinol A (**4.15**) but lacks the heterocyclic THP ring, demonstrates high potency against both drug-sensitive and drug-resistant *Plasmodium falciparum*. However, testing of several analogues show that both isonitriles make significant contributions to the activity of these isocyanoterpenes. Replacement of the C-5 isonitrile with a trisubstituted olefin as in **4.51** results in a decrease in activity, while replacement of the C-10 tertiary isonitrile with a vinylidene (**4.52**), ketone (**4.53**), or methyl substituent (**4.54**) results in a similar decrease in potency. Wood's major contribution from this work showed that the heterocyclic ring appended to the decalin core of the kalihinane family of natural products is not critical.

Table 4.5 Vanderwal's IC_{50} Values of Simplified Isocyanoterpenes against *P. falciparum*

				
4.16; kalihinol B	4.55; 3:1 olefin ratio	4.56	4.57	4.58
3D7 = 8.4 nM Dd2 = 4.6 nM	3D7 = 139 nM Dd2 = 144 nM	3D7 = 175 nM Dd2 = 123 nM	3D7 = 1.9 nM Dd2 = 1.6 nM	3D7 = 244 nM Dd2 = 416 nM
				
4.50	4.59	4.60	4.61	
3D7 = 12 nM Dd2 = 16 nM	3D7 = 2.9 nM Dd2 = 31 nM	3D7 = 15 nM Dd2 = 17 nM	3D7 = 1,150 nM Dd2 = 958 nM	
				
4.51; (±)-10-isocyano-4-cadinene	(±) 4.62	4.63; 7:1 olefin ratio	4.64; 5.6:1 olefin ratio	
3D7 = 705 nM Dd2 = 247 nM	3D7 = 180 nM Dd2 = 45 nM	3D7 = 138 nM Dd2 = 200 nM	3D7 = 312 nM Dd2 = 529 nM	

3D7 is a chloroquine-sensitive strain of *Plasmodium falciparum*

Dd2 is a chloroquine-resistant strain of *Plasmodium falciparum*

In 2017, the Vanderwal group expanded the list of isonitrile-containing analogues that exhibited bioactivity against *Plasmodium falciparum* (Table 4.5). They had previously shown that kalihinol B (**4.16**) has highly potent activity against drug-resistant *P. falciparum*.⁴⁶ Similar to the results obtained by the Wood group, the Vanderwal group observed an order of magnitude decrease in activity by replacing the C-10 isonitrile with an alkene, as in **4.51**. To determine whether alternative terpene scaffolds could be decorated with isonitriles

and retain reactivity, they found that sclareolide-derived isonitriles **4.57** and **4.58** exhibited similar activity to the natural products. This suggests that the terpene scaffold may just be a vehicle for the isonitrile; in a similar experiment, the Puri group found that adamantyl isonitrile is also active against *Plasmodium falciparum*.⁴⁷

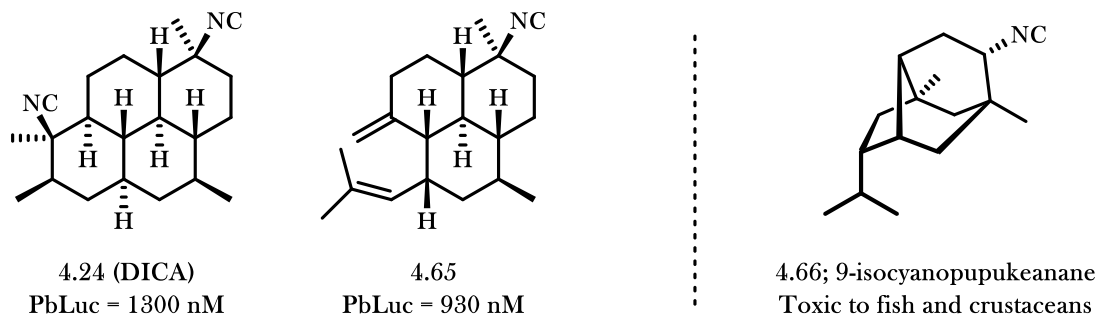
The Vanderwal group also expanded upon the testing of decalin analogues. They found that the stereochemistry of the C-10 tertiary isonitrile has little effect on the potency of the analogues (**4.50** and **4.59**) and that the relative position of the α -hydroxy isonitrile is relatively insignificant (**4.50** and **4.60**). However, the *bis*-axial *bis*-isonitrile **4.61** suffers from severely decreased activity for reasons that are currently unclear. As expected, replacement of either isonitrile with unsaturation results in a significant decrease in activity.

The relationship between the structure of isonitrile-containing terpenes and their activity against *Plasmodium falciparum* remains poorly understood. With exceptions in each case, general observations include: (1) analogues with two isonitriles display more potent activity than monosubstituted terpenes, (2) the configuration of the aliphatic portion of analogues can have a significant effect on the activity, and (3) the isonitrile is in all cases more potent than the corresponding isocyanate, isothiocyanate, *N*-formamide, and amine. Further studies are required to better understand the highly-complex structure-activity relationship of these compounds.

4.3.4 Mechanism of Action for Antiplasmodial Isocyanoterpenes

There is evidence to support that isocyanoterpenes act to prevent hemozoin formation in parasitic cells as well, albeit by a different mechanism. It is believed that the isonitrile functionality coordinates to the iron atom of free heme; there is a correlation between the coordination of the isonitrile to the iron atom of heme, measured by UV-vis, and the potency of the antimalarial isonitrile.⁴⁸ Furthermore, it was shown that DICA inhibits the *in vitro* formation of β -hematin, an oxidized dimer of heme naturally produced by red blood cells, from free heme.⁴⁹ To further investigate the proposed mechanism of action, Wright and coworkers determined through 3D-QSAR and receptor modeling that the proposed target requires a hydrophobic portion of the binding, fulfilled by the terpene fragment, and also contains portions that can participate in electrostatic interactions.⁴⁸

Table 4.6 Shenvi's Liver-stage Active ICTs and 9-isocyanopupukeanane



Liver-stage *Plasmodium falciparum* do not feed upon hemoglobin and therefore do not need to biocrystallize heme to detoxify the cell. Based on the mechanism of action proposed above, therefore, isocyanide-based terpenes should not be active against liver-stage parasites. However, Shenvi and co-workers found in 2016 that isocyanoterpenes **4.24** (DICA) and **4.65** are also highly active against liver-stage *Plasmodium berghei*, indicating that there is an additional or alternative mechanism of action (Table 4.6).⁵⁰ Further investigation into the mechanism of action(s) of isocyanoterpenes would provide insight into the feasibility of their use as antimalarial drugs.

4.4 Other Bioactivities of the Isocyanoterpenes

In addition to the evolutionarily advantageous activities discussed in section 4.2.4, researchers have also discovered additional bioactivity from isocyanoterpenes natural products. One such example was uncovered following the observation that nudibranch mollusks release a mucus that is lethal to fish and crustaceans.⁵¹ Nudibranchs are brightly colored and lack armored exoskeletons, thus leaving them susceptible to attack from predators, but are not fed upon. They fend off predators by releasing a mucus rich in 9-isocyanopupukeanane (**4.66**; Table 4.6) when threatened. It was found that the ICT was obtained from their sponge diet; the concentration of **4.66** in the mucus increases when the amount of *Hymenioaidon* sponge in their diet increases.⁵²

Although fish toxicity is not a phenotype often pursued in medicinal research, this observation opened the door for further investigations into the peculiar bioactivities of isocyanoterpenes. 7,20-

diisocyanoadociane (DICA) was found to have both Gram-negative and Gram-positive bioactivity,⁵³ vasodilative activity,⁵⁴ antifungal activity, antialgal activity, antitubular activity, and activity in the reduction of photosynthesis.⁵⁵ The kalihinanes also expressed anthelmintic,⁵⁶ antifouling,^{27b,57} antimicrobial,^{11,58} antifungal,^{11,59,60} and cytotoxic^{57c,60a,61} activity. Although a wealth of bioactivity has been observed from ICTs, they remain known primarily for their antiplasmodial activity. Interestingly, most ICTs are relatively non-toxic to mammalian cells.

4.5 General Considerations for Isocyanoterpene Natural Product Synthesis

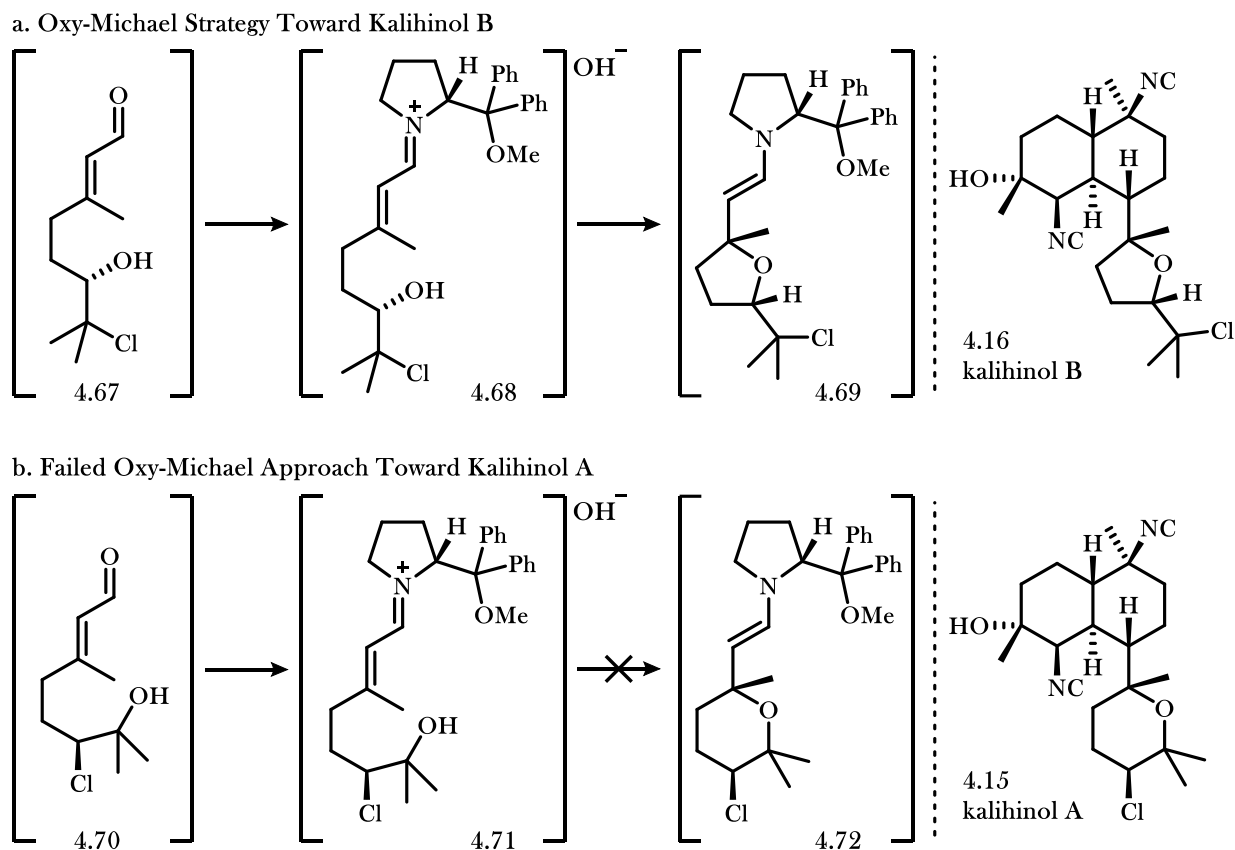
4.5.1 A Divergent Approach to All Isocyanoterpene Natural Products

The proposed biogenesis of the multitude of families of isocyanoterpenes involves initial formation of a decalin core and subsequent differentiation to three main families: the kalihinanes, amphilectanes, and isocycloamphilectanes. Nature has developed a technique for the development of a diverse class of natural products from a single precursor **4.10** (Figure 4.2) that should inspire the synthetic chemist. An attractive research program could be built around a universal strategy toward isocyanoterpene synthesis from a common precursor, which might accelerate a comprehensive investigation into the structure-activity relationship of ICTs.

Although inspirational, this level of thinking fails to consider the different challenges presented by each of these families of natural products. The kalihinanes are easily identified by the assortment of congested, stereodefined substituents that decorate the relatively simple core. In comparison, the 7,20-diisocyanoadociane natural product contains just two polar functional groups, but their selective installation on a unique all *trans*-fused perhydropyrene ring system presents its own challenge. The isonitrile functionalities are always installed in the last transformation from polar functional group precursors, which are located at different positions on the related natural product scaffolds (see Figure 4.1). An additional problem preventing a universal strategy therefore lies in the installation of these polar functionalities that differ in positioning, identity, and stereochemistry. For a universal strategy toward ICTs to be successful, each synthesis that diverges from a common precursor must then include a highly selective installation of polar

functionality. As one might imagine, each of the completed syntheses of these isocyanoterpenes stray from a universal approach and instead differ significantly in both synthetic precursor and general approach.

Figure 4.4 Vanderwal's Strategy Toward Kalihinol B and its Attempted Application to Kalihinol A



Even strategies geared toward the synthesis of two members of the same family of ICTs have proven difficult. In 2015, The Vanderwal group reported a total synthesis of kalihinol B involving a organocatalyst-controlled oxy-Michael addition of a secondary alcohol **4.68** into an eniminium conjugate acceptor to form the tetrahydrofuran heterocycle (Figure 4.4). During efforts to universalize this strategy, the Vanderwal group attempted to apply an analogous oxy-Michael addition toward the synthesis of kalihinol A, which instead contains a tetrahydropyran ring. It was found that the slow rate of ring-closure of **4.71** was surpassed by a faster decomposition pathway, and this strategy's application toward THP-containing kalihinanes was abandoned. Our experience attempting to apply the methodology from kalihinol B to a closely-related

member of the same family highlights the daunting task of developing a general synthesis strategy toward all ICTs. The highly differing successful strategies toward the kalihinanes and 7,20-diisocyanoadociane, each of which independently contribute toward our knowledge of ICT synthesis, will be discussed in chapters 5 and 7, respectively.

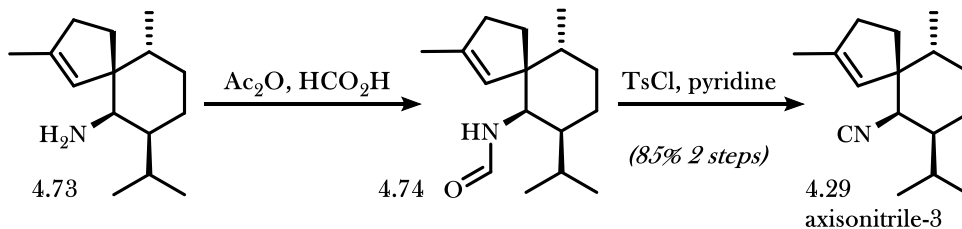
4.5.2 Isonitrile Installation

The number of strategies that may be considered when designing a synthesis of an isocyanoterpene natural product is limited by the number of methods by which isonitriles can be formed. Fortunately, several methodologies have been developed which install isonitriles both regio- and stereoselectively from a variety of precursors.

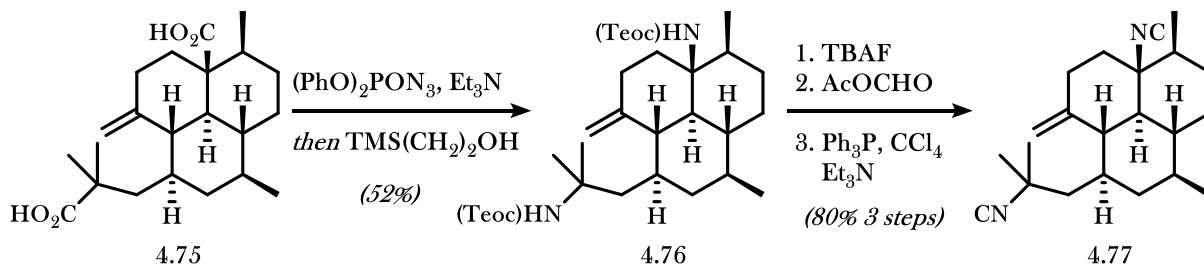
A classical method for isonitriles involves dehydration from the corresponding *N*-formylamine. This is among the most versatile of methods available for isonitrile installation, since there are countless known transformations that procure amine precursors. Furthermore, since the isonitrile is constructed from a previously installed C-N bond, epimerization is not a concern. Caine and Deutsch highlighted the applicability of this transformation in their synthesis of the first ICT axisonitrile-3 (**4.29**; Scheme 4.1a).⁶² From the amine precursor **4.78**, they formed the *N*-formylamine **4.74** using acetic anhydride and formic acid, which was then dehydrated with *p*-toluenesulfonyl chloride and pyridine to directly afford the isonitrile-containing natural product **4.29**. This method has similarly been used in both the synthesis of kalhinanes⁶³ and DICA.^{17,64} To accomplish this same transformation in a single step, the Shenvi group has demonstrated the use of difluoromethyl triflate as a mild reagent for the direct conversion of amines to isonitriles in their synthesis of kalihinol C.⁶⁵

Scheme 4.1 Isonitrile Syntheses from Amine Precursors

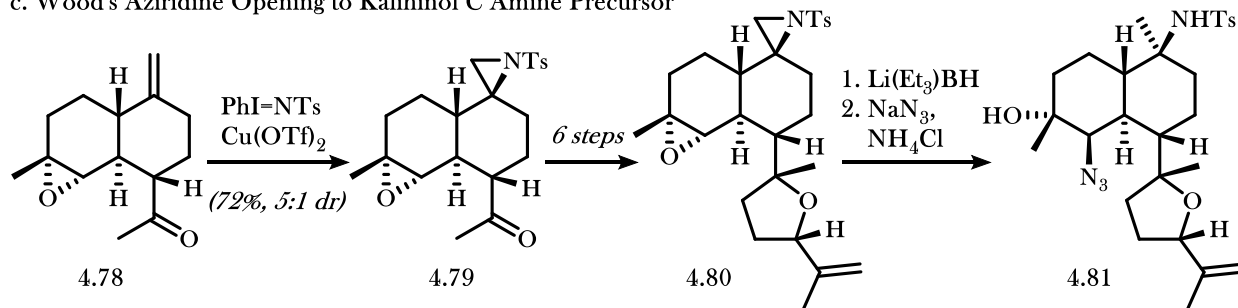
a. Caine and Deutsch's Formylation/Dehydration Isonitrile Installation



b. Piers's Curtius Rearrangement to Amphilectane Amine Precursor



c. Wood's Aziridine Opening to Kalihinol C Amine Precursor



The several known methods for the formation of secondary and tertiary amines provide additional variability in synthetic strategy. Free amines can be formed via the Curtius rearrangement from carboxylic acids, thus expanding the scope of isonitrile precursors to include ester, hydroxymethyl, nitrile, and carboxylic acid precursors. The Piers group has demonstrated the utility of esters as precursors to isonitriles in their synthesis of (+)-8-isocyano-10-cycloamphilectene (**4.77**; Scheme 4.1b).⁶⁶ Starting from diacid **4.75**, Piers performed a Curtius rearrangement to install the key stereodefined C-N bond. Following deprotection of **4.76**, *N*-formylation and dehydration then provided **4.77** in high yields from the ester precursor. Importantly, this reaction sequence involves stereospecific isonitrile formation since the carbon stereocenter does not participate in the reaction mechanism.

Wood and co-workers also disclosed a method for the formation of tertiary amines from vinylidene precursors (Scheme 4.1c).^{63a} In their synthesis of kalihinol C, they formed an *N*-tosylaziridine ring **4.79** via cyclization onto the 1,1-disubstituted olefin of **4.78**. The aziridine was carried forward until the end of the synthesis and ring opened to form the corresponding tertiary tosylamine **4.81**. The amine was then deprotected, acylated, and dehydrated to provide kalihinol C in an efficient manner. This method highlights a useful method by which “protected isonitriles” can be carried through the synthesis and unveiled toward the end where their reactivity will not inhibit construction of the rest of the natural product scaffold.

The other common method by which isonitriles can be installed involves attack of an electrophile or cation by inorganic cyanide mimics, similar to the nature’s own technique. In the case of primary or secondary isonitriles, their installation via the displacement of a leaving group is effective and stereoselective. However, the simple displacement of tertiary electrophiles under standard conditions is not a facile transformation. The Ritter reaction was an early solution to this problem: nucleophilic attack to a carbocation, most often formed via protonation of an electron-rich olefin, by a functionalized nitrile forms the key C–N bond. Importantly, the nucleophile must contain a substituent on the carbon atom, as inorganic cyanide is instead nucleophilic on carbon. As discussed in section 4.2.1, the tertiary isonitriles of isocyanoterpene natural products are believed to be installed in this manner, where a carbocation is formed and quenched with an enzyme-mediated isonitrile installation.

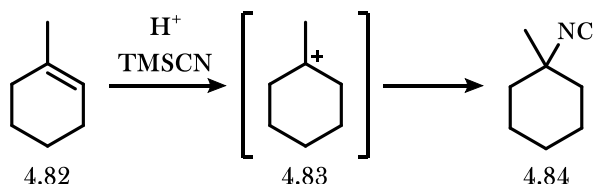
The Ritter method can be used for the stereoselective installation of tertiary isonitriles from precursors with scaffolds that bias the facial selectivity of nucleophilic attack (Figure 4.5a).⁶⁷ In the case of unhindered prochiral alkenes such as **4.83**; however, the symmetrical nature of the unoccupied carbocation orbital leads to low facial selectivity of nucleophilic attack. As a result, Ritter-type reactions generally suffer from low selectivity when used to install tertiary isonitriles.

In Corey and Magriotis’s synthesis of DICA, they highlight an alternate method for tertiary carbocation formation via Lewis acid-activated heterolytic cleavage of a tertiary trifluoroacetate functionality (Figure 4.5b).⁶⁸ When performed in the presence of trimethylsilyl cyanide (TMSCN) as a nucleophile, they found that the carbocation could be quenched by the nitrogen-atom to directly form tertiary isonitriles. Due

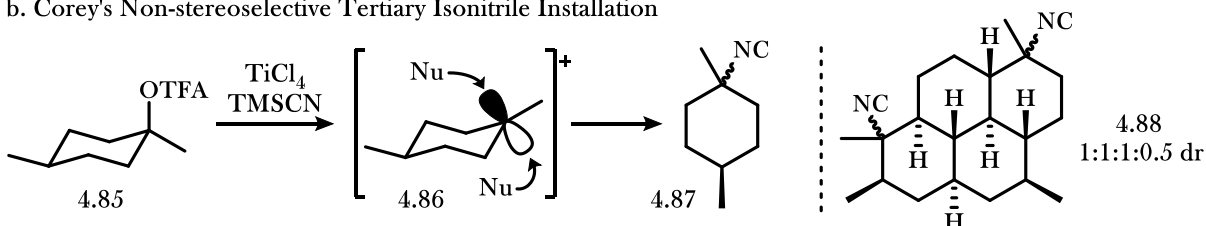
to the unbiased facial selectivity of TMSCN attack, however, they observed the formation of DICA accompanied by a mixture of its diastereomers. For several decades, the problem of stereoselective isonitrile installation from simple tertiary alcohol precursors remained unsolved.

Figure 4.5 Isonitrile Installation via Nucleophilic Attack

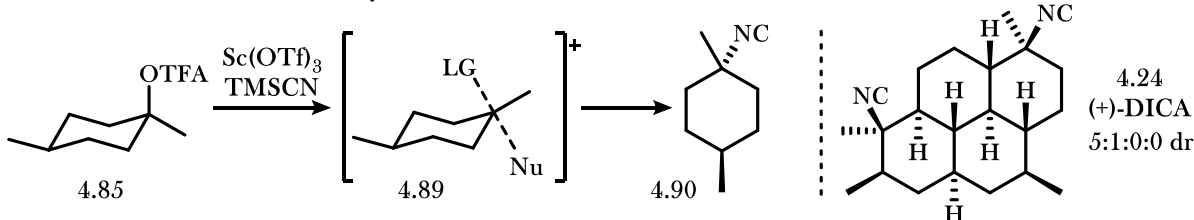
a. Ritter-type Installation of Tertiary Isonitriles



b. Corey's Non-stereoselective Tertiary Isonitrile Installation

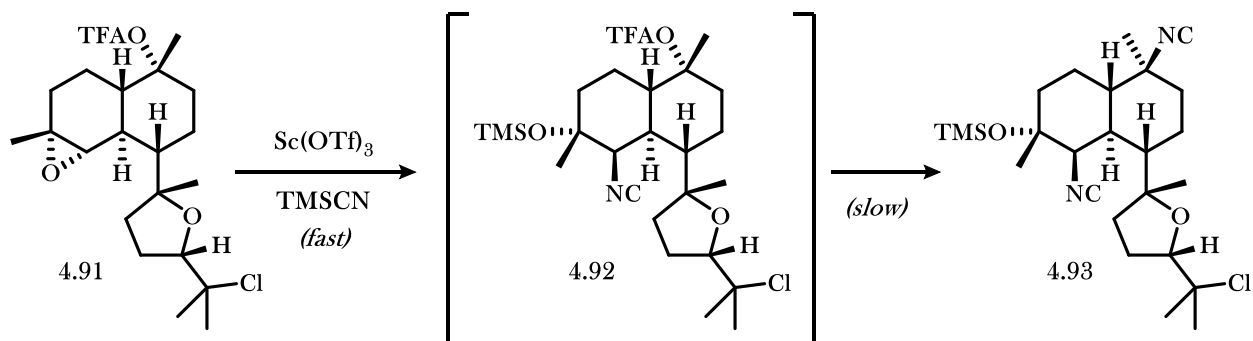


c. Shenvi's Stereoinvertive Tertiary Isonitrile Installation



In recent years, Shenvi and coworkers completed a synthesis of 7-isocyano-11(20),14-epiamphilectadiene involving installation of the tertiary isonitrile via a stereoselective invertive displacement of the stereodefined tertiary alcohol precursor.⁶⁹ This reaction proceeds through a mechanism very similar to that of Corey and co-workers but with higher stereoselectivity. The increased selectivity is attributed to the rapid rate of carbocation quenching that proceeds faster than the Lewis acid/trifluoroacetate tight ion pair's dissociation (see **4.89**). As a result, the leaving group still blocks a face of the prochiral carbocation at the time of C-N bond formation, preventing stereoretentive substitution. In a subsequent publication, the Shenvi group further investigates the scope and drawbacks of their valuable methodology.⁷⁰ This method has been used in their synthesis of DICA with improved selectivity (Figure 4.5c).

Scheme 4.6 Vanderwal's One-pot Bis-isonitrile Installation on Route to Kalihinol B



In 2015, the Vanderwal group extended the Shenvi methodology to include a one-pot *bis*-isonitrile installation via invertive displacement and epoxide opening en route to kalihinol B (Figure 4.6).⁴⁶ The addition of $\text{Sc}(\text{OTf})_3$ to trifluoroacetate **4.91** in TMSCN as a solvent rapidly opens the epoxide to the α -isocyano TMS-protected tertiary alcohol **4.92**, and a slower invertive displacement of the tertiary trifluoroacetate eventually forms the stereodefined tertiary isonitrile **4.93**. This inclusion of the Shenvi methodology in a one-pot installation of two dissimilar isonitriles represents a clever method for the procurement of the isonitrile motifs observed in the kalihinanes. In situations where a one-pot *bis*-isonitrile installation could not be performed, as stated in Shenvi's synthesis of the similar analogue kalihinol C, an aminolysis of the epoxide and above-described formylation/dehydration sequence could instead be utilized.⁶⁵

4.6 Conclusions

In just 45 years, the field of marine isocyanoterpenes has grown from the early identification of axisonitrile-1 to the creation of highly-potent antiplasmodial synthetic analogues with potential for use as medicinal therapies. Researchers have identified the biogenesis of the unique isonitrile substituent on sesqui- and diterpene scaffolds, discovered the valuable activity of ICT natural products against the *Plasmodium* genus of parasites that cause malaria, and developed several strategies to facilitate their synthesis in a laboratory setting. Despite all advancements in this growing field of interest, however, there remains an absence of understanding concerning the structure-activity relationship of these interesting natural products. Chapters 5-

8 will discuss various synthetic studies toward these isocyanoterpene natural products in an effort to better understand the structural features that are necessary to achieve medicinal value.

4.7 Notes and References

- (1) Cafiere, F.; Fattorusso, E.; Magno, S.; Santacroce, C.; Sica, D. *Tetrahedron*, **1973**, *29*, 4259–4262.
- (2) (a) Fattorusso, E.; Magno, S.; Mayol, L.; Santacroce, C.; Sica, D. *Tetrahedron* **1975**, *31*, 269–270.
(b) Fattorusso, E.; Mango, S.; Mayol, L.; Santacroce, C.; Sica, D. *Tetrahedron* **1974**, *30*, 3911–3913.
- (3) DiBlasio, B.; Fattorusso, E.; Magno, S.; Mayol, L.; Pedone, C.; Santacroce, C.; Sica, D. *Tetrahedron* **1976**, *32*, 473–478.
- (4) (a) Edenborough, M. S.; Herbert, R. B. *Nat. Prod. Rep.* **1988**, *5*, 229–245. (b) Lan, W.-J.; Wan, H.-P.; Li, G.-X.; Li, H. J.; Chen, Y. Y.; Liao, C. Z.; Cai, J. W. *Helv. Chim. Acta* **2008**, *91*, 426–434. (c) Jumaryatno, P.; Rands-Trevor, K.; Blanchfield, J. T.; Garson, M. J. *ARKIVOC* **2007**, *7*, 157–166. (d) Mitome, H.; Shirato, N.; Miyaoka, H.; Yamada, Y.; van Soest, R. W. M. *J. Nat. Prod.* **2004**, *67*, 833–837.
- (5) Garson, M. J.; Simpson, J. S. *Nat. Prod. Rep.* **2004**, *21*, 164–179.
- (6) Ciminiello, P.; Fattorusso, E.; Magno, S.; Mayol, L. *J. Org. Chem.* **1984**, *49*, 3949–3951.
- (7) (a) Burreson, B. J.; Christophersen, C.; Scheuer, P. J. *J. Am. Chem. Soc.* **1975**, *97*, 201–202. (b) Burreson, B. J.; Scheuer, P. J. *J. Chem. Soc., Chem. Commun.* **1974**, 1034–1035. (c) Burreson, B. J.; Christophersen, C.; Scheuer, P. J. *Tetrahedron* **1975**, *31*, 2015–2018.
- (8) Nakamura, H.; Kobayashi, J.; Ohizumi, Y.; Hirata, Y. *Tetrahedron Lett.* **1984**, *25*, 5401–5404.
- (9) Wratten, S. J.; Faulkner, D. J.; Hirotsu, K.; Clardy, J. *Tetrahedron Lett.* **1978**, 4345–4348.
- (10) Baker, J. T.; Wells, J. R.; Oberhänsli, W. E.; Hawes, G. B. *J. Am. Chem. Soc.* **1976**, *98*, 4010–4012.
- (11) Chang, C. W. J.; Patra, A.; Roll, D. M.; Scheuer, P. J.; Matsumoto, G. K.; Clardy, J. *J. Am. Chem. Soc.* **1984**, *106*, 4644–4646.

- (12) (a) Rodríguez, J.; Nieto, R. M.; Hunter, L. M.; Diaz, M. C.; Crews, P.; Lobkovsky, E.; Clardy, J. *Tetrahedron* **1994**, *50*, 11079–11090. (b) Chang, C. W. J.; Scheuer, P. J. *Comp. Biochem. Physiol.* **1990**, *97B*, 227–233.
- (13) (a) Fookes, C. J. R.; Garson, M. J.; MacLeod, J. K.; Skelton, B. W.; White, A. H. *J. Chem. Soc., Perkin Trans. 1*, **1988**, 1003–1011. (b) L. Minalde in ‘Marine Natural Products: Chemical and Biological Perspectives’, ed. P. J. Scheuer, Academic Press, London, 1978, Vol. 1, p. 204.
- (14) Garson, M. J. *J. Chem. Soc., Chem. Commun.* **1986**, 35–36.
- (15) Karuso, P.; Scheuer, P. J. *J. Org. Chem.* **1989**, *54*, 2092–2095.
- (16) Vennesland, B.; Conn, E. E.; Knowles, C. J.; Westley, J.; Wissing, J. *Cyanide in Biology*, Academic Press, London, 1981.
- (17) Simpson, J. S.; Garson, M. J. *Org. Biomol. Chem.* **2004**, *2*, 939–948.
- (18) Pfeifer, S.; Bär, H.; Zarnack, J. *Pharmazie*, **1972**, *27*, 536.
- (19) Dumdei, E. J.; Flowers, A. E.; Garson, M. J.; Moore, C. J. *Comp. Biochem. Physiol.* **1997**, *118A*, 1385.
- (20) Simpson, J. S. PhD thesis, The University of Queensland, 2000.
- (21) Simpson, J. S.; Garson, M. J. *Tetrahedron Lett.* **1998**, *39*, 5819–5822.
- (22) Garson, M. J. *Nat. Prod. Rep.* **1989**, *6*, 143–170.
- (23) Garson, M. J. *Chem. Rev.* **1993**, *93*, 1699–1733.
- (24) Garson, M. J.; Thompson, J. E.; Larsen, R. M.; Battershill, C. N.; Murphy, P. T.; Bergquist, P. R. *Lipids* **1992**, *27*, 378–388.
- (25) (a) Thompson, J. E.; Walker, R. P.; Wratten, S. J.; Faulkner, D. J. *Tetrahedron* **1982**, *38*, 1865–1873. (b) Faulkner, D. J.; Molinski, T. F.; Andersen, R. J.; Dumdei, E. J.; de Silva, E. D. *Comp. Biochem. Physiol.* **1990**, *97C*, 233.
- (26) Cimino, G.; De Rosa, S.; De Stefano, S.; Sodano, G. *Comp. Biochem. Physiol.* **1982**, *73B*, 471.

- (27) (a) Fusetani, N.; Hirota, H.; Okino, T.; Tomono, Y.; Yoshimura, E. *J. Nat. Toxins* **1996**, *5*, 249. (b) Okino, T.; Yoshimura, E.; Hirota, H.; Fusetani, N. *J. Nat. Prod.* **1996**, *59*, 1081–1083.
- (28) (a) Molina-Cruz, A.; Zilversmit, M. M.; Neafsey, D. E.; Hartl, D. L.; Barillas-Mury, C. *Annu. Rev. Genet.* **2016**, *50*, 447–465. (b) Sinka, M. E.; Bangs, M. J.; Manguin, S.; Coetzee, M.; Mbogo, C. M.; Hemingway, J.; Patil, A. P.; Temperley, W. H.; Gething, P. W.; Kabaria, C. W.; Okara, R. M.; Boeckel, T. V.; Godfray, H. C. J.; Harbach, R. E.; Hay, S. I. *Parasites & Vectors* **2010**, *3*, 117.
- (29) Gelb, M. H. *Curr. Opin. Chem. Biol.* **2007**, *11*, 440–445.
- (30) (a) Rich, S. M.; Leendertz, F. H.; Xu, G.; LeBreton, M.; Djoko, C. F.; Aminake, M. N.; Takang, E. E.; Diffo, J. L. D.; Pike, B. L.; Rosenthal, B. M.; Formenty, P.; Boesch, C.; Ayala, F. J.; Wolfe, N. D. *PNAS* **2009**, *106*, 14902–14907. (b) Perkins, D. J.; Were, T.; Davenport, G. C.; Kempaiah, P.; Hittner, J. B.; Ong'echa, J. M. *Int. J. Biol. Sci.* **2011**, *7*, 1427–1442. (c) Perlmann, P.; Troye-Blomberg, M. *Folia Biol.* **2000**, *46*, 210–218.
- (31) (a) Vogel, G. *Science* **2013**, *342*, 684–687. (b) White, N. J. *Trends in Parasitology* **2016**, *32*, 918–920. (c) Collins, W. E.; Jeffery, G. M. *Clin. Microbiol. Rev.* **2005**, *18*, 570–581.
- (32) Mohapatra, P. K.; Prakash, A.; Bhattacharyya, D. R.; Goswami, B. K.; Ahmed, A.; Sarmah, B.; Mahanta, J. *Indian J. Med. Res.* **2008**, *128*, 52–56.
- (33) Gerald, N.; Mahajan, B.; Kumar, S. *Eukaryot. Cell* **2011**, *10*, 474–482.
- (34) (a) Vaughan, A. M.; Aly, A. S. I.; Kappe, S. H. I. *Cell Host & Microbe* **2008**, *4*, 209–218. (b) Sturm, A.; Amino, R.; van de Sand, C.; Regen, T.; Regen, T.; Retzlaff, S.; Rennenberg, A.; Krueger, A.; Pollok, J.-M.; Menard, R.; Heussler, V. T. *Science* **2006**, *313*, 1287–1290.
- (35) Bledsoe, G. H. *Southern Medical Journal* **2005**, *98*, 1197–1204.
- (36) Tilley, L.; Dixon, M. W. A.; Kirk, K. *Int. J. Biochem. Cell Biol.* **2011**, *43*, 839–842.
- (37) Miller, L. H.; Ackerman, H. C.; Su, X.-z.; Wellem, T. E. *Nat. Med.* **2013**, *19*, 156–167.
- (38) Weissbuch, I.; Leiserowitz, L. *Chem. Rev.* **2008**, *108*, 4899–4914.

- (39) Wang, J.; Zhang, C.-J.; Chia, W. N.; Loh, C. C. Y.; Li, Z.; Lee, Y. M.; He, Y.; Yuan, L.-X.; Lim, T. K.; Liu, M.; Liew, C. X.; Lee, Y. Q.; Zhang, J.; Lu, N.; Lim, C. T.; Hua, Z.-C.; Liu, B.; Shen, H.-M.; Tan, K. S. W.; Lin, Q. *Nat. Commun.* **2015**, *6*, 10111.
- (40) Chopra, I.; Roberts, M. *Microbiol. Mol. Biol. Rev.* **2001**, *65*, 232-260.
- (41) Chulay, J. D.; Watkins, W. M.; Sixsmith, D. G. *Am. J. Trop. Med. Hyg.* **1984**, *33*, 325-330.
- (42) (a) Turschner, S.; Efferth, T. *Mini-Rev. Med. Chem.* **2009**, *9*, 206-214. (b) Ashley, E. A.; et al. *N. Engl. J. Med.* **2014**, *371*, 411-423. (c) Dondorp, A. M.; Nosten, F.; Poravuth, Y.; Das, D.; Physo, A. P.; Tarning, J.; Lwin, K. M.; Arie, F.; Hanpithakpong, W.; Lee, S. J.; Ringwald, P.; Silamut, K.; Imwong, M.; Chotivanich, K.; Lim, P.; Herdman, T.; An, S. S.; Yeung, S.; Singhasivanon, P.; Day, N. J. *N. Eng. J. Med.* **2009**, *361*, 455-467.
- (43) Flannery, E. L.; Chatterjee, A. K.; Winzeler, E. A. *Nat. Rev. Microbiol.* **2013**, *11*, 849-862.
- (44) Angerhofer, C. K.; Pezzuto, J. M.; König, G. M.; Wright, A. D.; Sticher, O. *J. Nat. Prod.* **1992**, *55*, 1787-1789.
- (45) König, G. M.; Wright, A. D.; Sticher, O.; Fronczek, F. *J. Nat. Prod.* **1992**, *55*, 633-638.
- (46) Daub, M. E.; Prudhomme, J.; Le Roch, K.; Vanderwal, C. D. *J. Am. Chem. Soc.* **2015**, *137*, 4912-4915.
- (47) Singh, C.; Srivastav, N. C.; Puri, S. K. *Bioorg. Med. Chem. Lett.* **2002**, *12*, 2277-2279.
- (48) Wright, A. D.; Wang, H.; Gurrath, M.; König, G. M.; Kocak, G.; Neumann, G.; Loria, P.; Foley, M.; Tilley, L. *J. Med. Chem.* **2001**, *44*, 873-885.
- (49) Young, R. M.; Adendorff, M. R.; Wright, A. D.; Davies-Coleman, M. T. *Eur. J. Med. Chem.* **2015**, *93*, 373-380.
- (50) Lu, H.-H.; Pronin, S. V.; Antonova-Koch, Y.; Meister, S.; Winzeler, E. A.; Shenvi, R. A. *J. Am. Chem. Soc.* **2016**, *138*, 7268-7271.
- (51) Johannes, R. E. *Veliger.* **1963**, *5*, 104-105.

- (52) Burreson, B. J.; Scheuer, P. J.; Finer, J.; Clardy, J. *J. Am. Chem. Soc.* **1975**, *97*, 4763–4764.
- (53) Kazlauskas, R.; Murphy, P. T.; Wells, R. J.; Blount, J. F. *Tetrahedron Lett.* **1980**, *21*, 315–318.
- (54) Morita, M.; Endo, M. *J. Pharmacobio-Dyn.* **1985**, *8*, s74.
- (55) Wright, A. D.; McCluskey, A.; Robertson, M. J.; MacGregor, K. A.; Gordon, C. P.; Guenther, J. *Org. Biomol. Chem.* **2011**, *9*, 400–407.
- (56) (a) Omar, S.; Albert, C.; Fanni, T.; Crews, P. *J. Org. Chem.* **1988**, *53*, 5971–5972. (b) Alvi, K. A.; Tenenbaum, L.; Crews, P. *J. Nat. Prod.* **1991**, *54*, 71–78.
- (57) (a) Okino, T.; Yoshimura, E.; Hirota, H.; Fusetani, N. *Tetrahedron Lett.* **1995**, *36*, 8637–8640. (b) Hirota, H.; Tomono, Y.; Fusetani, N. *Tetrahedron* **1996**, *52*, 2359–2368. (c) Xu, Y.; Li, N.; Jiao, W.-H.; Wang, R.-P.; Peng, Y.; Qi, S.-H.; Song, S.-J.; Chen, W.-S.; Lin, H.-W. *Tetrahedron* **2012**, *68*, 2876–2883.
- (58) Patra, A.; Chang, C. W. J.; Scheuer, P. J.; Van Duyne, G. D.; Matsumoto, G. K.; Clardy, J. *J. Am. Chem. Soc.* **1984**, *106*, 7981–7983. (b) Chang, C. W. J.; Patra, A.; Baker, J. A.; Scheuer, P. J. *J. Am. Chem. Soc.* **1987**, *109*, 6119–6123. (c) Bugni, T. S.; Singh, M. P.; Chen, L.; Arias, D. A.; Harper, M. K.; Greenstein, M.; Maiese, W. M.; Concepción, G. P.; Mangalindan, G. C.; Ireland, C. M. *Tetrahedron* **2004**, *60*, 6981–6988.
- (59) Patra, A.; Chang, C. W. J.; Scheuer, P. J.; Van Duyne, G. D.; Matsumoto, G. K.; Clardy, J. *J. Am. Chem. Soc.* **1984**, *106*, 7981–7983. (b) Chang, C. W. J.; Patra, A.; Baker, J. A.; Scheuer, P. J. *J. Am. Chem. Soc.* **1987**, *109*, 6119–6123. (c) Bugni, T. S.; Singh, M. P.; Chen, L.; Arias, D. A.; Harper, M. K.; Greenstein, M.; Maiese, W. M.; Concepción, G. P.; Mangalindan, G. C.; Ireland, C. M. *Tetrahedron* **2004**, *60*, 6981–6988.
- (60) (a) Fusetani, N.; Yasumuro, K.; Kawai, H.; Natori, T.; Brinen, L.; Clardy, J. *Tetrahedron Lett.* **1990**, *31*, 3599–3602. (b) Trimurtulu, G.; Faulkner, D. J. *J. Nat. Prod.* **1994**, *57*, 501–506.
- (61) Sun, J.-Z.; Chen, K.-S.; Yao, L.; Liu, H.-L.; Guo, Y.-W. *Arch. Pharm. Res.* **2009**, *32*, 1581–1584.

- (62) Caine, D.; Deutsch, H. *J. Am. Chem. Soc.* **1978**, *100*, 8030–8031.
- (63) (a) White, R. D.; Wood, J. L. *Org. Lett.* **2001**, *3*, 1825–1827. (b) White, R. D.; Keaney, G. F.; Slown, C. D.; Wood, J. L. *Org. Lett.* **2004**, *6*, 1123–1126. (c) Miyaoka, H.; Abe, Y.; Sekiya, N.; Mitome, H.; Kawashima, E. *Chem. Commun.* **2011**, *48*, 901–903. (d) Miyaoka, H.; Abe, Y.; Kawashima, E. *Chem. Pharm. Bull.* **2012**, *60*, 1224–1226.
- (64) Fairweather, K. A.; Mander, L. N. *Org. Lett.* **2006**, *8*, 3395–3398.
- (65) Reiher, C. A.; Shenvi, R. A. *J. Am. Chem. Soc.* **2017**, *139*, 3647–3650.
- (66) Schindeler, T. W. Ph.D. Dissertation, University of British Columbia, 1998.
- (67) Srikrishna, A.; Ravi, G.; Venkata Subbaiah, D. R. C. *Synlett* **2009**, 32–34.
- (68) Corey, E. J.; Magriotis, P. A. *J. Am. Chem. Soc.* **1987**, *109*, 287–289.
- (69) Pronin, S. V.; Shenvi, R. A. *J. Am. Chem. Soc.* **2012**, *134*, 19604–19606.
- (70) Pronin, S. V.; Reiher, C. A.; Shenvi, R. A. *Nature* **2013**, *501*, 195–199.

CHAPTER 5: BACKGROUND TO KALIHINOL A AND RELATED NATURAL PRODUCTS

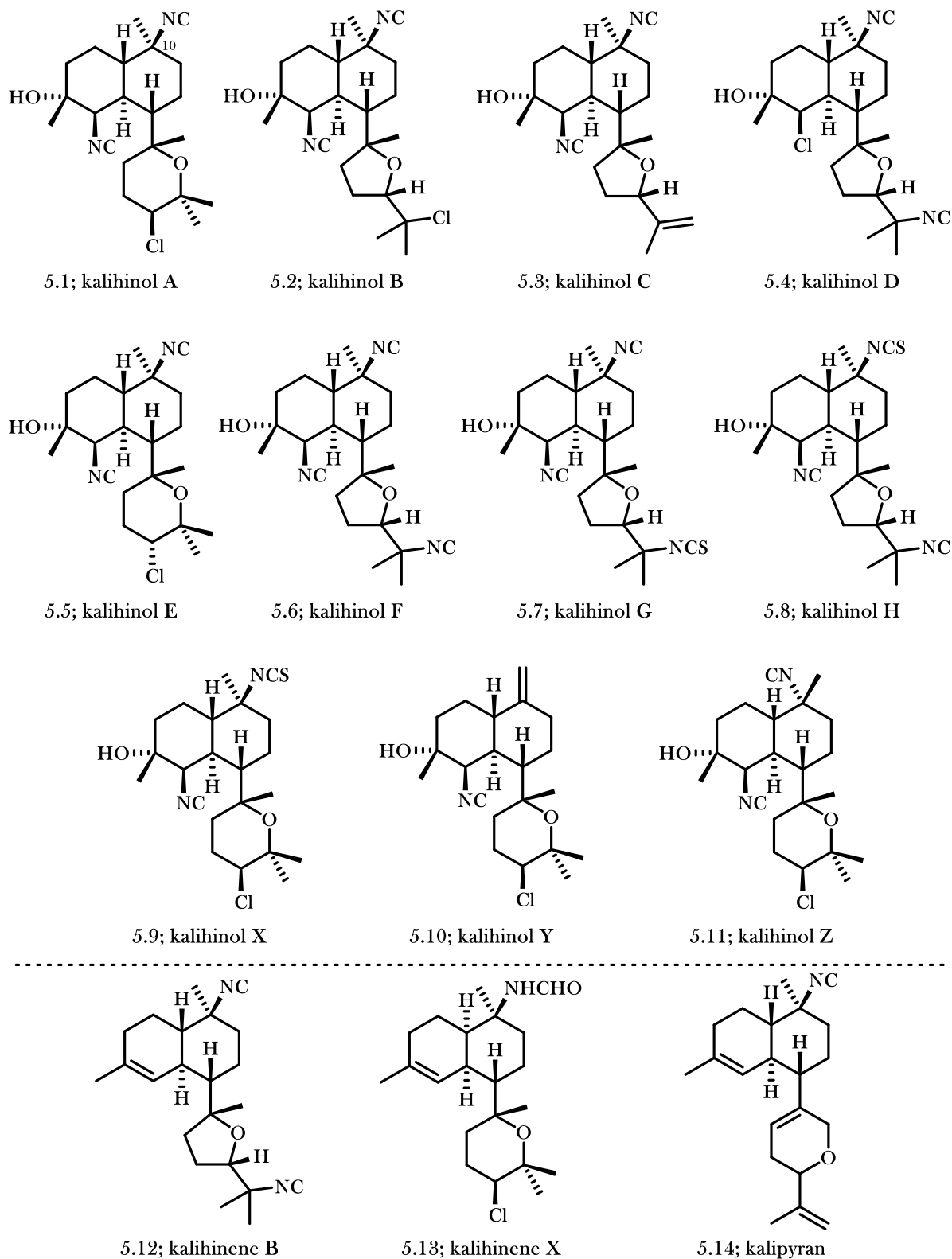
5.1 Introduction

As discussed in Chapter 4, the kalihinane family of natural products exhibits potent bioactivity against the malaria-causing parasite *Plasmodium falciparum*, thus stimulating interest in their potential use as medicinal agents. Although the kalihinanes can be isolated from nature, the small quantities obtained, in combination with the detrimental effects that natural product harvesting has on both host organisms and their ecosystem, necessitates the development of synthetic strategies. Efficient total syntheses of the kalihinanes not only allow for the acquisition of large quantities of the natural products but also introduces the ability to derivatize the natural product scaffolds to gain a better understanding of the relationship between molecular structure and bioactivity. In pursuit of this goal, several excellent total syntheses of the kalihinane family of natural products have been reported.

5.2 Isolation and Characterization of the Kalihinanes

Kalihinol A (**5.1**, Figure 5.1) was the first isolated member of the kalihinane family of natural products.¹ The sample was first obtained in 1981 from Scheuer and co-workers in Apra Harbor, Guam, and in 1984 their results were published. The *Acanthella* sponge (30 g) was freeze-dried and successively extracted with hexane, carbon tetrachloride, chloroform, and methanol. The carbon tetrachloride extract, containing 11.5 mg of kalihinol A (**5.1**), was found to have strong in vitro bioactivity against the fungus *Candida albicans*, which is known to cause infection in humans. After further investigation, this extract was also later found to also contain kalihinol B (**5.2**), kalihinol C (**5.3**), kalihinol E (**5.5**), and kalihinol F (**5.6**).²

Figure 5.1 Kalihinanes and Related Diterpenes



The relative structure of kalihinol A (**5.1**) was confirmed in the original report by X-ray crystallography, and the absolute stereochemistry was established in 1999 by Yamada and co-workers by circular dichroism spectroscopy.³ This secondary metabolite can be identified both by the *trans*-decalin core common to many marine isocyanoterpenes and the unique appended heterocyclic tetrahydropyran ring. Kalihinol A contains a tertiary alcohol on the aliphatic core, accompanied by both tertiary- and secondary-isonitriles. An equatorial chloride substituent is also observed on the heterocyclic ring, presumably introduced via epoxide-opening supported by the presence of α -oxidation. The kalihinane family of natural products then diversifies itself by the heterocyclic ring size and substituents that decorate the core. Kalihinol B (**5.2**), kalihinol C (**5.3**), and kalihinol F (**5.6**) distinguish themselves from the parent compound by their differentially-substituted THF ring. Kalihinol E (**5.5**) closely mimics kalihinol A but instead contains a stereoinverted axial chloride substituent on the heterocyclic ring.

Several additional kalihinanes were reported by Scheuer and co-workers in 1987.⁴ Kalihinol G (**5.7**) and kalihinol H (**5.8**) are analogous isothiocyanate derivatives of kalihinol B, and kalihinol X (**5.9**) is an isothiocyanate derivative of kalihinol A. Kalihinol D (**5.4**) contains a chloride in place of the decalin secondary-isonitrile of kalihinol A, whereas kalihinol Y (**5.10**) and kalihinol Z (**5.11**) are the elimination product and stereoisomer of the tertiary-isonitrile of kalihinol A, respectively. Since this time, additional isolation work had produced over fifty kalihinanes and related natural products, which again differ by connectivity and substituents. From this work, the kalihinenes (such as **5.12** and **5.13**), which possess a trisubstituted olefin in place of the isonitrile/alcohol pair on the decalin core, and the kalipyranes (such as **5.14**) which are identified by dihydropyran heterocyclic rings, were added to the diverse list of isocyanoterpene natural products.

5.3 Syntheses of the Kalihinanes and Related Natural Products

In addition to the promising bioactivity of the kalihinanes, their challenging structures have provoked a flood of effort toward their efficient total syntheses in a laboratory setting. Although initial efforts all focused around a similar Diels–Alder strategy, more recent endeavors have focused on broadening the methods by which the core of the kalihinanes can be accessed.

5.3.1 Yamada's Synthesis of Kalihinene X⁵

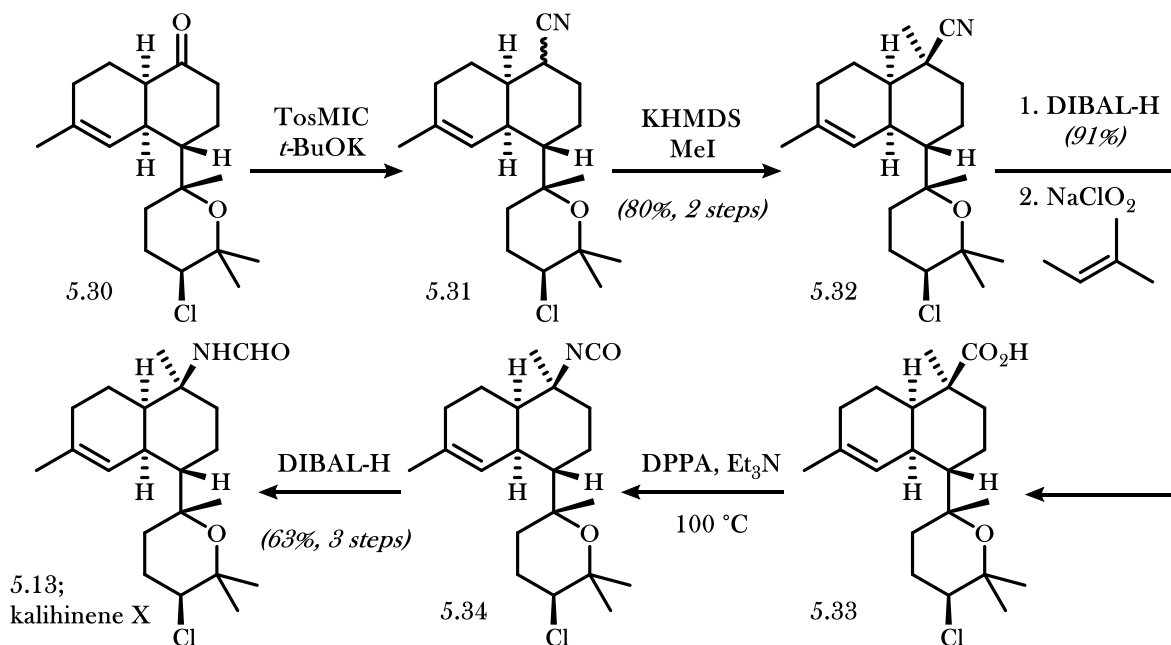
The first synthesis of a kalihinane-type natural product was accomplished in 2002 by Yamada and co-workers. Kalihinene X (**5.13**) belongs to the kalihinene class of natural products, differentiated from the more common kalihinanes by their trisubstituted olefin in place of the tertiary alcohol/isonitrile motif that defines the kalihinanes. Yamada's strategy, centered around a Diels–Alder cycloaddition to set the decalin core, was likely heavily influenced by Taber's synthesis of racemic torreyol⁶ which proceeds via a similar cycloaddition strategy.

The synthesis begins with stereodefined diol **5.15**, prepared in 97% ee in 4 steps from geranyl acetate,⁷ which is differentially protected at the more sterically hindered secondary alcohol via a three-step protection/protection/deprotection sequence (Scheme 5.1). The stereodefined epoxide **5.17** is then formed via a Sharpless asymmetric epoxidation of **5.16** and is subsequently opened by the stabilized anion formed by deprotonation of sulfone **5.18**. Following removal of the sulfur moiety by reduction with sodium amalgam and global acetate protection, the stereodefined chloride was installed via an Appel reaction to provide **5.22**. Acetate removal and protection of the less sterically-hindered alcohol as the pivalate provides access to intermediate **5.23**, which is then properly functionalized to accomplish ring closure of the tetrahydropyran (THP) ring via a two-step oxymercuration/reduction sequence to give **5.24**. With the heterocyclic ring completed, Yamada and co-workers began efforts toward formation of the decalin core.

The two non-cyclic oxygens of **5.24** were strategically protected early in the synthesis to allow for differentiation in their removal and functionalization at this point in the synthesis. The benzyl ether was first removed by reduction to provide the corresponding free alcohol, which was oxidized to the aldehyde **5.25**, converted to the allylic alcohol by treatment with a vinyl Grignard reagent, and again protected as the silyl ether **5.26**. The pivalate protecting group was then removed, oxidized to the aldehyde **5.27**, and converted in an *E*-selective manner to diene **5.28** via treatment with 2-methyl-2-propenyldiphenylphosphine oxide and deprotection. The allyl alcohol **5.28** was then deprotected and oxidized to the enone **5.29**, initiating a spontaneous intramolecular Diels-Alder cycloaddition to close the decalin core.

The carbonyl of the resulting decalone **5.30** was then converted to the nitrile **5.31** by treatment with TosMIC, and subsequent deprotonation followed by stereoselective methylation provided the tertiary nitrile (**5.32**; Scheme 5.2). A four-step sequence involving two stepwise redox manipulations to convert **5.32** to the corresponding carboxylic acid **5.33**, Curtius rearrangement to **5.34**, and isocyanate reduction formally interchanged the atoms of nitrile **5.32** to provide the formamide-containing product kalihinene X (**5.13**).

Scheme 5.2 Yamada's Completion of Kalihinene X



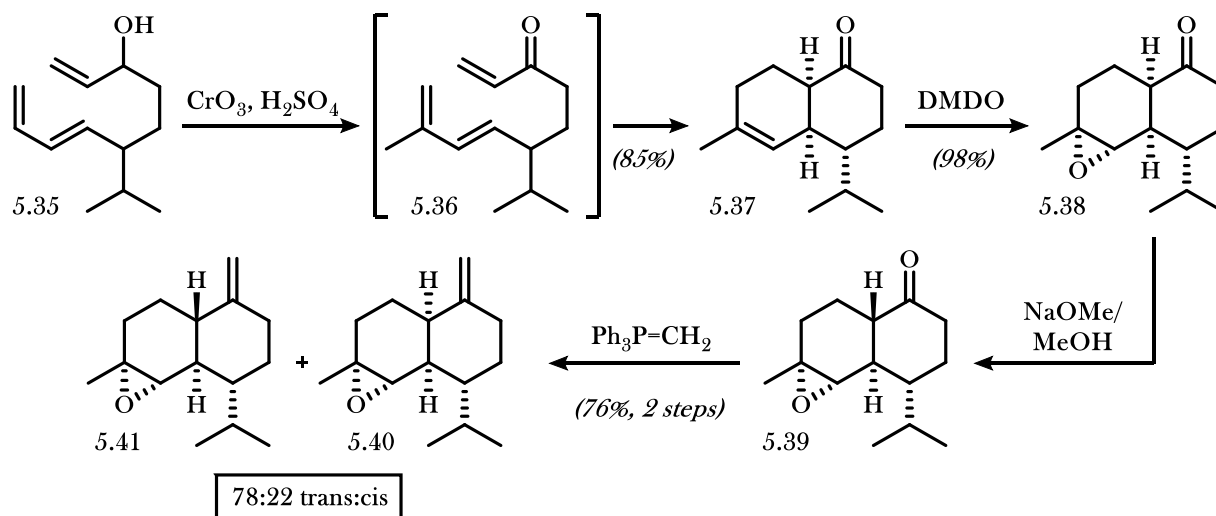
Yamada's synthesis of kalihinene X in 32 steps was an important initial feat in the field of kalihinane natural product synthesis, but also revealed the need for several key improvements. The Diels–Alder strategy, although highly effective in the synthesis of *cis*-decalin containing kalihinanes, does not provide immediate access to the *trans*-decalin motif and therefore cannot be directly applied to kalihinanes containing a *trans*-decalin. Furthermore, a six-step sequence is required to accomplish a functional group conversion from the Diels–Alder product ketone **5.30** to the stereodefined tertiary formamide **5.13**. In addition to inspiring further synthetic efforts, the completed synthesis of Yamada and co-workers also identified key transformations that must be developed to improve the way we access the kalihinanes.

5.3.2 Wood's Synthesis of (\pm)-Kalihinol C⁸

The first synthesis of a kalihinane containing the bis-isonitrile functionalities was completed by Wood and co-workers in 2004 in their synthesis of kalihinol C (**5.3**). The decalin core was formed by a similar cycloaddition to that of Yamada, but the problem of *trans*-decalin formation was solved by epimerizing the ketone α -stereocenter following cycloaddition. Furthermore, this synthesis introduced a method by which the α -isocyano tertiary alcohol motif can be installed.

A 2001 study published by Wood and co-workers⁹ introduced the strategy toward the decalin core that would later be used in their 2004 total synthesis of kalihinol C (Scheme 5.3). Formation of the decalin core was accomplished via a highly analogous method to Yamada's work and was therefore likely inspired by Taber's torreyol synthesis as well.⁶ The olefin resulting from cycloaddition of **5.36**, formed *in-situ* from **5.35** via oxidation, was subsequently epoxidized highly-selectively to provide **5.38**. Epimerization of the ketone α -stereocenter of **5.38** and Wittig methylenation prior to purification to form diastereomers **5.40** and **5.41** provided the *trans*- to *cis*-decalin products in ratio of 78:22, thereby providing an efficient method by which the *trans*-decalin motif can be procured.

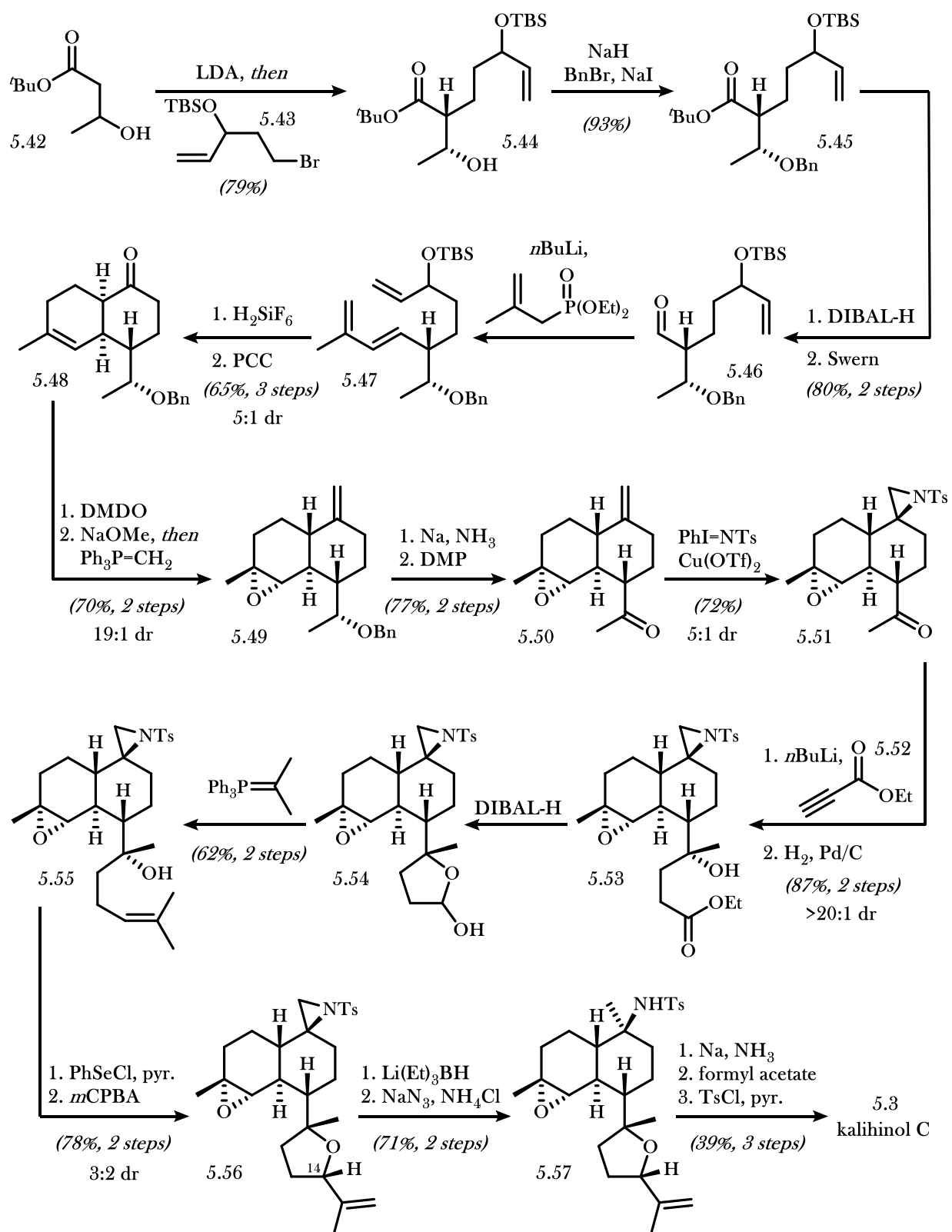
Scheme 5.3 Wood's Model Study Toward the Kalihinanes



In their synthesis of (\pm)-kalinol C, the Wood group begins with β -hydroxyester **5.42** as a racemic precursor (Scheme 5.4). A diastereoselective α -alkylation and subsequent benzylation of the secondary alcohol provides ester **5.45**, which is then converted to aldehyde **5.46** via a two-step reduction/oxidation sequence. Olefination of aldehyde **5.46** then provides diene **5.47** which closely resembled the decalin precursors of Yamada and Taber. Deprotection of the allyl silyl ether and oxidation again promotes a spontaneous Diels-Alder cycloaddition to form the *cis*-decalin core. Epoxidation with DMDO accomplishes a functionalization of the trisubstituted olefin of **5.48** with high selectivity for the convex face of the *cis*-decalin. Following epoxide installation, the epimerization/olefination sequence reported in their earlier study formed alkene **5.49** in a highly efficient 95:5 diastereomeric ratio.

Removal of the benzyl ether and oxidation of the secondary alcohol to **5.50** provided a ketone functional handle by which the heterocyclic ring can be appended. However, attempts to append the ring at this point in the sequence were unsuccessful due to reaction decomposition. To overcome this challenge, Wood and co-workers converted the alkene of **5.50** to the corresponding tosyl aziridine (**5.51**). The aziridine acts as a “protected amine”, allowing for installation of the key C-N bond without the detrimental effects of free amines. With the aziridine in place, the Wood group was then free to install the THF ring.

Scheme 5.4 Wood's Total Synthesis of Kalihinol C



The alkynyllithium species derived from **5.52** was found to add to ketone **5.51** with high selectivity to form the tertiary alcohol. Full hydrogenation of the alkyne formed ester **5.53**, which was then converted to lactol **5.54** by partial reduction and ring closure. The lactol was then olefinated to produce the trisubstituted alkene **5.55**, which subsequently participated in a selenoetherification to close the THF ring. Oxidation to the selenoxide followed by elimination provided the propylidene-substituted heterocycle **5.56** with low overall stereoselectivity at the C-14 position.

Following completion of the heterocyclic fragment, the remainder of the synthesis proceeded similarly to the Wood group's initial study. Opening of the epoxide with lithium triethylborohydride provided the ring-opened tosylamine, and epoxide azidation formed the α -azido tertiary alcohol **5.57**. A one-pot azide reduction and tosyl deprotection followed by a two-step bis-isonitrile installation from the free amines provided (\pm)-kalihinol C (**5.3**).

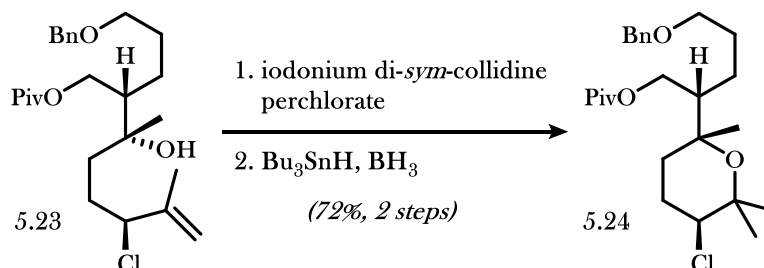
Wood's 26-step synthesis of racemic kalihinol C introduced crucial strategies by which key polar functionality can be introduced. The epoxidation and epoxide-opening strategy for formation of the α -isocyano tertiary alcohol motif is highly efficient and selective, and the epimerization of the *cis*-decalin to the *trans*-decalin framework provides a way in which the kalihinanes can be procured by a single Diels-Alder approach. However, the lengthy and non-stereoselective process by which the heterocyclic ring is installed indicates that further progress is necessary.

5.3.3 Miyaoka's Synthesis of Kalihinol A¹⁰

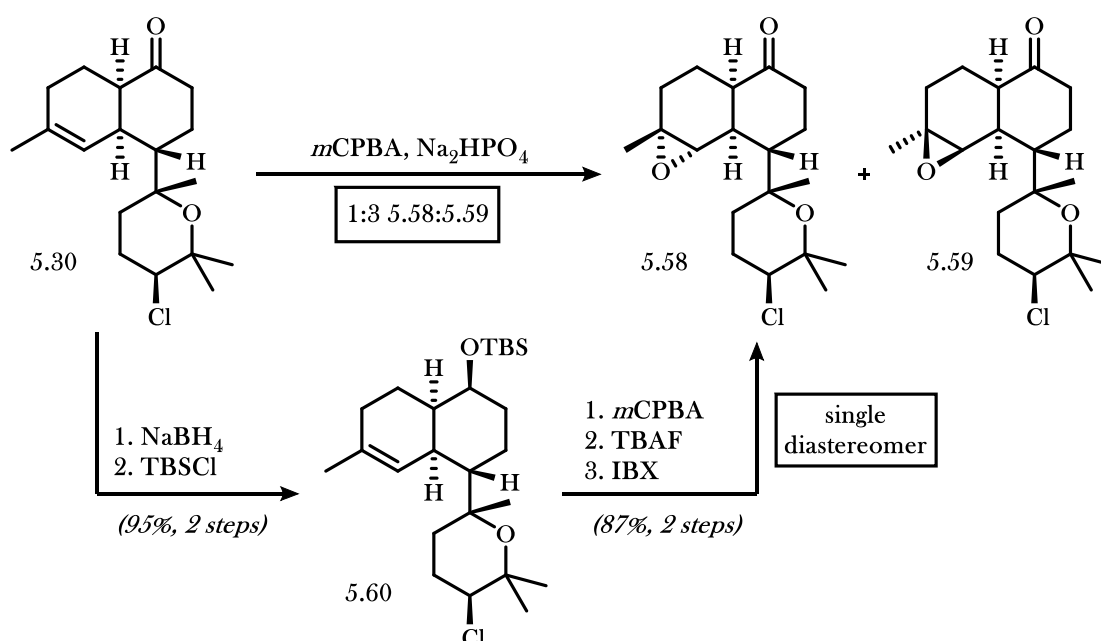
In 2011, Miyaoka and co-workers used the chemistry developed by Yamada and Wood to prepare Kalihinol A (**5.1**). Intermediate **5.23** was prepared according to Yamada's procedure, with minor changes to reagents, and an iodoetherification/reduction sequence was used to close the ring in 72% over two steps as opposed to Yamada's oxymercuration/reduction which proceeded in 41% over two steps (Scheme 5.5).

Scheme 5.5 Miyaoka's Contributions to the Synthesis of Kalihinanes

a. Iodoetherification/Reduction



b. Diastereoselective Epoxidation



c. Preparation of Kalihinol A



Following heterocycle formation, Miyaoka and co-workers then prepared the decalin core (**5.30**) according to the procedures developed by Wood and co-workers in their synthesis of kalihinol C. Unfortunately, epoxidation of trisubstituted olefin **5.30** proceeded with low diastereoselectivity, presumably

due to the increased steric bulk introduced by the THP ring in proximity to the desired reactive face of the olefin. To overcome this challenge, reduction and protection to form secondary silyl ether **5.60** blocked the undesired face of the trisubstituted olefin and promoted diastereoselective epoxidation. A deprotection/oxidation sequence then regenerated the ketone with the epoxide intact.

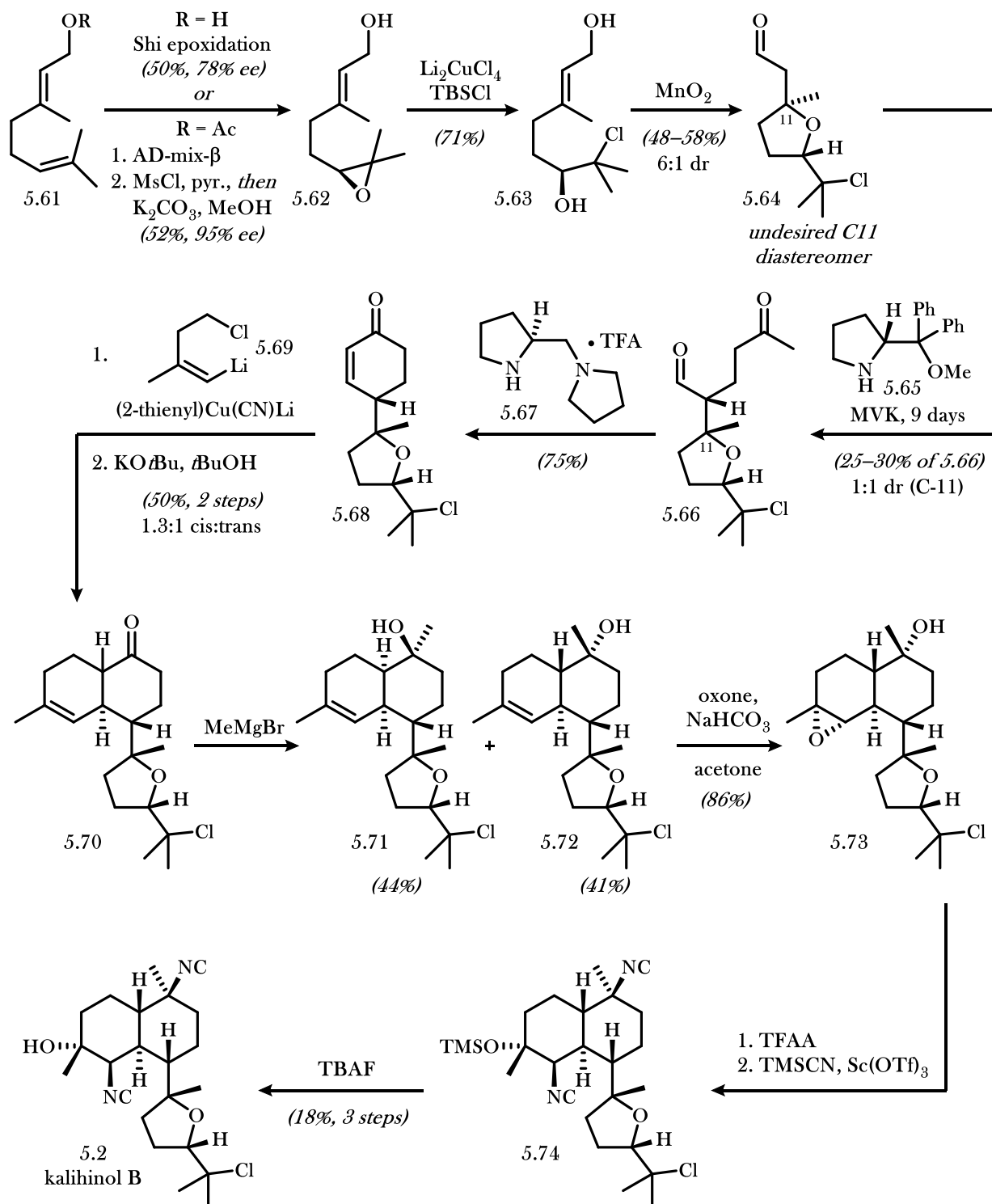
With the epoxide installed, Miyaoka then continued to use Wood's protocol to complete the natural product (**5.1**). Azidation of the epoxide installed the amino alcohol motif, and epimerization provided the *trans*-decalin core with high selectivity. The azidation/aziridination strategy used by Wood to complete kalihinol C was then used by Miyaoka with minor modifications to complete kalihinol A. Intermediates from the synthesis were also elaborated to make kalihinol Y and 10-*epi*-kalihinol I.¹¹

Although Miyaoka's 39-step synthesis of kalihinol A provided only marginal improvements to our understanding of efficient synthetic strategies toward the kalihinanes, their report represents completion of a synthetic target that had not yet been achieved despite its medicinal relevance. Miyaoka's main contribution to the field in this study highlights the 5-step sequence that can be used to facilitate diastereoselective epoxidation on *cis*-decalone frameworks that already contain the bulky heterocyclic ring. Aside from this contribution, Miyaoka's work is a combination of lessons learned from previous syntheses.

5.3.4 Vanderwal's Synthesis of Kalihinol B¹²

In 2015, the Vanderwal group published a total synthesis of kalihinol B (**5.2**) that expanded the toolbox for kalihinane synthesis. Rather than focusing on the Diels–Alder approach used by previous synthetic groups, this synthesis uses an organocatalyzed ring-closing cascade to set several key stereocenters followed by ring appendage via a tandem vicinal difunctionalization approach.

Scheme 5.6 Vanderwal's Synthesis of Kalihinol B



Starting from geranyl acetate (**5.61**), the key stereocenter of the tetrahydrofuran ring is installed using either an asymmetric Shi epoxidation or a two-step Sharpless dihydroxylation and epoxide formation (Scheme 5.6). The stereodefined epoxide **5.62** can then be opened regioselectively to the chlorohydrin **5.63**. Oxidation to form the α,β -unsaturated aldehyde spontaneously results in THF ring closure to form aldehyde **5.64** with the undesired stereoconfiguration at C-11. To overcome the innate selectivity of THF formation, condensation of proline-derived organocatalyst **5.65** equilibrates the C-11 stereocenter, indicating reversibility in THF formation, while also accomplishing an asymmetric addition to MVK to set the C-7 stereocenter of **5.66** with high selectivity. The Robinson annulation was then completed using organocatalyst **5.67**.

To append the final ring, a Piers-type annulation¹³ was performed involving a copper-catalyzed conjugate addition of organolithium **5.69** to enone **5.68**. The formed ketone then underwent an intramolecular alkyl halide displacement to provide a mixture of diastereomers of **5.70** about the decalin ring fusion. Although higher selectivity could be attained by epoxidizing the trisubstituted olefin of **5.70** prior to epimerization of the α -stereocenter, as observed by the Wood group, the subsequent methyl Grignard addition to the ketone would likely decompose the newly formed epoxide. Instead, formation of tertiary alcohols **5.71** and **5.72** prior to epoxidation provided a separable mixture of diastereomers.

Between the time of Wood and Vanderwal's syntheses, the Shenvi group developed a highly selective and functional group tolerant isonitrile installation from the corresponding stereoinverted trifluoroacetate (discussed in detail in Chapter 4). Following epoxidation and trifluoroacetate activation, the Vanderwal group used Shenvi's conditions to accomplish a one-pot *bis*-isonitrile installation via epoxide-opening and tertiary trifluoroacetate displacement to directly form **5.74**. Following desilylation of the tertiary alcohol, kalihinol B (**5.2**) was obtained.

Vanderwal's synthesis of kalihinol B, accomplished in 12 or 13 steps depending on one's preferred method for the formation of stereodefined epoxide **5.62**, was a major advancement in the field of kalihinane natural product synthesis. The strategy introduced a new way of envisioning the core that strayed from Diels-Alder cycloaddition disconnections that had previously dominated the field. Furthermore, Vanderwal's *bis*-

isonitrile installation significantly improved how we can access the kalihinane motif; previous syntheses involved separate isonitrile installations in a less efficient manner. Although the synthesis contained steps that proceeded with less-than-ideal stereoselectivity, Vanderwal's reported synthesis represents a significant strategic advancement in the field.

5.3.5 Shenvi's Synthesis of Kalihinol C¹⁴

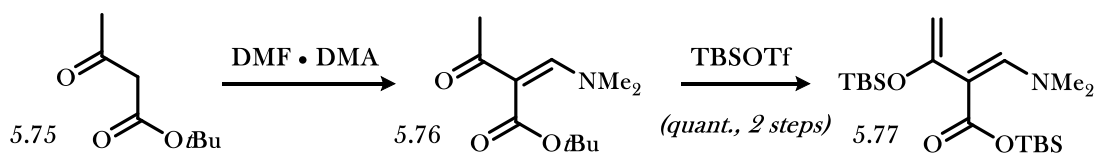
The Shenvi group recently reported a synthesis of kalihinol C that introduces a new way by which the complex core of the kalihinanes can be procured. Their strategy involves formation of the decalin core via two subsequent Diels–Alder cycloadditions from a dendralene-type precursor, a strategy initially used to target amphilectane and DICA natural products.

Enoxysilane **5.77**, which the authors refer to as a “heterodendralene”, is first made in two steps in quantitative yield from *tert*-butyl acetoacetate (**5.75**) via condensation with DMFDMA and subsequent enoxysilane formation (Scheme 5.7). The *bis*-dienophile **5.79** was formed via deprotonation of diethyl ethylphosphonate, condensation with ethyl geranylacetate (**5.78**) followed by *in situ* α -selenation, and subsequent selenoxide formation/elimination. A room temperature Diels–Alder cycloaddition was accomplished between the highly activated reaction partners providing the cyclic product **5.80**. The addition of hydrofluoric acid accomplished a double silyl deprotection and subsequent elimination of the β -ammonium substituent from the resulting ketone to provide **5.81**. A second Diels–Alder involving the newly generated α,β -unsaturated carboxylic acid formed the decalin framework in an efficient 70% yield over three steps.

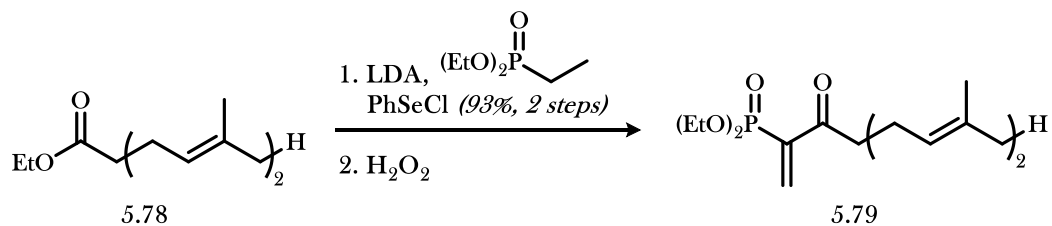
Dephosphonylation of **5.82** via modified Krapcho conditions then provided ketone **5.83**, which was converted to the tertiary alcohol by treatment with methylmagnesium chloride. Protonation of the enolate resulting from decarboxylation proceeds with high selectivity for *trans*-decalin formation, influenced largely by the inability of the strained tricyclic system to adopt a *cis*-decalin geometry. Lactone hydrolysis and subsequent decarboxylation provided the decalone **5.84** with the tertiary alcohol stereocenter, which was eventually used to form the heterocyclic THF ring, in place.

Scheme 5.7 Shenvi's Early Work Toward Kalihinol C

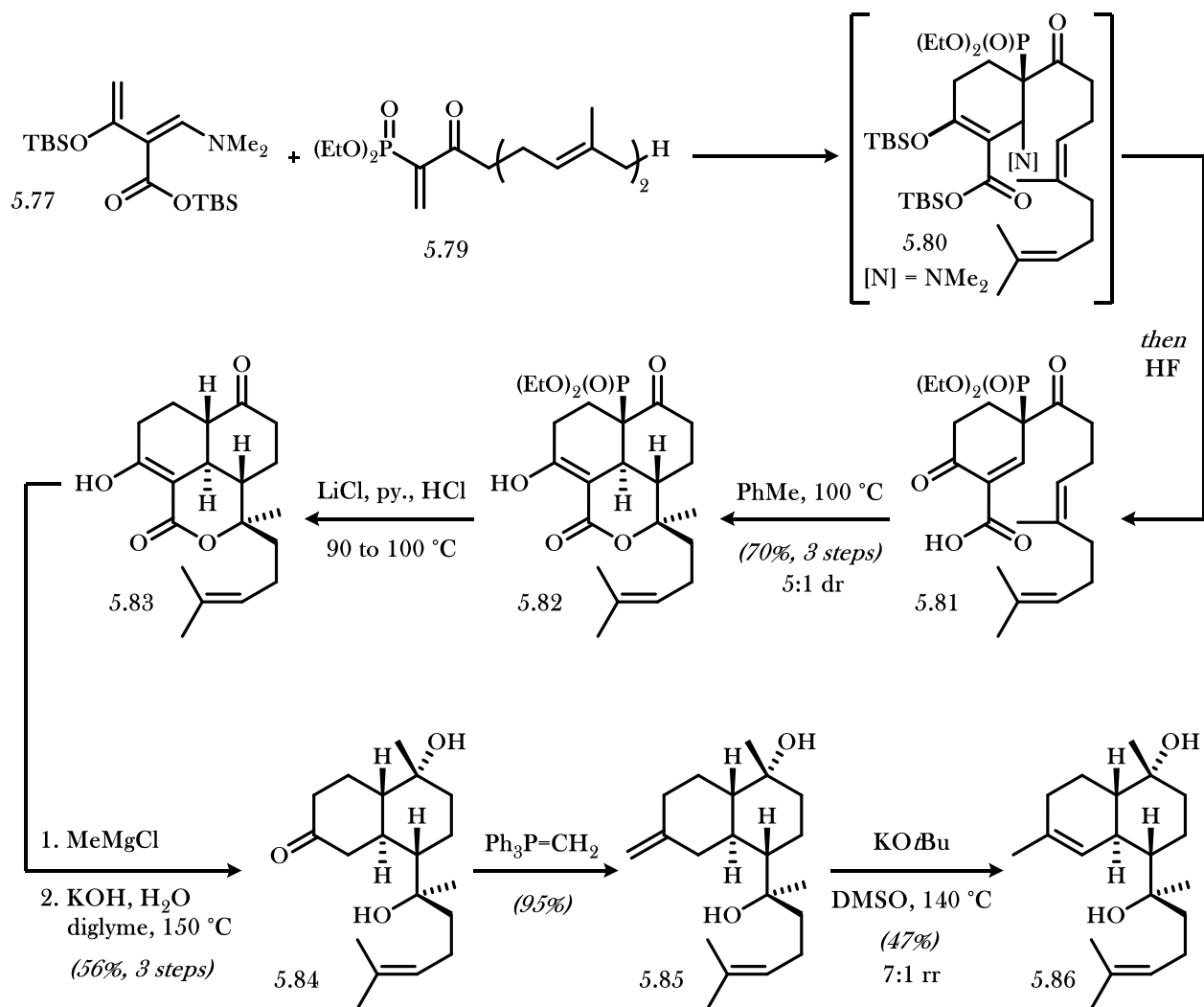
a. Synthesis of the Diene



b. Synthesis of the Dienophile



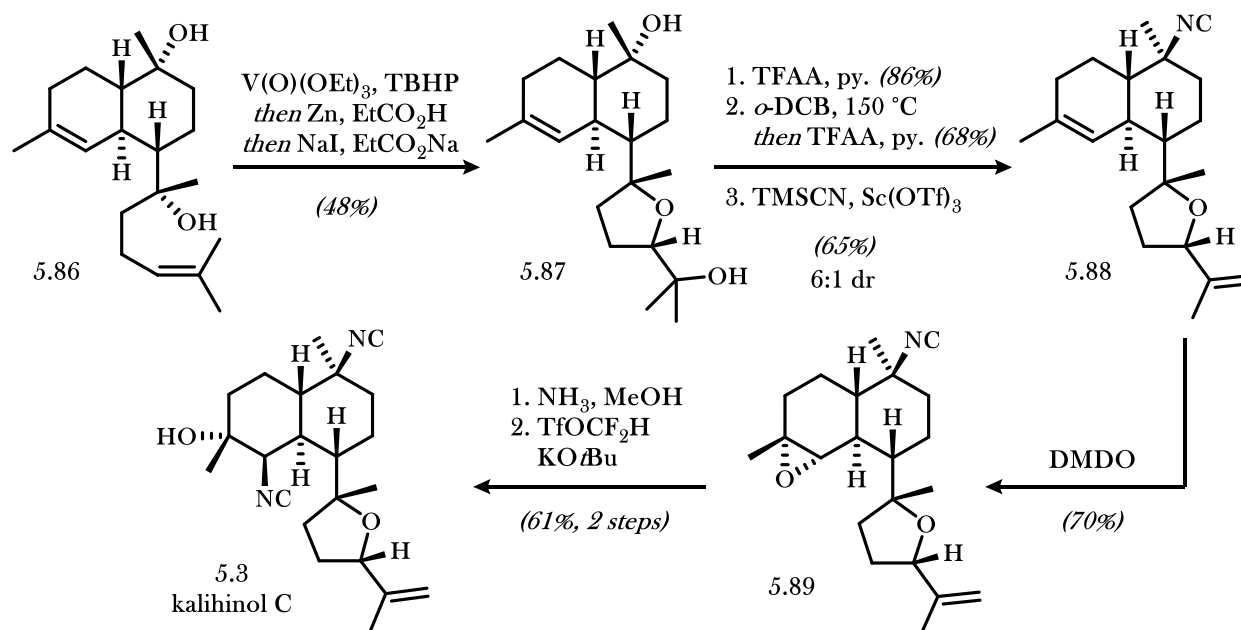
c. Diels-Alder Cascade



At this point, the ketone of decalone **5.84** was converted to the trisubstituted olefin of **5.86** in a two-step sequence. Olefination provided vinylidene **5.85**, but standard conditions for olefin isomerization selectively provided the undesired trisubstituted olefin. The Shenvi group remarkably found that use of the tertiary alkoxide as an intramolecular base accomplished olefin isomerization to selectively form **5.86** at elevated temperatures.

A one-pot, three-part sequence was then found necessary to construct the THF ring from the acyclic precursor (Scheme 5.8). A vanadium-directed epoxidation proceeded faster from the cyclic olefin as opposed to from the desired acyclic alkene of **5.86**. To overcome this obstacle, a procedure involving double epoxidation and a subsequent two-step “retro-epoxidation” via iodide epoxide-opening and an α -hydroxy organozinc elimination was found to be successful, and spontaneous THF formation followed. The tertiary alcohol resulting from ring-closure was eliminated to form the target exocyclic alkene. With the regenerated cyclic alkene in place, Reiher and Shenvi then performed their two-step stereoselective isonitrile installation to form the tertiary isonitrile **5.88**. The remaining isonitrile was installed via a three-step epoxidation, aminolysis, and isonitrile condensation to provide kalihinol C (**5.3**). The authors note that they were unable to accomplish the one-pot *bis*-isonitrile installation reported by Vanderwal.

Scheme 5.8 Shenvi's Completion of Kalihinol C



The Shenvi synthesis of kalihinol C is a masterful display of the bond- and stereocenter-forming power of dendralene Diels-Alder cascades. This 17-step synthesis accomplishes previously-elusive high *trans*-decalin selectivity by taking advantage of the strain introduced in the reactive conformations to form fused tricyclic systems. Furthermore, a highly selective formation of the tetrahydrofuran ring is accomplished. The authors also remark that the overall yield of kalihinol C is an order of magnitude higher than previous syntheses of the kalihinanes. The reported synthesis by Reiher and Shenvi further expands the methods available to synthetic chemists in pursuit of an ideal synthesis of the kalihinanes.

5.4 Conclusions

In just 16 years, significant improvements have been made in the field of isocyanoterpene natural product synthesis. Since the first synthesis of a kalihinane-type natural product by Yamada in 2002, several strategies have been developed that reduce the required synthetic steps and increase the efficiency of these syntheses. Original difficulties in selectively forming the *trans*-decalin and in installing the *bis*-isonitrile have been solved, and we can now access the kalihinanes and related scaffolds in just 12 steps. As we continue to improve upon our developed strategies, we approach a time when analogues can be rapidly procured and

analyzed for bioactivity. To accomplish this feat, the flexibility of reported synthetic strategies toward derivatization must also be studied.

As discussed in Chapter 4, kalihinanes possessing the six-membered THP heterocyclic ring are the most potent against *Plasmodium falciparum*. The methods described by Yamada and Miyaoka in their syntheses of kalihinene X and kalihinol A do provide access to the THP-containing scaffolds, but the high step count required to access them renders the syntheses implausible for analogue development. For this reason, a reliable and derivatizable method for the formation of THP-containing kalihinanes must be developed. Our efforts to accomplish this goal are detailed in Chapter 6.

5.5 Notes and References

- (1) Chang, C. W. J.; Patra, A.; Roll, D. M.; Scheuer, P. J.; Matsumoto, G. K.; Clardy, J. *J. Am. Chem. Soc.* **1984**, *106*, 4644-4646.
- (2) Patra, A.; Chang, C. W. J.; Scheuer, P. J.; Van Duyne, G. D.; Matsumoto, G. K.; Clardy, J. *J. Am. Chem. Soc.* **1984**, *106*, 7981-7983.
- (3) Shimomura, M.; Miyaoka, H.; Yamada, Y. *Tetrahedron Lett.* **1999**, *40*, 8015-8017.
- (4) Chang, C. W. J.; Patra, A.; Baker, J. A.; Scheuer, P. J. *J. Am. Chem. Soc.* **1987**, *109*, 6119-6123.
- (5) Miyaoka, H.; Shida, H.; Yamada, N.; Mitome, H.; Yamada, Y. *Tetrahedron Lett.* **2002**, *43*, 2227-2230.
- (6) Taber, D. F.; Gunn, B. P. *J. Am. Chem. Soc.* **1979**, *101*, 3992-3993.
- (7) Kodama, M.; Yoshio, S.; Tabata, T.; Deguchi, Y.; Sekiya, Y.; Fukuyama, Y. *Tetrahedron Lett.* **1997**, *38*, 4627-4630.
- (8) White, R. D.; Keaney, G. F.; Slown, C. D.; Wood, J. L. *Org. Lett.* **2004**, *6*, 1123-1126.
- (9) White, R. D.; Wood, J. L. *Org. Lett.* **2001**, *3*, 1825-1827.

- (10) Miyaoka, H.; Abe, Y.; Sekiya, N.; Mitome, H.; Kawashima, E. *Chem. Commun.* **2011**, 48, 901–903.
- (11) Miyaoka, H.; Abe, Y.; Kawashima, E. *Chem. Pharm. Bull.* **2012**, 60, 1224–1226.
- (12) Daub, M. E.; Prudhomme, J.; Le Roch, K.; Vanderwal, C. D. *J. Am. Chem. Soc.* **2015**, 137, 4912–4915.
- (13) Piers, E. *Pure Appl. Chem.* **1988**, 60, 107–114.
- (14) Reiher, C. A.; Shenvi, R. A. *J. Am. Chem. Soc.* **2017**, 139, 3647–3650.

6.1 Background and Inspiration

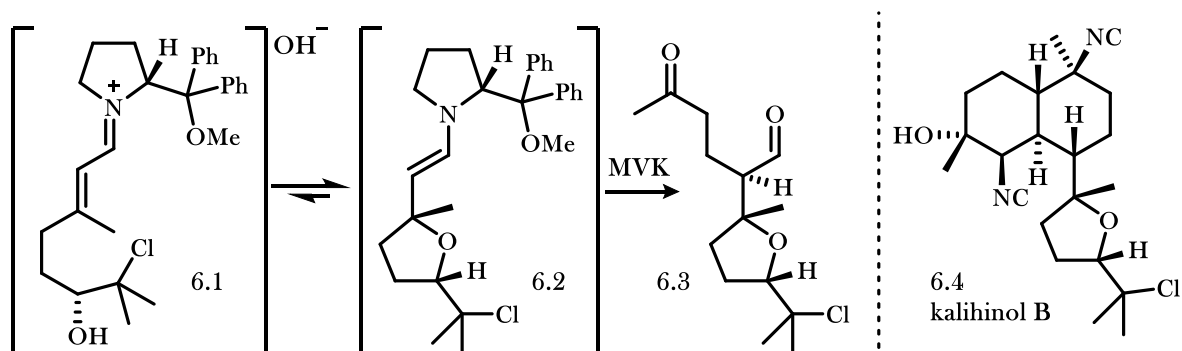
Despite the highly potent antiparasitic activity of kalihinol A (**6.8**; Figure 6.1a), an efficient method for its preparation is yet to be developed. The synthetic barrier likely lies in the congested tetrahydropyran ring functionality, since there have been several reported concise syntheses for tetrahydrofuran-containing kalihinanines. We therefore set out to develop an efficient method for formation of the key heterocyclic ring in a manner that would then provide convenient access to the kalihinane scaffold.

In the Vanderwal group's 2015 synthesis of kalihinol B (**6.4**; Figure 6.1b),¹ the heterocyclic tetrahydrofuran ring is formed via a ring-closing cyclization from a geraniol-derived α,β -unsaturated aldehyde. In this transformation, a chiral pyrrolidine-based organocatalyst forms the α,β -unsaturated iminium **6.1** *in situ*, which promotes an asymmetric oxy-Mannich cyclization to set the key stereocenter of **6.2**. The formed enamine intermediate is then removed from equilibrium via intermolecular conjugate addition to methyl vinyl ketone (MVK) to form **6.3**. As highlighted in Chapter 5, this conjugate addition cascade sets several key stereocenters with high stereoselectivity on route to the completed natural product.

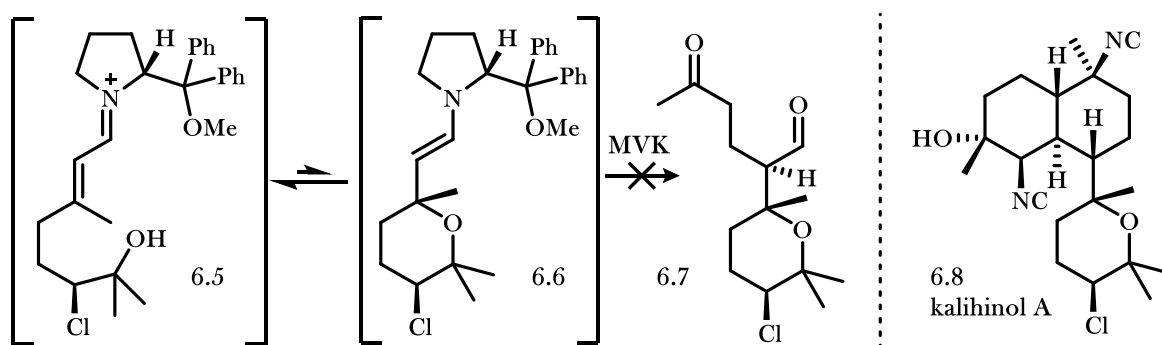
The decalin core of kalihinol A mimics that of kalihinol B, but the appended heterocyclic fragment is instead a six-membered tetrahydropyran (THP) ring. In an attempt to extend the successful conjugate addition cascade methodology to the synthesis of THP-containing kalihinanines, the Vanderwal group prepared **6.5** from the regioisomeric chlorohydrin containing a tertiary alcohol nucleophile. However, it was discovered that the initial oxy-Michael addition to form enamine **6.6** proceeded at a slower rate than a deprotonation of the eniminium **6.5** and subsequent nucleophilic addition of the resulting dienamine to MVK.

Figure 6.1 Successful Oxy-Mannich Cyclization and Attempted Application to Kalihinol A

a. Oxy-Michael Strategy Toward Kalihinol B



b. Failed Oxy-Michael Approach Toward Kalihinol A



The discrepancy in the rate of ring closure is likely due to both the intrinsically lower rate of bringing together more distant orbitals for ring closure and the sterically congested nature of the desired bond. The THP ring contains an ethereal oxygen situated between two fully-substituted carbon centers, and the diaxial interactions introduced by substituents on the product ring likely reduces the rate of its formation. To overcome byproduct formation, we began investigating alternative strategies incorporating well-precedented methodologies for the formation of sterically-congested THP rings. Since there remains no efficient synthesis of kalihinanes containing a THP ring, we believed that development of a strategy using well-precedented methods for ring closure would be a significant contribution to the field.

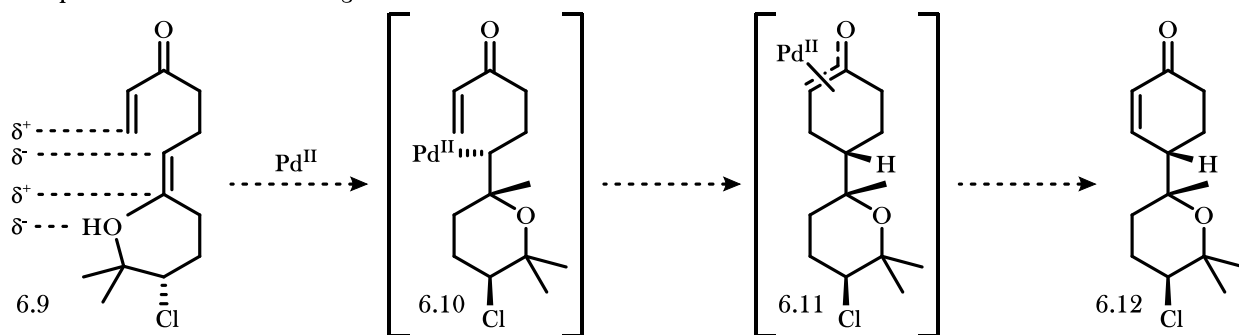
6.2 Original Cascade for the Formation of Two Rings

6.2.1 Proposed Core Formation

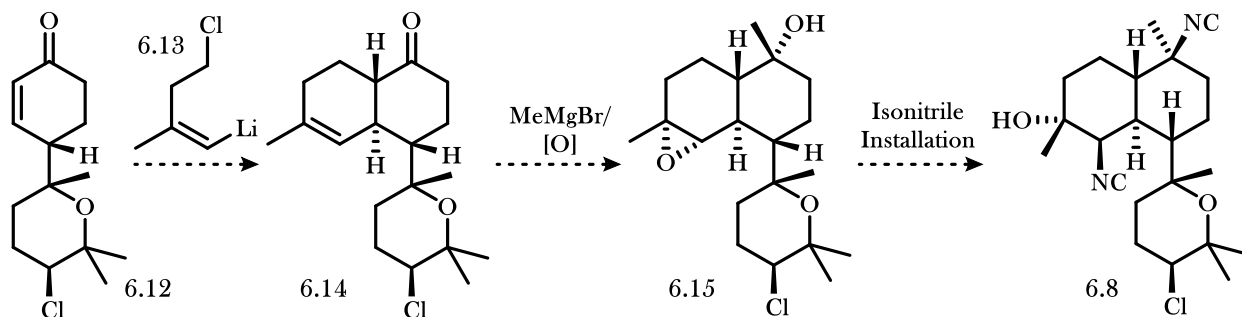
Our initial oxy-Mannich attempts described in Figure 6.1 showed that the equilibrium for THP formation lies toward the acyclic tertiary alcohol precursor. We figured that we could push the equilibrium forward by introducing functionality that will only react with a ring-closed THP equilibrium participant such as **6.10** (Figure 6.2a). Since our previous efforts proved that an *intermolecular* addition to MVK occurs at a faster rate than ring-closure, we postulated that an *intramolecular* conjugate addition only possible with the ring-closed intermediate **6.10** might facilitate the desired bond formations. With this in mind, we designed precursor **6.9**, which we believed possessed the properly matched functionality necessary to undergo a ring-closing cascade.

Figure 6.2 Matched Polarity of Cascade Precursor **6.9** and the Proposed Wacker/Heck/Saegusa Cascade

a. Proposed Mechanism for Ring Closure



b. Natural Product Completion Analogous to Our Synthesis of Kalihinol B



We postulated that the THP ring could first be closed via a Wacker-type oxy-palladation across the internal trisubstituted alkene of **6.9**. From there, we believed the resulting organopalladium species **6.10** might

then undergo a Heck-type carbopalladation across the pendant enone resulting in the formation of a second ring. The formed palladium enolate **6.11** could then undergo a Saegusa oxidation to regenerate the α,β -unsaturated cyclohexanone product (**6.12**).

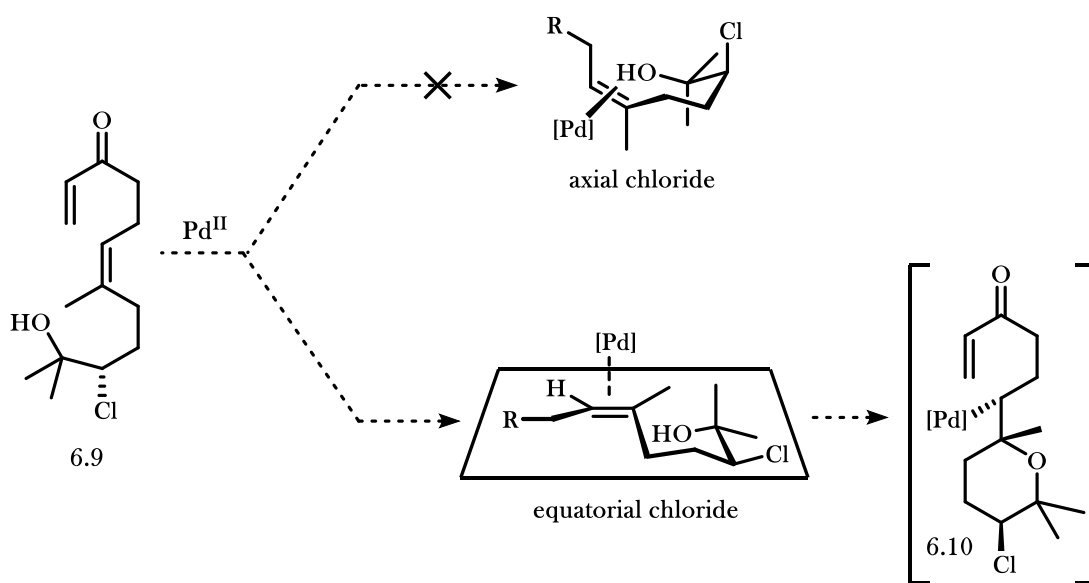
This proposed cascade is restricted to the use of palladium as the active catalyst due the required β -hydride elimination to regenerate the enone. The oxidation must be performed in the same process as C-C bond formation since the palladium enolate is formed regiospecifically; protonation of the enolate formed from the cascade would result in a symmetrical cyclohexanone species which could not be deprotonated selectively under standard conditions. Although the design of a synthetic route around a strict set of conditions for a key step is a high-risk endeavor, we were confident in the success of this transformation due to the well-developed and highly-versatile nature of palladium catalysis.

Oxypalladation to form tetrahydropyran rings has been studied by several research groups. If a strong base is present in the reaction mixture, alcohol deprotonation and subsequent O-Pd bond formation will occur. Upon heating in the presence of an alkene, a *syn*-carbopalladation can occur through a strained four-membered transition state. Although *syn*-oxypalladation have been extensively studied by the Wolfe group, they have only applied their methodology to the synthesis of five-membered tetrahydrofuran rings.² A rare of example of *syn*-oxypalladation to form tetrahydropyrans in moderate yields has been reported by Wang and co-workers.³

A more well-established method for oxypalladation of alkenes omits a strong base in the reaction mixture. Rather than initial Pd-O bond formation, the electrophilic palladium catalyst will instead coordinate to the electron-rich olefin and increase the π -system's susceptibility to nucleophilic attack. In a similar mechanism to the Wacker oxidation, in which alkenes can be converted to ketones via palladium-induced attack from water and subsequent β -hydride elimination, palladium coordination to the olefin will promote ring-closure to the tetrahydropyran. In contrast to *syn*-carbopalladations to form THP rings, there are several reported examples of THP formation in high yields via *anti*-carbopalladation.⁴ Due to the highly precedented history of *anti*-carbopalladations, we designed our cascade precursor **6.9** with a *cis*-alkene in order to form intermediate **6.10** with the proper relative stereochemistry.

The secondary chloride on the formed THP ring is crucial to the stereoselectivity of ring-closure (Figure 6.3). Prior to THP formation, the electrophilic palladium catalyst can coordinate to either face of the alkene of **6.9**. Since the oxygen nucleophile must attack from the opposing face of the palladium in an *anti* fashion, the resulting fully substituted carbon can be formed as either stereocenter. Fortunately, this reaction proceeds through a six-membered ring transition state in which substituents can have a significant impact on the reactive conformation. In this case, the secondary chloride will prefer to adopt an equatorial position in the reactive conformation to minimize diaxial interactions, which will relay stereoselectivity to the formed stereocenter of **6.10**.

Figure 6.3 Chloride-Directed Stereoselectivity in THP Formation



Following the Wacker/Heck/Saegusa cascade to form enone **6.12**, we postulated that the remainder of the synthesis of kalihinol A could proceed using the same strategy as our synthesis of kalihinol B (Figure 6.2b). The only difference separating kalihinol A and kalihinol B is the connectivity of the heterocyclic ring. Since the heterocyclic rings are both present in their completed form at this point in the synthesis, we were confident the rest of the synthetic manipulations would proceed with equal success. This proposed total synthesis of kalihinol A would represent a significant improvement over Miyaoka's previously reported

synthesis⁵ and would introduce a much-needed efficient method by which THP-containing kalihinanes can be procured.

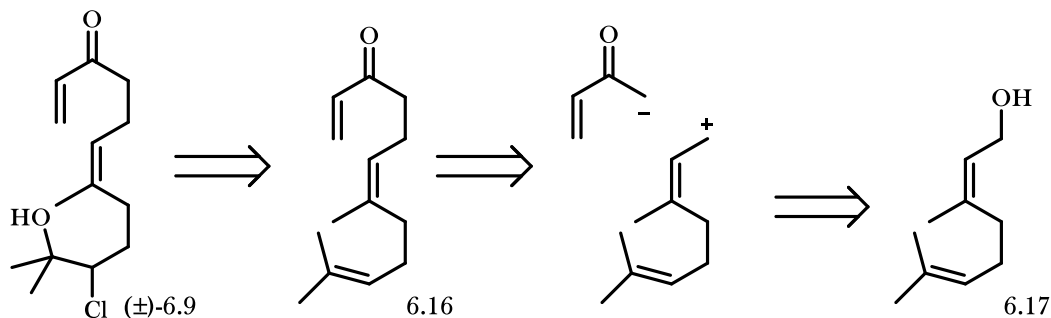
6.2.2 Synthesis of Carbon Framework via Allyl Halide Displacement

As discussed in Chapter 4, the terpenoid carbon framework of the kalihinanes is likely formed via cyclization from isoprene-derived building blocks. We also showed in our synthesis of kalihinol B that geraniol, a 10-carbon acyclic chain derived from two isoprene units, is an excellent precursor to the heterocyclic ring. We therefore designed the synthesis of acyclic cascade precursor **6.9** around transformations starting from a similar C10 fragment. Since a *cis*-olefin was necessary to achieve the desired product stereochemistry, we began our synthesis with nerol (**6.17**).

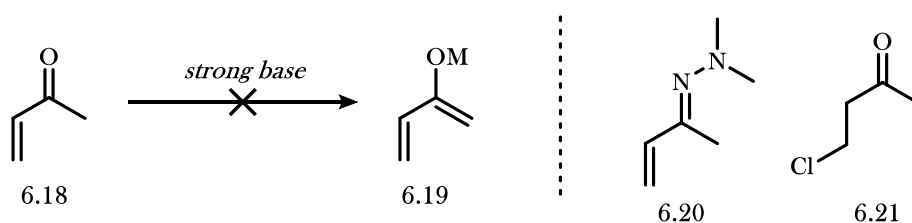
Our initial plan involved formation of the acyclic framework via allylation of a suitable nucleophile with an electrophile derived from nerol. An enolate derived from MVK (**6.18**), the ideal nucleophile in this situation, is not a feasible precursor owing to the conjugate acceptor's known tendency to polymerize under mildly acidic and basic conditions. We explored the application of MVK surrogates, specifically the MVK-derived hydrazone **6.20** and the β -chloro analogue **6.21**, but attempts to deprotonate resulted exclusively in decomposition. We therefore turned to more highly-precedented β -ketoester allylations toward acyclic cascade precursor **6.9**.

Scheme 6.1 Initial Methods Investigated for α -Carbonyl Allylation

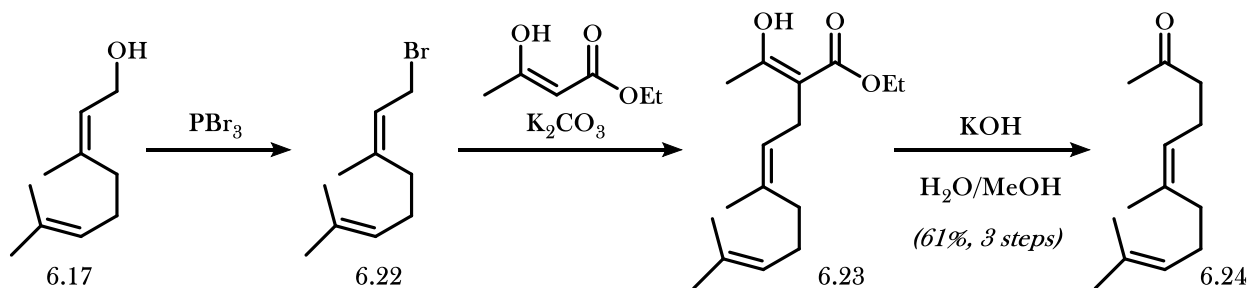
a. Proposed Route Toward Racemic Acyclic Precursor (\pm)-**6.9**



b. Unsuccessful Unstabilized Nucleophiles



c. Precedented β -Ketoester Nucleophilic Displacement

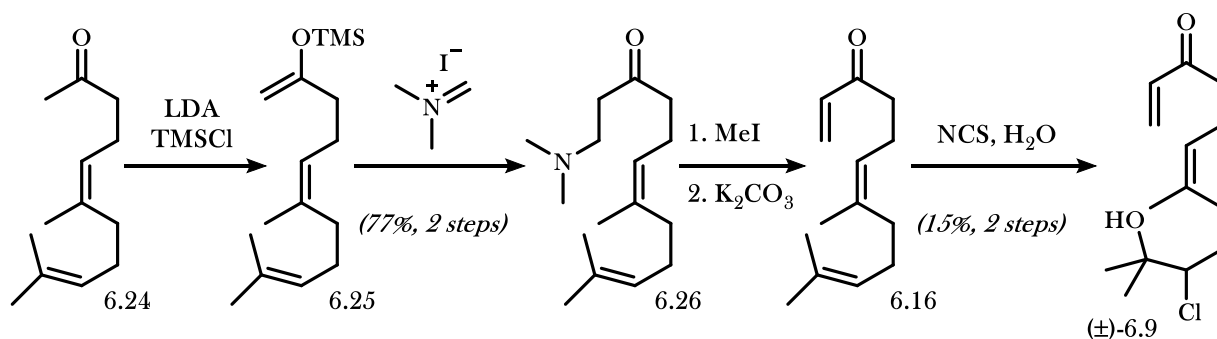


The functionalization of β -ketoesters is arguably one of the most efficient and dependable C-C bond forming reactions in organic chemistry. Due to a combination of the highly-dissociated electron-density of β -ketoesters and the correspondingly mild conditions at which they can be deprotonated, they differ significantly from simple ketone α -substitutions which require strong base and proceed through highly reactive intermediates. Inspired by the work of Snyder and co-workers,⁶ we decided to perform the known allylation of methyl acetoacetate with nerol bromide **6.22** to provide β -ketoester **6.23**, which could in turn be saponified and decarboxylated to form **6.24** in 61% over 3 steps (Scheme 6.1). With nerylacetone (**6.24**) in hand, we then investigated methods to form the enone of **6.9** selectively.

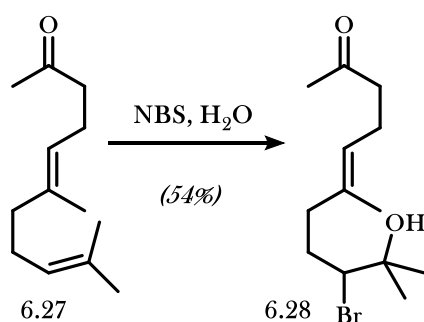
We first identified lithium diisopropylamide (LDA) as a sufficiently bulky base to selectively deprotonate nerylacetone (**6.24**) at the more accessible α -position (Scheme 6.2a). The formed enolate was quenched with trimethylsilyl chloride (TMSCl) to provide the resulting regiodefined enoxy silane **6.25** in high yield. We then found that the enoxy silane was sufficiently nucleophilic enough to add to Eschenmoser's salt, or *N,N*-dimethylmethyleiminium iodide,⁷ to cleanly provide tertiary amine **6.26** in 77% yield over 2 steps. The addition of methyl iodide then formed the β -ammonium ketone, which was eliminated to the enone product **6.16** following treatment with potassium carbonate as a base. The product was separated from charged byproducts via a hexane extraction from the crude solution in acetonitrile, providing the crude material with sufficient purity to carry forward to chlorohydrin formation.

Scheme 6.2 Formation of the Chlorohydrin Cascade Precursor

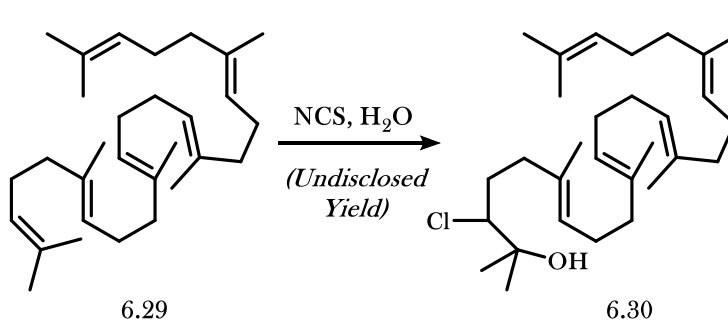
a. Successful Route Toward Chlorohydrin (\pm)-6.9



b. Corey's Bromohydrin Formation



c. Singh's Chlorohydrin Formation

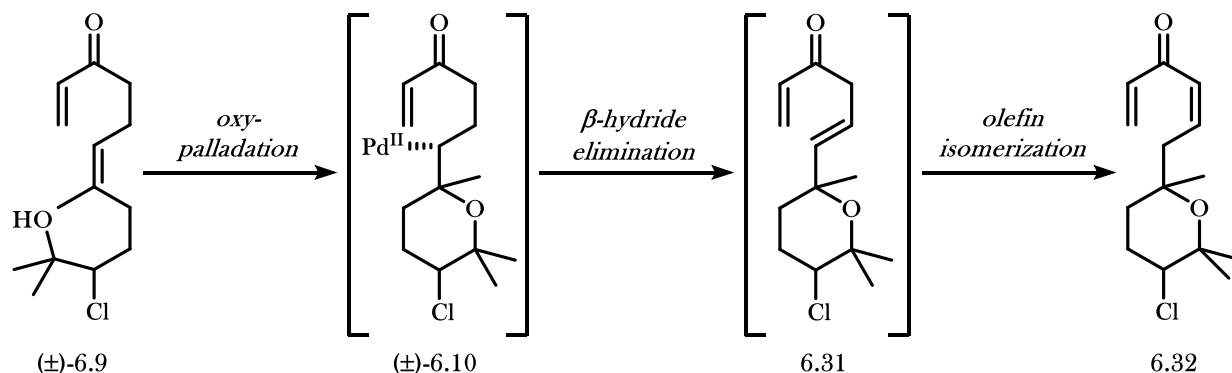


Among others, the Corey group has demonstrated the regioselective installation of bromohydrins on the terminus of geranylacetone **6.27** through the addition of electrophilic bromine in the presence of water (Scheme 6.2b).⁸ We believed that the added enone functionality of **6.16** would not react with an electrophilic halide source, therefore permitting the formation of **6.9** without undesired reactivity. However, the formation of chlorohydrins from isoprene-derived aliphatic chains is far less precedented; a single report of chlorohydrin formation from squalene oxide (**6.29**) via *N*-chlorosuccinimide activation is reported without yield in a footnote by Raina and Singh.⁹ Nevertheless, we found that the portionwise addition of *N*-chlorosuccinimide to enone **6.16** in the presence of water resulted in the formation of chlorohydrin **6.9** in *ca.* 20–25% yield accompanied by significant decomposition. The overall sequence of tertiary amine **6.26** to chlorohydrin **6.9** could be performed in a 15% yield over 3 steps. Although this method for chlorohydrin formation is both low yielding and non-stereoselective, the overall route provides rapid and reproducible access to cascade precursor **6.9**. We planned to reinitiate efforts toward an efficient and stereoselective synthesis of chlorohydrin **6.9** once we confirmed the Wacker/Heck/Saegusa cascade as a viable route toward THP-containing kalihinanes.

6.2.3 Early Cascade Attempts

Following isolation of chlorohydrin cascade precursor **6.9**, we then began efforts to accomplish the palladium catalyzed Wacker/Heck/Saegusa cascade. We found that Pd(PPh₃)₂Cl₂, a stable palladium (II) catalyst commonly used in oxypalladation reactions, was unable to accomplish the initial olefin functionalization. The switch to palladium (II) chloride, which lacks the stabilizing triphenylphosphine ligands and therefore possessed open binding sites, resulted in a complex mixture of unidentifiable products. The use of palladium (II) trifluoroacetate as a catalyst, however, produced small quantities of a product tentatively assigned as the bis-enone **6.32** (Figure 6.4). We observed differentiation of the *bis*-methyl substituents of the tertiary alcohol and the proton germinal to the chloride substituent indicating cyclization to the THP ring, and we believe product **6.32** is formed by β-hydride elimination of **6.10** and subsequent olefin isomerization.

Figure 6.4 Proposed Formation of Tentatively-Assigned Bis-Enone **6.32**



Attempts to introduce ligands to the palladium species to reduce the rate of β -hydride elimination eliminated all reactivity. At this point, we realized that a cascade not relying exclusively on the use of palladium would be beneficial to avoid β -hydride elimination byproducts. Although a more rigorous investigation into the formation of enone **6.12** could have been pursued, we instead changed our focus toward a similar cascade that would both expand our toolbox for plausible ring-closing reactions and result in an overall more efficient synthesis of the kalihinane core.

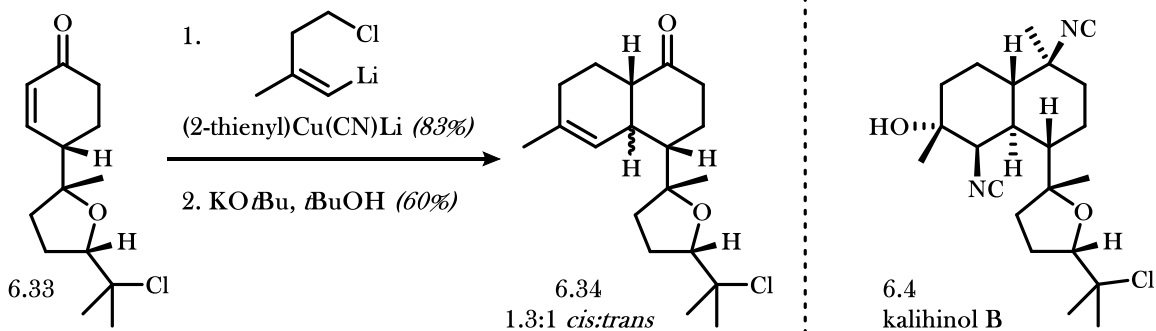
6.3 Revised Cascade for the Formation of Three Rings

6.3.1 Revised Cascade Strategy

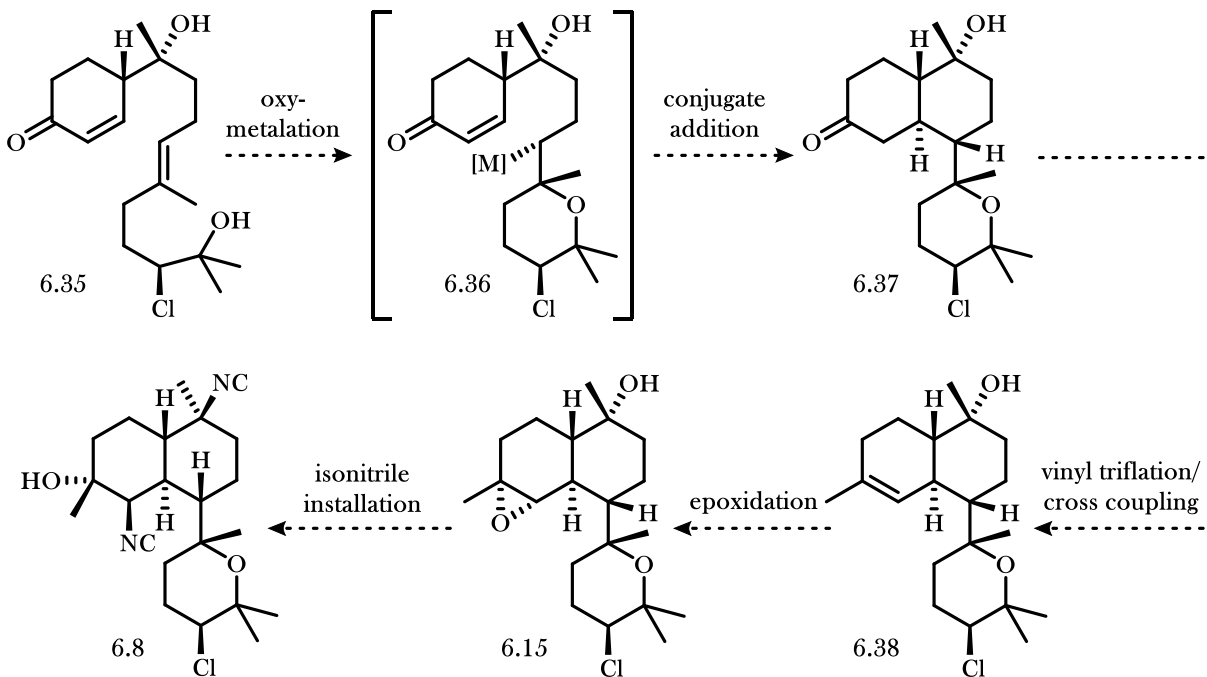
In our originally proposed cascade, the enone of **6.12** had to be regenerated as a functional handle to append the third ring of the kalihinane scaffold. Since we planned to form this enone via a Saegusa oxidation from the enolate intermediate, we were limited to palladium as a catalyst for the ring-closing cascade. However, if the ring were to be present prior to the ring-closing cascade, the Saegusa oxidation would be rendered unnecessary and the available choices of catalyst would be broadened. Additionally, the presence of the third ring would potentially allow for increased selectivity of the tandem vicinal difunctionalization, which proceeded with 1.3:1 dr favoring the undesired *cis* decalin in our synthesis of kalihinol **B** (Figure 6.5a).

Figure 6.5 Revised Strategy toward Kalihinol A

a. Poor Selectivity of Ring Annulation toward Kalihinol B



b. Revised Route to Form Full Kalihinane Core



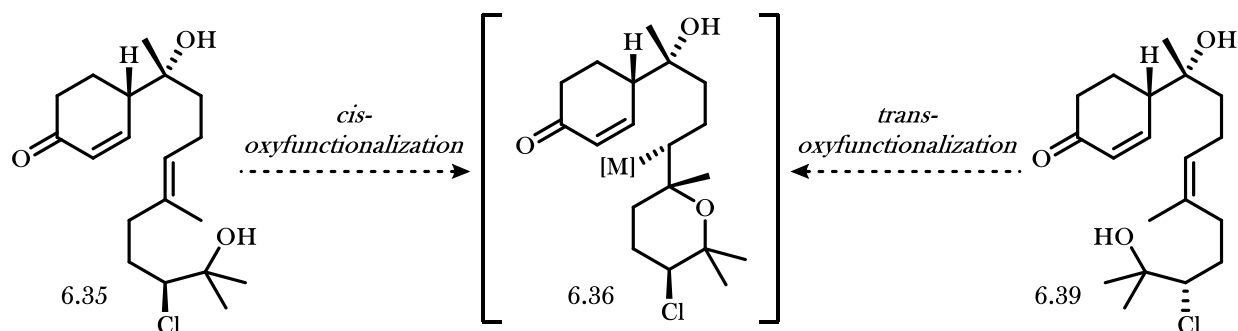
To circumvent these issues, we designed enone **6.35** as a precursor to the cascade (Figure 6.5b). Oxyfunctionalization across the internal olefin would provide a nucleophilic intermediate **6.36**, which might undergo an intramolecular 1,4-conjugate addition into the cyclohexanone fragment and complete the core. From there, a selective α -deprotonation and triflation would form a cross coupling partner to install the trisubstituted olefin of **6.38**, and remaining steps would proceed analogous to our synthesis of kalihinol B.

6.3.2 Mechanistic Considerations

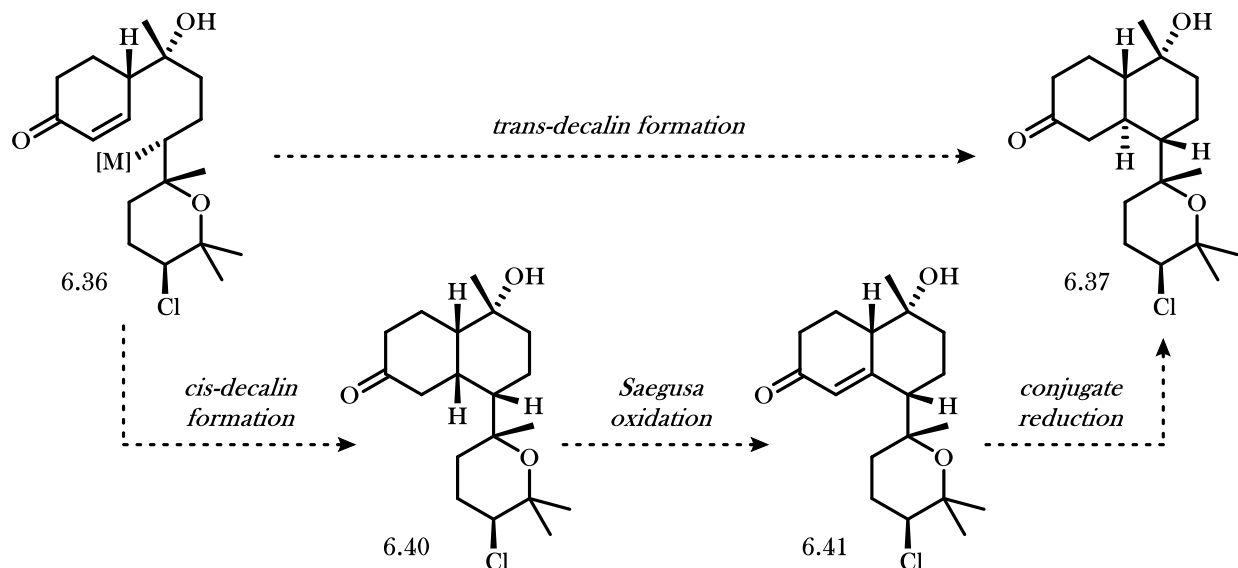
The E/Z identity of the internal alkene again has a direct impact on the stereocenter formed in the ring-closing cascade. If the THP ring-closing reaction were to proceed through an *anti* oxyfunctionalization mechanism, a substrate **6.39** containing a Z-alkene would be necessary. However, in the revised cascade, an alkylcopper species (**6.36**; Figure 6.6a; M = CuX, CuX₂) was identified as the most desirable conjugate addition precursor. Since oxycupration ring-closing transformations most often proceed through a *cis*-oxyfunctionalization mechanism, the acyclic precursor **6.35** must be constructed with an E-alkene.

Figure 6.6 Mechanistic Considerations for Stereocenter Formation

a. Impact of E/Z Alkene Isomer on Organometallic Stereocenter



b. Impact of Decalin Formation on Route



Following formation of the alkylcopper species, conjugate 1,4-addition could then proceed via attack of either prochiral face of the electron-deficient olefin of **6.36** (Figure 6.6b). Since no examples in the literature could be found involving a similar intramolecular organometallic ring-closing 1,4-addition, the selectivity of this transformation would need to be determined empirically. If the desired *trans*-decalin ring system were formed, the resulting ketone **6.37** could then be carried forward to the natural product. If the *cis*-decalin framework were instead observed (as shown by **6.40**), a Saegusa oxidation to the enone **6.41** and subsequent Birch reduction, hydrogenation, or hydrogen atom transfer could procure the *trans*-decalin isomer **6.37**. In the case of enone reduction, we were also aware that competing reduction of the secondary alkyl chloride could introduce difficulties.

6.4 Linear Route toward the Cascade Precursor

6.4.1 Early Installation of the Tertiary Alcohol

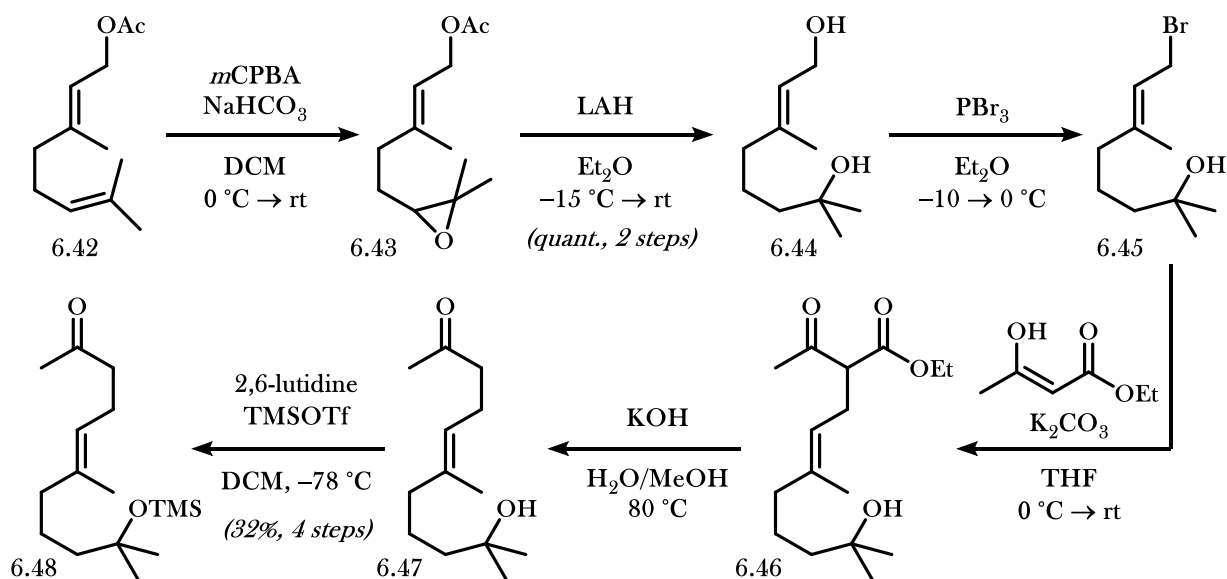
Upon considering the logistics of cascade development and optimization, we anticipated the formation of a complex mixture of diastereomers owing to modest selectivity in stereocenter formation. To minimize the number of stereocenters and reduce the complexity of characterization, we decided to omit the secondary chloride of **6.35** during our exploratory work. Following successful completion of the core, we planned to reproduce the optimized route with the chloride stereocenter installed.

Rather than install an epoxide late-stage and attempt an epoxide opening with harsh hydridic reagents to form the tertiary alcohol on a complex substrate, we instead found early installation of the tertiary alcohol to be most convenient. We found the desired functionality could be installed by epoxidation of geranyl acetate (**6.42**) and subsequent hydride opening of epoxide **6.43** at the less hindered position with lithium aluminum hydride (Scheme 6.3), which also accomplishes a one-pot acetate deprotection to unveil the allylic alcohol **6.44**.

The key C-C bond formation was then accomplished via a similar β -ketoester allylation as described in section 6.2.1. The allylic bromide **6.45** was formed selectively from the less-hindered primary allylic alcohol

using phosphorus tribromide, and then the C-C bond was formed with the addition of ethyl acetoacetate in the presence of potassium carbonate. A one-pot saponification/decarboxylation provided the geranylacetone derivative **6.47**. Since enone installation first involves formation of an enoxy silane requiring the use of strong base for α -deprotonation, the tertiary alcohol of **6.47** was first protected under mild conditions to remove the more acidic proton. The four-step sequence provided silylated geranylacetone derivative **6.48** in 32% isolated yield. The enone was then procured in a similar sequence to that of the nerol derivative **6.9**. Enoxy silane formation and addition into Eschenmoser's salt provided the tertiary amine **6.50** in 35% isolated yield (Scheme 6.4). Methylation to form the ammonium salt and elimination afforded enone **6.51** in sufficient purity to carry directly to the next step.

Scheme 6.3 Synthesis of Silylated Geranylacetone Derivative **6.48**

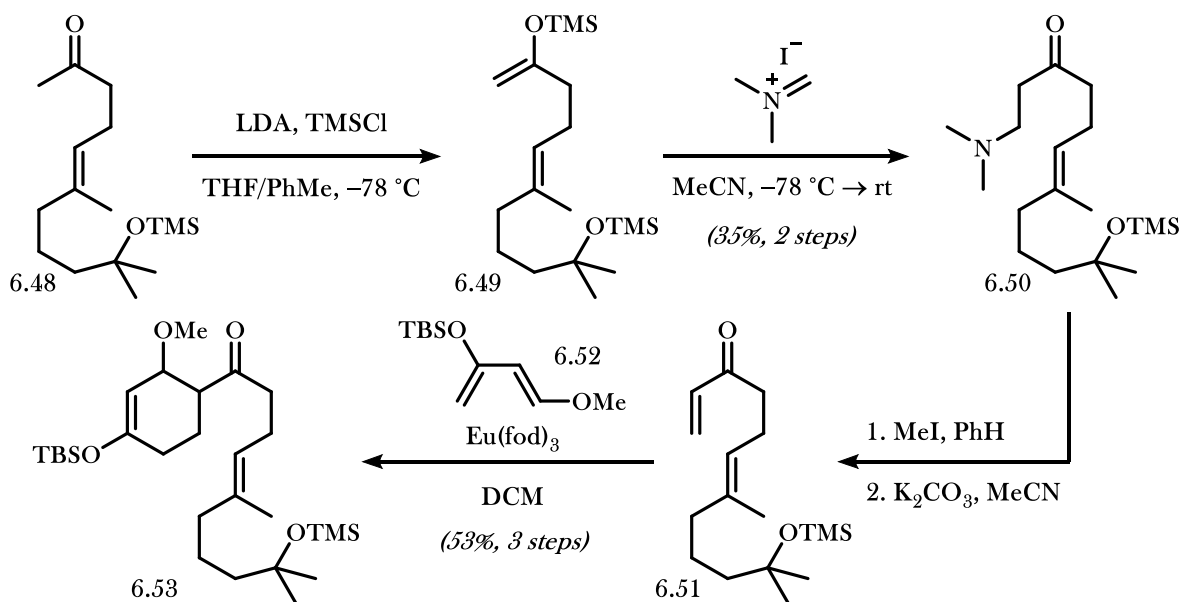


6.4.2 Diels-Alder with Danishefsky's Diene

Following dienophile **6.51** formation, conditions were then investigated to accomplish a Diels-Alder cycloaddition with Danishefsky's diene (**6.52**) while also retaining the enoxy silane functionality of the product **6.53** (Scheme 6.4). Unintentional silyl deprotection of **6.53** followed by expulsion of the methoxy substituent would form the cyclohexenone product, which would introduce susceptibility of alkene isomerization into

conjugation with the exocyclic ketone. Danishefsky and coworkers observed olefin isomerization in similar substrates following attempts to purify them by silica gel chromatography. A Diels–Alder transformation retaining the enoxy silane functionality of **6.53** would allow for installation of the tertiary alcohol selectively from the exocyclic ketone. Following tertiary alcohol formation, the enone could then be unveiled without risk of alkene isomerization.

Scheme 6.4 Dienophile Synthesis and Europium-Catalyzed Diels–Alder



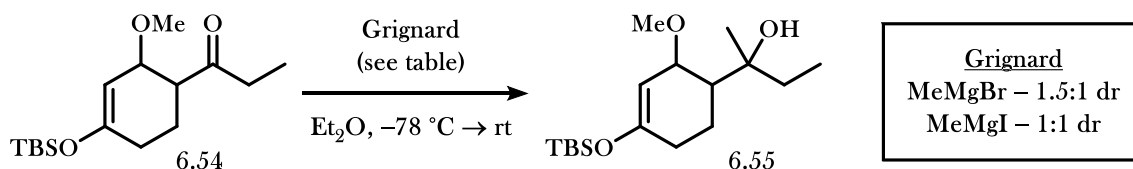
To date, the only Lewis acids that have demonstrated activation of dienophiles for [4+2] cycloadditions while retaining the enoxy silane functionality have been zinc (II) chloride¹⁰ and europium(III)-tris(1,1,1,2,2,3,3-heptafluoro-7,7-dimethyl-4,6-octanedionate), or $\text{Eu}(\text{fod})_3$.¹¹ We tested a variety of Lewis acids including the above and found that only $\text{Eu}(\text{fod})_3$ could provide cycloaddition product **6.53** without decomposition to the enone. The Diels–Alder product **6.53** could also be formed upon heating in the *absence* of Lewis acid, albeit in diminished yields. The overall three-step sequence from tertiary amine **6.50** provides enoxy silane **6.53** in 53% isolated yield.

6.4.3 Elaboration to the Precursor

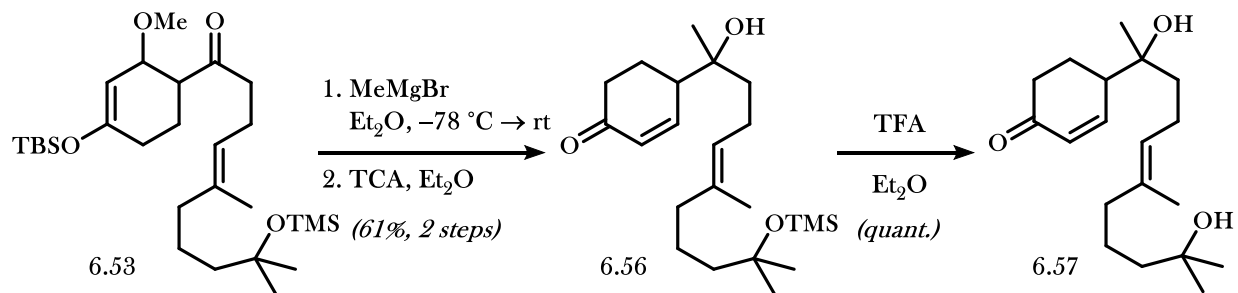
With the enoxy silane intact, the tertiary alcohol could then be formed from the ketone precursor. On test substrate **6.54** derived from Diels–Alder addition to ethyl vinyl ketone, methylmagnesium bromide added to the ketone to provide tertiary alcohol **6.55** as a 1.5:1 unidentified mixture of diastereomers, while methylmagnesium iodide provided a 1:1 mixture of diastereomers (Scheme 6.5).

Scheme 6.5 Completion of the Cascade Precursor

a. Impact of Halide on the Diastereoselectivity of Grignard Addition



b. Completion of the Cascade Precursor



On the full system, methylmagnesium bromide was found to cleanly add to ketone **6.53**, again providing an unidentified 1.5:1 ratio of a mixture of diastereomers. Addition of trichloroacetic acid resulted in hydrolysis to the vinylogous acetal to form **6.56** in 61% over 2 steps. Addition of trifluoroacetic acid (TFA) then deprotected the silyl ether to provide the cascade precursor **6.57** in quantitative yield as a mixture of diastereomers.

6.4.4 Route Summary

The route to the cascade precursor **6.57** is completed in 14 steps in a 3.6% overall yield. Importantly, the route uses well-precedented reactions with easily-optimized conditions that allowed for the initiation of

ring-closing investigations within a few months of the genesis of the project. However, there are several drawbacks to the synthesis up to this point. If the total synthesis were to be completed, the synthesis would amount to a total of 21 steps – significantly lengthier than our 13-step synthesis of kalihinol B. Additionally, our Diels–Alder cycloaddition to append the conjugate acceptor ring is not asymmetric under standard conditions, and all known asymmetric cycloadditions involving simple enones require acidic conditions which would likely deprotect the enoxy silane of the product. Furthermore, installation of the tertiary alcohol from the ketone precursor does not proceed with diastereoselectivity. While investigating ring-closing cascades (see section 6.7 and 6.8), we concurrently began a study into alternative strategies that would allow efficient access to precursor **6.57** as a single enantiomer and diastereomer.

6.5 Convergent Synthesis via Enolate Allylation

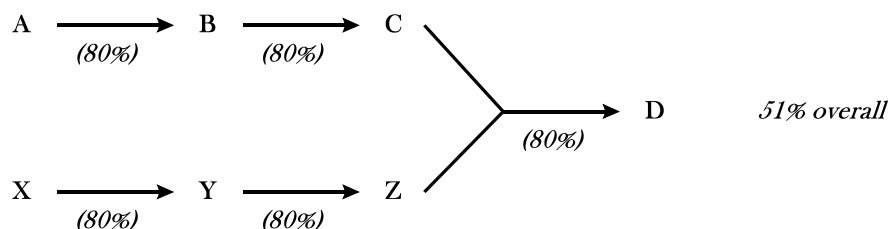
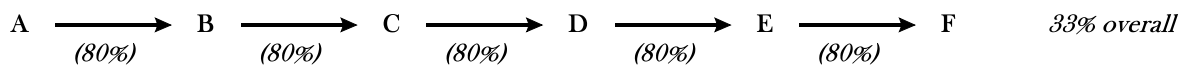
6.5.1 Motivation

To reduce the longest linear sequence required to procure cascade precursor **6.57**, we began investigations into convergent routes to make the key C–C bond that divides the molecule in half. Convergent syntheses are in most cases more efficient and higher yielding than linear routes; convergent strategies involving the same number of steps in identical yields can provide a final product in much higher overall yield as compared to linear strategies (Figure 6.7a).

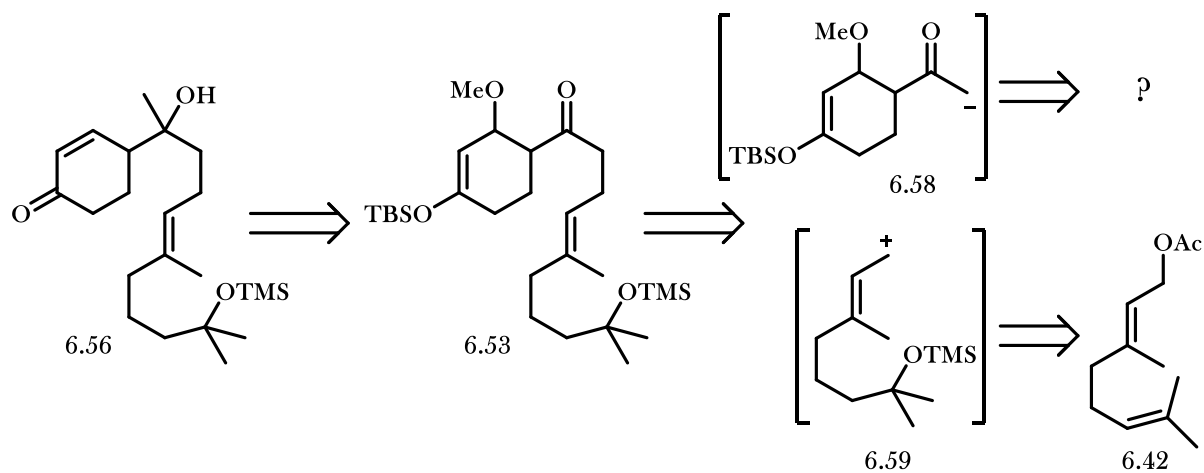
The linear strategy described in section 6.4 could be made convergent by instead displacing the allylic bromide **6.45** with a more complex nucleophile that already possesses the cyclohexenone ring. Since the nucleophilic carbon atom in this convergent strategy possesses α -oxygenation, we first investigated the allylation of enolate **6.58** (Figure 6.7b). With this proposed disconnection, the longest linear step count toward cascade precursor **6.57** could be improved from 14 steps to just 6 steps.

Figure 6.7 Linear vs. Convergent Strategies in Total Synthesis

a. Overall Yield Improvement with Convergent Strategies



b. Initial Convergent Strategy for Cascade Precursor Synthesis



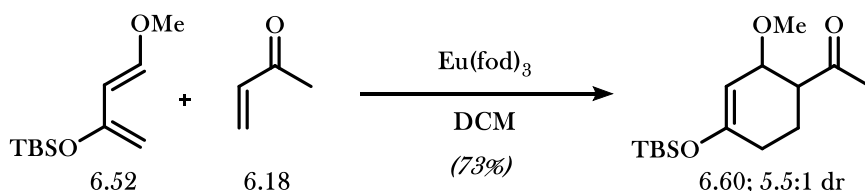
6.5.2 Enolate Allylation Attempts

The nucleophile precursor **6.60** was prepared using similar reactions than those used to append the conjugate acceptor ring onto enone **6.51**. A $\text{Eu}(\text{fod})_3$ catalyzed [4+2] cycloaddition involving MVK (**6.18**) and Danishefsky's diene (**6.52**) produced ketone **6.60** as a 5.5:1 mixture of diastereomers (Scheme 6.6a). Since the proposed enolate **6.58** is basic enough to deprotonate a tertiary alcohol, unlike our previous route utilizing a β -ketoester nucleophile, the alcohol of the electrophile had to be protected. Following bis-silyl protection of **6.44** under mild conditions and mono-deprotection of the less sterically-hindered primary allylic silyl ether,

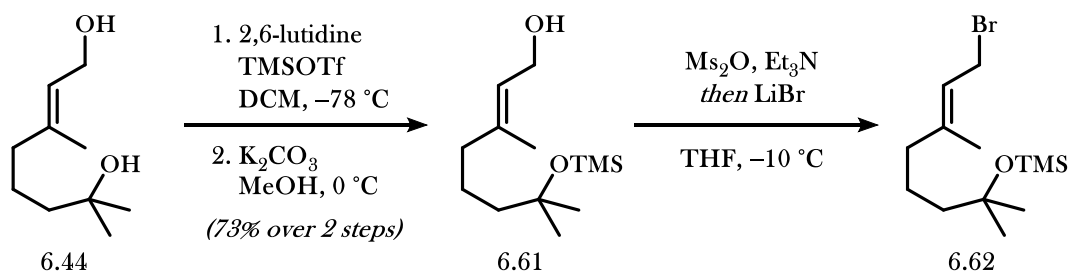
the allylic bromide **6.62** was formed via mesylation and bromide displacement (Scheme 6.6b). Efforts to accomplish α -deprotonation and enolate allylation of ketone **6.60** then commenced.

Scheme 6.6 *Synthesis of Coupling Partners for the Enolate Allylation Strategy*

a. Synthesis of the Ketone Precursor

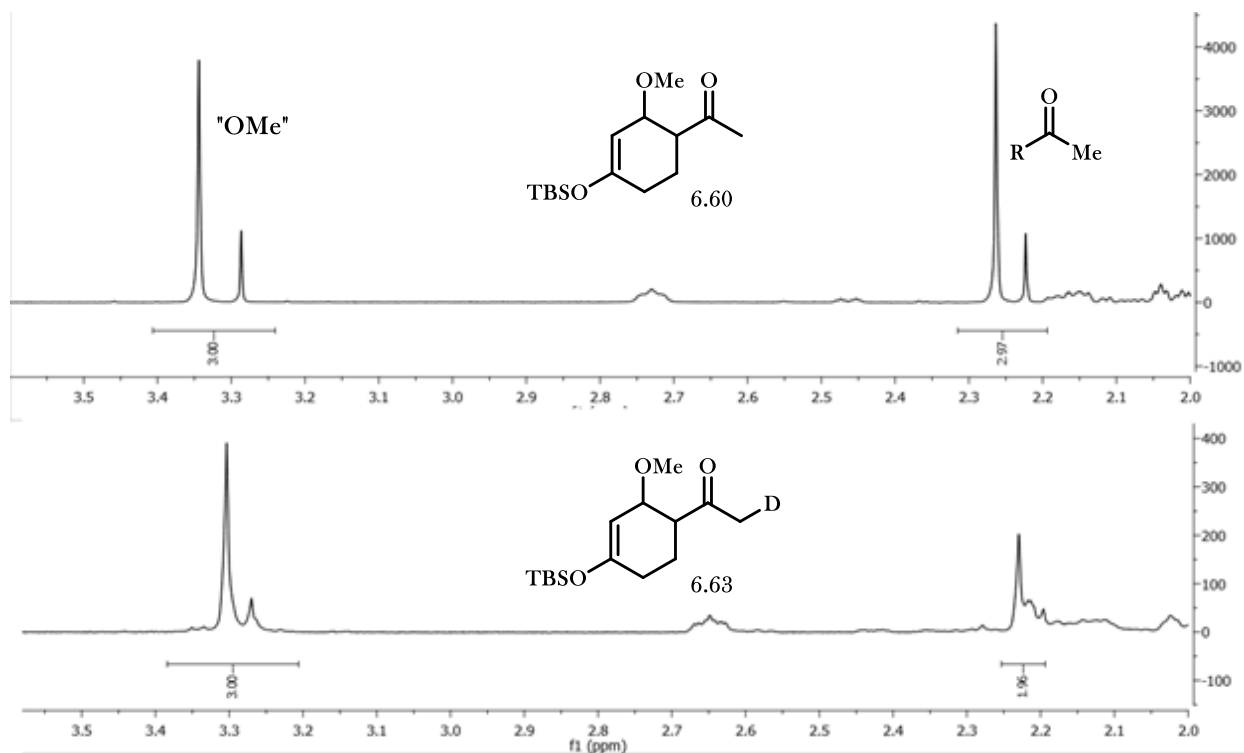


b. Synthesis of the Bromide Electrophile



The less sterically-hindered α -position of ketone **6.60** could be deprotonated selectively with strong hindered bases such as LDA or KHMDS. The regioselectivity of deprotonation was supported by ^1H NMR analysis following quenching of a formed lithium enolate intermediate with deuterium oxide (Figure 6.8). Treatment of the lithium enolate with geranyl bromide resulted in only trace quantities of allylation product **6.64** (8% isolated yield), likely due to the elevated temperatures necessary to accomplish halide displacement (Scheme 6.7). The introduction of HMPA, which coordinates to cationic counterions thereby increasing the nucleophilicity of anionic species, facilitated reactivity at colder temperatures but allowed for a slight increase in isolated yield of **6.64** to 13%.

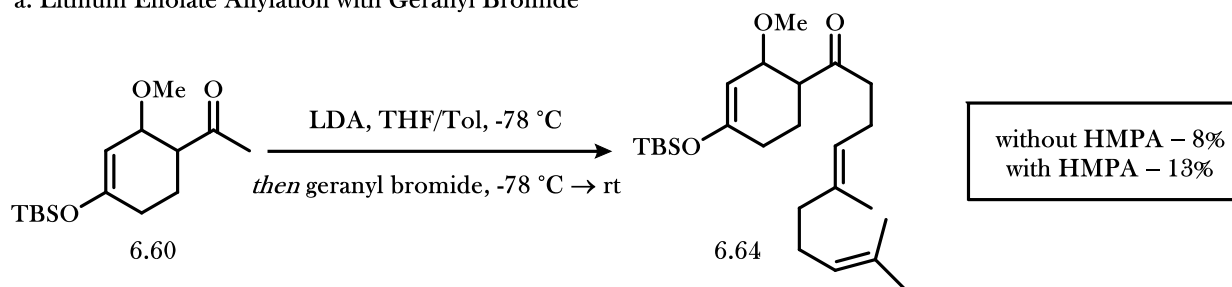
Figure 6.8 Selective Deprotonation of Ketone **6.60**



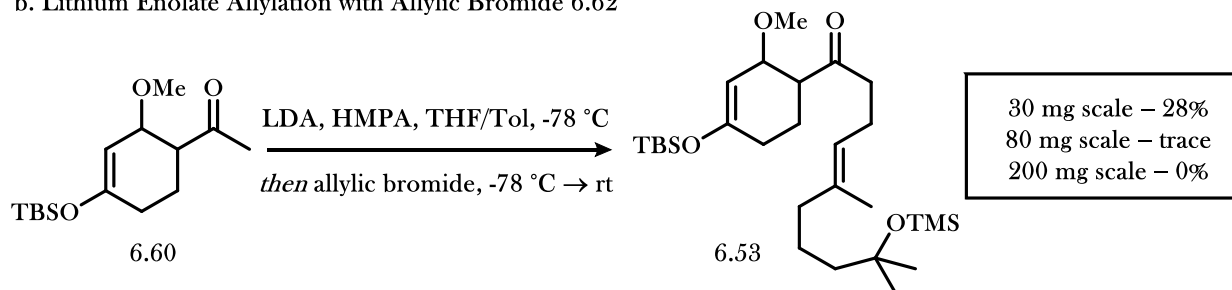
Use of allylic bromide **6.62**, which possesses substitution that corresponds to the desired cascade precursor **6.57**, increased the yield significantly for reasons that are unclear (Scheme 6.7b). Using identical conditions to those which afforded **6.64** in 13% yield, functionalization using allylic bromide **6.62** resulted in a 28% isolated yield of **6.53**. However, in addition to the low yields, these reactions also suffered from scalability issues; allylation produced trace product using 80 mg of starting material ketone **6.60**, and no product was observed on 200 mg scale. We therefore investigated other nucleophiles which might generate more desirable quantities of allylation product.

Scheme 6.7 Fragment Coupling via Enolate Allylation

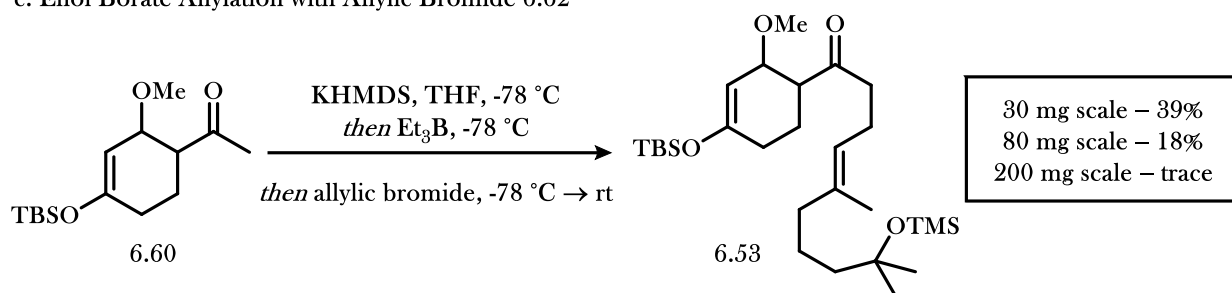
a. Lithium Enolate Allylation with Geranyl Bromide



b. Lithium Enolate Allylation with Allylic Bromide 6.62



c. Enol Borate Allylation with Allylic Bromide 6.62



Negishi and co-workers have previously demonstrated the utility of potassium enolborate intermediates as species that retain their high nucleophilic character but also benefit from significantly increased stability.¹² Their reported work includes the allylation of cyclohexanone-derived nucleophiles with geranyl- and neryl-derived electrophiles, providing strong precedent for our desired allylation. The nucleophiles are more stable at elevated temperatures, allowing for allylations to be run at temperatures that would cause decomposition with more common enolate nucleophiles. On small scale, we observed an exciting quantity of desired product (39%) using Negishi's methodology (Scheme 6.7c). However, as observed with the allylation of lithium enolates, we observed diminishing yields on larger scale. Additionally, allylation using enoxy silanes as nucleophiles and/or *in situ* generated allyl palladium electrophiles were unsuccessful.

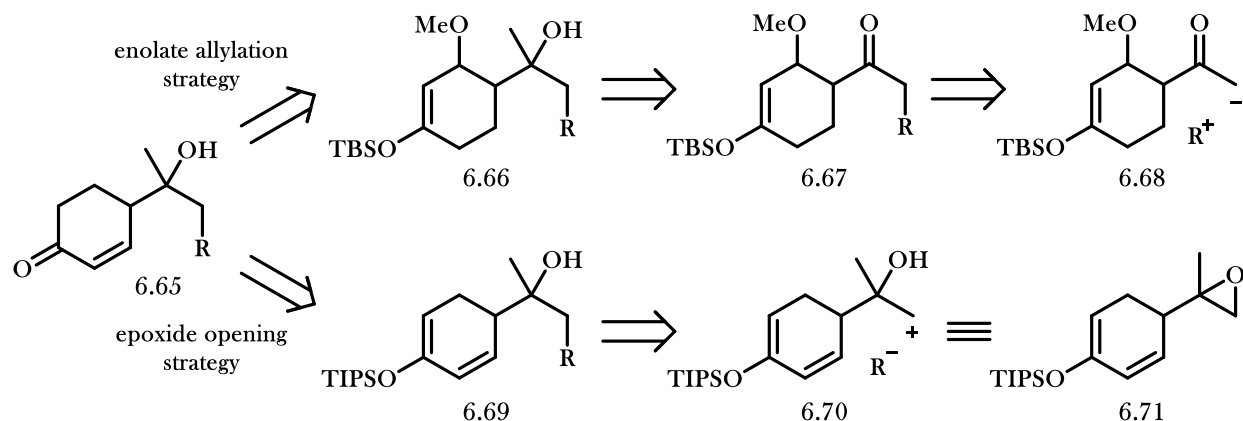
The α -allylation of carbonyls would allow for formation of the key C-C bond from easily accessed precursors and remains one of the most attractive disconnections toward the cascade precursor **6.56**. However, in addition to low yields and low scalability, there are other shortcomings that must be addressed. First, there currently lacks an enantioselective method for Diels-Alder cycloadditions involving methyl vinyl ketone as a dienophile. MacMillan and co-workers have developed an imidazolidinone organocatalyzed cycloaddition involving MVK that proceeds with moderate selectivity (61% ee with cyclopentadiene), but the reaction requires the addition of strong acid that would decompose the enoxy silane of the Danishefsky-type diene.¹³ If an enantioselective cycloaddition could be developed, there yet remains the issue of low diastereoselectivity in the formation of the tertiary alcohol of **6.56** from the ketone precursor. Due to a myriad of disadvantages to the formation of cascade precursor **6.56** via enolate allylation, we decided to pursue alternative strategies.

6.6 Convergent Synthesis via Epoxide Opening

6.6.1 Motivation

The inability to set both the α -stereocenter of **6.60** and the tertiary alcohol stereocenter derived from **6.53** via an enolate allylation pathway led us to pursue strategies by which those stereocenters were established prior to bond formation. We limited our search to disconnections retaining geranyl- and neryl-derived acyclic fragments, since methodologies to install the chlorohydrin had already been developed. We postulated that, in addition to an enolate functionalization disconnection, the oxygenation vicinal to the reactive carbon of the cyclic coupling partner might also suggest a disconnection involving epoxide opening.

Figure 6.9 Reversal of Polarity of Fragment Coupling

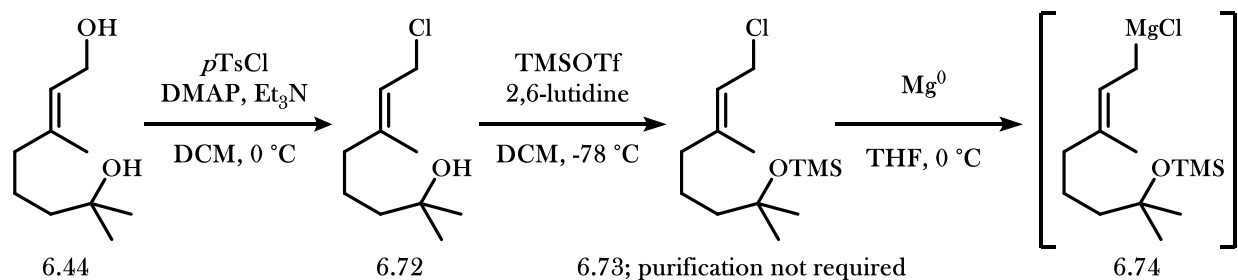


This approach might provide several improvements over the enolate allylation strategy. First, the stereochemistry of the cyclic stereocenter of **6.71** no longer depends on an asymmetric Diels–Alder cycloaddition and again opens the door for an enantioselective total synthesis of the kalihinanes (Figure 6.9). Furthermore, the stereocenter that bears the tertiary alcohol in **6.71** can be set prior to epoxide opening, no longer necessitating a (yet unsuccessful) diastereoselective Grignard addition to ketone **6.67**. The opening of epoxides with allylic Grignard reagents has been reported in abundance throughout the literature. To determine the feasibility of an epoxide-opening strategy, we began efforts to synthesize each coupling partner.

6.6.2 Synthesis of Allylic Nucleophile

Allylic chlorides are known to be more reliable precursors to allylic Grignard reagents than the corresponding allylic bromides. We therefore set allylic chloride **6.73** as the target nucleophile for the copper-catalyzed epoxide-opening toward the acyclic precursor. We initially attempted to form the allylic chloride directly from diol **6.44** via a selective activation and displacement of the allylic alcohol, analogous to our synthesis of the allylic bromide **6.62** with phosphorus tribromide (PBr_3). However, we were unable to accomplish a selective activation with dehydrative chlorinating reagents such as phosphorus trichloride (PCl_3). Instead, *p*-toluenesulfonyl chloride was found to selectively activate and displace the allylic alcohol to form allylic chloride **6.72** (Scheme 6.8).

Scheme 6.8 Formation of Allyl Grignard Nucleophile **6.74**

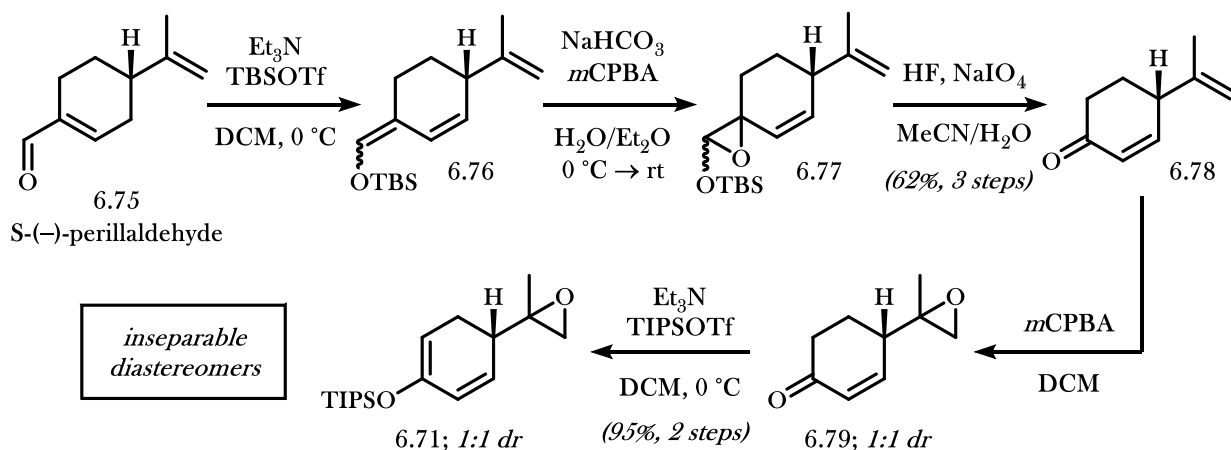


The remaining tertiary alcohol of **6.72** could be protected under mild conditions without undesired elimination of the allylic chloride, and the Grignard reagent **6.74** could be formed cleanly via addition of activated magnesium. With an efficient and scalable route to the nucleophilic fragment of the epoxide-opening transformation, we then turned our efforts toward a synthesis of the epoxide precursor.

6.6.3 Synthesis of Epoxide Precursor

We were pleased to discover that our target electrophilic epoxide closely resembles an intermediate procured by Razdan and co-workers in their synthesis of (-)-11-hydroxy- Δ^9 -tetrahydrocannabinol (THC; Scheme 6.9).¹⁴ They access epoxide **6.79** efficiently and scalably from S-(-)-perillaldehyde (**6.75**), an inexpensive commercially available terpene natural product with defined absolute stereochemistry. Extended dienoxysilane formation and selective epoxidation of the most kinetically reactive alkene of **6.76** provides epoxide **6.77** as a mixture of diastereomers. Deprotection of the silyl acetal **6.77** with hydrofluoric acid and subsequent oxidative cleavage with sodium periodate affords enone **6.78** as a single enantiomer. The Razdan group then again accomplished a regioselective, but not diastereoselective, epoxidation to provide **6.79** as a 1:1 mixture of diastereomers.

Scheme 6.9 Synthesis of a Mixture of Epoxide Diastereomers

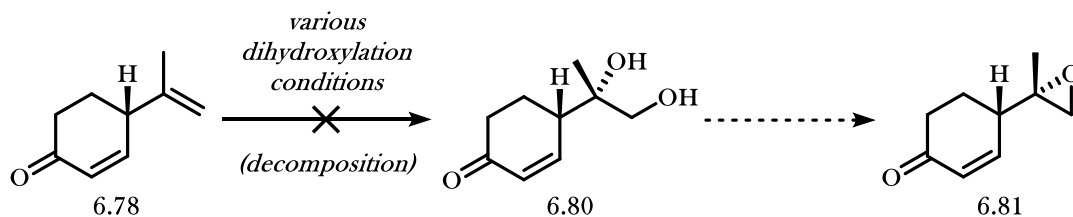


Although the reported route toward **6.79** provided the key framework for our epoxide-opening fragment coupling, there remained two main areas that required improvement. First, the enone of **6.79** is a more potent electrophile than the epoxide and would therefore likely react at a faster rate. This issue was quickly resolved via formation of the cross-conjugated dienoxysilane **6.71**, which could be easily deprotected following fragment coupling to unveil the enone.

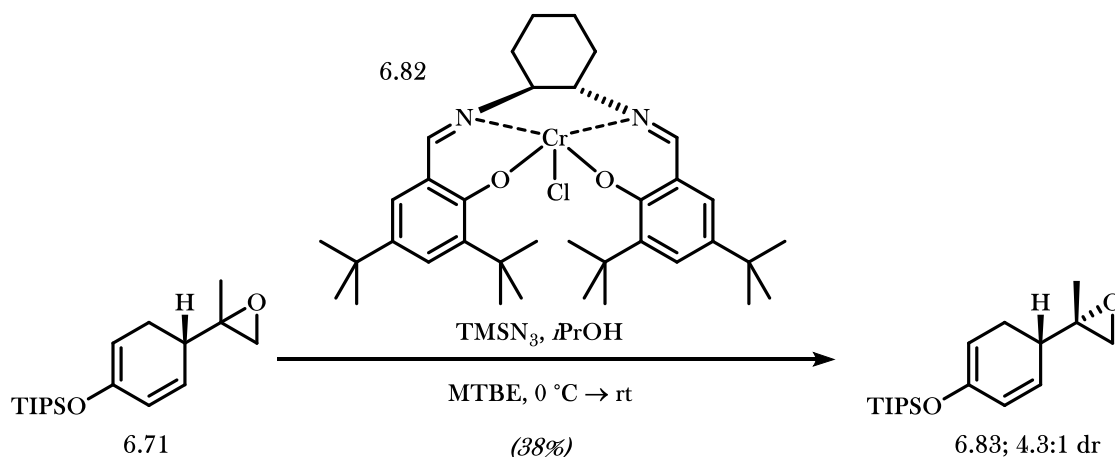
The remaining issue of the 1:1 diastereoselectivity of epoxide formation proved to be more problematic. To provide further difficulty, the diastereomers of both **6.79** and **6.71** (with TMS, TES, and TIPS silyl functionalities) could not be separated. If formation of a stereodefined epoxide could not be accomplished, the current route provides no benefit over our previous enolate allylation strategy with respect to the selective formation of the tertiary alcohol stereocenter.

Scheme 6.10 Methods for Synthesis of Stereodefined Epoxide **6.83**

a. Attempted Dihydroxylation and Subsequent Epoxide Formation



b. Epoxide Formation via Jacobsen's Kinetic Resolution



Since the allylic stereocenter does not impact the diastereoselectivity of epoxidation, we first explored enantioselective methods for formation of the correct diastereomer. Asymmetric epoxidations of 1,1-disubstituted olefins are notoriously known to proceed with low enantioselectivity and were not investigated. Asymmetric dihydroxylations have proven slightly more successful in certain cases,¹⁵ but we unexpectedly observed rapid decomposition of **6.78** upon introduction of dihydroxylation conditions (Scheme 6.10a). Identical dihydroxylation conditions introduced to S-(–)-perillaldehyde (**6.75**) resulted in clean reactivity, indicating the incompatibility of enone **6.78** with dihydroxylation conditions.

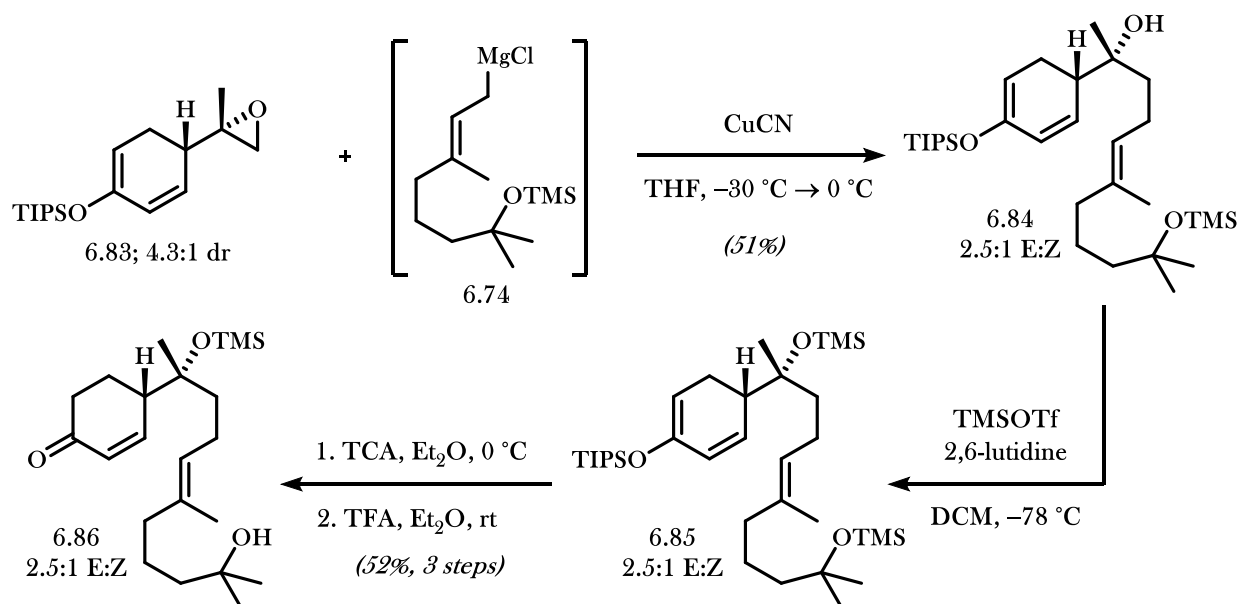
Based on the unlikelihood of a selective epoxide installation providing **6.83** as a single diastereomer, we changed our focus to methods that would allow for separation of the epoxide diastereomers. Jacobsen and co-workers have developed a kinetic resolution of 2,2-disubstituted epoxides which allows for the formation of a single diastereomer in high yields relative to their theoretical yield.¹⁶ Using the conditions reported by

Jacobsen, we could isolate enriched epoxide **6.83** in 38% yield as a 4.3:1 mixture of diastereomers (Scheme 6.10b). With the desired diastereomer in hand, we began pursuing epoxide-opening strategies toward the formation of the acyclic precursor.

6.6.4 Successful Epoxide Opening

We found that slow addition of allylic Grignard reagent **6.74** to epoxide **6.83** in the presence of a catalytic amount of copper (I) cyanide cleanly opened the epoxide to afford **6.84** in 51% yield (Scheme 6.11). Unfortunately, allylmagnesium halide species are not configurationally stable and provide **6.84** as a 2.5:1 E:Z mixture of olefin isomers. In cases where stereocenters resulting from ring-closure are formed stereospecifically, as described in section 6.7, this will lead to a mixture of diastereomers at that position. However, in cases where the stereocenter is destroyed as part of the reaction mechanism, as in section 6.8, the olefin mixture is inconsequential. If retention of E/Z configuration is necessary to achieve desired yields, allyllithium or allylbarium¹⁷ species have been shown to proceed without alkene isomerization. Silylation of the formed tertiary alcohol of **6.84** followed by a selective deprotection of the other two silyl functionalities provides silylated cascade precursor **6.86**.

Scheme 6.11 Completion of the Acyclic Precursor **6.86** via Epoxide-Opening Strategy



6.6.5 Route Summary

The formation of cascade precursor **6.86** via an epoxide-opening strategy demonstrates several advantages over our previously developed routes. Ten steps are required to form the cascade precursor, significantly shorter than the linear route (14 steps). Additionally, the two stereocenters can be formed selectively, and the yield (5.9% from perillaldehyde) is higher than those obtained from both of our previous strategies. Furthermore, this strategy allows for silyl protection of the spectator tertiary alcohol, which will prevent undesired reactivity. A drawback to our revised route remains the isomerization of the internal olefin, but replacement of allylmagnesium halide species with alternative metals could provide a solution to this problem. With the successful epoxide-opening strategy complete, we could then begin attempts to construct the core of THP-containing kalihinanes via various ring-closing transformations.

6.7 Ring-Closing Efforts via Heck Cascade

6.7.1 Initial Stepwise Strategy

Similar to our strategy described in Figure 6.2, we planned to close the ring system of THP-containing kalihinanes via oxymetalation and a 1,4-conjugate addition of the resulting organometallic species to a pendant enone. Due to the well-precedented propensity of organocopper species to add to enones in a 1,4-fashion, we began our investigation with oxymetallations involving copper-based catalysts. The Chemler group has demonstrated the utility of Cu(OTf)₂ to catalyze a *syn*-oxycupration to close tetrahydrofuran rings.¹⁸ However, oxymetalation to form six-membered THP rings has not yet been accomplished. Similarly, in our hands, we were unable to accomplish ring closure using a variety of copper catalysts. Attempts to accomplish an oxy-palladation and subsequent 1,4-addition were also unsuccessful, providing a complex mixture of unidentifiable products.

To simplify our experiments, we decided to instead pursue the formation of organometallic intermediate **6.36** by a more conventional means than through THP ring closure. If the heterocyclic ring could be closed to form an isolable intermediate that could then be easily converted to a nucleophilic

organometallic species, then analysis of the product mixture resulting from an attempted 1,4-addition would be simplified. There are a variety of transformations that can accomplish THP ring closure to form isolable intermediates. We decided to initially pursue the heavily precedented oxymercuration reaction for ring-closure.

6.7.2 Oxymercuration and 1,4-Addition Attempts

Oxymercuration has previously been shown to accomplish the formation of sterically congested THP rings in high yields and selectivities. In their synthesis of the cladiellin diterpenes, the Overman group showed the hindered bond-forming power of the oxymercuration reaction to close a large 9-membered ring starting material (**6.87**) to form a complex bicyclic product (**6.88**; Scheme 6.12a).¹⁹ The Yoshii group, en route to tetronomycin, showed that THP rings could be closed with high diastereoselectivity (Scheme 6.12b).²⁰ Importantly, Yoshii and co-workers also showed that, when mercury (II) acetate is used as an electrophilic metal source, the resulting organomercury acetate can be converted to the stable and isolable organomercury chloride through the addition of brine.

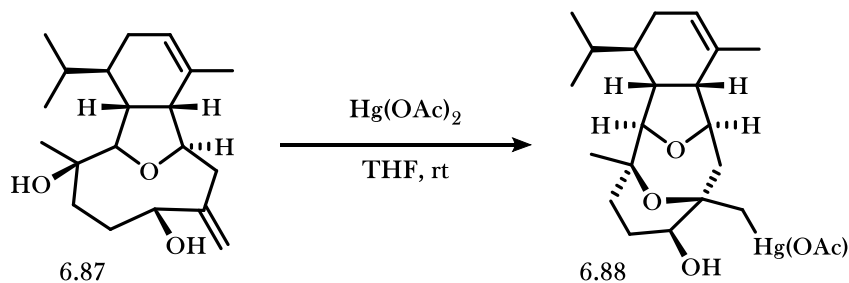
Once isolated, organomercury chloride intermediates can then be transmetallated to more reactive species that might participate in a 1,4-addition to the pendant enone. Kočovský and co-workers have converted organomercury halides directly to cuprate species that can then undergo 1,4-addition to a pendant α,β -unsaturated ester (Scheme 6.12c).²¹ Similarly, organomercury halide species can perform Heck reactions via organopalladium intermediates.²² Inspired by the stimulating precedent in the literature, we began efforts to use oxymercuration as a tool to study the 1,4-addition of organometallic nucleophiles to the pendant enone.

Oxymercuration of **6.57**, prepared via the original linear route as a mixture of diastereomers, proceeds smoothly upon addition of mercury (II) acetate and quenching with brine following complete ring-closure (Scheme 6.12d). The resulting organomercury chloride **6.93** is stable and can be purified by silica gel chromatography, although loss of material is observed. Unfortunately, efforts to transmetalate to organocuprates or organopalladium intermediates at low temperature resulted in rapid and exclusive ring-opening to regenerate acyclic precursor **6.57**. With clear evidence indicating that the rate of ring-opening is

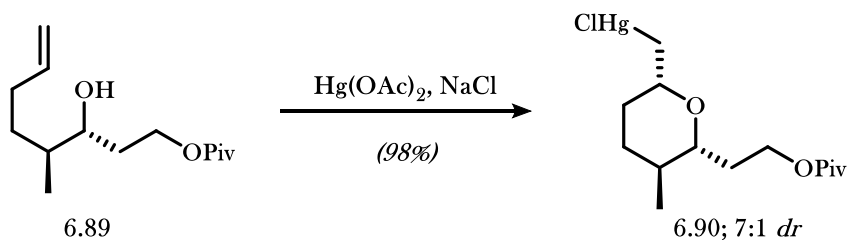
much faster than a 1,4-conjugate addition, we were forced to pursue C-C bond formation through other means.

Scheme 6.12 *Oxymercuration Precedent*

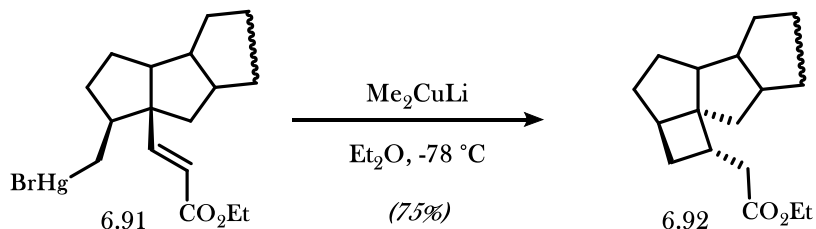
a. Overman's Synthesis of the Cladiellin Diterpenes (2001)



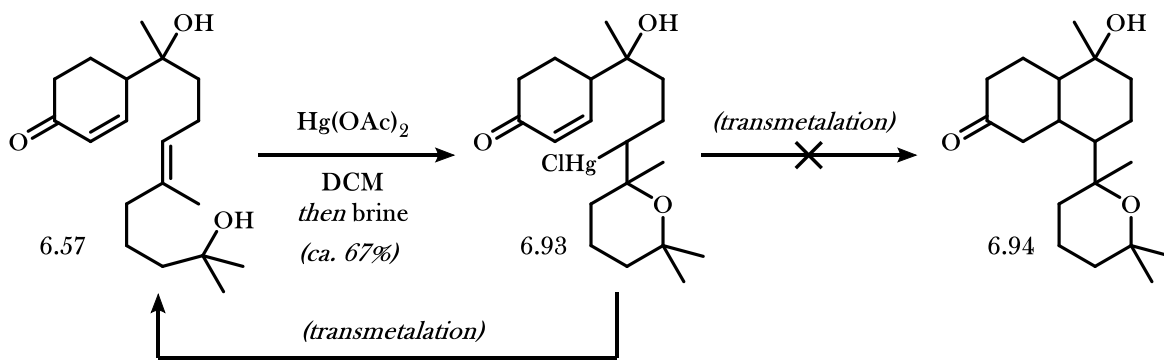
b. Yoshii's THP Formation on Route to Tetronomycin (1991)



c. Kocovský's Transmetalation to an Organocuprate (1992)



d. Oxymercuration and Observed Ring-Opening



6.8 Ring-Closing Efforts via Single-Electron Processes

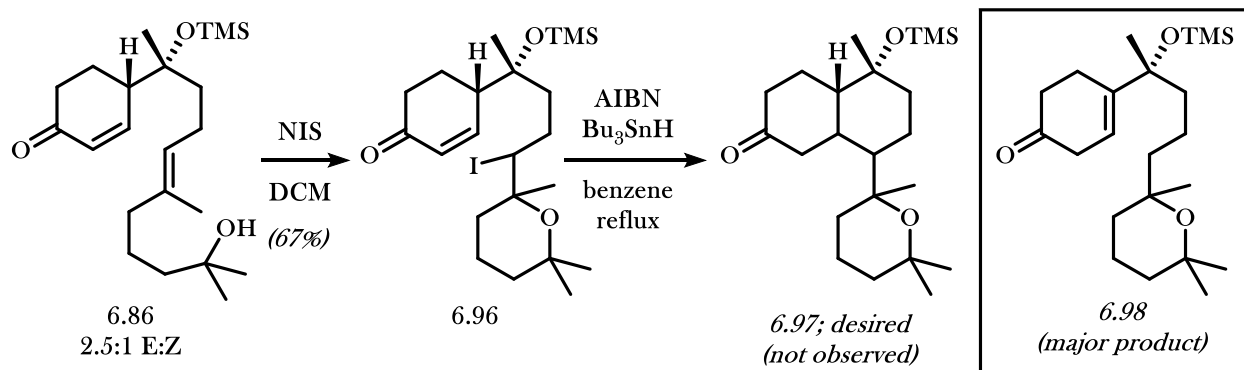
6.8.1 Rationale for Single-Electron Strategy

Metal-coordinated carbanion intermediates with α -alkoxy substituents will rapidly expel the α -leaving group due to the higher stability of anionic electron density on the more electronegative oxygen atom in the product. This leads to difficulty in generating nucleophilic species with α -alkoxides, as observed in section 6.7.2. To form a nucleophilic species capable of undergoing 1,4-addition to the pendant enone without extruding the α -alkoxide, we would have to facilitate reaction conditions that would produce a nucleophile more stable than the corresponding intermediate resulting from ring-opening. With this in mind, we turned to single-electron processes, which are unlikely to undergo β -scission to form a highly unstable oxygen-centered radical.

6.8.2 Initial Radical Precursor Formation

Initial attempts to accomplish radical cyclization from the organomercury chloride precursor **6.93** were unsuccessful; attempted homolysis of the C-Hg bond using UV light resulted in decomposition, and attempted formation of the radical using sodium borohydride resulted in rapid THP ring-opening presumably from the more electron-rich organomercury hydride complex. To form a more well-studied precursor to radical intermediates, we decided to investigate alkyl iodide **6.96** via a THP ring-closing iodoetherification (Scheme 6.13). Iodoetherification could be accomplished cleanly in 67% yield by treatment of the mono-silylated acyclic precursor **6.86** with *N*-iodosuccinimide. The resulting secondary alkyl iodide **6.96** was formed as a mixture of four diastereomers resulting from non-selective facial approach of the electrophilic iodide to the mixture of *E/Z* olefins.

Scheme 6.13 Iodoetherification and 1,5-Hydrogen Atom Abstraction



An initial attempt at radical formation with AIBN/ Bu_3SnH and subsequent addition to the conjugate acceptor produced no product. Instead, skipped enone **6.98** was isolated as the major product, likely resulting from a 1,5-hydrogen atom abstraction to form the highly stabilized tertiary allylic radical and subsequent hydrogen atom abstraction at the less-hindered position to propagate the radical chain. Attempts to change reactivity by modifying conditions, such as $\text{Et}_3\text{B}/\text{O}_2$ activation or use of Ph_3SnH as a hydrogen atom donor, failed to produce desired product.

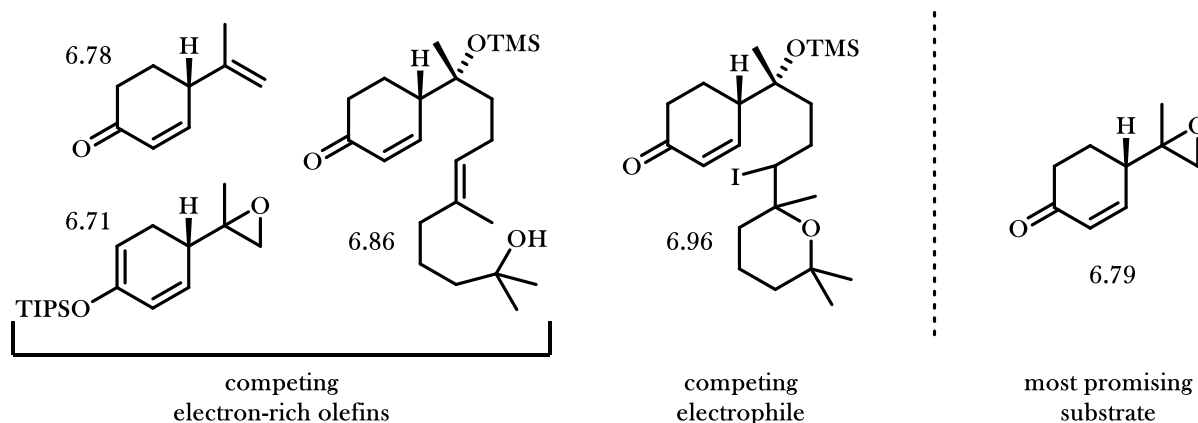
6.8.3 Attempts to Increase the Rate of 1,4-Radical Additions

Since the conditions by which the radical intermediate is formed should have no effect on the subsequent reactivity, we hoped to raise the relative rate of 1,4-radical addition by increasing the electron-accepting character of the enone. Inspired by Overman and coworkers' observation that α -chloroenones undergo 1,4-radical addition at higher rates than the analogous unfunctionalized enones,²³ we began efforts to install an α -chloride substituent on the enone.

Chloride substitutes are typically installed in the α -position of an enone via initial dichlorination and subsequent elimination of the β -chloride substituent. These conditions require high concentrations of chloride anion, limiting the functional group tolerability to those not susceptible to nucleophilic attack, and do not permit the presence of electron-rich olefins that would react a higher rate than the target enone. For these reasons, we were limited in the number of intermediates during our substrate synthesis that could

tolerate α -chloride installation (Figure 6.10). We identified **6.79** as the most promising substrate for α -chloride installation due to its absence of electron-rich olefins and easily displaced functional groups.

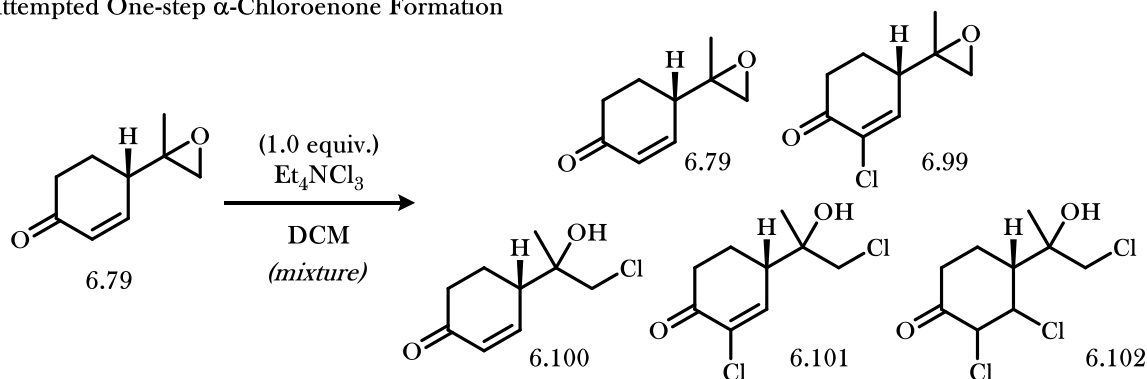
Figure 6.10 Potential Substrates for α -Chloroenone Formation



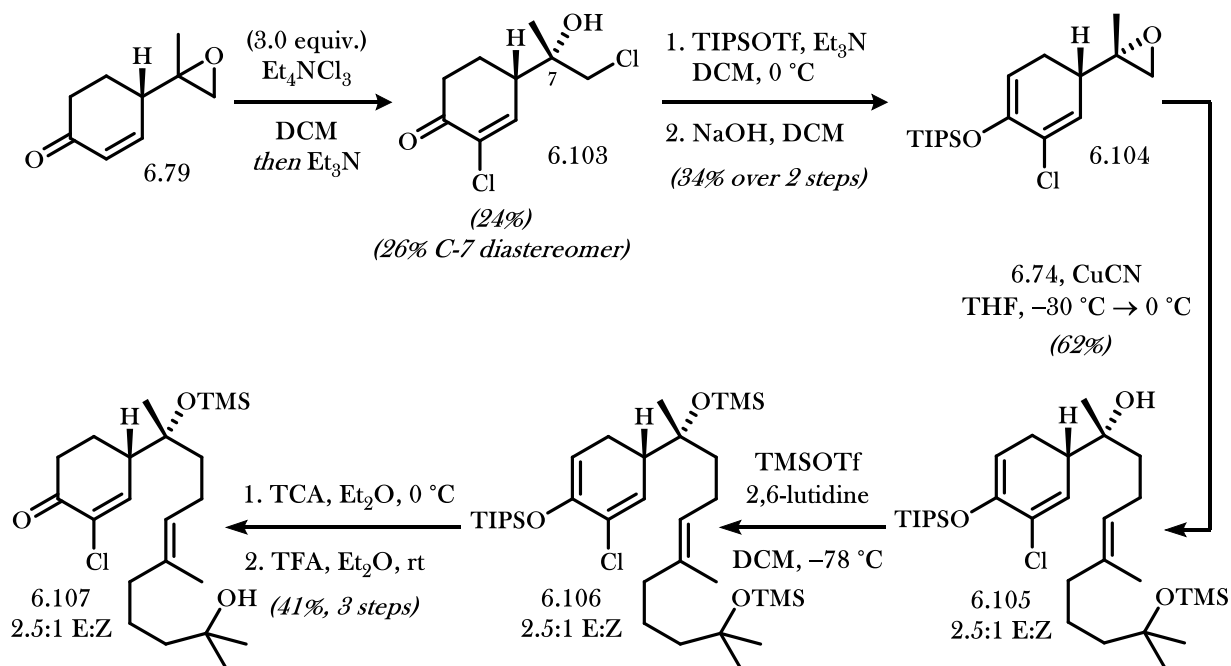
An initial attempt to α -functionalize enone **6.79** with one equivalent of Mioskowski's reagent, tetrabutylammonium trichloride, led to a complex mixture of products (Scheme 6.14a). However, the observation of a relatively clean mass spectrometry analysis of the crude product mixture beckoned for further investigation. Following careful chromatography to isolate each component of the mixture, we identified the components as a combination of mono-, di-, and tri-chloride installations involving both the enone and epoxide. Based on the presence of **6.100** in the crude mixture, we postulated that the rate of epoxide opening is comparable to enone functionalization and would therefore be difficult to prevent. Instead, we planned to form **6.99** via both a complete α -chloride installation and epoxide opening and subsequent epoxide regeneration via displacement.

Scheme 6.14 Synthesis and Testing of α -Chloroenone **6.107**

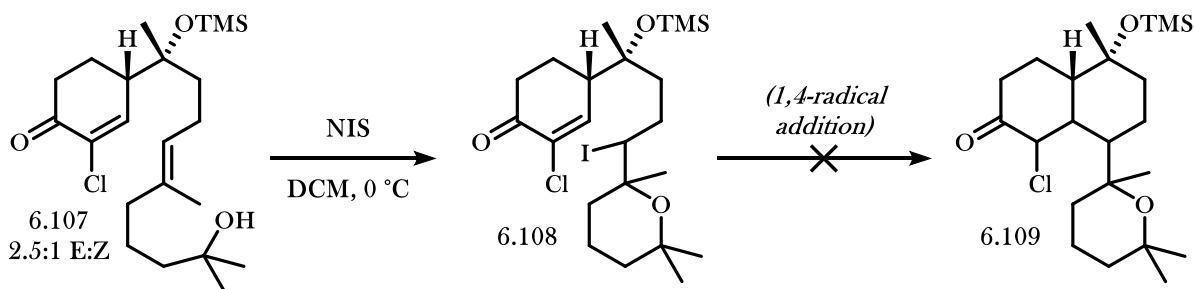
a. Attempted One-step α -Chloroenone Formation



b. Successful Multi-step α -Chloroenone Formation



c. Attempted Core Formation via Radical Cyclization



We eventually found that treatment of enone **6.79** with three equivalents of Mioskowski's reagent, followed by the addition of triethylamine to promote β -chloride elimination, accomplished clean conversion to chlorohydrin **6.103**, which could be isolated as a single diastereomer by silica gel chromatography (Scheme 6.14). Subsequent cross-conjugated dienoxysilane formation and closing of the epoxide via displacement of the primary alkyl chloride proceeded in low yield (34%), accompanied by significant decomposition. Further investigation into an efficient preparation of α -chloroenone **6.104** is warranted, but the developed conditions allowed us to prepare the epoxide-opening precursor in sufficient yields for the purpose of our investigation.

With a single diastereomer of the chlorinated epoxide fragment **6.104** in hand, we then accomplished the fragment coupling to provide **6.105** in 62% isolated yield. Subsequent silyl manipulations and iodoetherification provided the desired chloride analogue **6.108**. Unfortunately, in our attempts to promote radical conjugate addition, we exclusively observed product mixtures that again indicated 1,5-hydrogen atom abstraction. Attempts to further increase the electrophilicity of the enone using Lewis acidic conditions²⁴ failed to provide product as well.

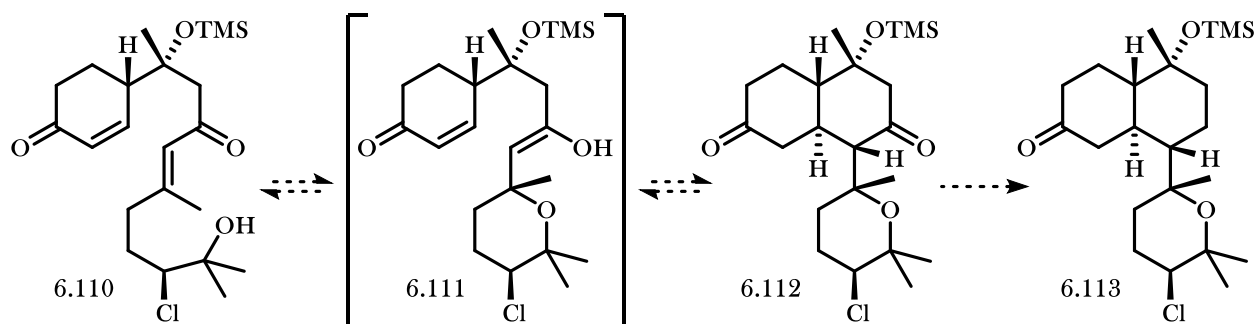
Although a radical 1,4-addition is a promising strategy for the formation of the kalihinane core, the competing 1,5-hydrogen atom abstraction pathway that proceeds at a faster rate would have to be eliminated. Substitution with an easily removed functional group, such as a halogen or ester, could prevent the formation of undesired byproduct. Unfortunately, the abstracted proton belongs to the stereocenter native to that of the S-(-)-perillaldehyde starting material, and so substitution at that position would require the development of a new strategy toward a substituted epoxide coupling partner. Accepting that radical addition from our current system could not be accomplished, we pursued an alternate strategy toward the THP-containing kalihinane core.

6.9 Ring-Closing Efforts via Michael Cascade

6.9.1 Motivation for Michael Cascade

In section 6.7, our discovery that carbanion formation in the presence of an α -alkoxide substituent leads rapidly and exclusively to THP ring opening is described. To overcome this issue, we hoped that stabilization of an anionic nucleophile formed via THP ring closure might increase its equilibrium presence and therefore might eventually permit 1,4-addition to the pendant enone. We designed acyclic precursor **6.110**, from which the kalihinane core could be formed via an oxy-Michael/Michael cascade (Figure 6.11).

Figure 6.11 Oxy-Michael/Michael Strategy Toward the Kalihinane Core



Initial conjugate addition of the tertiary alcohol of **6.110** to the acyclic enone would form enol **6.111** *in situ*, which is far more stable than an organometallic nucleophile. Furthermore, since the enol **6.111** is formed in equilibrium, extrusion of the β -leaving group would simply regenerate starting material **6.110** that could again undergo oxy-Michael addition.

6.9.2 Attempted Synthesis of Michael Cascade Precursor

Inspired by the success of the previously-developed epoxide-opening strategy, we hoped to form cascade precursor **6.110** by a similar mechanism. However, since the desired coupling product **6.110** contains a 1,3-dioxygenation motif, an epoxide-opening reaction must involve an umpolung-type nucleophile. We therefore designated dithiane precursor **6.116**, popularized by the Smith group as an acyl anion surrogate, as

a suitable nucleophile for epoxide-opening (Scheme 6.15a). Following formation of **6.118**, we hoped that hydrolysis to of the dithiane would provide acyclic precursor **6.110**.

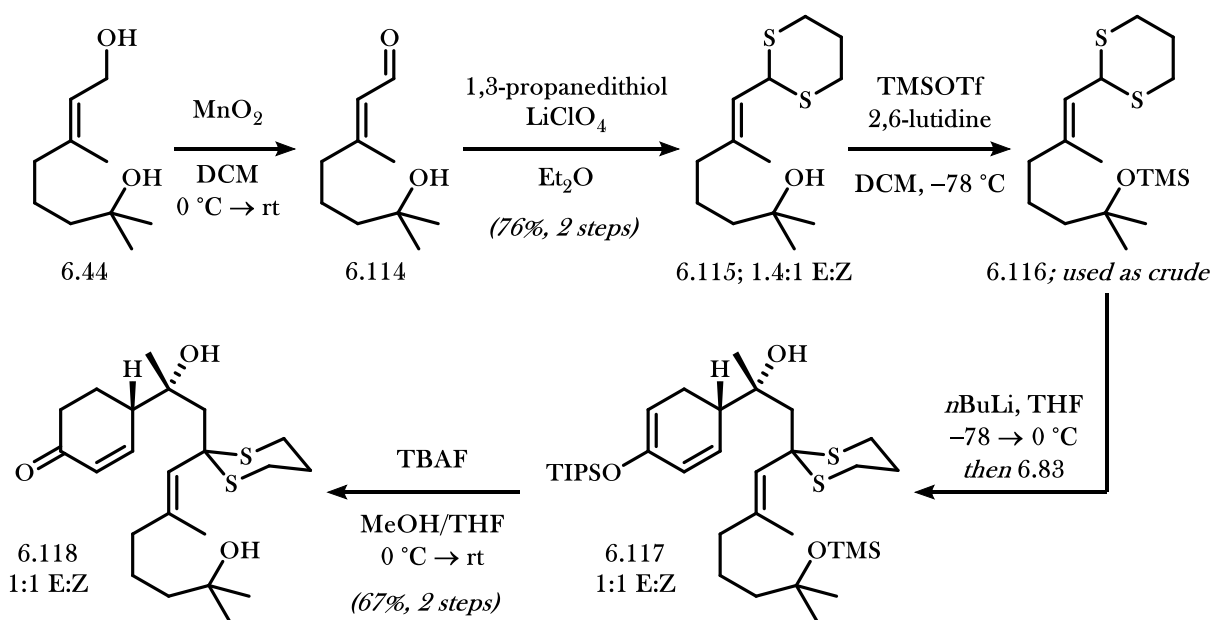
Starting again from diol **6.44**, we first prepared the α,β -unsaturated aldehyde **6.114** via oxidation with manganese (IV) oxide. We found condensation of 1,3-propanedithiol to proceed in the presence of a variety of Lewis acids to provide a 1.4:1 mixture of E:Z isomers. Dithianes prepared from the corresponding nerol-derived α,β -unsaturated aldehydes were also isolated as an identical mixture of isomers, indicating rapid isomer equilibration during the condensation reaction. The inseparable isomers were carried forward as a mixture.

Following silyl protection of the tertiary alcohol, deprotonation of the dithiane moiety with *n*-butyllithium and treatment with the stereodefined epoxide **6.83** produced coupling product **6.117**. Silyl protection of the formed tertiary alcohol of **6.117**, either in a separate pot or from the *in situ* generated alkoxide, resulted unexpectedly in decomposition. Since the dithiane represents the only difference between **6.117** and previously silylated substrates such as **6.84**, we suspect the dithiane moiety is unstable towards Lewis acids. We therefore removed the remaining silyl functionalities to form deprotected dithiane **6.118**.

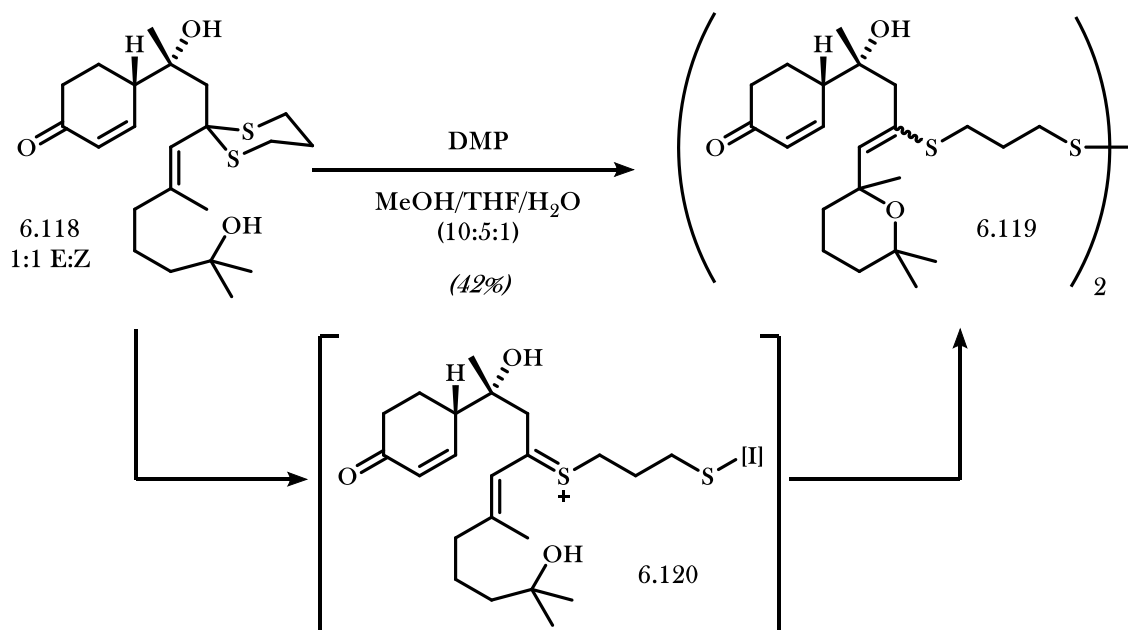
For dithiane hydrolysis to occur, a thiocarbenium intermediate **6.120** must first be formed which is vulnerable to nucleophilic attack by water (Scheme 6.15b). To increase the equilibrium presence of thiocarbenium ion, typical procedures for dithiane removal involve alkylation or oxidation of a sulfur substituent to increase its leaving group susceptibility. In our first attempt to hydrolyze the dithiane with the mild oxidant Dess–Martin periodinane in the presence of water, we instead unexpectedly observed THP ring closure and dimerization to form disulfide **6.119** in 42% yield. We suspect that the rate of intramolecular oxy-Michael addition into the α,β -unsaturated thiocarbenium **6.120** proceeds at a higher rate than intermolecular hydrolysis. Unable to complete the hydrolysis of the dithiane, we investigated methods that would instead take advantage of the vinyl sulfide products.

Scheme 6.15 Synthesis and Testing of the Michael Cascade Precursor

a. Dithiane Route Toward Acyclic Precursor 6.118



b. Attempted Oxidative Hydrolysis

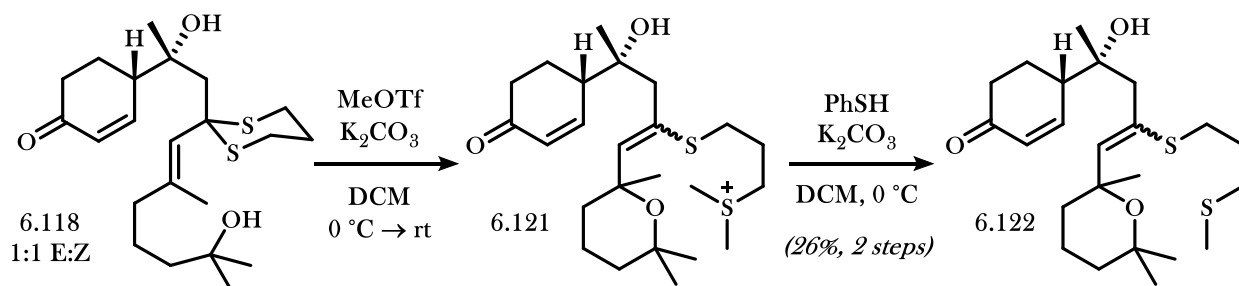


6.9.3 Use of Vinyl Sulfides as Nucleophiles for Ring-Closure

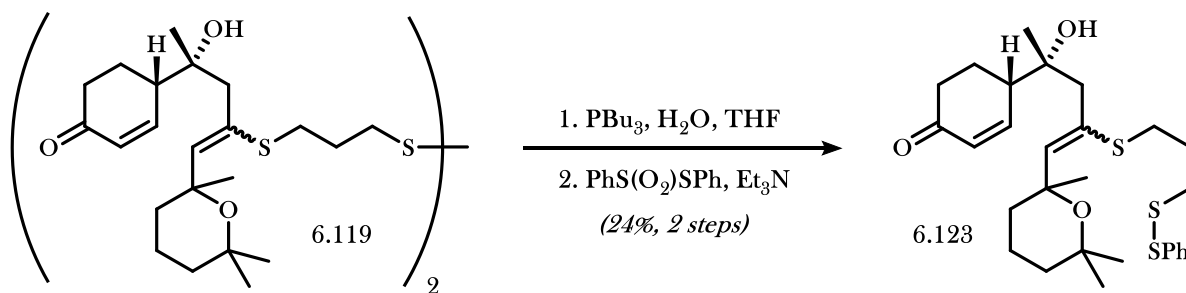
To simplify product analysis in the likely event of incomplete or nonselective reactivity for reactions involving the vinyl sulfide dimer, we developed monomer analogues as test substrates (Scheme 6.16a). Initial attempts to form methylated thioether **6.122** with methylating agents (MeI, MeOTf) were unsuccessful due to the higher rate of second methylation compared to the first. To form the desired product, *bis*-methylated product **6.121** was treated with deprotonated thiophenol to afford the monomethylated product **6.122**.

Scheme 6.16 Disulfide Analogue Synthesis and Attempted Ring Closure

a. Synthesis of the Methyl Capped Analogue



b. Synthesis of the Mixed Disulfide Analogue



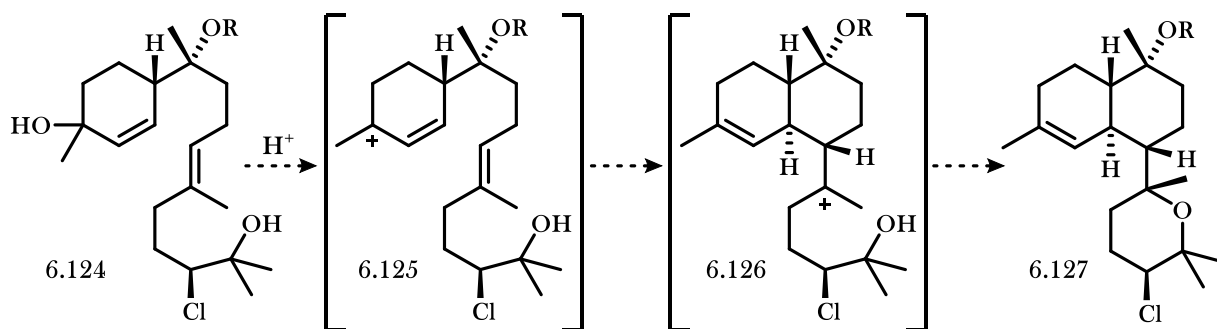
Additional analogues such as **6.123** could also be procured via tributylphosphine reduction of **6.119** to the monomeric thiols followed by trapping with electrophiles (Scheme 6.16b). Unfortunately, Lewis acid promoted vinyl sulfide 1,4-addition with all substrates under a variety of conditions led exclusively to uncharacterizable decomposition. Due to the absence of any isolable products indicating controlled reactivity after several attempts, we departed from our strategy involving dithiane intermediates.

6.10 Conclusions and Future Work

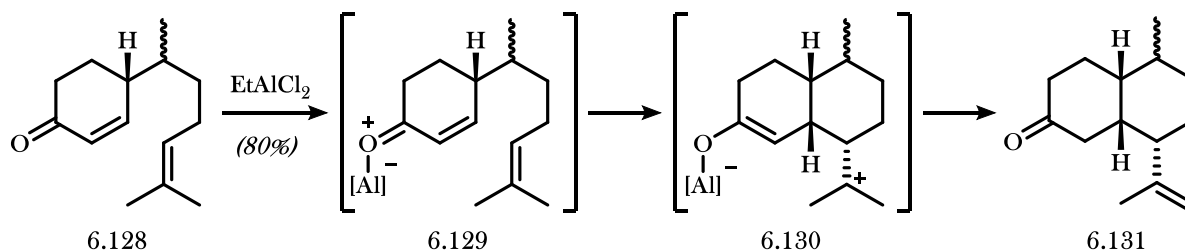
If a method can be developed to properly form the remaining C-C bond, the research described in Chapter 6 could contribute toward an efficient preparation of the THP-containing kalihinane core. Further work could focus on a π -cyclization to close the framework in one step from an acyclic precursor such as **6.124** (Scheme 6.17a). Formation of a tertiary allylic carbocation **6.125** could promote attack from the pendant trisubstituted olefin, which would subsequently be quenched by the pendant tertiary alcohol. However promising this strategy might be, work by Snider and co-workers showed that olefin attack to similar cyclohexenone fragment **6.128** resulted exclusively in *cis*-decalin formation (**6.131**; Scheme 6.17b).²⁵ Barring the unlikely case in which a longer chain length would reverse the selectivity of decalin formation, our substrate would likely proceed with the same selectivity.

Scheme 6.17 A Potential π -Cyclization to form the Kalihinane Core

a. Potential π -Cyclization Route Toward the Kalihinanes



b. Snider and Co-workers' *Cis*-decalin Formation via π -Cyclization



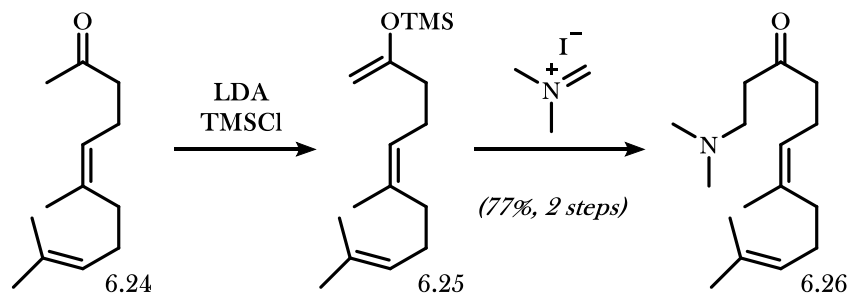
The strategy of attempting to bring together two functionalized rings connected by an acyclic chain to form a highly congested bond has proven difficult; several attempts at closing the central ring of THP-

containing kalihinanes have been unsuccessful. In future studies toward their synthesis, strategies involving outward bond-formation from a central core would likely be a safer strategy toward the kalihinanes. The work described herein not only describes several methods that accomplish key bond disconnections and set important stereocenters, but more importantly identify reactions that enable the efficient formation of the notoriously elusive kalihinane tetrahydropyran ring.

6.11 Experimental Procedures

Unless otherwise noted, all reactions were performed under an atmosphere of argon using flame-dried or oven-dried glassware and Teflon[®] coated stir bars. Anhydrous solvents were prepared by passage through columns of activated alumina. All amine bases were distilled from calcium hydride prior to use. All reagents were used as received or prepared according to literature procedures, unless otherwise noted. TMSOTf was distilled from calcium hydride prior to use. Microwave reactions were performed in a CEM Discover or Anton-Parr Monowave 300 microwave, as indicated. Reactions were monitored by thin-layer chromatography (TLC) using 250 μm EMD Millipore glass-backed TLC plates impregnated with a fluorescent dye, using UV (254 nm), KMnO_4 /heat, or *para*-anisaldehyde/heat as developing agents. Flash column chromatography was performed on EMD Millipore 60 \AA (0.040–0.063 mm) mesh silica gel, and flash column chromatography eluent mixtures are reported as %v/v. ^1H NMR spectra were recorded at 500 MHz on a Bruker 500 MHz (CRYO500 probe) instrument or at 600 MHz on a Bruker 600 MHz (AVANCE600 probe) instrument at 298 K. ^{13}C NMR spectra were recorded at 125 MHz on a Bruker 500 MHz (CRYO500 probe) at 298 K. Chemical shifts are reported in parts per million (ppm), referenced using residual undeuterated solvent (CHCl_3) at 7.26 ppm for ^1H and 77.16 ppm for ^{13}C spectroscopy. Chemical splitting is reported with the following designated peak multiplicities: ap = apparent, s = singlet, d = doublet, t = triplet, q = quartet, m = multiplet, br = broad. Coupling constants are reported in Hertz (Hz). IR spectra were recorded on a Varian 640-IR spectrometer using NaCl plates. High resolution mass spectra (HRMS) were recorded on a Waters LCT Premier spectrometer (using ESI-TOF) or Waters GCT Premier spectrometer (GC-CI), as indicated.

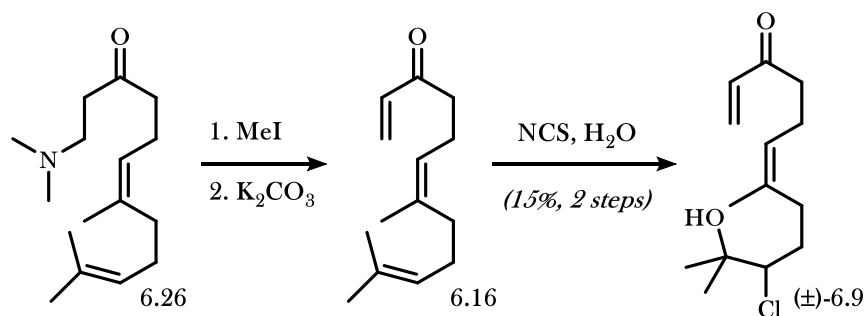
Amine 6.26



Enolate formation: To a flame dried flask with stir bar was added diisopropylamine (1.08 mL, 7.72 mmol, 1.5 equiv.) and anhydrous THF (7 mL) under argon. The solution was cooled to 0 °C and a [2.1 M] solution of *n*BuLi in hexane (3.4 mL, 7.20 mmol, 1.4 equiv.) was added dropwise over 10 minutes. After stirring for 5 minutes, the mixture was cooled to -78 °C and anhydrous THF (18.7 mL) was added slowly. At -78 °C, a solution of **6.24**²⁶ (1.0 g, 5.15 mmol, 1.0 equiv.) in anhydrous toluene (25.7 mL) was added dropwise over 1.5 hours. Following complete addition, the reaction mixture was stirred for 15 minutes and neat TMSCl (3.3 mL, 25.7 mmol, 5.0 equiv.) was added dropwise over 2 minutes. The reaction mixture was stirred for 2 hours at -78 °C, anhydrous Et₃N (3.3 mL) was added, and the cooling bath was removed. Once the reaction mixture reached 0 °C, it was poured into cold, saturated aqueous NaHCO₃ (50 mL). Hexanes (50 mL) were added, the phases were separated, and the organic phase was washed with cold, saturated aqueous NaHCO₃ (50 mL). The organic phase was dried with MgSO₄, filtered through cotton, and concentrated *in vacuo* to provide crude enoxy silane **6.25** a colorless oil (1.41 g). The crude mixture was used in the next step without purification.

Mannich reaction: To a flame dried flask with stir bar was added crude enoxy silane **6.25** (1.41 g) followed by anhydrous MeCN (8.5 mL). The solution was cooled to -40 °C, and to the solution was added N,N-dimethylmethylenimine iodide (952 mg, 5.15 mmol) portionwise as a solid. The reaction mixture was stirred for 16 hours while warming naturally to room temperature. Upon completion, the mixture was diluted with Et₂O (25 mL) and poured into saturated aqueous NaHCO₃ (25 mL). The layers were separated, and the aqueous layer was extracted with Et₂O (2 x 25 mL). The combined organic layers were dried with

MgSO₄, filtered through cotton, and concentrated *in vacuo* to a yellow oil. The crude mixture was dry loaded onto SiO₂ (*ca.* 10 g) and purified by silica gel chromatography (0–15% methanol in DCM) to afford **6.26** as an orange oil (994 mg, 77% over 2 steps): ¹H NMR (600 MHz, CDCl₃) δ 5.12–5.05 (m, 2H), 2.61–2.55 (m, 4H), 2.44 (t, *J* = 7.4 Hz, 2H), 2.29–2.21 (m, 2H), 2.23 (s, 6H), 2.07–2.01 (br, 4H), 1.68 (s, 3H), 1.67 (s, 3H), 1.60 (s, 3H).



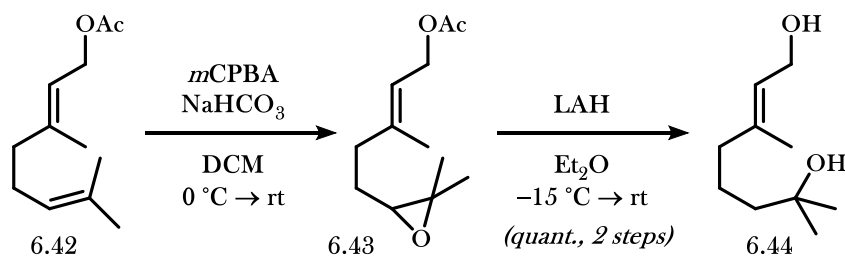
Enone (±)-6.9

Amine methylation: To a round bottom flask with stir bar was added amine **6.26** (994 mg, 3.95 mmol, 1.0 equiv.) followed by anhydrous benzene (4 mL). To the solution at room temperature was added methyl iodide (2 mL, 31.6 mmol, 8.0 equiv.). The reaction mixture was stirred for 3 hours and concentrated *in vacuo*. Hexanes (10 mL) were added, and the nonpolar layer was extracted with MeCN (3 x 10 mL). The combined MeCN extractions were filtered through cotton and concentrated *in vacuo* to a yellow solid (1.95 g). The crude ammonium mixture was used in the next step without further purification.

Ammonium elimination: To a round bottom flask with stir bar containing crude β-ammonium ketone (1.95 g) was added anhydrous MeCN (80 mL). Solid K₂CO₃ (1.09 g, 7.91 mmol) was added in two portions, and the reaction mixture was stirred for 1.5 hours. The polar layer was then extracted with hexanes (3 x 80 mL). The combined hexanes layers were then washed with [1 M] HCl (100 mL), and brine (2 x 100 mL). The organic layer was dried with MgSO₄, filtered through cotton, and concentrated *in vacuo* to provide crude **6.16** as a yellow oil (533 mg). The crude mixture was used in the next step without further purification.

Chlorohydrin formation: To a portion of crude enone **6.16** (30 mg) in a round bottom flask with stir bar was added THF (1.7 mL) and H₂O (830 μ L), and the solution was cooled to 0 °C. Solid *N*-chlorosuccinimide (20 mg, 0.145 mmol) was added in one portion with rapid stirring. The reaction mixture was warmed naturally to room temperature over 70 hours. Upon completion, EtOAc (5 mL) and H₂O (5 mL) were added. The layers were separated and the organic layer was washed with brine (2 mL). The organic layer was dried with MgSO₄, filtered through cotton, and concentrated *in vacuo* to a colorless oil. The crude mixture was purified by silica gel chromatography (20% EtOAc in hexanes) to afford **6.16** as a colorless oil (8.5 mg, 15% over 3 steps): ¹H NMR (500 MHz, CDCl₃) δ 6.35 (dd, *J* = 17.8, 10.7 Hz, 1H), 6.22 (d, *J* = 17.5 Hz, 1H), 5.83 (d, *J* = 10.5 Hz, 1H), 5.18 (t, *J* = 7.2 Hz, 1H), 3.78 (dd, *J* = 11.3, 1.4 Hz, 1H), 2.63 (td, *J* = 7.4, 1.7 Hz, 2H), 2.36 (dd, *J* = 14.6, 7.3 Hz, 2H), 2.32–2.21 (m, 2H), 2.00–1.91 (m, 1H), 1.67 (s, 3H), 1.66–1.60 (m, 1H), 1.30 (s, 3H), 1.29 (s, 3H); ¹³C NMR (126 MHz, CDCl₃) δ 200.4, 136.5, 134.8, 128.1, 125.1, 73.7, 72.7, 39.7, 31.2, 29.3, 26.3, 25.2, 23.2, 22.3.

Diol **6.44**

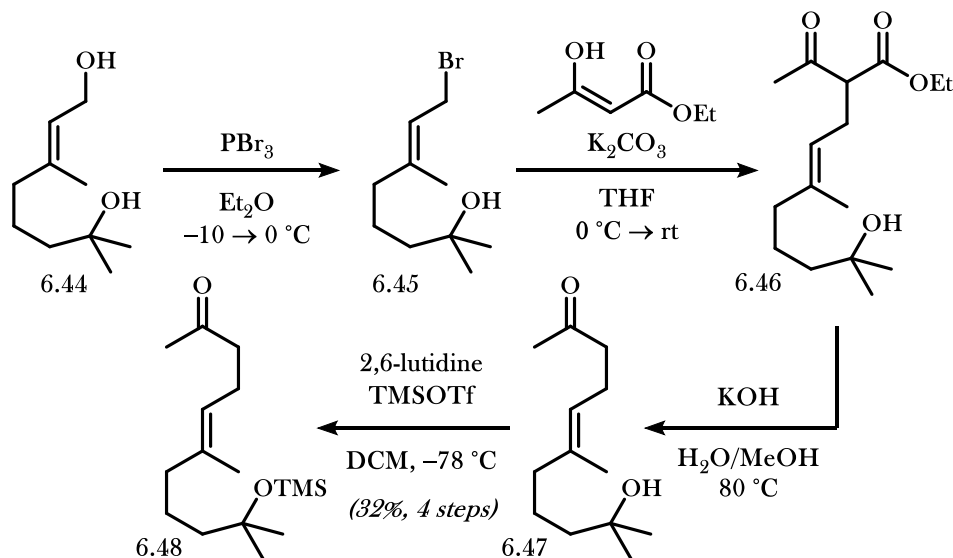


Epoxidation: To a round bottom flask with stir bar was added geranyl acetate **6.42** (15 mL, 70 mmol, 1.0 equiv.) and 250 mL of DCM, and the solution was cooled to 0 °C. A solution of *m*CPBA (19 g, 77 mmol, 1.1 equiv.) in DCM (100 mL) was added to the reaction mixture via dropping funnel over 30 minutes. After stirring for 30 minutes, a solution of *m*CPBA (1 g, 4.0 mmol, 0.06 equiv.) in DCM (30 mL) was added dropwise, and the reaction mixture was stirred for an additional 15 minutes. Upon completion, saturated aqueous sodium thiosulfate (50 mL) was added and the mixture was stirred vigorously for 30 minutes. The

layers were then separated, and the organic layer was washed with brine (100 mL). The organic phase was dried with MgSO₄, filtered through cotton, and concentrated *in vacuo* to provide crude **6.43** a colorless oil. The crude mixture was used in the next step without further purification.

Deprotection/epoxide opening: To a round bottom flask with stir bar was added Et₂O (200 mL) and LAH (6.7 g, 176 mmol). To the suspension at -15 °C was added a solution of crude epoxide **6.48** in Et₂O (150 mL) over 30 minutes. After 30 minutes at -15 °C, the bath was removed and the reaction was stirred for 6 hours. At this time, LAH (1.3 g, 34.1 mmol) was added as a solid to the reaction mixture at room temperature. The reaction mixture was stirred for 16 hours, at which time additional LAH (0.7 g, 18.4 mmol) was added as a solid at room temperature. After stirring for 10 hours, the reaction mixture was diluted with Et₂O (200 mL) and cooled to 0 °C. H₂O (8.7 mL), 15% aqueous NaOH (8.7 mL), and H₂O (26.1 mL) were added sequentially and the mixture was stirred for 30 minutes. MgSO₄ was added, the suspension was filtered, the filtrate was concentrated *in vacuo* to provide **6.44** as a pure colorless oil (12.9 g, *quant.*).

Ketone 6.48



Allyl bromide formation: To a flame dried round bottom flask with stir bar was added diol **6.44** (2.22 g, 12.9 mmol, 1.0 equiv.) and anhydrous Et₂O (6.5 mL) under argon. The solution was cooled to -10 °C,

and PBr_3 (612 μL , 2.90 mmol, 0.5 equiv.) was added dropwise over 20 minutes. The reaction mixture was stirred for 1 hour, warming naturally to 0 °C. Cold H_2O (10 mL) was poured into the reaction mixture, and the mixture was extracted with Et_2O (3 x 10 mL). The combined organic layers were washed with brine (10 mL), then dried with MgSO_4 , filtered through cotton, and concentrated *in vacuo* to provide crude **6.45** as a yellow oil (2.14 g). The crude mixture was used in the next step without purification.

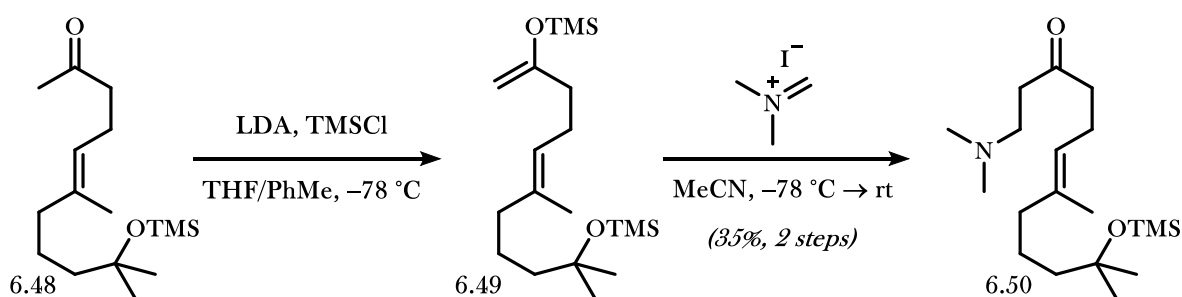
β -ketoester allylation: To a flame dried round bottom flask with stir bar was added methyl acetoacetate (1.16 mL, 9.10 mmol) and anhydrous THF (59 mL) under argon. The solution was cooled to 0 °C and NaH (437 mg, 60% w/w, 10.9 mmol) was added portionwise. The reaction mixture was then warmed to room temperature and stirred for 30 minutes. A solution of crude allyl bromide **6.45** (2.14 g) in anhydrous THF (14.5 mL) was then added dropwise over 10 minutes, and the reaction mixture was stirred for 16 hours at room temperature. Upon completion, the reaction mixture was cooled to 0 °C, and saturated aqueous NH_4Cl (100 mL) was added. The aqueous layer was extracted with EtOAc (3 x 100 mL), and the combined organic layers were washed with brine (100 mL), dried with MgSO_4 , filtered through cotton, and concentrated *in vacuo* to provide **6.46** as a yellow oil (2.27 g). The crude mixture was used in the next step without purification.

Decarboxylation: To a round bottom flask with stir bar was added β -ketoester **6.46** (2.27 g) and methanol (10 mL). To the solution was added a [5 M] aqueous solution of KOH (5 mL, 5.88 mmol), and the reaction mixture was stirred at 80 °C for 2 hours. Upon completion, the reaction mixture was cooled to room temperature, and saturated aqueous NH_4Cl (20 mL) was added. The mixture was extracted with Et_2O (3 x 20 mL), and the combined extracts were washed sequentially with NaHCO_3 (20 mL) and brine (20 mL). The organic extracts were dried with MgSO_4 , filtered through cotton, and concentrated *in vacuo* to provide **6.47** as a yellow oil (1.60 g). The crude mixture was used in the next step without purification.

Tertiary Alcohol Silylation: To a flame dried round bottom flask with stir bar was added alcohol **6.47** (1.60 g) and DCM (75 mL) under argon. The solution was cooled to -78 °C, and 2,6-lutidine (2.6 mL, 22.6 mmol) and TMSOTf (2.0 mL, 11.3 mmol) were added sequentially. The reaction mixture was stirred 1 hour

at $-78\text{ }^{\circ}\text{C}$. Upon completion, Et_3N (1 mL) and methanol (2.5 mL) were added, and the reaction mixture was warmed to room temperature. A 10% solution of EtOAc/hexanes (100 mL) was added, and the organic layer was washed sequentially with H_2O (50 mL), a 10% aqueous solution of citric acid (50 mL), and brine (50 mL). The organic layer was dried with MgSO_4 , filtered through cotton, and concentrated *in vacuo* to provide crude **6.48** as a yellow oil (1.60 g). The crude mixture was separated by silica gel chromatography (10% EtOAc in hexanes + 1% Et_3N to 50% EtOAc in hexanes + 1% Et_3N) to provide **6.48** as a colorless oil (1.17 g, 32% over 4 steps): ^1H NMR (500 MHz, CDCl_3) δ 5.07 (t, $J = 6.9$ Hz, 1H), 2.46 (t, $J = 7.5$ Hz, 2H), 2.27 (dd, $J = 14.5, 7.3$ Hz, 2H), 2.13 (s, 3H), 1.94 (dd, $J = 7.5, 6.6$ Hz, 2H), 1.46–1.32 (m, 4H), 1.19 (s, 6H), 0.09 (s, 9H).

Amine 6.50

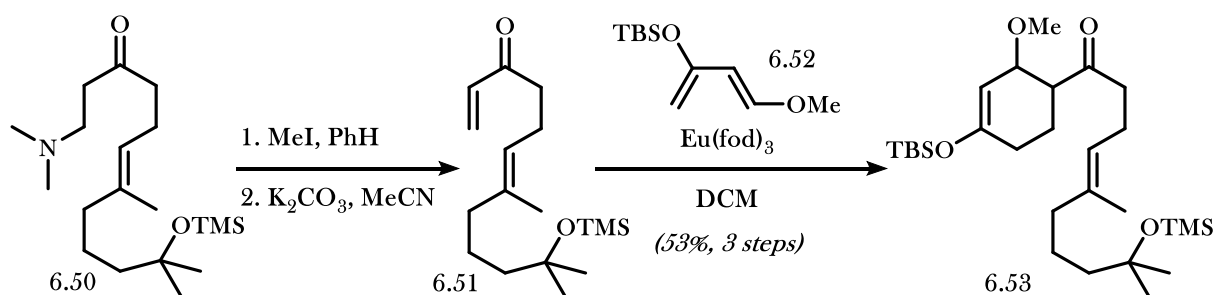


Enolate formation: To a flame dried flask with stir bar was added diisopropylamine (813 μL , 5.80 mmol, 1.4 equiv.) and anhydrous THF (5 mL) under argon. The solution was cooled to $0\text{ }^{\circ}\text{C}$ and a [2.8 M] solution of *n*BuLi in hexane (1.94 mL, 5.41 mmol, 1.3 equiv.) was added dropwise over 10 minutes. After stirring for 5 minutes, the mixture was cooled to $-78\text{ }^{\circ}\text{C}$ and anhydrous THF (14 mL) was added slowly. At $-78\text{ }^{\circ}\text{C}$, a solution of **6.48** (1.17 g, 4.11 mmol, 1.0 equiv.) in anhydrous toluene (19 mL) was added dropwise over 1.5 hours. Following complete addition, the reaction mixture was stirred for 15 minutes and neat TMSCl (2.5 mL, 19.3 mmol, 4.7 equiv.) was added dropwise over 2 minutes. The reaction mixture was stirred for 2 hours at $-78\text{ }^{\circ}\text{C}$, anhydrous Et_3N (3.0 mL) was added, and the cooling bath was removed. Once the reaction mixture reached $0\text{ }^{\circ}\text{C}$, it was poured into cold saturated aqueous NaHCO_3 (50 mL). Hexanes (50 mL) were added, the phases were separated, and the organic phase was washed with cold saturated aqueous NaHCO_3

(50 mL). The organic phase was dried with MgSO_4 , filtered through cotton, and concentrated *in vacuo* to provide crude **6.49** as a colorless oil. The crude mixture was used in the next step without purification.

Mannich reaction: To a flame dried flask with stir bar was added crude enoxy silane **6.49** followed by anhydrous MeCN (6.9 mL). The solution was cooled to $-40\text{ }^\circ\text{C}$, and to the solution was added N,N-dimethylmethyleiminium iodide (760 mg, 4.11 mmol) portionwise as a solid. The reaction mixture was stirred for 16 hours while warming naturally to room temperature. Upon completion, the mixture was diluted with Et_2O (25 mL) and poured into saturated aqueous NaHCO_3 (25 mL). The layers were separated, and the aqueous layer was extracted with Et_2O ($2 \times 25\text{ mL}$). The combined organic layers were dried with MgSO_4 , filtered through cotton, and concentrated *in vacuo* to provide crude **6.50** as a yellow oil (1.32 g). The crude mixture was purified by silica gel chromatography (0–15% methanol in DCM) to afford **6.50** as a yellow oil (495 mg, 35% over 2 steps): $^1\text{H NMR}$ (500 MHz, CDCl_3) δ 5.09–5.03 m, 1H), 2.72–2.63 (m, 4H), 2.47 (t, 7.4 Hz, 2H), 2.31–2.22 (m, 8H), 1.93 (dd, $J=7.5, 6.5\text{ Hz}$, 2H), 1.60 (s, 3H), 1.45–1.31 (m, 4H), 1.19 (s, 6H), 0.09 (s, 9H).

Ketone 6.53



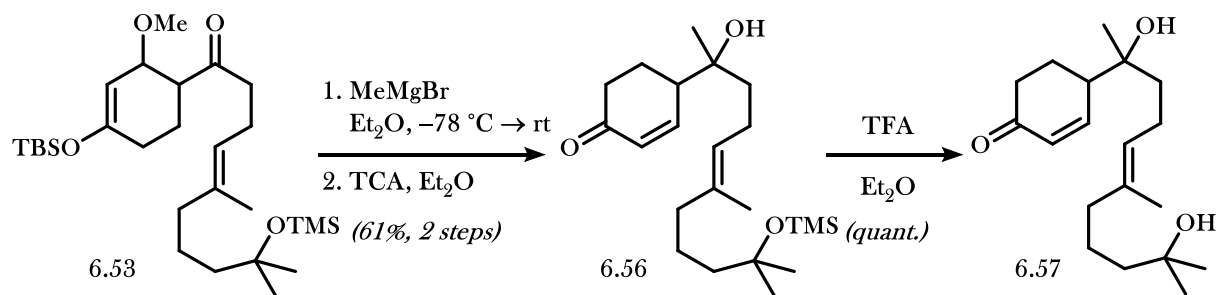
Amine methylation: To a round bottom flask with stir bar was added amine **6.50** (495 mg, 1.45 mmol, 1.0 equiv.) followed by anhydrous benzene (1.5 mL). To the solution at room temperature was added methyl iodide (721 μL , 11.6 mmol, 8.0 equiv.). The reaction mixture was stirred for 3 hours and concentrated *in vacuo*. Hexanes were added, and the nonpolar layer was extracted with MeCN ($3 \times 10\text{ mL}$). The combined

MeCN extractions were filtered through cotton and concentrated *in vacuo* to a yellow solid. The crude mixture was used in the next step without further purification.

Ammonium elimination: To a round bottom flask with stir bar containing crude β -ammonium ketone was added anhydrous MeCN (29 mL). Solid K_2CO_3 (400 mg, 2.90 mmol) was added in two portions, and the reaction mixture was stirred for 1.5 hours. The polar layer was then extracted with hexanes (3 x 50 mL). The combined hexanes layers were then washed with [1 M] HCl (50 mL), and brine (2 x 50 mL). The organic layer was dried with $MgSO_4$, filtered through cotton, and concentrated *in vacuo* to provide enone **6.51** as a yellow oil (300 mg). The crude mixture was used in the next step without further purification.

Diels-Alder cycloaddition: To a round bottom flask with stir bar was added crude enone **6.51** (300 mg), DCM (170 μ L), diene **6.52**²⁷ (553 mg, 2.58 mmol), and $Eu(fod)_3$ (52 mg, 0.05 mmol) under argon. The reaction mixture was stirred for 36 hours at room temperature. The reaction mixture was then diluted with Et_2O (1 mL) and H_2O (1 mL). The layers were separated, and the aqueous layer was extracted with Et_2O (2 x 1 mL). The combined organic extracts were dried with $MgSO_4$, filtered through cotton, and concentrated *in vacuo*. The crude mixture was purified by silica gel chromatography (5% EtOAc in hexanes) to afford **6.53** as a colorless oil (396 mg, 53% over 3 steps): 1H NMR (500 MHz, $CDCl_3$) δ 5.07 (t, J = 6.5 Hz, 1H), 4.98 (s, 1H), 4.25–4.15 (m, 1H), 3.28 (s, 3H), 2.62 (ddd, J = 10.9, 7.9, 3.2 Hz, 1H), 2.59–2.51 (m, 2H), 2.33–2.22 (m, 2H), 2.19–2.08 (m, 1H), 2.05–1.89 (m, 3H), 1.75–1.63 (m, 2H), 1.60 (s, 3H), 1.46–1.32 (m, 4H), 1.18 (s, 6H), 0.91 (s, 9H), 0.14 (s, 6H), 0.09 (s, 9H); ^{13}C NMR (126 MHz, $CDCl_3$) δ 212.4, 153.2, 136.4, 122.7, 103.5, 76.8, 73.9, 55.8, 51.7, 44.3, 42.8, 40.0, 29.8, 29.0, 25.6, 23.2, 22.6, 22.0, 18.0, 15.8, 2.6, -4.4, -4.5; IR (thin film) 2932, 2859, 1714, 1663, 1250, 839 cm^{-1} ; HRMS (ESI) m/z calculated for $C_{28}H_{54}O_4Si_2$ $[M+Na]^+$ 533.3458, found 533.3433.

Enone 6.57



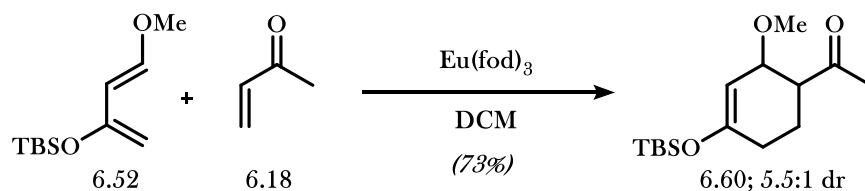
Grignard addition: To a flame dried vial with stir bar was added ketone **6.53** (200 mg, 0.39 mmol, 1.0 equiv.) and anhydrous Et₂O (560 μ L) under argon. The solution was cooled to -78 °C, and a [2.90 M] solution of MeMgBr in Et₂O (0.39 mmol, 1.0 equiv.) was added dropwise. The bath was removed and the reaction mixture was allowed to warm to room temperature. The reaction mixture was then diluted with Et₂O (2 mL) and saturated aqueous NH₄Cl (2 mL) was added. The layers were separated and the aqueous layer was extracted with Et₂O (2 x 2 mL). The combined organic extracts were washed with NaHCO₃ (1 mL) and brine (1 mL). The extracts were dried with MgSO₄, filtered through cotton, and concentrated *in vacuo* to a yellow oil (198 mg). The crude mixture was used in the next step without purification.

Mono-desilylation: To a vial with stir bar was added the crude enoxy silane (198 mg) and anhydrous Et₂O (3.7 mL) under argon at 0 °C. Trichloroacetic acid (316 mg, 1.88 mmol, 5.0 equiv., recrystallized from benzene) was added as a solid with vigorous stirring, and the reaction mixture was stirred at 0 °C for 1 hour. EtOAc (5 mL) and saturated aqueous NaHCO₃ (5 mL) were added, the layers were separated, and the organic layer was washed with brine (2 mL). The organic layer was dried with MgSO₄, filtered through cotton, and concentrated *in vacuo* to provide enone **6.56** as a yellow oil (180 mg). The crude mixture was purified by silica gel chromatography (15–25% EtOAc in hexanes) to afford pure **6.56** as a colorless oil (41.5 mg, 29%) and a mixture of diastereomers of **6.56** as a colorless oil (45.5 mg, 32%).

[Note: The mixture of mono-silylated material was deprotected and used for a span of explorational work, but a portion of the single diastereomer isolated was carried forward for the purpose of characterization.]

Silyl ether removal: To a vial with stir bar was added a portion of a single diastereomer of enone **6.56** (10 mg) and anhydrous Et₂O (260 μ L) under argon. TFA (25 μ L) was then added dropwise with vigorous stirring. The reaction mixture was stirred for 1 hour at room temperature. Upon completion, Et₂O (1 mL) and saturated aqueous NaHCO₃ (1 mL) were added, the layers were separated, and the aqueous layer was extracted with Et₂O (2 x 1 mL). The combined organic layers were then washed with brine (1 mL), dried with MgSO₄, filtered through cotton, and concentrated *in vacuo* to provide **6.57** as a thin film. The crude mixture was purified by silica gel chromatography (50% EtOAc in hexanes) to provide pure **6.57** as a colorless oil (9.1 mg, *quant.*): ¹H NMR (500 MHz, CDCl₃) δ 7.20 (d, *J* = 10.5 Hz, 1H), 6.09 (dd, *J* = 10.5, 2.8 Hz, 1H), 5.16 (t, *J* = 6.9 Hz, 1H), 2.58–2.50 (m, 2H), 2.37 (ddd, *J* = 16.7, 14.5, 5.1 Hz, 1H), 2.14 (dd, *J* = 15.3, 7.6 Hz, 2H), 2.11–2.04 (m, 1H), 1.99 (dd, *J* = 7.3, 6.3 Hz, 2H), 1.78–1.68 (m, 1H), 1.63 (s, 3H), 1.62–1.54 (m, 2H), 1.50–1.39 (m, 4H), 1.21 (s, 6H), 1.14 (s, 3H); ¹³C NMR (126 MHz, CDCl₃) δ 199.7, 152.0, 136.2, 130.2, 123.8, 74.1, 71.0, 46.1, 43.4, 40.0, 40.0, 37.4, 29.3, 24.7, 23.7, 22.6, 21.9, 16.0; IR (film) 3422 (br), 2936, 2968, 1669, 1380 cm⁻¹; HRMS (ESI) *m/z* calculated for C₁₉H₃₂O₃ [M + Na]⁺ 331.2249, found 331.2244.

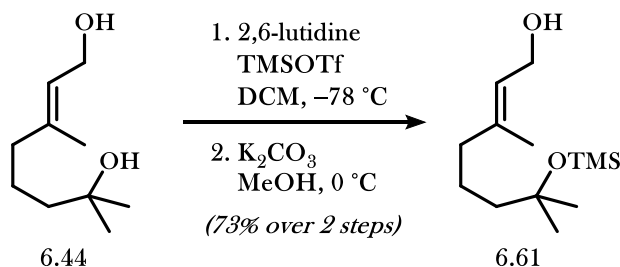
Ketone 6.60



To a flame dried round bottom flask with stir bar was added diene **6.52**²⁸ (2.96 g, 13.8 mmol, 1.0 equiv.) and anhydrous DCM (5.9 mL). Methyl vinyl ketone **6.18** (2.3 mL, 27.6 mmol, 2.0 equiv.) was added,

followed by $\text{Eu}(\text{fod})_3$ (715 mg, 0.69 mmol, 0.05 equiv.). The flask was sealed and the reaction mixture was stirred for 8 hours at room temperature. Upon completion, the mixture was diluted with DCM (200 mL) and saturated aqueous NaHCO_3 (150 mL). The layers were separated, and the aqueous layer was extracted with DCM (2 x 200 mL). The combined organic extracts were dried with MgSO_4 , filtered through cotton, and concentrated *in vacuo* to provide crude **6.60** as a yellow oil. The crude mixture was purified by silica gel chromatography (10–18% EtOAc in hexanes) to afford a 5.5:1 mixture of diastereomers of **6.60** as a slightly yellow oil (2.86 g, 73%): ^1H NMR (500 MHz, CDCl_3) δ 5.18 (d, $J = 5.3$ Hz, 0.15H, minor) 5.01 (s, 0.81H, major), 4.29 (d, $J = 5.8$ Hz, 0.81H, major), 4.23 (t, $J = 5.0$ Hz, 0.17H, minor), 3.32 (s, 2.52H, major), 3.27 (s, 0.47H, minor), 2.69 (ddd, $J = 10.7, 7.6, 3.4$ Hz, 0.81H, major), 2.45 (dt, $J = 12.3, 3.7$ Hz, 0.15H, minor), 2.25 (s, 2.48H, major), 2.21 (s, 0.47H, minor), 2.19–1.68 (m, 4H), 0.94–0.88 (m, 9H), 0.20–0.08 (m, 6H); ^{13}C NMR (126 MHz, CDCl_3) δ 210.7, 155.4, 103.3, 101.3, 76.7, 73.8, 55.7, 55.5, 52.2, 52.1, 29.8, 29.6, 28.9, 28.0, 25.64, 25.58, 23.0, 18.8, 18.0, -3.6, -4.4, -4.5; IR (film) 2930, 2894, 2858, 1714, 1662, 1364, 1192 cm^{-1} ; HRMS (ESI) m/z calculated for $\text{C}_{15}\text{H}_{28}\text{O}_3\text{Si}$ $[\text{M} + \text{Na}]^+$ 307.1705, found 307.1708.

Allylic Alcohol 6.61

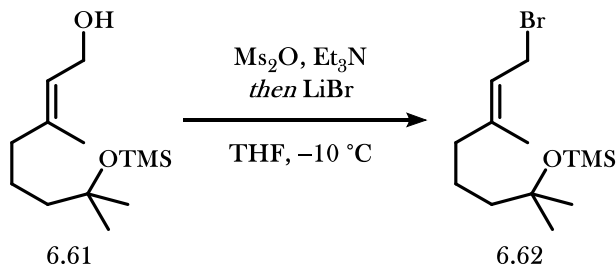


Bis-silylation: To a flame dried round bottom flask with stir bar was added diol **6.44** (6.0 g, 35 mmol, 1.0 equiv.) and DCM (350 mL) under argon. The solution was cooled to -78°C , and 2,6-lutidine (20.2 mL, 175 mmol, 5.0 equiv.) and TMSOTf (25.0 g, 112 mmol, 3.2 equiv.) were added sequentially. The reaction mixture was stirred for 5 hours at -78°C . Upon completion, Et_3N (20 mL) and methanol (120 mL) were added, and the reaction mixture was warmed to room temperature. A 10% solution of EtOAc/hexanes (500

mL) was added, and the organic layer was washed sequentially with H₂O (250 mL), a 10% aqueous solution of citric acid (250 mL), and brine (250 mL). The organic layer was dried with MgSO₄, filtered through cotton, and concentrated *in vacuo* to provide a colorless oil (9.1 g). The crude mixture was used in the next step without purification.

Mono-desilylation: To a flame dried round bottom flask with stir bar was added the crude disilane followed by MeOH (115 mL). The solution was cooled to 0 °C, and solid potassium carbonate (7.9 g, 57.4 mmol) was added in one portion. The reaction mixture was stirred for 30 minutes at 0 °C. Upon completion, saturated aqueous NH₄Cl (200 mL) was added, and the mixture was poured into DCM (300 mL). The layers were separated, and the aqueous layer was extracted with DCM (2 x 200 mL). The combined organic layers were dried with MgSO₄, filtered through cotton, and concentrated *in vacuo* to provide crude **6.61** as a slightly yellow oil. The crude mixture was purified by silica gel chromatography (10–20% EtOAc in hexanes) to afford **6.61** as a colorless oil (5.1 g, 73% over 2 steps): ¹H NMR (500 MHz, CDCl₃) δ 5.41 (t, *J* = 6.8 Hz, 1H), 5.15(dd, *J* = 5.6, 5.0 Hz, 2H), 2.00 (d, *J* = 7.8, 6.9 Hz, 2H), 1.67 (s, 3H), 1.51–1.42 (m, 2H), 1.42–1.35 (m, 2H), 1.20 (s, 6H), 0.09 (s, 9H); ¹³C NMR (126 MHz, CDCl₃) δ 140.0, 123.3, 73.9, 59.4, 44.3, 39.9, 29.8, 22.3, 16.1, 2.6; IR (film) 3326 (br), 2969, 1249, 1036 cm⁻¹; HRMS (ESI) *m/z* calculated for C₁₃H₂₈O₂Si [M + Na]⁺ 267.1756, found 267.1762.

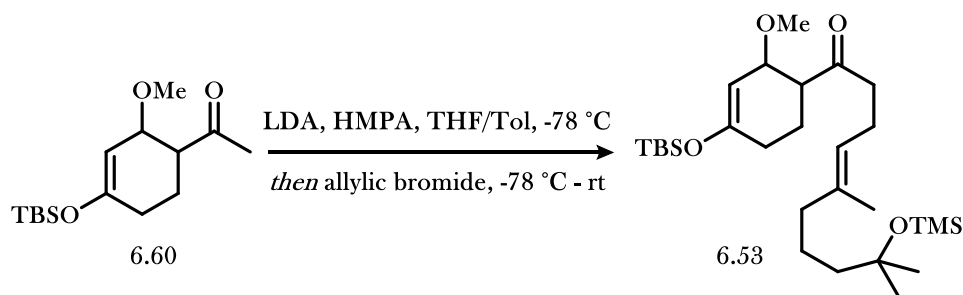
Allylic Bromide 6.62



To a flame dried vial with stir bar was added allylic alcohol **6.61** (51.3 mg, 0.21 mmol, 1.0 equiv.) and anhydrous THF (700 μL) under argon. The solution was cooled to -15 °C, and Et₃N (44 μL, 0.32 mmol,

1.5 equiv.) was added, followed by portionwise addition of solid MgSO_4 (43.9 mg, 0.25 mmol, 1.2 equiv.). After stirring for one hour at a temperature below $-10\text{ }^\circ\text{C}$, a solution of LiBr (23.7 mg, 0.27 mmol, 1.3 equiv.) in anhydrous THF (140 μL) was added dropwise. Following addition, the cold bath was removed and the reaction mixture was allowed to warm to room temperature naturally. After 2.25 hours, H_2O (1.3 mL) and Et_2O (2.2 mL) were added sequentially, and the layers were separated. The aqueous layer was extracted with Et_2O (2 x 2 mL), and the combined organic layers were dried with MgSO_4 , filtered through cotton, and concentrated *in vacuo* to provide crude **6.62** as a colorless oil (40.0 mg). The allylic bromide **6.62** could not be purified by silica gel chromatography and was therefore used directly in the next step.

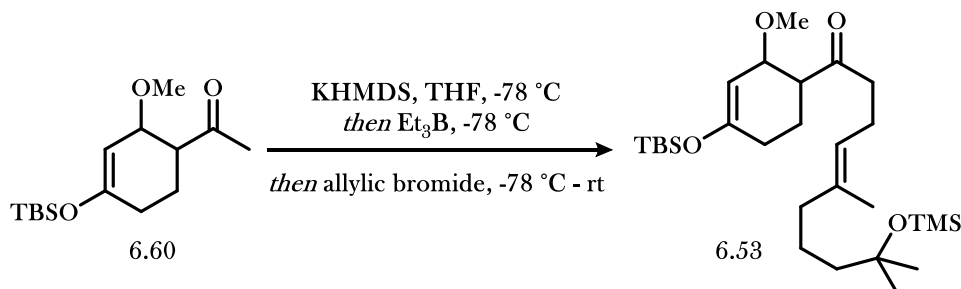
Ketone **6.53** via Lithium Enolate Allylation²⁹



To a flame dried round bottom flask with stir bar was added diisopropylamine (18 μL , 0.13 mmol, 1.2 equiv.) and anhydrous THF (250 μL) under argon. The solution was cooled to $-78\text{ }^\circ\text{C}$, and a [2.35 M] solution of *n*BuLi in hexanes (54 μL , 0.13 mmol, 1.2 equiv.) was added dropwise. After stirring for 20 minutes, a solution of ketone **6.60** (30 mg, 0.11 mmol, 1.0 equiv.) in anhydrous THF (800 μL) was added dropwise over 20 minutes. After stirring for an additional 30 minutes at $-78\text{ }^\circ\text{C}$, HMPA (40 μL , 0.23 mmol, 2.2 equiv.) was added. After stirring for 20 minutes at $-78\text{ }^\circ\text{C}$, a solution of allylic bromide **6.62** (40.0 mg, 0.13 mmol, 1.2 equiv.) in anhydrous THF (300 μL) was added dropwise. The reaction mixture was warmed to $0\text{ }^\circ\text{C}$ over the course of 2 hours, the bath was removed, and the reaction mixture was stirred for an additional 4 hours. Upon completion, the reaction mixture was quenched by the addition of H_2O (2 mL), and the mixture was extracted with Et_2O (3 x 2 mL). The combined organic extracts were washed with brine (2 mL),

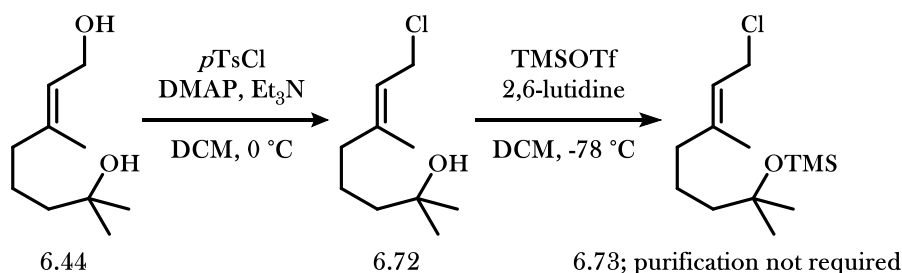
dried with MgSO_4 , filtered through cotton, and concentrated *in vacuo* to provide crude **6.53** a film. The crude product mixture was purified by silica gel chromatography (5% EtOAc in hexanes) to afford a **6.53** as a colorless oil (15 mg, 28%). The spectra obtained matched those reported above.

Ketone **6.53** via Enol Borate Allylation³⁰



To a flame dried vial with stir bar was added solid KHMDS (23 mg, 0.12 mmol, 1.1 equiv.) under argon. Anhydrous THF (150 μL) was added and the mixture was cooled to $-78\text{ }^\circ\text{C}$. A solution of ketone **6.60** (30 mg, 0.11 mmol, 1.0 equiv.) in anhydrous THF (200 μL) was then added over 15 minutes, and the reaction mixture was stirred for an additional 30 minutes at $-78\text{ }^\circ\text{C}$. A [1.0 M] solution of triethylborane in hexanes (116 μL , 0.12 mmol, 1.1 equiv.) was added dropwise, turning the reaction mixture bright yellow. After stirring at $-78\text{ }^\circ\text{C}$ for 15 minutes, a solution of allylic bromide **6.62** (65 mg, 0.21 mmol, 2.0 equiv.) in anhydrous THF (100 μL) was added. The reaction mixture was warmed to $-20\text{ }^\circ\text{C}$ and stirred for 5.5 hours. Upon completion, saturated aqueous NH_4Cl (1 mL) was added, and the mixture was warmed to room temperature. The aqueous phase was extracted with Et_2O (3 x 1 mL), and the combined organic extracts were washed with brine (1 mL). The organic phase was dried with MgSO_4 , filtered through cotton, and concentrated *in vacuo* to provide crude **6.53** a slightly yellow oil. The crude product mixture was purified by silica gel chromatography (4–5% EtOAc in hexanes) to afford a **6.53** as a colorless oil (20.6 mg, 39%). The spectra obtained matched those reported above.

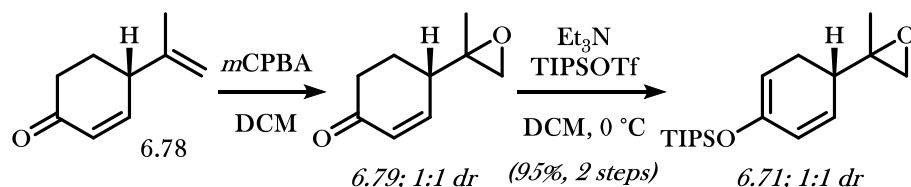
Allylic Chloride 6.73



*Allylic chloride formation:*³¹ To a flame dried round bottom flask with stir bar was added diol **6.44** (2.0 g, 11.61 mmol, 1.0 equiv.) and anhydrous DCM (8 mL) under argon. The solution was cooled to 0 °C, and DMAP (851 mg, 6.97 mmol, 0.6 equiv.), *p*-toluenesulfonyl chloride (2.65 g, 13.93 mmol, 1.2 equiv.), and Et₃N (1.6 mL, 11.61 mmol, 1.0 equiv.) were added sequentially. The cold bath was removed and the reaction mixture was stirred for 3.5 hours. Upon completion, the mixture was poured into Et₂O (100 mL) and washed sequentially with saturated aqueous NaHCO₃ (50 mL), saturated aqueous NH₄Cl (50 mL), and brine (50 mL). The organic phase was then dried with MgSO₄, filtered through cotton, and concentrated *in vacuo* to provide crude **6.72** as a slightly yellow oil (1.46 g). The crude product mixture was used in the next step without purification.

Tertiary alcohol silylation: To a flame dried round bottom flask with stir bar was added allylic chloride **6.72** (1.46 g) and DCM (76 mL) under argon. The solution was cooled to -78 °C, and 2,6-lutidine (3.5 mL, 30.6 mmol) and TMSOTf (2.8 mL, 15.3 mmol) were added sequentially. The reaction mixture was stirred 1 hour at -78 °C. Upon completion, Et₃N (1 mL) and methanol (2.5 mL) were added, and the reaction mixture was warmed to room temperature. A 10% solution of EtOAc/hexanes (100 mL) was added, and the organic layer was washed sequentially with H₂O (50 mL), a 10% aqueous solution of citric acid (50 mL), and brine (50 mL). The organic layer was dried with MgSO₄, filtered through cotton, and concentrated *in vacuo* to provide crude **6.73** as a yellow oil (1.89 g). The allylic chloride could not be purified by silica gel chromatography and was therefore used directly in the next step.

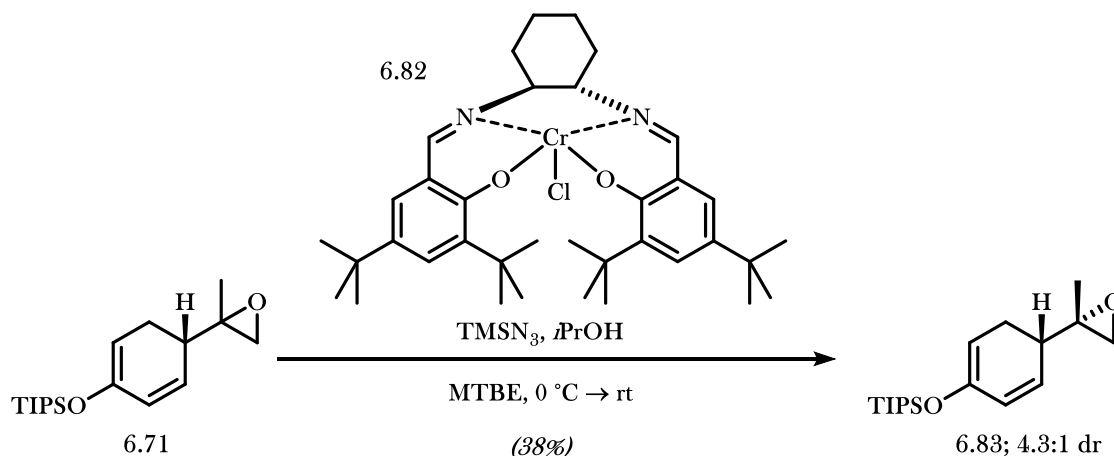
Epoxide 6.71



Selective epoxidation: To a round bottom flask with stir bar was added enone **6.78**³² (1.00 g, 7.34 mmol, 1.0 equiv.) followed by DCM (73 mL). Solid *m*CPBA (1.94 g, 8.08 mmol, 1.1 equiv.) was added portionwise over 10 minutes, and the reaction mixture was stirred overnight. In the morning, an additional 200 mg of *m*CPBA was added, and the reaction mixture was stirred until thin-layer chromatography indicated full conversion. Saturated aqueous sodium thiosulfate (100 mL) was added, and the mixture was stirred vigorously for 1 hour. The aqueous layer was extracted with DCM (3 x 100 mL), and the combined organic layers were dried with MgSO₄, filtered through cotton, and concentrated *in vacuo* to a slightly yellow oil (1.4 g). The crude product was used in the next step without purification.

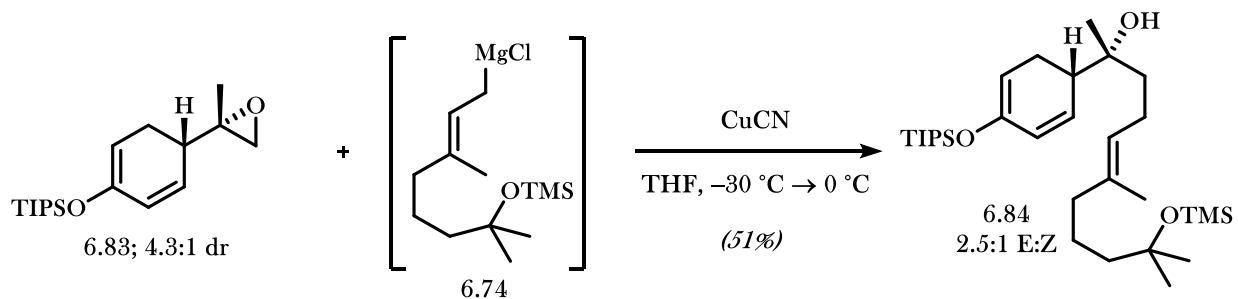
Dienoxy silane formation: To a flame dried round bottom flask with stir bar was added a portion of crude enone # (100 mg) followed by anhydrous DCM (3.3 mL) under argon. The solution was cooled to 0 °C, and Et₃N (183 μL, 1.31 mmol) was added, followed by the dropwise addition of TIPSOTf (194 μL, 0.72 mmol). The reaction mixture was stirred for 1.25 hours at 0 °C. Upon completion, methanol (20 μL) was added, the reaction mixture was warmed to room temperature, and saturated aqueous NaHCO₃ (5 mL) was added. The aqueous phase was extracted with Et₂O (3 x 5 mL), and the combined organic phases were washed with brine (5 mL), dried with MgSO₄, filtered through cotton, and concentrated *in vacuo* to a slightly yellow oil. The crude product mixture was purified by silica gel chromatography (5–10% EtOAc in hexanes) to afford a 1:1 mixture of diastereomers of **6.71** as a slightly yellow oil (153 mg, 95% over 2 steps).

Epoxide **6.83**³³



To a flame dried vial containing epoxide **6.71** (153 mg, 0.50 mmol, 1.0 equiv.) in anhydrous TBME (173 μ L) was added (*S,S*)-Cr(salen)Cl **6.82**³⁴ (6.3 mg, 0.01 mmol, 2 mol%). The mixture was cooled to 0 °C and isopropanol (21 μ L, 0.27 mmol, 0.55 equiv.) was added, followed by TMSN₃ (36 μ L, 0.27 mmol, 0.55 equiv.). The mixture was warmed to room temperature and stirred for 6 hours. Upon completion, the reaction mixture was pushed through a plug of silica gel and flushed with a 50% solution of ethyl acetate in hexanes. The mixture was concentrated *in vacuo* to provide crude **6.83** as a brown solid (157 mg). The reaction mixture was purified by silica gel chromatography (5% EtOAc in hexanes) to afford a 4.3:1 mixture of diastereomers of **6.83** as a colorless oil (58.7 mg, 38%). An analytically pure sample was obtained from careful chromatography: ¹H NMR (500 MHz, CDCl₃) δ 5.88–5.82 (m, 2H), 4.86–4.81 (m, 1H), 2.66 (d, *J* = 4.8 Hz, 1H), 2.59 (d, *J* = 4.8 Hz, 1H), 2.24–2.14 (m, 3H), 1.32 (s, 3H), 1.20–1.11 (m, 3H), 1.07 (d, *J* = 6.8 Hz, 18H); ¹³C NMR (126 MHz, CDCl₃) δ 148.2, 128.7, 127.6, 100.5, 58.8, 53.2, 40.6, 24.2, 18.9, 17.9, 12.5; IR (film) 2946, 2868, 1249, 839 cm⁻¹; HRMS (ESI) *m/z* calculated for C₁₈H₃₂O₂Si [M + Na]⁺ 331.2069, found 331.2059.

Dienoxy Silane 6.84

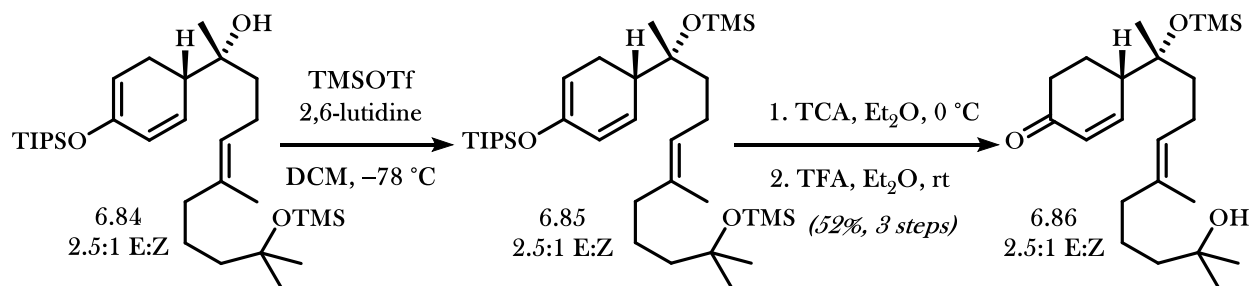


Allylic Grignard formation: To a flame dried round bottom flask with stir bar was added magnesium powder (229 mg, -20+100 mesh, ground with mortar and pestle). The flask was evacuated, filled with argon, evacuated, and flame dried with stirring. Upon cooling to room temperature, the flask was filled with argon, and 1.5 mL of anhydrous THF was added. The suspension was then subjected to three cycles of: sonication for *ca.* 60 seconds, gentle heating to *ca.* 60 °C, and addition *ca.* 5 μ L dibromoethane. Following the third repetition, addition of dibromoethane should result in visible formation of gaseous H₂. The suspension was then cooled to 0 °C, and, with vigorous stirring, a solution of allylic chloride **6.73** (501.8 mg, *ca.* 1.91 mmol) in 500 μ L anhydrous THF was then added slowly over 20 minutes to the magnesium suspension. Following complete addition, the cold bath was removed and the reaction mixture was stirred for 30 minutes at room temperature, and then transferred over via syringe to a flame dried flask under argon. The Grignard solution could be stored overnight at -20 °C. Titration prior to use with salicylaldehyde phenylhydrazone indicated a concentration of [0.46 M].

Allyl Nucleophile Epoxide Opening: To a flame dried vial with stir bar was added CuCN (3.7 mg, 0.042 mmol, 20 mol%) followed by anhydrous THF (350 μ L) under argon. A solution of epoxide **6.83** (65.1 mg, 0.21 mmol, 1.0 equiv.) in anhydrous THF (200 μ L) was added, and the suspension was cooled to -30 °C. A [0.46 M] solution of allylic Grignard **6.74** (554 μ L, 0.25 mmol, 1.2 equiv.) was added dropwise over 30 minutes. Following complete addition, the reaction mixture was warmed to 0 °C over 30 minutes and stirred at that temperature for 30 minutes. Upon completion, saturated aqueous NH₄Cl (1 mL) was added with vigorous stirring, followed by Et₂O (2 mL). The mixture was stirred under air for 20 minutes until a bilayer

formed. The layers were separated, and the organic layer was washed with brine (1 mL). The organic phase was dried with MgSO_4 , filtered through cotton, and concentrated *in vacuo* to provide crude **6.84** as a colorless oil. The crude product mixture was purified by silica gel chromatography (2–3% EtOAc in hexanes) to afford a 2.5:1 mixture of E/Z isomers of **6.84** as a colorless oil (57.6 mg, 51%): ^1H NMR (500 MHz, CDCl_3) δ 5.97–5.90 (m, 1H), 5.86–5.80 (m, 1H), 5.14 (t, J = 6.9 Hz, 1H), 4.89–4.83 (m, 1H), 2.47–2.36 (m, 1H), 2.28–2.04 (m, 4H), 2.01 (t, J = 6.7 Hz, 0.56H, minor), 1.95 (t, J = 6.7 Hz, 1.50H, major), 1.68 (s, 0.77H, minor), 1.56 (s, 2.20H, major), 1.55–1.50 (m, 2H), 1.46–1.34 (m, 4H), 1.19 (s, 6H), 1.18–1.12 (m, 5H), 1.10–1.04 (m, 24H), 0.10 (s, 9H); ^{13}C NMR (126 MHz, CDCl_3) δ 148.5, 136.1, 135.9, 129.34, 129.29, 127.39, 127.37, 124.9, 124.1, 100.9, 74.61, 74.58, 74.0, 73.9, 44.6, 44.4, 43.7, 40.1, 40.1, 39.8, 32.0, 29.9, 24.3, 23.7, 22.6, 22.0, 17.9, 17.7, 12.5, 12.3, 2.6; IR (film) 3448 (br), 2944, 2867, 1249, 884 cm^{-1} ; HRMS (ESI) m/z calculated for $\text{C}_{31}\text{H}_{60}\text{O}_3\text{Si}_2$ $[\text{M} + \text{Na}]^+$ 559.3979, found 559.3957.

Enone 6.86



Tertiary alcohol silylation: To a flame dried round bottom flask with stir bar was added tertiary alcohol **6.84** (57.6 mg, 0.11 mmol, 1.0 equiv.) and DCM (1.1 mL) under argon. The solution was cooled to $-78\text{ }^\circ\text{C}$, and 2,6-lutidine (62 μL , 0.54 mmol, 5.0 equiv.) and TMSOTf (58 μL , 0.32 mmol, 3.0 equiv.) were added sequentially. The reaction mixture was stirred 1 hour at $-78\text{ }^\circ\text{C}$. Upon completion, Et_3N (50 μL) and methanol (125 μL) were added, and the reaction mixture was warmed to room temperature. A 10% solution of EtOAc/hexanes (2 mL) was added, and the organic layer was washed sequentially with H_2O (1 mL), a 10% aqueous solution of citric acid (1 mL), and brine (1 mL). The organic layer was dried with MgSO_4 , filtered

through cotton, and concentrated *in vacuo* to provide **6.85** as a colorless oil. The crude product was used in the next step without further purification.

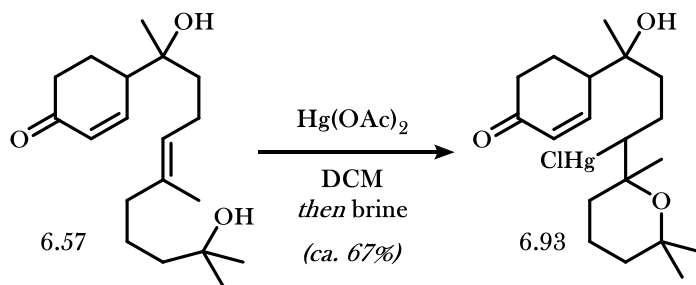
*[Note: The crude product mixture prepared above was combined with the crude product mixture of a reaction prepared in the same manner as above from 46.3 mg from tertiary alcohol **6.84**. The yield of **6.86** is reported based on the combined theoretical yield.]*

Dioxy silane deprotection: To a vial with stir bar was added crude trisilane **6.85** (88 mg) followed by Et₂O (2.9 mL). The solution was cooled to 0 °C, and trichloroacetic acid (243 mg, 1.44 mmol) was added as a solid. The reaction mixture was stirred for 1.5 at 0 °C. Upon completion, Et₂O (2 mL) was added, by slow addition of saturated aqueous NaHCO₃ (2 mL). The layers were separated, and the aqueous layer was extracted with Et₂O (3 x 2 mL). The combined organic extracts were washed with brine (2 mL), dried with MgSO₄, filtered through cotton, and concentrated *in vacuo* to provide a yellow oil. The crude product mixture was used in the next step without purification.

Tertiary alcohol deprotection: To a vial with stir bar was added the crude disilane followed by Et₂O (1.4 mL). Trifluoroacetic acid (0.5 mL) was added dropwise to the solution, and the reaction mixture was stirred for 1 hour. Et₂O (2 mL) was added, followed by saturated aqueous NaHCO₃ (2 mL). The layers were separated, and the aqueous layer was extracted with Et₂O (3 x 2 mL). The combined organic extracts were washed with brine (2 mL), dried with MgSO₄, filtered through cotton, and concentrated *in vacuo* to provide crude **6.86** as a yellow oil. The crude product mixture was purified by silica gel chromatography (20–27% EtOAc in hexanes) to afford a 2.5:1 mixture of E/Z isomers of **6.86** as a colorless oil (38.0 mg, 52% over 3 steps): ¹H NMR (500 MHz, CDCl₃) δ 7.12–7.05 (m, 1H), 6.05 (d, *J* = 10.4 Hz, 1H), 5.09 (t, *J* = 6.9 Hz, 1H), 2.57 (d, *J* = 11.1 Hz, 1H), 2.49 (d, *J* = 16.5 Hz, 1H), 2.33 (td, *J* = 14.6, 5.1 Hz, 1H), 2.16–2.06 (m, 1H), 2.01–1.93 (m, 3H), 1.72–1.56 (m, 4H), 1.56–1.48 (m, 2H), 1.48–1.37 (m, 4H), 1.20 (s, 6H), 1.14 (s, 3H), 0.14 (s, 9H); ¹³C NMR (126 MHz, CDCl₃) δ 199.9, 153.3, 153.2, 135.5, 135.3, 129.8, 124.7, 123.9, 77.7, 70.9, 70.8, 45.6, 43.6, 43.4, 40.4, 40.1, 40.0, 37.4, 32.0, 29.2, 24.7, 24.5, 23.3, 22.61, 22.57, 21.9, 21.8, 15.9, 2.5; IR

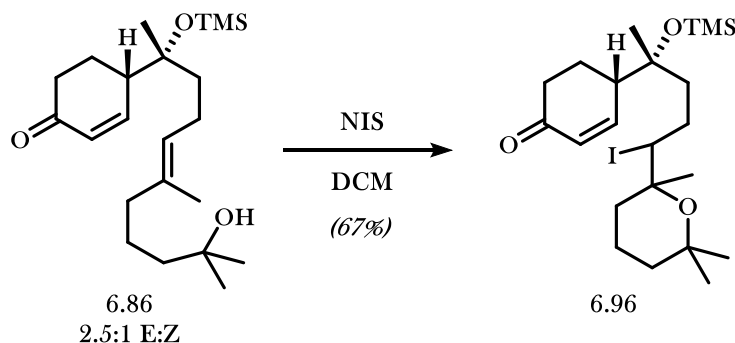
(film) 3450(br), 2964, 1683, 1251 cm^{-1} ; HRMS (ESI) m/z calculated for $\text{C}_{22}\text{H}_{40}\text{O}_3\text{Si}$ $[\text{M} + \text{Na}]^+$ 403.2644, found 403.2654.

Organomercury **6.93**³⁵



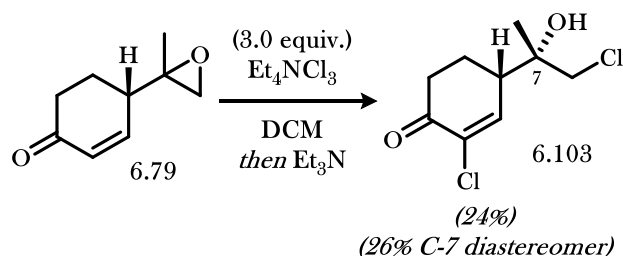
To a flame dried vial with stir bar was added solid $\text{Hg}(\text{OAc})_2$ (6.9 mg, 0.022 mmol, 1.3 equiv.), and the vial was filled with argon. Anhydrous DCM (270 μL) was added, followed by a solution of tertiary alcohol **6.57** (5.0 mg, 0.016 mmol, 1.0 equiv.) in anhydrous DCM (270 μL). The reaction mixture was stirred for 15 minutes at room temperature. Upon completion, brine (500 μL) was added and the mixture was stirred vigorously for 30 minutes. Upon completion, DCM (1 mL) and H_2O (1 mL) were added, the layers were separated, and the aqueous layer was extracted with DCM (2 x 1 mL). The combined organic layers were dried with MgSO_4 , filtered through cotton, and concentrated *in vacuo* to provide crude **6.93** as a thin film (6.6 mg, *ca.* 67%). The crude product was used in the next step without purification. Diagnostic characterization data is provided for the crude material: ^1H NMR (500 MHz, CDCl_3) δ 7.19–7.13 (m, 1H), 6.11 (d, J = 10.4 Hz, 1H), 2.83 (dt, J = 12.2, 4.2 Hz, 1H); ^{13}C NMR (126 MHz, CDCl_3) δ 199.33, 199.31, 151.20, 151.18, 130.53, 130.50, 73.95, 73.04, 46.2, 46.1, 42.9, 42.7, 37.3, 36.9, 34.1, 27.1, 26.3, 23.93, 23.86, 16.7; ^{13}C NMR (126 MHz, C_6D_6) δ 197.5, 150.4, 150.3, 130.7, 76.6, 16.1, 73.3, 73.2, 72.7, 46.4, 45.9, 42.5, 42.51, 42.49, 37.64, 37.56, 37.02, 36.99, 36.90, 36.85, 34.2, 27.1, 26.1, 24.9, 24.8, 23.6, 23.3, 23.0, 22.9, 17.0 ;IR (film) 3416 (br), 2966, 2928, 1665, 1219 cm^{-1} ; HRMS (ESI) m/z calculated for $\text{C}_{19}\text{H}_{31}\text{O}_3\text{HgCl}$ $[\text{M} + \text{Na}]^+$ 567.1599, found 567.1573.

Alkyl Iodide 6.96



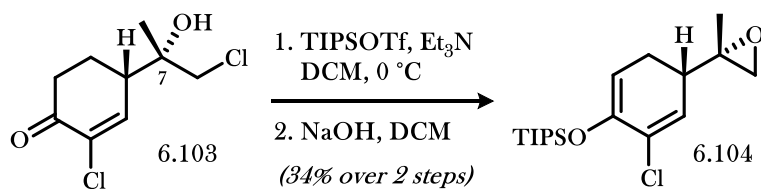
To a vial with stir bar as added tertiary alcohol **6.86** (5 mg, 0.013 mmol, 1.0 equiv.) and anhydrous DCM (260 μ L). *N*-iodosuccinimide (4.4 mg, 0.020, 1.5 equiv.) was added as a solid, and the reaction mixture was stirred for 1 hour at 0 °C. Upon completion, saturated aqueous sodium thiosulfate (1 mL) was added, and the mixture was stirred vigorously until colorless. The aqueous layer was extracted with hexanes (3 x 1 mL). The combined organic extracts were washed with brine (1 mL), dried with MgSO₄, filtered through cotton, and concentrated *in vacuo*. The crude product mixture was purified by silica gel chromatography (3–4.5% EtOAc in hexanes) to afford a mixture of diastereomers of **6.96** as a thin film (4.4 mg, 67%). A portion of the major diastereomer was isolated for characterization: ¹H NMR (500 MHz, CDCl₃) δ 7.12 (dt, *J* = 10.4, 1.8 Hz, 1H), 6.08 (dd, *J* = 10.4, 2.3 Hz, 1H), 3.91 (d, *J* = 11.2 Hz, 1H), 2.59–2.48 (m, 2H), 2.41–2.26 (m, 2H), 2.07–2.00 (m, 1H), 1.96 (ddd, *J* = 14.2, 12.4, 4.4 Hz, 1H), 1.81 (dt, *J* = 13.1, 4.1 Hz, 1H), 1.78–1.57 (m, 4H), 1.50–1.40 (m, 3H), 1.38 (s, 3H), 1.37–1.31 (m, 1H), 1.20 (s, 3H), 1.17 (s, 3H), 1.16 (s, 3H), 0.16 (s, 9H); ¹³C NMR (126 MHz, CDCl₃) δ 200.0, 153.3, 129.9, 74.3, 72.7, 54.5, 45.0, 41.2, 37.4, 36.6, 36.3, 32.6, 29.7, 28.2, 27.9, 25.0, 24.3, 21.6, 16.6, 2.5; IR (film) 2921, 2850, 1687, 839 cm⁻¹; HRMS (ESI) *m/z* calculated for C₂₂H₃₉O₃SiI [M + Na]⁺ 529.1611, found 529.1609.

Chlorohydrin **6.103**



To a round bottom flask with stir bar was added epoxide **6.79** (300 mg, 1.97 mmol, 1.0 equiv.) and anhydrous DCM (20 mL) under argon. The solution was cooled to 0 °C, and tetraethylammonium trichloride (1.26 g, 5.32 mmol, 2.7 equiv.) was added as a solid in three portions over 10 minutes. Following complete addition, the cold bath was removed and the reaction mixture was stirred at room temperature for 3 hours. Upon completion, neat triethylamine (500 μL) was added dropwise over 1 minute, and the reaction mixture was stirred for an additional 3 hours. Upon completion, the reaction mixture was poured into Et_2O (30 mL) and washed sequentially with saturated aqueous NaHCO_3 (30 mL) and brine (30 mL). The organic phase was dried with MgSO_4 , filtered through cotton, and concentrated *in vacuo* to provide crude **6.94** as brown oil. The crude product mixture was purified by silica gel chromatography (10–33% EtOAc in hexanes) to afford **6.103** as a colorless oil (108 mg, 24%): ^1H NMR (500 MHz, CDCl_3) δ 7.39–7.35 (m, 1H), 3.66, (d, J = 11.6, 1H), 3.61 (d, J = 11.6, 1H), 2.97 (ddd, J = 11.4, 4.2, 2.4 Hz, 1H), 2.75 (dt, J = 16.7, 3.4 Hz, 1H), 2.52 (ddd, J = 16.7, 14.6, 5.0 Hz, 1H), 2.10–2.02 (m, 1H), 1.81–1.70 (m, 1H), 1.21 (s, 3H); ^{13}C NMR (126 MHz, CDCl_3) δ 190.9, 146.8, 133.0, 73.2, 52.6, 45.6, 37.3, 24.5, 21.0; IR (film) 3463 (br), 2960, 1694, 1094 cm^{-1} ; HRMS (ESI) m/z calculated for $\text{C}_9\text{H}_{12}\text{O}_2\text{Cl}_2$ $[\text{M} + \text{Na}]^+$ 245.0112, found 245.0117.

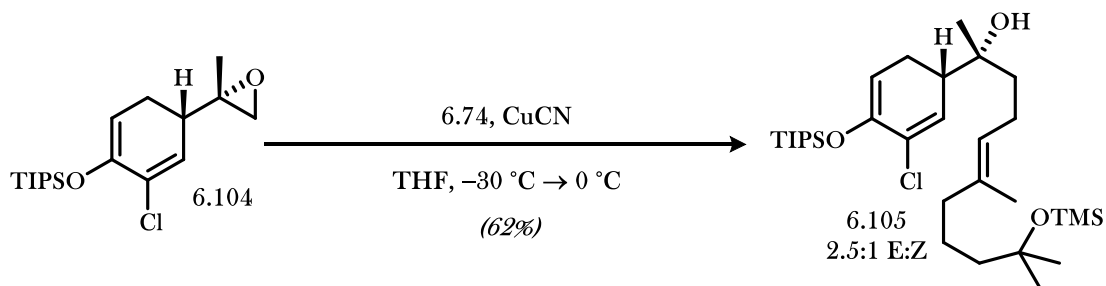
Epoxide 6.104



Enoxy Silane Formation: To a flame dried round bottom flask with stir bar was added chlorohydrin **6.103** (108 mg, 0.48 mmol, 1.0 equiv.) and anhydrous DCM (2.4 mL) under argon. The solution was cooled to 0 °C, and triethylamine (134 μ L, 0.96 mmol, 2.0 equiv.) was added, followed by dropwise addition of TIPSOTf (130 μ L, 0.48 mmol, 1.0 equiv.). The reaction mixture was stirred at 0 °C for 1.5 hours. Upon completion, the reaction mixture was diluted with DCM (10 mL) and quenched with saturated aqueous NaHCO₃ (10 mL). The phases were separated, and the aqueous layer was extracted with DCM (2 x 10 mL). The combined organic extracts were washed with H₂O (10 mL), dried with MgSO₄, filtered through cotton, and concentrated *in vacuo* to a yellow oil (190 mg). The crude product mixture was carried forward to the next step without purification.

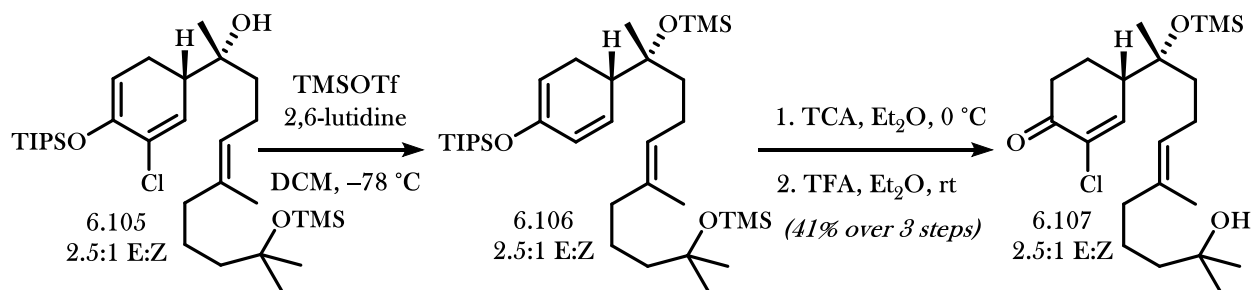
Epoxide Closing: To a flame dried round bottom flask with stir bar was added the crude chlorohydrin (190 mg) and anhydrous DCM (4.8 mL). Powdered NaOH (58 mg, 1.45 mmol, ground with mortar and pestle) was added in one portion as a solid, and the vial was sealed. The reaction mixture was stirred for 3 hours at room temperature. Upon completion, H₂O (5 mL) was added, the phases were separated, and the organic phase was washed with brine (5 mL). The organic layer was dried with MgSO₄, filtered through cotton, and concentrated *in vacuo* to provide crude **6.104** as a yellow oil (140 mg). The crude product mixture was purified by silica gel chromatography (3% EtOAc in hexanes) to afford **6.104** as a colorless oil (55.5 mg, 34% over 2 steps): ¹H NMR (500 MHz, CDCl₃) δ 5.99 (d, *J* = 3.7 Hz, 1H), 4.96 (t, *J* = 4.8 Hz, 1H), 2.65 (d, *J* = 4.7 Hz, 1H), 2.60 (d, *J* = 4.7 Hz, 1H), 2.32 (ddd, *J* = 12.8, 9.0, 3.7 Hz, 1H), 2.24–2.16 (m, 2H), 1.33 (s, 3H), 1.22 (heptet, *J* = 7.6 Hz, 3H), 1.10 (dd, *J* = 7.5, 1.8 Hz, 18H); ¹³C NMR (126 MHz, CDCl₃) δ 145.0, 130.1, 125.5, 102.0, 58.3, 53.0, 42.3, 24.1, 19.0, 18.0, 12.6; IR (film) 2944, 2867, 883 cm⁻¹; HRMS (ESI) *m/z* calculated for C₁₈H₃₁O₂ClSi [M + Na]⁺ 365.1680, found 365.1696.

Tertiary Alcohol **6.105**



To a flame dried round bottom flask with stir bar was added CuCN (3.3 mg, 0.036 mmol, 20 mol%) followed by anhydrous THF (300 μ L) under argon. A solution of epoxide **6.104** (62 mg, 0.18 mmol, 1.0 equiv.) in anhydrous THF (200 μ L) was added, and the suspension was cooled to -30 °C. A [0.38 M] solution of allylic Grignard **6.74** (960 μ L, 0.36 mmol, 2.0 equiv.) was added dropwise over 30 minutes. Following complete addition, the reaction mixture was warmed to 0 °C over 30 minutes and stirred at that temperature for 30 minutes. Upon completion, saturated aqueous NH₄Cl (1 mL) was added with vigorous stirring, followed by Et₂O (2 mL). The mixture was stirred under air for 20 minutes until a bilayer formed. The layers were separated, and the organic layer was washed with brine (1 mL). The organic phase was dried with MgSO₄, filtered through cotton, and concentrated *in vacuo* to provide crude **6.105** as a colorless oil. The crude product mixture was purified by silica gel chromatography (3–5% EtOAc in hexanes) to afford a 2.5:1 mixture of E/Z isomers of **6.105** as a colorless oil (64 mg, 62%): ¹H NMR (500 MHz, CDCl₃) δ 6.07 (dd, *J* = 3.6, 3.2 Hz, 1H), 5.13 (dd, *J* = 6.7, 6.2 Hz, 1H), 5.01–4.96 (m, 1H), 2.58–2.49 (m, 1H), 2.16–1.91 (m, 5H), 1.68 (s, 0.91H, minor), 1.61 (s, 2.16H, major), 1.55–1.48 (m, 2H), 1.47–1.32 (m, 5H), 1.26–1.17 (m, 10H), 1.11 (d, *J* = 7.3 Hz, 18H), 1.05 (s, 3H), 0.10 (s, 9H); ¹³C NMR (126 MHz, CDCl₃) δ 145.2, 136.3, 136.1, 129.6, 126.40, 126.35, 124.6, 123.8, 102.3, 102.2, 74.31, 74.28, 74.0, 73.9, 45.8, 44.5, 44.3, 40.0, 39.9, 39.7, 29.8, 24.3, 23.5, 23.3, 22.6, 22.0, 21.8, 18.0, 17.7, 15.9, 12.6, 2.6; IR (film) 3439 (br), 2945, 2867, 1248, 883 cm⁻¹; HRMS (ESI) *m/z* calculated for C₃₁H₅₉ClO₃Si₂ [M + Na]⁺ 593.3589, found 593.3587.

Enone 6.107

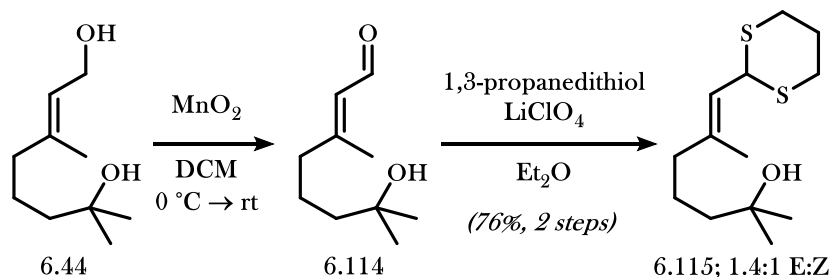


Tertiary alcohol silylation: To a flame dried round bottom flask with stir bar was added tertiary alcohol **6.105** (64 mg, 0.11 mmol, 1.0 equiv.) and DCM (1.1 mL) under argon. The solution was cooled to -78 °C, and 2,6-lutidine (39 μ L, 0.34 mmol, 3.0 equiv.) and TMSOTf (30 μ L, 0.17 mmol, 1.5 equiv.) were added sequentially. The reaction mixture was stirred 1 hour at -78 °C. At this point, thin-layer chromatography analysis indicated incomplete conversion, so 2,6-lutidine (39 μ L, 0.34 mmol, 3.0 equiv.) and TMSOTf (30 μ L, 0.17 mmol, 1.5 equiv.) were added sequentially. Upon completion, Et₃N (50 μ L) and methanol (125 μ L) were added, and the reaction mixture was warmed to room temperature. A 10% solution of EtOAc/hexanes (2 mL) was added, and the organic layer was washed sequentially with H₂O (1 mL), a 10% aqueous solution of citric acid (1 mL), and brine (1 mL). The organic layer was dried with MgSO₄, filtered through cotton, and concentrated *in vacuo* to provide crude **6.106** as a colorless oil. The crude product was used in the next step without further purification.

Dienoxy silane deprotection: To a vial with stir bar was added crude trisilane **6.106** followed by Et₂O (2.2 mL). The solution was cooled to 0 °C, and trichloroacetic acid (155 mg, 1.12 mmol) was added as a solid. The reaction mixture was stirred for 1.5 at 0 °C. Upon completion, Et₂O (2 mL) was added, by slow addition of saturated aqueous NaHCO₃ (2 mL) The layers were separated, and the aqueous layer was extracted with Et₂O (3 x 2 mL). The combined organic extracts were washed with brine (2 mL), dried with MgSO₄, filtered through cotton, and concentrated *in vacuo* to provide a yellow oil. The crude product mixture was used in the next step without purification.

Tertiary alcohol deprotection: To a vial with stir bar was added the crude disilane followed by Et₂O (1.1 mL). Trifluoroacetic acid (0.4 mL) was added dropwise to the solution, and the reaction mixture was stirred for 2 hours. Et₂O (2 mL) was then added, followed by saturated aqueous NaHCO₃ (2 mL), and solid NaHCO₃ was added until bubbling upon addition ceased. The layers were separated, and the organic layer washed with brine (1 mL), dried with MgSO₄, filtered through cotton, and concentrated *in vacuo* to provide crude **6.107** as a colorless oil. The crude product mixture was purified by silica gel chromatography (20–33% EtOAc in hexanes) to afford a 2.5:1 mixture of E/Z isomers of **6.107** as a colorless oil (19.0 mg, 41% over 3 steps): ¹H NMR (500 MHz, CDCl₃) δ 7.26–7.23 (m, 1H), 5.09 (t, *J* = 6.8 Hz, 1H), 2.76–2.70 (m, 2H), 2.45 (ddd, *J* = 16.8, 14.4, 5.1 Hz, 1H), 2.17–1.94 (m, 5H), 1.79–1.70 (m, 1H), 1.69 (s, 0.84H, minor), 1.61 (s, 2.32H, major), 1.58–1.51 (m, 2H), 1.49–1.39 (m, 4H), 1.21 (s, 6H), 1.18 (s, 3H), 0.17 (s, 9H); ¹³C NMR (126 MHz, CDCl₃) δ 191.6, 149.3, 149.2, 135.8, 135.6, 132.1, 124.5, 123.7, 77.1, 71.0, 70.9, 47.6, 43.6, 43.4, 40.3, 40.1, 40.0, 37.6, 32.1, 29.30, 29.27, 29.25, 24.9, 24.30, 24.38, 23.3, 22.62, 22.59, 21.9, 21.8, 16.0, 2.51, 2.48; IR (film) 2965, 1698, 1251 cm⁻¹; HRMS (ESI) *m/z* calculated for C₂₂H₃₉O₃ClSi [M + Na]⁺ 437.2255, found 437.2238.

Dithiane 6.115

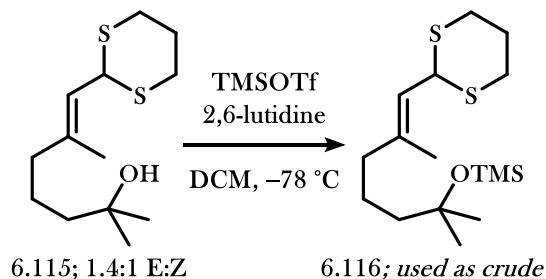


Allylic Alcohol Oxidation: To a round bottom flask with stir bar was added diol **6.44** (300 mg, 1.74 mmol, 1.0 equiv.) and DCM (3.4 mL). To the stirring solution was added activated MnO₂ (1.5 g, 17.4 mmol, 10 equiv.). The reaction mixture was stirred at room temperature for 1 hour. Upon completion, the mixture

was filtered through Celite and concentrated to provide crude **6.114** as a colorless oil (295 mg). The crude product mixture was used in the next step without purification.

Dithiane Formation: To a flame dried round bottom flask with stir bar was added a portion of α,β -unsaturated aldehyde **6.114** (100 mg) followed by anhydrous Et₂O (150 μ L) under argon. 1,3-propanedithiol (118 μ L, 1.18 mmol) was then added to the solution. To the reaction mixture was then added a solution of LiClO₄ (125 mg, 1.18 mmol) in anhydrous Et₂O (440 μ L). The reaction mixture was stirred for 24 hours at room temperature. Upon completion, H₂O (1 mL) was added, and the aqueous layer was extracted with Et₂O (3 x 1 mL). The combined organic extracts were dried with MgSO₄, filtered through cotton, and concentrated *in vacuo* to provide crude **6.115** as a colorless oil. The crude product mixture was purified by silica gel chromatography (20–33% EtOAc in hexanes) to afford a 2.5:1 mixture of E/Z isomers of **6.115** as a colorless oil (119 mg, 76% over 2 steps).

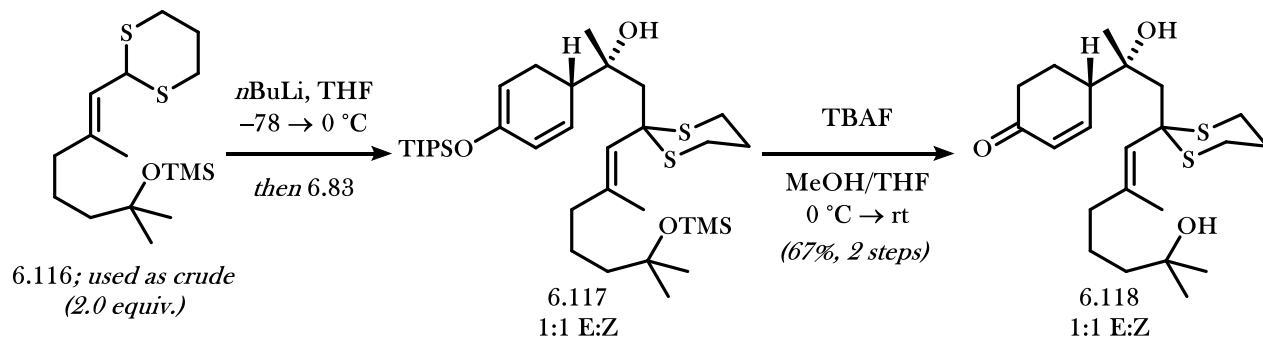
Dithiane **6.116**



To a flame dried round bottom flask with stir bar was added dithiane **6.115** (100 mg, 0.38 mmol, 1.0 equiv.) and DCM (3.8 mL) under argon. The solution was cooled to -78 °C, and 2,6-lutidine (178 μ L, 1.54 mmol, 4.0 equiv.) and TMSOTf (139 μ L, 0.77 mmol, 2.0 equiv.) were added sequentially. The reaction mixture was stirred 1 hour at -78 °C. Upon completion, Et₃N (100 μ L) and methanol (250 μ L) were added, and the reaction mixture was warmed to room temperature. A 10% solution of EtOAc/hexanes (10 mL) was added, and the organic layer was washed sequentially with H₂O (5 mL), a 10% aqueous solution of citric acid (5 mL), and brine (5 mL). The organic layer was dried with MgSO₄, filtered through cotton, and concentrated

in vacuo to provide crude **6.116** as a yellow oil (101 mg). The crude mixture was used in the next step without further purification.

Enone 6.118

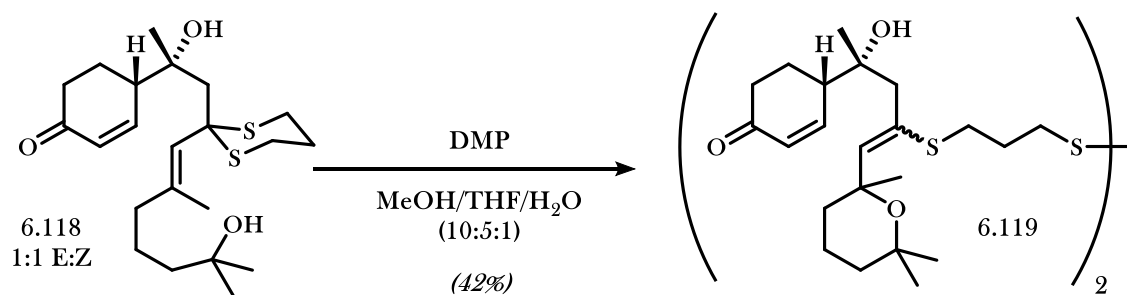


*Dithiane Epoxide Opening:*³⁶ To a flame dried round bottom flask with stir bar was added dithiane **6.116** (137.8 mg, 0.41 mmol, 1.05 equiv.) and anhydrous THF (410 μL) under argon. The solution was cooled to $-78 \text{ } ^\circ\text{C}$, and a [2.42 M] solution of *n*-butyllithium in hexanes (163 μL , 0.40 mmol, 1.0 equiv.) was added dropwise. The reaction mixture was stirred for 5 minutes, warmed to $0 \text{ } ^\circ\text{C}$ and stirred for 30 minutes, and then cooled again to $-78 \text{ } ^\circ\text{C}$. A solution of epoxide **6.83** (122 mg, 0.40 mmol, 1.0 equiv.) in anhydrous THF (274 μL) was then added dropwise, and the reaction mixture was stirred for 45 minutes at $-78 \text{ } ^\circ\text{C}$. Upon completion, saturated aqueous NH_4Cl (500 μL) was added and the mixture was warmed to room temperature. H_2O (2 mL) was added, the layers were separated, and the aqueous layer was extracted with EtOAc (3 x 1 mL). The combined organic extracts were dried with MgSO_4 , filtered through cotton, and concentrated *in vacuo* to provide crude **6.117** as a yellow oil (243 mg). The crude product mixture was carried forward to the next step without further purification.

Global Silyl Deprotection: To a vial with stir bar was added crude disilane **6.117** (243 mg), methanol (1.6 mL), and THF (200 μL). The reaction mixture was cooled to $0 \text{ } ^\circ\text{C}$ and a [1.0 M] solution of TBAF in THF (790 μL , 0.79 mmol) was added dropwise over 2 minutes. The reaction mixture was stirred for 10 minutes, the cold bath was removed, and the reaction mixture was stirred for 16 hours at room temperature.

Upon completion, saturated aqueous NH_4Cl (5 mL) was added, and the organic layer was extracted with Et_2O (3 x 5 mL). The combined organic layers were washed with H_2O (5 mL) and brine (5 mL), then dried with MgSO_4 , filtered through cotton, and concentrated *in vacuo* to provide crude **6.118** as a brown oil (244 mg). The crude product mixture was purified by silica gel chromatography (50% EtOAc in hexanes) to afford a 1:1 mixture of E/Z isomers of **6.118** as a colorless oil (109 mg, 67% over 2 steps): ^1H NMR (500 MHz, CDCl_3) δ 7.28–7.22 (m, 1H), 6.09 (two isomers, d, $J=2.6$ Hz, 1H), 5.49 (two isomers, s, 1H), 3.14–2.93 (m, 2H), 2.85–2.73 (m, 2H), 2.65 (ddd, $J=9.2, 4.2, 2.0$ Hz, 1H), 2.61–2.50 (m, 2H), 2.35 (t, $J=14.3$ Hz, 2H), 2.23–2.14 (m, 1H), 2.11–1.90 (m, 4H), 1.80–1.71 (m, 2H), 1.56–1.32 (m, 6H), 1.25 (two isomers, s, 3H), 1.22 (two isomers, s, 6H); ^{13}C NMR (126 MHz, CDCl_3) δ 199.6, 151.83, 151.78, 144.2, 143.5, 130.3, 127.8, 127.6, 75.1, 70.9, 70.8, 50.8, 50.6, 48.4, 48.3, 47.0, 46.7, 43.8, 43.3, 41.8, 37.5, 33.6, 29.4, 29.3, 28.4, 28.3, 28.2, 28.1, 25.2, 25.04, 24.97, 24.6, 24.5, 22.8, 22.6, 18.5; IR (film) 3422 (br), 2966, 2934, 1671, 1378 cm^{-1} ; HRMS (ESI) m/z calculated for $\text{C}_{22}\text{H}_{36}\text{O}_3\text{S}_2$ $[\text{M} + \text{Na}]^+$ 435.2003, found 435.2009.

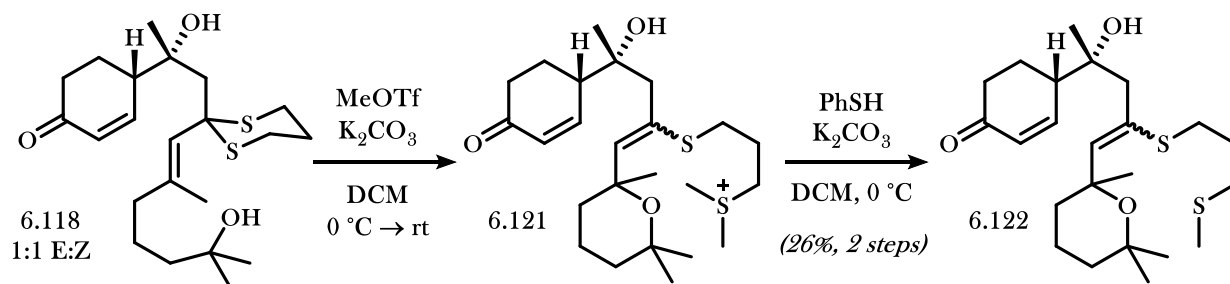
Vinyl Sulfide **6.119**



To a vial with stir bar was added dithiane **6.118** (50 mg, 0.12 mmol, 1.0 equiv.) followed by methanol (837 μL), THF (413 μL), and H_2O (81 μL). To the stirring solution was added DMP (51.4 mg, 0.12 mmol, 1.0 equiv.) as a solid in a single portion. After stirring for 2 hours at room temperature, additional DMP (15 mg, 0.04 mmol, 0.3 equiv.) was added. After stirring for 1 hour at room temperature, additional DMP (15 mg, 0.04 mmol, 0.3 equiv.) was added. After stirring for 1 additional hour at room temperature, thin-layer chromatography indicated reaction completion. DCM (2 mL) was added, and the solution was added

dropwise to saturated aqueous NaHCO₃ (2 mL). The layers were separated, and the aqueous layer was extracted with DCM (2 x 2 mL). The combined organic extracts were dried with MgSO₄, filtered through cotton, and concentrated *in vacuo* to provide crude **6.119** as a colorless oil. The crude product mixture was purified by silica gel chromatography (50–70% EtOAc in hexanes) to afford a mixture of diastereomers of **6.119** as a colorless oil (20.8 mg, 42%). Diagnostic NMR peaks: ¹H NMR (500 MHz, CDCl₃) δ 7.22 (dd, *J* = 23.5, 2.5 Hz, 2H), 6.07 (td, *J* = 10.6, 2.3 Hz, 2H), 5.47 (s, 2H), 2.87–2.73 (m, 8H), 2.59–2.46 (m, 3H), 2.43–2.30 (m, 2H), 2.22 (d, *J* = 15.8 Hz, 2H); ¹³C NMR (126 MHz, CDCl₃) δ 199.8, 199.7, 152.5, 152.0, 130.1, 129.9, 127.21, 127.17, 126.6, 125.9, 75.9, 75.6, 75.3, 74.6, 70.92, 70.92, 47.5, 44.7, 44.1, 44.01, 43.95, 43.92, 37.7, 37.5, 37.41, 37.37, 37.0, 29.4, 29.3, 28.9, 28.8, 28.2, 27.8, 27.7, 25.2, 24.0, 23.2, 21.9, 18.7, 18.6.

Vinyl Sulfide **6.122**



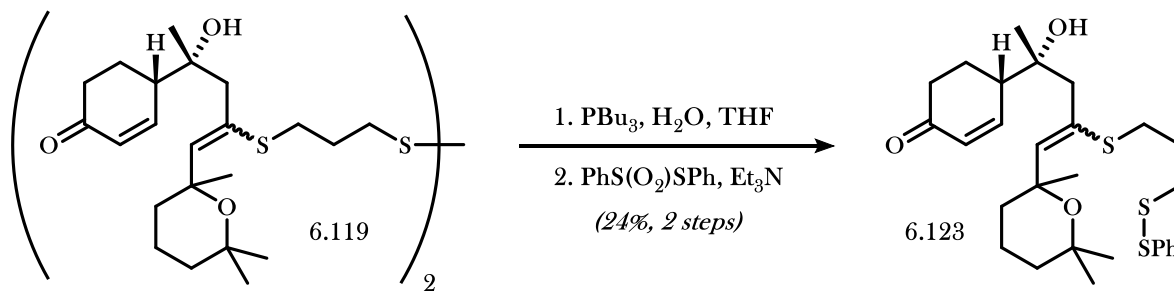
*[Note: The procedure described below includes an unsuccessful attempted one-pot formation of thioether **6.122**. A full workup and resubjection was necessary to accomplish demethylation.]*

Dithiane Bis-Methylation: To a flame dried vial with stir bar was added dithiane **6.118** (10 mg, 0.024 mmol, 1.0 equiv.), anhydrous DCM (350 μL), and potassium carbonate (10 mg, 0.072 mmol, 3.0 equiv.) under argon. The suspension was cooled to 0 °C, and a solution of MeOTf (10.5 μL, 0.096 mmol, 4.0 equiv.) in DCM (50 μL) was added dropwise. The bath was removed and the reaction mixture was stirred for 1 hour at room temperature. A solution of MeOTf (10.5 μL, 0.096 mmol, 4.0 equiv.) in anhydrous DCM (50 μL)

was added dropwise, the reaction mixture was stirred for 1 hour at room temperature, and an additional solution of MeOTf (10.5 μ L, 0.096 mmol, 4.0 equiv.) in anhydrous DCM (50 μ L) was added dropwise. After 1 hour, thin-layer chromatography analysis indicated complete conversion. The reaction was cooled to 0 $^{\circ}$ C, and a solution of thiophenol (9.8 μ L, 0.096 mmol, 4.0 equiv.) in anhydrous DCM (100 μ L) was added. The reaction was warmed to room temperature, and an additional 200 μ L of neat thiophenol was added. Demethylation to **6.122** was not observed after several hours. H₂O (2 mL) was added, and the aqueous layer was extracted with DCM (3 \times 2 mL). The combined organic layers were dried with MgSO₄, filtered through cotton, and concentrated *in vacuo* to a colorless oil. The crude product mixture, which was found to contain significant quantities of thiophenol, was used in the next step without further purification.

Thionium Demethylation: To a vial with stir bar was added the above crude mixture, anhydrous DCM (400 μ L), and solid potassium carbonate (6.6 mg, 0.048 mmol) at 0 $^{\circ}$ C under argon. The reaction mixture was stirred for 15 minutes at 0 $^{\circ}$ C, the cold bath was removed, and the reaction mixture was stirred at room temperature for 4 hours. Upon completion, H₂O (2 mL) and DCM (2 mL) were added, the layers were separated, and the organic layer was washed with saturated aqueous NaHCO₃ (2 mL). The organic layer was dried with MgSO₄, filtered through cotton, and concentrated *in vacuo* to provide crude **6.122** as a thin film. The crude product mixture was purified by silica gel chromatography (20–33% EtOAc in hexanes) to afford a mixture of diastereomers of **6.122** as a colorless oil (2.7 mg, 26%): (see spectra); IR (film) 3448 (br), 2966, 2919, 1680, 1376 cm⁻¹; HRMS (ESI) *m/z* calculated for C₂₃H₃₈O₃S₂ [M + Na]⁺ 449.2160, found 449.2165.

Mixed Disulfide **6.123**



To a vial with stir bar was added dimer **6.119** (37.1 mg, 0.045 mmol, 1.0 equiv.) and THF (1.85 mL) under argon. Tributylphosphine (25 μL , 0.10 mmol, 2.2 equiv.) and H_2O (19 μL) were then added sequentially. The reaction mixture was stirred for 1 hour at room temperature. Upon completion, triethylamine (19 μL , 0.14 mmol, 3.0 equiv.) was added, followed by *S*-phenyl benzenethiosulfonate (28.2 mg, 0.11 mmol, 2.5 equiv.). The reaction mixture was stirred at room temperature for 1.5 hours. Upon completion, EtOAc (5 mL) and saturated aqueous NaHCO_3 (5 mL) were added, and the layers were separated. The organic layer was extracted with EtOAc (2 \times 5 mL), and the combined organic extracts were washed with brine (5 mL). The organic layer was then dried with MgSO_4 , filtered through cotton, and concentrated *in vacuo* to provide crude **6.123** as a colorless oil. The crude product mixture was purified by silica gel chromatography (33% EtOAc in hexanes) to afford a mixture of diastereomers of **6.123** as a thin film (10.9 mg, 24%): (see spectra); IR (film) 3441 (br), 2927, 2966, 1680, 1375, 740 cm^{-1} ; HRMS (ESI) m/z calculated for $\text{C}_{28}\text{H}_{40}\text{O}_3\text{S}_3$ $[\text{M} + \text{Na}]^+$ 543.2037, found 543.2024.

6.12 Notes and References

- (1) Daub, M. E.; Prudhomme, J.; Le Roch, K.; Vanderwal, C. D. *J. Am. Chem. Soc.* **2015**, *137*, 4912-4915.
- (2) (a) Josephine S. Nakhla, Jeff W. Kampf, John P. Wolfe. *J. Am. Chem. Soc.* **2006**, *128*, 2893-2901.
(b) Michael B. Hay and John P. Wolfe. *Tetrahedron Lett.* **2006**, *47*, 2793-2796. (c) John P. Wolfe. *Synlett* **2008**, *19*, 2913-2937. (d) Josephine S. Nakhla, Jeff W. Kampf, John P. Wolfe. *J. Am. Chem. Soc.* **2006**, *128*, 2893-2901.
- (3) Zhang, Z. Pan, C.; Wang, Z. *Chem. Commun.* **2007**, 4686-4688.
- (4) (a) Semmelhack, M. F.; Kim, C. R.; Dobler, W.; Meier, M. *Tetrahedron Lett.* **1989**, *30*, 4925-4928.
(b) White, J. D.; Kuntiyong, P.; Lee, T. H. *Org. Lett.* **2006**, *8*, 6039-6042.
- (5) Miyaoka, H.; Abe, Y.; Sekiya, N.; Mitome, H.; Kawashima, E. *Chem. Commun.* **2011**, *48*, 901-903.
- (6) Snyder, S. A.; Treitler, D. S.; Brucks, A. P. *J. Am. Chem. Soc.* **2010**, *132*, 14303-14314.
- (7) Schreiber, J.; Maag, H.; Hashimoto, N.; Eschenmoser, A. *Angew. Chem. Int. Ed.* **1971**, *10*, 330-331.
- (8) Corey, E. J.; Sodeoka, M. *Tetrahedron Lett.* **1991**, *32*, 7005-7008.
- (9) Raina, S.; Singh, V. K. *Tetrahedron* **1995**, *51*, 2467-2476.
- (10) (a) Seth, P. P.; Totah, N. I. *Org. Lett.* **1999**, *1*, 1411-1414. (b) Kitana, Y.; Morita, A.; Kumamoto, T.; Ishikawa, T. *Helv. Chim. Acta* **2002**, *85*, 1186-1195.
- (11) Masuda, T.; Anraku, K.; Kimura, M.; Sato, K.; Okamoto, Y.; Otsuka, M. *Synthesis* **2012**, *44*, 909-919.
- (12) (a) Negishi, E.; Chatterjee, S. *Tetrahedron Lett.* **1983**, *24*, 1341-1344. (b) Negishi, E.; Matsushita, H.; Chatterjee, S.; John, R. A. *J. Org. Chem.* **1982**, *47*, 3188-3190.
- (13) Northrup, A. B.; MacMillan, D. W. C. *J. Am. Chem. Soc.* **2002**, *124*, 2458-2460.
- (14) Siegel, C.; Gordon, P. M.; Razdan, R. K. *J. Org. Chem.* **1989**, *54*, 5428-5430.

- (15) Chen, Y.; Xiong, Z.; Zhou, G.; Liu, L.; Li, Y. *Tetrahedron: Asymmetry* **1998**, *9*, 1923–1928.
- (16) Lebel, H.; Jacobsen, E. N. *Tetrahedron Lett.* **1999**, *40*, 7303–7306.
- (17) Yanagisawa, A.; Habaue, S.; Yasue, K.; Yamamoto, H. *J. Am. Chem. Soc.* **1994**, *116*, 6130–6141.
- (18) (a) Miller, Y.; Miao, L.; Hosseini, A. Z.; Chemler, S. R. *J. Am. Chem. Soc.* **2012**, *134*, 12149–12156.
(b) Bovino, M. T.; Liwosz, T. W.; Kendel, N. E.; Miller, Y.; Tyminska, N.; Zurek, E.; Chemler, S. R. *Angew. Chem. Int. Ed.* **2014**, *53*, 6383–6387.
- (19) MacMillan, D. W. C.; Overman, L. E.; Pennington, L. D. *J. Am. Chem. Soc.* **2001**, *123*, 9033–9044.
- (20) Hori, K.; Hikage, N.; Inagaki, A.; Mori, S.; Nomura, K.; Yoshii, E. *J. Org. Chem.* **1992**, *57*, 2888–2902.
- (21) Kocovsky, P.; Srogl, J. *J. Org. Chem.* **1992**, *57*, 4565–4567.
- (22) Heck, R. F. *J. Am. Chem. Soc.* **1968**, *90*, 5518–5526.
- (23) (a) Schnermann, M. J.; Overman, L. E. *Angew. Chem. Int. Ed.* **2012**, *51*, 9576–9580. (b) Garnsey, M. R.; Slutskyy, Y.; Jamison, C. R.; Zhao, P.; Lee, J.; Rhee, Y. H.; Overman, L. E. *J. Org. Chem.* **2017**, Article ASAP.
- (24) Renaud, P.; Gerster, M. *Angew. Chem. Int. Ed.* **1998**, *37*, 2562–2579.
- (25) Snider, B. B.; Rodini, D. J.; Van Straten, J. *J. Am. Chem. Soc.* **1980**, *102*, 5872–5880.
- (26) Ketone **6.24** was prepared according to: Snyder, S. A.; Treitler, D. S.; Brucks, A. P. *J. Am. Chem. Soc.* **2010**, *40*, 14303–14314.
- (27) Diene **6.52** was prepared according to: Choi, J.; Park, H.; Yoon, H. J.; Kim, S.; Sorensen, E. J.; Lee, C. *J. Am. Chem. Soc.* **2014**, *136*, 9918–9921.
- (28) Diene **6.52** was prepared according to: Nakagawa, M.; Uchida, H.; Ono, K.; Kimura, Y.; Yamabe, M.; Watanabe, T.; Tsuji, R.; Akiba, M.; Terada, Y.; Nagaki, D.; Ban, S.; Miyashita, N.; Kano, T.; Theeraladanon, C.; Hatakeyama, K.; Arisawa, M.; Nishida, A. *Heterocycles* **2003**, *59*, 721–733.

- (29) Conditions inspired by: Knight, J. D.; Coltart, D. M. *Tetrahedron Lett.* **2013**, *54*, 5470-5472.
- (30) Conditions inspired by: (a) Negishi, E.; Chatterjee, S. *Tetrahedron Lett.* **1983**, *24*, 1341-1344. (b) Negishi, E.; Matsushita, H.; Chatterjee, S.; John, R. A. *J. Org. Chem.* **1982**, *47*, 3188-3190.
- (31) Conditions inspired by: Bertrand, C.; Hélène, M.; Dominique, M.; Guy, O. *Bull. Chem. Soc. Jpn.* **1988**, *61*, 141-148.
- (32) Enone **6.78** prepared according to: Siegel, C.; Gordon, P. M.; Razdan, R. K. *J. Org. Chem.* **1989**, *54*, 5428-5430.
- (33) Conditions inspired by: Lebel, H.; Jacobsen, E. N. *Tetrahedron Lett.* **1999**, *40*, 7303-7306.
- (34) Catalyst prepared according to: Martinez, L. E.; Leighton, J. L.; Carsten, D. H.; Jacobsen, E. N. *J. Am. Chem. Soc.* **1995**, *117*, 5897-5898.
- (35) Conditions inspired by: Kocovsky, P.; Grech, J. M.; Mitchell, W. L. *J. Org. Chem.* **1995**, *60*, 1482-1483.
- (36) Conditions inspired by: Hanessian, S.; Focken, T.; Oza, R. *Org. Lett.* **2010**, *12*, 3172-3175.

CHAPTER 7: ISOLATION AND SYNTHETIC STRATEGIES TOWARD 7,20-DIISOCYANOADOCIANE

7.1 Introduction

In Chapter 4, the potent bioactivity of (+)-7,20-diisocyanodociane (**7.1**; (+)-DICA) against *Plasmodium falciparum*, a parasite responsible for the most malaria-related deaths per year in the world, was discussed. However, (+)-DICA is isolated in trace yields from its host organisms, which highlights the need for synthetic designs to procure appreciable quantities for medicinal study. While the kalihinanes, described in detail in chapters 4 and 5, are identified by their highly congested assortment of stereocenters and diverse functionality, (+)-DICA and related natural products display contrasting features. The all-*trans* tetracyclic framework of (+)-DICA decorated with just two polar functional groups causes synthetic considerations to focus mainly on stereoselective bond-formation from non-intuitive precursors. Since the limited functionality on (+)-DICA does not suggest an obvious series of disconnections, the reported total syntheses differ significantly in their overall strategy.

7.2 Isolation and Characterization of DICA

(+)-DICA was first isolated and identified in the 1970s in a collaborative effort by the Wells and Oberhänsli groups.¹ The sponge *Cymbastella hooperi*, referred to at the time as *Adocia sp.* but since corrected,² was freeze-dried, milled, and extracted with cold petroleum ether to provide (+)-DICA in 2% yield. The crystalline material was analyzed by single-crystal x-ray crystallography and the structure was determined to be that of **7.1**. High resolution mass spectrometry analysis indicated a mass of 324.2565 m/z, in agreement with the molecular formula of (+)-DICA, and the optical rotation was found to be $[\alpha]^{22}_{\text{D}} +47.4^{\circ}$ (*c* 0.7, DCM). The isonitrile functionalities were supported by IR frequencies at 2130 and 2140 cm^{-1} , and the methyl groups geminal to the isonitriles were identified by fine C-N splitting. Further support for the isonitrile moieties involved hydrolysis to and characterization of the corresponding *bis*-formamide. Full ^1H , ^{13}C , and 2D NMR analyses were later published to further support the structure of (+)-DICA.³

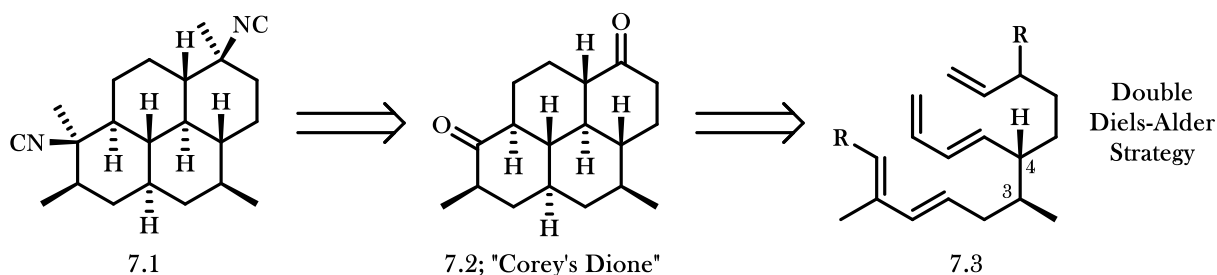
7.3 Previous Syntheses of 7,20-Diisocyanoadociane

7.2.1 Corey's Total Synthesis of (+)-DICA

The first synthesis of (+)-DICA was completed by Corey and Magriotis in 1987.⁴ In addition to providing a way by which the scaffold of (+)-DICA could be procured, the authors also hoped to determine the absolute configuration via a synthesis of the nonracemic natural product. Prior to the completion of this synthesis, the absolutely stereochemistry of (+)-DICA had not been determined.

Corey and Magriotis structured their endgame around the formation of the *bis*-isonitrile **7.1** in a non-diastereoselective manner from the corresponding diketone precursor (**7.2**) (Figure 7.1). The strategy for the formation of this precursor to (+)-DICA was built around the formation of the perhydropyrene structure via two Diels–Alder cycloaddition disconnections.

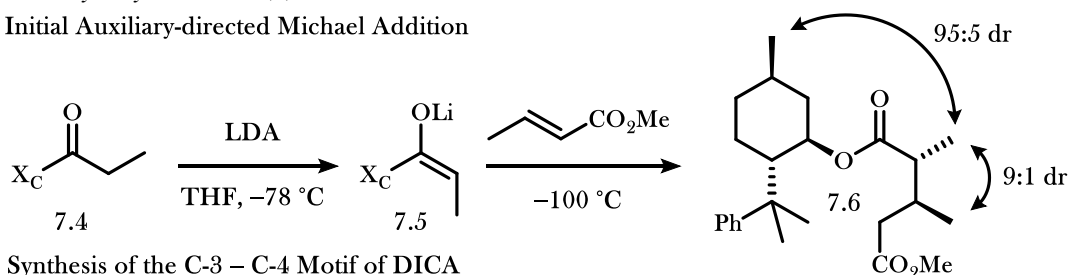
Figure 7.1 Corey's Strategy toward (+)-DICA



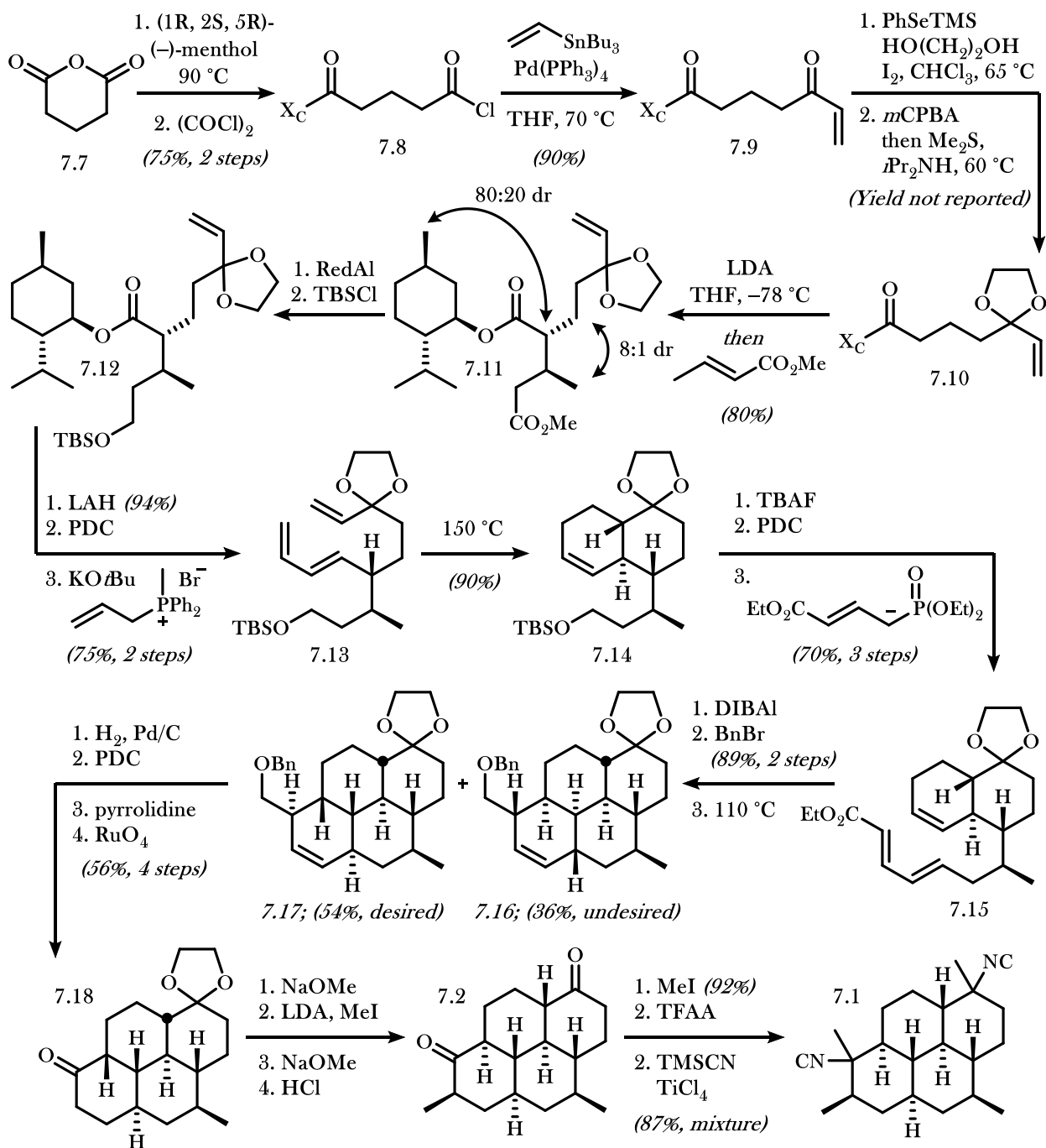
To accomplish a synthesis of nonracemic DICA by this approach, the absolute and relative configuration of the C3–C4 motif would first have to be established. The key stereocenters were formed using Corey's previously reported chiral auxiliary-directed asymmetric Michael addition to methyl crotonate.⁵ In their initial publication using the nucleophile **7.4** derived from propionic acid and menthol, this Michael addition formed the desired product **7.6** with excellent diastereoselectivity (Scheme 7.1a). However, when applied to the synthesis of (+)-DICA, which required use of more complex nucleophile **7.10**, the product following chiral auxiliary removal was determined to have only a 60% ee (Figure 7.1b). Although higher diastereoselectivity could be accomplished using the bulkier (–)-phenmenthol chiral auxiliary, the

Scheme 7.1 Corey's Synthesis of (+)-DICA

a. Corey's Initial Auxiliary-directed Michael Addition



b. Corey's Synthesis of the C-3 – C-4 Motif of DICA



(-)-menthol-derived nucleophile was used in this synthesis due to its low cost and chiral influence sufficient enough to determine the absolute stereochemistry of (+)-DICA. Using this methodology, key intermediate **7.11** was formed in 80% yield as an 8:1 ratio of diastereomers.

With the stereochemistry of **7.11** established, a series of functional group manipulations were then performed to install proper unsaturated precursors to the first Diels–Alder cycloaddition. Reduction and protection of the ester of **7.11** formed silyl ether **7.12**, which would remain protected until it would eventually be used to install functionality for the second Diels–Alder cycloaddition. Removal of the chiral auxiliary, oxidation to the aldehyde, and Wittig alkenylation provided diene **7.13**, which then participated in a thermal [4+2] cycloaddition to provide the cyclohexene Diels–Alder product **7.14** in 90% yield. As part of Corey’s clever strategy, the alkene resulting from the cycloaddition would later act as the dienophile in a subsequent Diels–Alder ring formation.

Deprotection and oxidation of the silyl ether of **7.14** and alkenylation using triethyl (*E*)-lithio-4-phosphonocrotonate provided diene **7.15** in 70% yield over three steps, which was then reduced and protected to provide the Diels–Alder precursor. Heating provided cycloaddition products **7.16** and **7.17** in high combined yield as a mixture of diastereomers resulting from low selectivity of facial approach by the diene to the dienophile. A four-step retro-homologation sequence from the desired **7.17** then provided ketone **7.18** in 56% yield. A series of steps involving epimerization, methyl installation, epimerization, and ketal removal then provided the all-*trans* perhydropyrene scaffold **7.2**. Using the protocol described in Chapter 4, the isonitriles were then installed via a diaxial *bis*-tertiary alcohol formation and subsequent non-stereoselective tertiary isonitrile installation to provide a mixture of diastereomers of **7.1**, including (+)-DICA. The natural product was isolated following HPLC purification, but a yield of (+)-DICA was not reported.

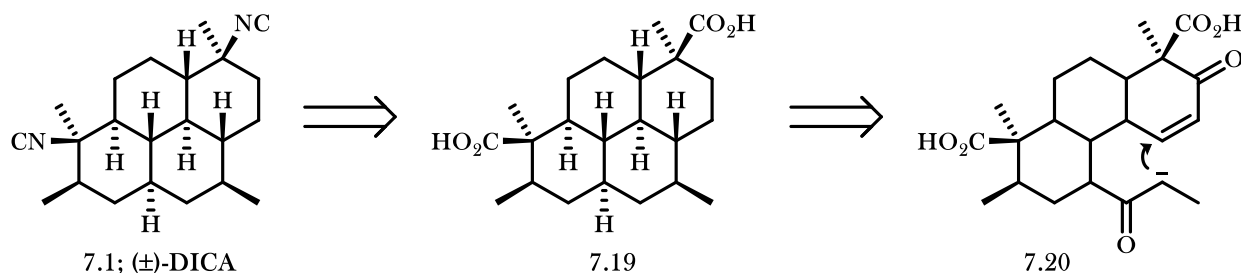
The first synthesis of (+)-DICA by Corey and Magriotis not only confirmed the absolute configuration of the natural product, but also did so in a highly strategic manner. The double Diels–Alder strategy is a clever method for the formation of the perhydropyrene scaffold, and it rapidly provides access to the complex core. Although problems with the synthesis exist, the authors propose solutions to each problem in their

publication; the ee of the natural product could be improved by using a (-)-phenmenthol chiral auxiliary, and they suggest the diastereoselectivity of the second Diels-Alder could be improved by changing the terminal substituent of the diene. Furthermore, the synthesis highlights the need for stereoselective methods for tertiary isonitrile installation from ketone precursors, an issue that has since been resolved by Shenvi and Pronin.⁶

7.2.2 Mander's Synthesis of (\pm)-DICA

Fairweather and Mander reported a second synthesis of racemic DICA aimed at installing the *bis*-isonitrile motif with high selectivity to improve upon the synthesis of Corey and Magriotis.⁷ To do this, they planned to form the amine precursors to the isonitriles via a Curtius rearrangement from the corresponding diacid precursor **7.19** (Figure 7.2). Their strategy, which employs numerous protecting groups and several multi-step sequences as synthetic detours to overcome undesired reactivity, is headlined by an intramolecular Michael addition to complete the tetracyclic core. At the time, the synthesis of Fairweather and Mander was the only strategy that provided DICA as a single diastereomer.

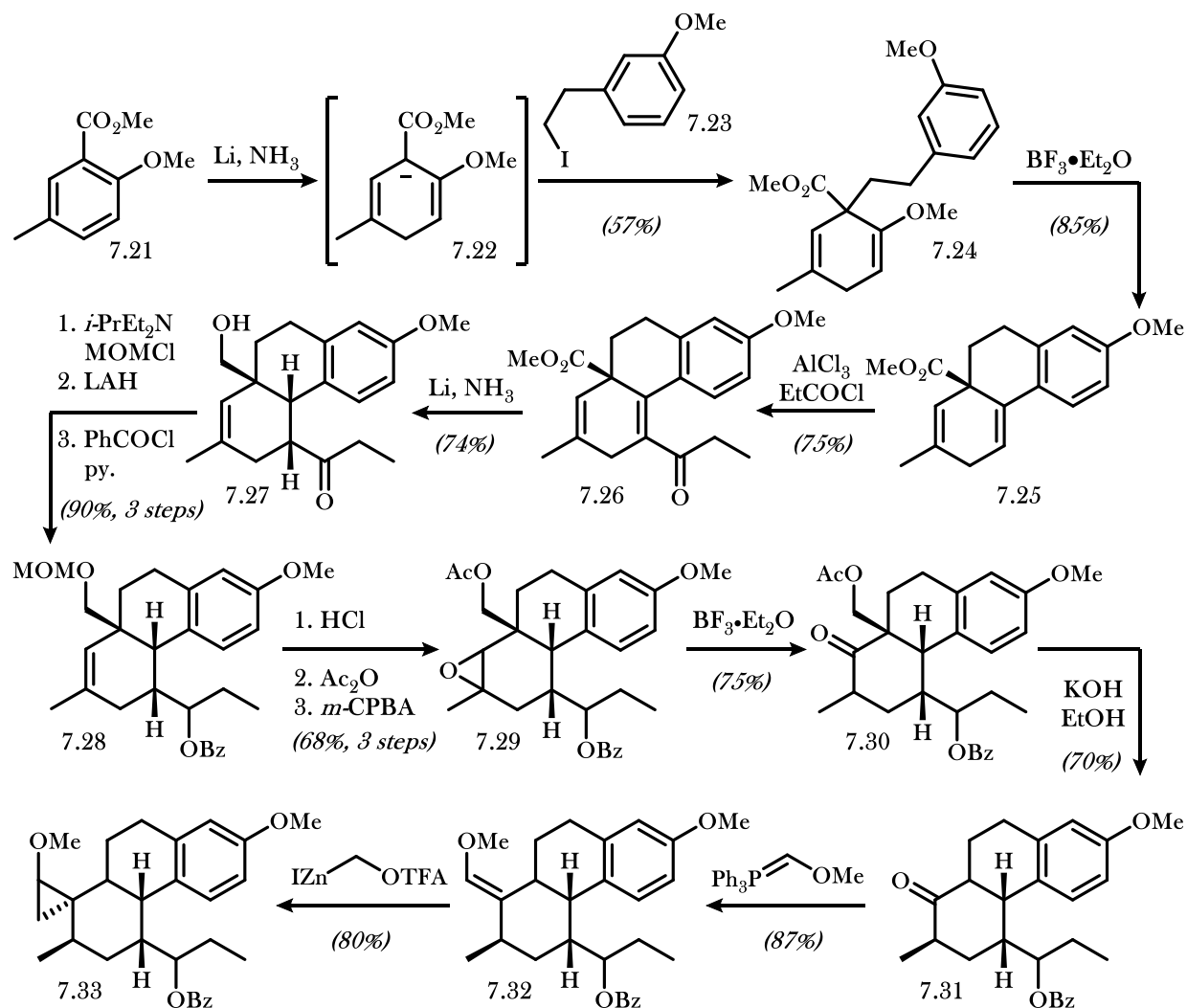
Figure 7.2 Mander's Curtius Rearrangement Approach to (\pm)-DICA



Starting from methyl benzoate **7.21**, the tricyclic fragment **7.25** was formed in a two-step Birch alkylation followed by Lewis acid-promoted ring closure. Friedel-Crafts acylation then formed **7.26**, which was subsequently reduced under dissolving metal conditions to provide cyclohexenone **7.27** (Scheme 7.2). The differentially protected epoxide **7.29** was then formed in a rather nonstrategic five-step protection/reduction/protection/deprotection/protection sequence and ensuing epoxidation. Following treatment with Lewis acid, a Meinwald rearrangement afforded the α -methylated ketone **7.30**, which would

eventually be used as a functional handle to install a tertiary isonitrile. A one-pot α -methyl epimerization and deacylative retro-aldol provided ketone **7.31**.

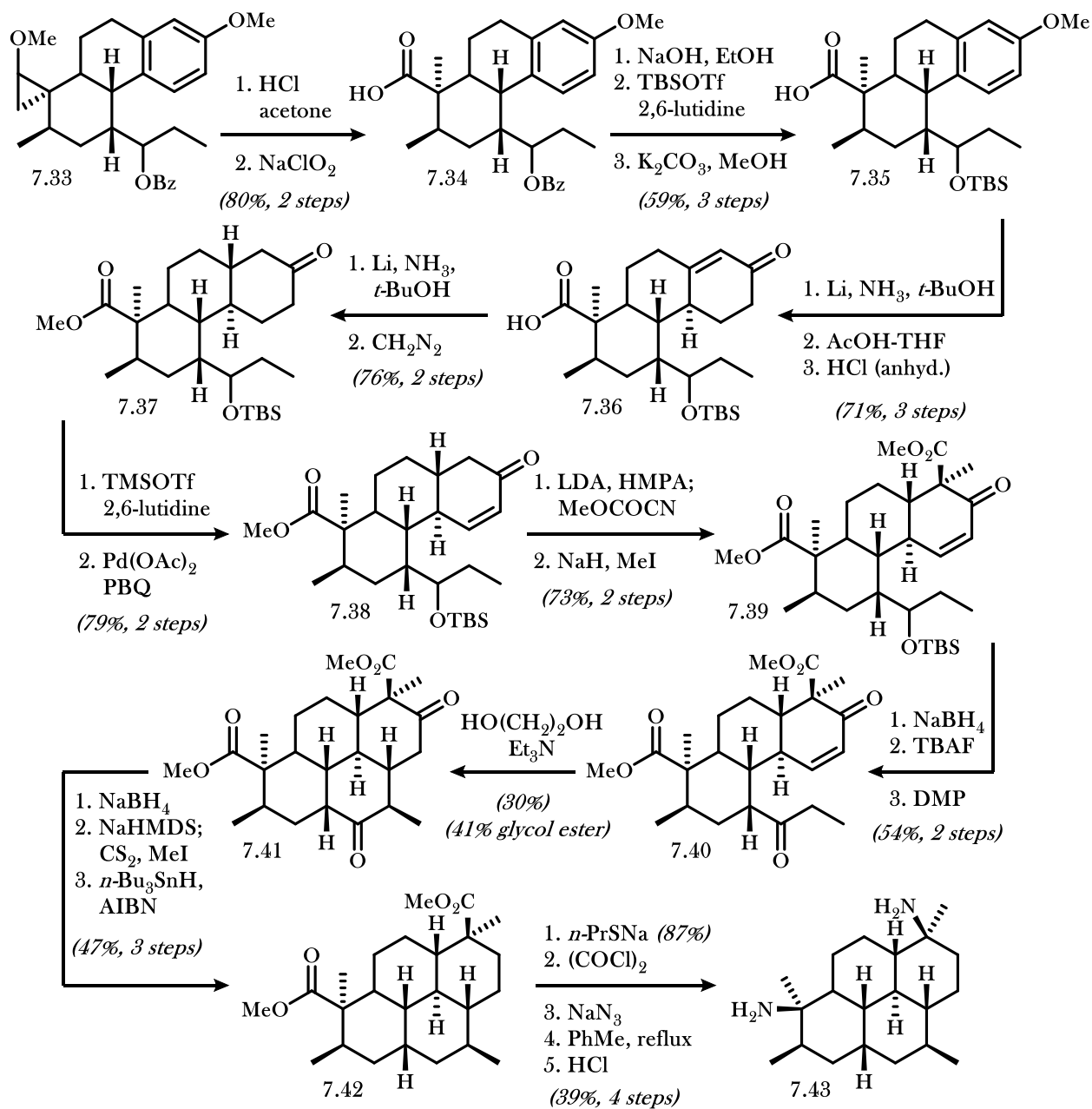
Scheme 7.2 Mander's Formal Synthesis of (\pm)-DICA



To form the isonitrile with high selectivity, Fairweather and Mander avoided formation of the tertiary alcohol and instead performed a Wittig olefination and Simmons–Smith cyclopropanations to provide **7.33**. Heating to reflux in strong acid provided ring-opened product, which was oxidized to the corresponding carboxylic acid via Lindgren oxidation to provide stereodefined tertiary carboxylate **7.34** (Scheme 7.3). Prior to isonitrile formation, completion of the tetracyclic core was first necessary.

A three-step protecting group swap provided silyl ether **7.35**, which was subjected to Birch reduction conditions and a two-step hydrolysis/isomerization sequence to provide enone **7.36**. An additional dissolving metal reduction then reduced the enone, and the carboxylic acid was converted to the methyl ester **7.37**.

Scheme 7.3 Mander's Completion of the Formal Synthesis of (\pm)-DICA



Enone **7.38** was formed by a two-step Saegusa oxidation sequence, and a two-step double α -functionalization provided ketoester **7.39**. To prevent oxy-Michael reactivity, the enone was reduced to the allylic alcohol, the silyl ether was deprotected, and a one-pot *bis*-oxidation to the dicarbonyl **7.40** was performed. Heating of **7.40** under weakly basic conditions provided the tetracyclic core **7.41** as a mixture of methyl and glycolic esters. In a separate sequence from each product of ring closure, the carbonyls were removed via reduction to the corresponding secondary alcohols and radical deoxygenation, and the esters were dealkylated and converted to the bis(acyl azide). Curtius rearrangement and hydrolysis of the resulting isocyanates provided the *bis*-amine **7.43**, which has been shown to be a precursor to the natural product.⁸

Fairweather and Mander accomplished their goal of forming each stereocenter of (\pm)-DICA with high selectivity. However, the conversion of the carbonyls to the isonitriles via a Curtius rearrangement takes at least ten-steps, and in this synthesis, the strategy required additional protection/deprotection steps while the authors functionalized the rest of the core. Corey's and Mander's methods for tertiary isonitrile installation from the corresponding ketone each have their own benefits and limitations, and one could choose to employ either method to suit their needs.

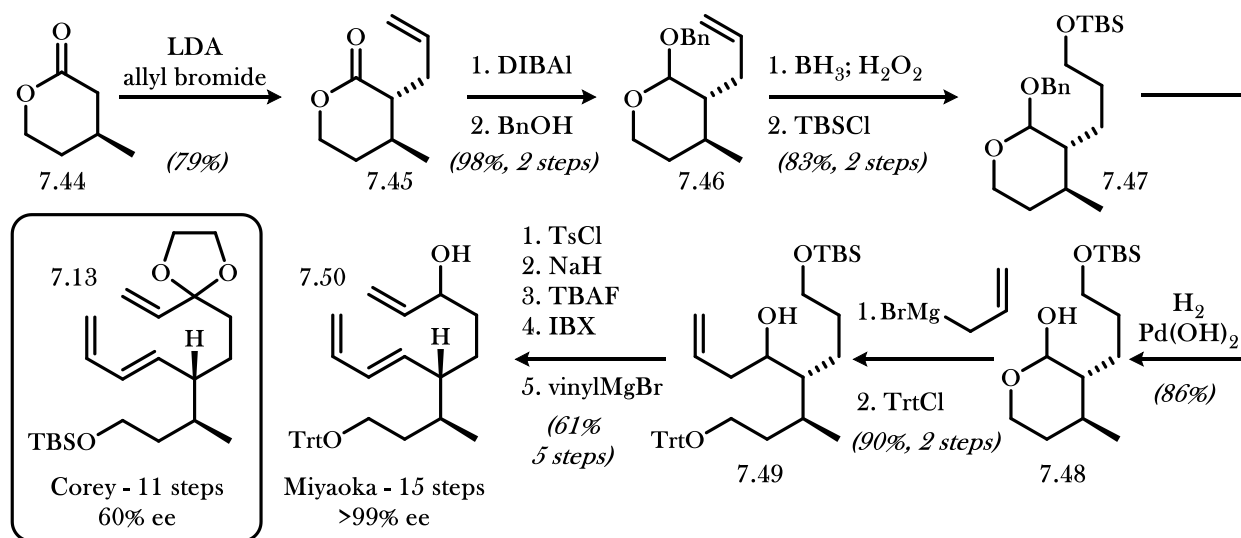
Aside from the isonitrile installation, Mander's synthesis also suffers from the high dependence on protecting groups and multi-step sequences to accomplish small functional group modifications. Although the lack of functionality on (\pm)-DICA presents a challenge in designing a strategy toward its procurement, it also allows for the use of promiscuous reaction conditions due to the decreased likelihood of side-reactivity. However, in Mander's synthesis, the formation of highly-functionalized intermediates en route to (\pm)-DICA introduces the challenge of adverse reactivity, and, as a result, protecting groups and indirect functional group manipulations play a key role.

7.2.3 Miyaoka's Synthesis of (+)-DICA

In 2011, Miyaoka and co-workers reported a synthesis of (+)-DICA nearly identical to that of Corey and Magriotis.⁹ Aside from minor changes to reaction conditions and functional group manipulations, the only difference in synthetic strategy involves formation of the C3-C4 fragment, which Corey procured via the

asymmetric Michael addition described in section 7.2.1. Miyaoka instead formed this fragment from known lactone **7.44** via a diastereoselective α -alkylation and ring-opening allylation to eventually provide **7.50** (Scheme 7.4).

Scheme 7.4 Miyaoka's Formation of the C-3 - C-4 Stereocenter Motif Toward (+)-DICA



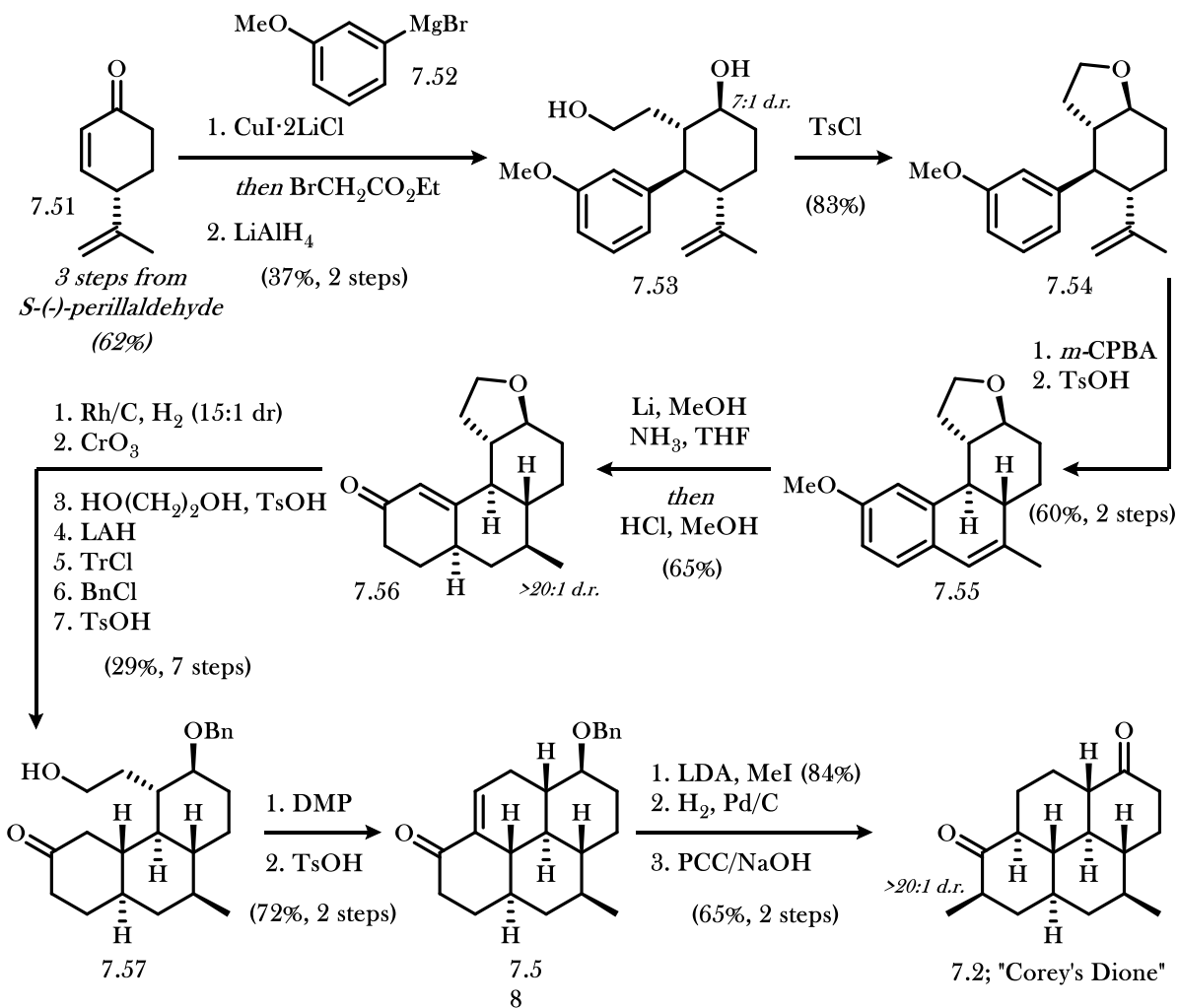
Although Miyaoka's synthesis of Diels-Alder precursor **7.50** requires an additional four steps to procure, the material can be provided with nearly perfect enantioselectivity and therefore is a valuable contribution to the field of ICT total synthesis. The remainder of the synthesis will not be discussed, however, since it proceeds in a highly analogous manner to the synthesis of Corey and Magriotis described above.

7.2.4 Vanderwal's Formal Synthesis of (+)-DICA

In 2016, Roosen and Vanderwal completed a formal synthesis of (+)-DICA using Corey's dione (**7.2**) as a synthetic target.¹⁰ The strategy was based on a tandem vicinal difunctionalization approach also used by the Vanderwal group in their total synthesis of fellow isocyanoterpene kalihinol B.¹¹ Starting from enone **7.51**, available in three steps from commercially available S-(-)-perillaldehyde,¹² the Vanderwal group accomplished a conjugate addition of methoxyarene nucleophile **7.52**, followed by quenching of the enolate

intermediate with ethyl bromoacetate (Scheme 7.5). The crude dicarbonyl product was then reduced with lithium aluminum hydride to provide diol **7.53** in 37% yield with good diastereoselectivity.

Scheme 7.5 Vanderwal's Formal Synthesis of (+)-DICA



Diol **7.53** was then converted to the tetrahydrofuran **7.54** to protect each alcohol from reaction conditions in the subsequent several steps. Epoxidation of the isopropylidene provided a mixture of epoxide diastereomers, which then condensed onto the electron-rich aromatic ring to provide **7.55** via a one-pot Meinwald rearrangement¹³ and Friedel-Crafts condensation. Roosen and Vanderwal then accomplished a 4-electron reduction of **7.55**, involving diastereoselective reduction of the styrenyl olefin and reduction of the

electron-rich aromatic ring. The crude cyclohexadiene product was then hydrolyzed and isomerized to provide **7.56** in 65% yield.

With enone **7.56** in hand, the Vanderwal group then had to elaborate their intermediate to prepare for an aldol condensation from primary alcohol **7.57** to provide **7.58**. Hydrogenation with rhodium on carbon provided the corresponding cyclohexanone intermediate with high diastereoselectivity, and chromium trioxide converted the tetrahydrofuran ring to the lactone. Conversion of the ketone to the ketal protected it from subsequent treatment with LAH, which again opened the lactone to the diol. From there, a three-step protection/protection/deprotection sequence was implemented resulting in mono-protected product **7.57**. The seven-step sequence preparing intermediate **7.57** for aldol condensation was accomplished in 29% yield.

With the proper functionality in place, Roosen and Vanderwal then accomplished a two-step ring-closing sequence involving oxidation of primary alcohol **7.57** and subsequent acid-catalyzed aldol condensation to provide **7.58** in 72%. Inspired by the endgame of Corey and Magriotis, Roosen and Vanderwal installed the α -methyl functionality in 84% yield, reduced the enone alkene while simultaneously removing the benzyl protecting group, and then oxidized under basic epimerizing conditions to provide Corey's dione (**7.2**) in 65% with excellent diastereoselectivity.

Vanderwal's 21-step formal synthesis of **7.2** can be extrapolated to a 24-step synthesis of (+)-DICA using Corey's unselective endgame. The strengths of this synthesis include the high diastereoselectivity at which each stereocenter of the core is formed, the strategic manner in which multiple stereocenters are formed from a 4-electron Birch reduction, and the use of the tetrahydrofuran ring as a protecting group for sensitive functionality while the rest of the core is constructed. However, the synthesis also suffers from several drawbacks as well. The formal synthesis target **7.2** has been shown by Corey to proceed with poor diastereoselectivity when elaborated to the natural product and has since been replaced by Shenvi's endgame as an ideal approach for the completion of the natural product. Furthermore, the seven-step sequence converting tetrahydrofuran **7.56** to the aldol condensation precursor **7.57** involves several protections and redox manipulations. Our efforts to improve upon this formal synthesis are described in Chapter 8.

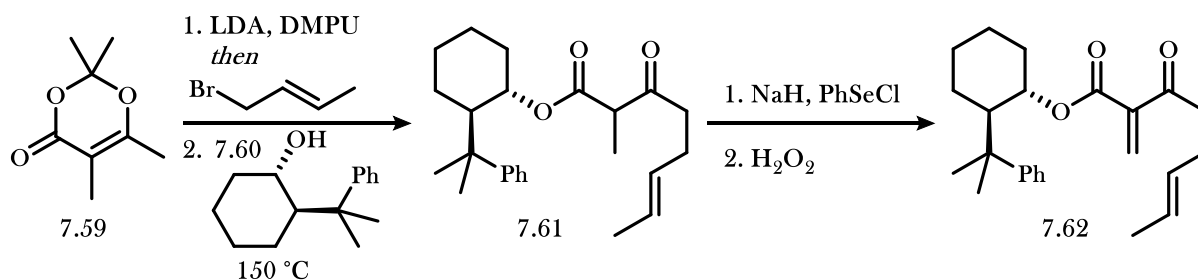
7.2.5 Shenvi's Synthesis of (+)-DICA

In 2016, the Shenvi group applied their Danishefsky-type dendralene double Diels–Alder strategy to the synthesis of (+)-DICA.¹⁴ Using a similar disconnection approach as their 2012 synthesis of racemic isocyanoamphilectene,¹⁵ Shenvi and co-workers prepared a complex tricyclic fragment rapidly and stereoselectively from relatively simple precursors. However, the synthesis of (+)-DICA was performed in an asymmetric manner via early incorporation of a chiral auxiliary which directed the facial selectivity of the initial Diels–Alder. Furthermore, the opposing stereochemistry at the C-1 position, installed in their original synthesis via conjugate addition, was instead set via HAT-reduction of the of the already-substituted enone, which proceeded with the same facial selectivity. To complete the synthesis, a sequence was developed to append the fourth ring and install the addition isonitrile in a selective manner.

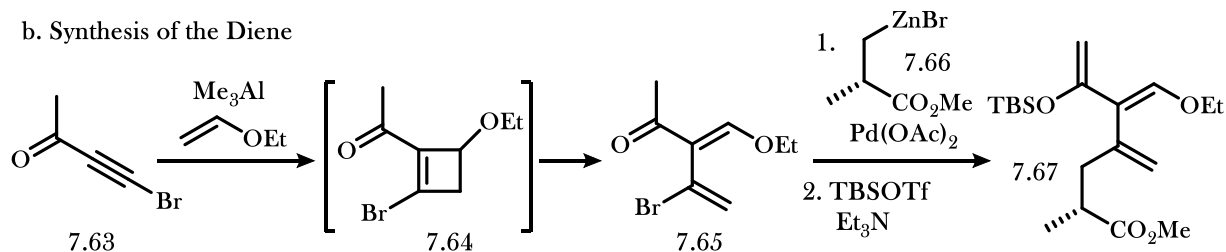
The synthesis begins with formation of both the diene **7.67** and dienophile **7.62** for the key intermolecular Diels–Alder transformation. The dienophile is formed in a four-step sequence beginning with γ -allylation of dioxanone **7.59**, and subsequent ring-opening transesterification with chiral auxiliary **7.60** forms β -ketoester **7.61** (Scheme 7.6a). Installation of an α -selenide and selenoxide elimination provides doubly-activated enone **7.62**, which is used directly in the Diels–Alder reaction without purification.

Scheme 7.6 Synthesis of the Diels–Alder Components

a. Synthesis of the Dienophile



b. Synthesis of the Diene



The Danishefsky-type dendralene **7.67** was formed in just three steps via a remarkably clever sequence (Scheme 7.6b). A formal [2+2] cycloaddition involving ethyl vinyl ether and ynone **7.63** provides cyclobutene intermediate **7.64**, which undergoes a spontaneous electrocyclic ring-opening to provide dienone **7.65**. The vinyl bromide is then alkylated via Negishi coupling with **7.66**. To form the diene that will eventually react in the first cycloaddition, the ketone was converted to the corresponding enoxy silane **7.67** via addition of TBSOTf. With the two complex Diels–Alder components in hand, Shenvi and co-workers then performed their key complexity-building step toward (+)-DICA.

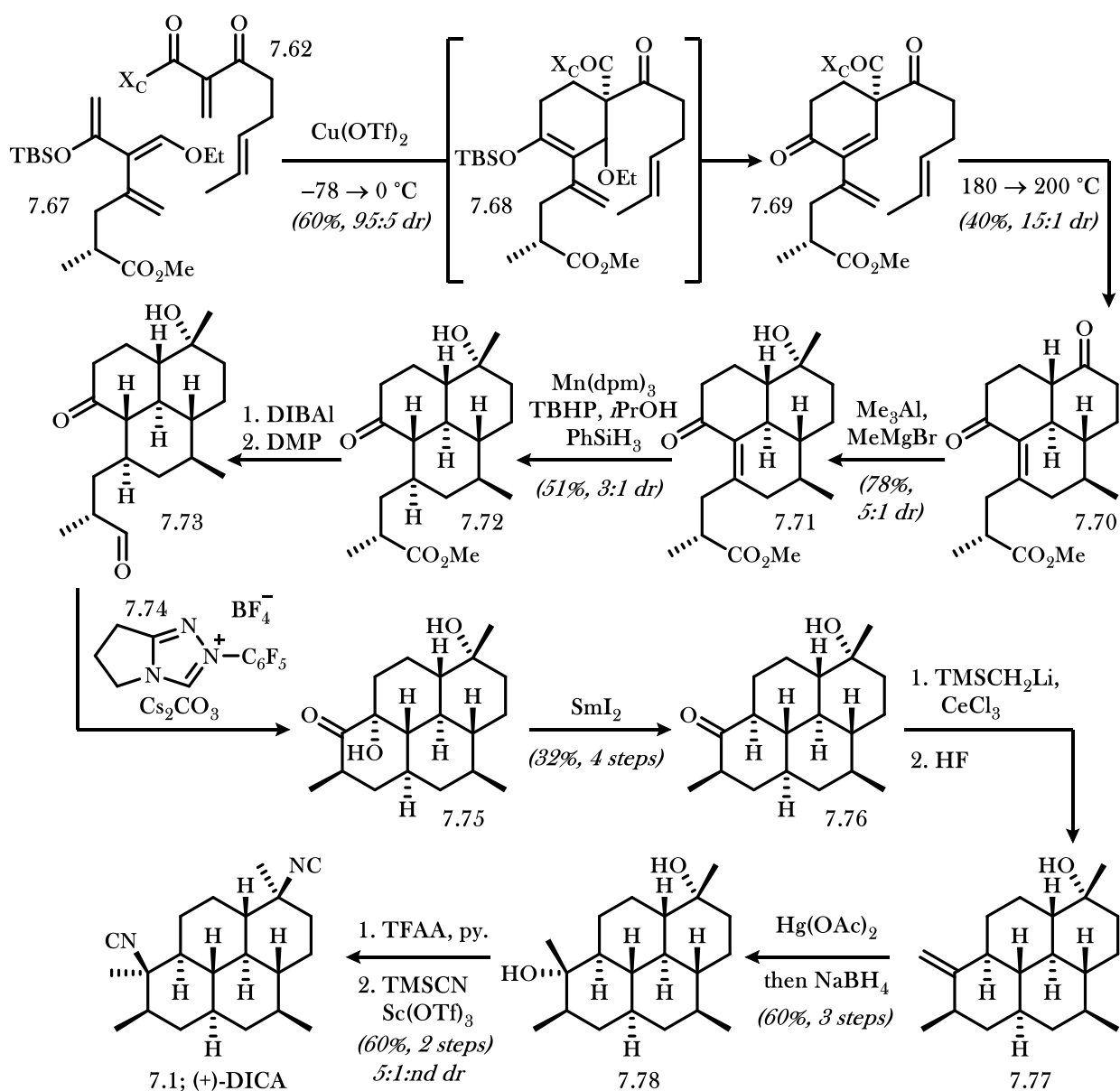
The cycloaddition between **7.62** and **7.67** proceeded in reasonable yield with very high diastereoselectivity relative to the chiral auxiliary, and the formed enoxy silane decomposed to the corresponding enone **7.69** under the reaction conditions via β -methoxy extrusion (Scheme 7.7). The resulting diene could then participate in a second Diels–Alder cycloaddition with the pendant alkene to provide the tricyclic product **7.70**. Under these reaction conditions, the chiral auxiliary was also removed to provide the ketone via a retro-heteroene/decarboxylation pathway. From this point forward, the reactivity strayed from that of the synthesis of isocyanoamphilectane and had to be developed anew.

Chemoselective tertiary alcohol installation provided **7.71** without adverse reactivity involving the enone, and a reduction of the enone was accomplished using hydrogen atom transfer (HAT) conditions to provide the thermodynamically-preferred stereoisomer **7.72**. Global reduction with DIBAL and subsequent oxidation provided aldehyde **7.73**, which then participated in an umpolung *N*-heterocyclic carbene-catalyzed nucleophilic addition to the ketone to provide α -hydroxyketone **7.75**. Samarium(II) iodide reduction effected deoxygenation of the α -ketol to provide ketone **7.76**.

At this point, the ketone **7.76** had to be converted to the equatorial tertiary alcohol **7.78** as a precursor to the stereoinvertive isonitrile installation developed previously by Shenvi and Pronin.⁶ Unfortunately, standard conditions for this transformation employing Yamamoto's bulky MAD aluminum Lewis acid and a variety of nucleophiles provided only the axial alcohol. To circumvent this issue, Shenvi and co-workers converted the ketone to vinylidene **7.77** in a two-step Peterson olefination sequence. Taking

advantage of the observed preferred face of attack, they then employed an oxymercuration/reduction to give the desired equatorial alcohol **7.78**. Using their two-step activation/invertive displacement methodology, Shenvi and co-workers then installed the tertiary isonitriles to provide **7.1** with high selectivity.

Scheme 7.7 Shenvi's Synthesis of (+)-DICA



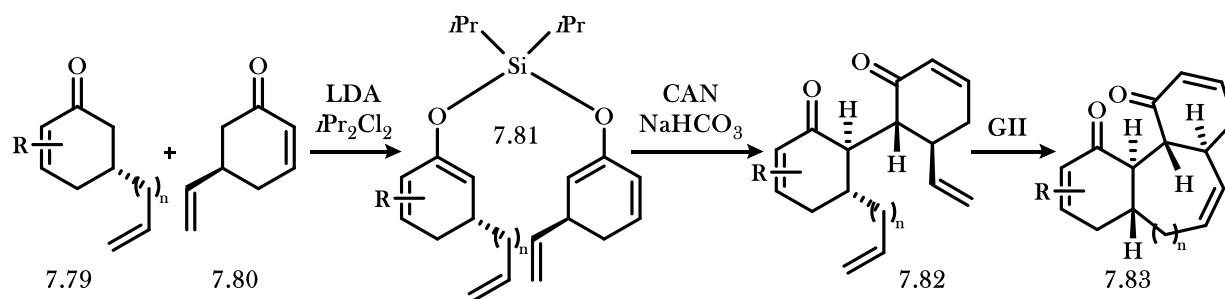
The synthesis of (+)-DICA reported by Shenvi and co-workers is a truly strategic synthesis of this natural product focusing on a minimum number of complexity-building transformations. The Danishefsky-

type dendralene Diels–Alder provides access to a tricyclic precursor to (+)-DICA in just two steps from acyclic precursors and sets each stereocenter with high selectivity. Closure of the fourth ring is accomplished by a unique unpolung transformation, and installation of the isonitriles demonstrates improvements over the strategies employed by both Corey and Mander. Although the potential improvements to the synthesis are limited in number, the sequence employing three redox manipulations in four steps to form ketone **7.76** might be shortened, and a one-step equatorial alcohol formation from ketone **7.76** would greatly improve the synthesis. Despite the slight room for improvement, the synthesis of (+)-DICA reported by Shenvi and co-workers makes significant contributions to the field of ICT total synthesis.

7.2.6 Thomson's Formal Synthesis of DICA

In 2018, Robinson and Thomson developed a method for the formation of tricyclic products such as **7.83** from simple cyclohexenone precursors and applied their methodology to a formal total synthesis of (+)-DICA.¹⁶ Their methodology begins with formation of a *bis*-dienoxysilane **7.81** formation by treating two enone precursors with dichlorodiisopropylsilane and lithium diisopropylamide (Figure 7.3). Following formation of the mixed silane, addition of ceric ammonium nitrate promotes an oxidative ring closing reaction to provide the 1,4-diketone **7.82**. The tricyclic product **7.83** is then completed via a ring-closing alkene metathesis. The overall sequence provides products of varying ring size and substitution in generally useful yields considering the complexity of the products. The utility of this strategy is then demonstrated with its application to a concise synthesis of (+)-DICA.

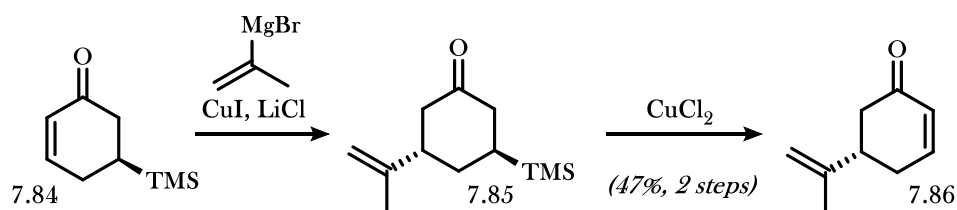
Figure 7.3 Robinson and Thomson's Oxidative Enone Coupling



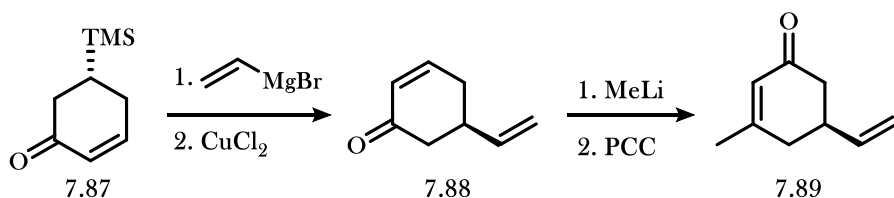
The cyclohexenone components for the key oxidative tricycle formation were first procured from relatively simple cyclohexenone building blocks. Fragment **7.86** was formed in a two-step substrate-directed diastereoselective conjugate addition to provide cyclohexanone **7.85**, and an oxidative elimination generated the desired enone **7.86** in 47% over 2 steps (Scheme 7.8a). Fragment **7.89** was generated by a similar strategy beginning with a conjugate addition to form **7.88**. 1,2-addition of methyllithium followed by an oxidative transposition provided cyclohexenone **7.89** in 39% yield over 4 steps (Scheme 7.8b).

Scheme 7.8 Thomson's Formal Synthesis of (+)-DICA

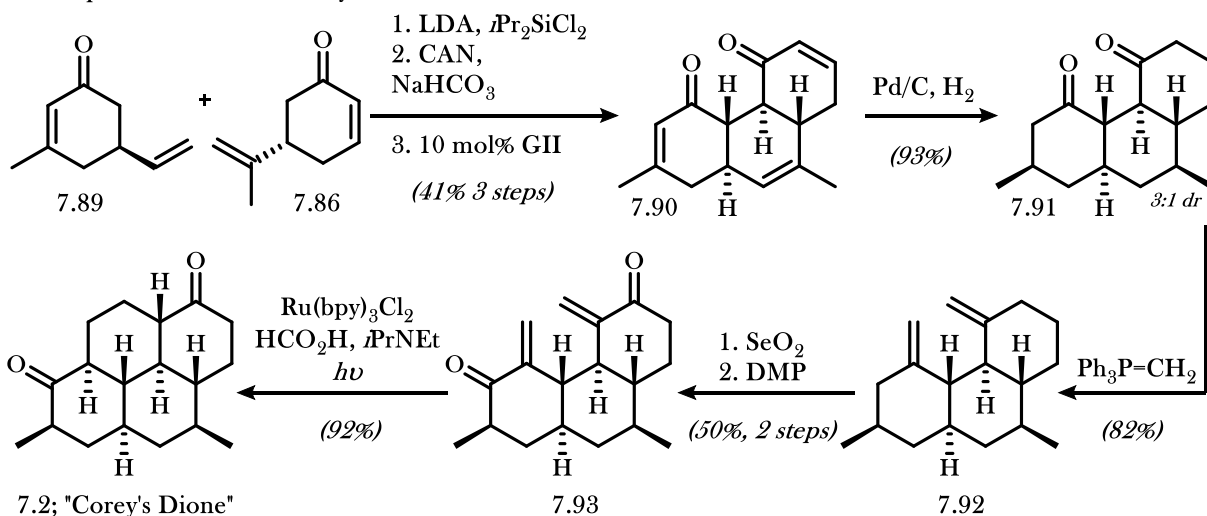
a. Synthesis of Fragment A



b. Synthesis of Fragment B



c. Completion of the Formal Synthesis



With the coupling partners in hand, they then performed a three-step oxidative cyclization/metathesis sequence to provide tricyclic product **7.90** with high diastereoselectivity in 41% over three steps. A global hydrogenation provided saturated tricycle **7.91** with modest diastereoselectivity, and a Wittig methylenation of the desired diastereomer provided *bis*-vinylidene **7.92** in high yield. A *bis*-allylic oxygenation and subsequent oxidation provided *bis*-enone **7.93** in 50% over 2 steps. To complete the formal synthesis, Robinson and Thomson then accomplished a reductive enone coupling using Yoon's protocol¹⁷ to afford tetracycle **7.2** in an impressive 92% yield. As described in section 7.2.1, Corey's dione can be elaborated over a three-step sequence to a mixture of diastereomers including (+)-DICA.

The work of Robinson and Thomson demonstrates a combination rarely observed in methodology-based synthesis where a strategy does not have to bend to incorporate its defining key step. The oxidative enone coupling and alkene metathesis sequence provides a portion of the core in high yield, high diastereoselectivity, and with the proper functionality installed to complete the formal synthesis in a straightforward manner. The pseudo-symmetrical structure of (+)-DICA has begged for a dimerization-based strategy to be explored, and the authors have provided an excellent initial example of a synthesis completed via coupling of two similar fragments. Although the formal synthesis still relies on Corey's inefficient endgame toward the completed natural product, the work reported by Robinson and Thomson makes a significant contribution to the myriad of strategies by which the core of (+)-DICA can be procured.

7.3 Conclusions

The potent and noteworthy bioactivity of (+)-7,20-diisocyanoadociane has led to a variety of synthetic efforts toward its efficient synthesis in a laboratory setting. Since the syntheses of Corey and Mander, both of which provided access to DICA with their own advantages but suffered from significant drawbacks, synthetic approaches have improved to be both concise and stereoselective. Although current strategies can access (+)-DICA as a single diastereomer in a succinct manner, a multitude of a strategies will be necessary to allow derivatization for further biological testing. As a result, the need for additional and improved syntheses toward (+)-DICA remains.

7.4 Notes and References

- (1) Baker, J. T.; Wells, J. R.; Oberhänsli, W. E.; Hawes, G. B. *J. Am. Chem. Soc.* **1976**, *98*, 4010–4012.
- (2) van Soest, W. M.; Desqueyroux-Faúdez, R.; Wright, A. D.; König, G. M. *Bull. Ins. R. Sci. Nat. Belg. Biol.* **1996**, *66*, 103.
- (3) König, G. M.; Wright, A. D. *Magn. Reson. Chem.* **1995**, *33*, 694–697.
- (4) Corey, E. J.; Magriotis, P. A. *J. Am. Chem. Soc.* **1987**, *109*, 287–289.
- (5) Corey, E. J.; Peterson, R. T. *Tetrahedron Lett.* **1985**, *26*, 5025–5028.
- (6) Pronin, S. V.; Reiher, C. A.; Shenvi, R. A. *Nature* **2013**, *501*, 195–199.
- (7) Fairweather, K. A.; Mander, L. N. *Org. Lett.* **2006**, *8*, 3395–3398.
- (8) Simpson, J. S.; Garson, M. J. *Org. Biomol. Chem.* **2004**, *2*, 939–948.
- (9) Miyaoka, H.; Okubo, Y.; Muroi, M.; Mitome, H.; Kawashima, E. *Chem. Lett.* **2011**, *40*, 246–247.
- (10) Roosen, P. C.; Vanderwal, C. D. *Angew. Chem. Int. Ed.* **2016**, *55*, 7180–7183.
- (11) Daub, M. E.; Prudhomme, J.; Le Roch, K.; Vanderwal, C. D. *J. Am. Chem. Soc.* **2015**, *137*, 4912–4915.
- (12) Siegel, C.; Gordon, P. M.; Razdan, R. K. *J. Org. Chem.* **1989**, *54*, 5428–5430.
- (13) Meinwald, J.; Labana, S. S.; Chadha, M. S. *J. Am. Chem. Soc.* **1963**, *85*, 582–585.
- (14) Lu, H.-H.; Pronin, S. V.; Antonova-Koch, Y.; Meister, S.; Winzeler, E. A.; Shenvi, R. A. *J. Am. Chem. Soc.* **2016**, *138*, 7268–7271.
- (15) Pronin, S. V.; Shenvi, R. A. *J. Am. Chem. Soc.* **2012**, *134*, 19604–19606.
- (16) Robinson, E. E.; Thomson, R. J. *J. Am. Chem. Soc.* **2018**, *140*, 1956–1965.
- (17) Du, J. N.; Espelt, L. R.; Guzei, I. A.; Yoon, T. P. *Chem. Sci.* **2011**, *2*, 2115–2119.

CHAPTER 8: A SECOND-GENERATION SYNTHESIS OF (+)-7,20-DIISOCYANOADOCIANE

8.1 Introduction and Motivation

Studies toward natural product total synthesis often identify ideal bond disconnections that cannot be fashioned by known methodologies. In cases such as these, the development of new synthetic methodologies is vital. Following the development of new strategies to form previously-elusive bonds, the opportunity to merge previously reported strategies with modern methodologies presents itself. In the work described below, we redesign our strategy toward (+)-7,20-diisocyanoadociane to not only incorporate improvements designed in hindsight from our first-generation synthesis, but also to include modern methodologies for stereodefined tertiary isonitrile installation, resulting in a significantly more efficient and scalable synthesis.

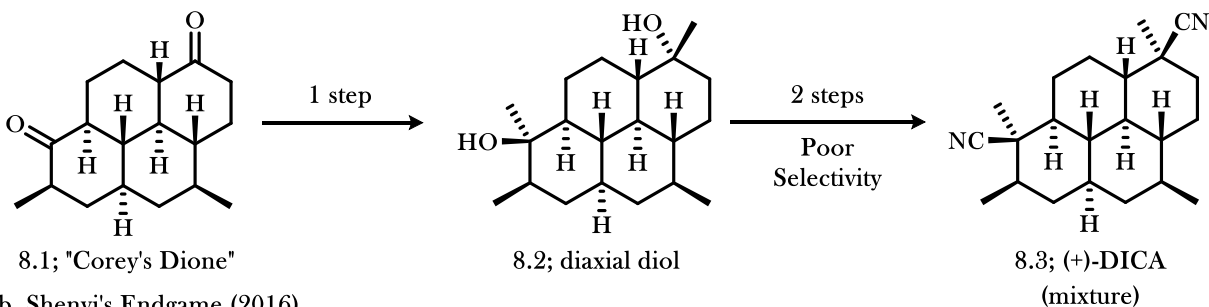
8.1.1 Original Strategy and Room for Improvement

In our 2016 formal synthesis of (+)-7,20-diisocyanoadociane (**DICA**),¹ described in detail in Chapter 7, we disclosed a 21-step route toward Corey's dione (**8.1**; Figure 8.1) using a 4-electron Birch reduction as a key step to establish multiple stereocenters with high selectivity. However, Corey's dione (**8.1**), initially reported as an intermediate in Corey and Magriotis's total synthesis of (+)-**DICA**,¹ is further elaborated to the completed natural product using a now-obsolete methodology for tertiary isonitrile installation. From ketone **8.1**, Corey formed the *bis*-axial alcohol **8.2**, and then accomplished a non-diastereoselective *bis*-isonitrile installation to provide (+)-**DICA** (**8.3**) as a complex diastereomeric mixture.

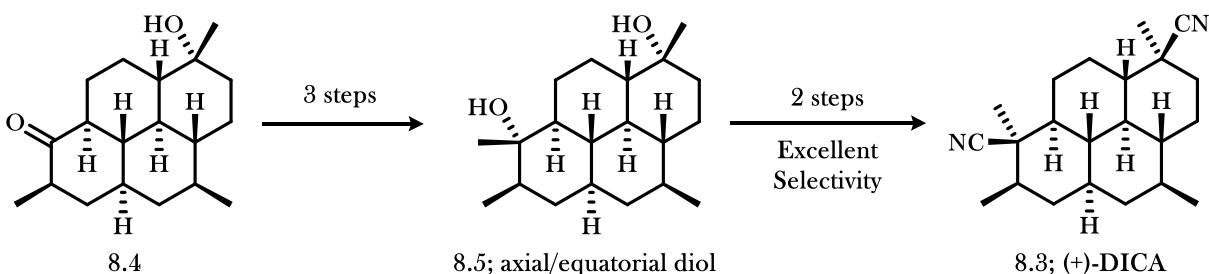
At the time, Corey's endgame included the best method available for the formation of the tertiary isonitriles. However, recent advances in the field reported by Pronin and Shenvi allow for the stereoinvertive installation of tertiary isonitriles with good selectivity.² In their 2016 synthesis of (+)-**DICA**, they showcase the impact of their methodology and procure (+)-**DICA** with high diastereoselectivity from stereodefined *bis*-tertiary alcohol **8.5**.³ Following the disclosure of Pronin and Shenvi's methodology, the incorporation of a highly efficient method for isonitrile installation now becomes a requirement in the synthesis of isocyanoterpene natural products.

Figure 8.1 Reported Endgames to (+)-DICA

a. Corey's Endgame (1987)



b. Shenvi's Endgame (2016)



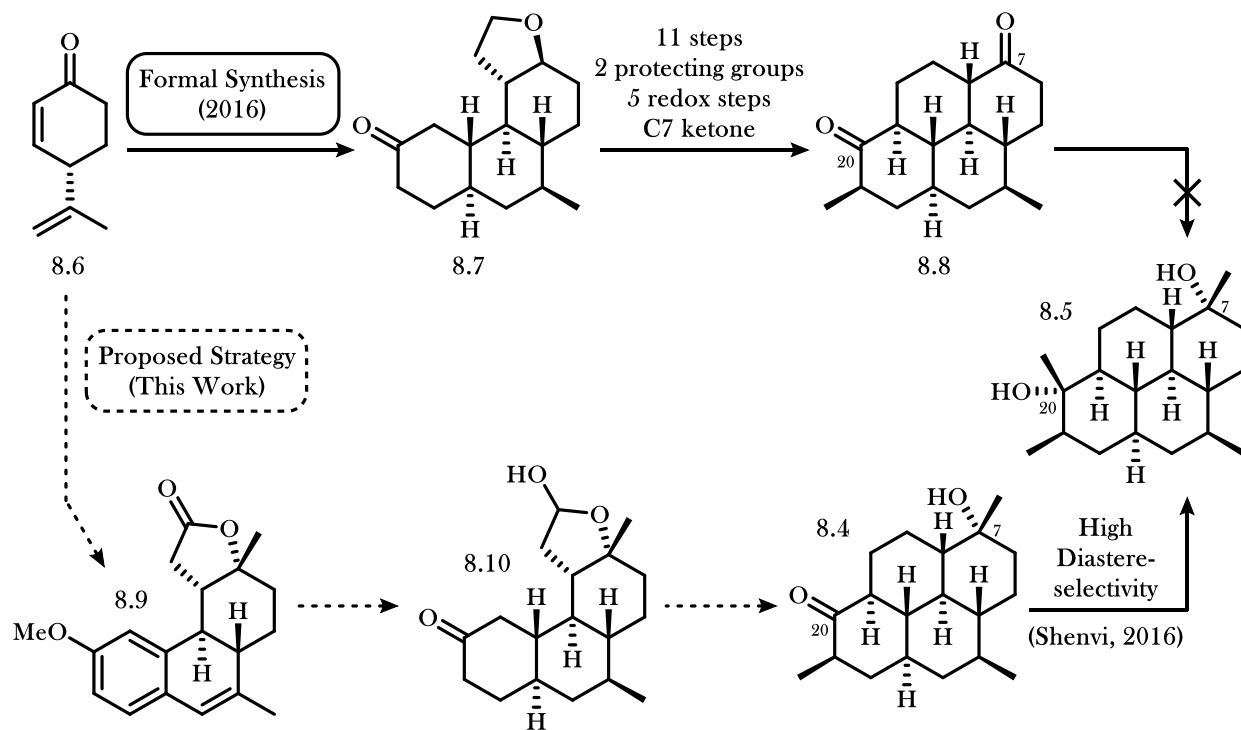
Since the tertiary isonitriles of (+)-DICA possess opposing arrangements about their parent cyclohexane ring (one axial and one equatorial isonitrile substituent), the corresponding *bis*-tertiary alcohols of its precursor must therefore also possess one axial and one equatorial alcohol. However, since the two ketone functionalities of Corey's dione (**8.1**) experience similar steric and electronic environments, it would likely be difficult to accomplish a selective tertiary alcohol formation from a single ketone while leaving the other intact. As observed in Corey's synthesis, exposure of dione **8.1** to an organometallic nucleophile forms the tertiary alcohol pair with *bis*-axial configurations. Since there currently lacks a method for the formation of configurationally-differentiated diol **8.5** from dione **8.1**, Corey's dione is no longer the most strategic precursor on route to (+)-DICA.

8.1.2 Proposed Revised Route

To improve upon our previous synthesis of (+)-DICA, we planned to use the general strategy of our initial synthesis to access strategic precursor **8.5** (Figure 3.2). Rather than attempting to set the two alcohol stereocenters in successive reactions from Corey's dione (**8.1**), we thought it would be advantageous to instead install the axial C-7 tertiary alcohol stereocenter early in the synthesis, which would allow us to install the C-

20 equatorial tertiary alcohol upon completion of the tetracyclic core without risk of adverse reactivity. Since our initial route already involves reactivity at the C-7 position when the ketone resulting from tandem vicinal functionalization is reduced to secondary alcohol, we identified this point in the synthesis as an ideal time for tertiary alcohol installation.

Figure 8.2 Proposed Revised Strategy Toward (+)-DICA



We also hoped that the revised route could strengthen a less-efficient portion of our original synthesis as well. We targeted a seven-step sequence in our original synthesis involving conversion of tetrahydrofuran **8.7** to the tetracyclic product **8.8** as a weakness that could be significantly improved. The inefficiency of the sequence is a result of the ring possessing an improper oxidation state for aldol condensation and the need to protect the C-7 secondary alcohol while leaving the less-sterically hindered primary alcohol unprotected. As a result, this sequence involves several redox manipulations and the use of two separate protecting groups to differentiate the alcohols.

We believed we could accomplish our goals for a revised synthesis by designing a route that passes through lactone **8.9**. This intermediate contains the stereodefined C-7 stereocenter, set via organometallic addition to the ketone resulting from our initial tandem vicinal difunctionalization, thereby providing access to the use of Shenvi's endgame for stereoselective isonitrile installation. However, this lactone is not in the correct oxidation state to participate in an aldol condensation later in the synthesis, so a reduction would be required. Rather than facilitating a full reduction to the ring-opened diol analogous to our original route, we instead pursued more strategic use of the lactone functionality.

With the C-7 stereocenter now fully-substituted, it is no longer susceptible to oxidation prior to the aldol condensation and therefore does not need to be protected. In the presence of the unprotected C-7 alcohol, oxidation of the primary alcohol to the aldehyde would likely lead to the formation of lactol **8.10** in equilibrium. We noticed that lactol **8.10** is a single oxidation state away from that of our lactone precursor **8.9**, and therefore might be procured by more strategic means. Since the nucleophilic partner for the aldol condensation is prepared by a Birch reduction sequence, we hoped that we could also accomplish lactone reduction to the lactol in an overall 6-electron reduction step.

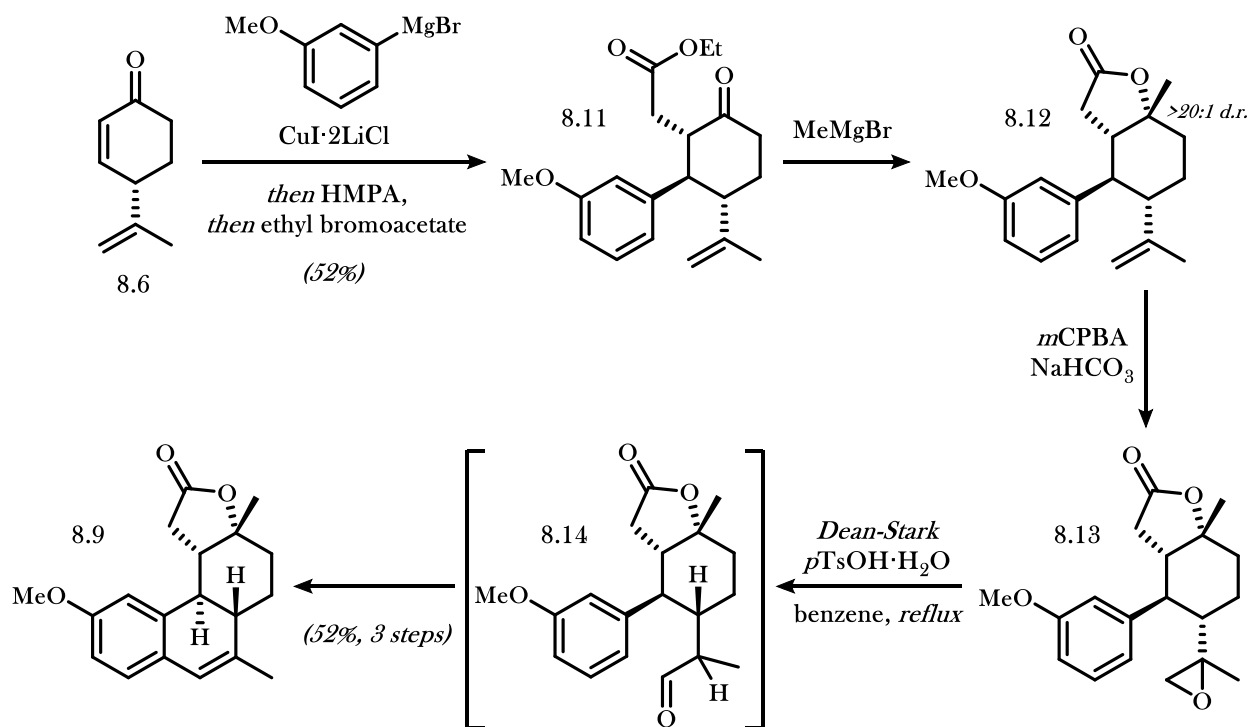
8.2 Initial Des-Methyl Strategy toward (+)-DICA

8.2.1 Early Work and C-7 Stereocenter Installation

Our revised synthesis of (+)-DICA began with the identical tandem vicinal difunctionalization of **8.6** used previously to set two key stereocenters in high diastereoselectivity (Scheme 8.1). Rather than reduce the dicarbonyl intermediate **8.11** to the diol as performed in our previous synthesis, the dicarbonyl product was isolated. We discovered that methylmagnesium bromide addition to the ketone functionality proceeded with high diastereoselectivity, and the formed alkoxide spontaneously closed onto the pendant ester to cleanly provide the lactone **8.12**. An attempt at a one-pot conjugate addition/enolate trapping/lactone formation sequence did provide product in low yields and could be a source of further investigation to reduce the number of steps toward (+)-DICA.

The crude product mixture was then subjected to a two-step formal dehydrative C-C coupling sequence utilized in our previous synthesis. Epoxidation of the alkene provided epoxide **8.13** as a mixture of diastereomers, and subsequent heating in the presence of catalytic acid accomplished a one-pot Meinwald rearrangement and Friedel-Crafts condensation to provide the styrenyl product **8.9**. With the tetracyclic product **8.9** in hand, we could then begin efforts to accomplish a 6-electron Birch reduction.

Scheme 8.1 Formation of the Des-Methyl Lactone-Containing Birch Precursor



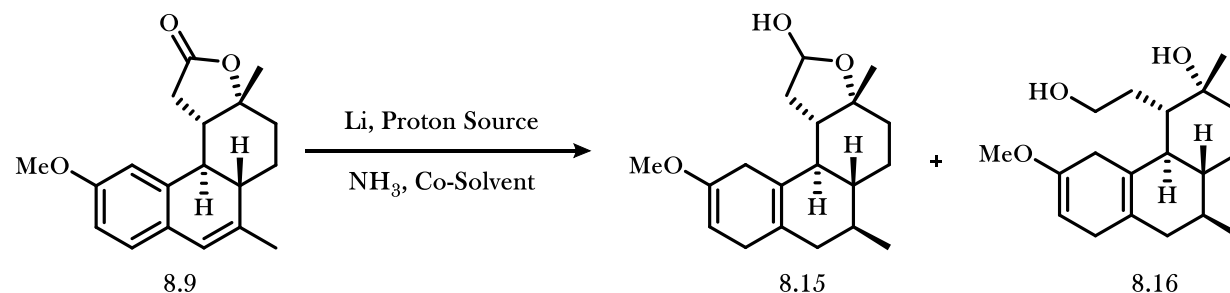
8.2.2 Des-Methyl Birch Reduction

The difficulty of the Birch reduction lies in the preservation of the lactone moiety under conditions necessary to accomplish reduction of the electron-rich aromatic ring. Reduction of the styrenyl olefin and lactone of **8.9** proceed at a rapid rate owing to the highly stabilized radical anion intermediates formed and the lack of aromatization energy that must be overcome. However, reduction of electron-rich aromatic rings is far slower by comparison. Although the extended reaction times are typically not detrimental to product yield, the presence of the lactone introduces complications; the highly basic conditions intrinsic to Birch reductions increase the presence of the free aldehyde in equilibrium, which can be reduced under the reaction

conditions. To afford a high yield of Birch product **8.15** (Table 8.1), we would have to accomplish rapid aromatic reduction while somehow preventing opening and reduction of the lactol.

Initial testing of the Birch reduction using conditions employed in our original synthesis resulted in rapid and complete formation of diol prior to aromatic ring reduction. Attempts to accomplish full reduction to diol **8.16** were unsuccessful; only *ca.* 40% of the aromatic ring was reduced to cyclohexadiene **8.16** after several hours in the presence of lithium (Entry 1; Table 8.1). Attempts to accomplish complete reduction of silylated **8.16** were similarly unsuccessful (see Experimental Procedures). Due to the highly nonpolar character of lactone **8.9** and observation of insolubility prior to addition of lithium, we hypothesized that solubility considerations would have a key effect on conversion. Increasing the ratio of THF to NH₃ from 1:4 to 1:2 increased consumption of the aromatic ring to *ca.* 75% (Entry 2), but we could not drive it to further conversion. Attempts to further increase the ratio of THF to NH₃ resulted in the observation of biphasic reaction mixtures.

Table 8.1 Birch Reduction Conditions on the Des-Methyl Substrate



Entry	Proton Source	Co-Solvent	Co-Solvent:NH ₃	Total Concentration	Reduction Product	Reverse Add'n	Arene Reduction	NMR Yield
1	MeOH	THF	1:4	0.020 M	8.16	--	40%	
2	MeOH	THF	1:2	0.007 M	8.16	--	75%	
3	<i>t</i> BuOH	THF	1:5	0.008 M	8.15	--	46%	
4	<i>t</i> BuOH	THF	1:3	0.008 M	8.15	--	55%	
5	<i>t</i> BuOH	THF	1:1	0.005 M	8.15	Yes	89%	
6	<i>t</i> BuOH	dioxane	1:3	0.020 M	8.15	Yes	88%	
7	<i>t</i> BuOH	DME	1:3	0.020 M	8.15	Yes	>95%	40%
8	<i>s</i> BuOH	DME	1:3	0.020 M	8.15	Yes	86%	36%
9	<i>n</i> PrOH	DME	1:3	0.020 M	8.16	Yes	--	--

Unable to procure higher yields by increasing the solubility of intermediates, we turned to investigating other reaction condition variables. Unexpectedly, replacement of methanol as a proton source with *tert*-butanol eliminated lactol opening and reduction completely and afforded lactol product **8.15** with *ca.* 46% reduction of the aromatic ring (Entry 3). This result is rather counterintuitive; the increased pK_a of *tert*-butanol relative to methanol would likely increase the ratio of deprotonated lactol in the reaction mixture, thereby increasing the equilibrium presence of free aldehyde. Since the use of aniline as a proton source also results exclusively in the formation of diol **8.16**, we suspect the bulky nature of *tert*-butanol as a proton source is the foundation of the observed discrepancy. Further studies are warranted to determine the exact cause for this observed difference in reactivity.

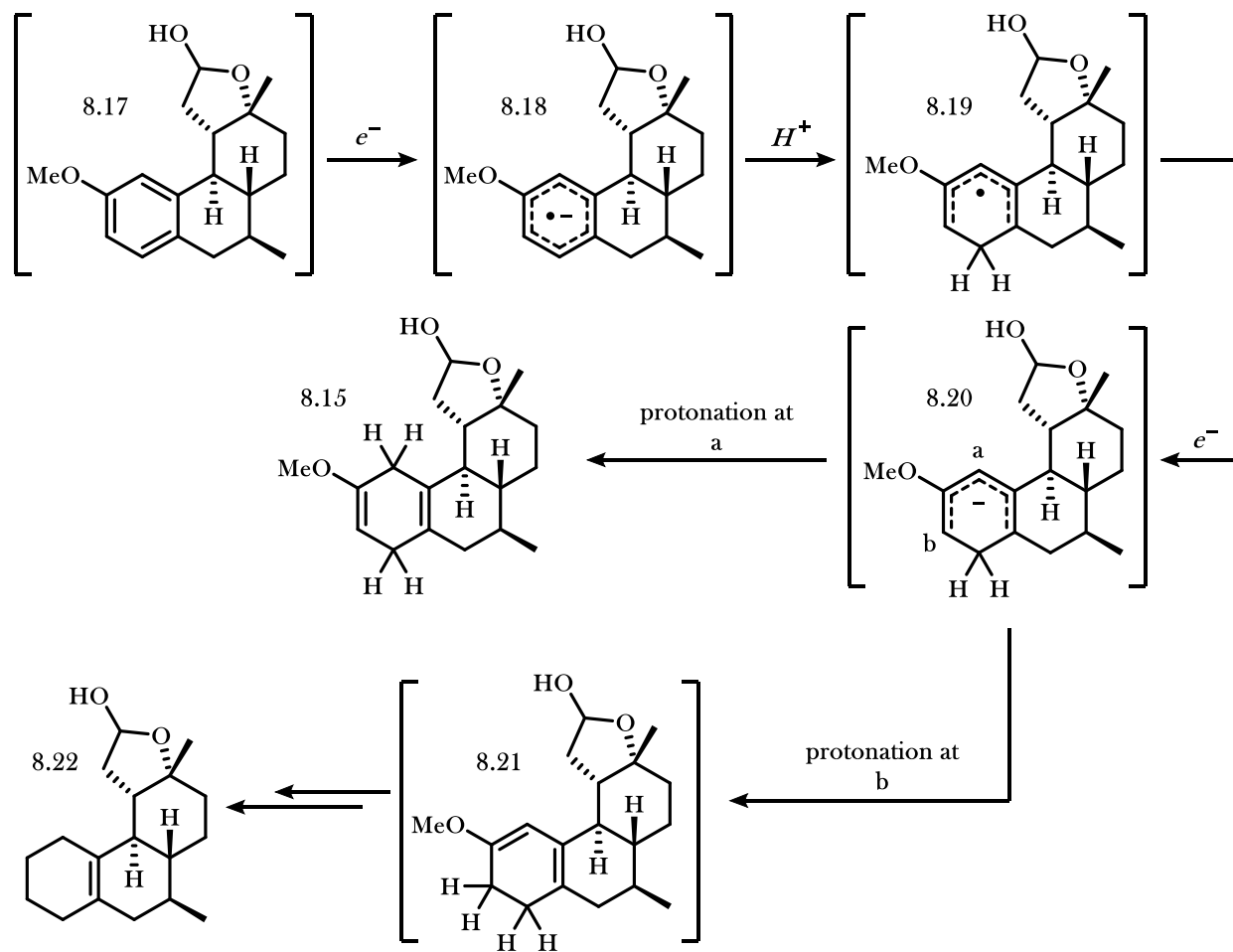
Inspired by our previous observation that intermediate solubility is crucial to accomplish conversion, we again increased the ratio of THF to NH₃ and observed only a slight increase in arene consumption (*ca.* 55%; Entry 4). To overcome this issue, an investigation into the experimental setup was necessary. Under commonly used Birch reduction conditions, each component of the reaction mixture is added prior to lithium addition (substrate, proton source, ammonia, and co-solvent). Although our substrate is soluble in THF, addition of **8.9** as a solution in THF to ammonia results in the immediate formation of an insoluble suspension. We postulated that instantaneous reduction was necessary upon introduction of the solution of **8.9** in THF to the ammonia solution, before **8.9** solidified out of the reaction mixture as a powder. To accomplish this, we instead added **8.9** as a solution in THF to a mixture of ammonia, *tert*-butanol, and dissolved lithium. Using this experimental setup, we observed *ca.* 89% consumption of the aromatic ring (Entry 5). By changing the solvent to 1,2-dimethoxyethane, we were able to accomplish complete aromatic ring consumption (Entry 7).

Our initial excitement over seemingly clean conversion was quenched upon the isolation of low quantities of the enone following hydrolysis and purification. After a thorough investigation into the product mixture, we identified cyclohexene **8.22** as a product formed in a *ca.* 1:1 ratio with cyclohexadiene **8.15**. Because the byproduct **8.22** does not contain the diagnostic ¹H peaks of the cyclohexadiene (vinyl proton

and methyl ether protons), we previously did not observe its presence. We found that this infrequently observed byproduct⁴ results from passage down an alternative mechanistic pathway during arene reduction.

Following a series of single-electron reductions and anion protonations from **8.17**, pentadienyl anion **8.20** is formed as part of the reduction mechanism (Figure 8.3). Since protonation is slow to occur at substituted positions owing to steric hindrance, protonation will occur at either *ortho*-position relative to the methyl ether. Typically, protonation at position *a* will occur more rapidly than at position *b* due to the relative HOMO orbital coefficients. However, in circumstances where pendant functional groups of the substrate provide steric hindrance to protonation at position *a*, protonation at position *b* is observed. The resulting conjugated cyclohexadiene **8.21** is susceptible to further reduction under Birch conditions, eventually resulting in the formation of cyclohexene **8.22**.

Figure 8.3 Proposed Mechanism Toward Cyclohexene Byproduct **8.22**

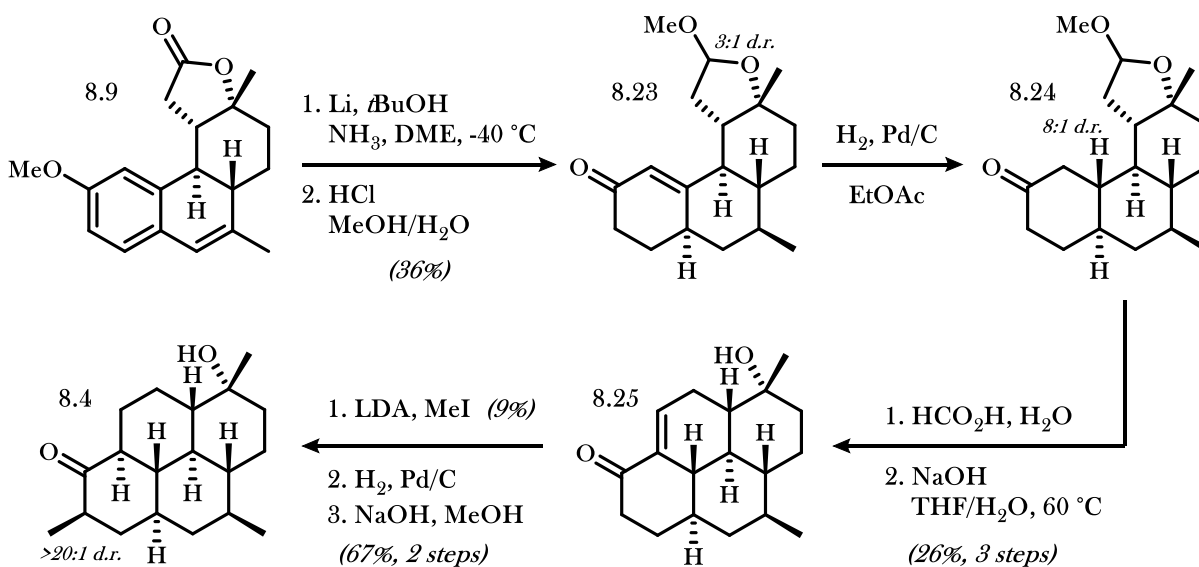


We hoped that the addition of a less sterically-hindered proton source that could better access position *a* would increase the ratio of product **8.15** to byproduct **8.22**. However, we found *sec*-butanol to have little impact on the product yield (Entry 8; Table 8.1), and the use of isopropanol resulted in lactol opening and reduction (Entry 9). Unable to further improve the yield, we pushed forward with our optimized conditions. Birch reduction and subsequent hydrolysis provided methyl acetal **8.23** in 36% yield (Scheme 8.2). Although the lactol could be procured via hydrolysis in solvents other than methanol in diminished yields, the acetal was formed intentionally because of its increased stability relative to the corresponding lactol.

8.2.3 Completion of the Formal Synthesis

The cyclohexenone **8.23** was hydrogenated using Pd/C as a catalyst to provide cyclohexanone **8.24** in an 8:1 diastereomeric ratio. Attempts to accomplish an aldol condensation directly from acetal **8.24** were unsuccessful, so the acetal was hydrolyzed to the corresponding lactol. Although the tetracyclic core could not be formed under acidic conditions, we found that heating in the presence of aqueous sodium hydroxide provided product **8.25** in 26% yield over three steps. Attempts to optimize conditions to provide better yields, including employing alternative bases, were unsuccessful.

Scheme 8.2 Completion of the Des-Methyl Formal Synthesis



We planned to complete the formal synthesis in an analogous manner to our original synthesis. Because precursor **8.25** contains a more acidic proton than the ketone α -position, the α -methylation of the ketone would have to proceed via formation of the dianion intermediate. A single attempt to accomplish an α -methylation of ketone **8.25** provided the *mono*-methylated product in just 9% yield, accompanied by a significant amount of the geminally *bis*-methylated ketone as the major product. Although this reaction could likely be optimized to provide higher yield of the *mono*-methylated product, these efforts were found to be unnecessary based on the results described in section 3.3 below. The α -methylated product could then be hydrogenated and epimerized under basic conditions to provide **8.4** in 67%. Since ketone **8.4** is used as an intermediate in Shenvi's synthesis of DICA, its formation completes a formal synthesis.

8.2.4 Route Summary

Our revised formal synthesis of (+)-DICA accomplishes the two main goals that provoked its inception; this new route targets a more strategic precursor (**8.4**) with the C-7 stereocenter already in place, the improves upon the 7-step sequence from Birch reduction product to the tetracyclic core. Incorporating Shenvi's 5-step endgame strategy, this shortens our synthesis to 20 steps and has the potential to significantly increase the overall efficiency. However, there remain several areas for improvement.

Although the Birch reduction accomplishes the selective formation of several key stereocenters, the reaction suffers from significant byproduct formation and only provides enone **8.23** in 36% yield over two steps. Furthermore, the formation of the tetracyclic via base-catalyzed aldol condensation is inefficient, providing the product enone **8.25** in 26% over three steps. Although we believe the yield of the ketone α -methylation could be improved, the 9% yield of our initial attempt is unacceptable for a simple transformation. Although less detrimental to the overall synthesis, the need to hydrolyze acetal **8.24** to the lactol prior to cyclization is less than strategic.

Overall, the revised formal synthesis of (+)-DICA supports our hypothesis that the intermediate formation of lactone **8.9** not only shortens the number of steps to make the tetracyclic core but also provides access to tertiary alcohol **8.4** as a strategic precursor to (+)-DICA.

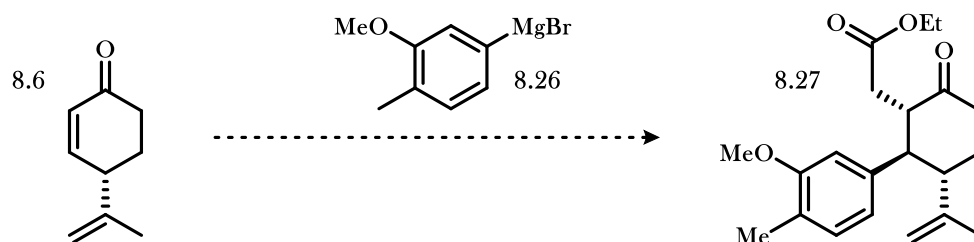
8.3 Early Installation of Methyl Group

8.3.1 Effects of Early Methyl Incorporation

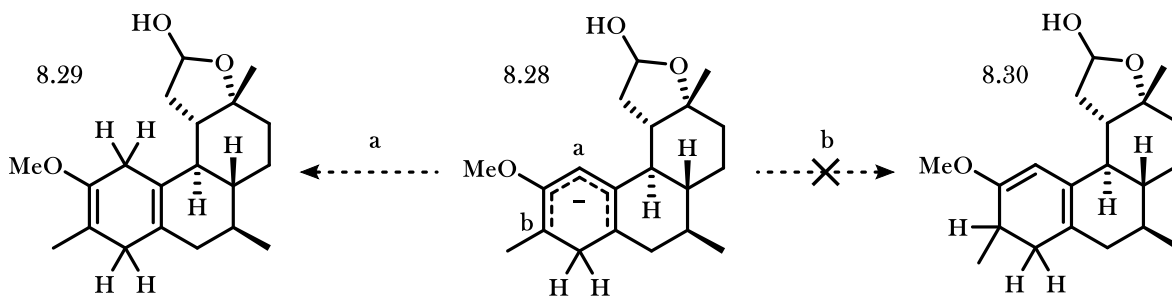
Following the completion of our revised synthesis, we began seeking solutions to the shortcomings described in section 3.2.4. When considering the ketone α -methylation, we noted that the ring to which the methyl group is bound is introduced in the initial conjugate addition to enone **8.6**. If the nucleophilic precursor to the conjugate addition already contains the methyl substituent, then the step required to install it would no longer be necessary (Figure 8.4a). By using **8.26** as a Grignard precursor, we could eliminate a potential 9% yield and lower the overall step count.

Figure 8.4 Impact of Initial Introduction of Methyl Group on the Arene Ring

a. Use of Methylated Aryl Grignard Reagent **8.26**



b. Potential Byproduct Suppression in Birch Reduction



When considering the downstream effects of early methyl incorporation, we acknowledged the added difficulty that we would likely encounter during efforts to reduce the more electron-rich aromatic ring. However, we then recalled that the presence of a substituent on the ring would prevent protonation at that position over the course of a Birch reduction (Figure 8.4b). With protonation unlikely to occur at the now-substituted undesired position **b** from pentadienyl anion **8.28**, byproduct formation should be diminished.

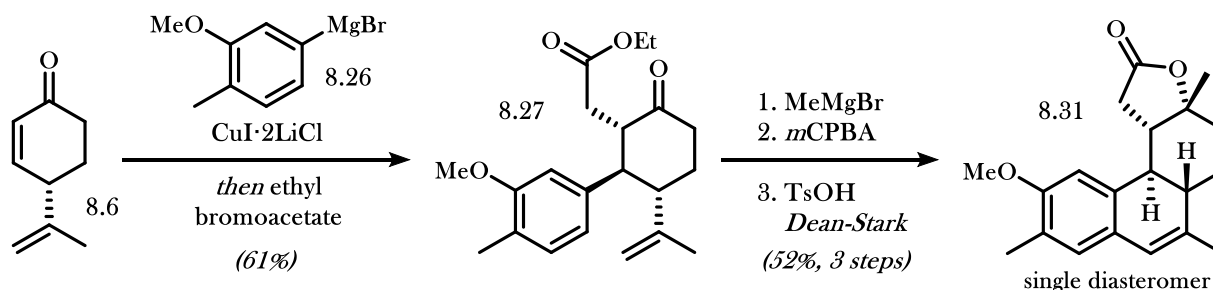
The early incorporation of a methyl substituent on the aromatic ring should thereby significantly improve the efficiency of our synthesis.

8.3.2 Revised Birch Reduction

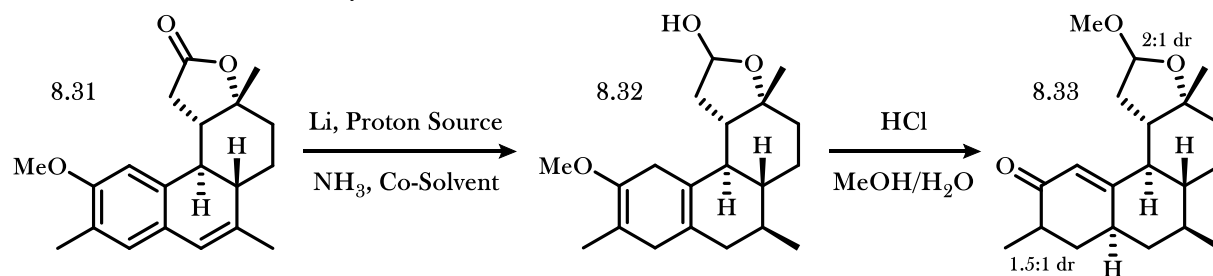
The newly revised route begins using identical conditions to those of the initial route described above. The tandem vicinal difunctionalization of enone **8.6** provided dicarbonyl **8.27** in a slightly-improved 62% yield, and the subsequent three-step sequence for to provide Birch reduction precursor **8.31** proceeded with identical 52% yield.

Scheme 8.3 Early Work and Birch Reduction with the Methyl-Containing Substrate

a. Synthesis of the Birch Precursor



b. Birch Reduction of the Methylated Precursor



Entry	Proton Source	Co-Solvent	Co-Solvent: NH_3	Total Concentration	Reduction Product	Reverse Add'n	Arene Reduction	Isolated Yield of 8.33
1	<i>t</i> BuOH	DME	1:3	0.020 M		(insoluble in DME)		
2	<i>t</i> BuOH	dioxane	1:2.5	0.019 M		(slow reduction; decomposition)		
3	<i>s</i> BuOH	dioxane	1:2.5	0.019 M	8.32	Yes	>95%	70%

Unfortunately, our previously optimized conditions for the Birch reduction were ineffective; Birch precursor **8.31** was insoluble in DME and could not be added to the reaction mixture as a solution. After a

short screen, we identified 1,4-dioxane as a solvent capable of dissolving **8.31** that could be used in a Birch reduction. Subjecting **8.31** to Birch conditions using 1,4-dioxane as a solvent, however, resulted in no product formation, as the rate of lactol opening and reduction was faster than the rate of aryl reduction. After an analysis of Birch reduction precedent, we found literature suggesting that the rate of arene reduction is increased in the presence of less sterically-hindered proton sources, suggesting a proton-coupled electron transfer mechanism.⁵ Indeed, we found that use of *sec*-butanol, previously identified as the least sterically-hindered proton source that would not cause lactol opening and reduction, significantly improved the rate of arene reduction. Furthermore, the cyclohexene byproduct was not observed by mass spectroscopy or HPLC analysis, indicating selective protonation of pentadienyl anion **8.28**. Following hydrolysis, the enone **8.33** was isolated in 70% yield over two steps.

8.3.3 Completion of the Formal Synthesis

Hydrogenation of enone **8.33** provided cyclohexanone **8.34**, and subsequent hydrolysis of the acetal afforded the corresponding lactol. To our surprise, conditions previously found to accomplish an aldol condensation provided none of product **8.35**. Increasing the temperature or concentration of base were similarly ineffective and resulted exclusively in decomposition. We postulated that the presence of the α -methyl substituent increases the stability of an enolate formed via deprotonation from that position, and therefore decreases the equilibrium presence of the enolate productive toward product formation. Since the yield of the aldol condensation from *des*-methyl substrate **8.24** is already low, it is conceivable that even a small equilibrium shift could result in the complete suppression of product formation.

Scheme 8.4 Attempted Application of the Base-Catalyzed Aldol Condensation

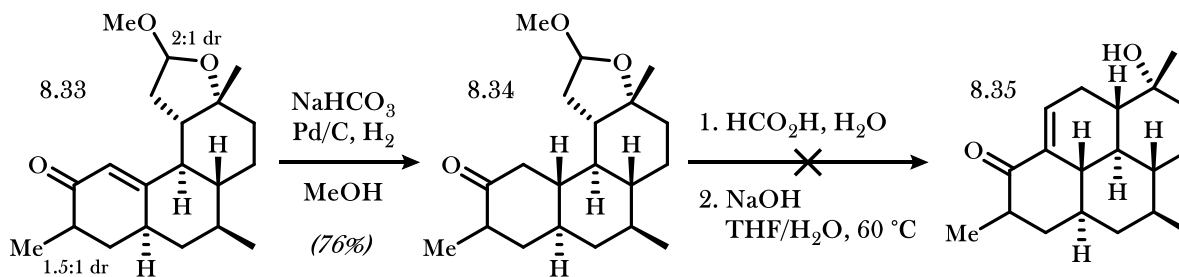
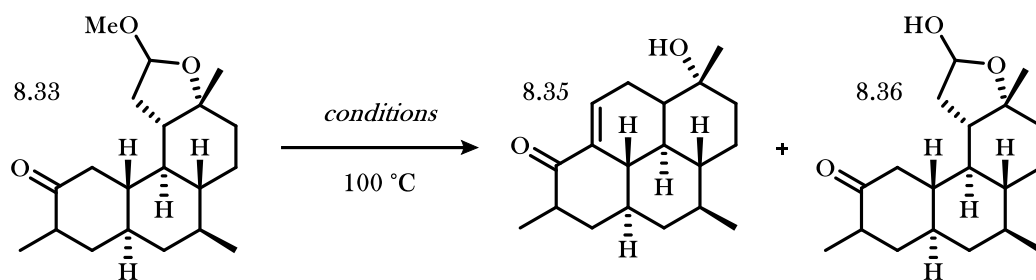


Table 8.2 Enamine-Mediated Aldol Condensation



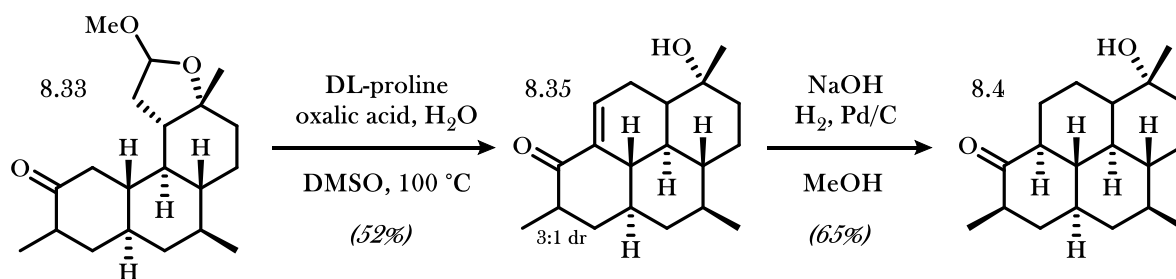
Entry	Amine (Equiv.)	Solvent	Concentration	Water Equiv.	Acid (Equiv.)	NMR Yield 8.35	NMR Yield 8.36
1	pyrrolidine (5)	DMF	[0.05 M]	5	AcOH (113)	17%	12%
2	pyrrolidine (5)	DMSO	[0.05 M]	5	AcOH (113)	26%	10%
3	pyrrolidine (5)	DMSO	[0.05 M]	5	oxalic acid (20)	34%	10%
4	piperidine (5)	DMSO	[0.05 M]	5	oxalic acid (20)	11%	27%
5	morpholine (5)	DMSO	[0.05 M]	5	oxalic acid (20)	32%	18%
6	DL-proline (5)	DMSO	[0.05 M]	5	oxalic acid (20)	30%	20%
7	DL-proline (5)	DMSO	[0.05 M]	5	oxalic acid (10)	29%	2%
8	DL-proline (5)	DMSO	[0.05 M]	5	oxalic acid (40)	27%	1%
9	DL-proline (5)	DMSO	[0.05 M]	2	oxalic acid (20)	12%	2%
10	DL-proline (5)	DMSO	[0.05 M]	15	oxalic acid (20)	17%	4%
11	DL-proline (2)	DMSO	[0.05 M]	5	oxalic acid (20)	24%	12%
12	DL-proline (25)	DMSO	[0.05 M]	5	oxalic acid (20)	63%	4%
13	DL-proline (12)	DMSO	[0.10 M]	1	oxalic acid (10)	53%	15%

We took this result as an opportunity to improve upon our previously developed method for ring-closure. We identified enamine catalysis as a promising method for formation of **8.35**; formation of the more substituted enamine from the ketone of **8.33** is highly disfavored owing to the introduction of allylic strain, and the less-substituted enamine should therefore be formed selectively as a result. Initially, product **8.35** formation was observed using pyrrolidine as an amine source and acetic acid to presumably aid in acetal opening (Entry 1; Table 8.2). The amount of identifiable material recovered in the crude product mixture was low, indicating a prominent decomposition pathway. We found that DMSO provided slightly improved overall yields (Entry 2). After a short screen, oxalic acid was determined to be the most efficient acid for this transformation (Entry 3), and DL-proline provided the cleanest reactivity (Entry 6). Although increasing the concentrations of acid (Entries 7 and 8) and water (Entries 9 and 10) had little effect on the yield of desired

product, we discovered that a large excess of DL-proline was necessary to afford cyclization product **8.35** in good yield (Entry 12). The equivalents of DL-proline could be decreased by increasing the reaction concentration to [0.10 M] (Entry 13).

Although large amine loadings are necessary to obtain high yields of cyclization product **8.35**, the reaction rate does not significantly increase upon incorporation of additional amine. We suspect that the decomposition typically observed under these reaction conditions results from the *in situ* formation of a highly reactive aldehyde, and we suggest decomposition of the aldehyde is reduced in the presence of high equivalencies of proline due to possible formation of the corresponding aldimine. Further studies are necessary to identify the exact mechanism of this transformation.

Scheme 8.5 Improved Completion of the Formal Synthesis

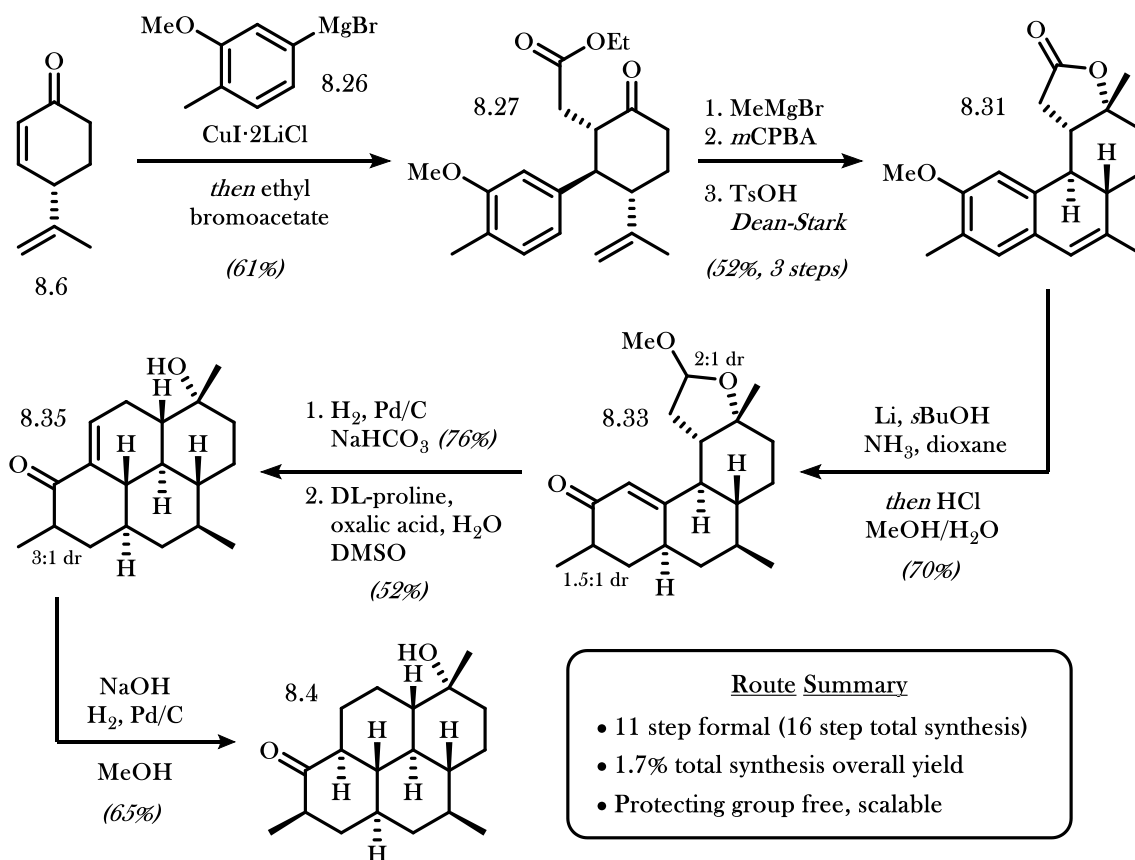


We found that, under the same conditions as Entry 13, enone **8.35** could be isolated in 52% yield. With the tetracyclic core in hand, we then found that a one-pot hydrogenation/epimerization of the α -stereocenter from **8.35** provides the completed formal synthesis target **8.4** in 65% yield.

8.3.4 Route Summary

Use of an aromatic ring nucleophile already containing a methyl substituent provides numerous benefits to the overall synthetic sequence. The yield of the Birch reduction and subsequent hydrolysis is significantly increased to 70% compared to the 36% yield obtained from *des*-methyl substrate **8.9**. The tetracyclic core can then be formed in an increased yield, and no longer requires an additional step to

Scheme 8.6 Completed Route Toward Formal Synthesis Product **8.4**



hydrolyze acetal **8.33** to the corresponding lactol. Furthermore, early introduction of the methyl substituent eliminates the low-yielding α -methylation of ketone **8.25**. This sequence provides Shenvi's intermediate (**8.4**) in just 11 steps from the S-($-$)-perillaldehyde starting material. Perhaps the most valuable contribution of this work, however, involves the application of our previous synthetic strategy to the formation of a formal synthesis product that allows for the stereoselective installation of the two isonitrile functionalities.

8.4 Improved Endgame

Using Shenvi's protocol for completion of the natural product, the equatorial alcohol is formed in three steps from **8.4** via olefination to the corresponding vinylidene in a two-step Peterson olefination sequence, followed by oxymercuration/reduction. With the tertiary equatorial alcohol in hand, activation as the *bis*-trifluoroacetate and invertive displacement installs the isonitriles to form (+)-DICA (**8.3**). Although

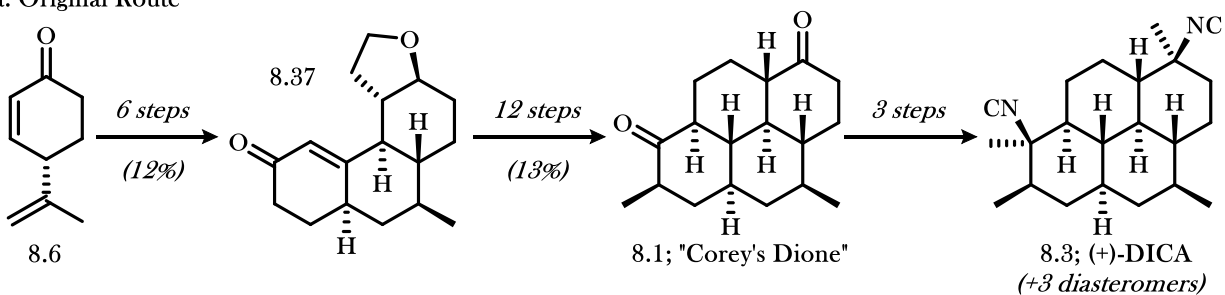
this endgame provides access to (+)-DICA rapidly and efficiently, the three-step sequence for tertiary alcohol formation leaves room for improvement. Efforts are currently underway within the Vanderwal group for a one-step tertiary alcohol formation. Once formed, the two-step stereoselective isonitrile installation remains the most effective way to then access the completed natural product.

8.5 Conclusions and Future Work

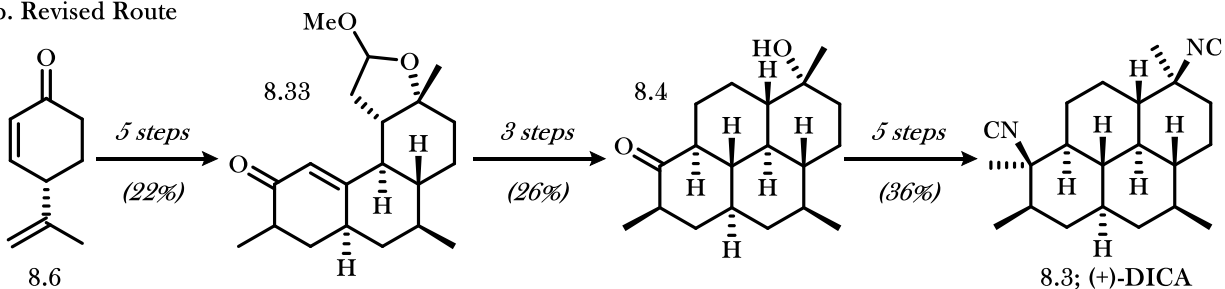
The work reported herein details significant improvements over Roosen and Vanderwal's original formal synthesis of DICA. Starting from the same precursor **8.6**, the Birch reduction product is now procured in one fewer step while increasing the overall yield from 12% to 22%. With the methyl acetal in place, the formal synthesis is then completed in just an additional three steps in 26% overall yield, as compared to the 12 steps in 13% yield accomplished in the original synthesis. With the stereodefined tertiary alcohol in place, (+)-DICA can then be procured in high diastereoselectivity using Shenvi's protocol, as opposed to the nondiastereoselective procedure used by Corey from intermediate **8.1**.

Figure 8.5 Summary of our Syntheses of (+)-DICA

a. Original Route



b. Revised Route

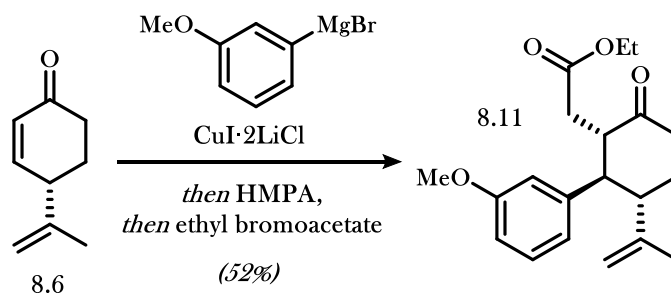


Although there is room for improvement within the endgame, we argue that the synthesis of (+)-DICA described herein is now the most efficient protocol for the synthesis of this valuable natural product in a laboratory setting.

8.6 Experimental Procedures

Unless otherwise noted, all reactions were performed under an atmosphere of argon using flame-dried or oven-dried glassware and Teflon coated stir bars. Anhydrous solvents were prepared by passage through columns of activated alumina. All amine bases were distilled from calcium hydride prior to use. All reagents were used as received or prepared according to literature procedures, unless otherwise noted. TMSOTf was distilled from calcium hydride prior to use. Microwave reactions were performed in a CEM Discover or Anton-Parr Monowave 300 microwave, as indicated. Reactions were monitored by thin-layer chromatography (TLC) using 250 μm EMD Millipore glass-backed TLC plates impregnated with a fluorescent dye, using UV (254 nm), $\text{KMnO}_4/\text{heat}$, or *para*-anisaldehyde/heat as developing agents. Flash column chromatography was performed on EMD Millipore 60 \AA (0.040–0.063 mm) mesh silica gel, and flash column chromatography eluent mixtures are reported as %v/v. ^1H NMR spectra were recorded at 500 MHz on a Bruker 500 MHz (CRYO500 probe) instrument or at 600 MHz on a Bruker 600 MHz (AVANCE600 probe) instrument at 298 K. ^{13}C NMR spectra were recorded at 125 MHz on a Bruker 500 MHz (CRYO500 probe) at 298 K. Chemical shifts are reported in parts per million (ppm), referenced using residual undeuterated solvent (CHCl_3) at 7.26 ppm for ^1H and 77.16 ppm for ^{13}C spectroscopy. Chemical splitting is reported with the following designated peak multiplicities: ap = apparent, s = singlet, d = doublet, t = triplet, q = quartet, m = multiplet, br = broad. Coupling constants are reported in Hertz (Hz). IR spectra were recorded on a Varian 640-IR spectrometer using NaCl plates. High resolution mass spectra (HRMS) were recorded on a Waters LCT Premier spectrometer (using ESI-TOF) or Waters GCT Premier spectrometer (GC-CI), as indicated.

Ketone 8.11



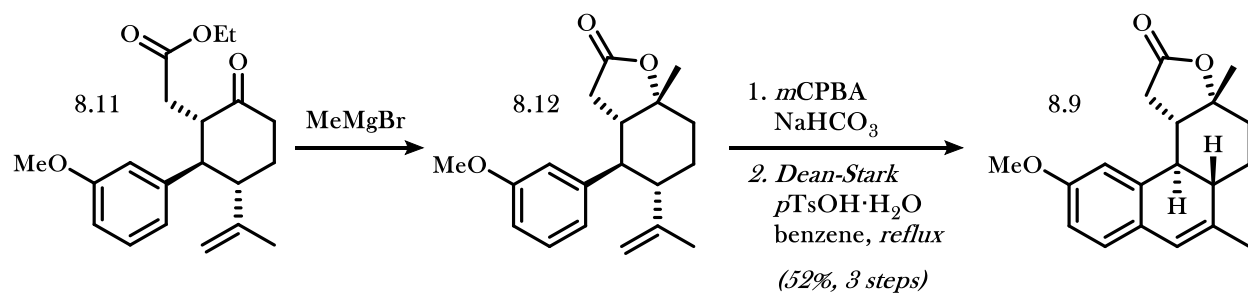
Preparation of the Grignard solution: To a flame dried round bottom flask with stir bar was added magnesium powder (885 mg, -20+100 mesh, ground with mortar and pestle). The flask was evacuated, filled with argon, evacuated, and flame dried with stirring. Upon cooling to room temperature, the flask was filled with argon, and 14 mL of anhydrous THF was added. The suspension was then subjected to three cycles of: sonication for *ca.* 60 seconds, gentle heating to *ca.* 60 °C, and addition *ca.* 20 μL dibromoethane. Following the third repetition, addition of dibromoethane should result in visible formation of gaseous H_2 . With vigorous stirring, a solution of 3-bromoanisole (3.5 mL, 27.64 mmol) in 3.5 mL anhydrous THF was then added slowly over 20 minutes to the magnesium suspension, maintaining an internal temperature of 55–60 °C. Following complete addition, the reaction mixture was stirred for 30 minutes, and then transferred over via cannula to a flame dried flask under argon. The Grignard solution could be stored overnight at -20 °C. Titration prior to use with salicylaldehyde phenylhydrazone indicated a concentration of [1.20 M].

Preparation of the catalyst solution: A [0.25 M] solution of $\text{CuI} \cdot 2\text{LiCl}$ was prepared by adding LiCl (381.6 mg, 9.00 mmol) to a 50 mL round bottom flask with stir bar, evacuating, and flame drying while stirring. Upon cooling to room temperature, the flask was removed from vacuum and CuI (856.8 mg, 4.50 mmol) was added as a solid. The mixture was evacuated and filled with argon. To the solid mixture was added 18 mL of anhydrous THF, and the suspension was stirred vigorously until dissolved.

Conjugate addition and enolate trapping: To a three-neck flame dried round bottom flask under argon with internal thermometer was added 18 mL of anhydrous THF followed by 6.8 mL of a [1.20 M] aryl magnesium bromide solution (8.128 mmol, 1.23 equiv.). The solution was cooled to -78 °C and 2.7 mL of

a [0.25 M] solution of CuI • 2LiCl (0.661 mmol, 0.1 equiv.) was added dropwise over 5 minutes. After stirring at -78 °C for 10 minutes, a solution of enone **8.6**⁶ (900 mg, 6.608 mmol, 1.0 equiv.) in anhydrous THF (5.4 mL) was added dropwise over 15 minutes. Following addition, the resulting yellow reaction mixture was stirred for 2 hours at -78 °C. The cooling bath was removed and the reaction mixture was stirred for 1 hour while cooling to room temperature naturally. The reaction mixture was then cooled to -78 °C, HMPA (2.34 mL, 13.4 mmol, 2.0 equiv.) was added over 2 minutes, and the suspension was stirred vigorously for 1 hour at -78 °C to fully dissolve the HMPA. Freshly distilled ethyl bromoacetate (2.70 mL, 24.4 mmol, 3.7 equiv.) was then added dropwise over 5 minutes. After stirring for 10 minutes at -78 °C, the bath was removed and the reaction mixture was stirred for 24 hours at room temperature. Upon completion, the reaction mixture was poured into 100 mL of a 1:1 mixture of H₂O:NH₄Cl(sat., aq.). The layers were separated, and the aqueous layer was extracted with ethyl acetate (2 x 100 mL). The combined organic layers were then washed with brine (2 x 50 mL), dried with MgSO₄, filtered through cotton, and concentrated *in vacuo* to a yellow oil. The crude product mixture was purified by silica gel chromatography (5–15% EtOAc in hexanes) to afford **8.11** as a colorless oil (1.13g, 52%). The functionality on **8.11** experiences restricted rotation, and two ¹³C peaks are missing; ¹H NMR (600 MHz, CDCl₃) δ 7.20 (t, *J* = 7.4 Hz, 1H), 6.73 (t, *J* = 6.6 Hz, 2H), 6.66 (s, 1H), 4.58 (d, *J* = 14.0 Hz, 2H), 4.06–3.95 (m, 2H), 3.78 (s, 3H), 3.16–3.08 (m, 1H), 2.85 (td, *J* = 11.7, 2.6 Hz, 1H), 2.71 (t, *J* = 11.7 Hz, 1H), 2.67 (td, *J* = 13.6, 5.9 Hz, 1H), 2.56 (d, *J* = 13.5 Hz, 1H), 2.44 (dd, *J* = 16.7, 9.1 Hz, 1H), 2.15–2.07 (m, 1H), 1.96 (dd, *J* = 16.8, 3.2 Hz, 1H), 1.88 (ddd, *J* = 26.0, 13.5, 3.7 Hz, 1H), 1.49 (s, 3H), 1.18 (t, *J* = 7.1 Hz, 3H); ¹³C NMR (126 MHz, CDCl₃) δ 209.6, 172.6, 159.6, 145.7, 142.8, 129.5, 112.8, 111.7, 60.3, 55.2, 53.5, 52.3, 51.3, 41.3, 32.3, 32.2, 19.5, 14.1; IR (film) 2930, 1714, 1153 cm⁻¹; HRMS (ESI) *m/z* calculated for C₂₀H₂₆O₄ [M + Na]⁺ 353.1729, found 353.1728.

Lactone 8.9



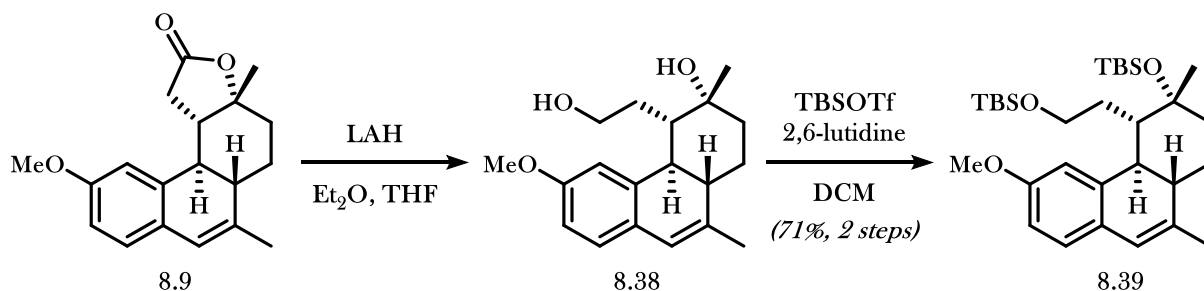
Grignard addition and lactone formation: To a flame dried round bottom flask with stir bar under argon was added ketone **8.11** (2.50 g, 7.57 mmol, 1.0 equiv.) followed by 37.8 mL of anhydrous THF. The reaction mixture was cooled to 0 °C, and a [2.55 M] solution of methyl magnesium bromide (3.26 mL, 8.32 mmol, 1.1 equiv.) was added dropwise over 10 minutes. The reaction mixture was stirred for 2 hours at 0 °C, then the bath was removed and the reaction mixture was stirred at room temperature for 1 hour. Upon completion, the reaction mixture was diluted with Et₂O (100 mL) and poured into saturated, aqueous NH₄Cl (100 mL). The layers were separated, and the aqueous layer was extracted with Et₂O (2 x 100 mL). The combined organic layers were dried with MgSO₄, filtered through cotton, and concentrated *in vacuo* to provide crude **8.12** as a viscous oil. The crude mixture was used in the next step without further purification.

Isopropylidene epoxidation: To a round bottom flask with stir bar was added the crude lactone **8.12** followed by 126 mL of DCM. Solid NaHCO₃ (8.26 g, 98.4 mmol) was added, followed by batch wise addition of mCPBA (3.73 g, 70% w/w, 15.1 mmol) over 10 minutes. The reaction mixture was capped with outlet needle and stirred for 16 hours. Upon completion, sodium thiosulfate (100 mL) was added, and the biphasic mixture was stirred vigorously for 1 hour. The mixture was then extracted with EtOAc (3 x 100 mL), and the combined extracts were washed sequentially with saturated aqueous NaHCO₃ (100 mL) and brine (100 mL). The organic extracts were then dried with MgSO₄, filtered through cotton, and concentrated *in vacuo* to a colorless foam. The crude mixture was used in the next step without purification.

Meinwald rearrangement and Friedel-Crafts condensation: To a round bottom flask with stir bar was attached a Dean-Stark apparatus with condenser. To the reaction flask was added 150 mL of benzene and

TsOH•H₂O (173 mg, 0.91 mmol). The solution was refluxed for 30 minutes to remove water, and then cooled to *ca.* 50 °C. To the acidic solution was added dropwise a solution of crude epoxide in 10 mL benzene over 5 minutes. The reaction mixture was refluxed for 1.5 hours, then cooled to room temperature and poured into saturated aqueous NaHCO₃ (300 mL). The biphasic mixture was extracted with Et₂O (100 mL and 200 mL, sequentially), and the combined organic layers were washed with brine (100 mL). The organic extracts were dried with MgSO₄, filtered through cotton, and concentrated *in vacuo* to a brown solid. The crude product mixture was dry loaded onto silica and purified by silica gel chromatography (10–20% EtOAc in hexanes) to afford **8.9** as an off-white solid (1.15g, 51% over 3 steps): ¹H NMR (500 MHz, CDCl₃) δ 6.97 (d, *J*= 8.2 Hz, 1H), 6.72 (dd, *J*= 8.2, 2.3 Hz, 1H), 6.56 (s, 1H), 6.27 (s, 1H), 3.81 (s, 3H), 3.25 (dd, *J*= 17.4, 7.0 Hz, 1H), 2.54 (dd, *J*= 10.7, 7.0 Hz, 1H), 2.40–2.28 (m, 2H), 2.06–1.92 (m, 2H), 1.88 (s, 3H), 1.55–1.50 (m, 2H), 1.47 (s, 3H); ¹³C NMR (126 MHz, CDCl₃) δ 176.2, 158.2, 137.9, 137.1, 128.9, 126.2, 123.6, 111.5, 109.8, 84.8, 55.4, 44.3, 42.4, 39.6, 38.7, 34.8, 27.8, 23.5, 20.4; IR (film) 2926, 1754, 1606, 1494, 1224, 933, 728 cm⁻¹; HRMS (ESI) *m/z* calculated for C₁₉H₂₂O₃ [M + Na]⁺ 321.1467, found 321.1461.

Bis-silanol **8.39**

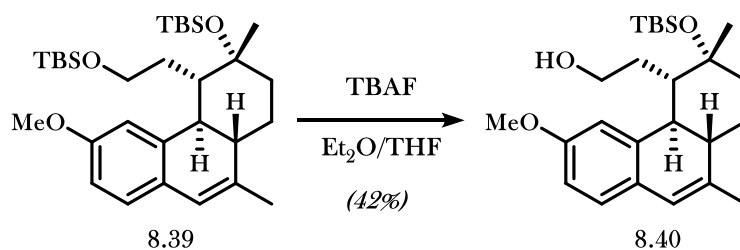


*Lactone Reduction:*⁷ To a vial with stir bar was added anhydrous Et₂O (460 μL) followed by a [4M] of LAH in Et₂O (84 μL, 0.34 mmol, 2 equiv.). To the stirrer mixture was then added a solution of lactone **8.9** (50 mg, 0.17 mmol, 1.0 equiv.) in anhydrous THF (500 μL) dropwise over 5 minutes. The reaction mixture was stirred for 2 hours at room temperature, then diluted with 2 mL Et₂O and cooled to 0 °C. To the reaction mixture was sequentially added: *ca.* 12 μL of water, *ca.* 12 μL of 15% aqueous sodium hydroxide,

and *ca.* 36 μL of water. The mixture was stirred for 30 minutes, MgSO_4 was added, and the suspension was filtered through Celite. Concentrated *in vacuo* afforded the crude mixture as a colorless oil. The crude mixture was used in the next step without further purification.

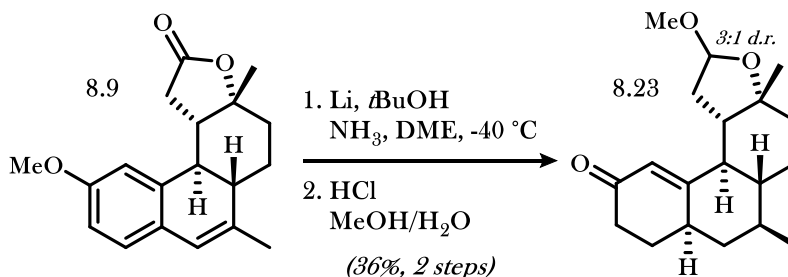
Bis-silyl protection: To a vial with stir bar containing crude diol **8.38** under argon was added DCM (1.7 mL). The solution was cooled to 0 °C, and 2,6-lutidine (117 μL , 1.01 mmol) and TBSOTf (116 μL , 0.504 mmol) were added sequentially. The bath was removed, and the reaction mixture was stirred for 1 hour. At this time, TLC analysis indicated incomplete conversion, so additional 2,6-lutidine (117 μL , 1.01 mmol) and TBSOTf (116 μL , 0.504 mmol) were added sequentially at room temperature. The reaction mixture stirred for 16 hours. Upon completion, the reaction mixture was diluted with a 10% solution of EtOAc in hexanes (2 mL) and washed sequentially with H_2O (1 mL), a 10% citric acid solution (1 mL), and brine (1 mL). The organic extracts were then dried with MgSO_4 , filtered through cotton, and concentrated *in vacuo* to a brown oil. The crude mixture was purified by silica gel chromatography (2.0–2.5% EtOAc in hexanes) to afford **8.39** as a white wax (63.6 mg, 71% over 2 steps): ^1H NMR (500 MHz, CDCl_3) δ 7.03 (d, J = 1.5 Hz, 1H), 6.90 (d, J = 8.2 Hz, 1H), 6.67 (dd, J = 8.2, 2.2 Hz, 1H), 6.25 (s, 1H), 4.02 (ddd, J = 10.1, 10.1, 6.9 Hz, 1H), 3.94 (ddd, J = 10.1, 10.1, 5.2 Hz, 1H), 3.80 (s, 3H), 2.46 (t, J = 12.5 Hz, 1H), 2.17–2.08 (m, 1H), 1.94–1.66 (m, 5H), 1.87 (s, 3H), 1.55 (dd, J = 11.2, 7.2 Hz, 1H), 1.41–1.33 (m, 1H), 1.34 (s, 3H), 0.90 (s, 9H), 0.89 (s, 9H), 0.14 (s, 6H), 0.08 (s, 3H), 0.07 (s, 3H); ^{13}C NMR (126 MHz, CDCl_3) δ 157.7, 141.11, 141.06, 130.0, 125.0, 123.3, 111.8, 110.1, 74.8, 64.2, 55.2, 44.5, 44.0, 41.0, 39.9, 33.2, 30.4, 26.2, 26.0, 22.4, 19.9, 18.8, 18.3, -1.6, -2.2, -5.2, -5.3; IR (film) 2955, 2930, 2856, 1254, 835 cm^{-1} ; HRMS (ESI) m/z calculated for $\text{C}_{31}\text{H}_{54}\text{O}_3\text{Si}_2$ $[\text{M} + \text{Na}]^+$ 553.3510, found 553.3488.

Primary Alcohol **8.40**⁸



To a vial with stir bar containing bis-silane **8.39** (43 mg, 0.081 mmol, 1 equiv.) in THF (8.4 mL) was added a [1 M] solution of TBAF in THF (267 μ L, 0.267 mmol, 3.3 equiv.) at room temperature. The reaction mixture was stirred for 16 hours, and Et₂O (10 mL) and H₂O (10 mL) were added. The layers were separated, and the organic layer was washed with brine (3 mL), dried with MgSO₄, filtered through cotton, and concentrated *in vacuo* to a colorless oil. The crude mixture was purified by silica gel chromatography (10–15% EtOAc in hexanes) to afford **8.40** as a colorless oil (14.3 mg, 42%): ¹H NMR (600 MHz, CDCl₃) δ 6.96 (d, *J* = 1.6 Hz, 1H), 6.91 (d, *J* = 8.1 Hz, 1H), 6.68 (dd, *J* = 8.2, 2.3 Hz, 1H), 6.26 (s, 1H), 4.05 (ddd, *J* = 10.2, 10.2, 6.6 Hz, 1H), 3.97 (10.2, 10.2, 5.4 Hz, 1H), 3.81 (s, 3H), 2.48 (t, *J* = 12.2 Hz, 1H), 2.26–2.16 (m, 1H), 1.92–1.78 (m, 3H), 1.87 (s, 3H), 1.76–1.66 (2H), 1.57 (dd, *J* = 11.2, 7.4, 2H), 1.38 (dd, *J* = 13.3, 3.5 Hz, 1H), 1.35 (s, 3H), 0.90 (s, 9H), 6.22 (sm, 6H); ¹³C NMR (126 MHz, CDCl₃) δ 157.6, 141.2, 141.0, 130.1, 125.1, 123.3, 111.3, 109.9, 74.7, 63.9, 55.3, 44.6, 43.9, 40.9, 39.8, 33.2, 30.3, 26.2, 22.3, 19.9, 18.8, -1.6, -2.2; IR (film) 3423 (br), 2931, 2955, 1253, 1031, 834, 772 cm⁻¹; HRMS (ESI) *m/z* calculated for C₂₅H₄₀O₃Si [M + Na]⁺ 439.2644, found 439.2638.

Cyclohexenone **8.23**

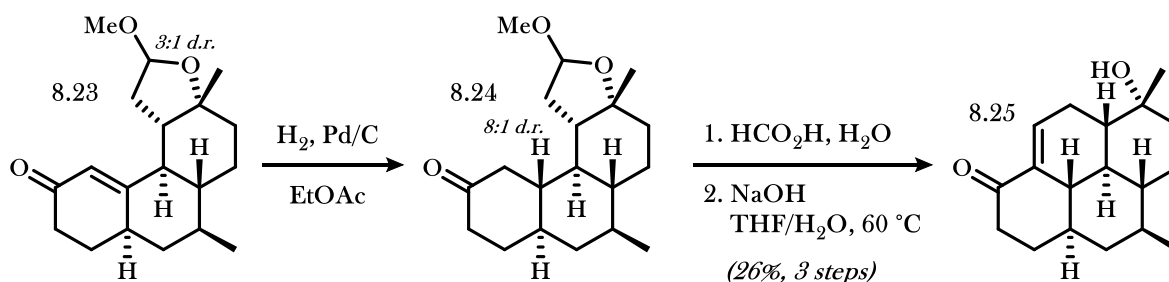


Birch reduction: A three-neck round bottom flask with glass stir bar, internal thermometer, cold finger condenser, and septum was cooled to -78 °C. Ammonia (34 mL) was condensed into the reaction flask, and lithium chunks (311 mg, 45.1 mmol, 50 equiv.) were added over 2 minutes. After stirring for 10 minutes at -78 °C, *tert*-butanol (6.0 mL, 63 mmol, 70 equiv.) and 1,2-dimethoxyethane (6.0 mL) were added. The reaction mixture was warmed to reflux, and a solution of arene **8.9** (269 mg, 0.90 mmol, 1.0 equiv.) in 1,2-dimethoxyethane (5.0 mL) was added dropwise over 2 minutes. The reaction mixture was then refluxed until colorless (*ca.* 20 minutes). To the reaction mixture was then added *tert*-butanol (4.3 mL, 45 mmol, 50 equiv.), followed by lithium chunks (311 mg, 45.1 mmol, 50 equiv.). The reaction mixture was refluxed until colorless (*ca.* 2 hours). Upon completion, solid NH₄Cl (5.8 g, 108 mmol, 120 equiv.) was added, and the reaction mixture was warmed to room temperature over 3 hours to allow ammonia to evaporate. To the reaction mixture was then added H₂O (30 mL). The biphasic mixture was then extracted with EtOAc (3 x 20 mL), and the combined organic extracts were washed with brine (2 x 10 mL). The organic extracts were then dried with MgSO₄, filtered through cotton, and concentrated *in vacuo* to a colorless oil. An NMR yield could be determined by addition of butylated hydroxytoluene as an external standard. The crude mixture (with BHT) was used in the next step without further purification.

Methyl ether hydrolysis and acetal formation: To a vial of crude acetal with stir bar was added methanol (11.8 mL), followed by a [6.0 M] solution of HCl (1.07 mL). The reaction mixture was capped and stirred overnight. In the morning, the reaction mixture was poured into saturated aqueous NaHCO₃ (20 mL), and the mixture was extracted with EtOAc (3 x 20 mL). The combined organic extracts were washed with

brine (10 mL), then dried with MgSO₄, filtered through cotton, and concentrated *in vacuo* to a colorless oil. The crude mixture was purified by silica gel chromatography (15–20% EtOAc in hexanes) to afford a 3:1 mixture of diastereomers of **8.23** as a colorless oil (100.4 mg, 37% over 2 steps): ¹H NMR (500 MHz, CDCl₃) δ 5.79–5.75 (m, 1H), 5.01 (major, dd, *J* = 5.9, 5.1 Hz, 0.75H), 4.98 (minor, d, *J* = 6.2 Hz, 0.25H), 3.36 (major, s, 2.25H), 3.32 (minor, s, 0.75H), 2.55 (minor, quintet, *J* = 6.8 Hz, 0.25H), 2.44–2.25 (m, 4H), 2.22–2.10 (m, 1H), 2.09–2.00 (contains major, m, 1.75H), 1.94–1.78 (m, 3H), 1.73–1.60 (m, 2H), 1.47–1.14 (m, 8H), 0.97 (minor, d, *J* = 6.4 Hz, 0.75H), 0.96 (major, d, *J* = 6.5 Hz, 2.25H); ¹³C NMR (126 MHz, CDCl₃) δ 199.9, 167.8, 121.7, 121.6, 105.2, 104.6, 83.1, 81.8, 55.5, 55.1, 50.4, 49.1, 48.8, 48.7, 43.6, 43.4, 43.2, 41.3, 40.1, 38.8, 37.3, 36.9, 35.1, 35.0, 34.8, 34.7, 29.4, 28.9, 28.4, 28.1, 26.2, 25.9, 19.23, 19.20; IR (film) 2927, 1672, 1100, 1032 cm⁻¹; HRMS (ESI) *m/z* calculated for C₁₉H₂₈O₃ [M + Na]⁺ 327.1936, found 327.1931.

Enone **8.25**



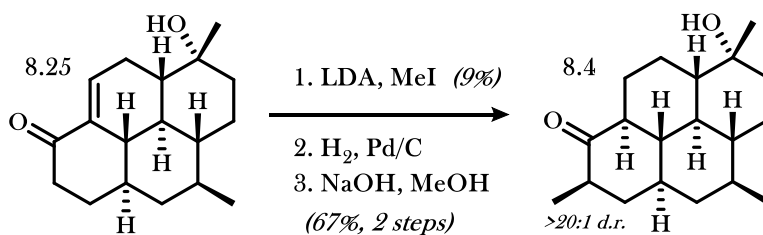
Enone reduction: To a vial with stir bar containing enone **8.23** (24 mg, 0.079 mmol, 1.0 equiv.) was added EtOAc (5 mL) followed by Pd/C (5 wt. %, 7 mg). The vial was capped, and a hydrogen balloon and vent needle were introduced to the system. A stream of hydrogen gas was bubbled through the suspension for 60 seconds, then the needle was pulled to the gaseous space above the reaction mixture, and the vent needle was removed. The reaction mixture was stirred for 2 hours. Upon completion, the reaction mixture was diluted with EtOAc (5 mL) and filtered through Celite. The filtrate was then concentrated *in vacuo* to a thin film. The crude mixture was used in the next step without further purification.

[Note: A one-pot hydrolysis/aldol condensation was attempted below. The hydrolysis to the lactol was successful, but the subsequent aldol condensation resulted in no conversion. The recovered crude mixture was then resubjected to aldol condensation conditions to yield product.]

Acetal hydrolysis: To a vial with stir bar containing crude ketone **8.24** was added H₂O (60 μ L) and formic acid (140 μ L). The reaction was stirred at room temperature for 1 hour. Upon completion, 100 μ L of water was added, followed by a NaOH pellet (120 mg) with rapid stirring. THF was added (400 μ L), and the reaction mixture was sealed and stirred at 50 °C for 16 h. TLC indicated no conversion to product. H₂O (2 mL) and EtOAc (2 mL) were added. The layers were separated, and the aqueous layer was extracted with EtOAc (2 x 2 mL). The combined organic layers were washed sequentially with saturated aqueous NH₄Cl (1 mL) and brine (1 mL). The organic extracts were then dried with MgSO₄, filtered through cotton, and concentrated *in vacuo* to a brown oil.

Aldol condensation: To a vial with stir bar containing the above crude mixture was added THF (400 μ L), followed by a [6 M] aqueous solution of NaOH (200 μ L). The vial was sealed and heated to 60 °C for 16 hours. Upon completion, H₂O (2 mL) and EtOAc (2 mL) were added. The layers were separated, and the aqueous layer was extracted with EtOAc (2 x 2 mL). The combined organic layers were washed sequentially with saturated aqueous NH₄Cl (1 mL) and brine (1 mL). The organic extracts were then dried with MgSO₄, filtered through cotton, and concentrated *in vacuo* to a brown oil. The crude product mixture was purified by silica gel chromatography (17–20% EtOAc in hexanes) to afford **8.25** as a thin film (5.7 mg, 26% over 3 steps): ¹H NMR (500 MHz, CDCl₃) δ 6.82 (dd, J = 7.1, 3.4 Hz, 1H), 2.56 (ddd, J = 17.6, 4.3, 1.8 Hz, 1H), 2.39–2.26 (m, 3H), 1.90–1.70 (m, 5H), 1.52–1.20 (m, 8H), 1.19 (s, 3H), 1.10 (m, 2H), 0.98–0.91 (m, 1H), 0.95 (d, J = 6.6 Hz, 3H), 0.91–0.83 (m, 1H), 0.75 (ddd, J = 22.4, 10.4, 3.7 Hz, 1H); ¹³C NMR (126 MHz, CDCl₃) δ 200.4, 136.7, 136.1, 70.0, 47.36, 47.30, 43.44, 42.5, 42.0, 39.9, 39.6, 39.3, 36.9, 30.1, 28.2, 25.6, 24.5, 19.6; IR (film) 3461 (br), 2924, 2864, 1683, 1618, 1260 cm⁻¹; HRMS (ESI) m/z calculated for C₁₈H₂₆O₂ [M + Na]⁺ 297.1830, found 297.1830.

Ketone 8.4

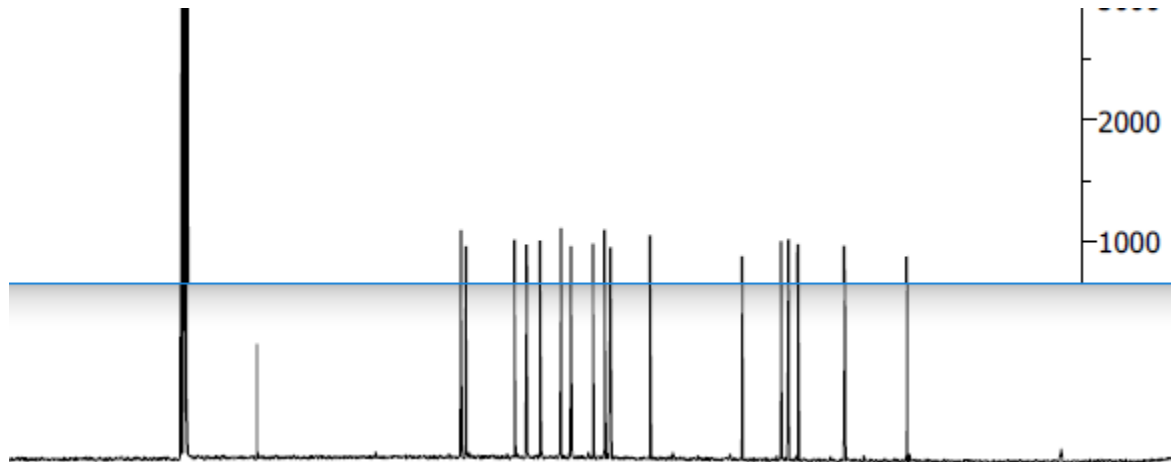


Methylation: To a solution of *N,N*-diisopropylamine (25 μ L, 0.175 mmol, 2.5 equiv.) in anhydrous THF (167 μ L) at 0 $^{\circ}$ C under argon was added dropwise a [2.45 M] solution of *n*BuLi in hexanes (65 μ L, 0.158 mmol, 2.25 equiv.). The reaction mixture was stirred for 10 minutes, and then cooled to -78° C. A solution of enone **8.25** (19.3 mg, 0.07 mmol, 1.0 equiv.) in anhydrous THF (250 μ L) was added dropwise over 5 minutes. To the vial containing trace enone **8.25** was added anhydrous THF (44 μ L), and the solution was transferred dropwise to the reaction mixture. The reaction mixture was stirred for 10 minute at -78° C, and HMPA (17 μ L) was added. Once the HMPA solubilized, a solution of MeI (16.6 μ L, 0.266 mmol, 3.8 equiv.) in anhydrous THF (20 μ L) was added. The cold bath was removed and the reaction mixture was allowed to warm to room temperature naturally. After 50 minutes, the vial cap was removed and saturated aqueous NH₄Cl (1.5 mL) was added. The aqueous layer was extracted with EtOAc (3 \times 1 mL). The combined organic extracts were washed with brine (2 \times 1 mL), and then dried with MgSO₄, filtered through cotton, and concentrated *in vacuo* to a brown oil. The crude product mixture was purified by silica gel chromatography (10–15% EtOAc in hexanes) to afford the methylated product as a thin film (1.8 mg, 9%). The film was immediately used in the next step.

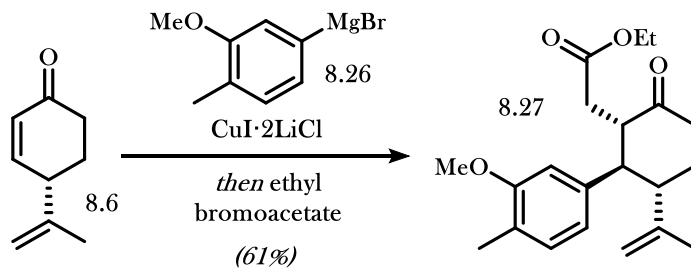
Hydrogenation: To a vial with stir bar containing crude enone (1.8 mg) was added EtOAc (400 μ L) followed by a catalytic portion of Pd/C (5 wt. %). The vial was capped, and vent needle was introduced to the system. The mixture was added to a Parr bomb pressure vessel and H₂ gas (900 psi) was introduced to the system. The reaction mixture was stirred for 2 hours. Upon completion, the reaction mixture was diluted with EtOAc (2 mL) and filtered through Celite. The filtrate was then concentrated *in vacuo* to a thin film. The crude mixture was used in the next step without further purification.

Epimerization: To a vial with stir bar containing crude ketone prepared above was added MeOH (100 μ L) followed by a [0.13 M] solution of NaOH in MeOH (100 μ L). The reaction mixture was heated to 50 $^{\circ}$ C for 30 minutes and cooled to room temperature. EtOAc (1 mL) and saturated aqueous NH_4Cl (1 mL) were added, and the layers were separated. The aqueous layer was extracted with EtOAc (2 \times 1 mL), and the combined organic extracts were washed with brine (1 mL). The crude extracts were dried with MgSO_4 , filtered through cotton, and concentrated *in vacuo* to a thin film. The crude product mixture was purified by silica gel chromatography (10–15% EtOAc in hexanes) to afford **8.4** as a thin film (1.2 mg, 67% over 2 steps). The pure product matched literature values, except for a single peak.⁹ Shenvi and co-workers indicate a ^{13}C peak at δ 52.6 ppm, whereas we observe a peak at δ 53.0. Since the overlaid spectra of our (top) and Shenvi's (bottom) intermediates match perfectly, and each ^{13}C other peak matches the reported data, we are confident in the identity of our product.

Figure 8.6 Overlaid ^{13}C Spectra of Vanderwal (top) and Shenvi (bottom) Intermediates



Ketoester 8.27



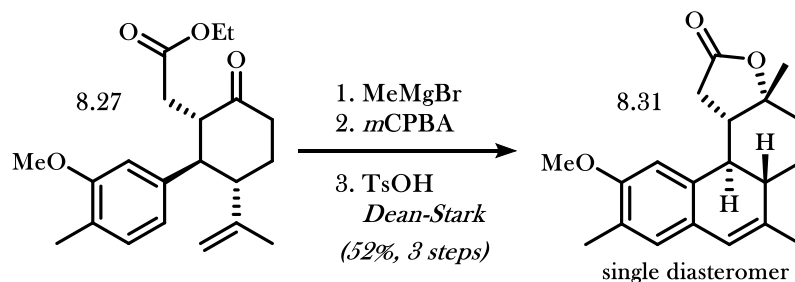
Preparation of the Grignard solution: To a flame dried round bottom flask with stir bar was added magnesium powder (3.71 g, -20+100 mesh, ground with mortar and pestle). The flask was evacuated, filled with argon, evacuated, and flame dried with stirring. Upon cooling to room temperature, the flask was filled with argon, and 58.5 mL of anhydrous THF was added. The suspension was then subjected to three cycles of: sonication for *ca.* 60 seconds, gentle heating to *ca.* 60 °C, and addition *ca.* 50 μL dibromoethane. Following the third repetition, addition of dibromoethane should result in visible formation of gaseous H_2 . With vigorous stirring, a solution of 2-methyl-5-bromoanisole (23.4 g, 116 mmol) in 14.7 mL anhydrous THF was then added slowly over 20 minutes to the magnesium suspension, maintaining an internal temperature of 50–55 °C. Following complete addition, the reaction mixture was stirred for 30 minutes, and then transferred over via cannula to a flame dried flask under argon. The Grignard solution could be stored overnight at -20 °C. Titration prior to use with salicylaldehyde phenylhydrazone indicated a concentration of [1.29 M].

Preparation of the catalyst solution: A [0.25 M] solution of $\text{CuI} \cdot 2\text{LiCl}$ was prepared by adding LiCl (622 mg, 14.7 mmol, 20 mol%) to a 50 mL round bottom flask with stir bar, evacuating, and flame drying while stirring. Upon cooling to room temperature, the flask was removed from vacuum and CuI (1.40 g, 7.3 mmol, 10 mol%) was added as a solid. The mixture was evacuated and filled with argon twice. To the solid mixture was added 29.4 mL of anhydrous THF, and the suspension was stirred vigorously until dissolved.

Conjugate addition and enolate trapping: To a three-neck flame dried round bottom flask under argon with internal thermometer was added 200 mL of anhydrous THF followed by 67 mL of a [1.29 M] aryl magnesium bromide solution (86.4 mmol, 1.18 equiv.). The solution was cooled to -78 °C and the above

[0.25 M] solution of $\text{CuI} \cdot 2\text{LiCl}$ (7.3 mmol, 0.1 equiv.) was transferred to the reaction pot over 25 minutes to form a yellow-green solution. After stirring at $-78\text{ }^{\circ}\text{C}$ for 15 minutes, a solution of enone **8.6** (10 g, 73.4 mmol, 1.0 equiv.) in anhydrous THF (60 mL) was added via cannula over 25 minutes, maintaining an internal temperature below $-75\text{ }^{\circ}\text{C}$. Following addition, the resulting yellow reaction mixture was stirred for 2 hours at $-78\text{ }^{\circ}\text{C}$. The cooling bath was removed and the reaction mixture was stirred for 1 hour while cooling to room temperature naturally. The reaction mixture was then cooled to $-78\text{ }^{\circ}\text{C}$, HMPA (26.1 mL, 150 mmol, 2.0 equiv.) was added over 10 minutes, maintaining an internal temperature below $-75\text{ }^{\circ}\text{C}$, and the suspension was stirred vigorously for 45 minutes at $-78\text{ }^{\circ}\text{C}$ to fully dissolve the HMPA. Freshly distilled ethyl bromoacetate (29.9 mL, 270 mmol, 3.7 equiv.) was then added dropwise over 10 minutes, maintaining an internal temperature below $-75\text{ }^{\circ}\text{C}$. After stirring for 10 minutes at $-78\text{ }^{\circ}\text{C}$, the bath was removed and the reaction mixture was stirred for 27 hours at room temperature. Upon completion, the reaction mixture was poured into 1.5 L of a 1:1 mixture of $\text{H}_2\text{O}:\text{NH}_4\text{Cl}(\text{sat.}, \text{aq.})$. The layers were separated, and the aqueous layer was extracted with ethyl acetate (2 x 500 mL). The combined organic layers were then washed with brine (2 x 400 mL), dried with MgSO_4 , filtered through cotton, and concentrated *in vacuo* to a green oil. The crude product mixture was dry loaded onto SiO_2 (76 g) and purified by silica gel chromatography (0-10% EtOAc in hexanes) to afford **8.27** as a viscous, slightly yellow oil (15.4 g, 61%): ^1H NMR (600 MHz, CDCl_3) δ 7.02 (d, $J=7.5$ Hz, 1H), 6.62 (d, $J=6.62$ Hz, 1H), 6.56 (s, 1H), 4.59 (d, $J=12.5$ Hz, 2H), 3.99 (qd, $J=7.3, 3.7$ Hz, 2H), 3.80 (s, 3H), 3.12 (ddd, $J=12.4, 9.2, 3.4$ Hz, 1H), 2.86 (td, $J=11.6, 3.4$ Hz, 1H), 2.69 (t, $J=11.5$ Hz, 1H), 2.68 (ddd, $J=13.8, 13.5, 6.0$ Hz, 1H), 2.56 (dt, $J=13.5, 3.2$ Hz, 1H), 2.46 (dd, $J=16.7, 9.1$ Hz, 1H), 2.16 (s, 3H), 2.14-2.08 (m, 1H), 1.96 (dd, $J=16.8, 3.5$ Hz, 1H), 1.88 (ddd, $J=26.3, 13.5, 4.4$ Hz, 1H), 1.50 (s, 3H), 1.17 (t, $J=7.2$ Hz, 3H); ^{13}C NMR (126 MHz, CDCl_3) δ 209.7, 172.7, 157.7, 146.0, 139.9, 130.5, 125.1, 119.9, 112.7, 109.5, 60.3, 55.3, 53.6, 52.5, 51.4, 41.3, 32.3, 19.5, 15.9, 14.1; IR (film) 2931, 1714, 1646, 1612, 1584, 1510, 1461, 1415, 1376, 1326, 1255, 1194, 1153, 1039, 890 cm^{-1} ; HRMS (ESI) m/z calculated for $\text{C}_{21}\text{H}_{28}\text{O}_4$ $[\text{M} + \text{Na}]^+$ 367.1885, found 367.1883.

Lactone 8.31

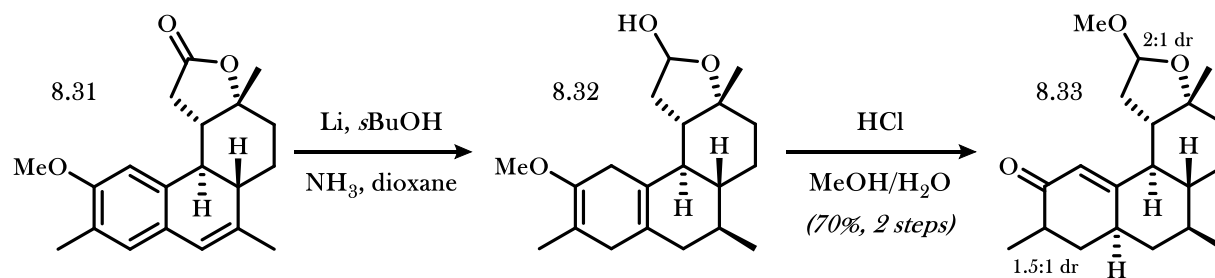


Grignard addition and lactone formation: To a flame dried round bottom flask with stir bar under argon was added ketone **8.27** (15.4 g, 44.6 mmol, 1.0 equiv.) followed by 223 mL of anhydrous THF. The reaction mixture was cooled to 0 °C, and a [2.76 M] solution of methyl magnesium bromide (17.8 mL, 49.1 mmol, 1.1 equiv.) was added dropwise over 20 minutes via syringe pump. The reaction mixture was stirred for 2 hours at 0 °C, then the bath was removed and the reaction mixture was stirred at room temperature for 1.5 hours. Upon completion, the reaction mixture was diluted with Et₂O (200 mL) and poured into cold, saturated aqueous NH₄Cl (400 mL). The layers were separated, and the aqueous layer was extracted with Et₂O (2 x 400 mL). The combined organic layers were washed with brine (300 mL), dried with MgSO₄, filtered through cotton, and concentrated *in vacuo* to a slightly yellow foam. The crude mixture was used in the next step without further purification.

Isopropylidene epoxidation: To a round bottom flask with stir bar was added the crude lactone followed by 446 mL of DCM. Solid NaHCO₃ (22.5 g, 268 mmol) was added, followed by batchwise addition of *m*CPBA (16.5 g, 70% w/w, 66.9 mmol) over 3 minutes. The reaction mixture was capped with outlet needle and stirred for 16 hours. Upon completion, 200 mL of EtOAc was added, followed by 400 mL of sodium thiosulfate (sat., aq.), and the biphasic mixture was stirred vigorously for 1 hour. The layers were separated, and the aqueous layer was extracted with EtOAc (2 x 300 mL). The combined extracts were washed sequentially with saturated aqueous NaHCO₃ (200 mL) and brine (200 mL). The organic extracts were then dried with MgSO₄, filtered through cotton, and concentrated *in vacuo* to a slightly yellow foam. The crude mixture was used in the next step without purification.

Meinwald rearrangement and Friedel-Crafts condensation: To a round bottom flask with stir bar was attached a Dean-Stark apparatus with condenser. To the reaction flask was added 445 mL of benzene and TsOH•H₂O (509 mg, 2.68 mmol). The solution was refluxed for 1 hour to remove water, and then cooled to *ca.* 50 °C. To the acidic solution was added dropwise a solution of crude epoxide in 20 mL benzene over 10 minutes. The reaction mixture was refluxed for 2 hours, then cooled to room temperature and poured into a biphasic mixture of saturated aqueous NaHCO₃ (400 mL) and 400 mL EtOAc. The biphasic mixture was separated, and the organic layer was washed with brine (300 mL). The organic extract was dried with MgSO₄, filtered through cotton, and concentrated *in vacuo* to a yellow solid. The crude solid was dissolved in 100 mL CHCl₃, warmed to reflux, and 100 mL MeOH was added in a single portion with stirring. The solution was cooled to -20 °C for 16 hours. The cold solution was then filtered, and the filtered solids were washed with cold MeOH and dried under a stream of air to afford 5.4 g of **8.31** as white needles. The mother liquor was concentrated *in vacuo*, dry loaded onto SiO₂, and purified by silica gel chromatography (10–20% EtOAc in hexanes) to afford 1.8 g of **8.31** as a white solid. The purified samples were combined to provide **8.31** as a white solid (7.2 g, 52% over 3 steps): ¹H NMR (600 MHz, CDCl₃) δ 6.83 (s, 1H), 6.48 (s, 1H), 6.23 (s, 1H), 3.84 (s, 3H), 3.27 (dd, *J* = 17.3, 7.1 Hz, 1H), 2.55 (dd, *J* = 10.8, 7.3 Hz, 1H), 2.51 (d, *J* = 17.5 Hz, 1H), 2.38–2.29 (m, 2H), 2.18 (s, 3H), 2.05–2.00 (m, 1H), 1.96 (t, *J* = 13.5 Hz, 1H), 1.88 (s, 3H), 1.59–1.51 (m, 2H), 1.49 (s, 3H); ¹³C NMR (126 MHz, CDCl₃) δ 176.1, 156.2, 137.8, 133.8, 128.5, 128.1, 124.7, 123.7, 106.4, 84.9, 55.7, 44.2, 42.4, 39.8, 38.7, 34.8, 27.9, 23.5, 20.4, 15.6; IR (film) 2930, 1750, 1271, 1220, 937, 751 cm⁻¹; HRMS (ESI) *m/z* calculated for C₂₀H₂₄O₃ [M + Na]⁺ 335.1623, found 335.1620; mp: 232–234 °C.

Cyclohexenone **8.33**



Birch Reduction: To a flame dried three-neck 500 mL round bottom flask under argon was attached two septa and a cold finger condenser containing a dry ice/acetone bath at $-78\text{ }^{\circ}\text{C}$. The flask was added to a dry ice/acetone bath precooled to $-78\text{ }^{\circ}\text{C}$, and ammonia (*ca.* 200 mL) was condensed into the flask. Upon complete addition, a septum was removed and quickly replaced with a distillation head, which was in turn attached to the following reaction apparatus: a flame dried three-neck 500 mL round bottom flask cooled to $-78\text{ }^{\circ}\text{C}$ under argon containing the above-described distillation head, an air-tight mechanical stirrer, and a cold finger containing a dry ice/acetone bath at $-78\text{ }^{\circ}\text{C}$. The liquid ammonia was distilled into the reaction apparatus by lowering the initial $-78\text{ }^{\circ}\text{C}$ bath, with distillation proceeding until the distilled ammonia aligned with a pre-measured 120 mL mark on the reaction flask. Upon completion, the distillation flask was again cooled to $-78\text{ }^{\circ}\text{C}$, and the distillation head was removed from the reaction apparatus and replaced with a septum through which a cold-temperature thermometer had been inserted. To the reaction apparatus at $-78\text{ }^{\circ}\text{C}$ was then added solid lithium (1.1 g, 160 mmol, 50 equiv.) and *s*BuOH (20.6 mL, 224 mmol, 70 equiv.) and the reaction mixture was stirred for 10 minutes at $-78\text{ }^{\circ}\text{C}$. In a separate flame dried 100 mL round bottom flask with stir bar, lactone **8.31** (1.0 g, 3.2 mmol, 1.0 equiv.) was added, followed by anhydrous 1,4-dioxane (50 mL). The suspension was warmed to $35\text{ }^{\circ}\text{C}$ with stirring. Once dissolved, the dioxane solution was transferred to the reaction apparatus slowly over 45 minutes, maintaining a reaction temperature below $-70\text{ }^{\circ}\text{C}$. After stirring for 10 minutes below $-70\text{ }^{\circ}\text{C}$, the bath was removed and replaced with an acetone bath precooled to $-60\text{ }^{\circ}\text{C}$. The reaction mixture was warmed to $-45\text{ }^{\circ}\text{C}$ slowly over 30 minutes, maintaining a bath temperature only *ca.* $5\text{ }^{\circ}\text{C}$ warmer than the reaction temperature. Once the temperature reached $-45\text{ }^{\circ}\text{C}$, the

reaction mixture turned colorless indicating absence of dissolved lithium. To the reaction mixture at $-45\text{ }^{\circ}\text{C}$ was added *s*BuOH (14.7 mL, 160 mmol, 50 equiv.) and solid lithium (1.1 g, 160 mmol, 50 equiv.). The bath temperature was allowed to rise to *ca.* $-30\text{ }^{\circ}\text{C}$, bringing the reaction mixture to a gentle reflux. After refluxing for 1 hour, the reaction mixture turned colorless, indicating consumption of lithium. *After cooling the reaction mixture to $-45\text{ }^{\circ}\text{C}$ to lower the internal air pressure*, solid NH_4Cl (17.1 g) was added slowly, followed by EtOAc (100 mL). The cold bath and cold finger were removed from the reaction apparatus, and the mixture was allowed to warm to room temperature naturally overnight. In the morning, EtOAc (50 mL) was added, and the mixture was poured into H_2O (150 mL). The layers were separated, and the aqueous layer was extracted with EtOAc (2 x 125 mL). The combined organic layers were washed with brine (2 x 200 mL), then dried with MgSO_4 , filtered through cotton, and concentrated *in vacuo* to provide crude **8.32** as a colorless oil. The crude product mixture was used in the next step without further purification.

Hydrolysis/Isomerization: To crude **8.32** in a round bottom flask with stir bar was added methanol (44 mL) followed by a dropwise addition of [6M] aqueous HCl (4.0 mL) over 2 minutes. The reaction mixture was stirred for 16 hours. Upon completion, the reaction mixture was diluted with EtOAc (125 mL) and poured slowly into saturated aqueous NaHCO_3 (250 mL). The layers were separated, and the aqueous layer was extracted with EtOAc (2 x 125 mL). The combined organic layers were washed with brine (2 x 125 mL), dried with MgSO_4 , filtered through cotton, and concentrated *in vacuo* to a slightly yellow oil. The crude product mixture was purified by silica gel chromatography (10-20% EtOAc in hexanes) to afford a mixture of four diastereomers of **8.33** as a white wax (717 mg, 70% over 2 steps). Two sets of two diastereomers could be isolated by careful chromatography for characterization, however the relative ratio of diastereomers of isolated product pairs do not reflect that of the combined product mixture.

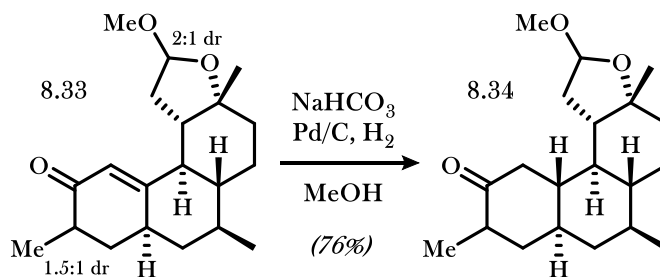
Less polar set of diastereomers: ^1H NMR (600 MHz, CDCl_3) δ 5.77 (s, minor, 0.4H), 5.72 (major, s, 0.6H), 5.02 (major, t, $J = 4.8\text{ Hz}$, 0.6H), 4.99 (minor, t, $J = 4.8\text{ Hz}$, 0.4H), 3.40-3.33 (m, 3H), 2.48-2.24 (m, 3H), 2.13-1.75 (m, 6H), 1.70 (major, t, $J = 11.3\text{ Hz}$, 0.6H), 1.59 (minor, t, $J = 11.5\text{ Hz}$, 0.4H), 1.46-1.19 (m, 5H), 1.30 (s, 3H), 1.13-1.08 (m, 3H), 1.08-0.75 (m, 2H), 0.99-0.93 (m, 3H); ^{13}C NMR (126 MHz, CDCl_3) δ

167.2, 165.4, 122.6, 120.2, 105.3, 105.2, 81.9, 81.8, 55.6, 55.5, 50.6, 49.3, 49.3, 47.5, 44.7, 44.0, 43.6, 42.6, 40.5, 39.8, 39.7, 39.0, 38.8, 37.7, 37.5, 37.1, 36.7, 36.2, 34.7, 34.6, 29.0, 28.8, 26.5, 25.7, 19.23, 19.20, 15.1, 14.4.

More polar set of diastereomers: ^1H NMR (600 MHz, CDCl_3) δ 5.76 (major, s, 0.7H), 5.70 (minor, s, 0.3H), 5.00–4.95 (m, 1H), 3.34–3.30 (m, 3H), 2.57 (major, app. quintet, J = 6.9 Hz, 0.7H), 2.53 (minor, app. quintet, J = 6.8 Hz, 0.3H), 2.50–2.25 (m, 3H), 2.11–2.01 (m, 2H), 1.96–1.79 (m, 3H), 1.66 (major, d, J = 13.8 Hz, 0.7H), 1.62 (minor, d, J = 13.8 Hz, 0.3H), 1.51–1.35 (m, 2H), 1.35–1.23 (m, 3H), 1.20–1.16 (m, 3H), 1.13–1.08 (m, 3H), 0.98–0.93 (m, 3H), 0.93–0.74 (m, 2H); ^{13}C NMR (126 MHz, CDCl_3) δ 168.2, 166.5, 122.1, 119.9, 104.7, 104.5, 82.3, 83.0, 55.1, 55.0, 49.5, 49.3, 48.2, 47.9, 44.6, 42.7, 41.6, 41.2, 39.7, 39.6, 39.0, 38.6, 38.5, 37.9, 37.3, 37.3, 36.4, 36.2, 35.04, 34.99, 31.6, 29.6, 29.2, 26.2, 25.5, 19.3, 19.2.

Mixture: IR (film) 2926, 1669, 1452, 1373, 1097, 733 cm^{-1} ; HRMS (ESI) *submitted*.

Ketone **8.34**

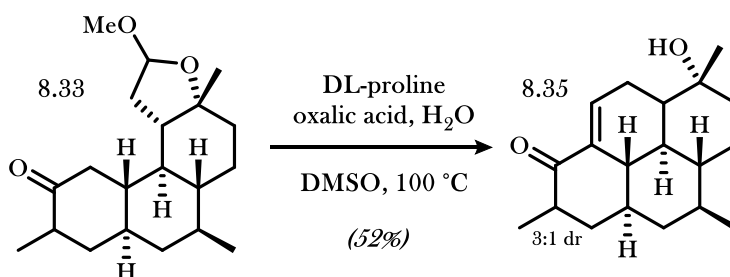


To a round bottom flask with stir bar was added enone **8.33** (830 mg, 2.6 mmol, 1.0 equiv.) followed by methanol (150 mL). Solid NaHCO_3 (547 mg, 6.5 mmol, 2.5 equiv.) was added, followed by Pd/C (5 wt %, 274 mg). The flask was capped with a septum, and a hydrogen balloon and vent needle were introduced to the system. A stream of hydrogen gas was bubbled through the suspension for 5 minutes with stirring, then the needle was pulled to the gaseous space above the reaction mixture, and the vent needle was removed. The reaction mixture was stirred for 3 hours. Upon completion, the reaction mixture was diluted with EtOAc (300 mL) and filtered through Celite. The filtrate was then concentrated *in vacuo* to a white solid. The crude

mixture was purified by silica gel chromatography (8–10% EtOAc in hexanes) to afford **8.34** as a white solid (636 mg, 76%).

8.34 is isolated as a mixture of four diastereomers, leading to fractional integration numbers corresponding to individual diastereomers. The integrations are reported as observed: ^1H NMR (600 MHz, CDCl_3) δ 4.91–4.87 (m, 1H), 3.32–3.26 (m, 3H), 2.59 (dd, $J = 12.6, 3.9$ Hz, 0.39H), 2.54–2.46 (m, 1H), 2.46–2.38 (m, 0.79H), 2.36–2.27 (m, 0.86H), 2.16 (app. dt, $J = 28.4, 13.2$ Hz, 0.48H), 2.04 (t, $J = 12.9$ Hz, 0.40H), 2.01–1.91 (m, 0.91H), 1.87–1.79 (m, 0.69H), 1.79–1.31 (6.82H), 1.27 (app. d, $J = 4.3$ Hz, 2.26H), 1.23–1.07 (m, 4.62H), 1.07–0.99 (m, 0.68H), 0.97 (app. dd, $J = 6.5, 2.0$ Hz, 1.90H), 0.94–0.86 (m, 3.65H), 0.84–0.50 (m, 1.94H); ^{13}C NMR (126 MHz, CDCl_3) δ 215.9, 215.4, 213.2, 212.7, 104.4, 104.21, 104.15, 84.41, 84.39, 83.3, 83.2, 54.7, 54.62, 54.55, 51.9, 51.5, 51.1, 50.3, 49.6, 49.5, 48.7, 47.24, 47.22, 47.02, 46.99, 46.6, 46.5, 44.9, 44.8, 44.6, 44.4, 44.3, 44.0, 43.7, 43.11, 43.09, 43.0, 42.9, 42.71, 42.67, 42.6, 42.5, 42.2, 42.0, 41.7, 41.6, 41.2, 42.1, 40.0, 39.7, 38.0, 37.8, 37.0, 36.8, 35.87, 35.75, 35.1, 35.0, 34.1, 33.9, 30.2, 30.1, 29.6, 29.5, 24.3, 24.2, 23.42, 23.38, 19.87, 29.86, 17.7, 17.5, 14.13, 14.12, IR (film) 2910, 1705, 1455, 1372, 1022 cm^{-1} ; HRMS (ESI) *submitted*.

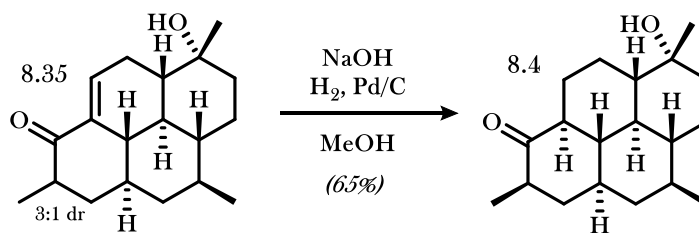
Enone 8.35



To a round bottom flask with stir bar was added **8.33** (100 mg, 0.31 mmol, 1.0 equiv.) under argon. DMSO (2.5 mL) was added, followed by a solution of H_2O (5.6 μL) in DMSO (500 μL). Proline (431 mg, 3.7 mmol, 12 equiv.) was added as a solid, followed by addition of oxalic acid (281 mg, 3.1 mmol, 10 equiv.) as a solid. The reaction mixture was added to an oil bath preheated to $100\text{ }^\circ\text{C}$ and stirred under argon for 5

hours. Upon completion, the reaction mixture was cooled to room temperature and poured into saturated aqueous NaHCO₃ (50 mL). The aqueous phase was extracted with EtOAc (3 x 50 mL), and the combined organic layers were washed with brine (2 x 50 mL). The organic extracts were then dried with MgSO₄, filtered through cotton, and concentrated *in vacuo* to a yellow oil. The crude product mixture was purified by silica gel chromatography (10–16% EtOAc in hexanes) to provide **8.35** as a white foam (46.4 mg, 52%). ¹H NMR (600 MHz, CDCl₃) δ 6.77 (minor, dd, *J* = 4.2, 3.0 Hz, 0.23H), 6.66 (major, dd, *J* = 4.0, 3.2 Hz, 0.76H), 2.56 (dq, *J* = 9.8, 7.5, 2.4 Hz, 0.23H), 2.37–2.18 (m, 2.81H), 1.85 (ddd, *J* = 13.2, 5.8, 2.6 Hz, 1H), 1.81–1.65 (m, 4H), 1.65–1.18 (m, 8H), 1.14 (s, 3H), 1.11–1.05 (m, 1H), 1.02 (d, *J* = 6.8 Hz, 3H), 0.91 (d, *J* = 6.5 Hz, 3H), 0.96–0.83 (m, 1H), 0.76–0.64 (m, 1H); ¹³C NMR (126 MHz, CDCl₃) δ 204.0, 202.9, 137.0, 136.5, 135.6, 134.9, 69.8, 48.0, 47.3, 47.2, 47.0, 43.9, 43.3, 42.7, 42.3, 41.9, 41.4, 39.8, 39.5, 39.0, 37.0, 36.90, 36.87, 33.9, 28.1, 25.6, 25.4, 24.5, 19.5, 18.5, 15.6; IR (film) 3485 (br), 2904, 1679, 1619, 1212 cm⁻¹; HRMS (ESI) *submitted*.

Ketone 8.4



To a vial with stir bar containing **8.35** (30 mg, 0.10 mmol, 1.0 equiv.) was added 2 mL of a [0.2M] solution of NaOH in MeOH, followed by Pd/C (5 wt. %, 11 mg). The vial was capped and a hydrogen balloon and vent needle were introduced to the system. A stream of hydrogen gas was bubbled through the suspension for 1 minute with stirring, the needle was pulled to the gaseous space above the reaction mixture, and the vent needle was removed. The reaction mixture was stirred for 24 hours. Upon completion, the reaction mixture was diluted with EtOAc (5 mL) and filtered through Celite. To the filtrate was added saturated aqueous NH₄Cl (5 mL), the layers were separated, and the aqueous layer was extracted with EtOAc (2 x 5 mL). The

combined organic extracts were washed with brine (5 mL), dried with MgSO₄, filtered through cotton, and concentrated *in vacuo* to a white solid (25 mg). The crude mixture was purified by silica gel chromatography (15% EtOAc in hexanes) to afford **8.4** as a white solid (19.7 mg, 65%). The pure product matched literature values, with the caveat mentioned above in our initial formation of **8.4**.¹⁰

8.7 Notes and References

- (1) Corey, E. J.; Magriotis, P. A. *J. Am. Chem. Soc.* **1987**, *109*, 287-289.
- (2) Pronin, S. V.; Reiher, C. A.; Shenvi, R. A. *Nature* **2013**, *501*, 195-199.
- (3) Lu, H.-H.; Pronin, S. V.; Antonova-Koch, Y.; Meister, S.; Winzeler, E. A.; Shenvi, R. A. *J. Am. Chem. Soc.* **2016**, *138*, 7268-7271.
- (4) (a) Nagase, H.; Imaide, S.; Hirayama, S.; Nemoto, T.; Fujii, H. *Bioorg. Med. Chem. Lett.* **2012**, *22*, 5071-5074. (b) Cambie, R. C.; Metzler, M. R.; Rutledge, P. S.; Woodgate, P. D. *J. Org. Chem.* **1990**, *298*, 117-131.
- (5) Birch, A. J.; Subba Rao, G. S. R. Reductions by Metal-Ammonia Solutions and Related Reagents. In *Advances In Organic Chemistry, Methods and Results*; Taylor, E. C., Ed.; Wiley-Interscience: New York, 1972; pp 1-65.
- (6) Siegel, C.; Gordon, P. M.; Razdan, R. K. *J. Org. Chem.* **1989**, *54*, 5428-5430.
- (7) Procedure modified from: Toyota, M.; Yokota, M.; Ihara, M. *J. Am. Chem. Soc.* **2001**, *123*, 1856-1861.
- (8) Procedure modified from: Plonska-Ocypa, K.; Sicinski, R. R.; Plum, L. A.; Grzywacz, P.; Frelek, J.; Clagett-Dame, M.; DeLuca, H. F. *Bioorg. Med. Chem.* **2009**, *17*, 1747-1763.
- (9) Lu, H.-H.; Pronin, S. V.; Antonova-Koch, Y.; Meister, S.; Winzeler, E. A.; Shenvi, R. A. *J. Am. Chem. Soc.* **2016**, *138*, 7268-7271.

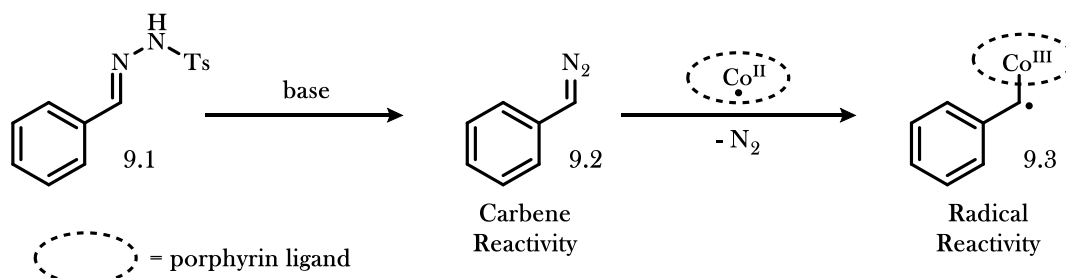
- (10) Lu, H.-H.; Pronin, S. V.; Antonova-Koch, Y.; Meister, S.; Winzeler, E. A.; Shenvi, R. A. *J. Am. Chem. Soc.* **2016**, *138*, 7268-7271.

CHAPTER 9: CATALYTIC SYNTHESIS OF INDOLINES BY HYDROGEN ATOM TRANSFER TO COBALT(III)-CARBENE RADICALS

9.1 Introduction, Motivation, and Relevant Background

Identifying new reactivity of well-known functional groups broadens their versatility in organic synthesis. Prior to recent discoveries, the diazo functional group (see 9.2) had generally been considered a precursor to discrete carbenes or metallocarbenes. These carbene intermediates have been shown to participate in a variety of two-electron processes including cyclopropanations, 1,2-shifts, and bond insertions.¹ However, the discovery of Co(II)-metalloradical catalysis, which unlocks radical-type reactivity from carbene precursors, has invalidated the one-dimensional stereotype of carbenes and has enabled carbene precursors to perform a variety of single-electron processes.

Figure 9.1 Unlocking Radical Reactivity from Carbene Precursors



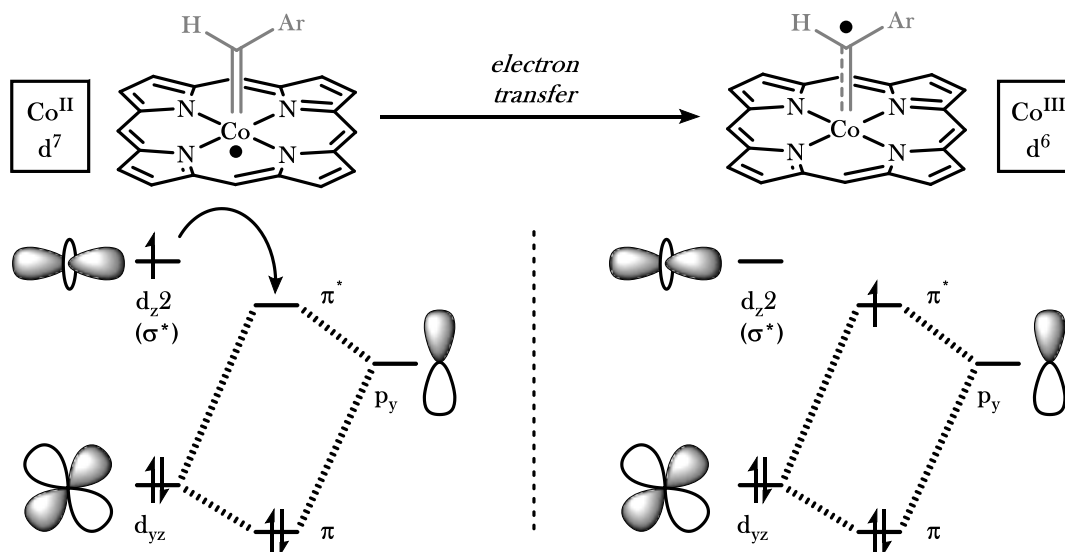
9.1.1 Introduction to Radical Carbenes

The unique reactivity of radical carbene intermediates is made possible by the unique orbital configurations of the components that come together to produce them. A planar ligand, such as a porphyrin or salen, coordinated to the cobalt(II) precursor causes the single-electron to occupy the d_{z^2} orbital of the complex. When the cobalt(II) complex interacts with a carbene intermediate, this same d_{z^2} orbital of the metal interacts with fully-occupied sp^2 orbital of the carbene to form a two-center, three-electron bond. Since this initial interaction is of bond order 0.5 and therefore can be described as only a weak interaction, the

electron occupying the σ^* orbital is typically labeled as occupying the d_{z^2} orbital from which it comes (see Figure 9.2, left side).

The weak interaction described above brings the d_{z^2} orbital of the metal and the unoccupied p orbital of the carbene into proximity, facilitating the formation of a π -bond. The energy of the resulting π^* orbital lies just below the energy of the above-described d_{z^2} orbital, prompting a metal-to-carbon electron transfer from the d_{z^2} orbital to the p orbital of the carbon atom. The resulting carbon-centered radical (Figure 9.2, right side) has then been observed to undergo single electron-type reactivity. Although computational studies suggest a more concerted process than the one described above, the stepwise representative process is described for simplification.

Figure 9.2 Formation of Cobalt(III)-Carbene Radical Intermediates



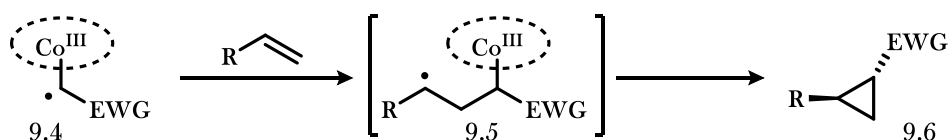
9.1.3 Typical Reactions of Radical Carbenes

Cobalt(III)-carbene radicals (**9.3**) are best described as one-electron reduced Fischer-type carbenes.² These intermediates retain the reactive nature of radicals, but with a decreased susceptibility toward carbene dimerization.² This carbon-centered radical has been shown to participate in various single-electron reactions including 1,2-addition (Figure 9.3a)³ and radical recombination (Figure 9.3c). In a recent example, the de Bruin group disclosed the formation of indene products (**9.13**) from radical carbene precursors (**9.11**) which

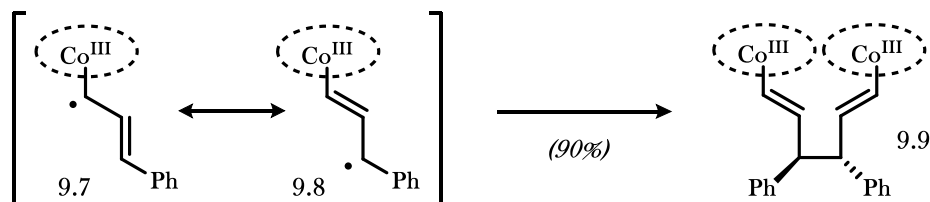
undergo a formal 1,2-addition to a pendant olefin, likely proceeding through an electrocyclic-type pathway (Figure 9.3c).⁴ Despite the extent to which the radical reactivity of these intermediates has been explored, the only reported example in this context of hydrogen atom transfer, a fundamental radical transformation, utilized as a strategy in C-C bond formation is limited to the formation of highly specific sulfolane or sultone derivatives.⁵

Figure 9.3 Commonly Observed Reactions of Carbene Radicals

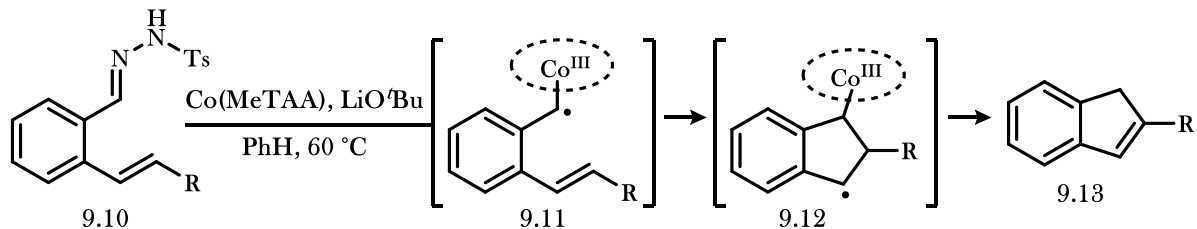
a. Typical Cyclopropanations via Carbene Radical Catalysis



b. Observed Radical Recombination of Carbene Radicals



c. De Bruin's Indene Formation via Cobalt(III)-Carbene Radical Catalysis

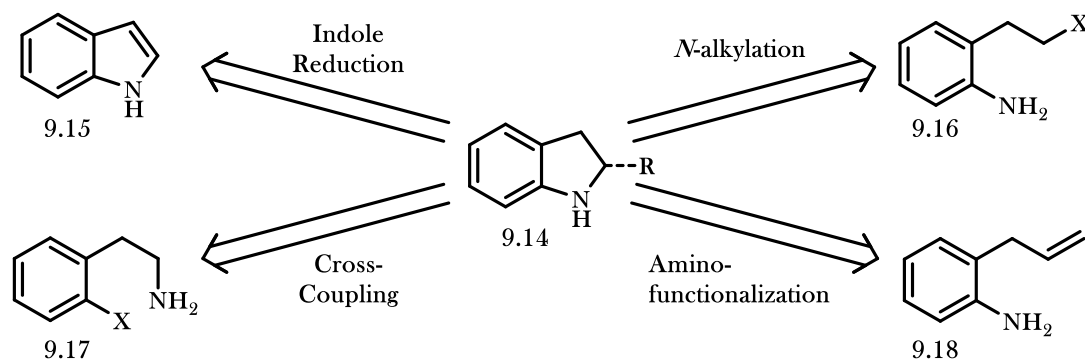


9.1.2 Application to Indoline Synthesis

The indoline heterocycle (**9.14**) is commonly observed among both natural products and pharmaceutical scaffolds, and the need to access this important motif has led to the development of a variety of methods by which it can be obtained. Simple indolines can be efficiently prepared from indole precursors (**9.15**) in high yields, but this transformation requires the use of strongly acidic, strongly hydridic, or highly pressurized conditions.^{6,7} Several dependable and versatile methods have also been reported employing Pd,^{8,9}

Cu,^{10,11} Ni,¹² Ti,¹³ and amines¹⁴ as ring-closing catalysts from precursors such as **9.17**. Furthermore, a variety of methods to form indolines involving radical ring-closing,¹⁵ alkylation,¹⁶ formal 1,2-addition across olefins,^{17,18,19} benzyne functionalization,²⁰ and [4+2] cycloadditions²¹ each present their own advantages.

Figure 9.4 Conventional Methods for Indoline Formation

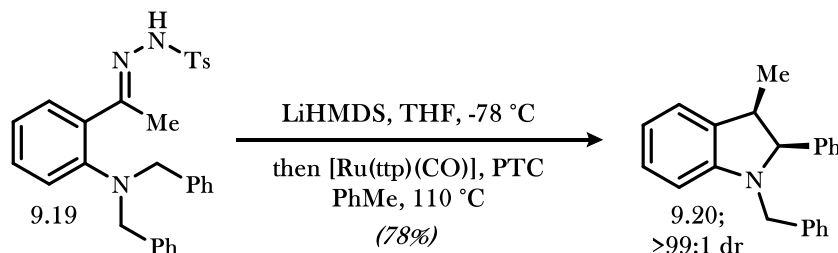


However, several of these existing methods suffer from functional group intolerance, the necessity of using expensive noble transition metal catalysts, harsh reaction conditions, and/or require the use of protecting groups that require tedious conditions for their removal. For this reason, there remains a need for new, efficient, and broadly applicable catalytic routes to expand the currently available methods for indoline synthesis from readily available starting materials.

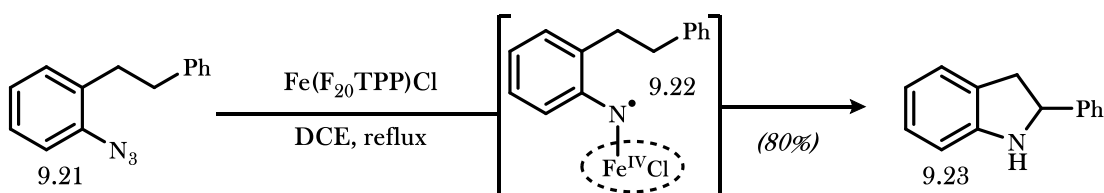
Although carbene or nitrene precursors have previously been used in the synthesis of indolines,²² such as Che and co-workers' synthesis of **9.20** (Figure 9.5a), each method has been proposed to proceed by standard two-electron bond insertion mechanisms commonly observed from these complexes. Cobalt(III) nitrene radicals, which are formed via an analogous decomposition of azide functional groups, have been shown to undergo C-H abstraction in the formation of C-N bonds, but generally have been limited in application to tailor-made starting materials.²³ To date, the only disclosed method for indoline formation via metalloradical catalysis was disclosed by the Che group, in which they invoked a mechanism involving C-H abstraction by the analogous iron(IV) nitrene radical **9.22** to lead to formation of the key C-N bond of indole **9.23** (Figure 9.5b).²⁴

Figure 9.5 Cobalt(III)-Carbene Radical Catalysis Applied to Indoline Formation

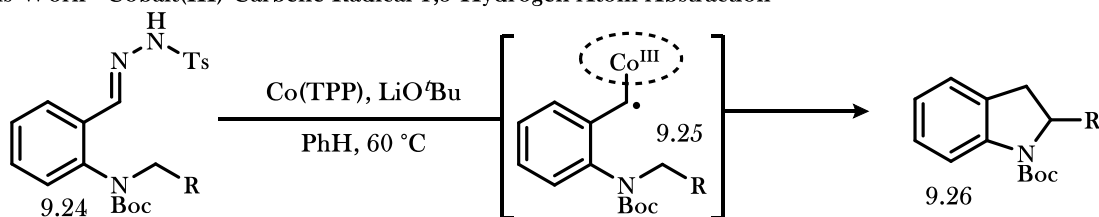
a. Che et al. - Ruthenium Carbenoid 1,2-Insertion



b. Che et al. - Iron(IV)-Nitrene Radical 1,5-Hydrogen Atom Abstraction



c. This Work - Cobalt(III)-Carbene Radical 1,5-Hydrogen Atom Abstraction

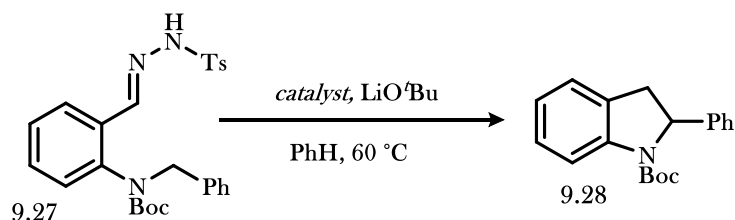


Despite their promising potential, carbene radicals have not yet been used in the synthesis of nitrogen-containing heterocycles. We herein disclose a method for the synthesis of indolines (**9.26**) by exploiting our observation that cobalt radical intermediates undergo 1,5-hydrogen atom abstraction reactions (Figure 9.5c).

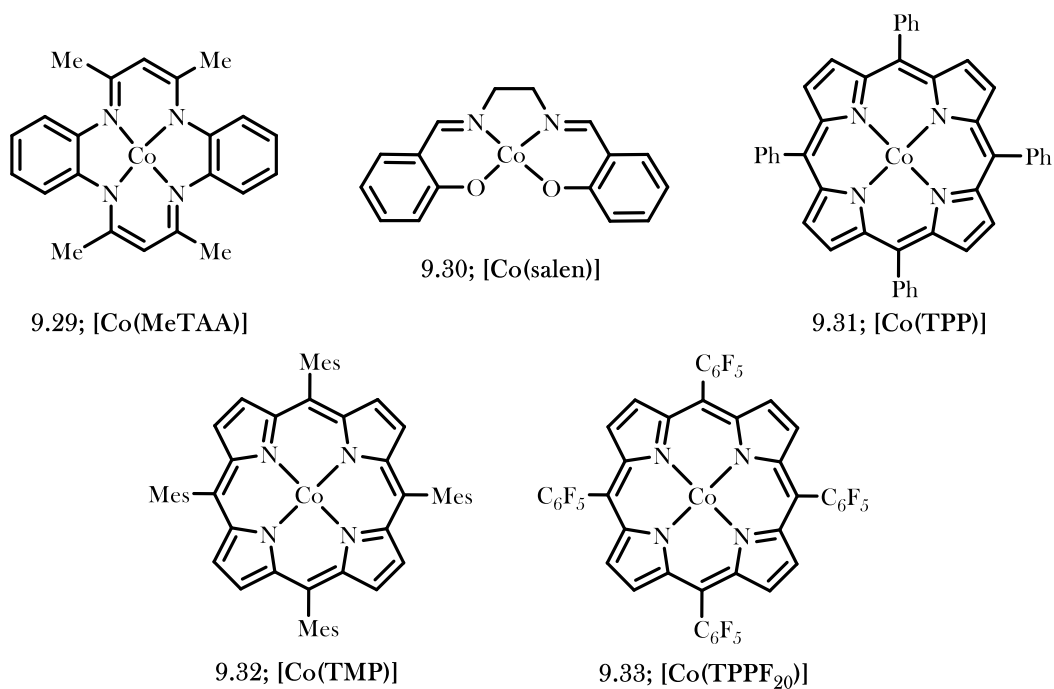
9.2 Optimization of Conditions

We began our investigation using the N-benzyl substituted hydrazone **9.27** as a test substrate, designed to facilitate 1,5-hydrogen atom abstraction through stabilization of the intermediate benzylic radical (Table 1). We initially found that heating of the tosyl hydrazone in the presence of lithium *tert*-butoxide as a base resulted exclusively in carbene dimerization products in the absence of a metal catalyst (Table 9.1, entry 1). However, the addition of [Co^{II}(MeTAA)] (**9.29**), a high-spin metalloradical catalyst with known propensity to form radicals from carbene precursors,⁴ resulted in conversion to the desired indoline product

Table 9.1 Optimization of Conditions for Indoline Formation



Entry	Catalyst	Catalyst		time (h)	NMR Yield
		Loading (mol %)	Base (equiv)		
1	-	-	1.7	18	-
2	[Co(MeTAA)] (9.29)	5	1.7	18	83%
3	[Co(salen)] (9.30)	5	1.7	18	76%
4	[Co(TPP)] (9.31)	5	1.7	18	>99%
5	[Co(TMP)] (9.32)	5	1.7	18	>99%
6	[Co(TPPF ₂₀)] (9.33)	5	1.7	18	>99%
7	CoCl ₂	25	1.7	18	trace
8	Rh ₂ (OAc) ₄	25	1.7	18	-
9	[Co(TPP)] (9.31)	5	1.2	18	35%
10	[Co(TPP)] (9.31)	5	3.0	18	65%
11	[Co(TPP)] (9.31)	5	1.7	6	95%
12	[Co(TPP)] (9.31)	1	1.7	18	90%



in 83% yield (entry 2). [Co^{II}(salen)] complexes (such as **9.30**) also facilitated ring-closure, but at reduced and somewhat less reproducible yields (entry 3). After establishing porphyrins as more reliable ligands, we determined the commercially available and air- and moisture-stable catalyst [Co^{II}(TPP)] (**9.31**) to be superior in this context, leading to quantitative yield of the indoline product (entry 4). More electron rich ([Co^{II}(TMP)]) (**9.32**) or electron deficient ([Co^{II}(TPPF₂₀))] (**9.33**) cobalt porphyrins gave similar results and provide no specific advantages over the commercially available [Co^{II}(TPP)] (**9.31**) catalyst (entries 4–6). Using CoCl₂ as a catalyst led to formation of only trace quantities of the indoline product, suggesting that planar (porphyrin-like) ligands are essential (entry 7). Additionally, introduction of rhodium(II) acetate dimer to facilitate 1,2-carbene insertion²⁵ resulted in no indoline product, perhaps because the lithium *tert*-butoxide base necessary to accomplish diazo formation from the tosylhydrazone precursor causes catalyst decomposition (entry 8).

The molar ratio of lithium *tert*-butoxide has a significant effect on the yield of this transformation. Decreasing the amount of base to 1.2 equivalents limits the yield to 35%, whereas the addition of three equivalents of base decreases the yield to 65% (entries 9–10). We postulate that this need for superstoichiometric base is related to the low solubility of lithium *tert*-butoxide in benzene. In addition to reagent optimization, we also found that near-quantitative yields could be acquired with shorter reaction times of 6 hours (entry 11), and the catalyst loading could be decreased to 0.01 equivalents with only a slight decrease in yield (entry 12).

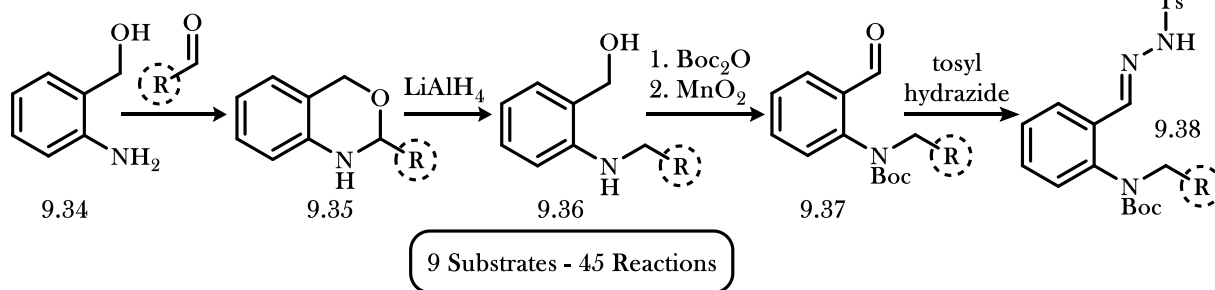
9.3 Substrate Synthesis

Our original route toward the *N*-derivatized substrates involved an initial condensation of **9.34** with the properly functionalized aldehyde to form hemiaminal intermediates of type **9.35** (Figure 9.6). Reduction with lithium aluminum hydride produced ring opened benzyl alcohol **9.36**, which was then protected as the carbamate, oxidized to the aldehyde **9.37**, and converted to the tosyl hydrazone **9.38** via treatment with tosyl hydrazide. The use of safe, reliable transformations throughout this route allowed us to quickly procure material for the reaction optimization described in section 9.3.

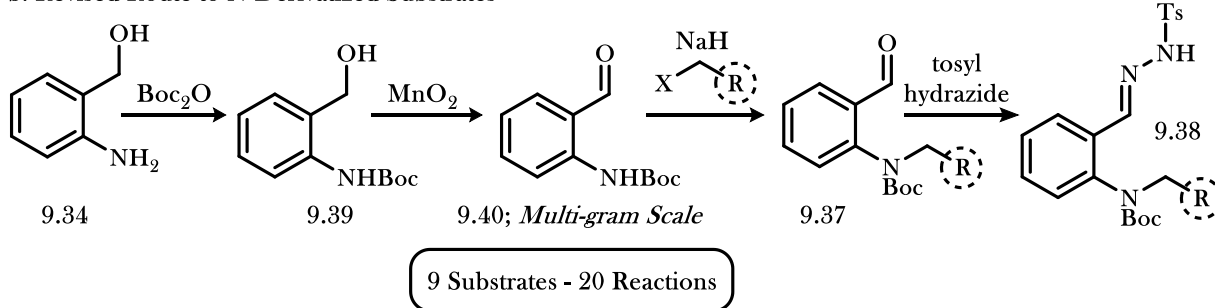
We planned to build a library that contained nine substrates with differential substitution on the aniline nitrogen. The use of our initial route to obtain the nine substrates would require 45 reactions in total. To shorten the amount of time and resources required to build our library, we instead pursued a strategy that would allow for the derivatization of intermediates later in the sequence. By moving two steps previously at the end of our original synthesis to a point prior to derivatization, we could significantly improve the efficiency of our library-building efforts.

Figure 9.6 Strategies toward the *N*-Derivatized Substrates

a. Initial Route to *N*-Derivatized Substrates



b. Revised Route to *N*-Derivatized Substrates

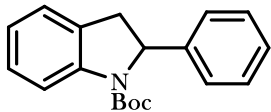
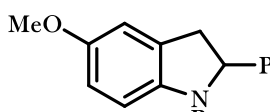
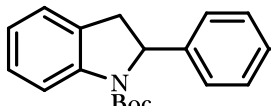
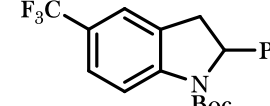
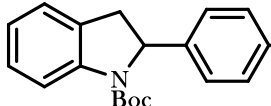
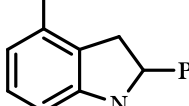
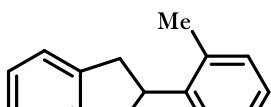
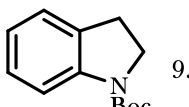
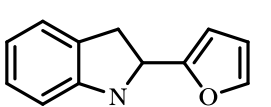
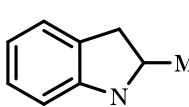
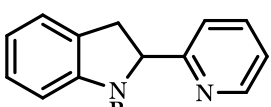
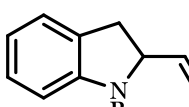


Starting with the same 2-aminobenzyl alcohol **9.34**, we found that carbamate **9.39** formation and benzyl alcohol oxidation could provide benzaldehyde derivative **3.40** on multi-gram scale. From there, derivatization was accomplished via deprotonation of the carbamate and subsequent nucleophilic displacement upon addition of a suitable nucleophile to form intermediates of type **9.37**. The tosyl hydrazone **9.38** could be formed directly from the crude mixture and recrystallized to provide pure samples for testing the proposed reaction scope. By developing a new sequence that allows for late-stage differentiation, we cut the number of steps required to build a 9-substrate library from 45 total steps to 20 total steps.

9.4 Scope Analysis (conducted by Dr. Monalisa Goswami; see section 9.7)

To explore the versatility of this transformation, we designed our library to involve substituents that might have steric or electronic implications on the proposed reaction mechanism (Table 9.2). We found that the electron density on the *N*-benzyl ring (entries 1–3) has little effect on the yield of the reaction. Additionally, the introduction of a bulky ortho substituent on the benzylic functionality (entry 4) did not prevent the ring-closure. The formed radical is also sufficiently stabilized by both electron-rich and electron-poor heterocycles (entries 5 and 6, respectively). The surprisingly low impact of the electronic environment of the *N*-benzyl substituent supports the proposed radical mechanism. Electron donating, electron withdrawing, and sterically-hindering substituents on the aniline moiety are also well tolerated (entries 7–9). A clear limitation of this methodology involves the need for substituents at the nitrogen atom that provide sufficient stabilization of the

Table 9.2 Substrate Scope for Indoline Formation

Entry	Product	Yield	Entry	Product	Yield
1		98%	7		81%
2		92%	8		96%
3		96%	9		80%
4		97%	10		0%
5		95%	11		0%
6		95%	12		80%

proposed radical intermediate. We found that a 1,5-hydrogen atom abstraction to form primary (entry 10) and secondary (entry 11) radicals was not possible, suggesting that the carbene radical intermediate is not reactive enough to generate the required N-CH•R radical intermediates in absence of aromatic R-substituents providing resonance stabilization. However, we found the allylic radical to be sufficiently stabilized to provide 80% yield of the desired vinyl indoline product (entry 12). Functionalization of the aniline ring also provided substituted indoline products in high yields.

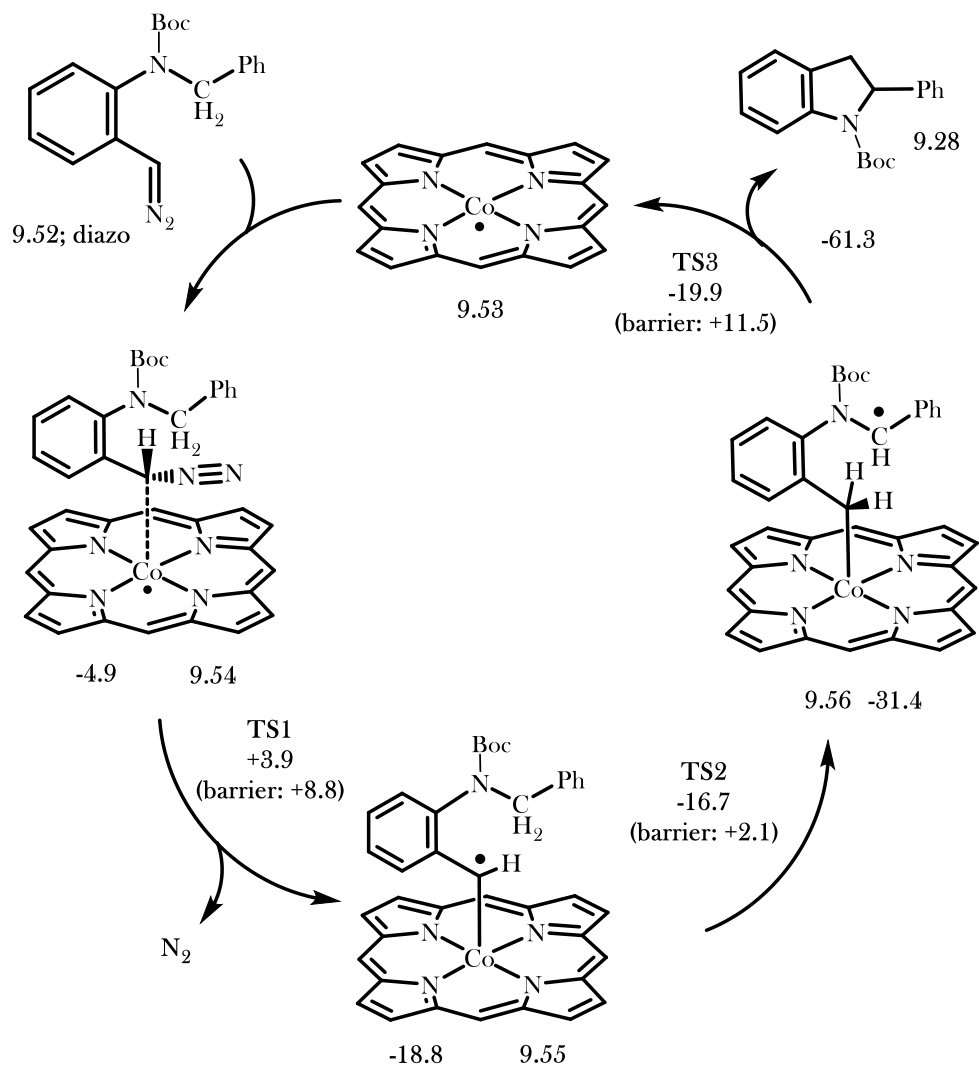
Varying substitution on the aniline ring has a more significant effect on product yield as compared to varying substitution on the benzyl ring (entries 2 and 3). We postulate that the electronics mainly influence the presumed rate-limiting step of converting the tosyl hydrazone substrate into the diazo compound. Substituents on the aniline ring should have a significant influence on this polar two-electron step, as opposed to radical-type steps.

9.5 Reaction Mechanism (investigated by Dr. Monalisa Goswami and Prof. Bas de Bruin; see section 9.7)

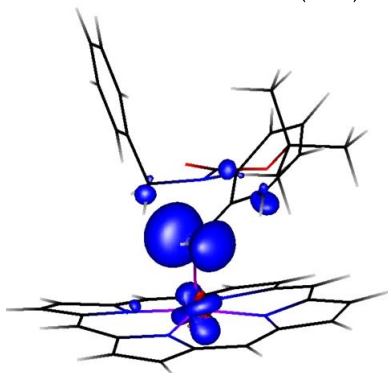
To support our proposed mechanism for indoline formation, we conducted DFT calculations to measure the relative energies of all transition states and intermediates throughout the reaction mechanism. The radical displacement to regenerate the catalyst **9.53** is the highest barrier transition state for the reaction (11.5 kcal/mol). The surprisingly low energetic barriers for the transformation suggest that the rate-limiting step is the decomposition of the tosyl hydrazone to the diazo species **9.52**, which is known to require heating. This suggestion is corroborated by the observation that, when the reaction is run at 60 °C within an NMR spectrometer, only the tosyl hydrazone and indoline product **9.28** can be observed. Overall, the sequence following diazo formation results in an energy benefit of 61.3 kcal/mol, indicating a highly exothermic process.

Figure 9.7 Computational Data for Indoline Formation

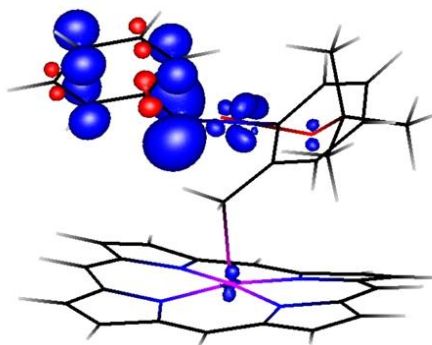
a. Proposed Mechanism Supported by DFT Calculations



b. Radical Carbene Intermediate (9.55)



c. Benzylic Radical Following HAT (9.56)



9.6 Conclusions

In this work, we report a novel route for the synthesis of several substituted indolines which have relevance to both natural product and pharmaceutical scaffolds. The reaction initiates efficiently via a $[\text{Co}^{\text{II}}(\text{Por})]$ -catalyzed pathway by activation of an in situ-formed diazo compound to form a carbene radical. The ensuing 1,5-hydrogen atom transfer step transforms the reactive carbene radical into a more stabilized conjugated radical, which then liberates the desired N-heterocyclic product with regeneration of the catalyst via a ring closing radical displacement step. This reaction uses inexpensive, commercially available reagents and allows for the use of tosyl hydrazones as safe, stable precursors to diazo compounds.²⁶ To the best of our knowledge, this is the first example of a cobalt(III)-carbene radical mediated C-H activation/rebound mechanism for the synthesis of N-heterocyclic organic products. The metalloradical catalyzed indoline synthesis in this work represents an example of a formal intramolecular carbene insertion reaction into a benzylic C-H bond, but proceeds via a radical mechanism and displays highly controlled reactivity of the key $\text{Co}(\text{III})$ -carbene radical intermediates involved.

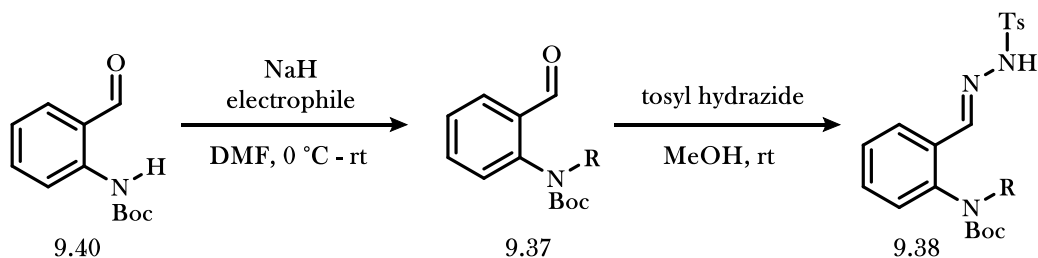
9.7 Acknowledgments

The work described in this chapter was done in collaboration with Dr. Monalisa Goswami and Prof. Bas de Bruin at the University of Amsterdam. The genesis of the research project, optimization of reaction conditions, and synthesis of the substrate library was performed by the author of this thesis. Substrate testing was performed by Dr. Monalisa Goswami, and computational data was produced by Dr. Monalisa Goswami and Prof. Bas de Bruin.

9.8 Experimental Procedures

Unless otherwise noted, all manipulations were performed under a nitrogen atmosphere using standard Schlenk techniques. All solvents used for catalysis were dried over and distilled from sodium (benzene, toluene) or CaH₂ (dichloromethane, hexane, ethyl acetate, methanol, acetonitrile). Solvent used for cobalt catalysis reactions degassed prior to use. Reactions were monitored by thin-layer chromatography (TLC) using Merck TLC 60_{F254} plates, and visualized using ultraviolet light. All chemicals were purchased from commercial sources and used as received unless otherwise mentioned. [Co^{II}(MeTAA)]²⁷ and [Co^{II}(Salophen)] **1**²⁸ were synthesized according to literature methods. Flash column chromatography was performed using Sigma-Aldrich 60 Å (60-100 mesh) silica gel, and flash column chromatography eluent mixtures are reported at %v/v. All NMR spectra were recorded at 293 K. Individual peaks are reported as: multiplicity (s = singlet, d = doublet, t = triplet, q = quartet, m = multiplet), integration, coupling constant (Hz). All ¹H NMR spectra were measured on a Bruker Avance 400 (400 MHz) or Mercury 300 (300 MHz), referenced internally to residual solvent resonance of CDCl₃ (δ = 7.26 ppm), or dms_o-d₆ (δ = 2.50 ppm). Bruker Avance 400 (101 MHz) or Bruker Avance 500 (126 MHz), referenced internally to residual solvent resonance of CDCl₃ (δ = 77.0 ppm) or dms_o-d₆ (δ = 39.52). ¹⁹F spectra measured on a Mercury 300 (300 MHz), were referenced externally against CFCl₃. High Resolution Mass spectra were measured on an AccuTOF LC, JMS-T100LP Mass spectrometer (JEOL, Japan). FD/FI probe (FD/FI) is equipped with FD Emitter, Carbotec or Linden (Germany), FD 10 μm. Current rate 51.2 mA/min over 1.2 min FI Emitter, Carbotec or Linden (Germany), FI 10 μm. Flashing current 40 mA on every spectra of 30 ms. Typical measurement conditions are: Counter electrode -10kV, Ion source 37V.

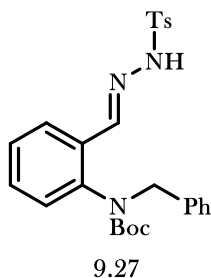
General Procedure for Substrate Synthesis



To a suspension of NaH (1.0 mmol, 1 equiv.) in DMF (0.67 mL) at 0 °C was added dropwise over 5 minutes a solution of *t*-butyl(2-formylphenyl)carbamate (**9.40**) (221 mg, 1.0 mmol, 1 equiv.) and a suitable electrophile (1.3 mmol, 1.3 equiv.) in DMF (1.5 mL). The reaction mixture warmed naturally to room temperature while stirring overnight. Upon completion, the reaction mixture was cooled to 0 °C and a saturated aqueous solution of NH₄Cl was added dropwise over 5 minutes. The mixture was extracted with ethyl acetate (3 x 5 mL) and the combined organic layers were dried over MgSO₄, filtered through cotton, and concentrated *in vacuo* to provide **9.37**.

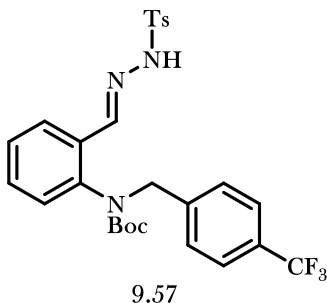
The crude reaction mixture was immediately dissolved in methanol (5 mL), and *p*-toluenesulfonyl hydrazide (205 mg, 1.1 mmol, 1.1 equiv.) was added in one portion as a solid. The reaction mixture was stirred vigorously overnight at room temperature, during which time a precipitate formed. Upon completion, the reaction mixture was filtered, and the solids were washed sequentially with methanol and hexanes to afford the corresponding substrate **9.38** as a pure compound.

Hydrazone 9.27



9.27 was prepared as a white solid in 59% yield according to the above general procedure using benzyl bromide as the electrophile. ^1H NMR (500 MHz, CDCl_3 -*d*) δ 11.57 (s, 1H), 7.79 (s, 1H), 7.77 - 7.68 (d, J = 7.1 Hz, 2H), 7.60 (m, 1H), 7.40 (d, J = 7.2 Hz, 2H), 7.31 (m, 1H), 7.29 - 7.04 (m, 6H), 4.30 - 4.50 (br, 2H), 2.35 (s, 3H), 1.00 - 1.60 (br, 9H); ^{13}C NMR (126 MHz, CDCl_3) δ 153.8, 143.4, 143.3, 140.5, 137.2, 136.2, 131.1, 130.3, 129.7, 128.3, 128.2, 127.6, 127.3, 127.1, 125.3, 79.9, 52.8, 27.7, 21.0; HRMS (FD) m/z calculated for $\text{C}_{26}\text{H}_{29}\text{N}_3\text{O}_4\text{S}$ [M] 479.1879, found 479.1875.

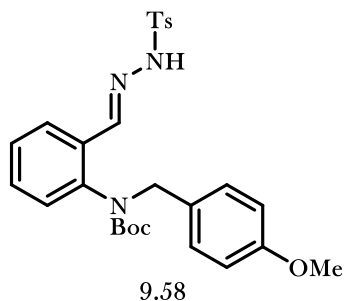
Hydrazone 9.57



9.57 was prepared as a white solid in 17% yield according to the above general procedure using *p*-trifluoromethylbenzyl bromide as the electrophile. ^1H NMR (400 MHz, $\text{DMSO-}d_6$) δ 11.58 (s, 1H), 7.81 (s, 1H), 7.73 (d, J = 8.0 Hz, 2H), 7.68 - 7.56 (m, 3H), 7.43 - 7.29 (m, 5H), 7.24 (m, 1H), 7.11 (d, J = 7.7 Hz, 1H), 5.05 - 4.49 (m, 2H), 2.34 (s, 3H), 1.52 - 0.98 (m, 9H); ^{13}C NMR (75 MHz, $\text{DMSO-}d_6$) δ 153.9, 143.4, 143.2, 142.3, 140.5, 136.2, 130.9, 130.5, 129.7, 128.8, 128.5, 128.1, 127.7, 127.4, 127.1, 126.0, 125.5,

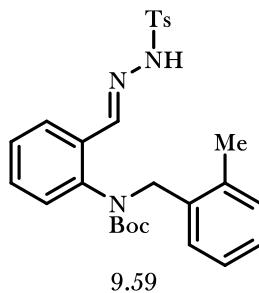
125.25 (q, $J = 3.8$), 122.4, 80.2, 52.5, 27.7, 21.0; ^{19}F NMR (282 MHz, $\text{DMSO-}d_6$) δ -60.9; HRMS (FD) m/z calculated for $\text{C}_{27}\text{H}_{28}\text{F}_3\text{N}_3\text{O}_4\text{S}$ [M]: 547.1753, found: 547.1755.

Hydrazone 9.58



9.58 was prepared as a white solid in 40% yield according to the above general procedure using *p*-methoxybenzyl bromide as the electrophile: ^1H NMR (500 MHz, $\text{DMSO-}d_6$) δ 11.55 (s, 1H), 7.87–7.64 (m, 3H), 7.60 (br, 1H), 7.38 (d, $J = 6.5$ Hz, 2H), 7.30 (br, 1H), 7.23 (br, 1H), 7.13–6.97 (m, 3H), 6.77 (d, $J = 5.7$ Hz, 2H), 4.90–4.23 (br, 2H), 3.69 (s, 3H), 2.34 (s, 3H), 1.76–0.87 (br, 9H); ^{13}C NMR (75 MHz, $\text{DMSO-}d_6$) δ 158.4, 153.8, 143.4, 140.5, 136.2, 131.1, 130.3, 129.7, 129.1, 127.8, 127.1, 125.3, 113.7, 79.8, 54.9, 52.1, 27.8, 21.0; HRMS (FD) m/z calculated for $\text{C}_{27}\text{H}_{31}\text{N}_3\text{O}_5\text{S}$ [M]: 509.1984, found: 509.1994.

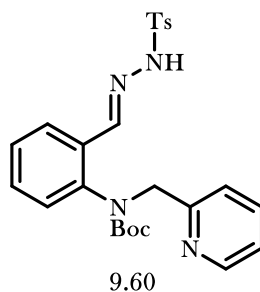
Hydrazone 9.59



9.59 was prepared as a white solid in 57% yield according to the above general procedure using 2-methylbenzyl bromide as the electrophile: ^1H NMR (500 MHz, $\text{DMSO-}d_6$) δ 11.58 (s, 1H), 7.85–7.67 (m, 3H), 7.58 (d, $J = 7.7$ Hz, 1H), 7.46–7.36 (m, 2H), 7.38–7.19 (m, 2H), 7.14–7.03 (m, 3H), 7.06–6.92 (m,

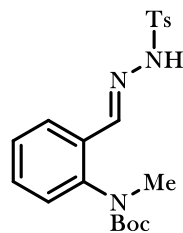
2H), 4.92–4.40 (m, 2H), 2.35 (s, 3H), 2.10 (s, 3H), 1.66–0.94 (br, 9H); ^{13}C NMR (126 MHz, $\text{DMSO-}d_6$) δ 153.6, 143.4, 143.1, 140.3, 136.2, 136.0, 134.9, 131.3, 130.2, 130.1, 129.7, 127.4, 127.1, 125.7, 125.3; HRMS (FD) m/z calculated for $\text{C}_{27}\text{H}_{31}\text{N}_3\text{O}_4\text{S}$ [M $^+$]: 493.2035, found 493.2038.

Hydrazone 9.60



9.60 was prepared as a white solid in 41% yield according to the above general procedure using 2-(bromomethyl)pyridine hydrobromide as the electrophile. To solubilize the salt prior to addition, triethylamine was added dropwise to the solution of substrate in DMF until no further insolubles were observed: ^1H NMR (300 MHz, $\text{DMSO-}d_6$) δ 11.59 (s, 1H), 8.40 (s, 1H), 7.99 (s, 1H), 7.77 (d, $J = 8.0$ Hz, 2H) 7.72–7.58 (m, 2H), 7.40 (d, $J = 8.0$ Hz, 2H), 7.37–7.15 (m, 5H), 4.96–4.40 (br, 2H), 2.35 (s, 3H), 1.40–0.95 (br, 9H); ^{13}C NMR (75 MHz, $\text{DMSO-}d_6$) δ 157.4, 156.8, 153.7, 148.9, 143.9, 143.4, 142.9, 141.0, 136.7, 136.2, 131.1, 130.4, 129.7, 129.5, 127.7, 127.4, 127.2, 127.1, 125.3, 122.4, 121.9, 79.9, 54.8, 27.1, 21.0; HRMS (FD) m/z calculated for $\text{C}_{25}\text{H}_{28}\text{N}_4\text{O}_4\text{S}$ [M $^+$] 480.1831, found 481.1853.

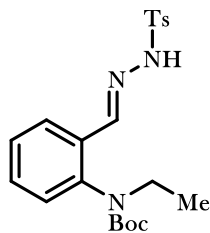
Hydrazone 9.61



9.61

9.61 was prepared as a white solid in 8% yield according to the above general procedure using methyl iodide as the electrophile: ^1H NMR (300 MHz, $\text{DMSO-}d_6$) δ 11.51 (s, 1H), 7.86 (d, $J = 4.4$ Hz, 1H), 7.83–7.61 (m, 3H), 7.50–7.36 (m, 3H), 7.36–7.12 (m, 2H), 3.05 (s, 3H), 2.35 (s, 3H), 1.66–0.92 (br, 9H); ^{13}C NMR (126 MHz, $\text{DMSO-}d_6$) δ 153.7, 143.4, 143.2, 142.3, 136.1, 130.7, 130.5, 129.7, 127.2, 125.3, 79.5, 37.2, 27.7, 21.0; HRMS (FD) m/z calculated for $\text{C}_{20}\text{H}_{25}\text{N}_3\text{O}_4\text{S}$ [M] 403.1566, found: 403.1566.

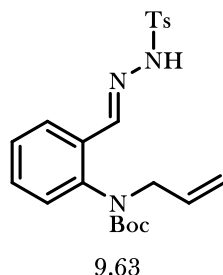
Hydrazone 9.62



9.62

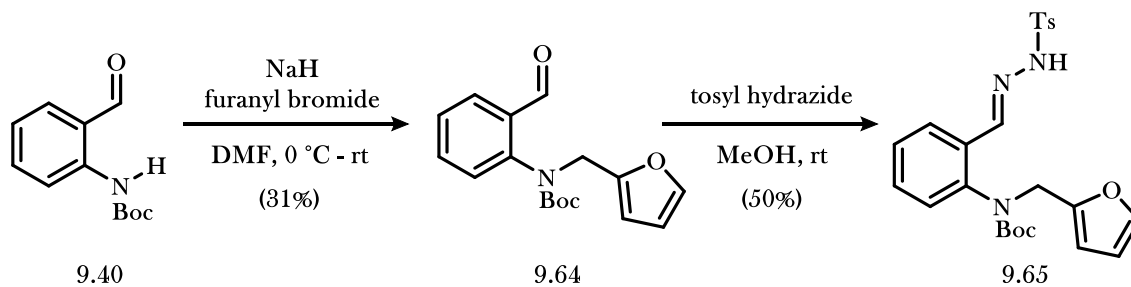
9.62 was prepared as a white solid in 58% yield according to the above general procedure using ethyl iodide as the electrophile: ^1H NMR (400 MHz, $\text{DMSO-}d_6$) δ 11.55 (s, 1H), 7.89 (s, 1H), 7.74 (d, $J = 8.2$ Hz, 2H), 7.69 (dd, $J = 7.8, 1.2$ Hz, 1H), 7.44–7.36 (m, 3H), 7.30 (t, $J = 7.5$ Hz, 1H), 7.20 (dd, $J = 7.9, 0.6$ Hz, 1H), 3.71–3.38 (m, 2H), 2.35 (s, 3H), 1.61–1.00 (br, 9H), 0.93 (t, $J = 6.3$ Hz, 4H); ^{13}C NMR (75 MHz, $\text{DMSO-}d_6$) δ 153.3, 143.5, 143.4, 140.7, 136.1, 131.4, 130.7, 129.7, 128.0, 127.23, 127.15, 125.2, 79.4, 45.1, 44.2, 27.8, 21.0, 13.1; HRMS (FD) m/z calculated for $\text{C}_{21}\text{H}_{27}\text{N}_3\text{O}_4\text{S}$ [M] 417.1722, found 417.1752.

Hydrazone 9.63



9.63 was prepared as a white solid in 63% yield according to the above general procedure using allyl bromide as the electrophile: ^1H NMR (300 MHz, DMSO- d_6) δ 11.54 (s, 1H), 7.88 (s, 1H), 7.74 (d, J = 16.3 Hz, 2H), 7.67 (dd, J = 7.8, 1.7 Hz, 1H), 7.43–7.34 (m, 3H), 7.28 (t, J = 7.5 Hz, 1H), 7.19 (dd, J = 7.9, 1.3 Hz, 1H), 5.88–5.63 (m, 1H), 5.08–4.92 (m, 2H), 4.21–3.97 (m, 2H), 2.35 (s, 3H), 1.59–0.95 (br, 9H); ^{13}C NMR (75 MHz, DMSO- d_6) δ 153.4, 143.5, 143.4, 140.7, 136.2, 133.4, 131.2, 130.5, 129.7, 128.0, 127.24, 127.16, 125.3, 118.1, 79.7, 53.3, 52.2, 27.7, 21.0; HRMS (FD) m/z calculated for $\text{C}_{22}\text{H}_{27}\text{N}_3\text{O}_4\text{S}$ [M] 429.1722, found 429.1729.

Hydrazone 9.65

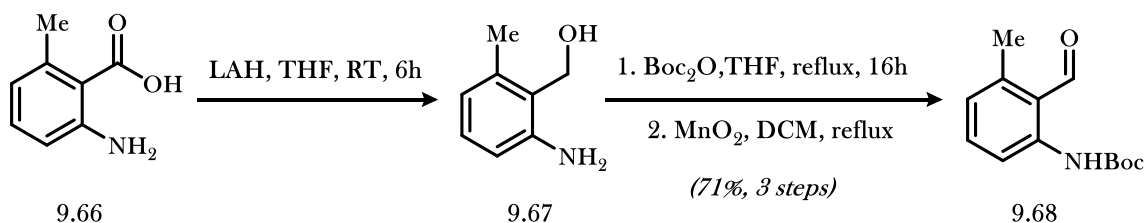


To a suspension of NaH (1.0 mmol, 1 equiv.) in DMF (0.67 mL) at 0 °C was added dropwise over 5 minutes a solution of *t*-butyl(2-formylphenyl)carbamate (**9.40**) (221 mg, 1.0 mmol, 1 equiv.) and furanyl bromide (1.3 mmol, 1.3 equiv.) in DMF (1.5 mL). The reaction mixture warmed naturally to room temperature while stirring overnight. Upon completion, the reaction mixture was cooled to 0 °C and a saturated aqueous solution of NH_4Cl was added dropwise over 5 minutes. The mixture was extracted with ethyl acetate (3 x 5 mL) and the combined organic layers were dried over MgSO_4 , filtered through cotton,

and concentrated *in vacuo* to provide **9.64**. The crude residue was purified via flash column chromatography (10% ethyl acetate in hexanes) and subsequently recrystallized using warm hexanes to give the corresponding aldehyde **51** in 31% yield as a white crystalline solid: $^1\text{H NMR}$ (300 MHz, CDCl_3) δ 9.81 (s, 1H), 7.85 (d, $J = 7.8$ Hz, 1H), 7.59 (td, $J = 7.8, 1.5$ Hz, 1H), 7.39 (t, $J = 7.6$ Hz, 1H), 7.31 (s, 1H), 7.24 – 7.11 (br, 1H), 6.25 (br, 1H), 6.14 (d, $J = 3.0$ Hz, 1H), 5.17–4.55 (m, 2H), 1.80–1.07 (br, 9H); $^{13}\text{C NMR}$ (75 MHz, CDCl_3) δ 190.0, 154.4, 150.4, 144.1, 142.4, 134.7, 133.1, 128.1, 127.6, 110.4, 109.3, 80.1, 46.5, 28.1; HRMS (FD) m/z calculated for $\text{C}_{17}\text{H}_{19}\text{NO}_4$ [M] 301.1314, found: 301.1320.

The product **9.64** was dissolved in methanol (5 mL), and *p*-toluenesulfonyl hydrazide (205 mg, 1.1 mmol, 1.1 equiv.) was added in one portion as a solid. The reaction mixture was stirred vigorously overnight at room temperature, during which time a precipitate formed. Upon completion, the reaction mixture was filtered, and the solids were washed sequentially with methanol and hexanes to afford **9.65** as a white solid in 50% yield: $^1\text{H NMR}$ (300 MHz, $\text{DMSO-}d_6$) δ 11.57 (s, 1H), 7.78–7.68 (m, 3H), 7.62 (d, $J = 7.4$ Hz, 1H), 7.45 (br, 1H), 7.39 (d, $J = 8.2$ Hz, 2H), 7.33 (d, $J = 6.9$ Hz, 1H), 7.30–7.22 (m, 1H), 7.08 (d, $J = 7.8$ Hz, 1H), 6.26 (br, 1H), 6.09 (br, 1H), 4.78–4.60 (m, 2H), 2.35 (s, 3H), 1.55–0.95 (br, 9H); $^{13}\text{C NMR}$ (75 MHz, $\text{DMSO-}d_6$) δ 153.6, 150.4, 144.7, 143.6, 142.7, 136.3, 131.5, 130.5, 129.8, 127.5, 127.3, 125.5, 110.6, 108.9, 80.1, 27.8, 21.1; HRMS (FD) m/z calculated for $\text{C}_{24}\text{H}_{27}\text{N}_3\text{O}_5\text{S}$ [M] 469.1671, found: 469.1681.

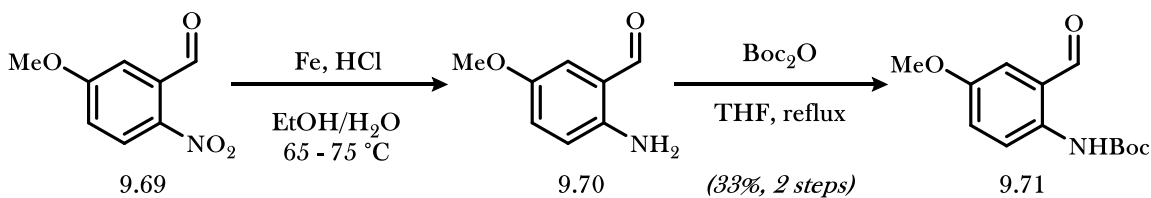
Aldehyde **9.68**



To a solution of 2-amino-6-methylbenzoic acid (**9.66**) (1.0 g, 6.6 mmol, 1 equiv.) in THF (14 mL) at 0 °C was added LAH (16 mmol, 2.4 equiv.) portionwise as a solid. An additional 14 mL of THF was added slowly and the reaction was let to stir for 6 hours, warming to room temperature naturally during this time.

Upon completion, the reaction mixture was filtered through a plug of Celite, washed with Et₂O, and concentrated to give the corresponding benzyl alcohol **9.67**. The crude residue was dissolved in THF (13 mL), and Boc₂O (1.6 g, 7.3 mmol, 1.1 equiv.) was added in a single portion. The reaction mixture was heated to reflux and stirred for 16 hours. Upon completion, the reaction mixture was concentrated to a brown oil containing the corresponding carbamate. To the crude residue was added DCM (13 mL), and MnO₂ (5.7 g, 66 mmol, 10 equiv.) was added in a single portion. The reaction mixture was heated to reflux and stirred vigorously for 16 hours. Upon completion, the reaction mixture was filtered through Celite and washed with DCM. The filtrate was concentrated *in vacuo*, and the resulting crude residue was purified via flash column chromatography (0-5% ethyl acetate in hexanes) to give the corresponding aldehyde **9.68** in 71% yield as a pale yellow powder: ¹H NMR (400 MHz, CDCl₃) δ 10.87 (s, 1H), 10.35 (s, 1H), 8.26 (d, *J* = 8.6 Hz, 1H), 7.35 (dd, *J* = 8.0, 8.0 Hz, 1H), 6.77 (d, *J* = 7.5 Hz, 1H), 2.58 (s, 3H), 1.50 (s, 9H); ¹³C NMR (75 MHz, CDCl₃) δ 193.8, 153.0, 143.1, 142.6, 136.1, 124.4, 118.8, 116.8, 80.7, 28.3, 19.3; HRMS (FD) *m/z* calculated for C₁₃H₁₇NO₃ [M] 235.1208, found: 235.1215.

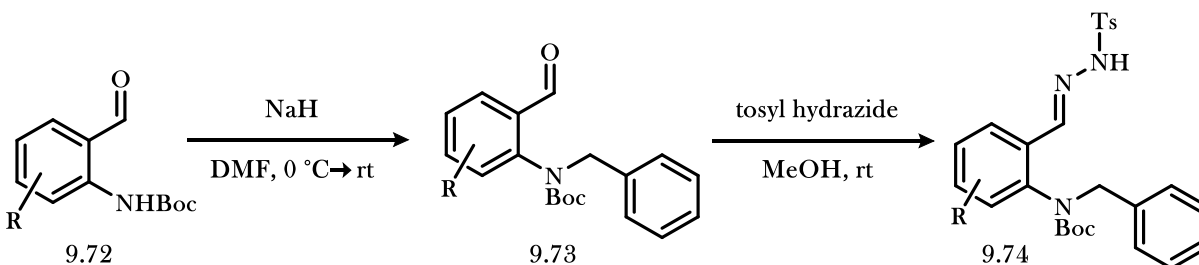
Aldehyde **9.71**



To a round bottom flask was sequentially added aldehyde **9.69** (1.00 g, 5.52 mmol, 1 equiv.), absolute ethanol (16.5 mL), iron powder (1.23 g, 22.1 mmol, 4 equiv.) and [0.1M] HCl (2.8 mL, 0.28 mmol, 0.05 equiv.). The reaction mixture was heated to 65 °C for 2 hours, followed by heating at 75 °C for 2 hours. Following complete reduction, the reaction mixture was cooled to room temperature, quenched with saturated aqueous NaHCO₃ (10 mL), and extracted with CH₂Cl₂ (3 × 10 mL). The combined organic layers were dried with MgSO₄, filtered, and concentrated to give crude **9.70** as a brown oil.

The crude product mixture was immediately dissolved in dry THF (5.5 mL), and Boc_2O (2.5 mL, 11.0 mmol, 2 equiv.) was added in one portion. The reaction mixture was heated at 50 °C for 24 hours, at which point thin-layer chromatography indicated low conversion. An additional 2 mL of Boc_2O was added, and the reaction mixture was heated to reflux for 72 hours. Upon completion, the reaction mixture was concentrated and immediately purified by silica gel chromatography (10% ethyl acetate in hexanes) to afford **9.71** in 33% as a bright yellow solid: ^1H NMR (400 MHz, CDCl_3) δ 10.10 (s, 1H), 9.86 (s, 1H), 8.39 (d, $J=9.2$ Hz, 1H), 7.15 (dd, $J=9.1, 2.9$ Hz, 1H), 7.11 (d, $J=2.9$ Hz, 1H), 3.84 (s, 3H), 1.53 (s, 9H); ^{13}C NMR (101 MHz, CDCl_3) δ 194.6, 154.1, 153.1, 135.5, 122.5, 121.8, 120.0, 119.1, 80.7, 55.7, 28.3; HRMS (FD) m/z calculated for $\text{C}_{13}\text{H}_{17}\text{NO}_4$ [M] 251.1158, found 251.1169.

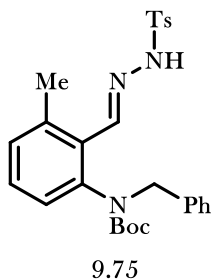
General Procedure for Synthesis of Aniline Derivatives



To a flame-dried Schlenk vial was added sodium hydride (217 mg, 5.42 mmol, 60% w/w dispersion in mineral oil, 1.2 equiv.). The vial was evacuated and filled with nitrogen three times, and DMF (3.3 mL) was added. The suspension was cooled to 0 °C, and a solution of the aldehyde **9.72** (1.00 g, 4.52 mmol, 1 equiv.) and benzyl bromide (805 μL , 6.78 mmol, 1.2 equiv.) in DMF (7.5 mL) was added dropwise over 10 minutes. Following addition, the reaction mixture was removed from the water bath and stirred overnight. Upon completion, the reaction mixture was diluted with ethyl acetate (20 mL) and saturated aqueous ammonium chloride (10 mL) was added dropwise. The layers were separated, and the aqueous layer was extracted with ethyl acetate (2 x 10 mL). The combined organic layers were dried with MgSO_4 , filtered, and concentrated to provide **9.73** as a yellow oil.

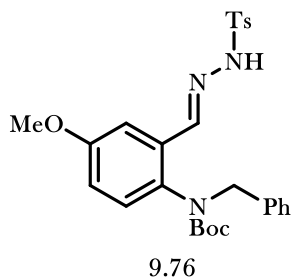
The yellow oil was immediately dissolved in dry methanol (9 mL), and tosyl hydrazide (926 mg, 4.97 mmol, 1.1 equiv.) was added. The reaction mixture was capped and stirred vigorously overnight. Upon completion, the reaction mixture was filtered, the precipitate was washed sequentially with methanol and hexanes, and dried under a stream of air to afford the corresponding substrate **9.74** as a pure compound.

Hydrazone **9.75**



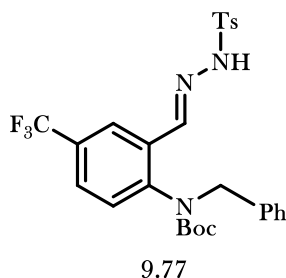
9.75 was prepared as a white solid in 65% yield according to the above general procedure using **9.68** as the aldehyde precursor: ^1H NMR (400 MHz, DMSO- d_6) δ 11.55 (s, 1H), 7.94 (s, 1H), 7.73 (d, J = 8.2 Hz, 2H), 7.39 (d, J = 8.0 Hz, 2H), 7.33–7.18 (m, 3H), 7.18–7.02 (m, 4H), 6.78 (d, J = 7.7 Hz, 1H), 4.80 (d, J = 15.3 Hz, 1H), 4.24 (br, 1H), 2.33 (s, 3H), 2.22 (s, 3H), 1.66–0.90 (br, 9H); ^{13}C NMR (75 MHz, DMSO- d_6) δ 153.9, 144.9, 143.4, 141.6, 138.5, 136.2, 130.0, 129.6, 129.4, 129.0, 128.3, 128.2, 127.3, 127.2, 125.8, 79.7, 52.9, 27.8, 21.7, 21.0; HRMS (FD) m/z calculated for $\text{C}_{27}\text{H}_{31}\text{N}_3\text{O}_4\text{S}$ [M] 493.2035, found 493.2059.

Hydrazone 9.76



9.76 was prepared as a white solid in 60% yield according to the above general procedure using **9.71** as the aniline precursor: ¹H NMR (400 MHz, DMSO-*d*₆) δ 11.55 (s, 1H), 7.77–7.67 (m, 3H), 7.40 (d, *J* = 8.0 Hz, 2H), 7.28–7.15 (m, 3H), 7.11 (d, *J* = 7.5 Hz, 2H), 7.05 (s, 1H), 6.96 (d, *J* = 8.7 Hz, 1H), 6.88 (dd, *J* = 8.9, 2.3 Hz, 1H), 4.79–4.40 (m, 2H), 3.72 (s, 3H), 2.35 (s, 3H), 1.59–0.96 (br, 9H); ¹³C NMR (75 MHz, DMSO-*d*₆) δ 157.5, 154.2, 143.5, 143.2, 137.3, 136.1, 133.7, 132.1, 129.7, 129.1, 128.4, 127.4, 127.2, 116.2, 109.2, 79.7, 52.3, 53.0, 27.8, 21.0; HRMS (FD) *m/z* calculated for C₂₇H₃₁N₃O₅S [M] 509.1984, found 509.1990.

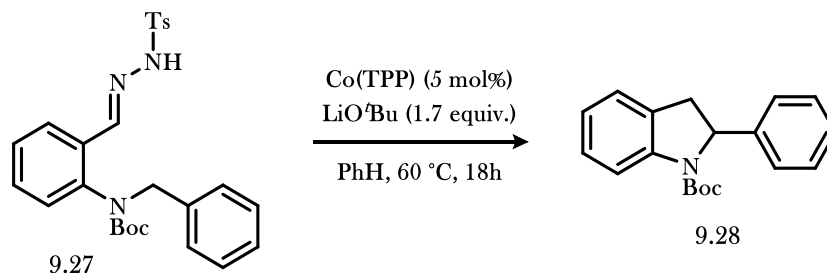
Hydrazone 9.77



9.77 was prepared as a white solid in 17% yield according to the above general procedure using *tert*-butyl(2-formyl-4-(trifluoromethyl)phenyl)carbamate as the aldehyde precursor, which was prepared according to literature procedure:²⁹ ¹H NMR (400 MHz, DMSO-*d*₆) δ 11.79 (s, 1H), 7.73–7.85 (m, 2H), 7.75–7.66 (m, 3H), 7.43–7.36 (m, 3H), 7.26–7.16 (m, 3H), 7.13 (d, *J* = 6.6 Hz, 2H), 4.92–4.57 (br, 2H), 2.35 (s, 3H), 1.53–0.90 (br, 9H); ¹³C NMR (75 MHz, DMSO-*d*₆) δ 153.2, 143.7, 143.6, 141.7, 136.9, 136.0, 132.3, 129.7,

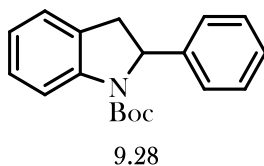
128.9, 128.4, 128.2, 127.5, 127.1, 126.8 (m), 124.7, 122.6, 121.7, 80.6, 52.5, 27.6, 20.9; ^{19}F NMR (282 MHz, $\text{DMSO-}d_6$) δ -61.26; HRMS (FD) m/z calculated for $\text{C}_{27}\text{H}_{28}\text{F}_3\text{N}_3\text{O}_4\text{S}$ [M] 547.1753, found: 547.1753.

General Procedure for Cobalt-Catalyzed Indoline Formation



To a flame dried Schlenk tube was added substrate (0.300 mmol) followed by the **[Co(TPP)]** (10 mg, 0.015 mmol, 5.0 mol%). The Schlenk tube was evacuated and back-filled with nitrogen three times, and evacuated prior to transfer to a glove box. Once inside a glove box, the reaction flask was slowly filled with nitrogen, and lithium *tert*-butoxide (40.8 mg, 0.510 mmol, 1.7 equiv.) was added to this Schlenk flask. The solids were dissolved in 6 mL of benzene and the reaction flask was removed from the glove box and transferred to an oil bath preheated to $60\text{ }^\circ\text{C}$. After 18 hours, the reaction mixture was cooled to room temperature, opened to air, and 6 mL of water was added in a single portion. The water layer was extracted 3 times with hexanes (3 x 6 mL). The organic portions were dried over MgSO_4 , filtered through cotton, and concentrated *in vacuo*. The crude residue was then purified via silica gel chromatography to provide the pure indoline product.

Indoline 9.28



9.28 was prepared as a white solid in 98% yield according to the above general procedure using **9.27** as the hydrazide precursor. Silica gel chromatography was performed using 10% ethyl acetate in hexanes as the eluent. The spectroscopic data matched literature values.³⁰

9.9 Notes and References

- (1) F. A. Carey, R. J. Sundberg, in *Advanced Organic Chemistry, Part B: Reactions and Synthesis*, 5th ed., Chapt. 10, Springer, 2007.
- (2) a) Dzik, W. I.; Xu, X.; Zhang, P. X.; Reek, J. N. H.; de Bruin, B. *J. Am. Chem. Soc.* **2010**, *132*, 10891–10902. b) Lu, H.; Dzik, W. I.; Xu, X.; Wojtas, L.; de Bruin, B.; Zhang, X. P. *J. Am. Chem. Soc.* **2011**, *133*, 8518–8521; c) Dzik, W. I.; Zhang, X. P.; de Bruin, B. *Inorg. Chem.* **2011**, *50*, 9896–9903; d) Dzik, W. I.; Reek, J. N. H.; de Bruin, B. *Chem.-Eur. J.* **2008**, *14*, 7594–7599; e) Lyaskovskyy, V.; de Bruin, B. *ACS Catal.* **2012**, *2*, 270–279; f) Russell, S. K.; Hoyt, J. M.; Bart, S. C.; Milsman, C.; Stieber, S. C. E.; Semproni, S. P.; DeBeer, S.; Chirik, P. J. *Chem. Sci.* **2014**, *5*, 1168–1174; g) Comanescu, C. C.; Vyushkova, M.; Iluc, V. M. *Chem. Sci.*, **2015**, *6*, 4570–4579; h) Sharon, D. A.; Mallick, D.; Wang, B.; Shaik, S. *J. Am. Chem. Soc.* **2016**, *138*, 9597–9610.
- (3) For 1,2-addition across olefins, see: a) Doyle, M. P. *Angew. Chem. Int. Ed.* **2009**, *48*, 850–852; b) Zhu, S. F.; Ruppel, J. V.; Lu, H. J.; Wojtas, L.; Zhang, X. P. *J. Am. Chem. Soc.* **2008**, *130*, 5042–5043; c) Zhu, S. F.; Perman, J. A.; Zhang, X. P. *Angew. Chem. Int. Ed.* **2008**, *47*, 8460–8463; d)

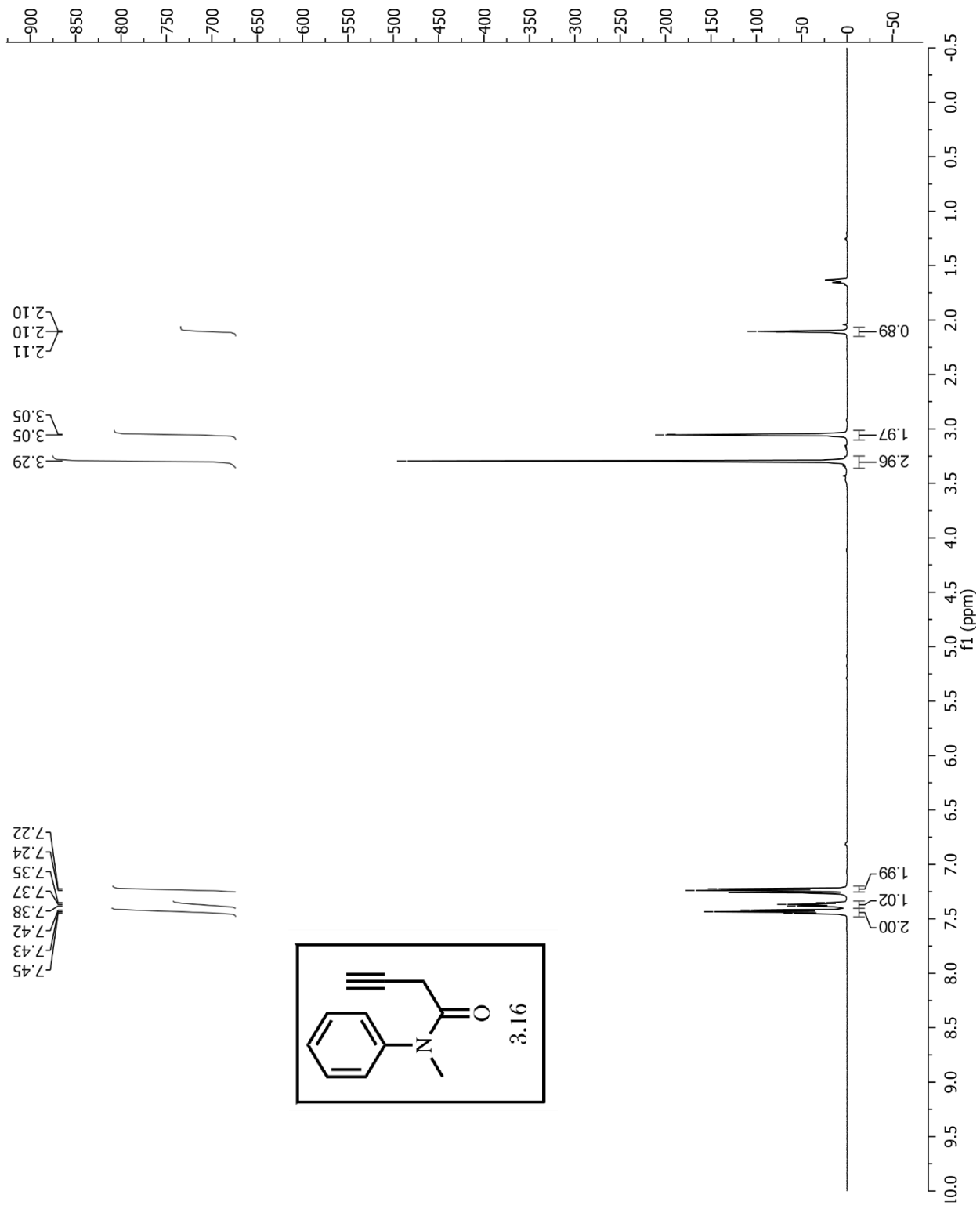
- Fantauzzi, S.; Gallo, E.; Rose, E.; Raoul, N.; Caselli, A.; Issa, S.; Ragaini, F.; Cenini, S. *Organometallics* **2008**, *27*, 6143–6151; e) Xu, X.; Zhu, S.; Cui, X.; Wojtas, L.; Zhang, X. P. *Angew. Chem. Int. Ed.* **2013**, *52*, 11857–11861; f) Zhang, J.; Jiang, J.; Xu, D.; Luo, Q.; Wang, H.; Chen, J.; Li, H.; Wang, Y.; Wan, X. *Angew. Chem. Int. Ed.* **2015**, *54*, 1231–1235; g) Paul, N. D.; Mandal, S.; Otte, M.; Cui, X.; Zhang, X. P.; de Bruin, B. *J. Am. Chem. Soc.* **2014**, *136*, 1090–1096.
- (4) Das, B. G.; Chirila, A.; Tromp, M.; Reek, J. N. H.; de Bruin, B. *J. Am. Chem. Soc.* **2016**, *138*, 8968–8975.
- (5) a) Lu, H.; Lang, K.; Jiang, H.; Wojtas, L.; Zhang, X. P. *Chem. Sci.* **2016**, *7*, 6934–6939; b) Griffin, J. R.; Wendell, C. I.; Garwin, J. A.; White, C. M. *J. Am. Chem. Soc.* **2017**, *139*, 13624–13627.
- (6) For methods for free indoline formation, see: a) Maryanoff, B. E.; McComsey, D. F.; Nortey, S. O. *J. Org. Chem.* **1981**, *46*, 355–360; b) Kotsuki, H.; Ushio, Y.; Ochi, M. *Heterocycles* **1987**, *26*, 1771–1774; c) Lunn, G. *J. Org. Chem.* **1987**, *52*, 1043–1046; d) Srikrishna, A.; Reddy, T. J.; Viswajanani, R. *Tetrahedron* **1996**, *52*, 1631–1636; e) Voutchkova, A. M.; Gnanamgari, D.; Jakobsche, C. E.; Butler, C.; Miller, S. J.; Parr, J.; Crabtree, R. H. *J. Organomet. Chem.* **2008**, *693*, 1815–1821; f) Tan, M.; Zhang, Y. *Tetrahedron Lett.* **2009**, *50*, 4912–4915; g) Kulkarni, A.; Zhou, W.; Török, B. *Org. Lett.* **2011**, *13*, 5124–5127; h) Wu, J.; Barnard, J. H.; Zhang, Y.; Talwar, D.; Robertson, C. M.; Xiao, J. *Chem. Commun.* **2013**, *49*, 7052–7054; i) Chen, F.; Surkus, A.-E.; He, L.; Pohl, M.-M.; Radnik, J.; Topf, C.; Junge, K.; Beller, M. *J. Am. Chem. Soc.* **2015**, *137*, 11718–11724; j) Talwar, D.; Li, H. Y.; Durham, E.; Xiao, J. *Chem.-Eur. J.* **2015**, *21*, 5370–5379.
- (7) For methods for Boc-protected indoline formation, see: a) Clarisse, D.; Fenet, B.; Fache, F. *Org. Biomol. Chem.* **2012**, *10*, 6587–6594; b) Srivari, C.; Basu, D.; Reddy, C. R. *Synthesis* **2007**, *10*, 1509–1512; c) Kuwano, R.; Sato, K.; Ito, Y. *Chem. Lett.* **2000**, *4*, 428–429.

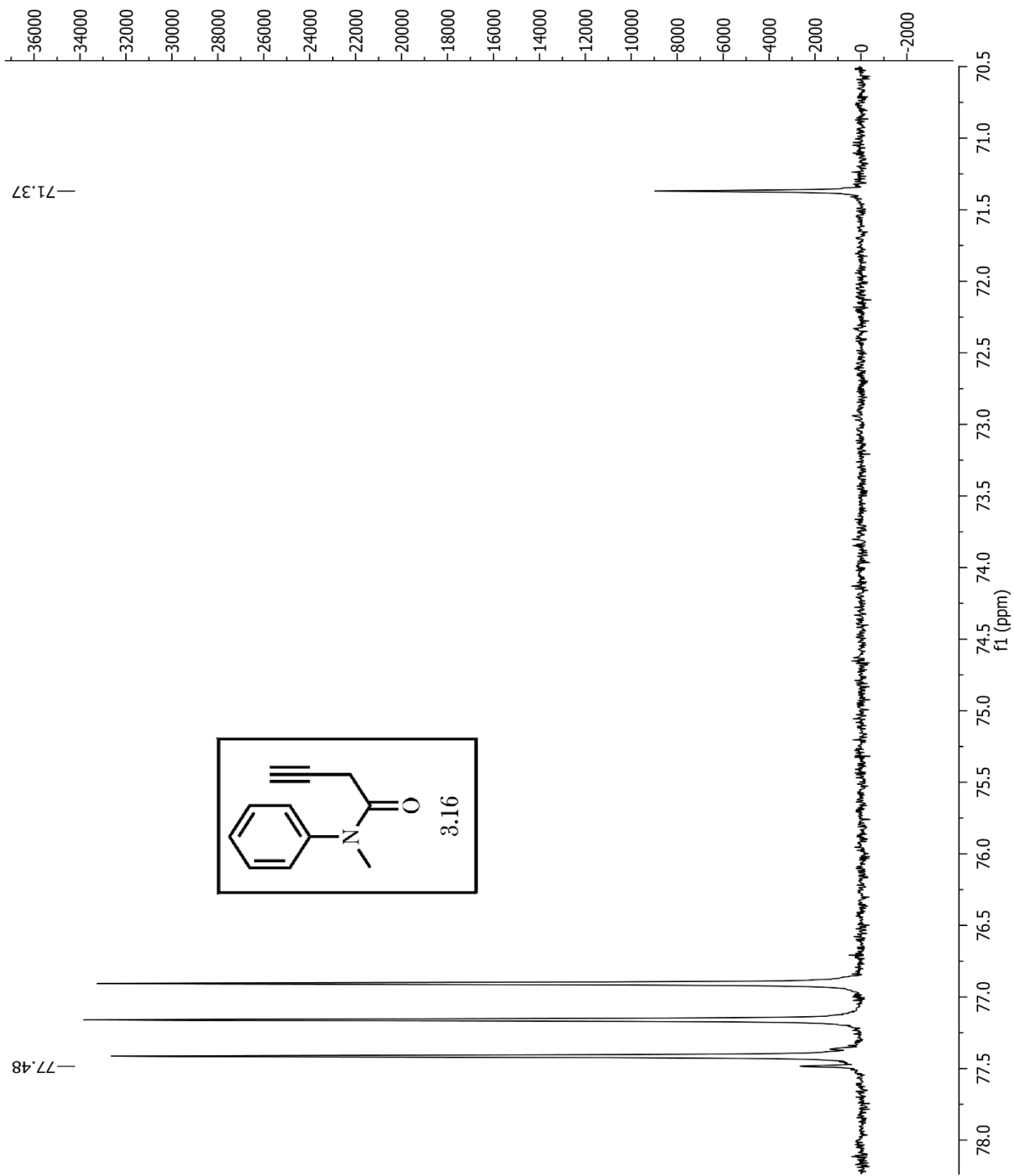
- (8) For palladium-catalyzed aryl-nitrogen couplings, see: a) Guram, A. S.; Rennels, R. A.; Buchwald, S. L. *Angew. Chem. Int. Ed.* **1995**, *34*, 1348-1350; b) Wolfe, J. P.; Rennels, R. A.; Buchwald, S. L. *Tetrahedron*, **1996**, *52*, 7525-7546.
- (9) For palladium-catalyzed aryl-carbon couplings, see: Watanabe, T.; Oishi, S.; Fujii, N.; Ohno, H. *Org. Lett.* **2008**, *10*, 1759-1762.
- (10) For copper-catalyzed aryl-nitrogen couplings: a) Klapars, A.; Huang, X.; Buchwald, S. L. *J. Am. Chem. Soc.* **2002**, *124*, 7421-7428; b) Yamada, K.; Kubo, T.; Tokuyama, H.; Fukuyama, T. *Synlett*. **2002**, *2*, 231-234.
- (11) For an aryl-N/C-N coupling cascade, see: Minatti, A.; Buchwald, S. L. *Org. Lett.* **2008**, *10*, 2721-2724.
- (12) Omar-Amrani, R.; Thomas, A.; Brenner, E.; Schneider, R.; Fort, Y. *Org. Lett.* **2003**, *5*, 2311-2314.
- (13) (a) Wipf, P.; Maciejewski, J. P. *Org. Lett.*, **2008**, *10*, 4383-4386. (b) Gansäuer, A.; Behlendorf, M.; von Laufenberg, D.; Fleckhaus, A.; Kube, C.; Sadasivam, D. V.; Flowers II, R. A. *Angew. Chem. Int. Ed.* **2013**, *51*, 2012, 4739-4742. (c) Gansäuer, A.; von Laufenberg, D.; Kube, C.; Dahmen, T.; Michelmann, A.; Behlendorf, M.; Sure, R.; Seddiqzai, M.; Grimme, S.; Sadasivam, D. V.; Fianu, G. D.; Flowers II, R. A. *Chem Eur. J.* **2015**, *21*, 280-289.
- (14) Zhao, Y.; Xu, M.; Zheng, Z.; Yuan, Y.; Li, Y. *Chem. Commun.* **2017**, *53*, 3721-3724.
- (15) a) Fuwa, H.; Sasaki, M. *Org. Lett.* **2007**, *9*, 3347-3350; b) Clive, D. L. J.; Peng, J.; Fletcher, S. P.; Ziffle, V. E.; Wingert, D. *J. Org. Chem.* **2008**, *73*, 2330-2344; c) Viswanathan, R.; Smith, C. R.; Prabhakaran, E. N.; Johnston, J. N. *J. Org. Chem.* **2008**, *73*, 3040-3046.
- (16) Wang, Z.; Wan, W.; Jiang, H.; Hao, J. *J. Org. Chem.* **2007**, *72*, 9364-9367.
- (17) For the use of aminometalation to build indolines, see: Nicolaou, K. C.; Roecker, A. J.; Pfefferkorn, J. A.; Cao, G.-Q. *J. Am. Chem. Soc.* **2000**, *122*, 2966-2967.

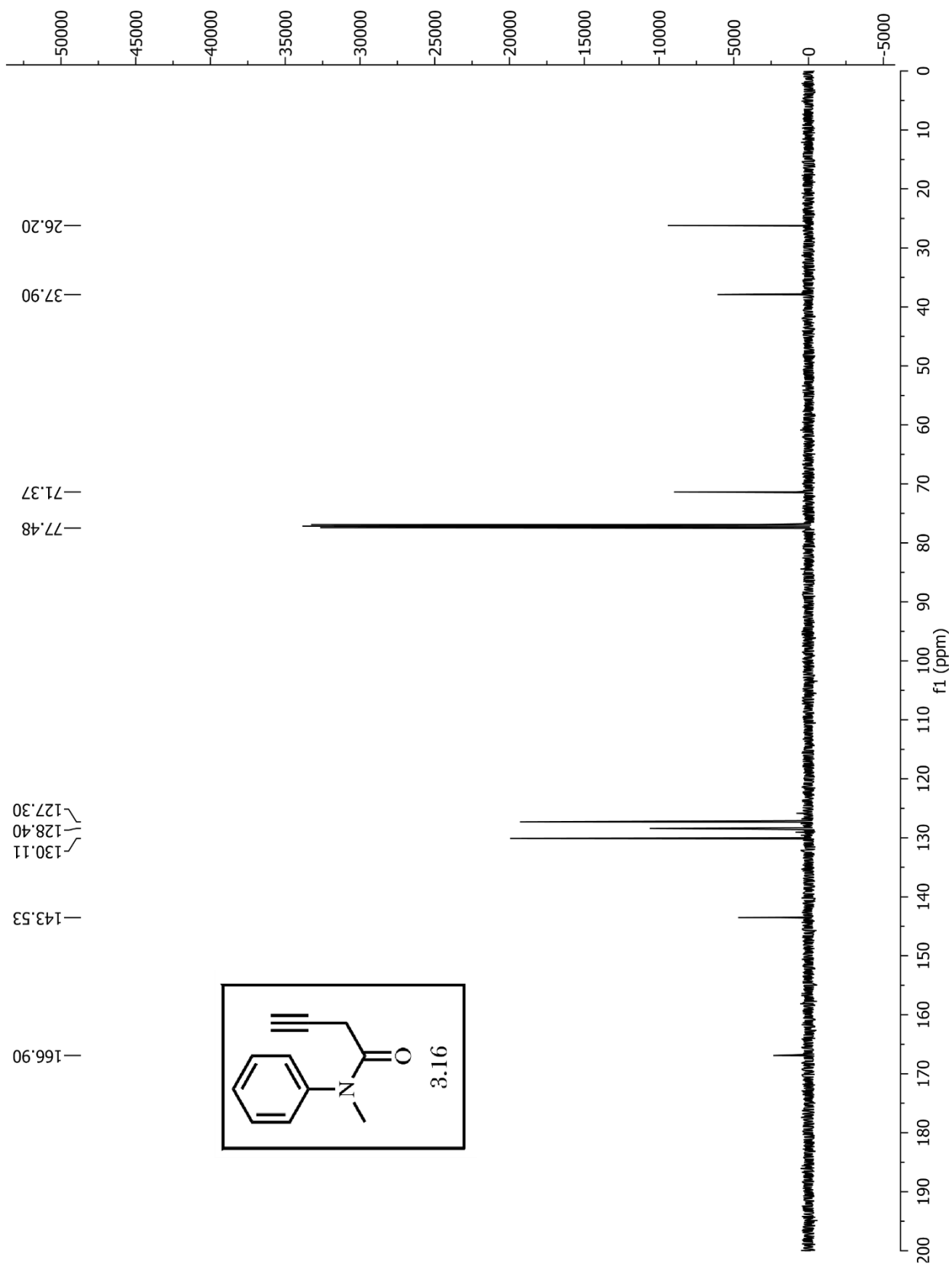
- (18) For indoline synthesis via carbolittiation, see: Gil, G. S.; Groth, U. M. *J. Am. Chem. Soc.* **2000**, *122*, 6789–6790.
- (19) For the use of hypervalent iodine in indoline synthesis, see: Correa, A.; Tellitu, I.; Domínguez, E.; SanMartin, R. *J. Org. Chem.* **2006**, *71*, 8316–8319.
- (20) For the use of benzyne intermediates in indoline synthesis, see: Golmore, C. D.; Allan, K. M.; Stoltz, B. M. *J. Am. Chem. Soc.* **2008**, *130*, 1558–1559.
- (21) Dunetz, J. R.; Danheiser, R. L. *J. Am. Chem. Soc.* **2005**, *127*, 5776–5777
- (22) a) Garner, R. *Tetrahedron Lett.* **1968**, *9*, 221–224; b) Cheung, W.-H.; Zheng, S.-L.; Yu, W.-Y.; Zhou, G.-C.; Chu, C.-M. *Org. Lett.* **2003**, *5*, 2535–2538; c) Krogsgaard-Larson, N.; Begtrup, M.; Herth, M. M.; Kehler, J. *Synthesis*, **2010**, *24*, 4287–4299; d) Mahoney, S. J.; Fillion, E. *Chem. Eur. J.* **2012**, *18*, 68–71. e) Reddy, A. C. S.; Choutipalli, V. S. K.; Ghorai, J.; Subramanian, V.; Anbarasan, P. *ACS Catal.* **2017**, *7*, 6283–6288; f) Alt, I. T.; Guttroff, C.; Plietker, B. *Angew. Chem. Int. Ed.* **2017**, *56*, 10582–10586.
- (23) a) Ruppel, J. V.; Kamble, R. M.; Zhang, X. P. *Org. Lett.* **2007**, *9*, 4889–4892; b) Lu, H.-J.; Li, C.-Q.; Jiang, H.-L.; Lizardi, C. L.; Zhang, X. P. *Angew. Chem., Int. Ed.* **2014**, *53*, 7028–7032.
- (24) Liu, Y.; Wei, J.; Che, C.-M. *Chem. Commun.* **2010**, *46*, 6926–6928.
- (25) a) Doyle, M. P. *Chem. Rev.* **1986**, *86*, 919–939; b) Davies, H. M. L.; Beckwith, R. E. J. *Chem. Rev.* **2003**, *103*, 2861–2904.
- (26) a) Bamford, W. R.; Stevens, T. S. *J. Chem. Soc.* **1952**, 4735–4740; b) Barluenga, J.; Valdes, C. *Angew. Chem., Int. Ed.* **2011**, *50*, 7486–7500; c) Shao, Z.; Zhang, H. *Chem. Soc. Rev.* **2012**, *41*, 560–572; d) Xiao, Q.; Zhang, Y.; Wang, J. *Acc. Chem. Res.* **2013**, *46*, 236–247; e) Yao, T.; Hirano, K.; Satoh, T.; Miura, M. *Angew. Chem., Int. Ed.* **2012**, *51*, 775–779; f) Hu, F.; Xia, Y.; Ye, F.; Liu, Z.; Ma, C.; Zhang, Y.; Wang, J. *Angew. Chem., Int. Ed.* **2014**, *53*, 1364–1367.

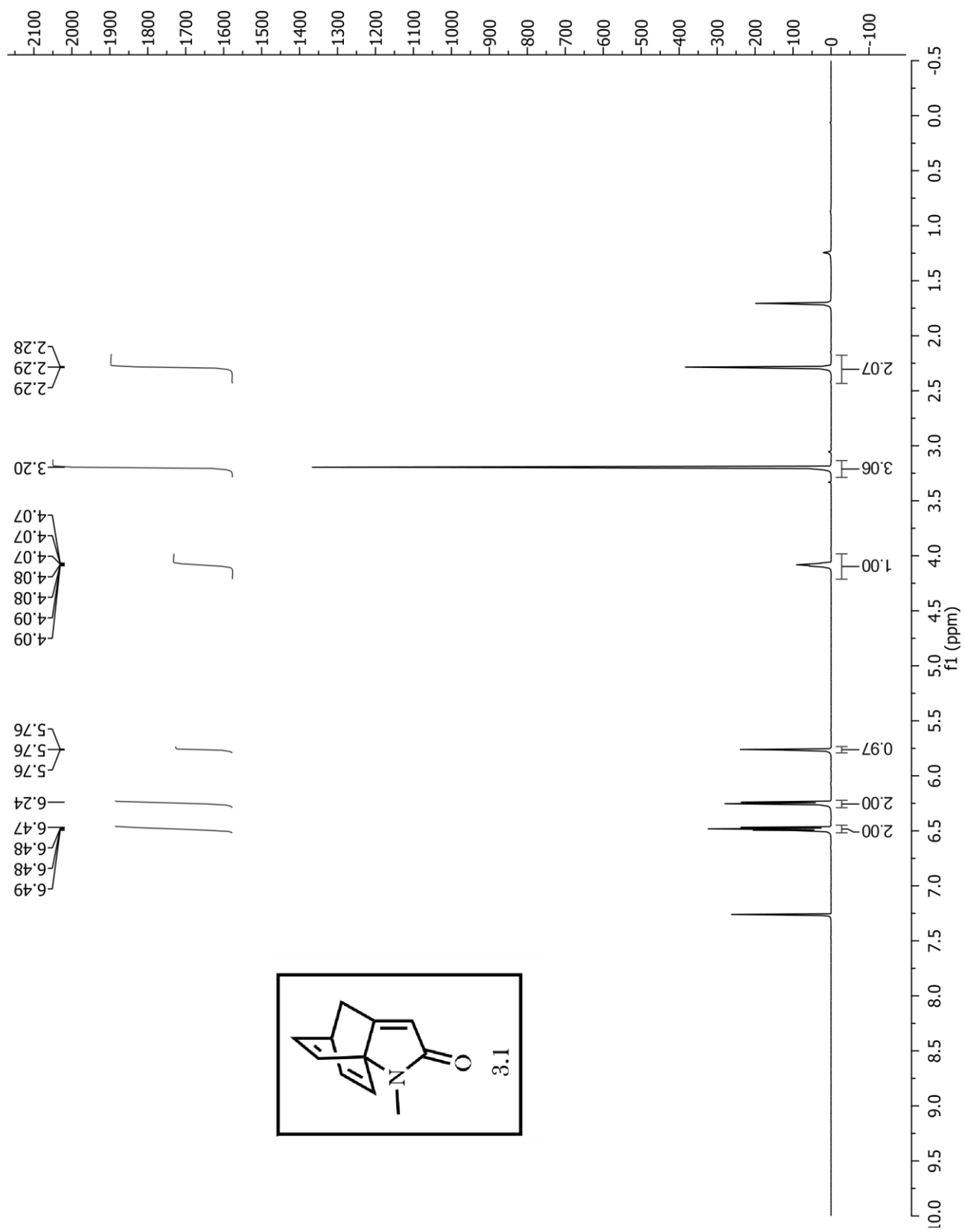
- (27) B. G. Das, A. Chirila, M. Tromp, J. N. H. Reek, B. de Bruin, *J. Am. Chem. Soc.*, **2016**, *138*, 8968-8975.
- (28) J. Wöltinger, J.-E. Bäckvall, A. Zsigmond, *Chem. Eur. J.* **1999**, *5*, 1460-1467.
- (29) P. Hewawasam, N. Chen, M. Ding, J. T. Natale, C. G. Boissard, S. Yeola, V. K. Gribkoff, J. Starrett, S. I. Dworetzky, *Bioorg. Med. Chem. Lett.* **2004**, *14*, 1615-1618.
- (30) H. Fuwa, M. Sasaki, *Org. Lett.* **2007**, *9*, 3347-3350.

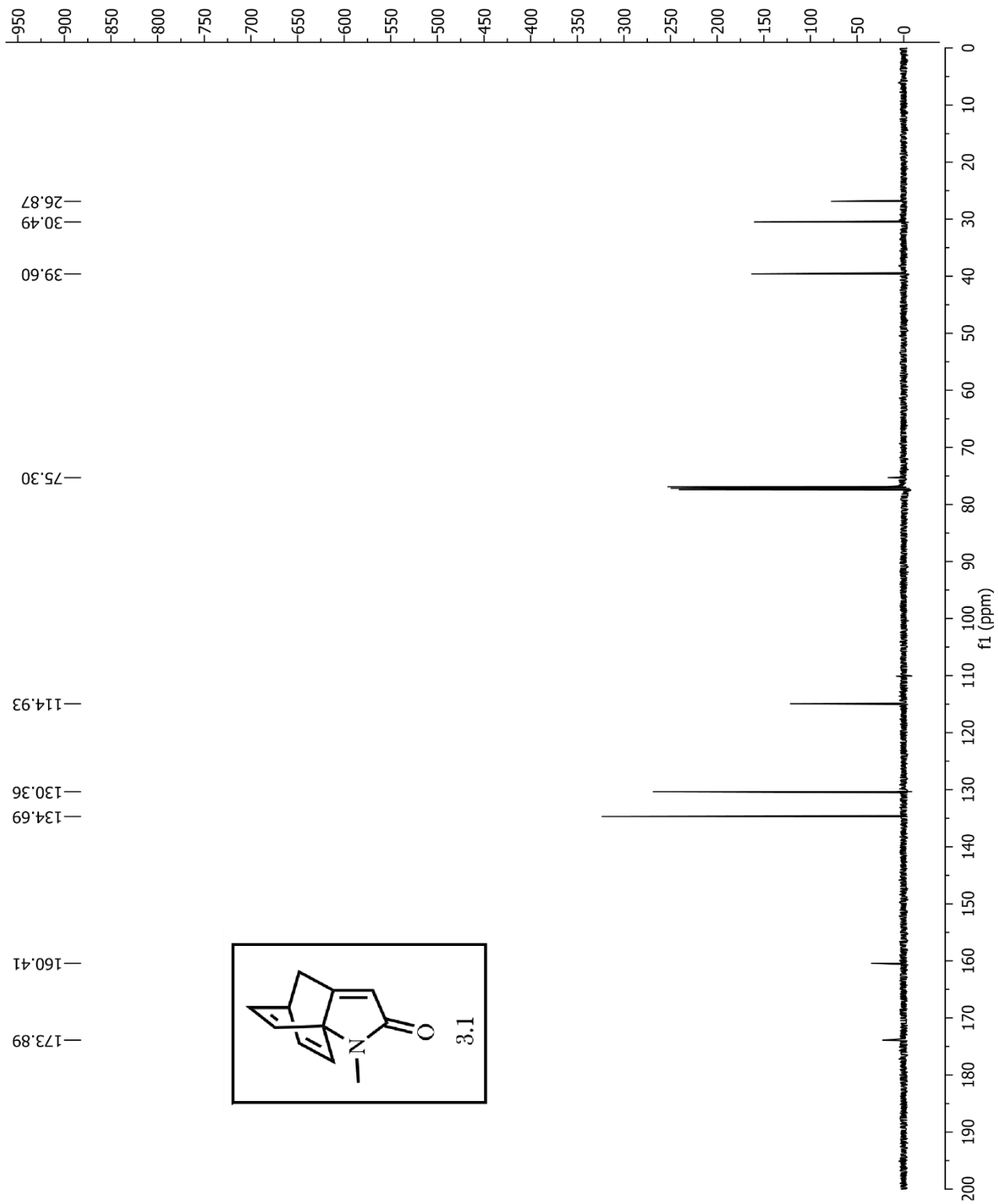
APPENDIX: NMR DATA

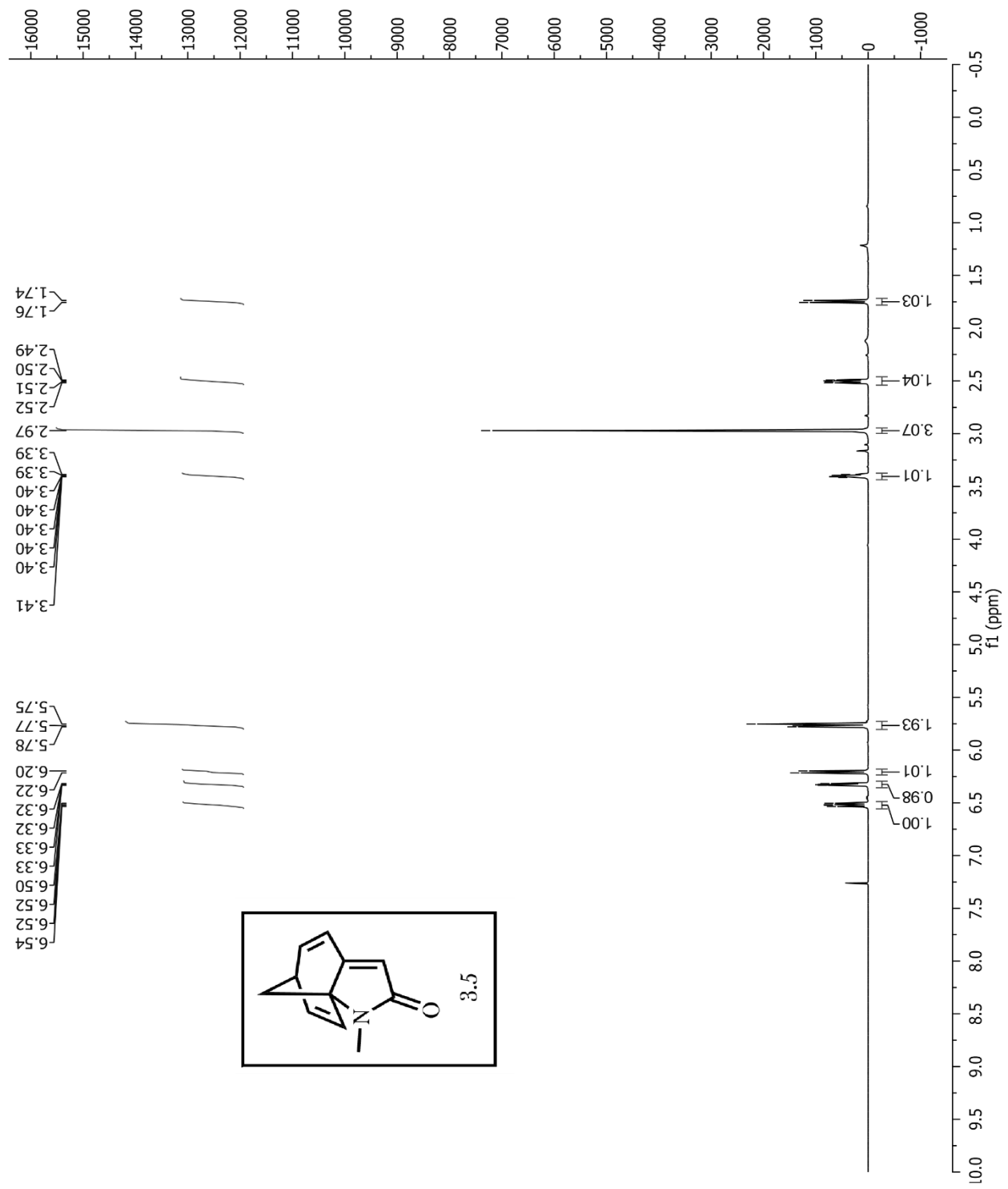


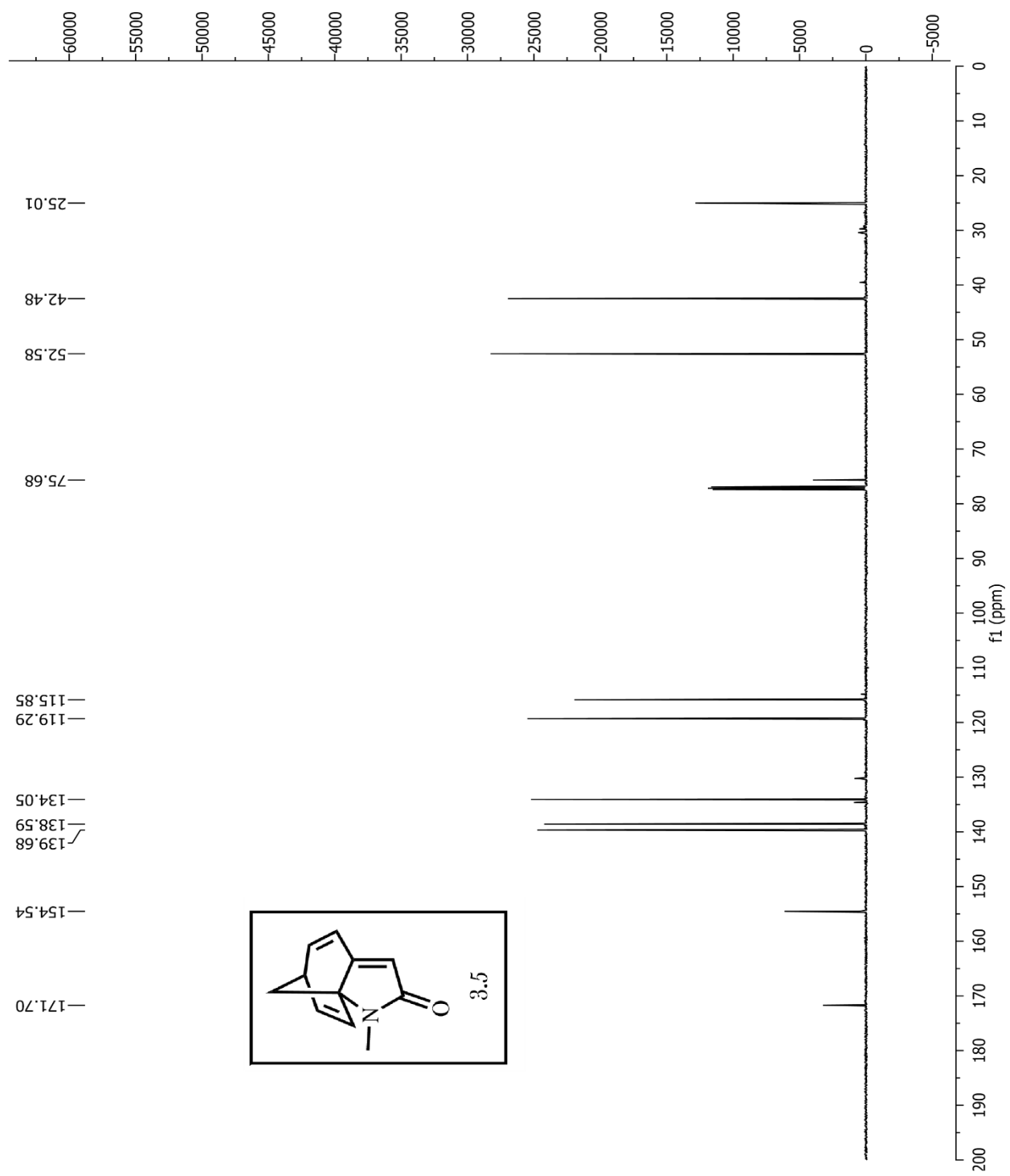


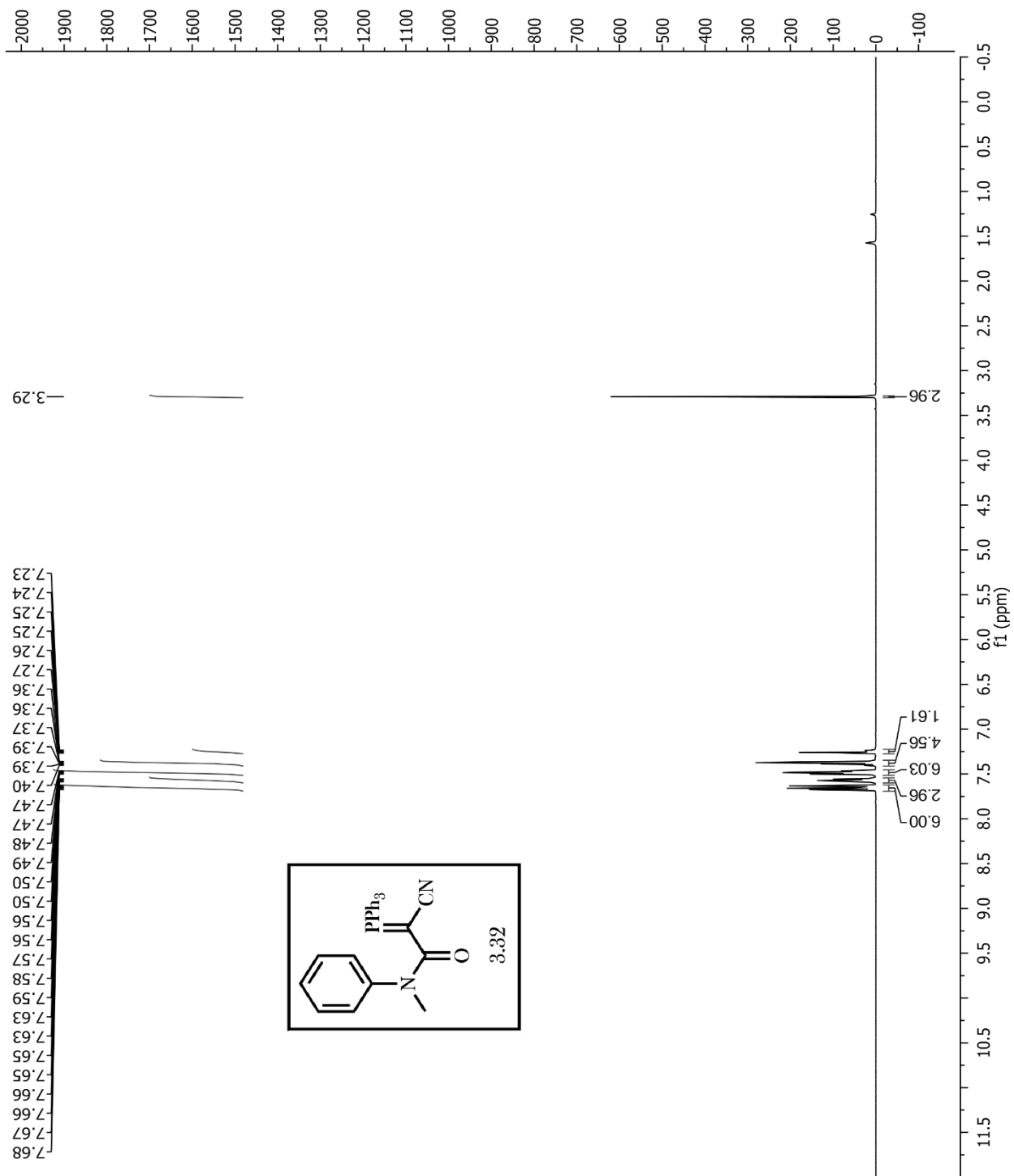


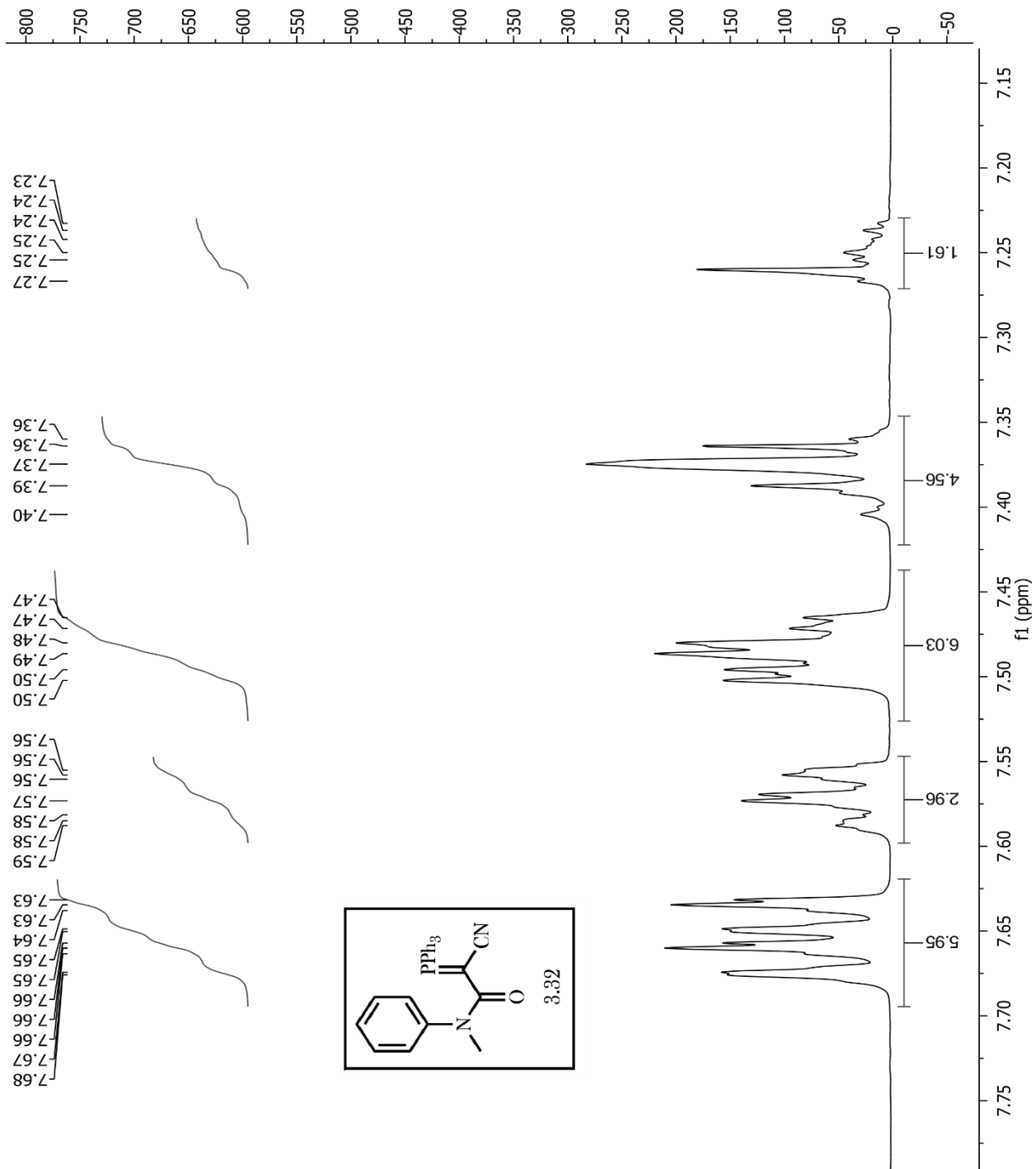


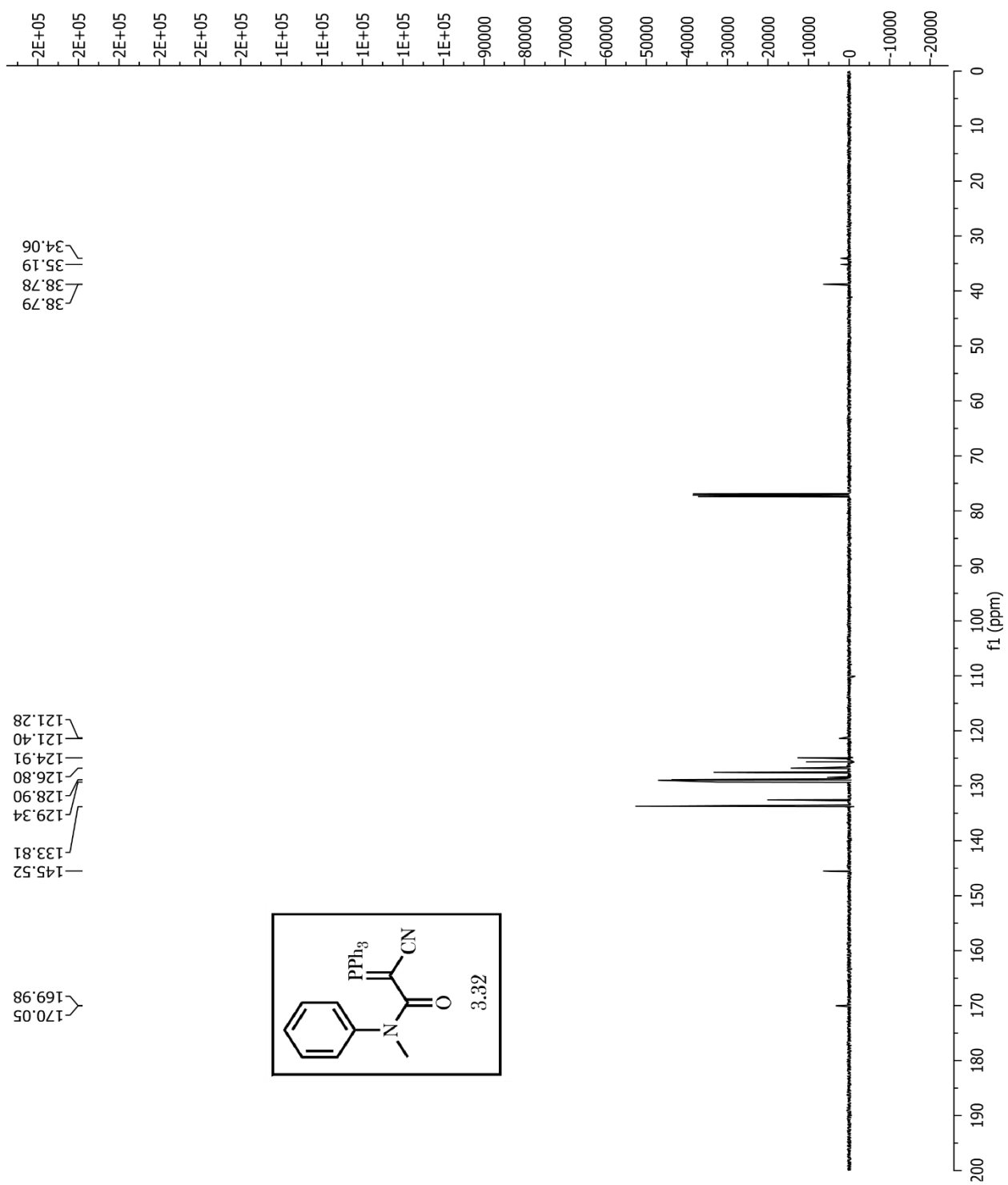


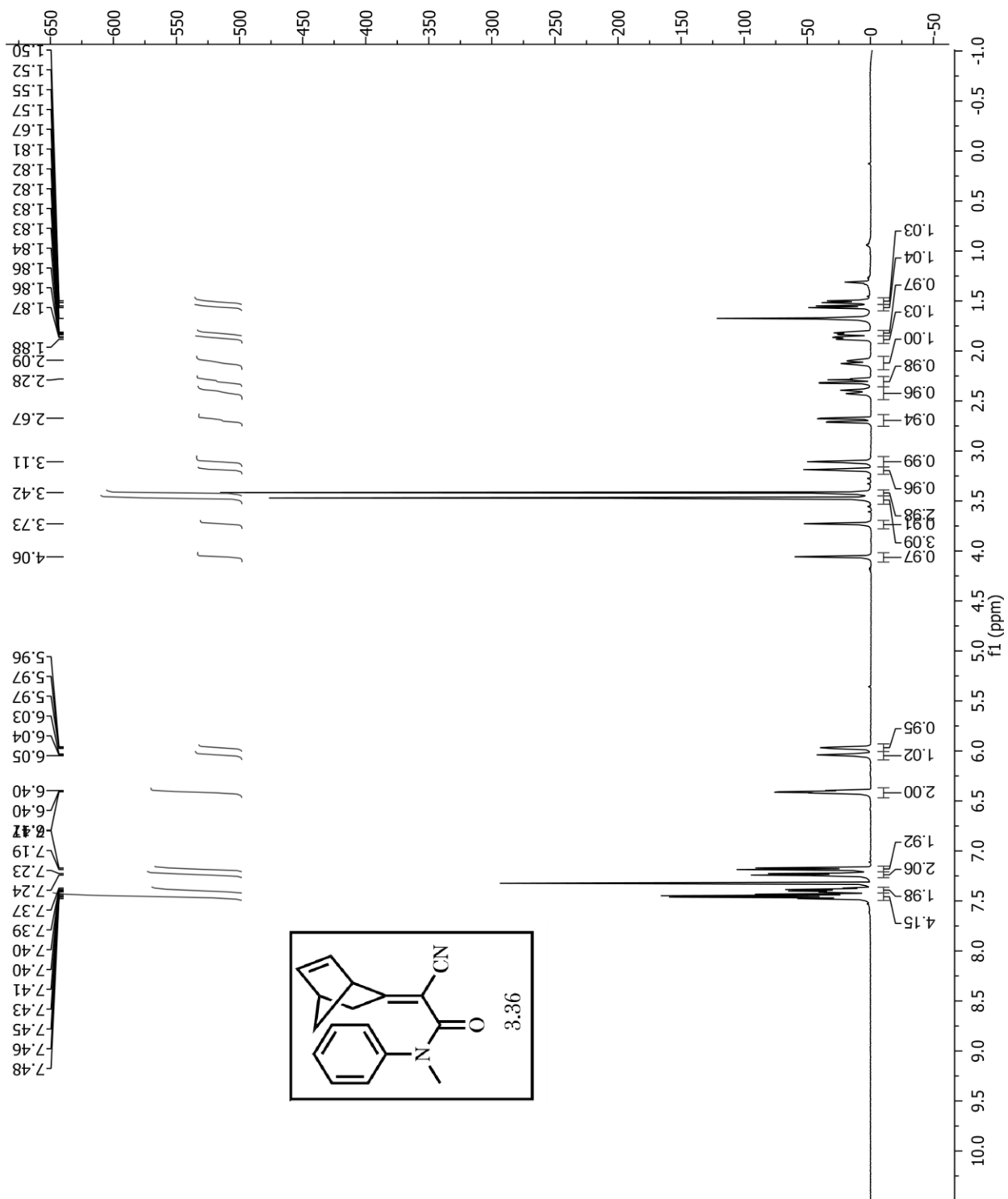


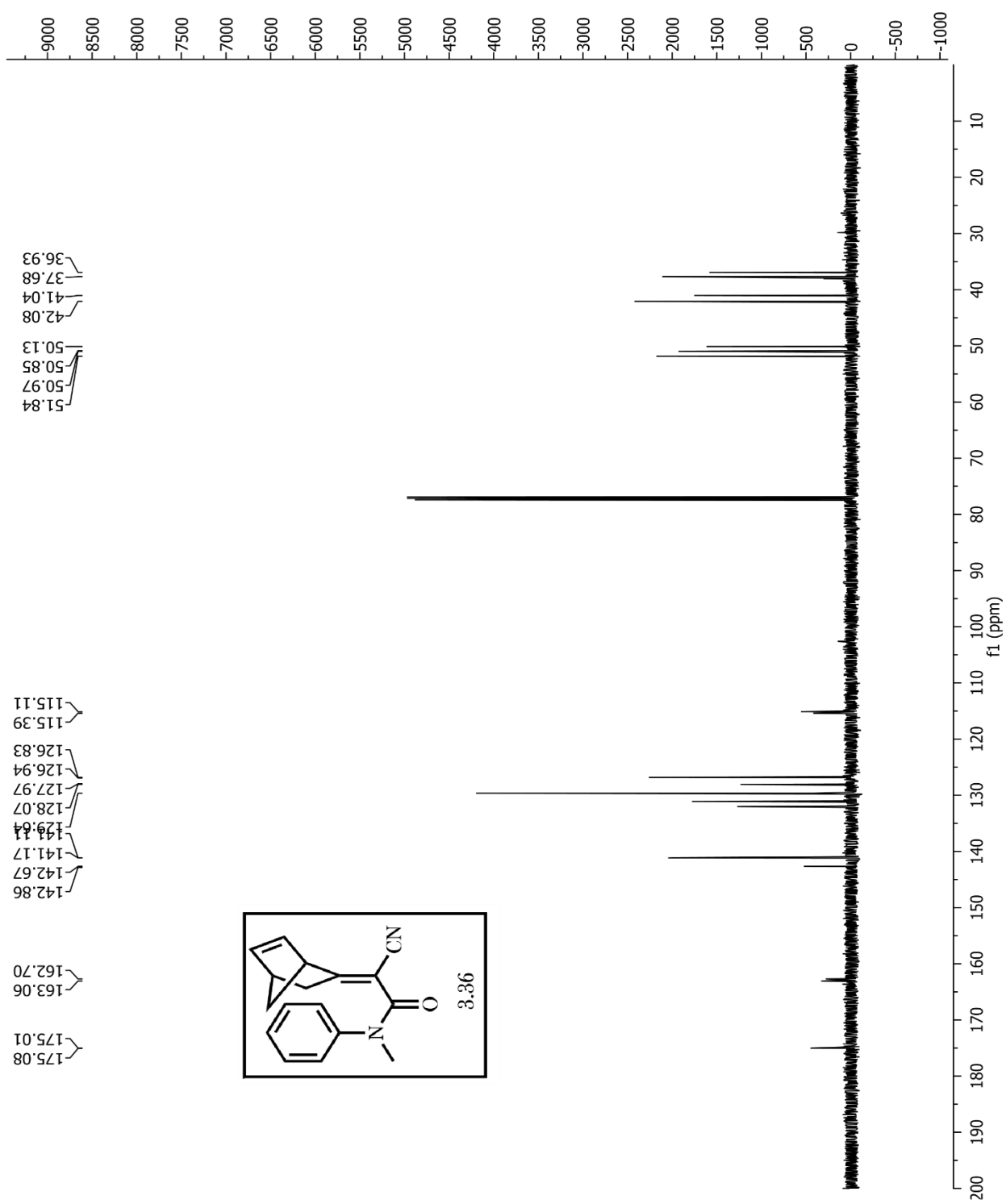


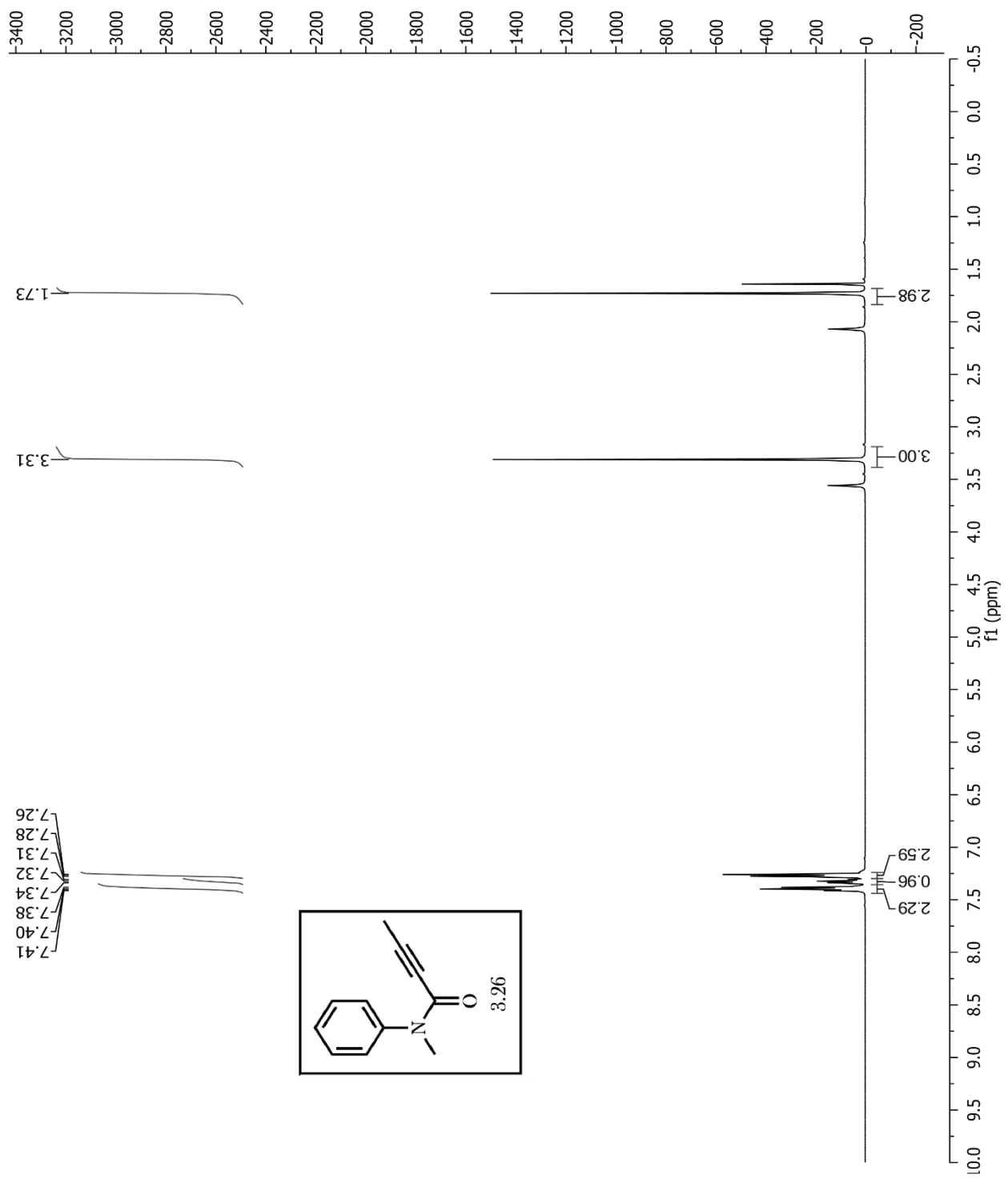


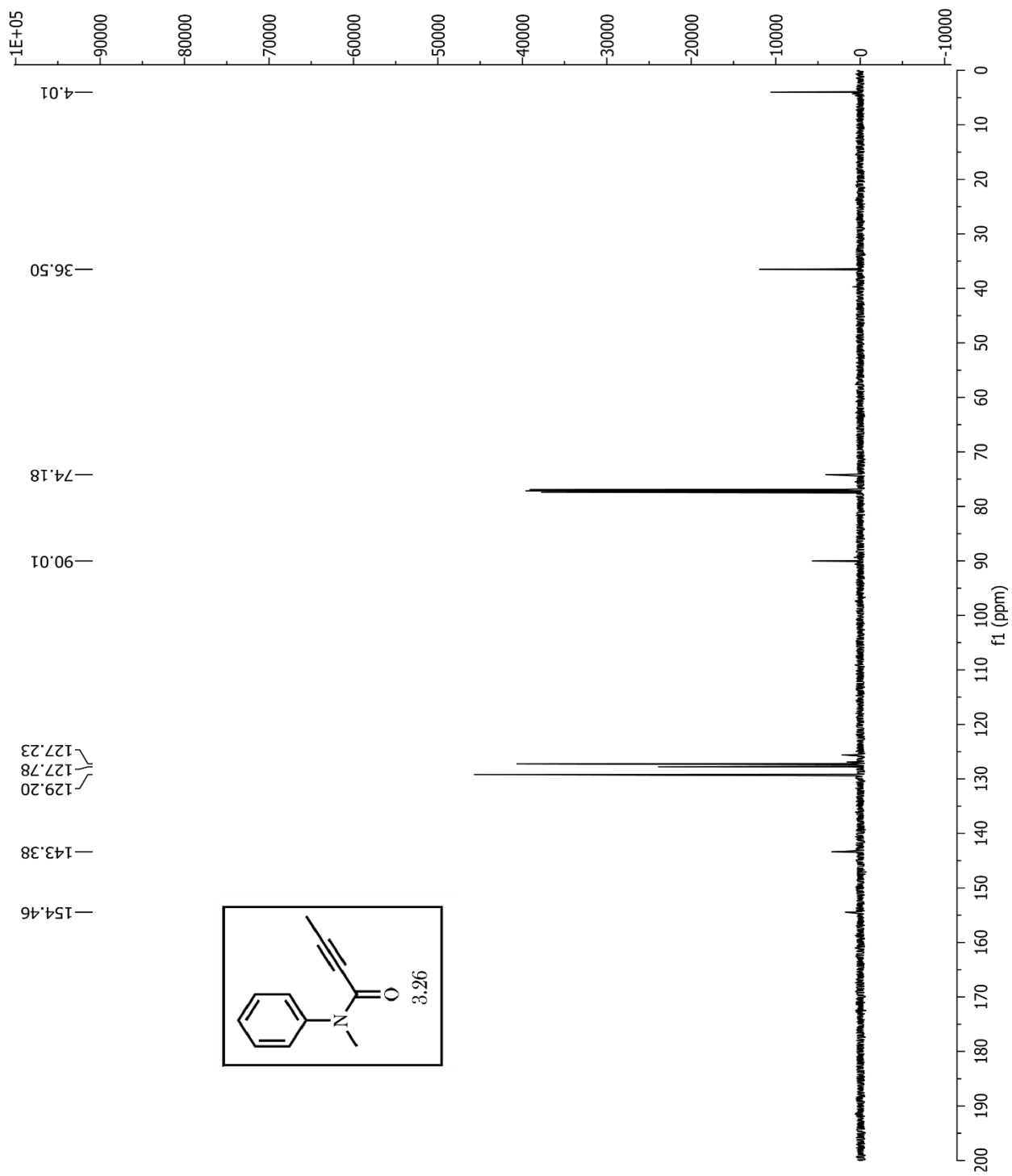


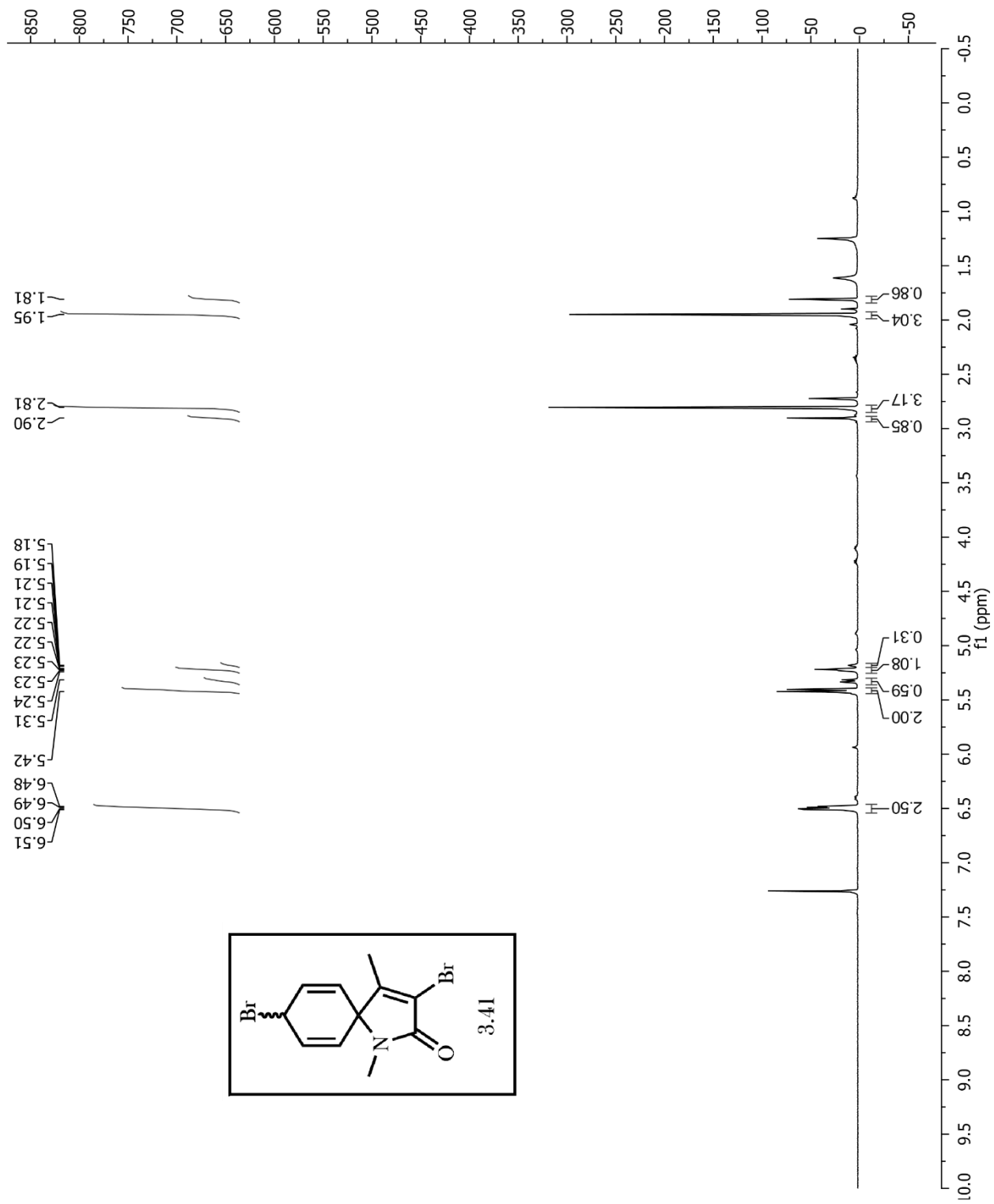


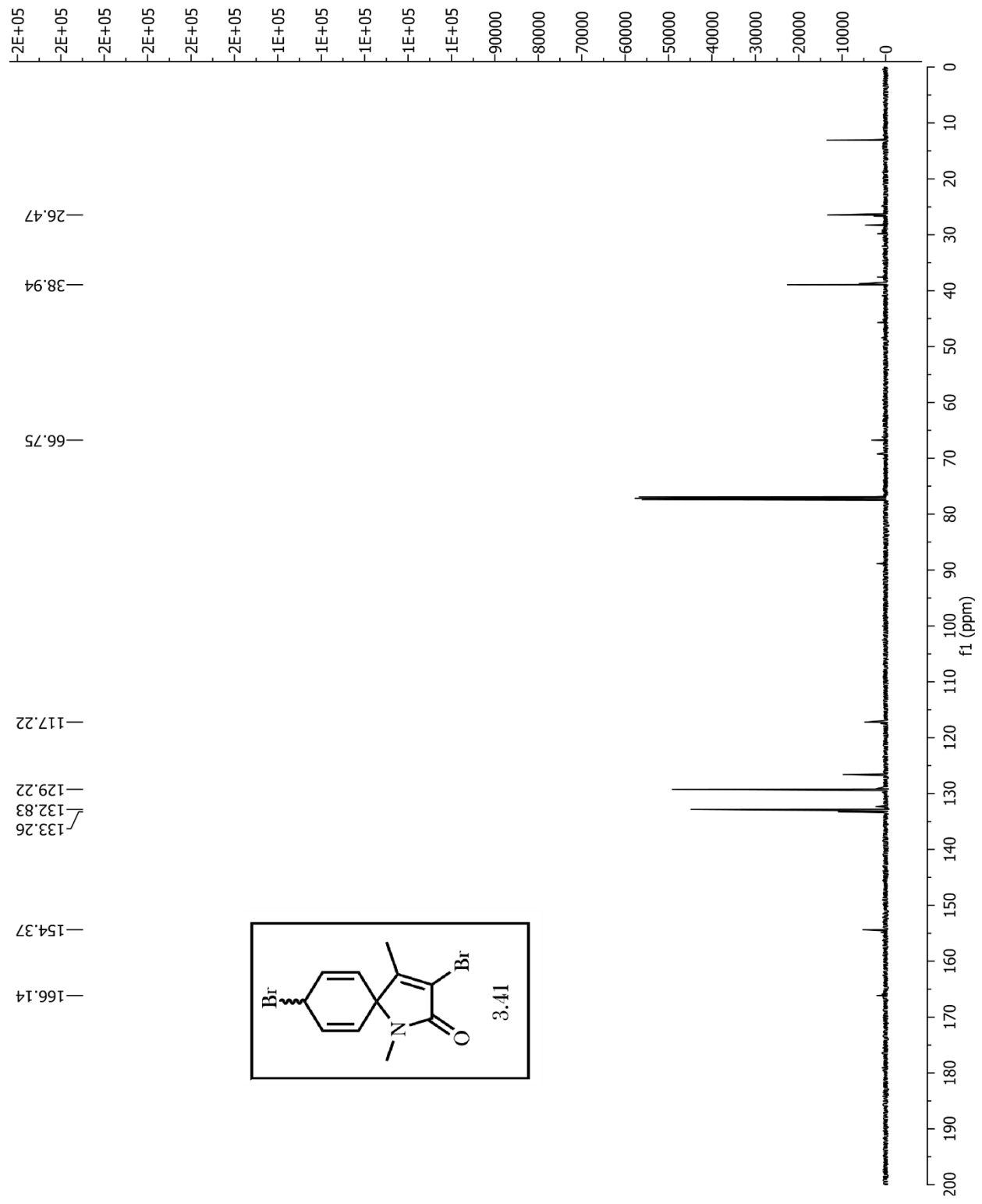


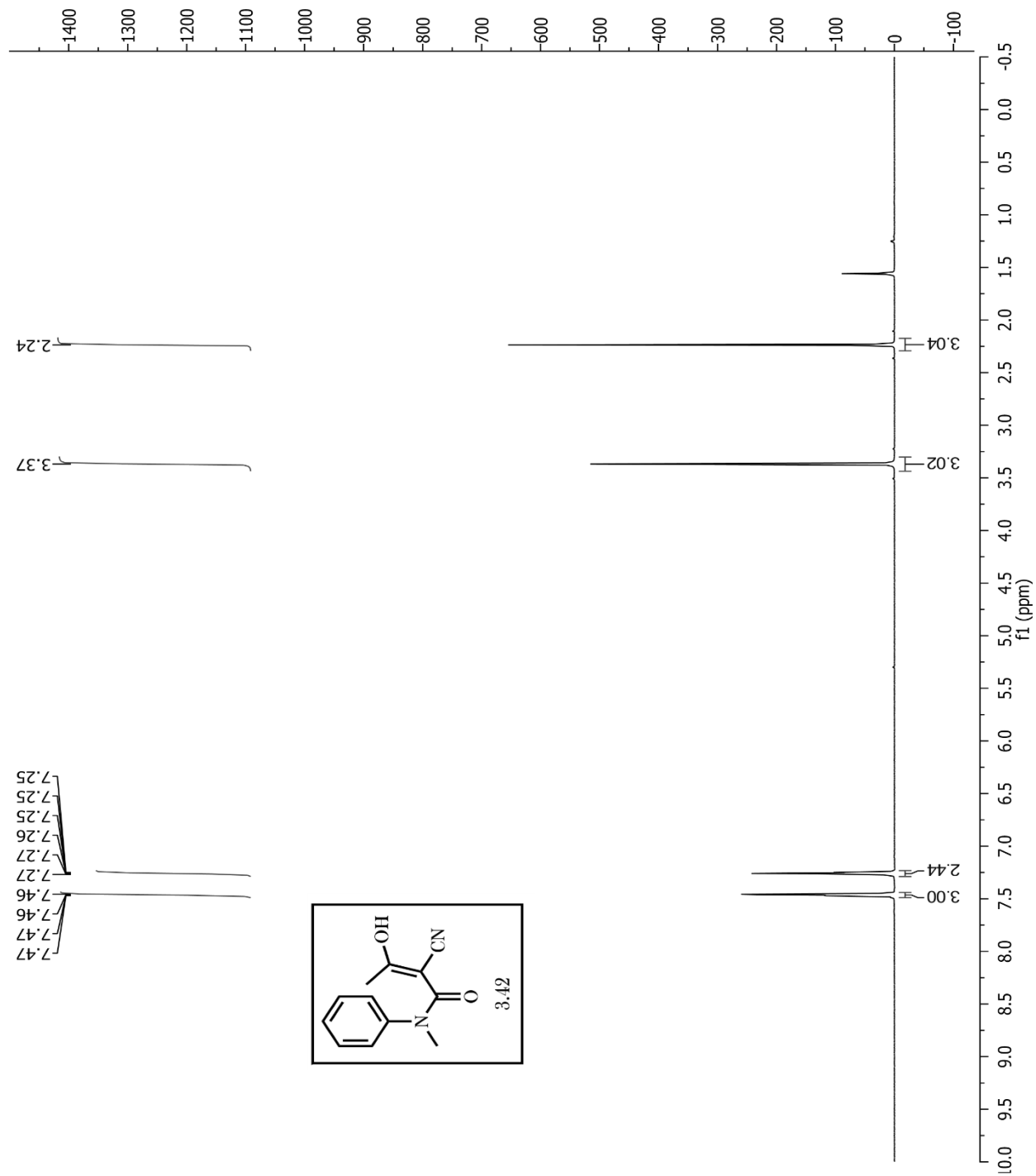


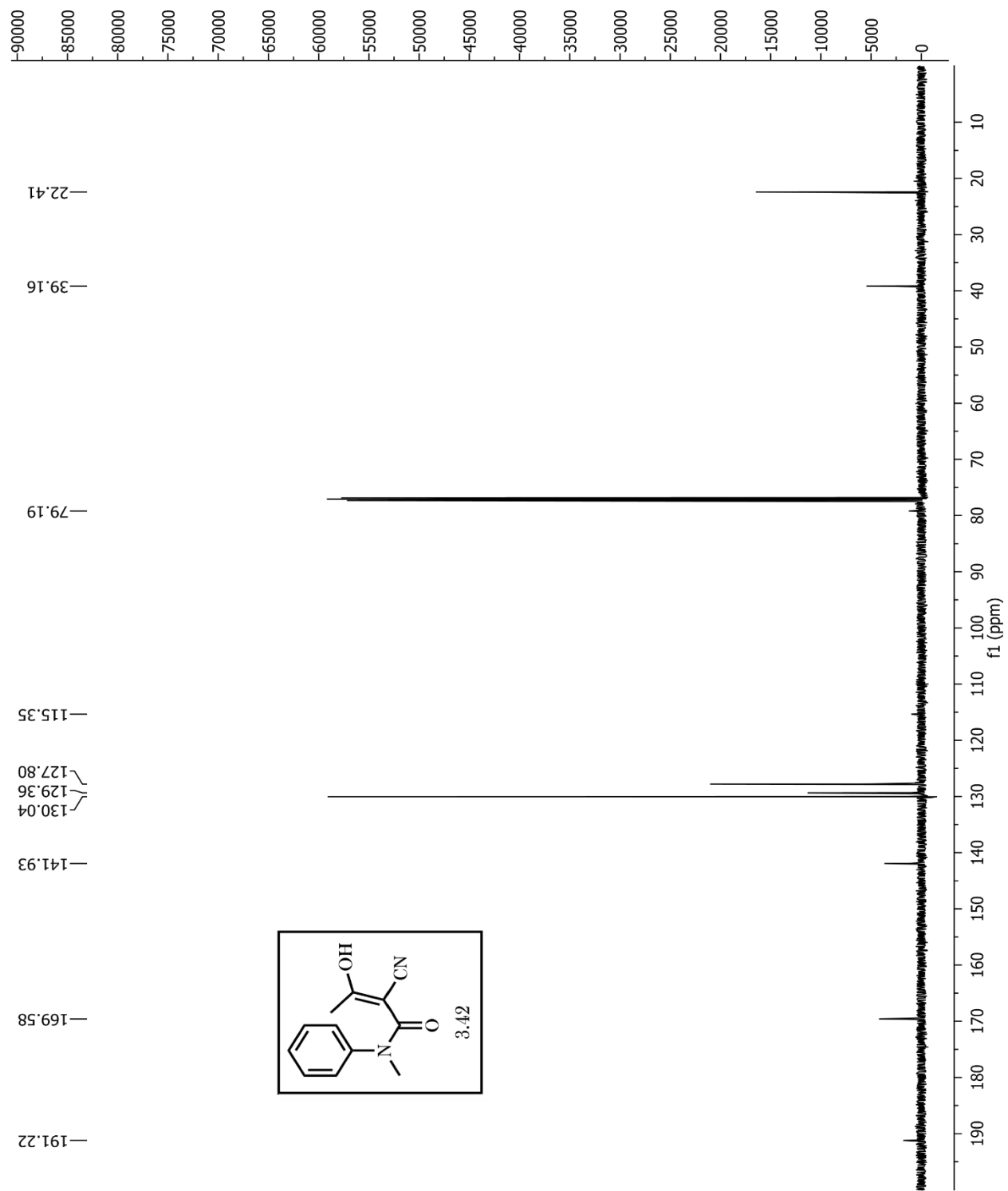


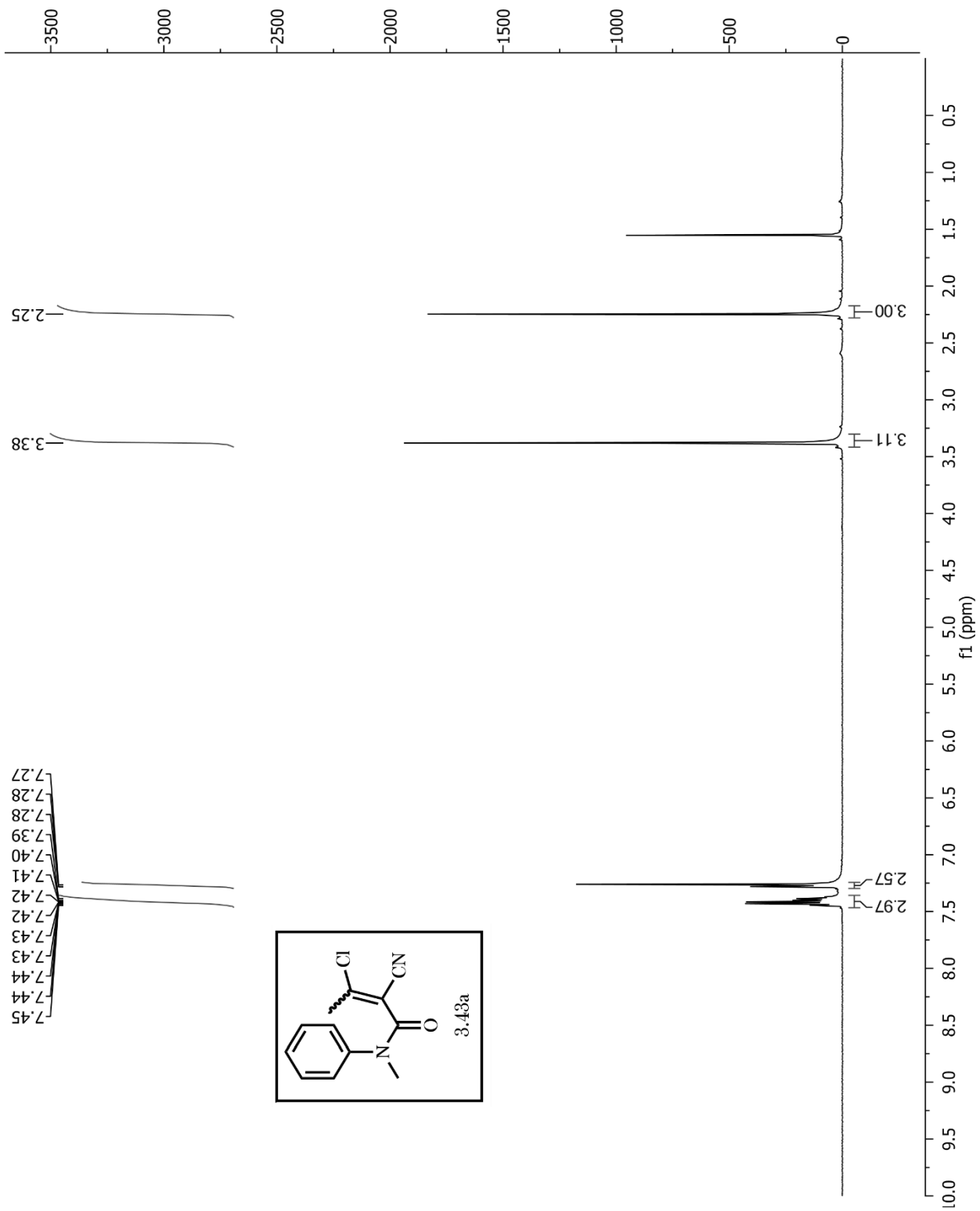


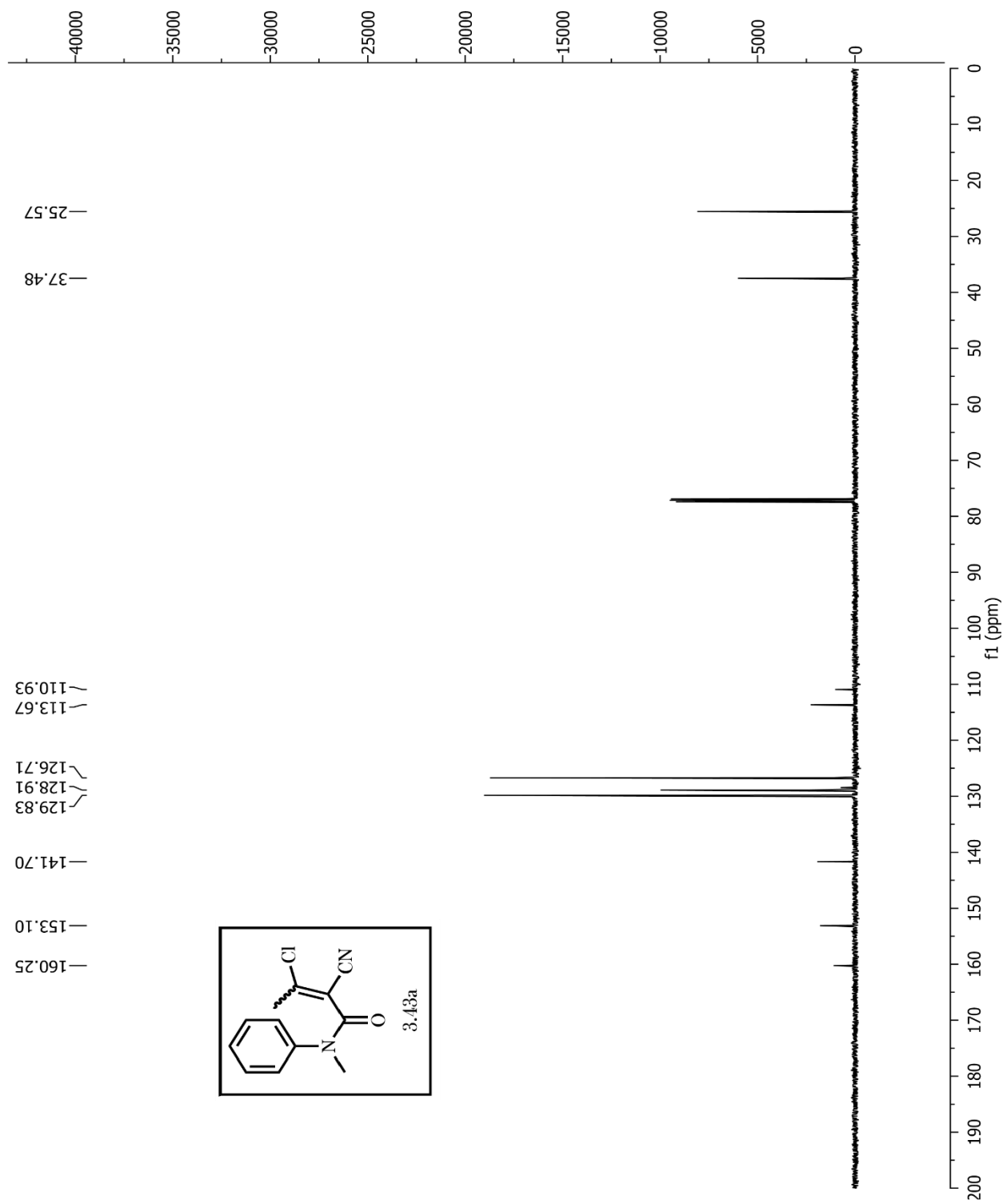


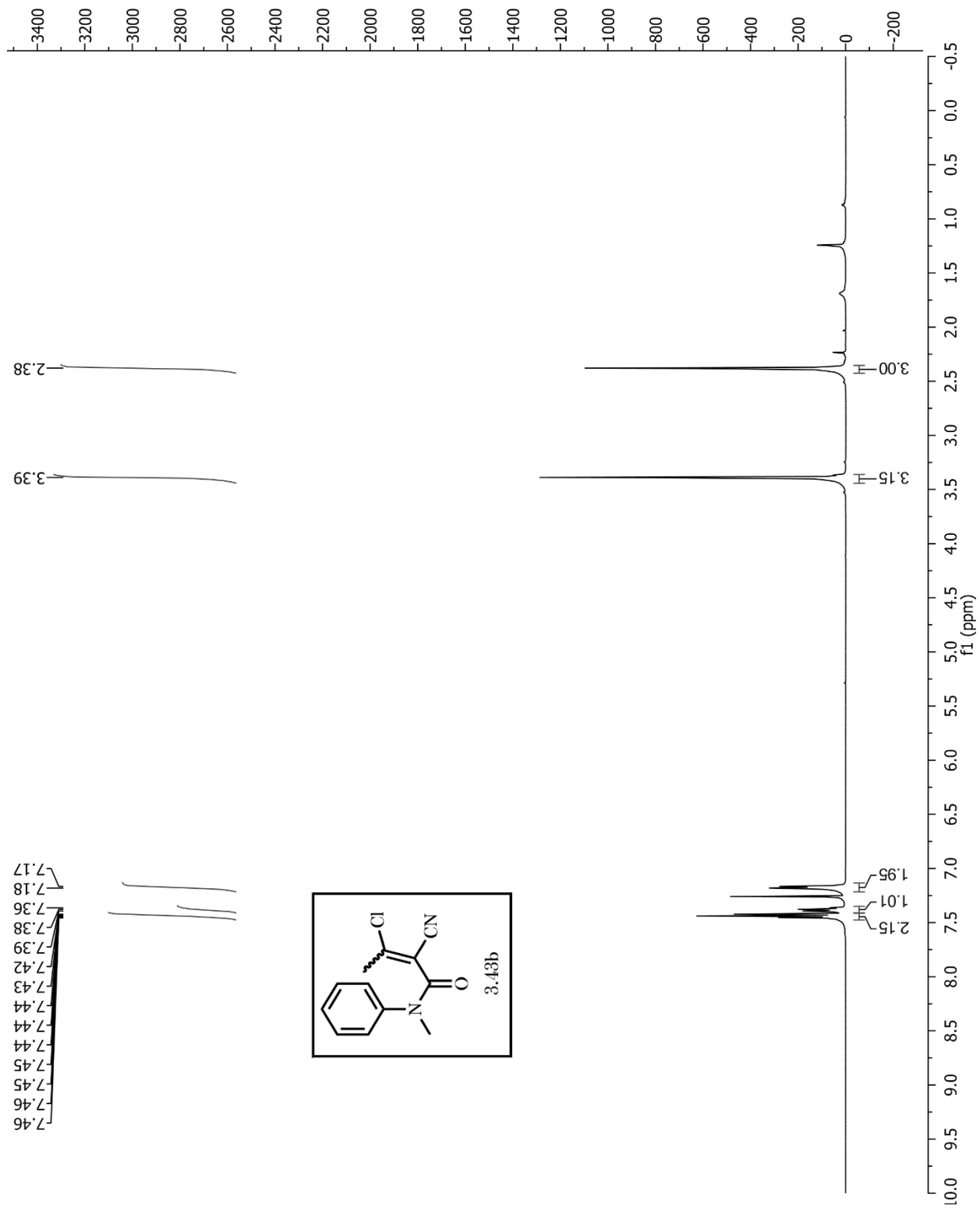


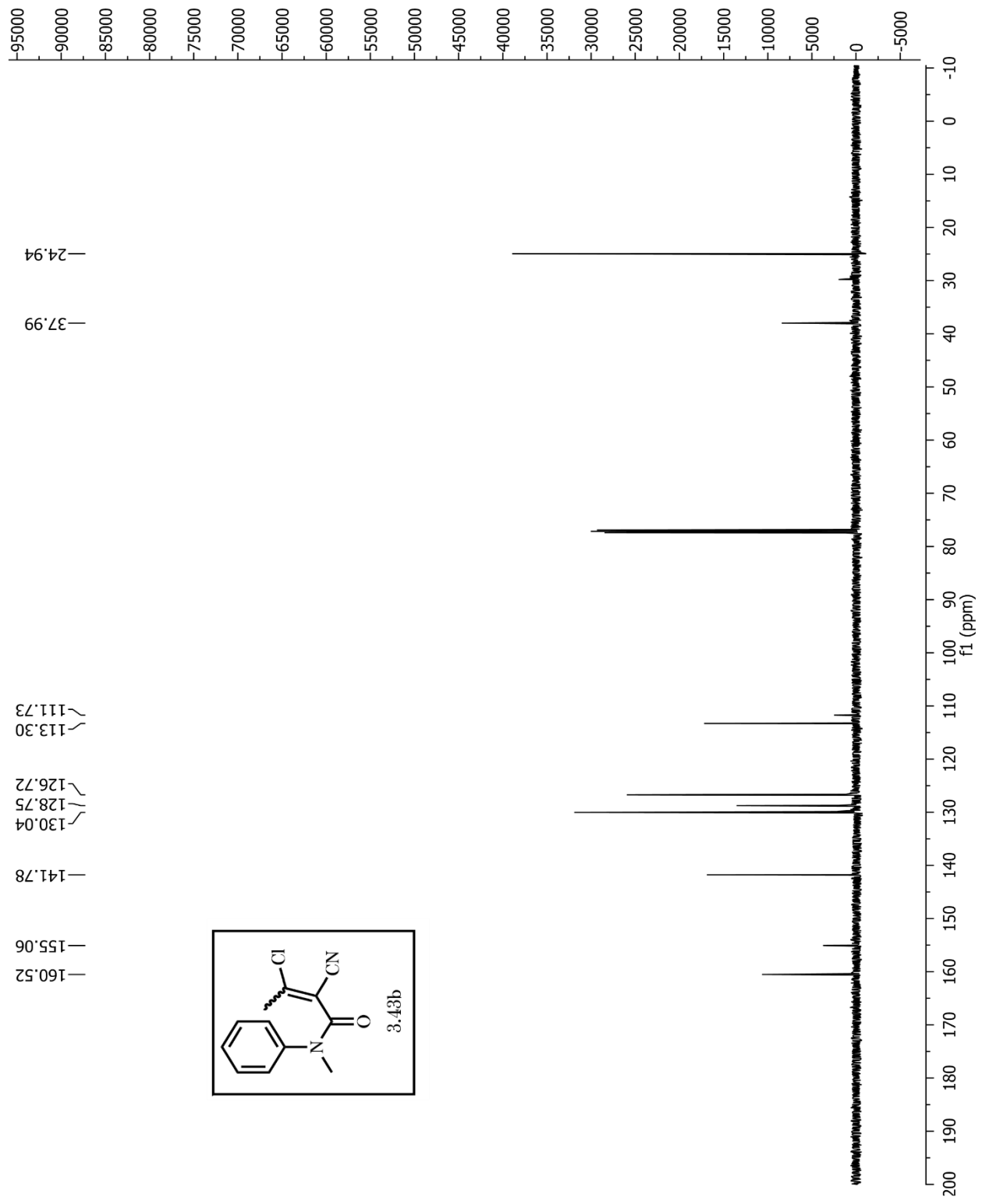


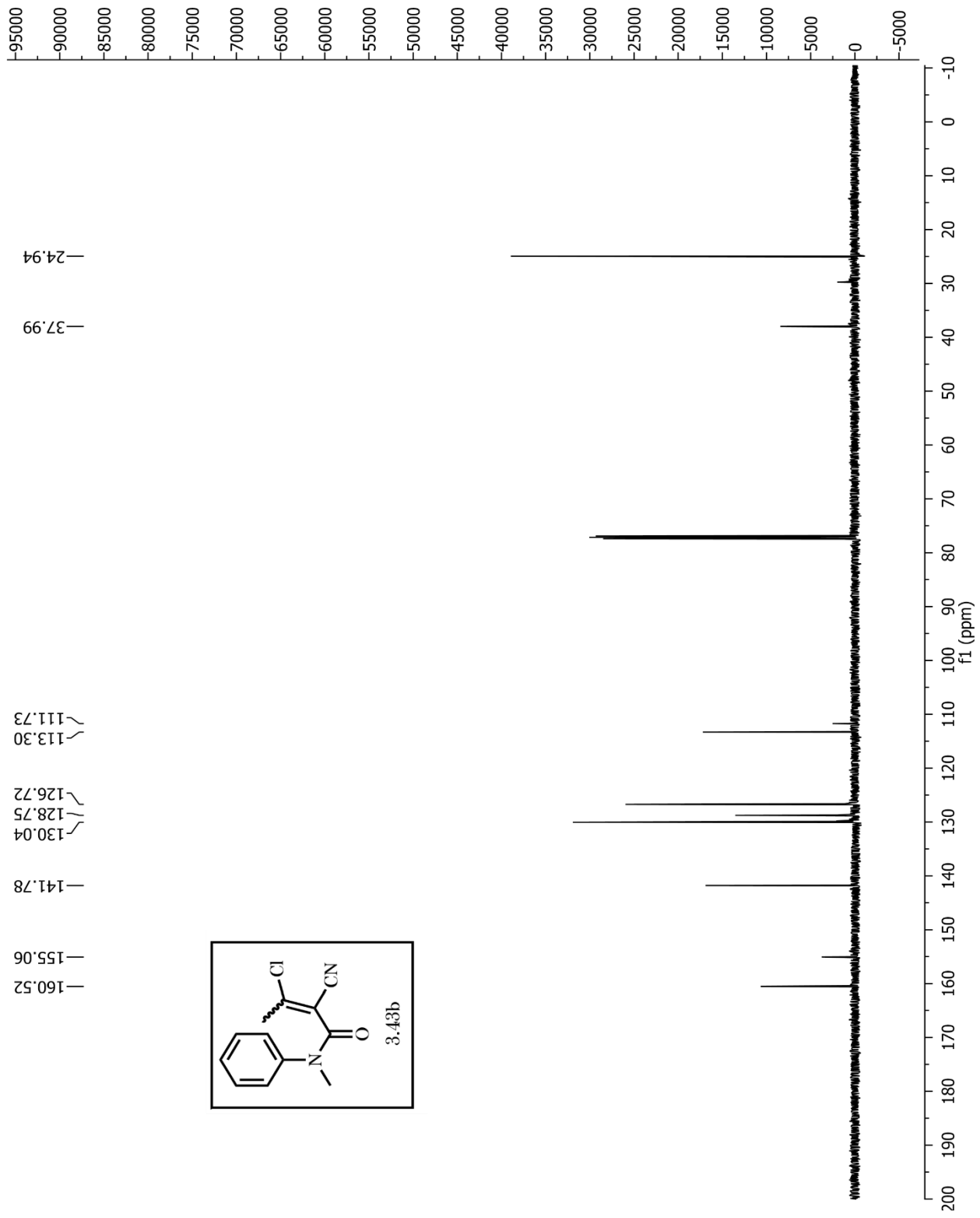


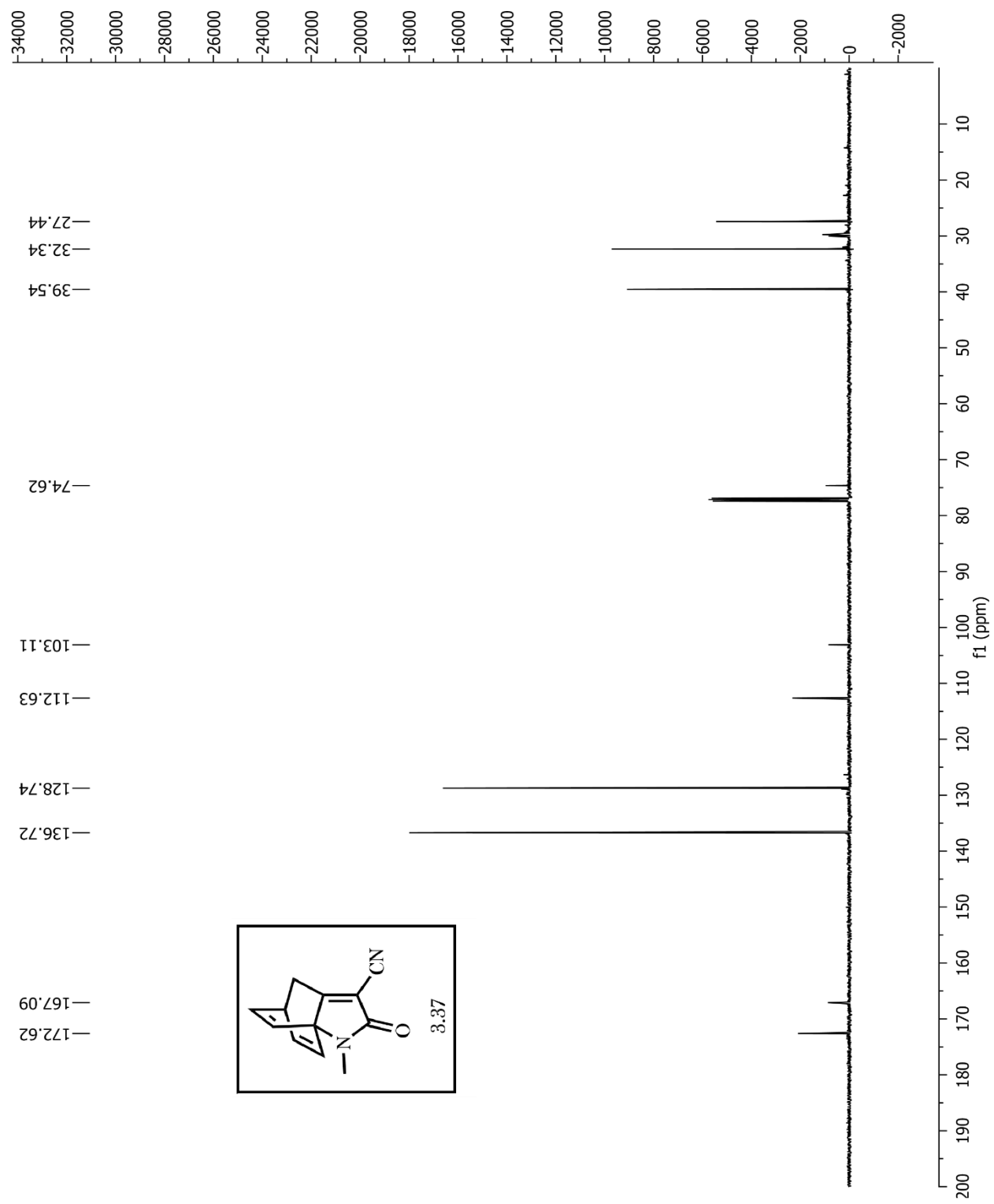


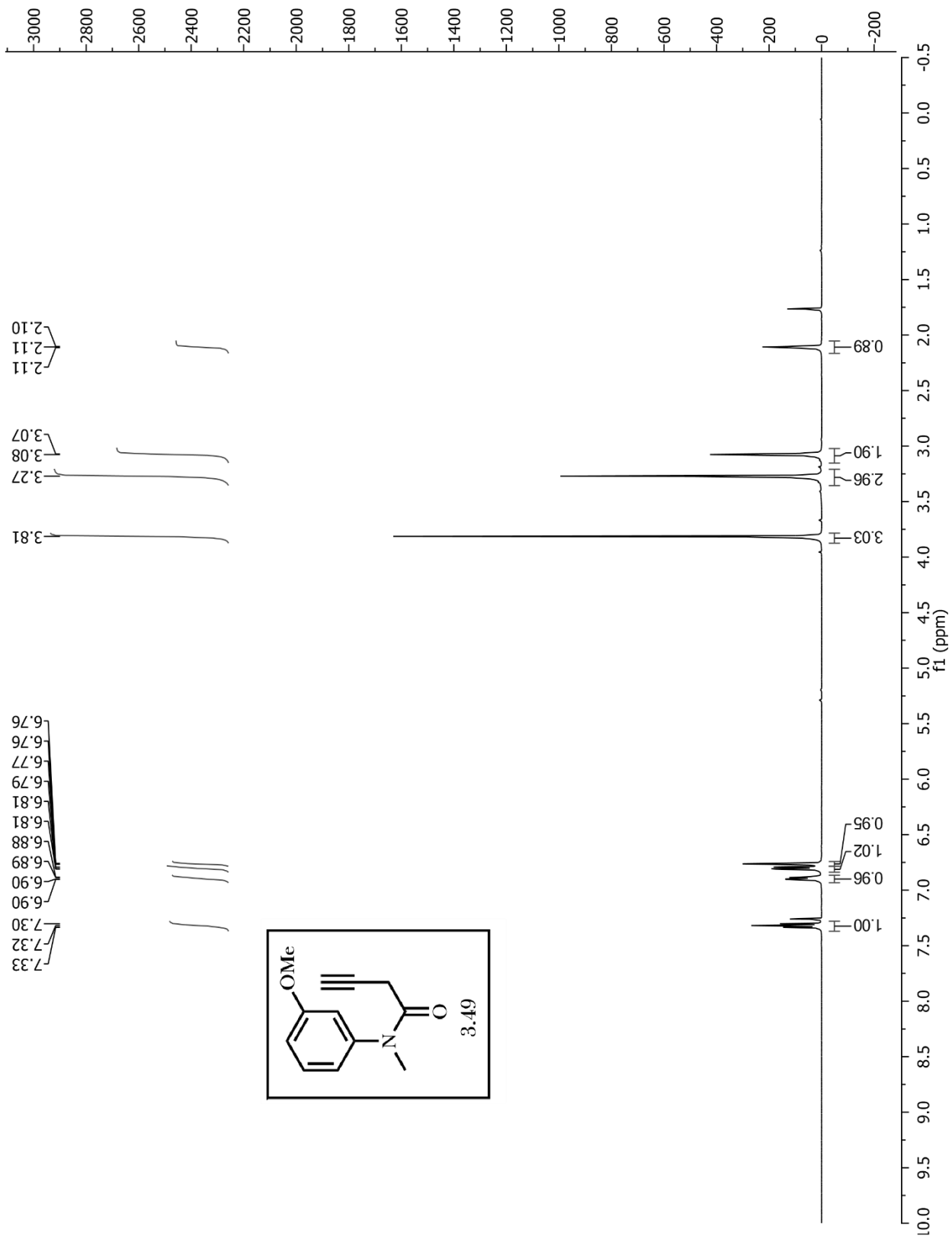


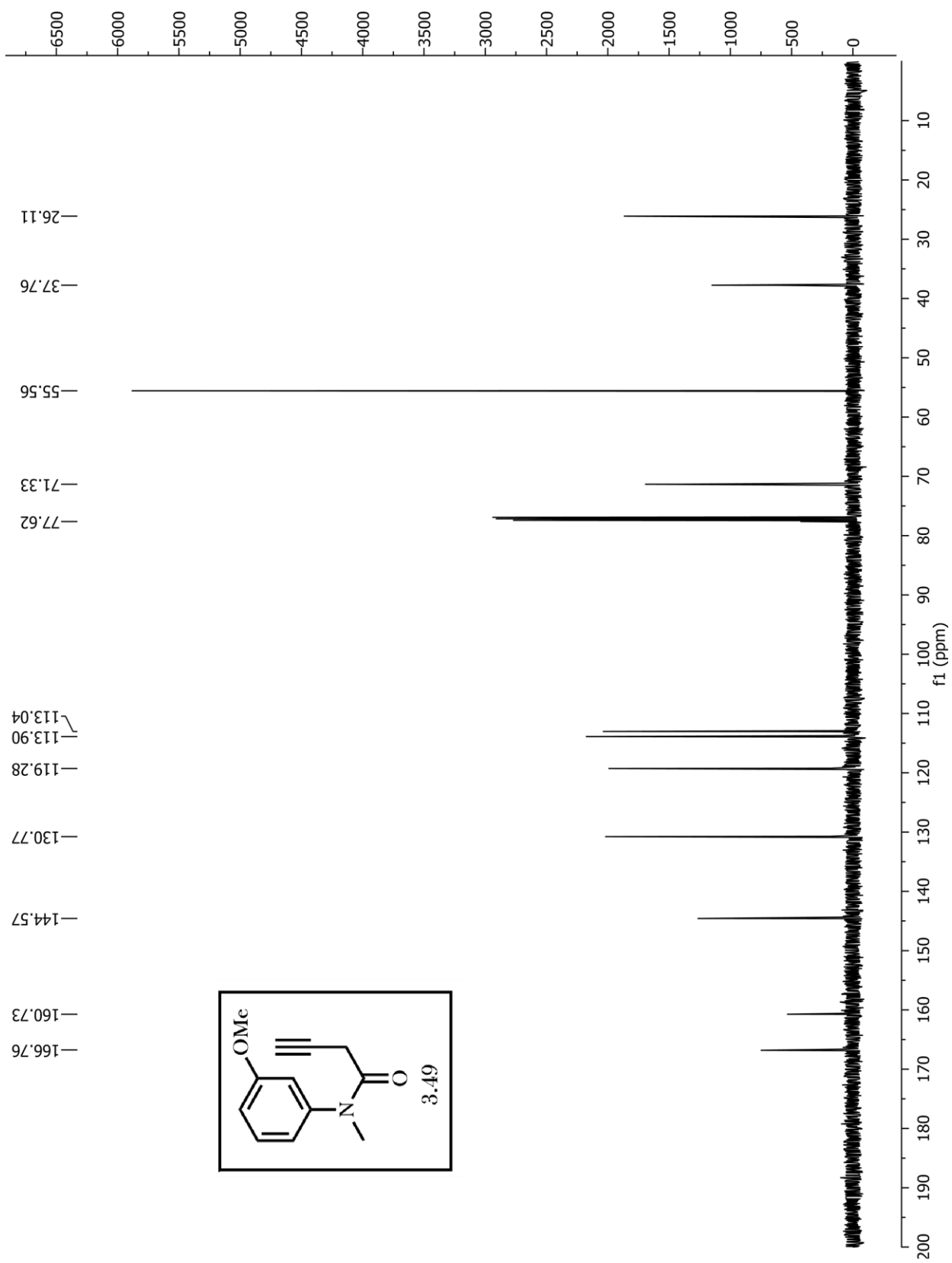


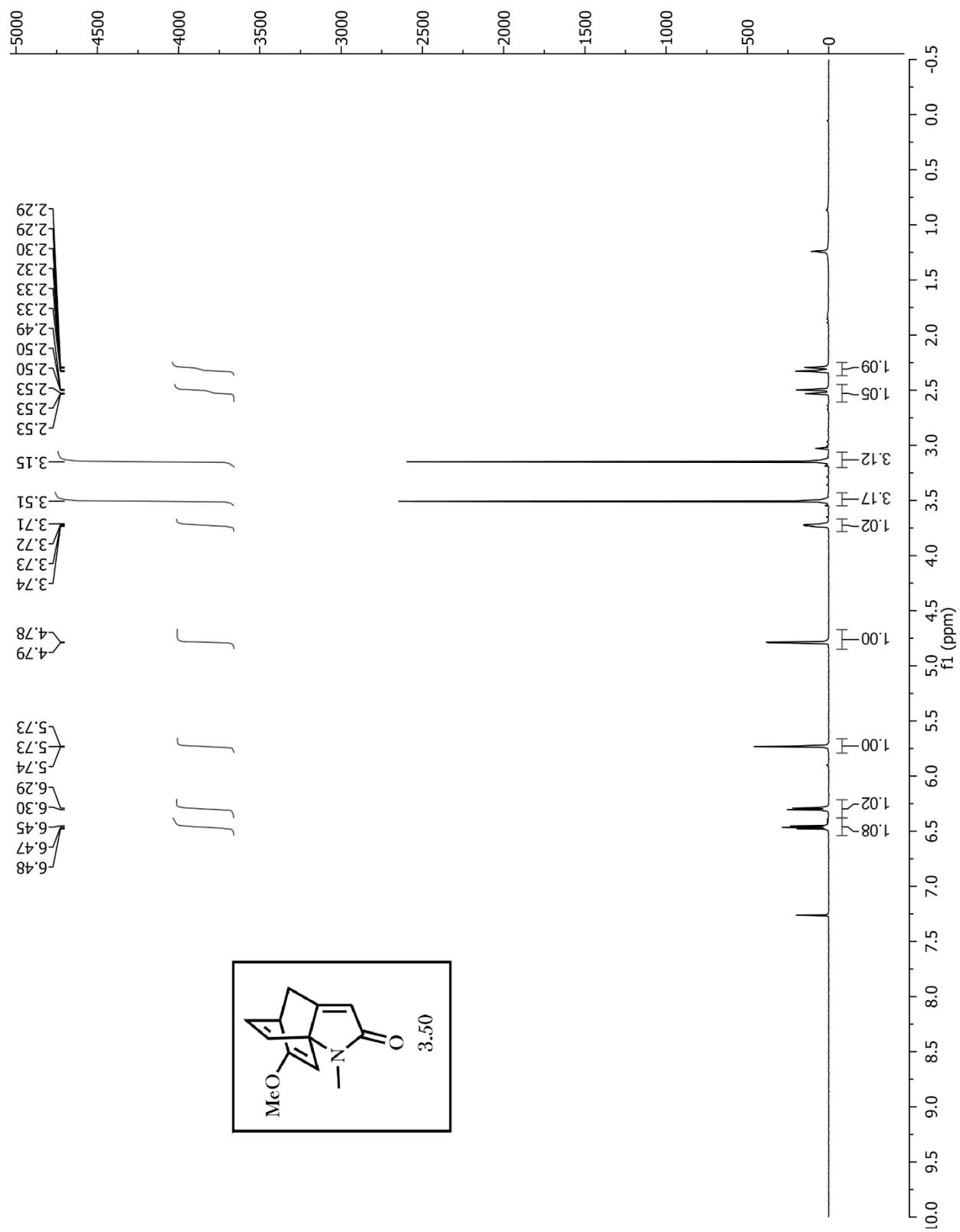


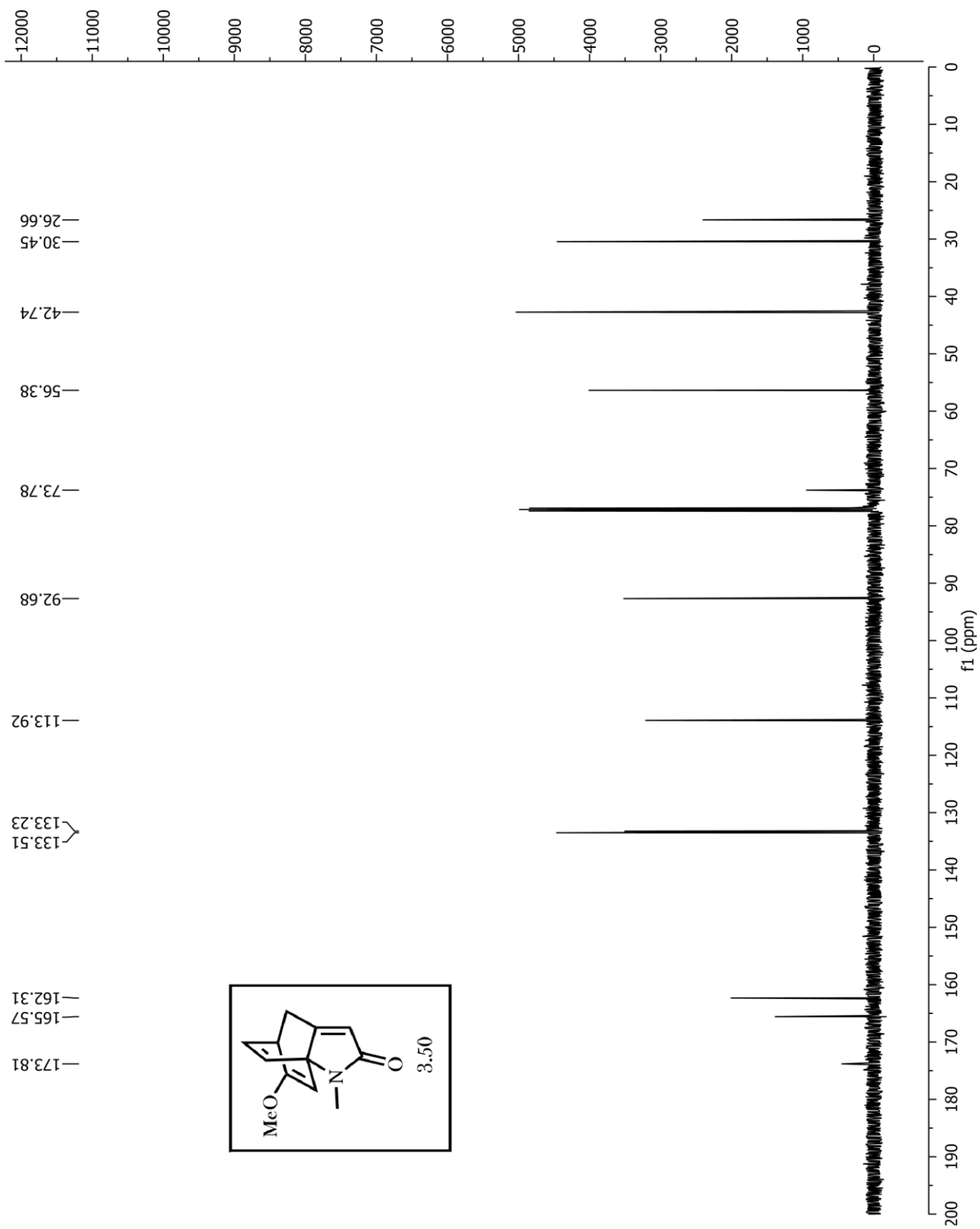


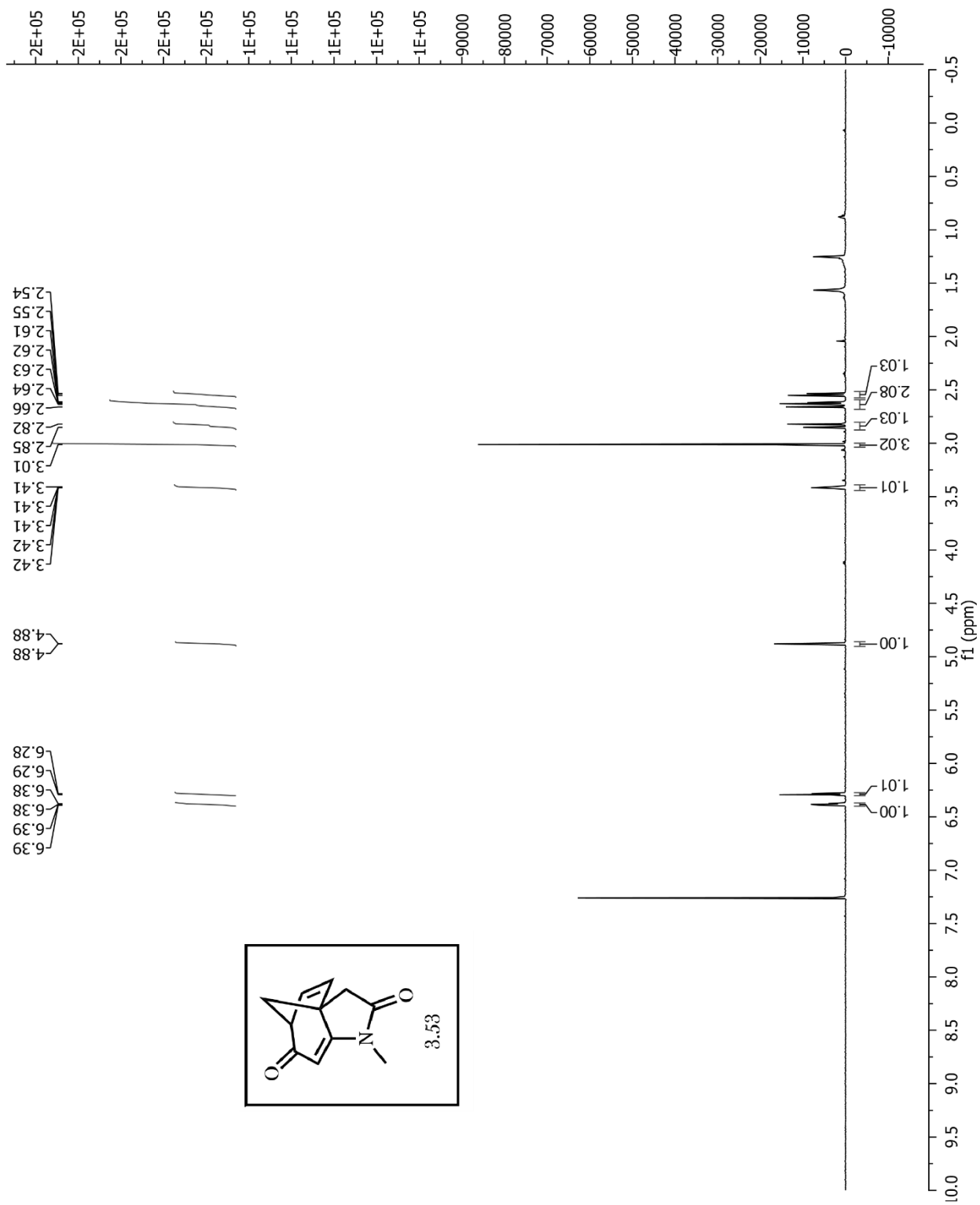


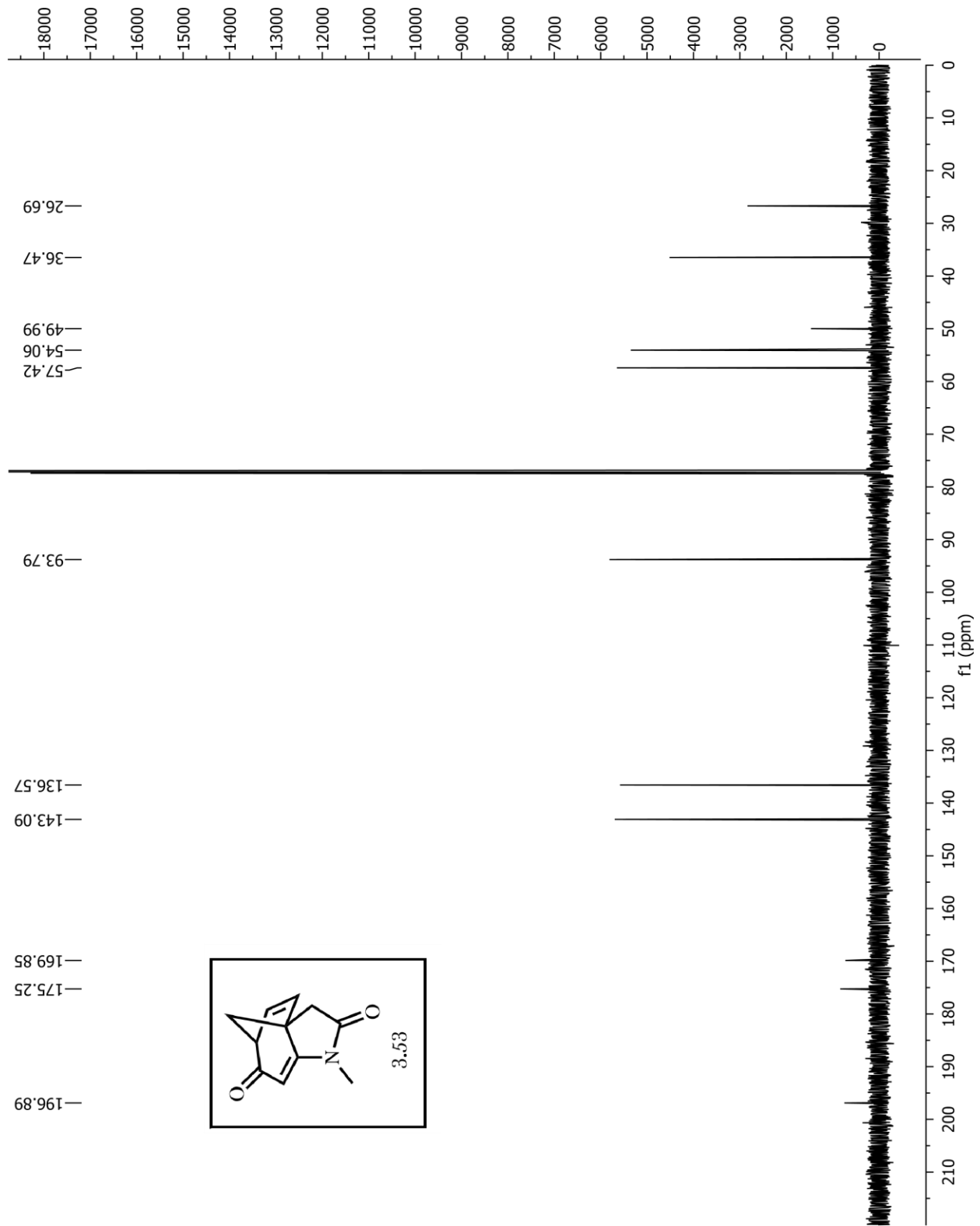


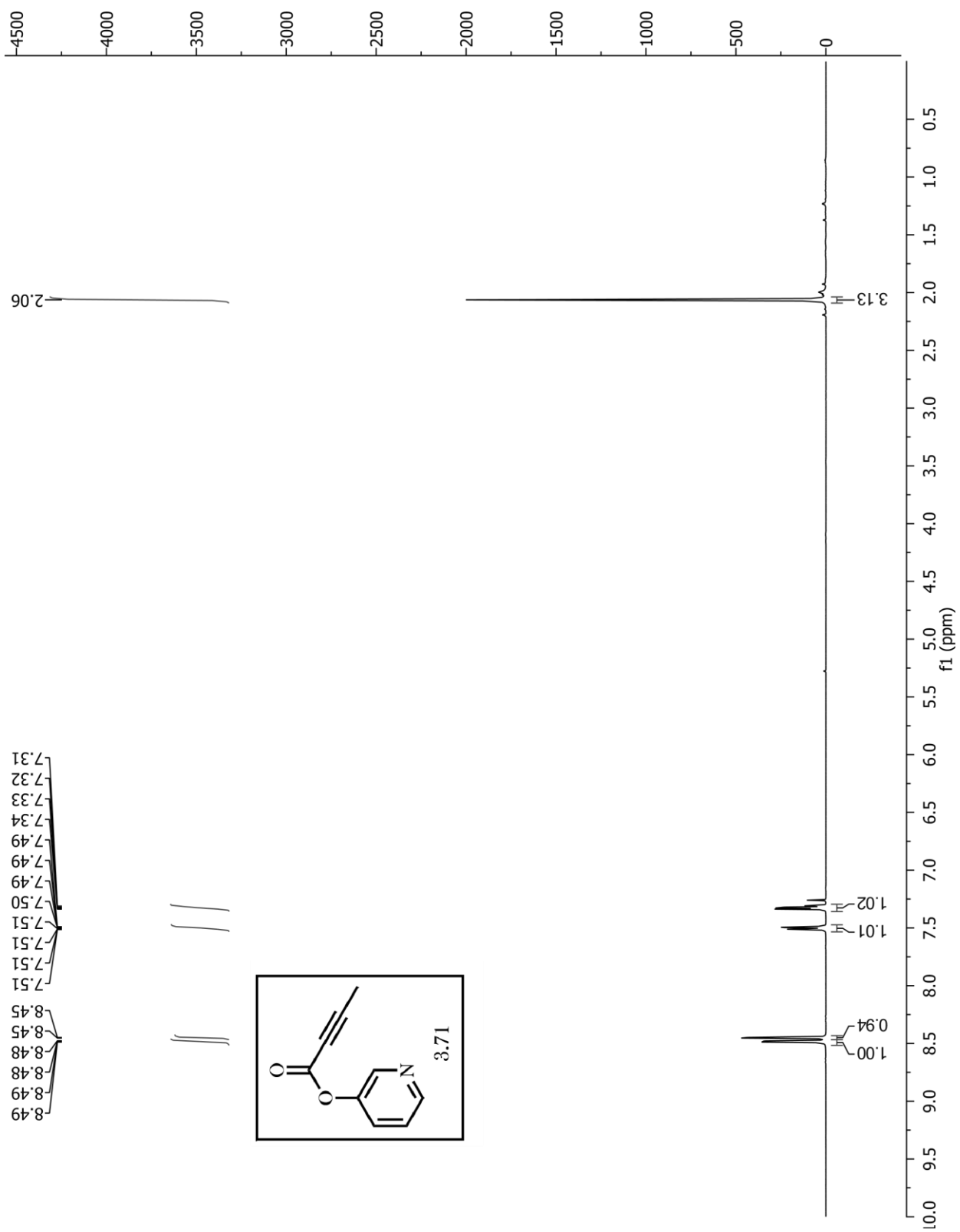


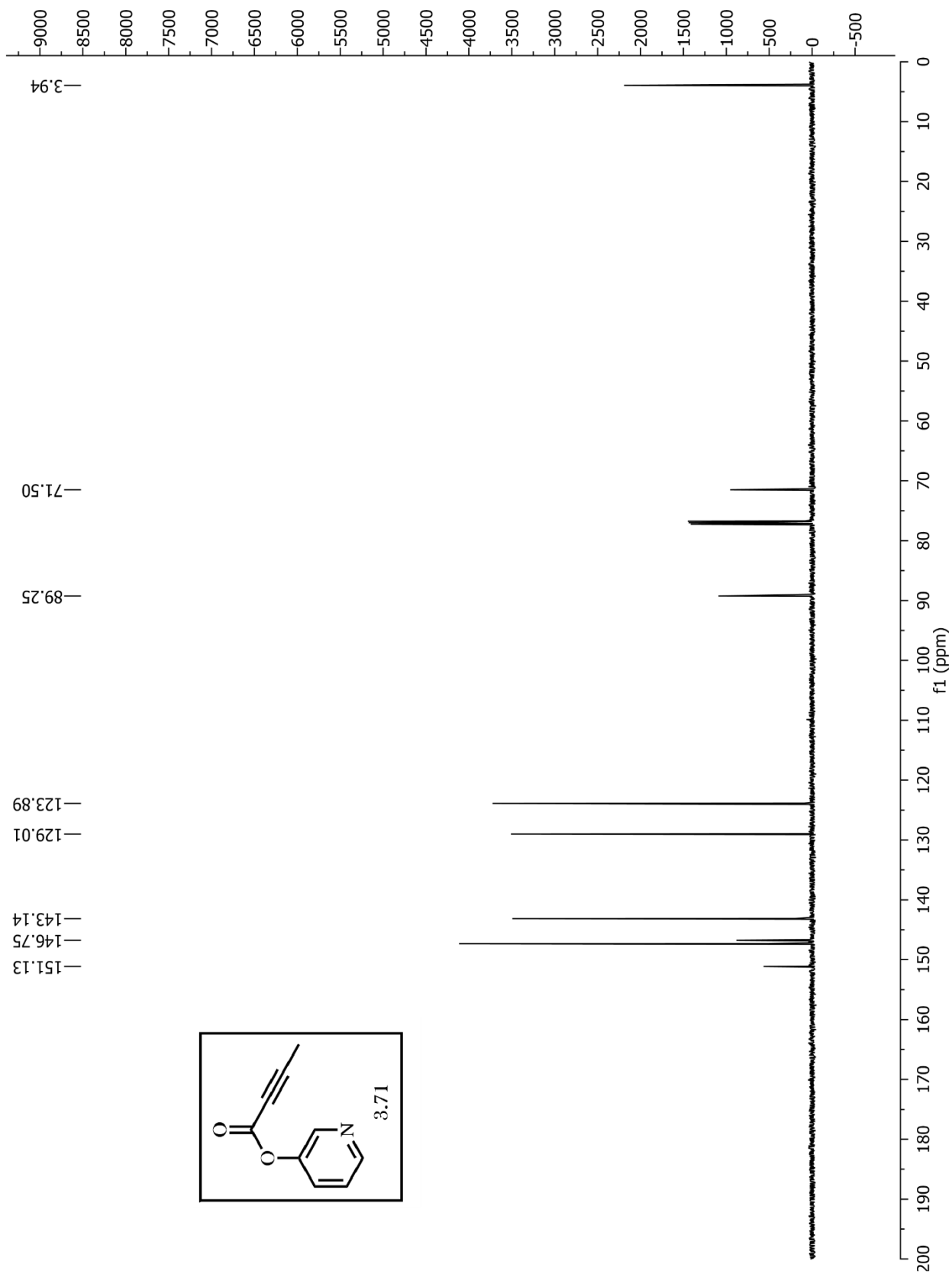


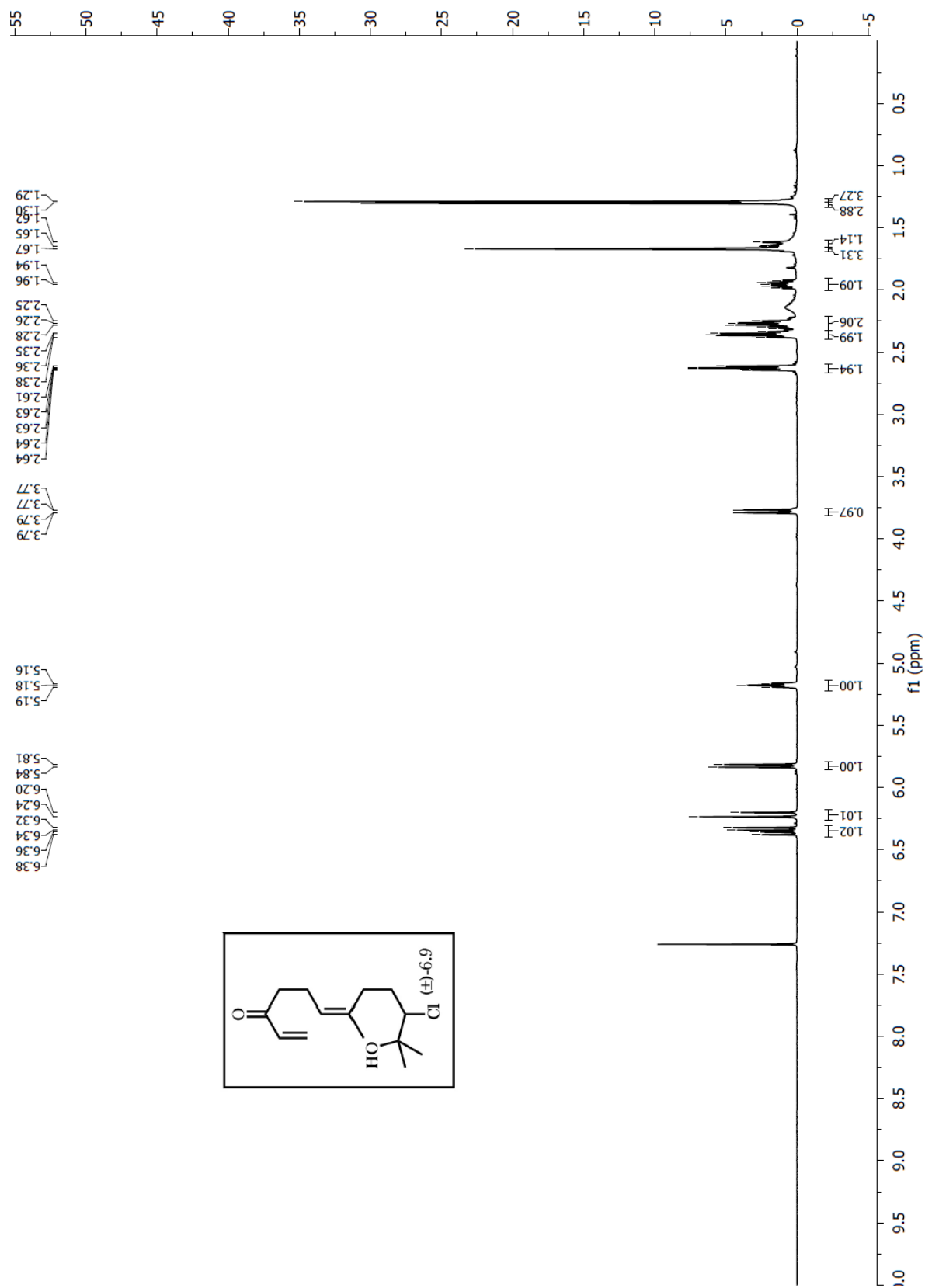


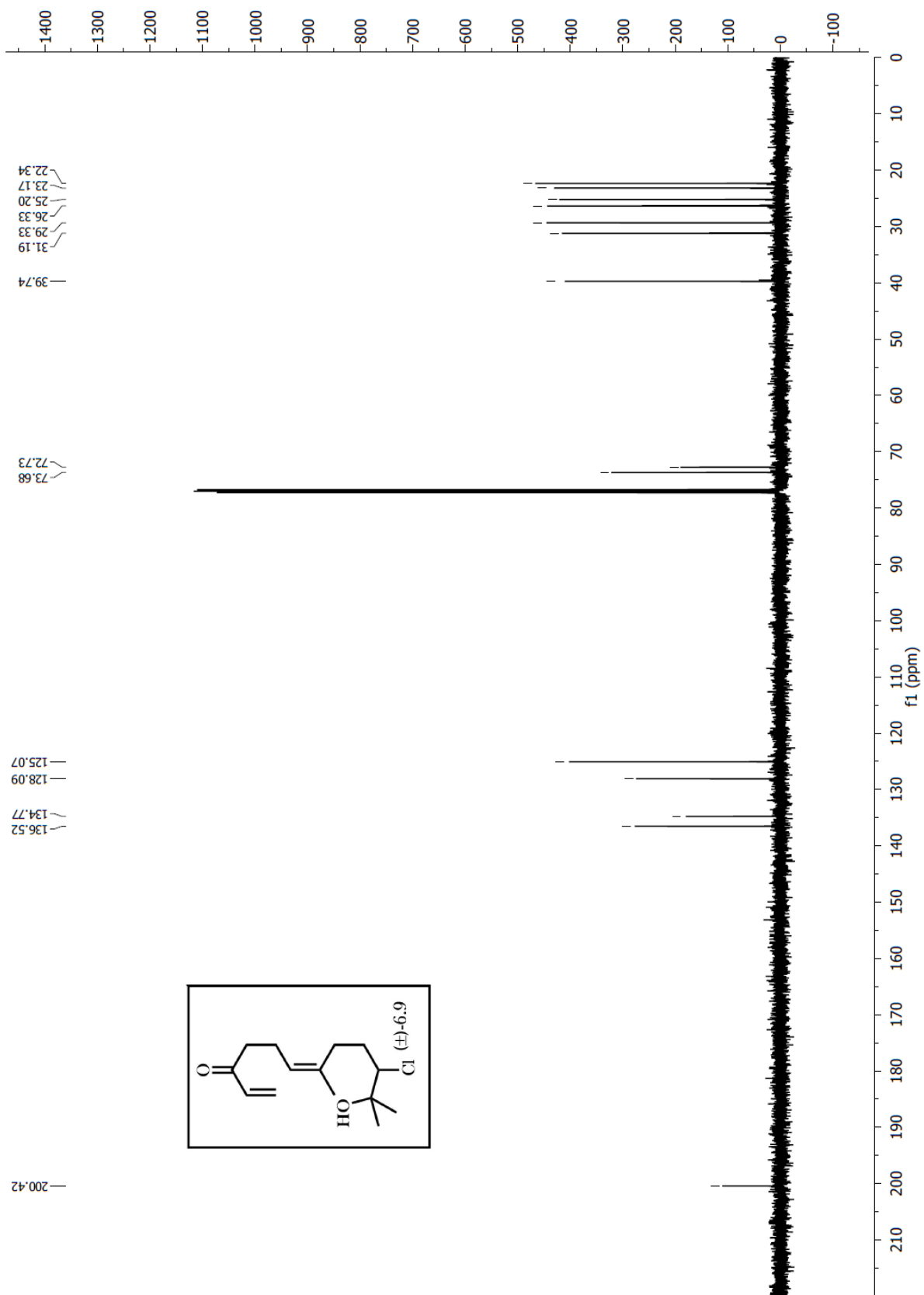


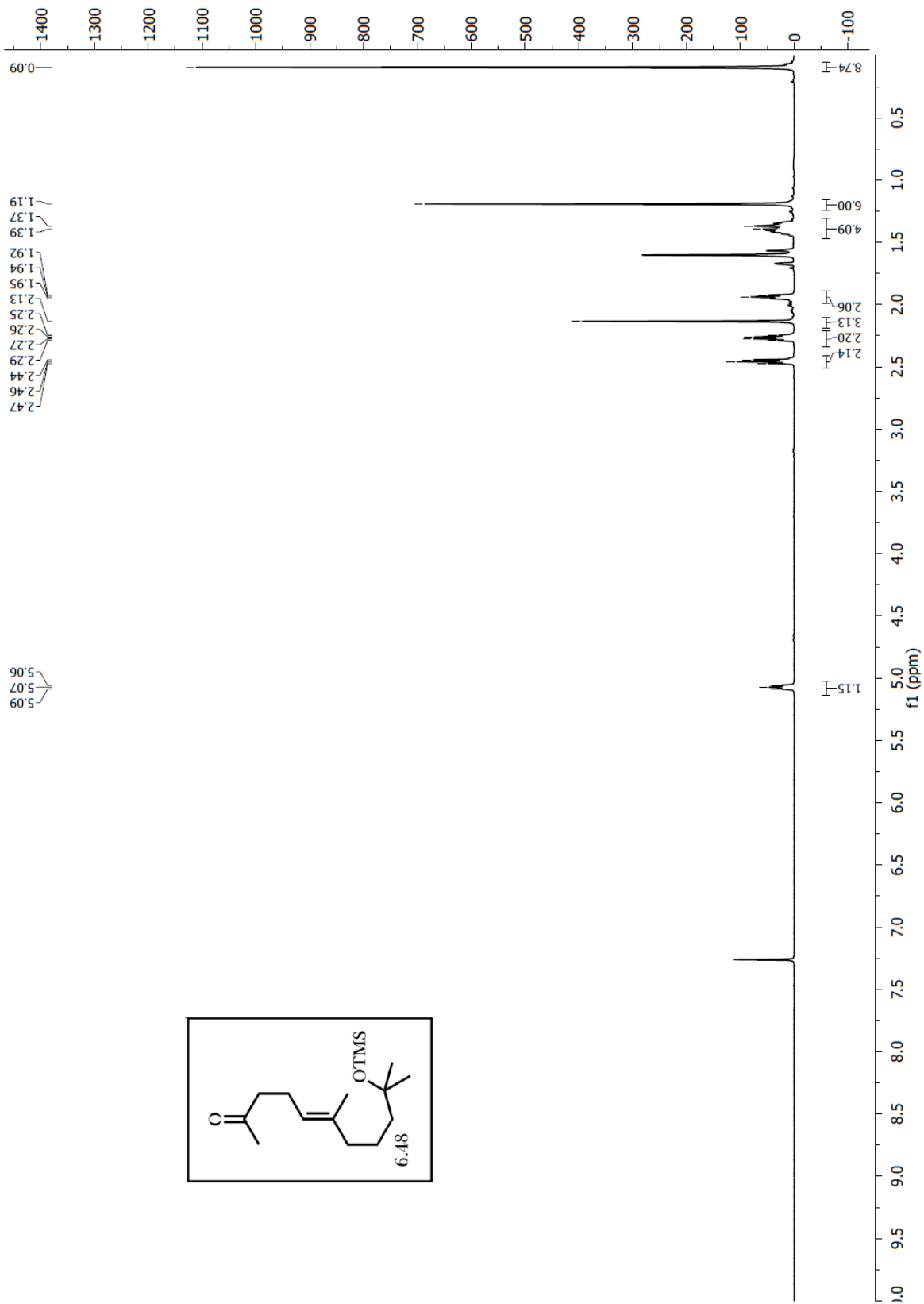


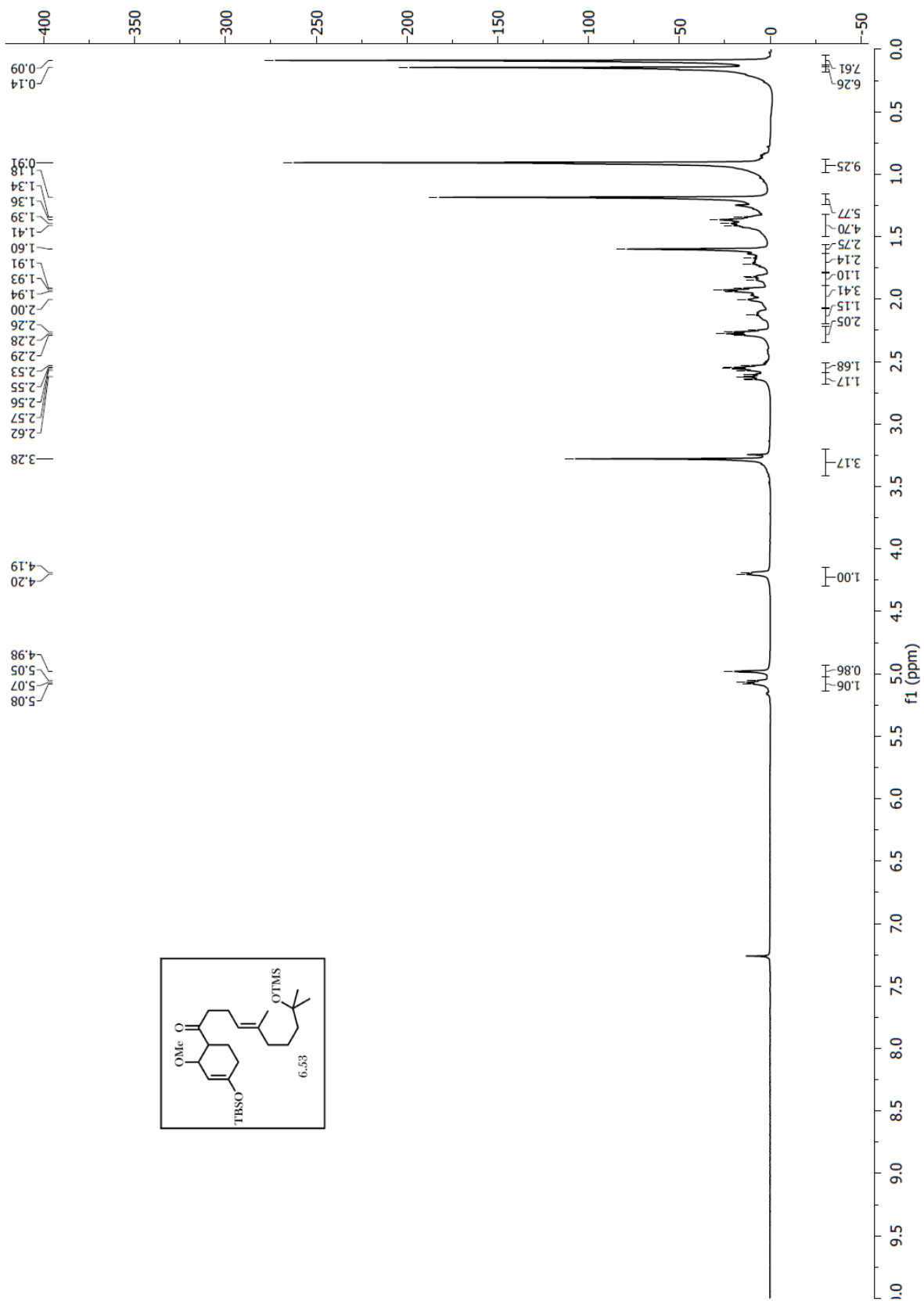


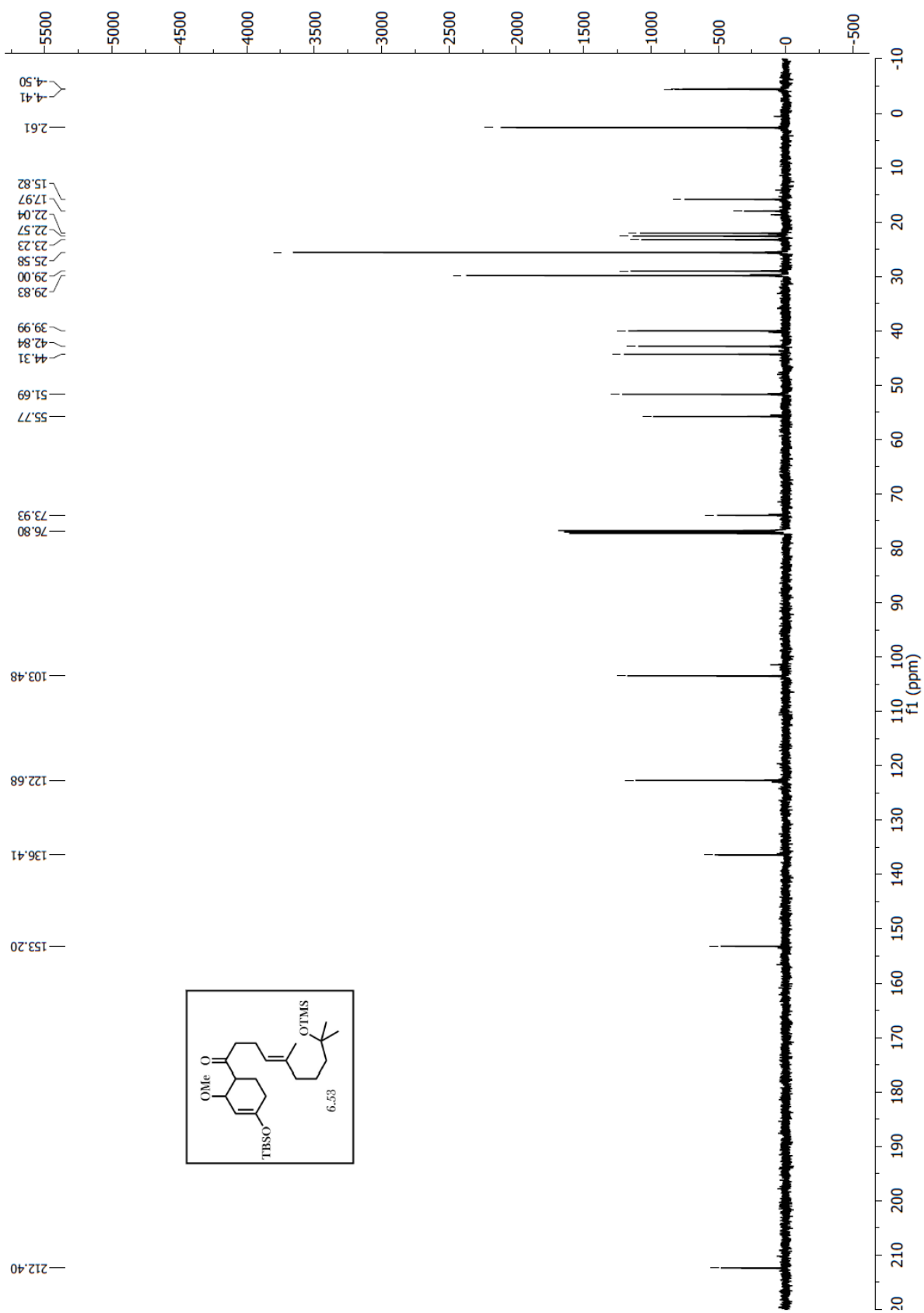


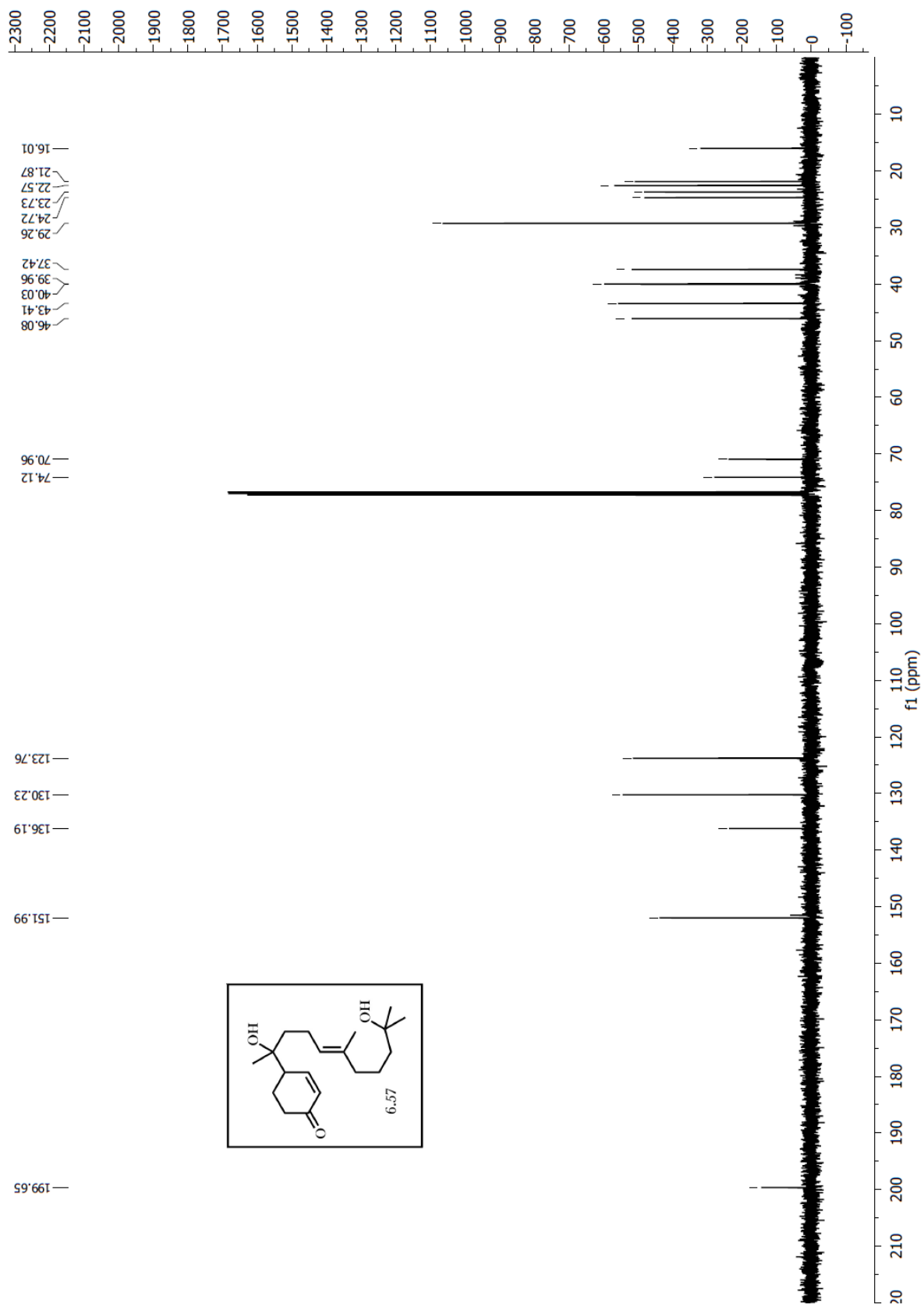


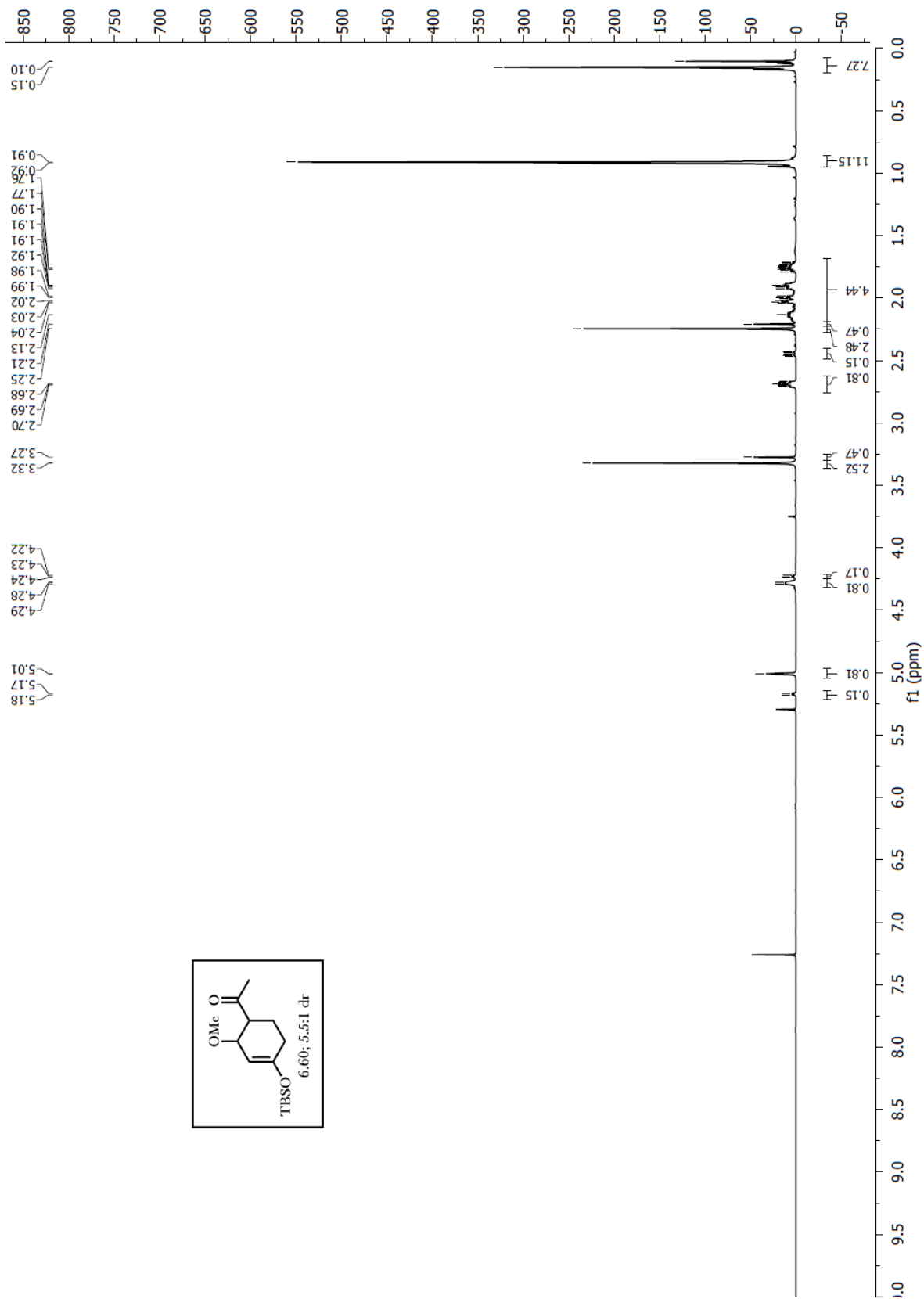


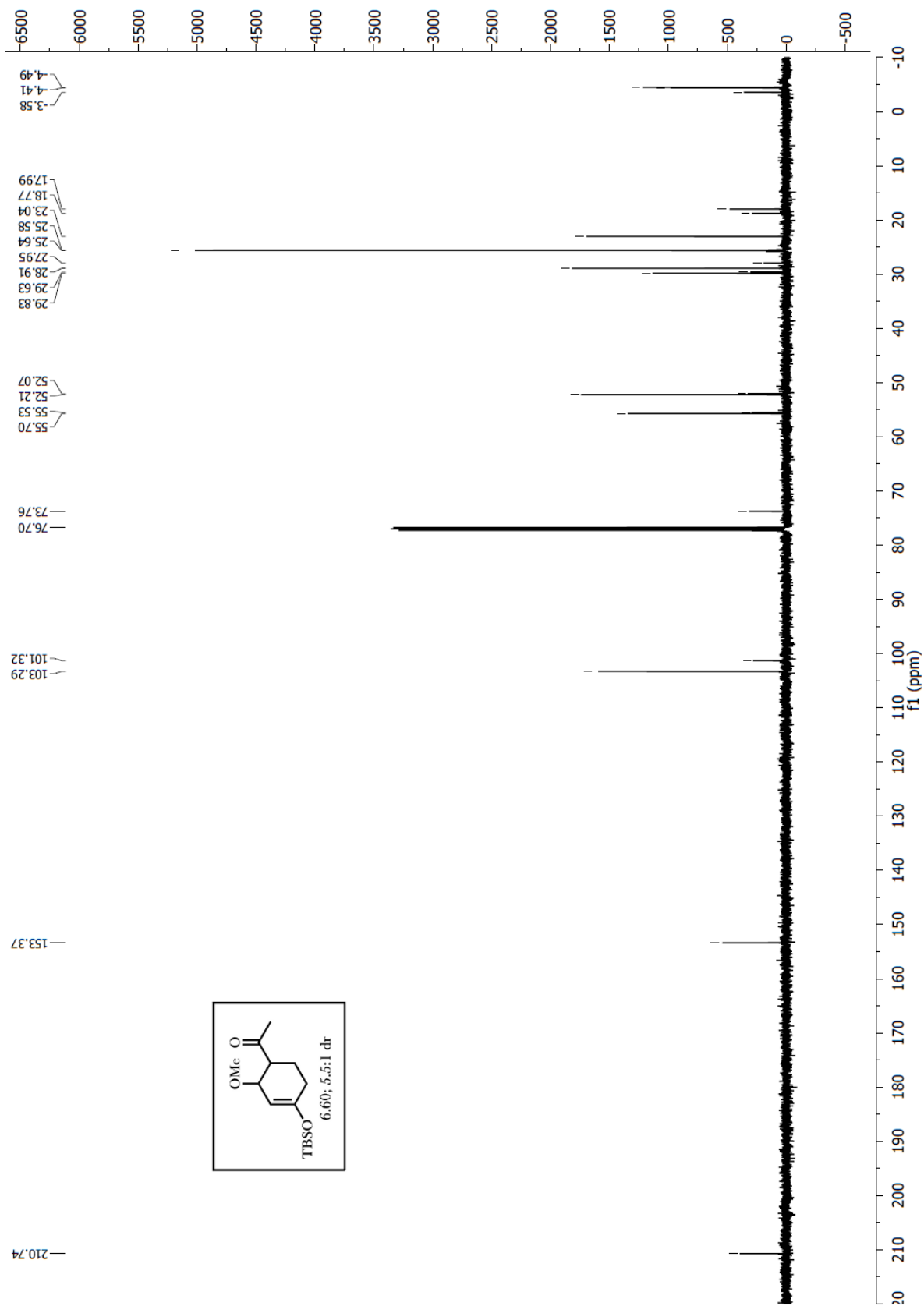


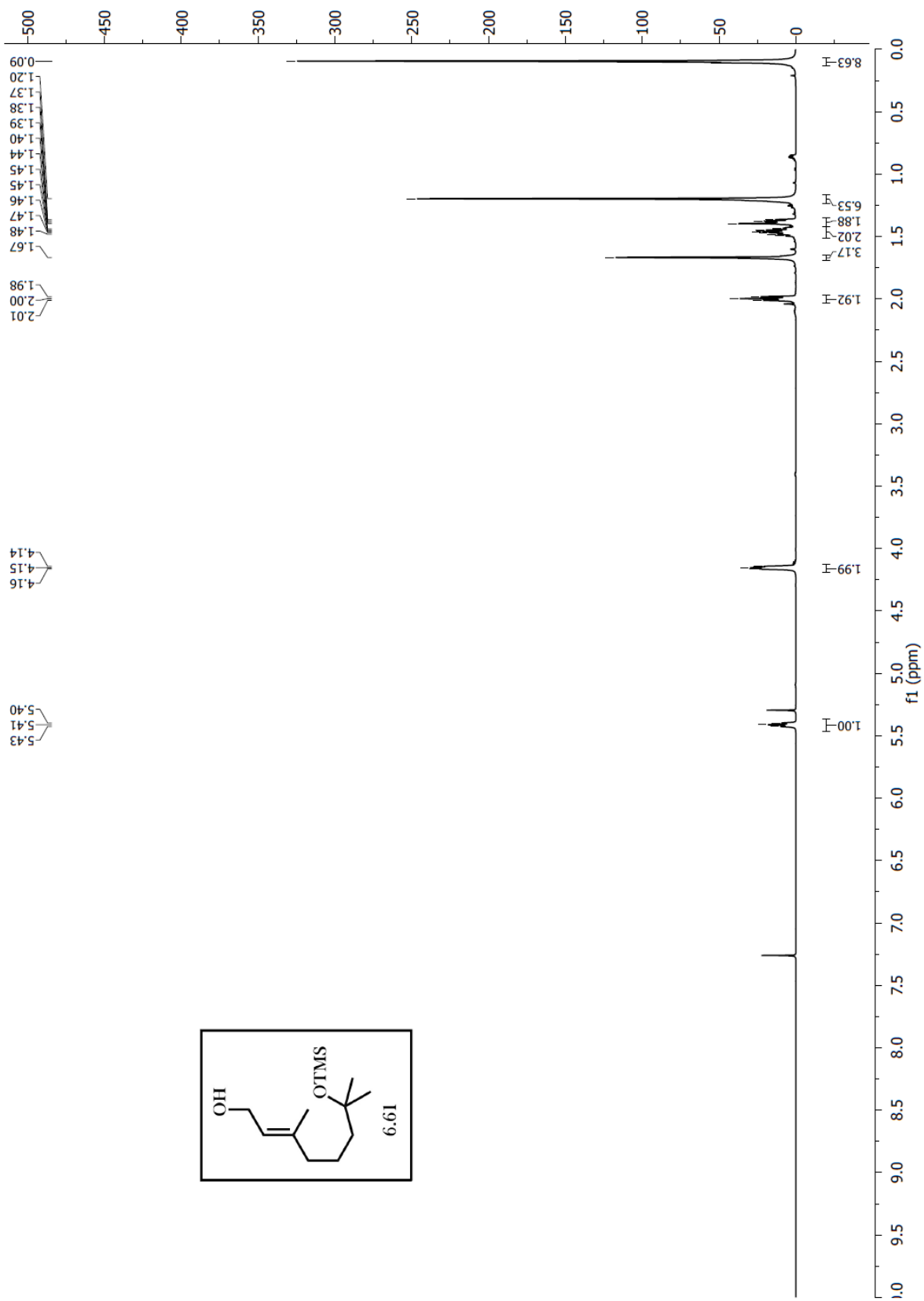


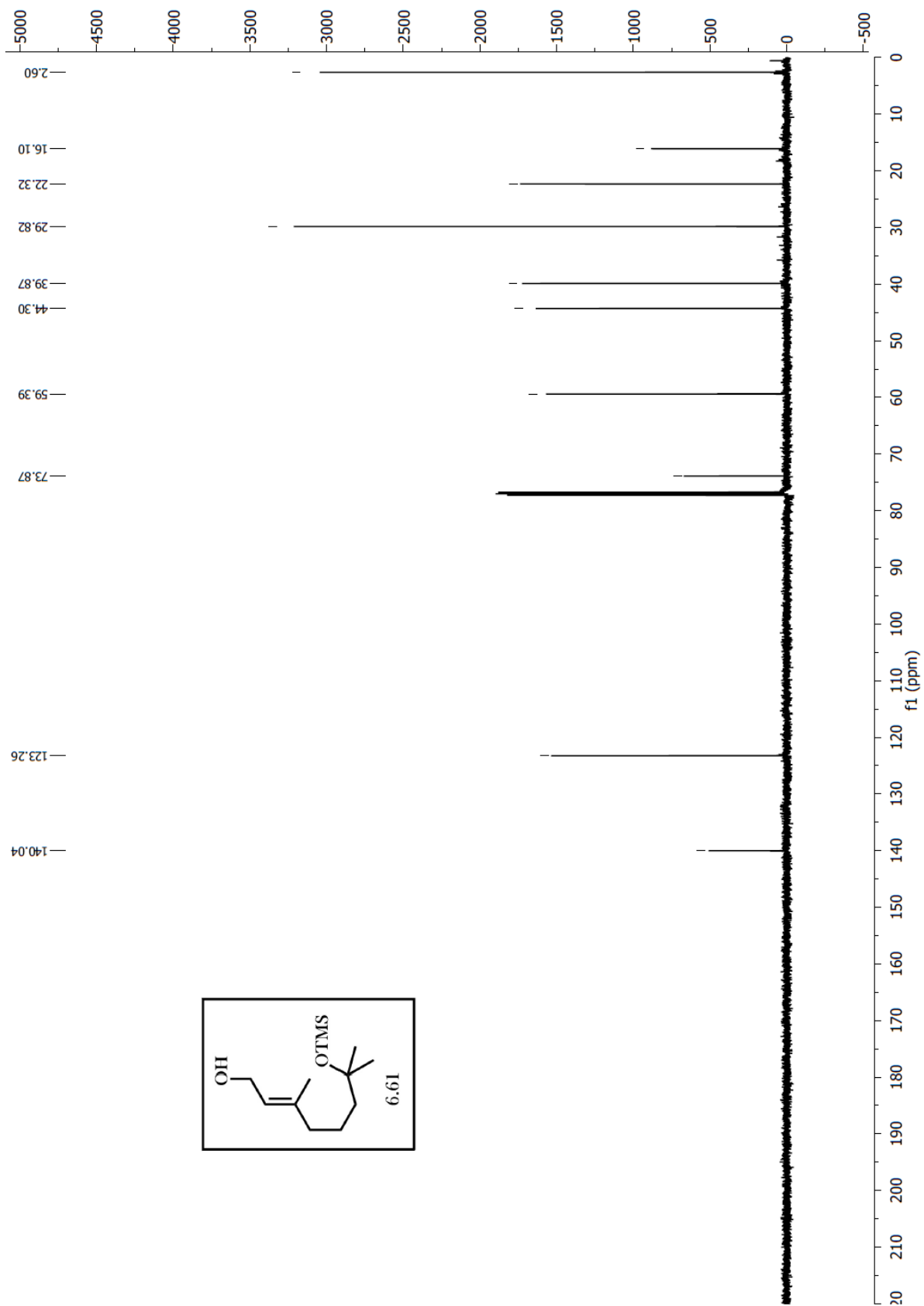


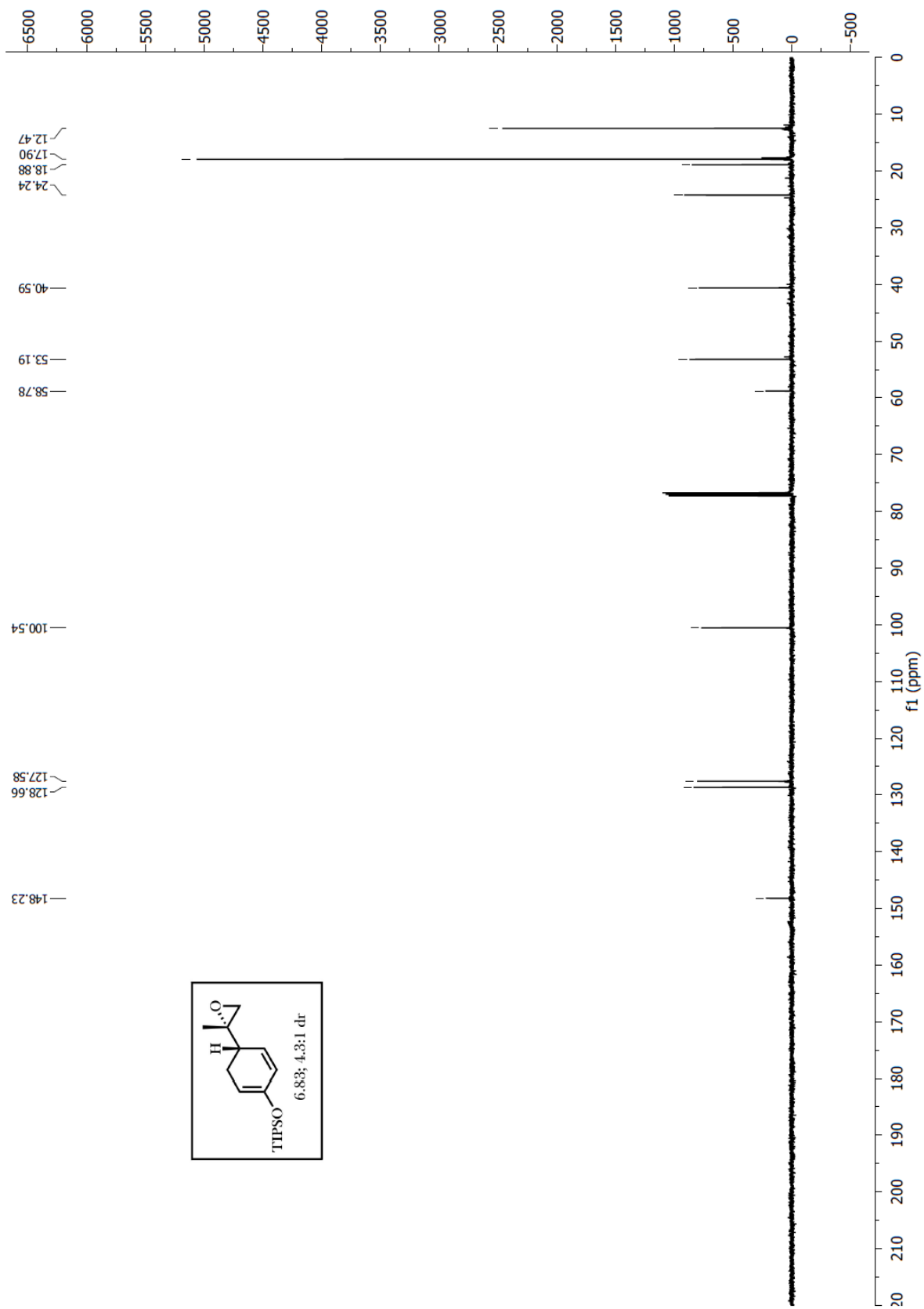


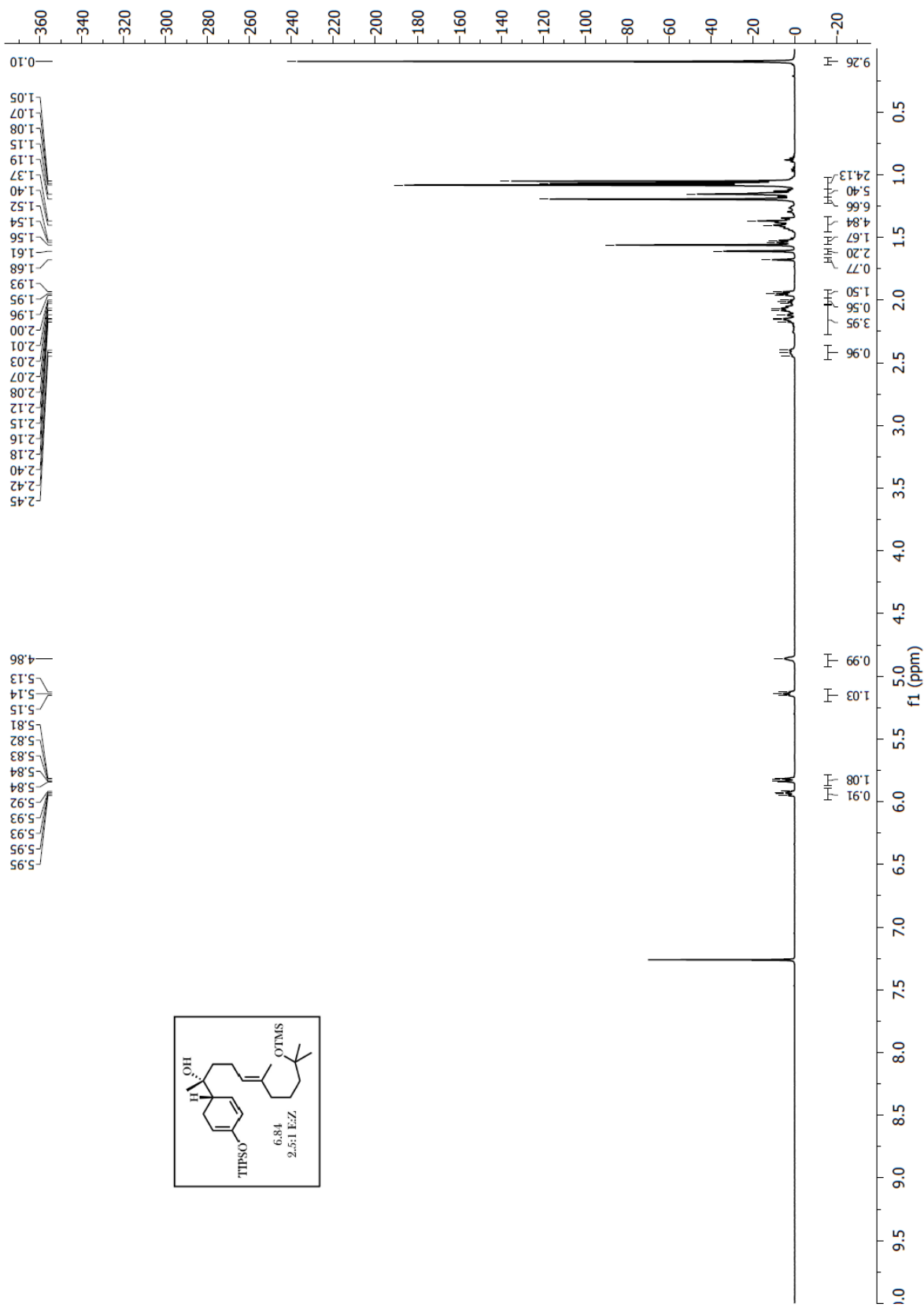


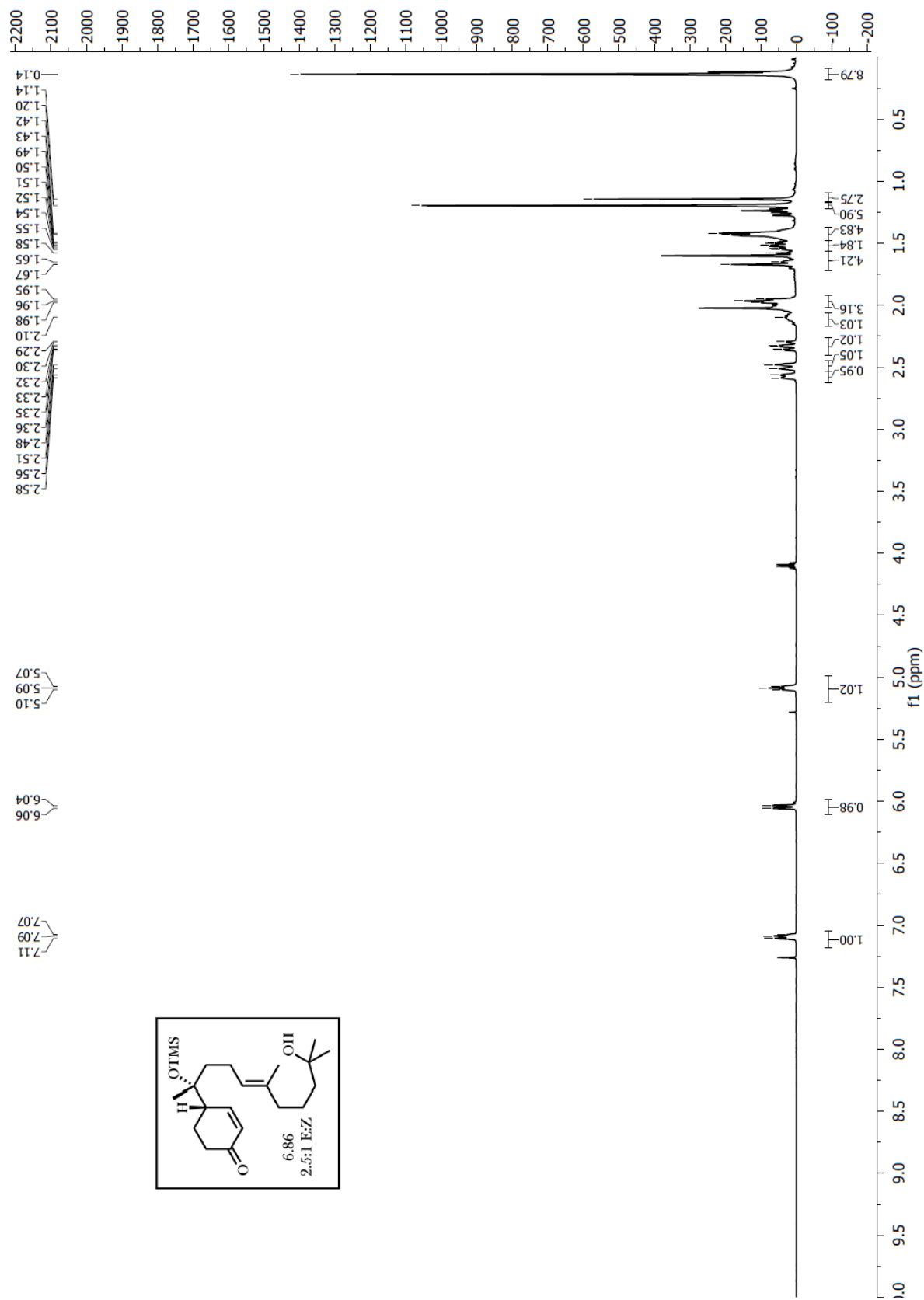


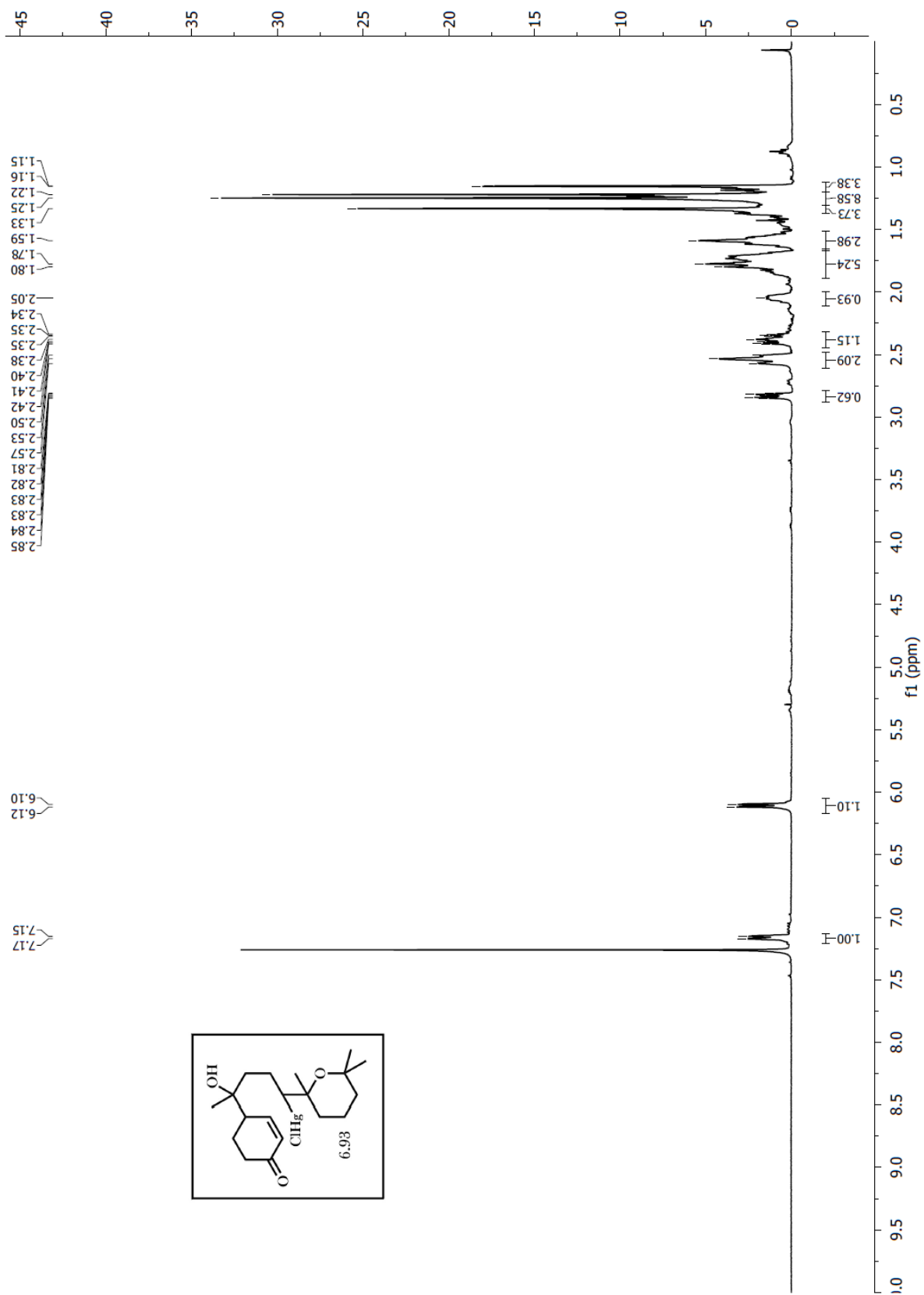


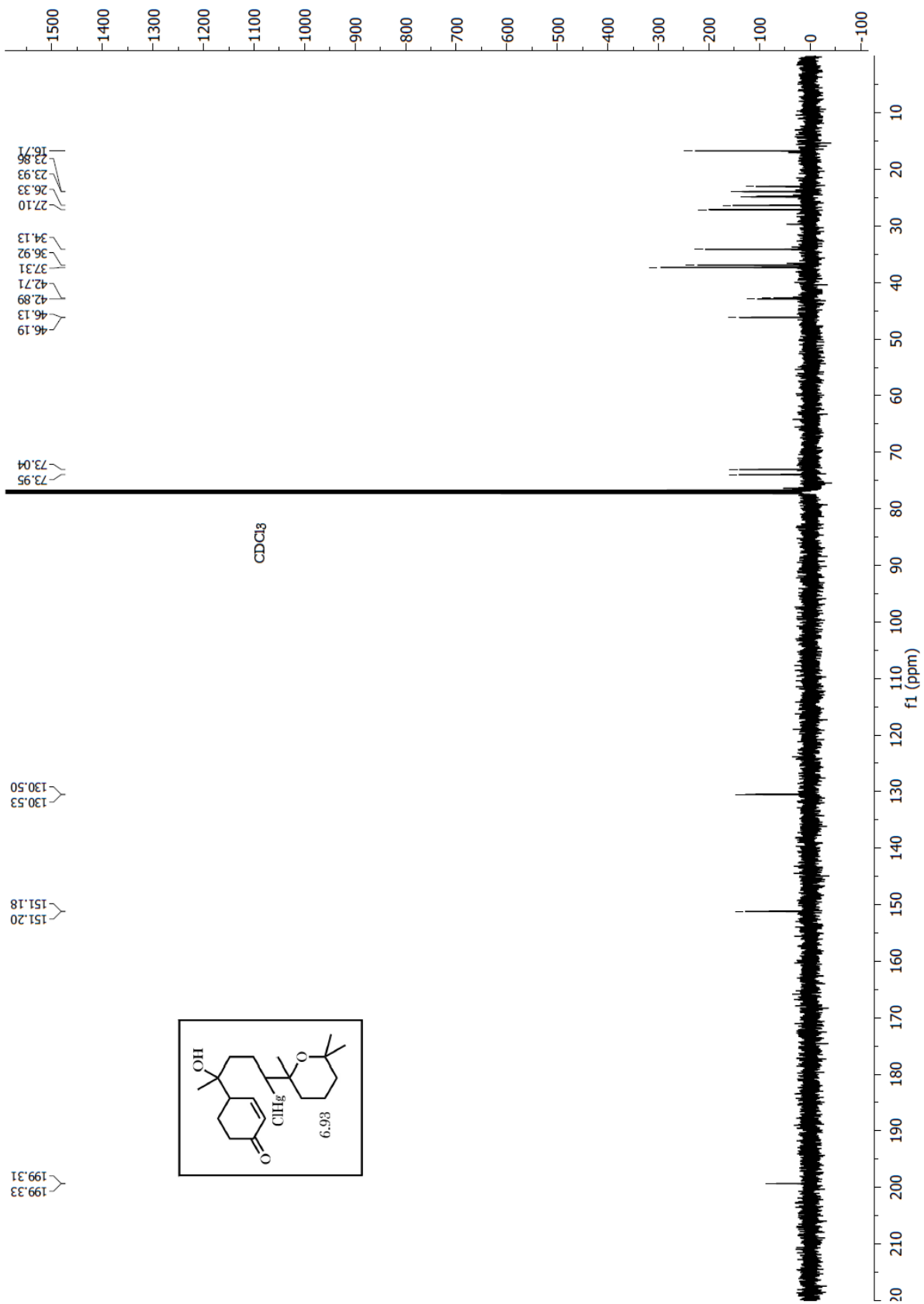


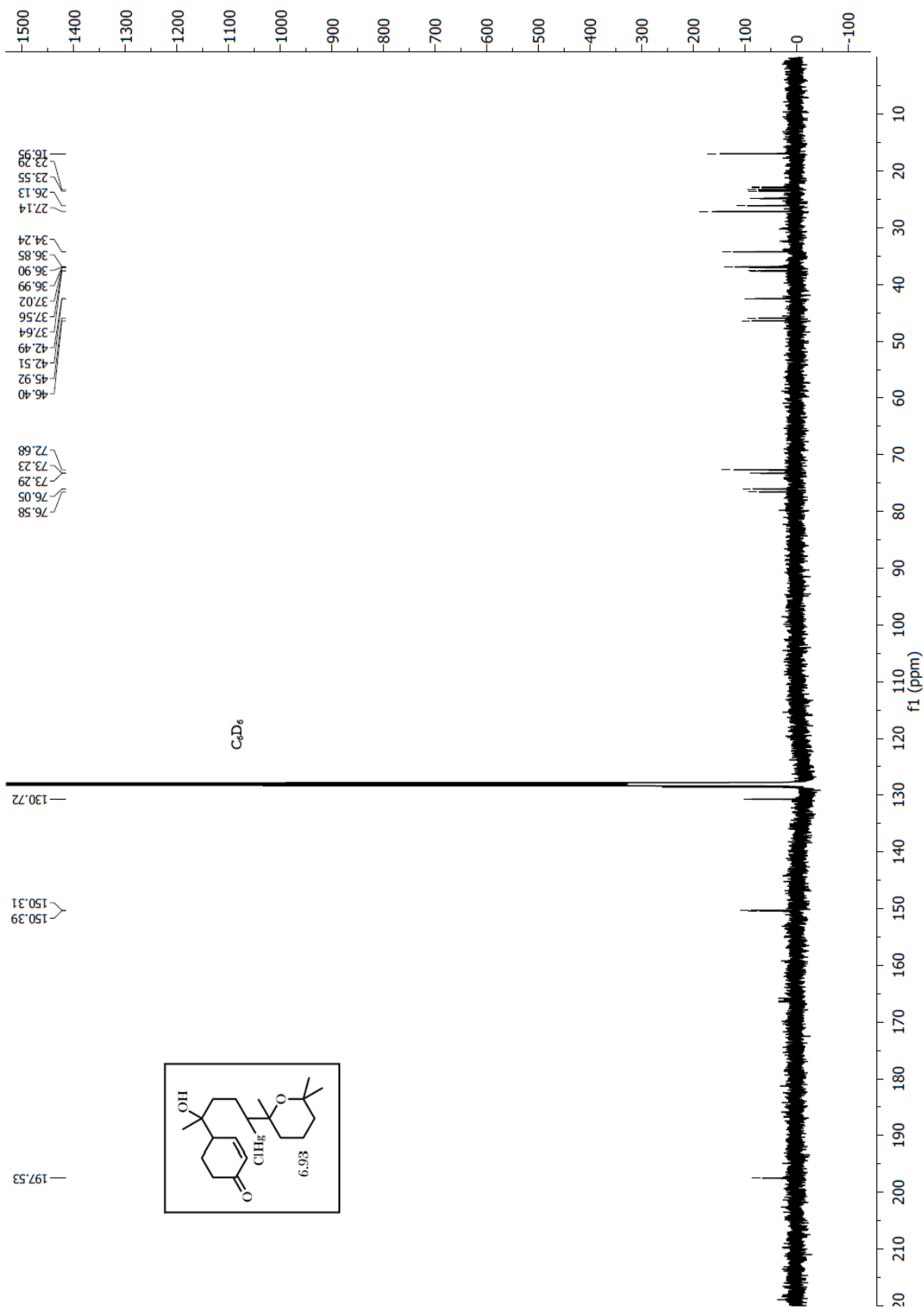


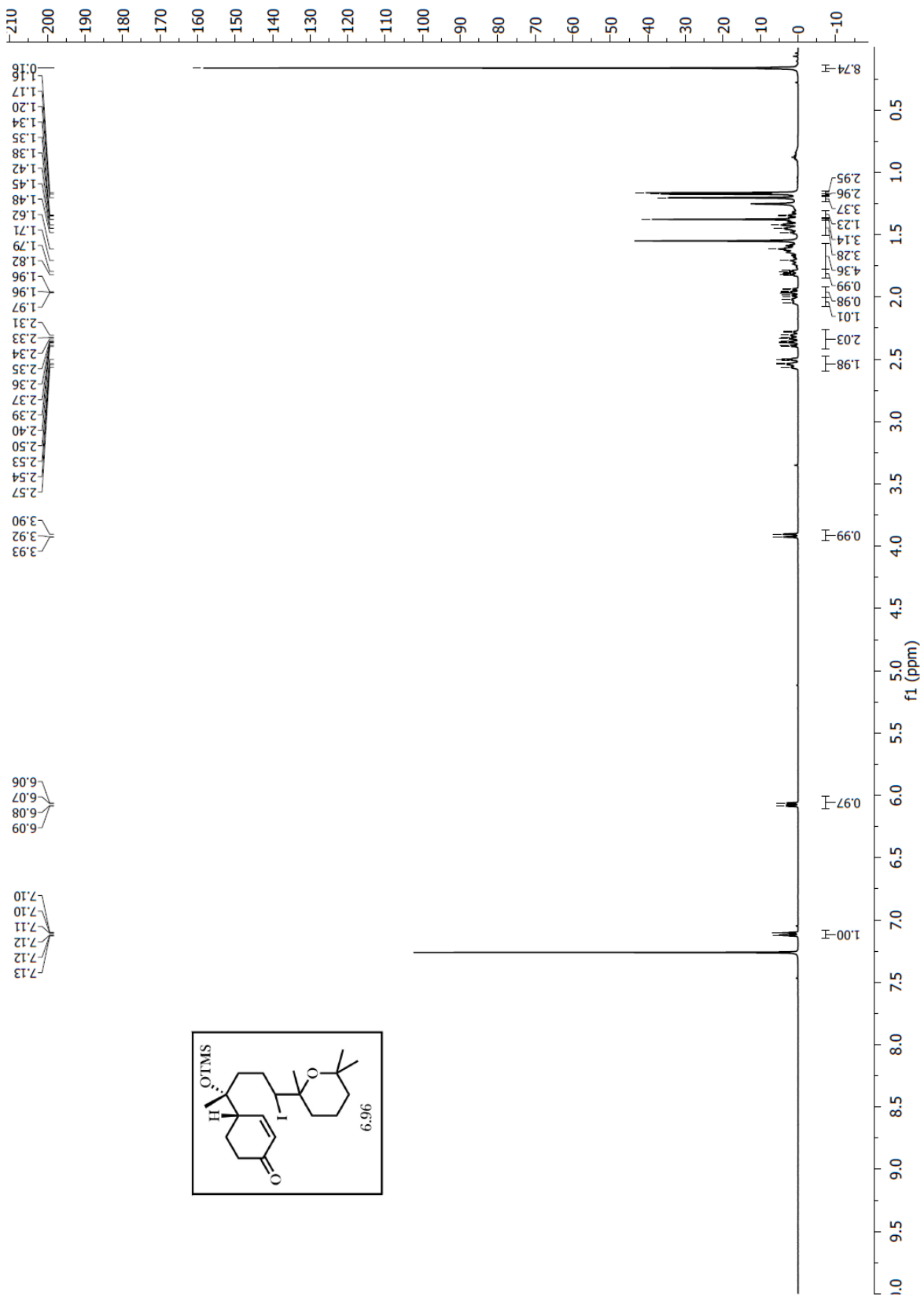


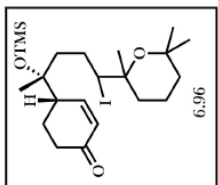
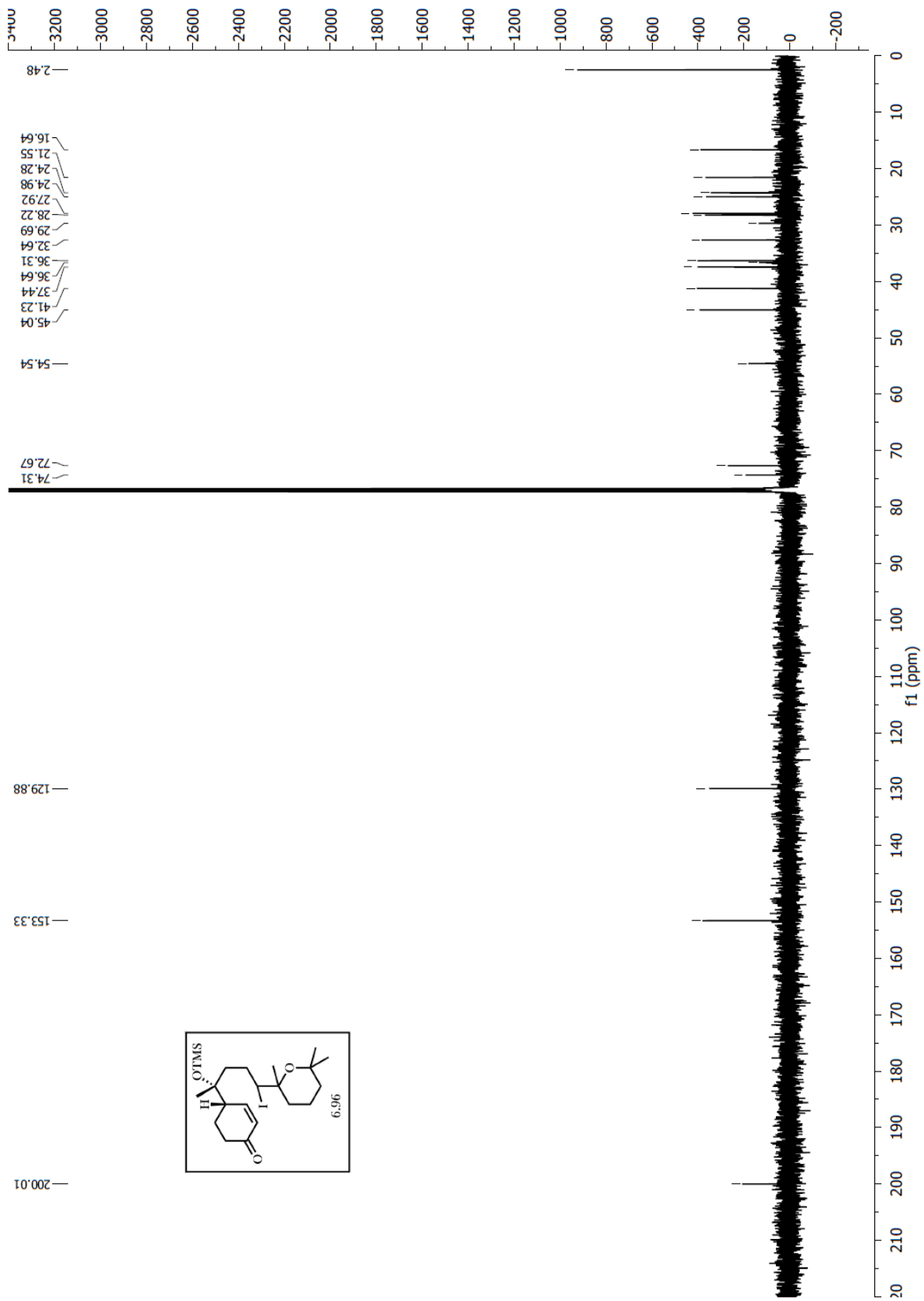


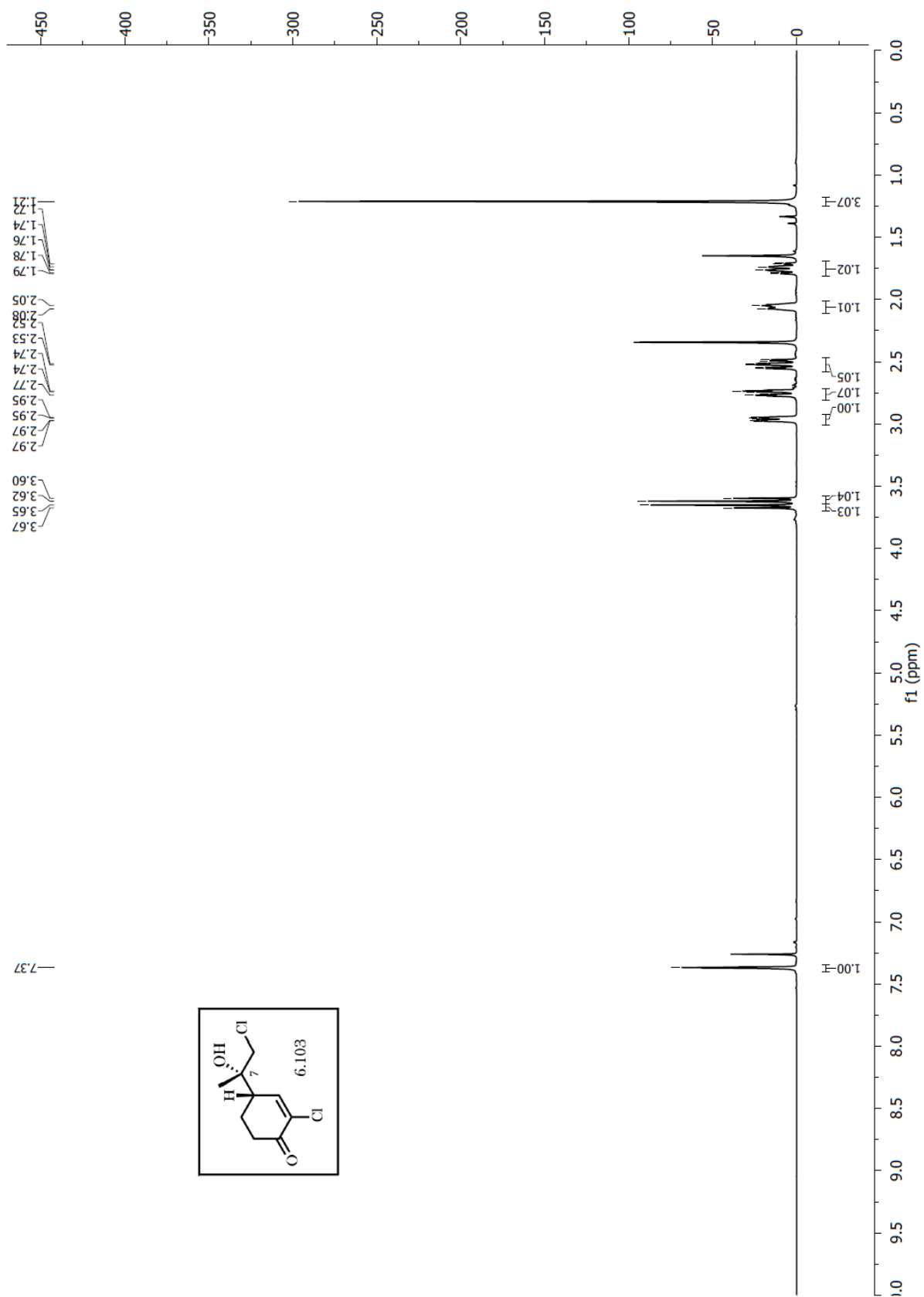


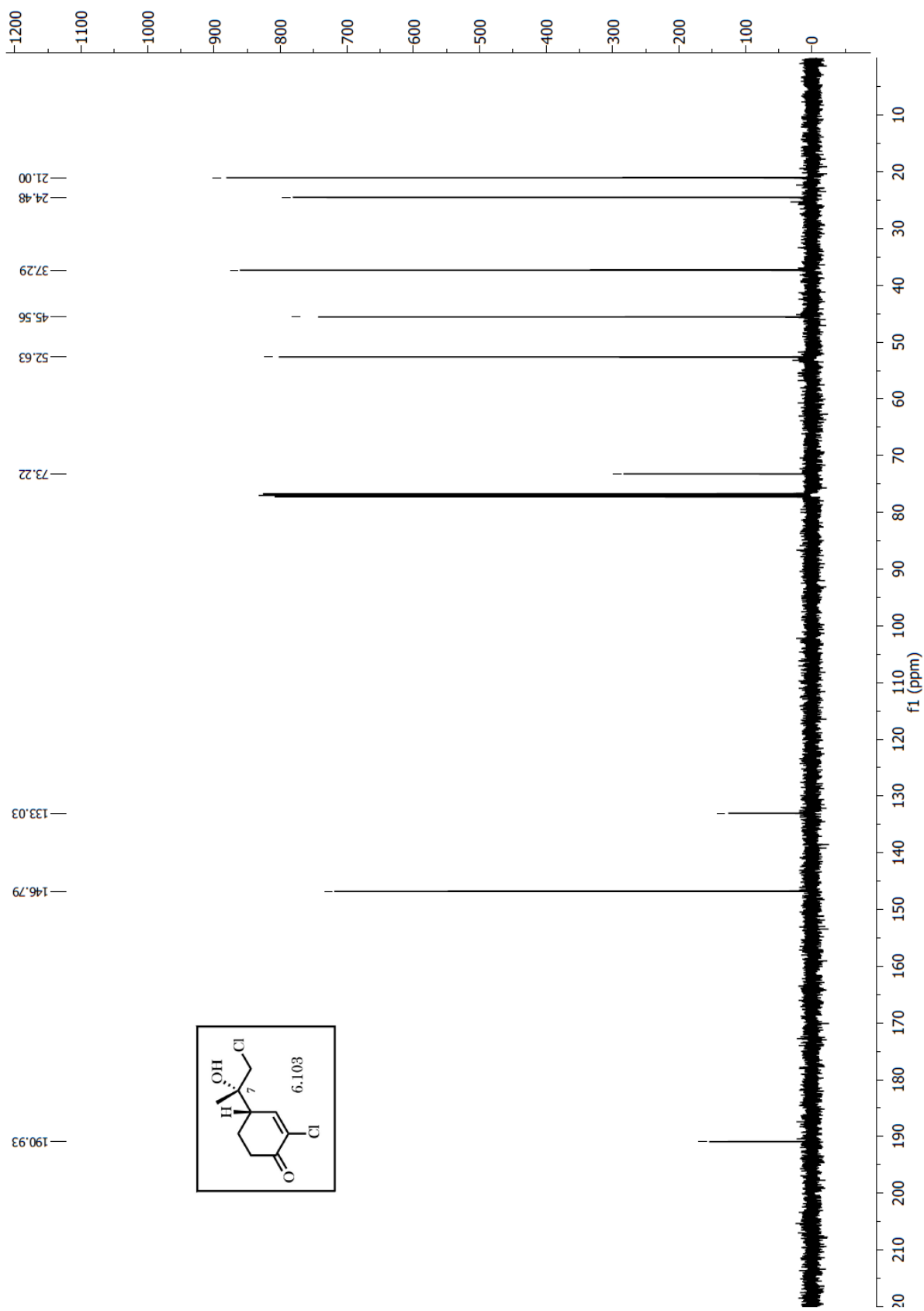


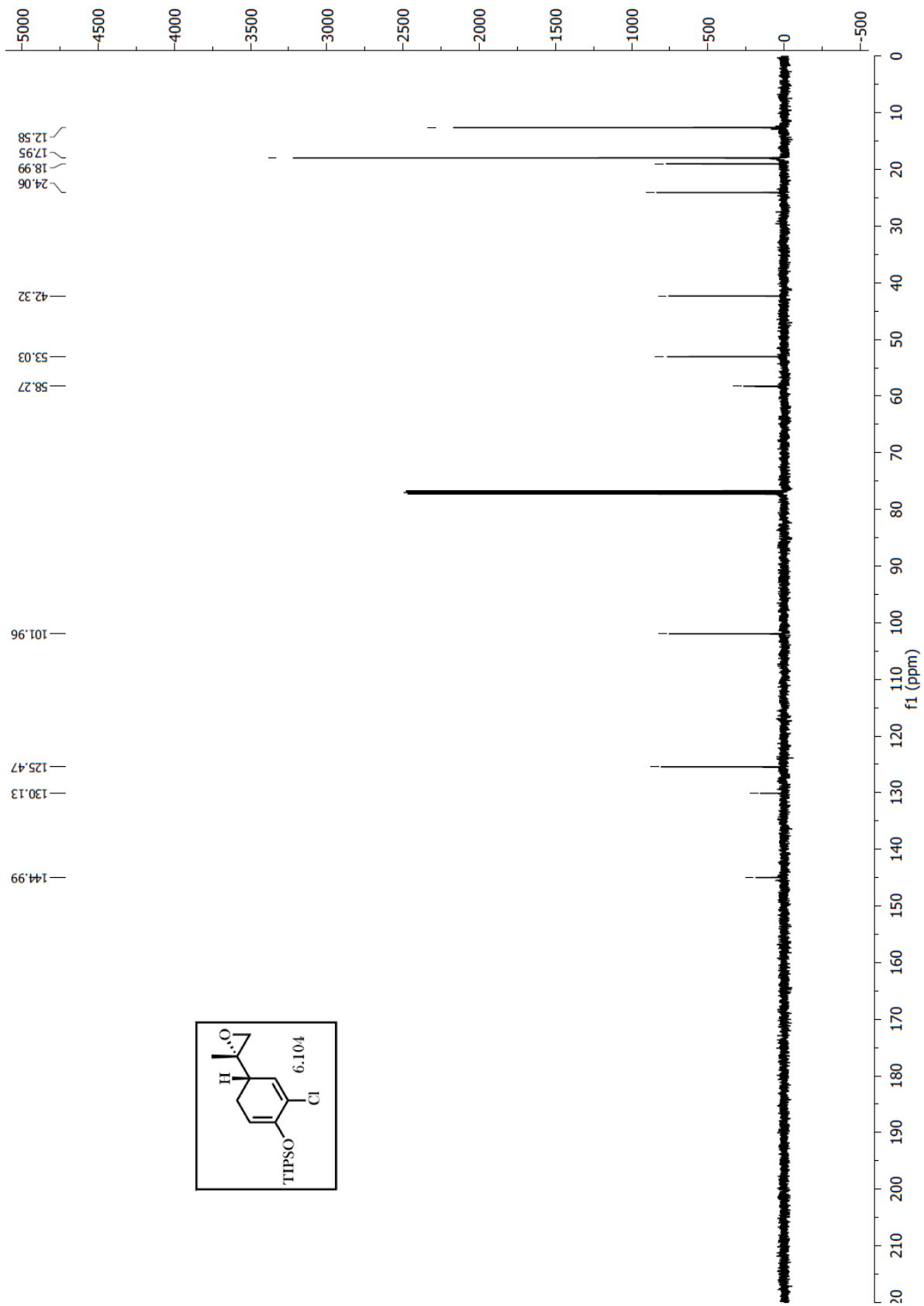


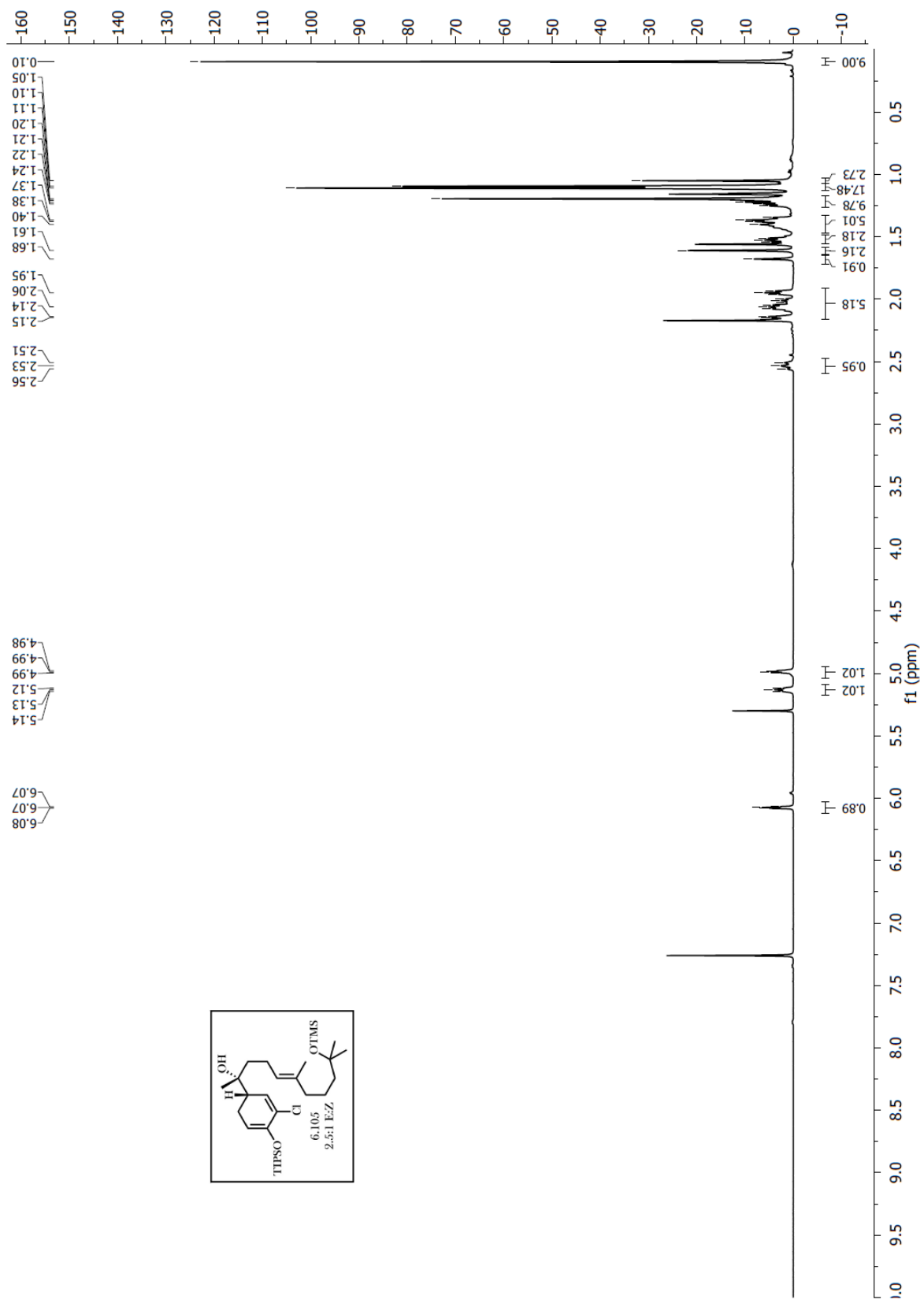


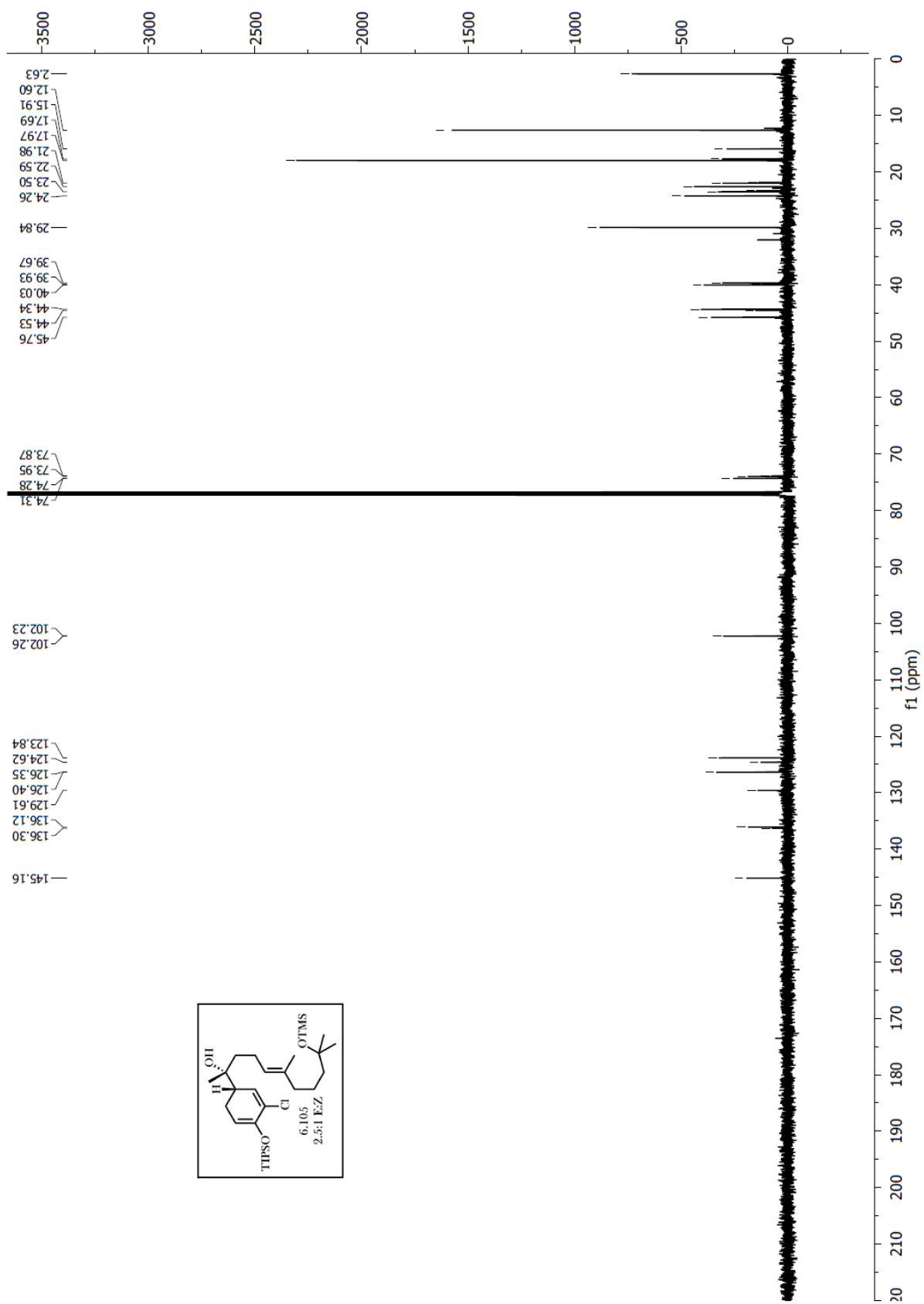


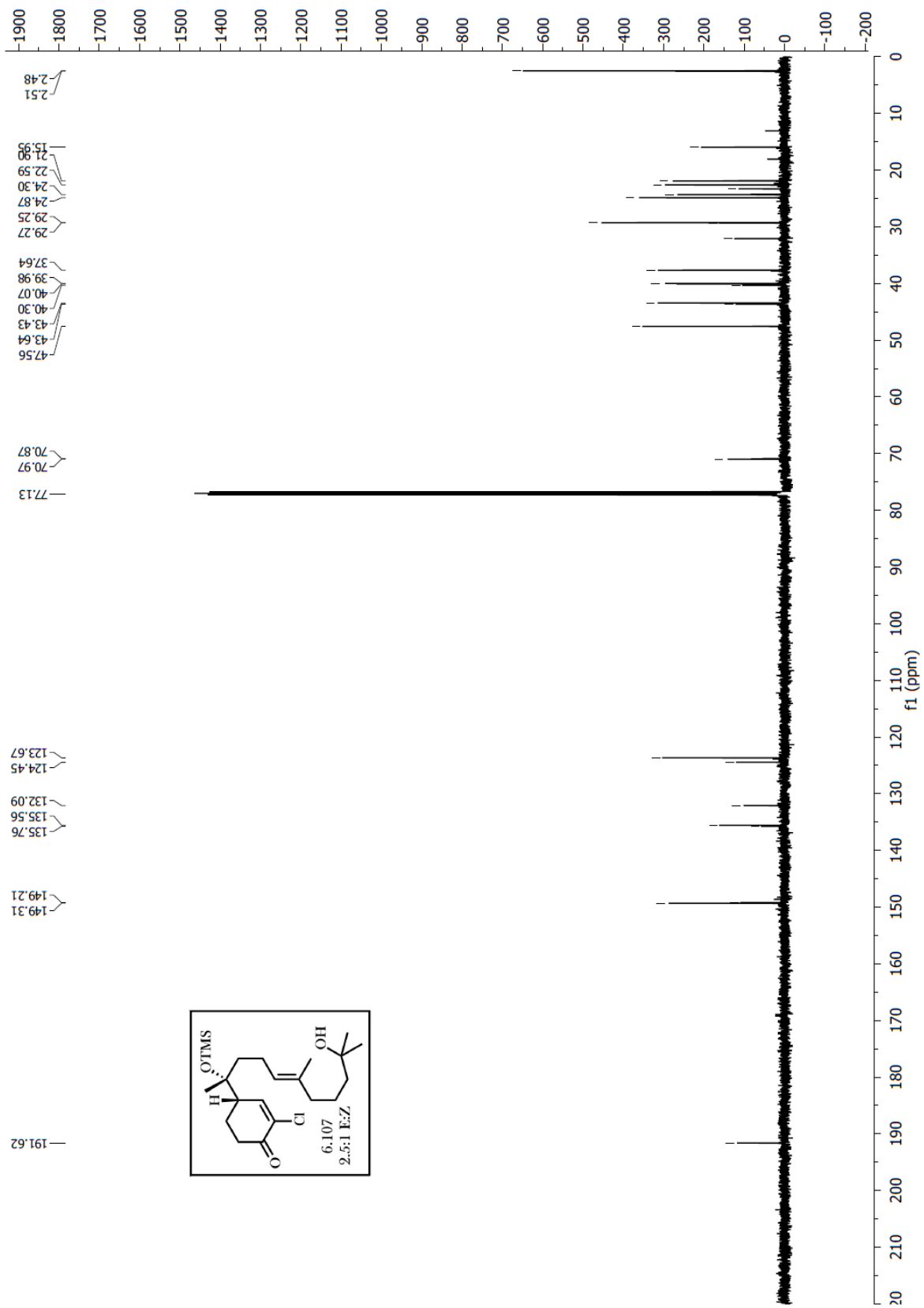


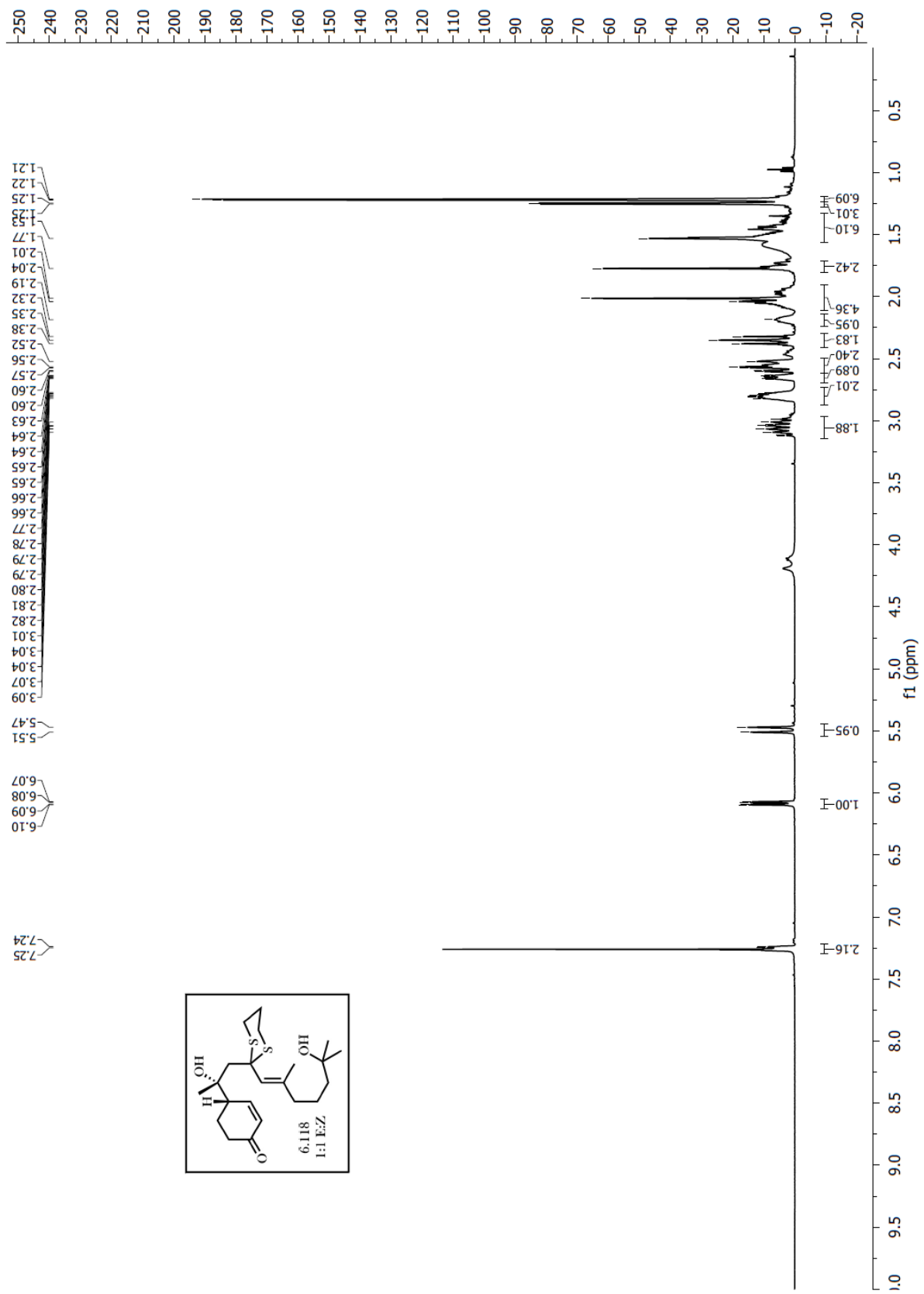


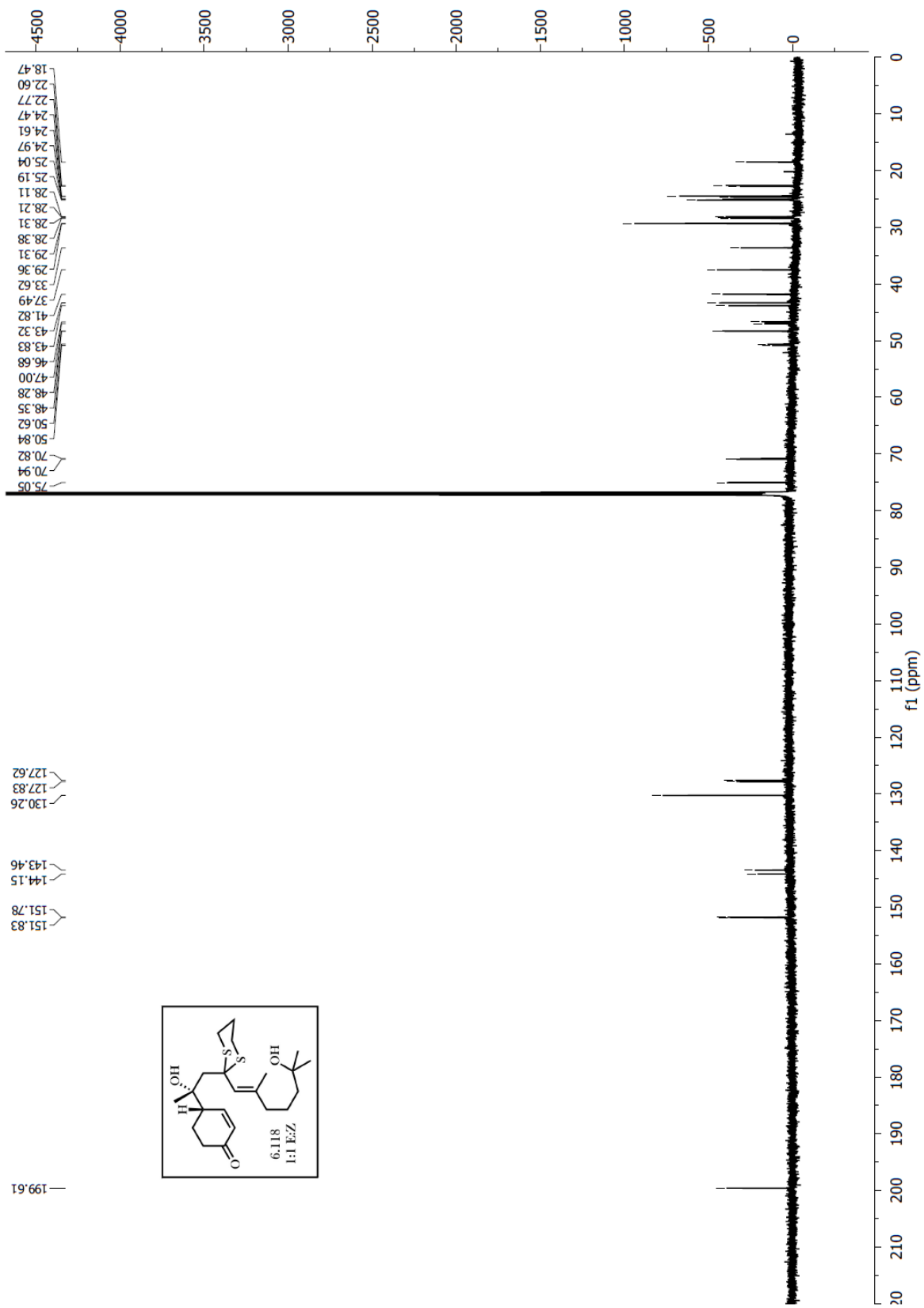


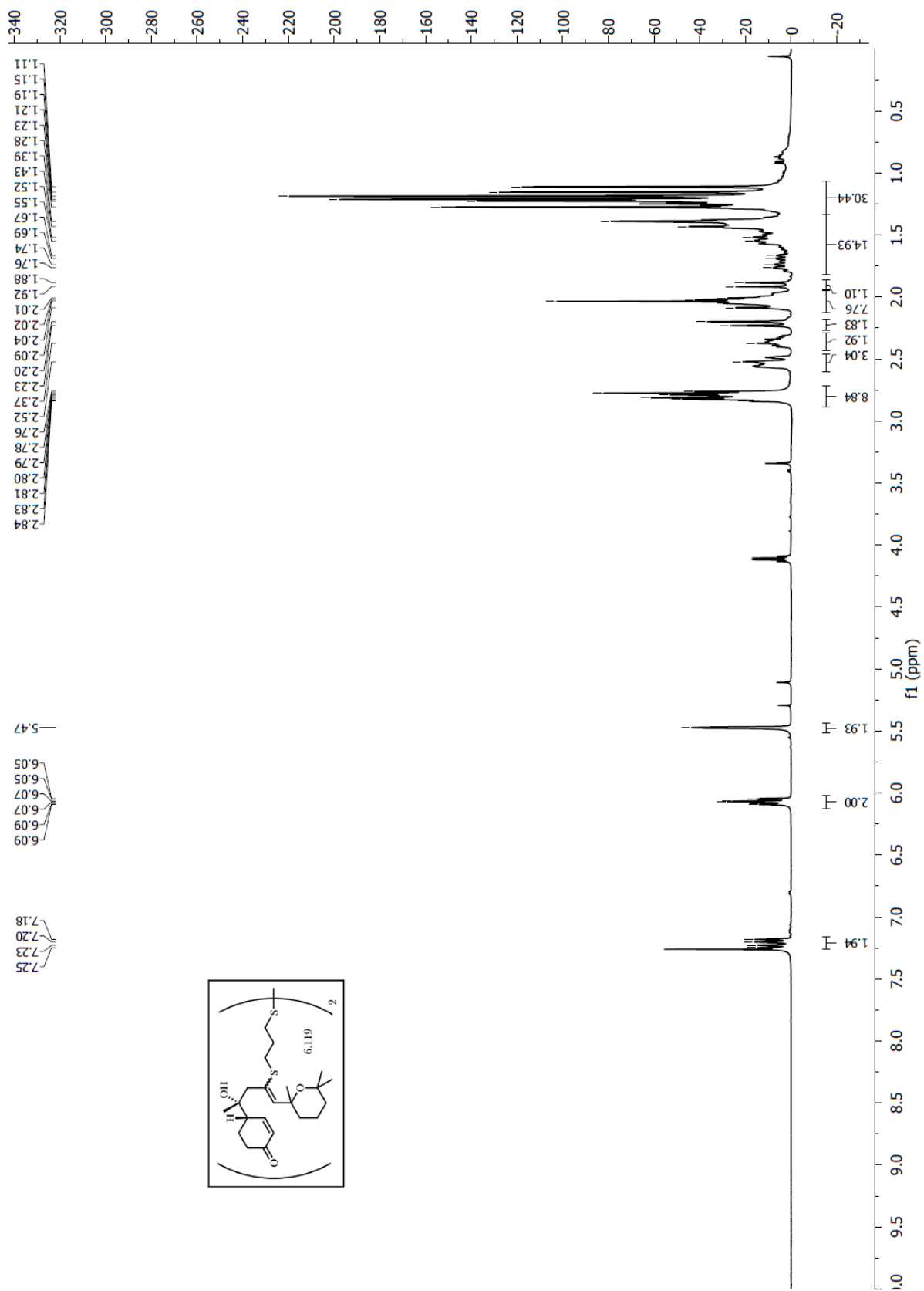


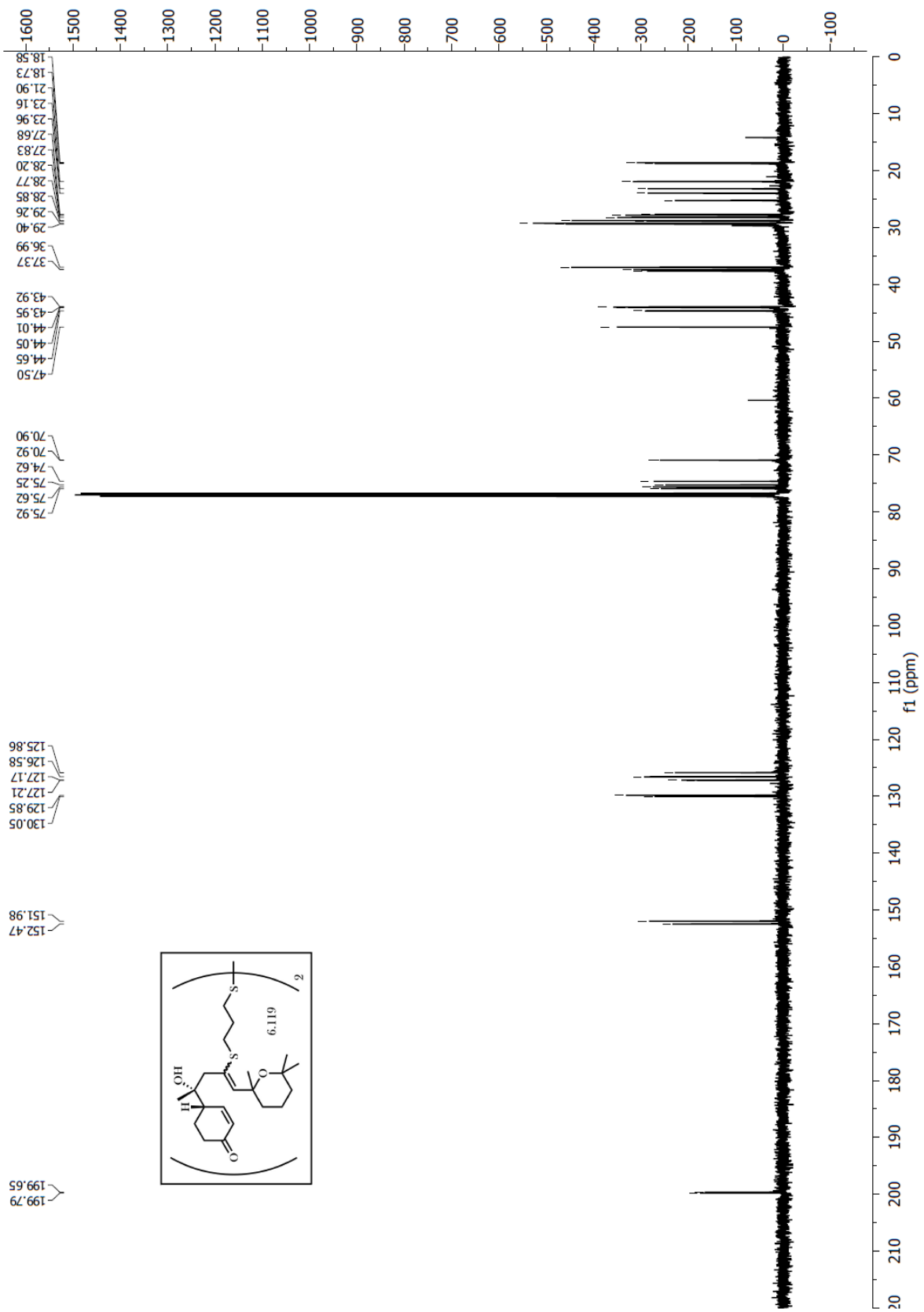


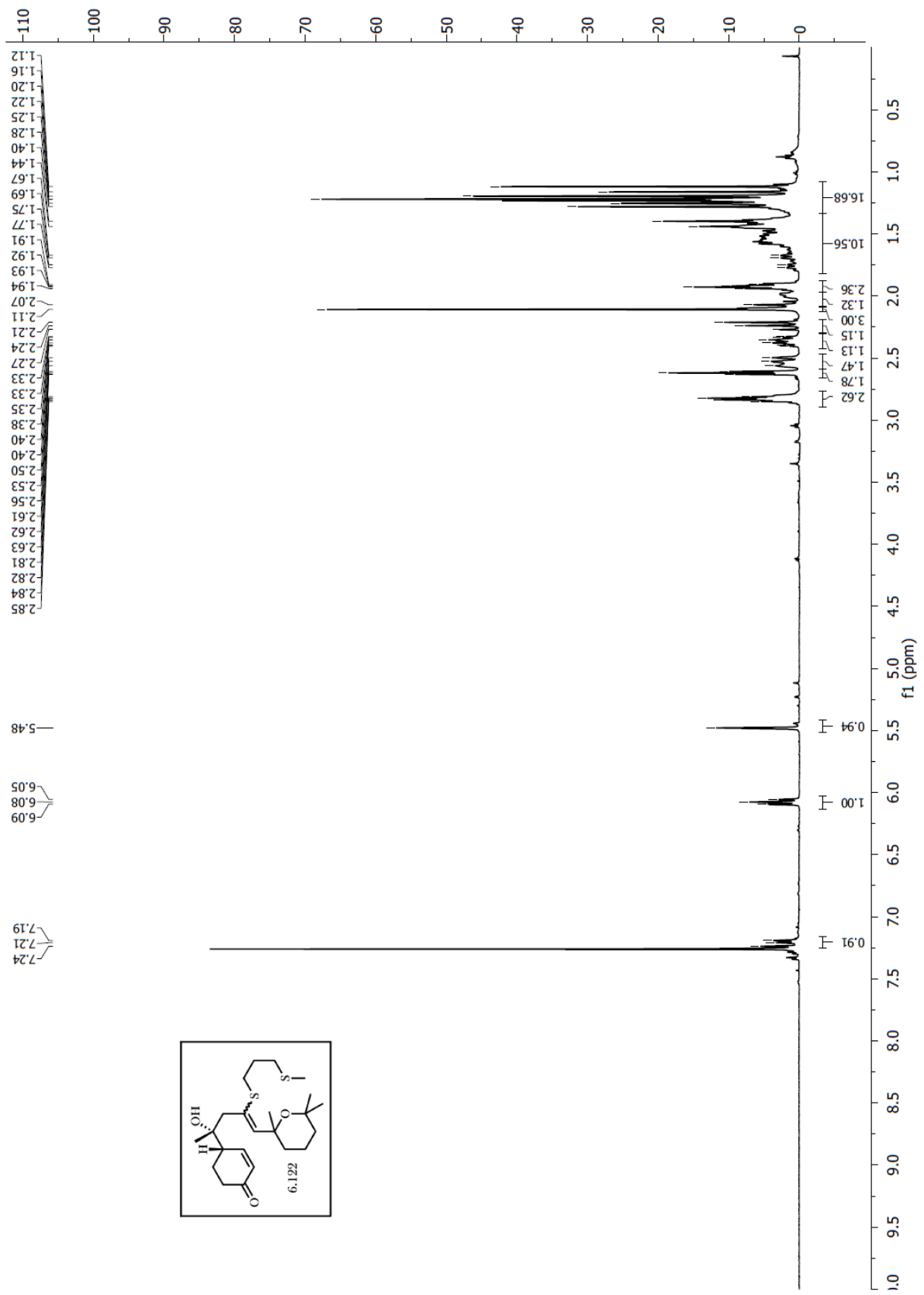


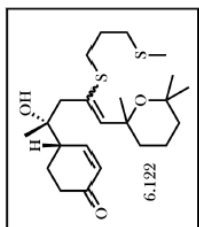
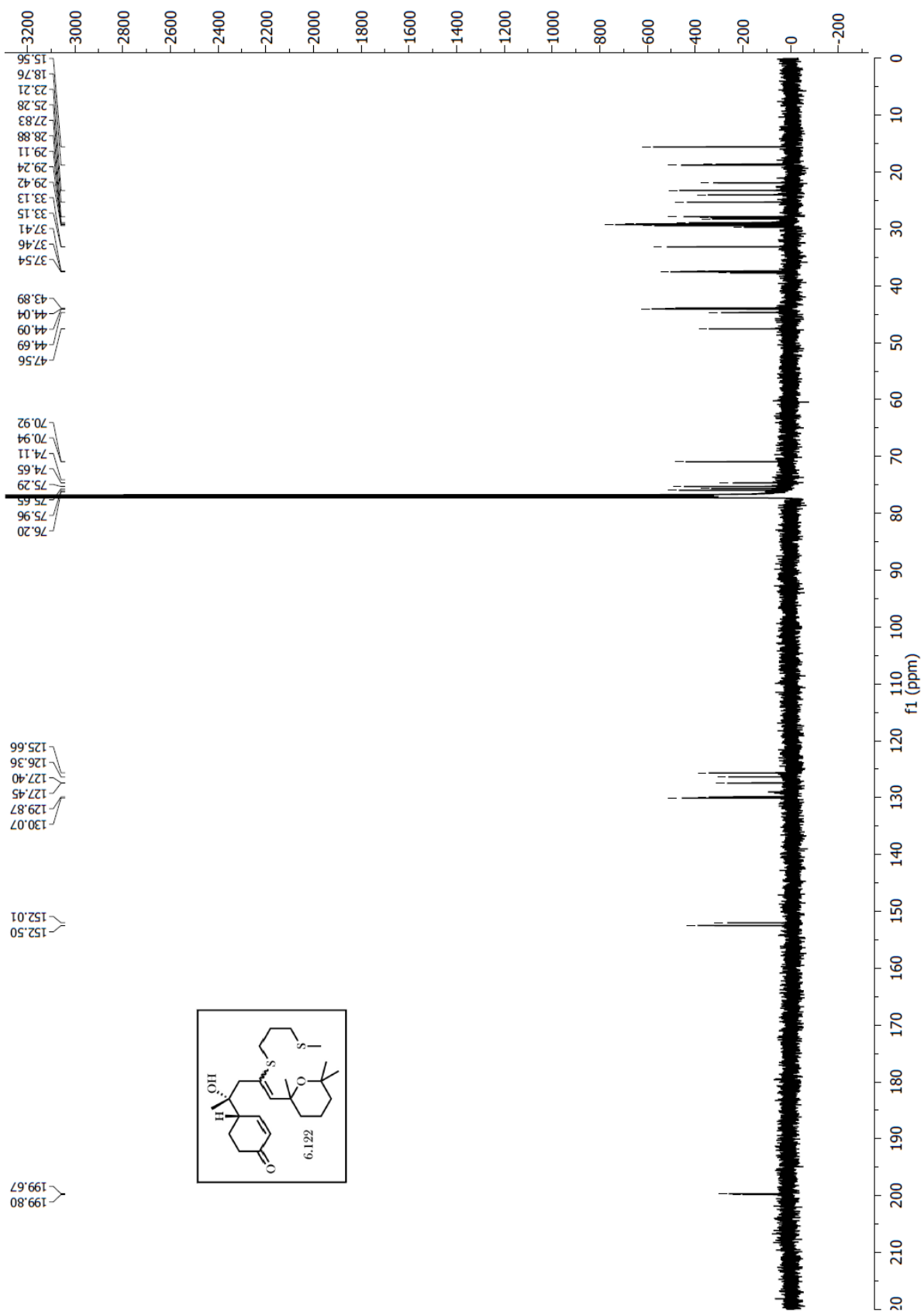


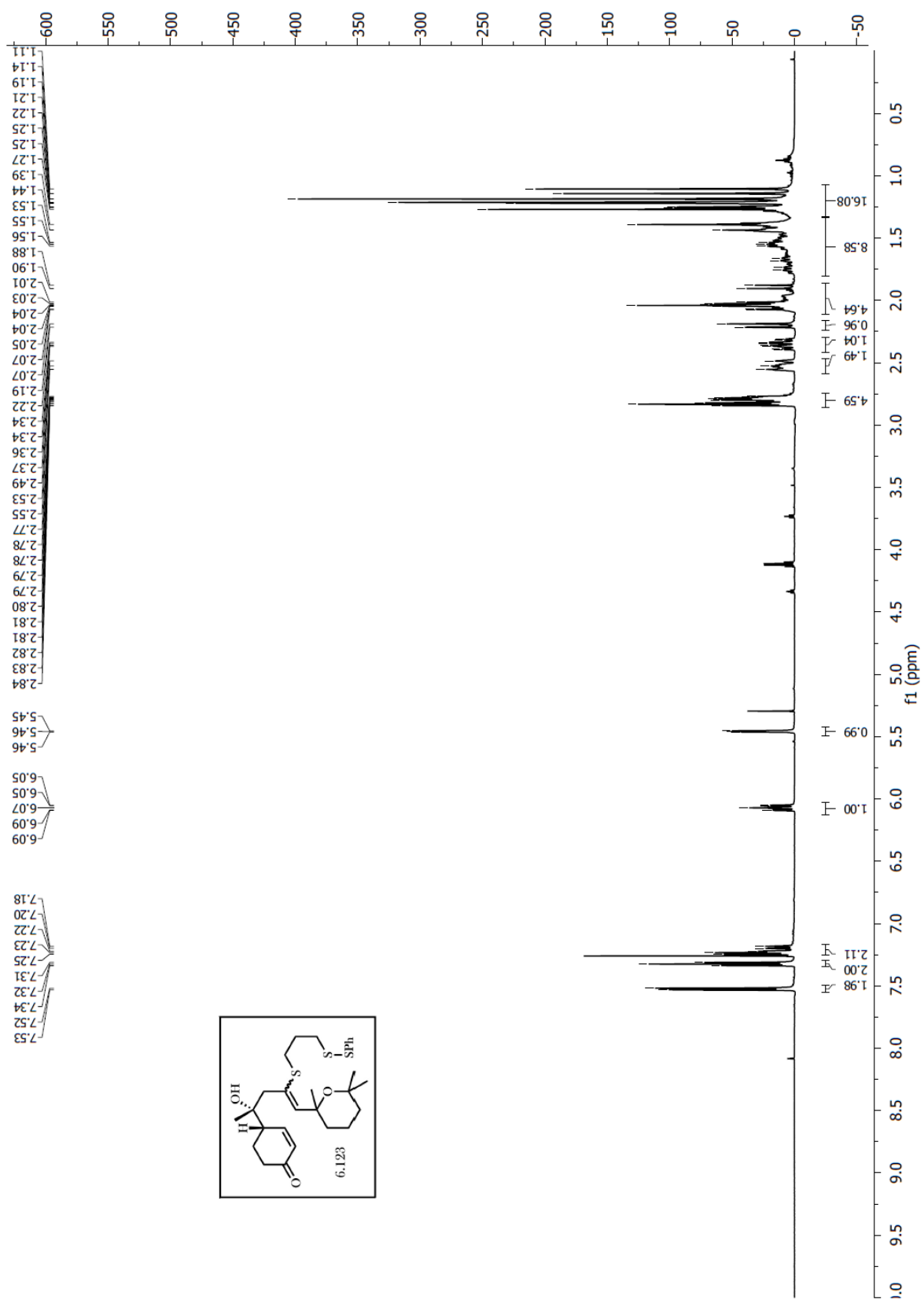


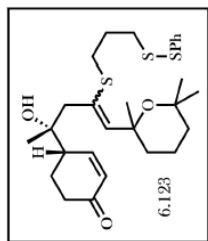
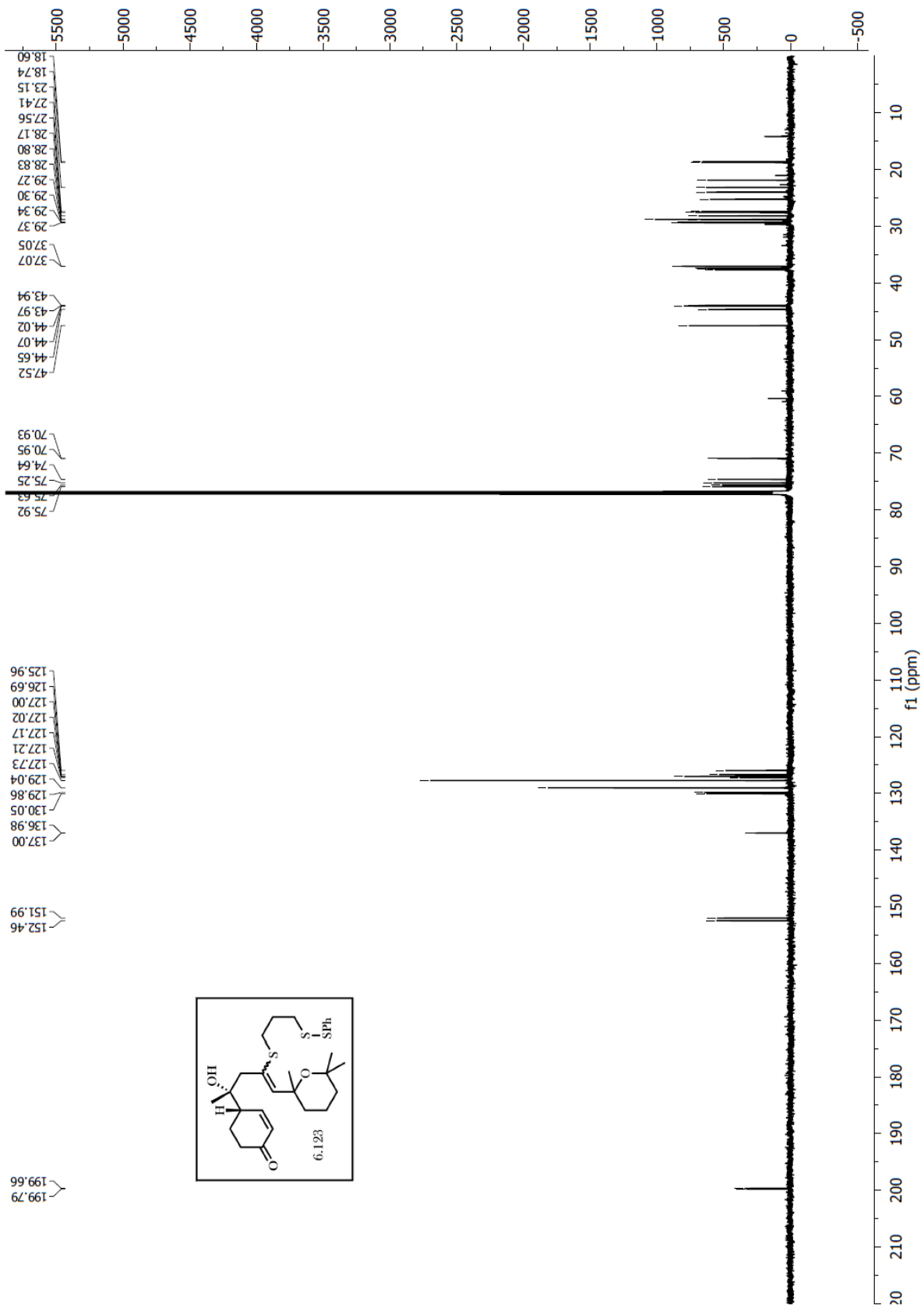


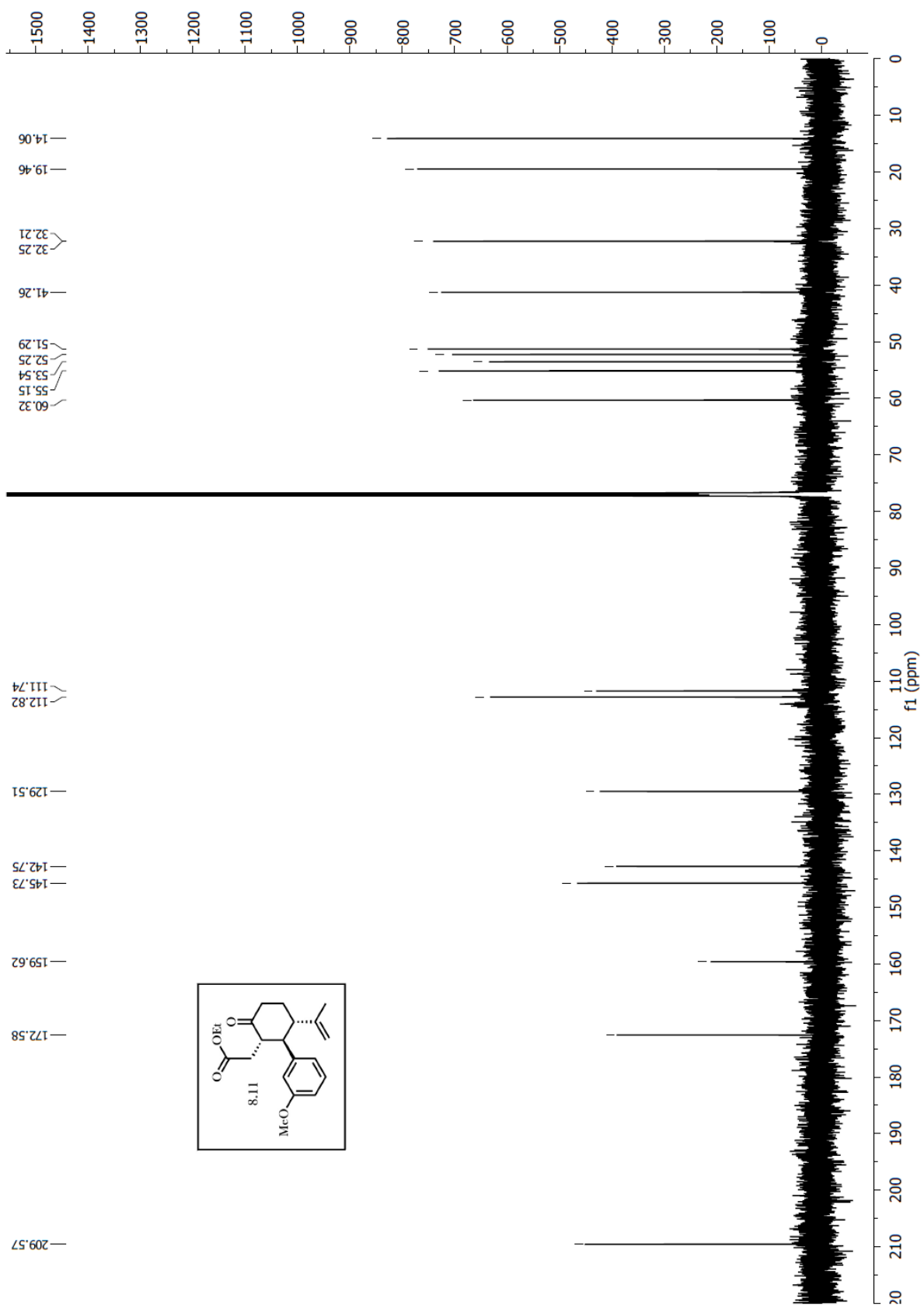


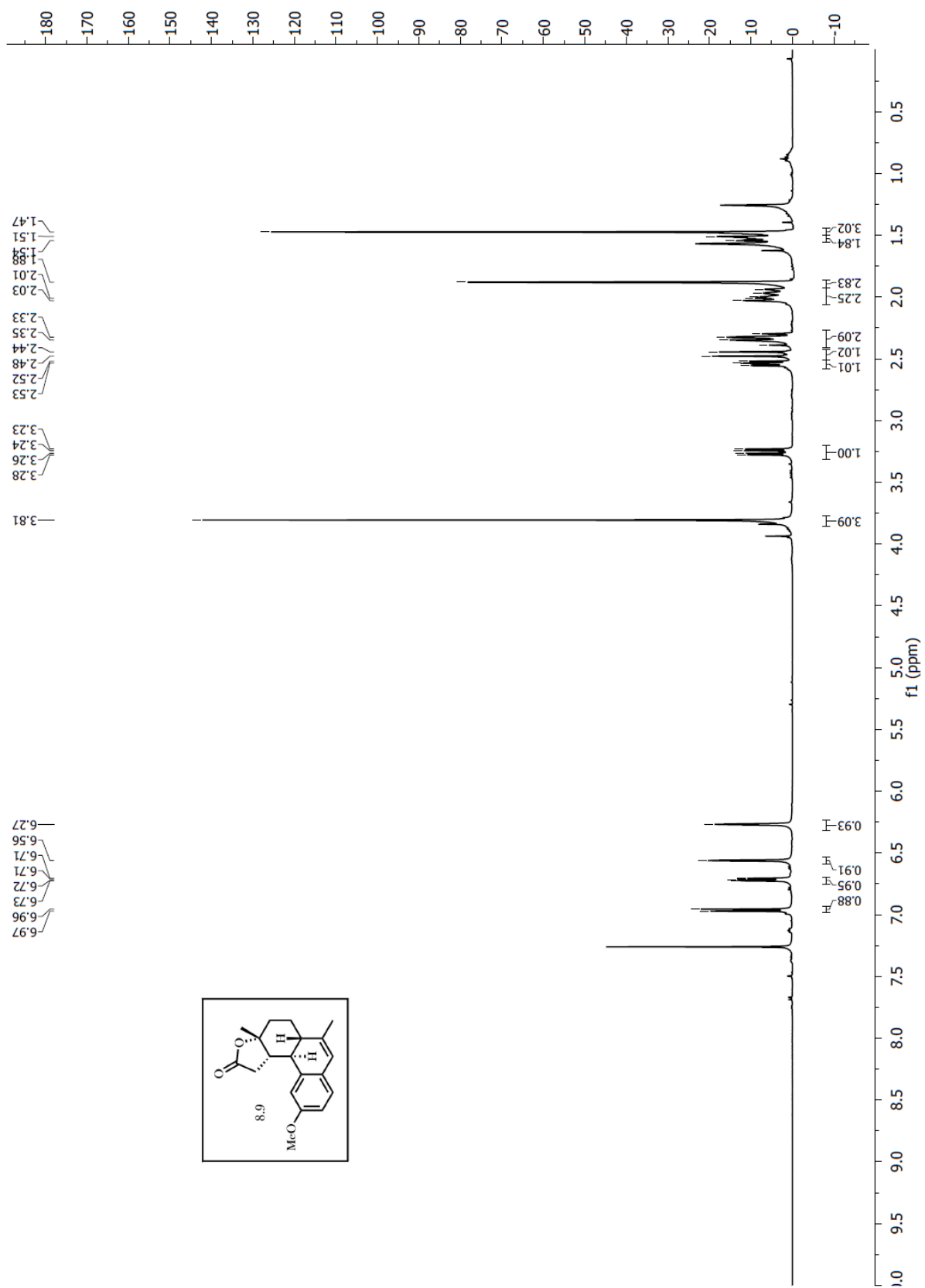


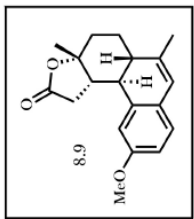
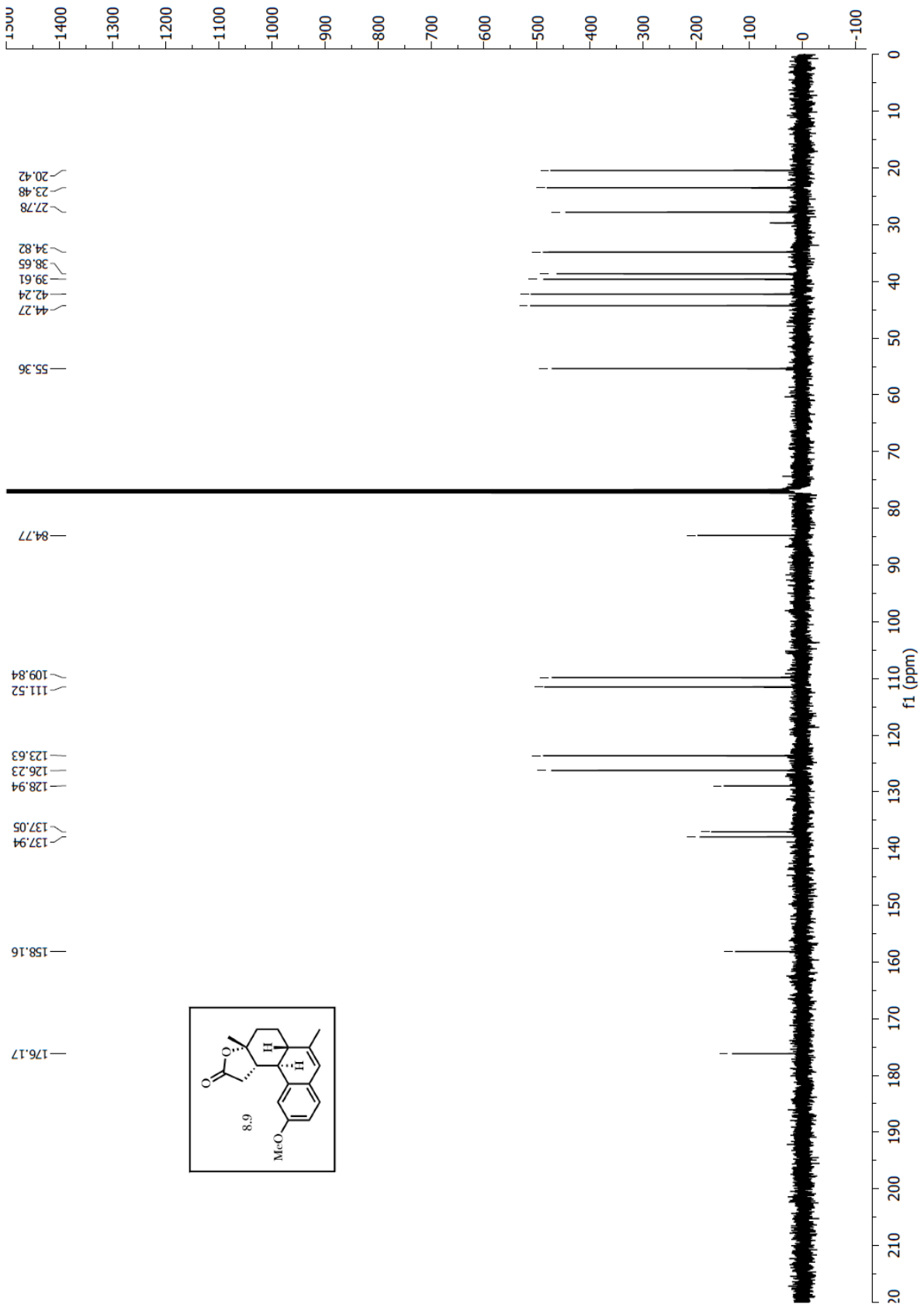


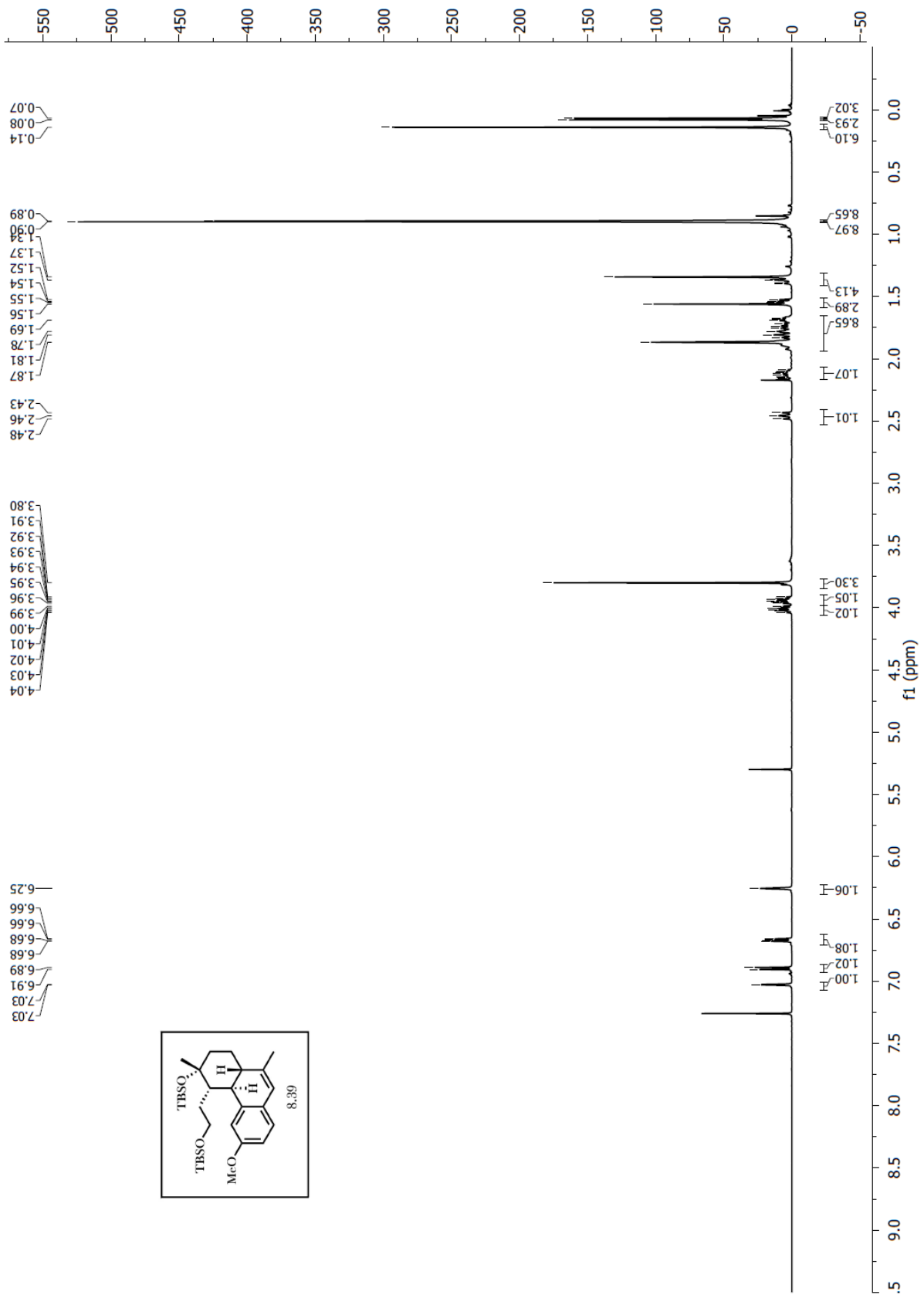


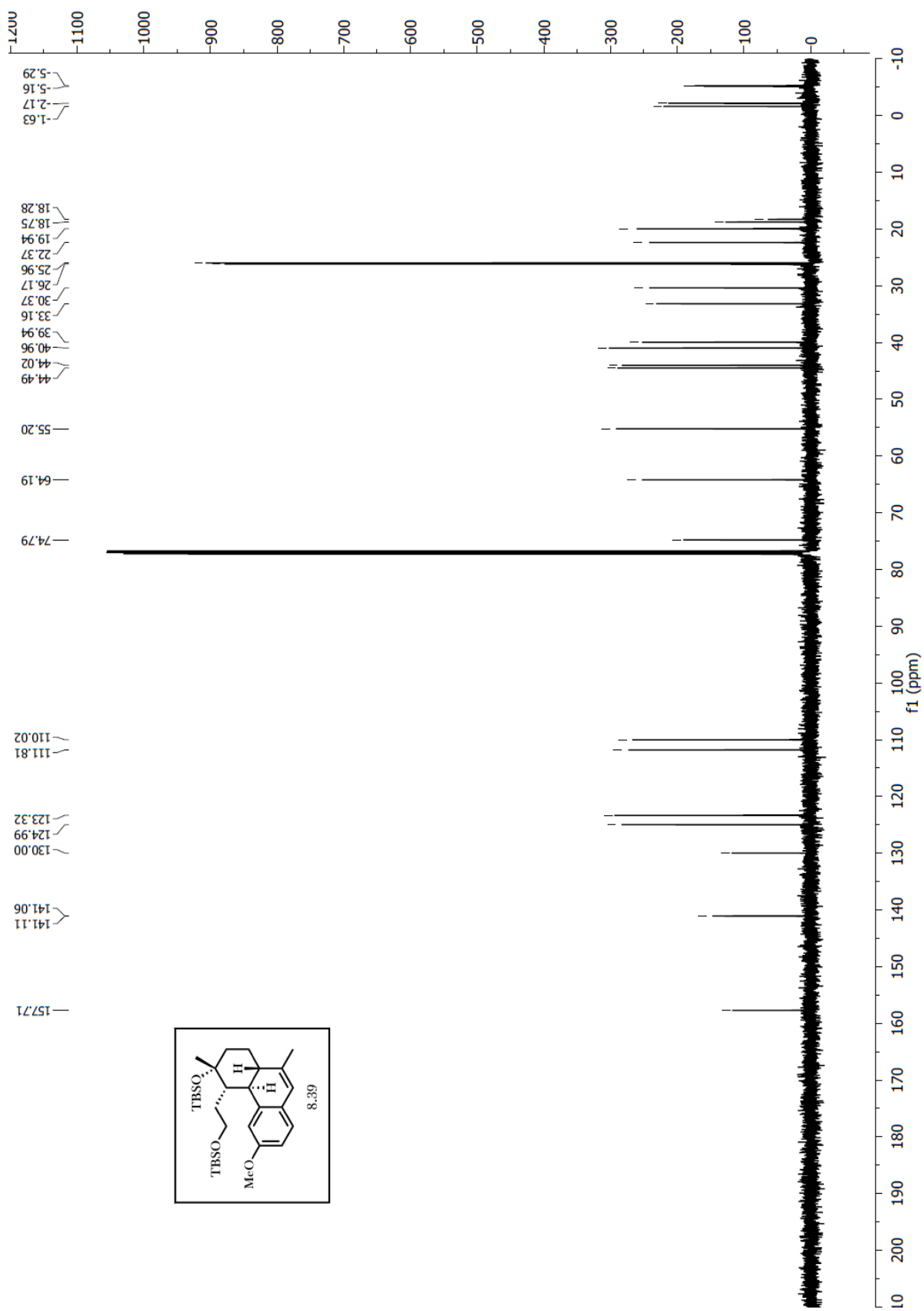


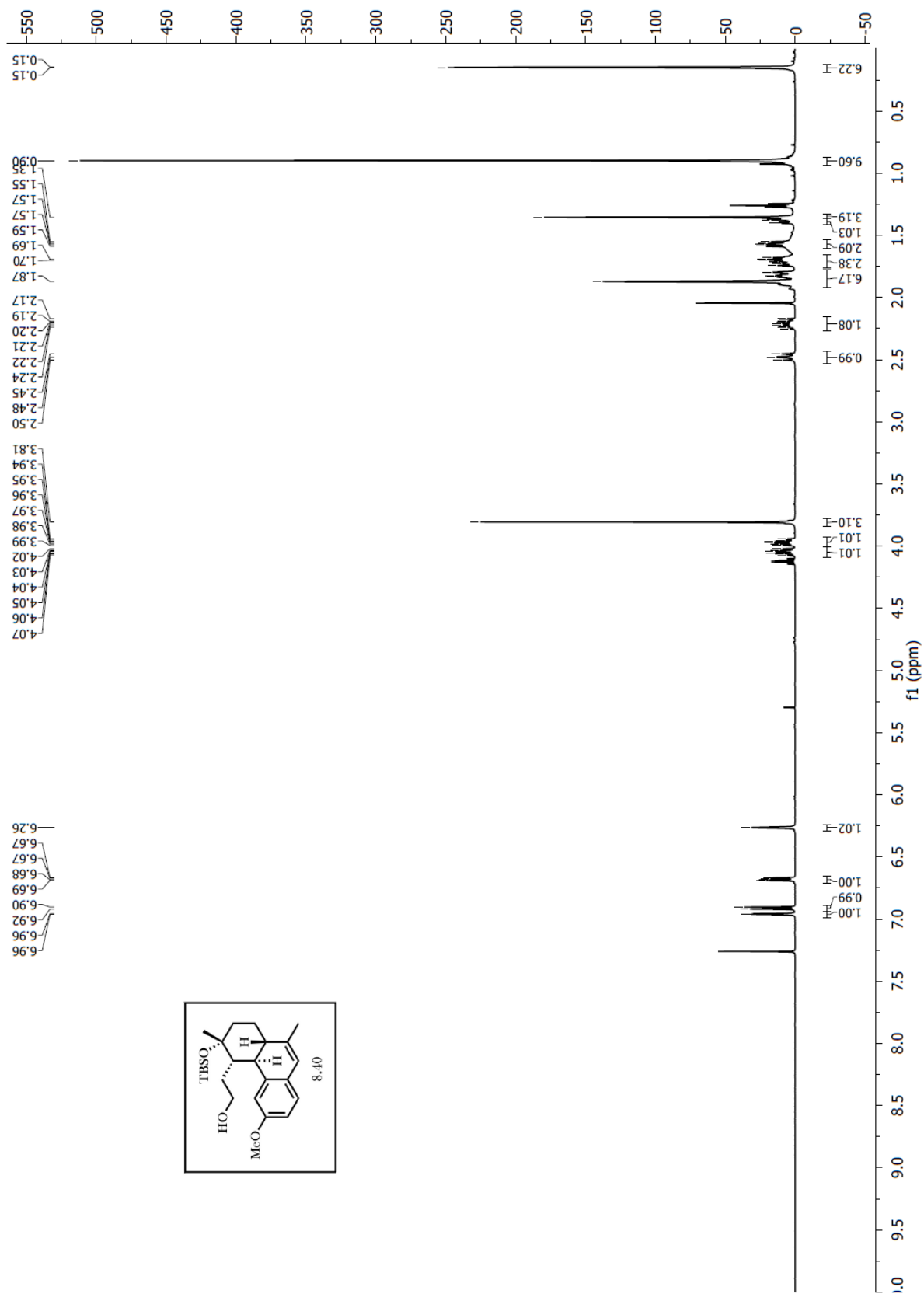


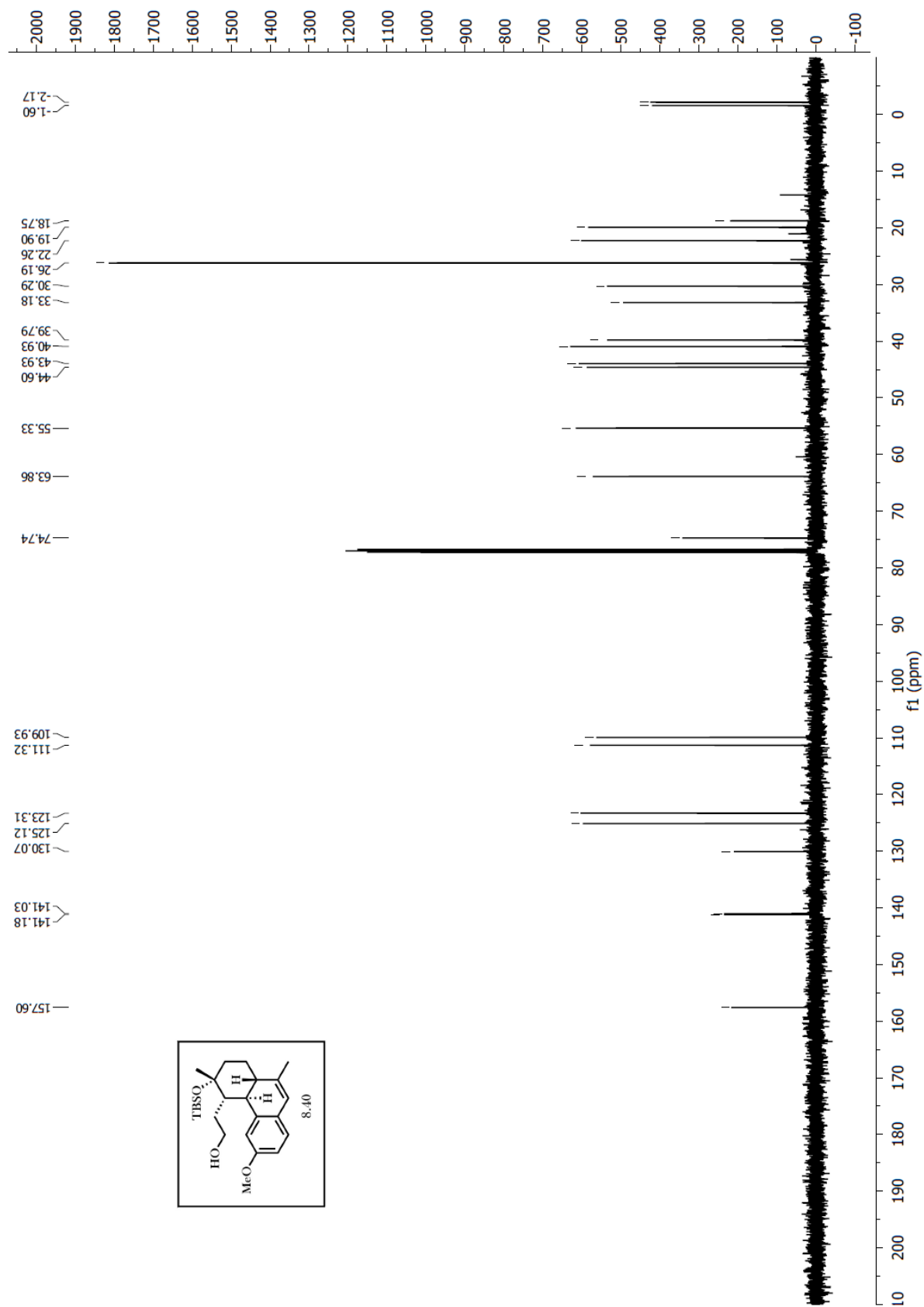


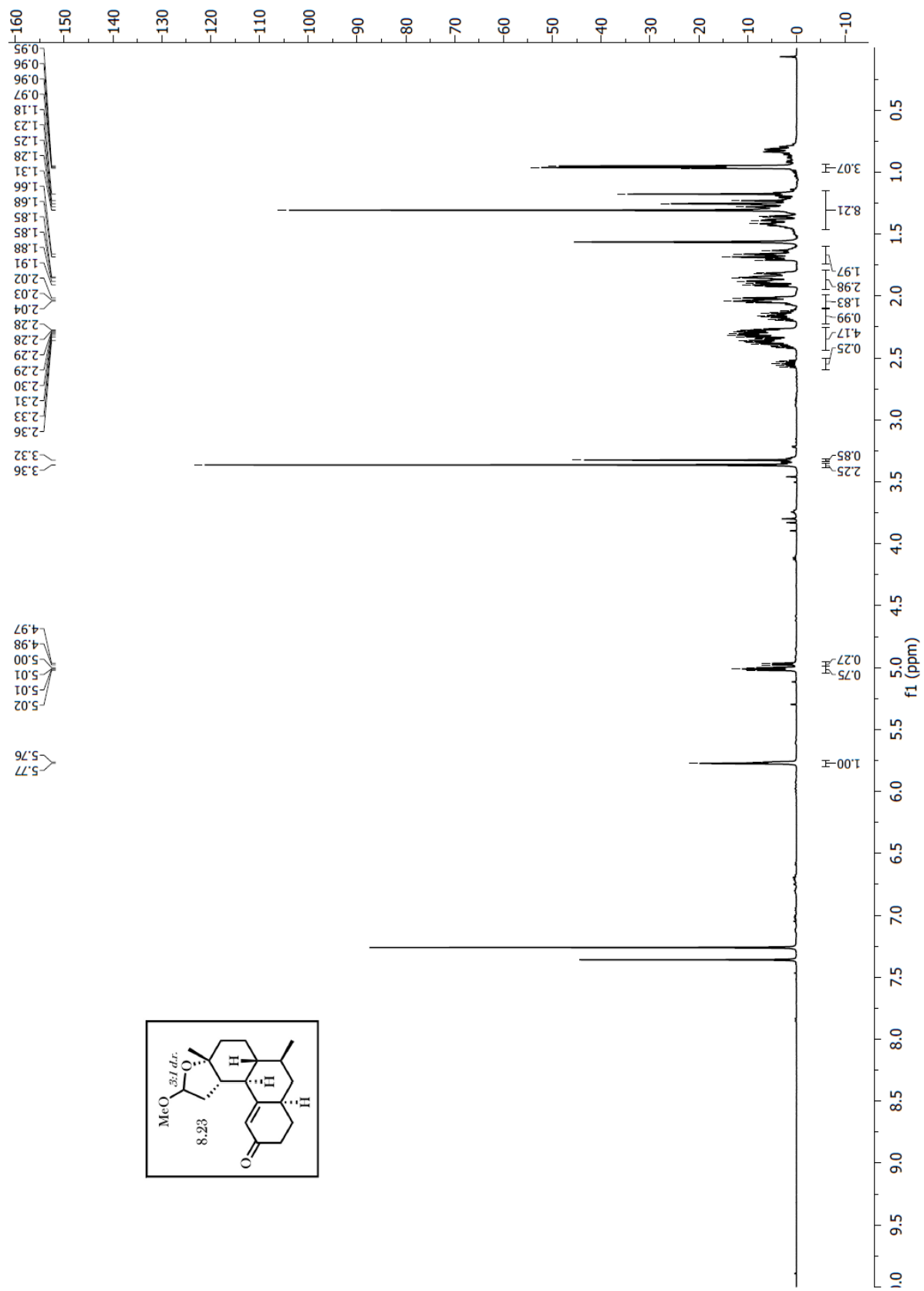


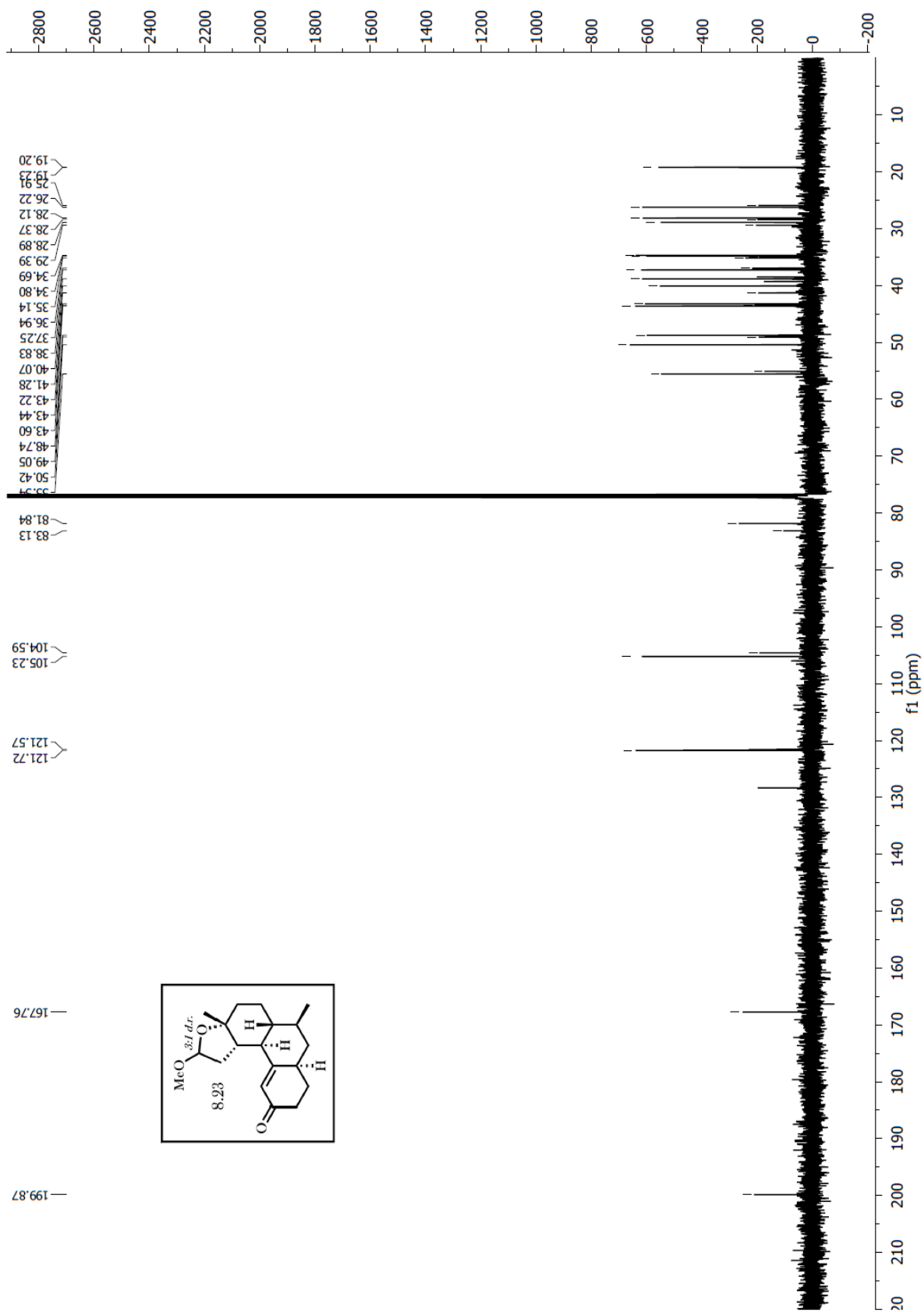


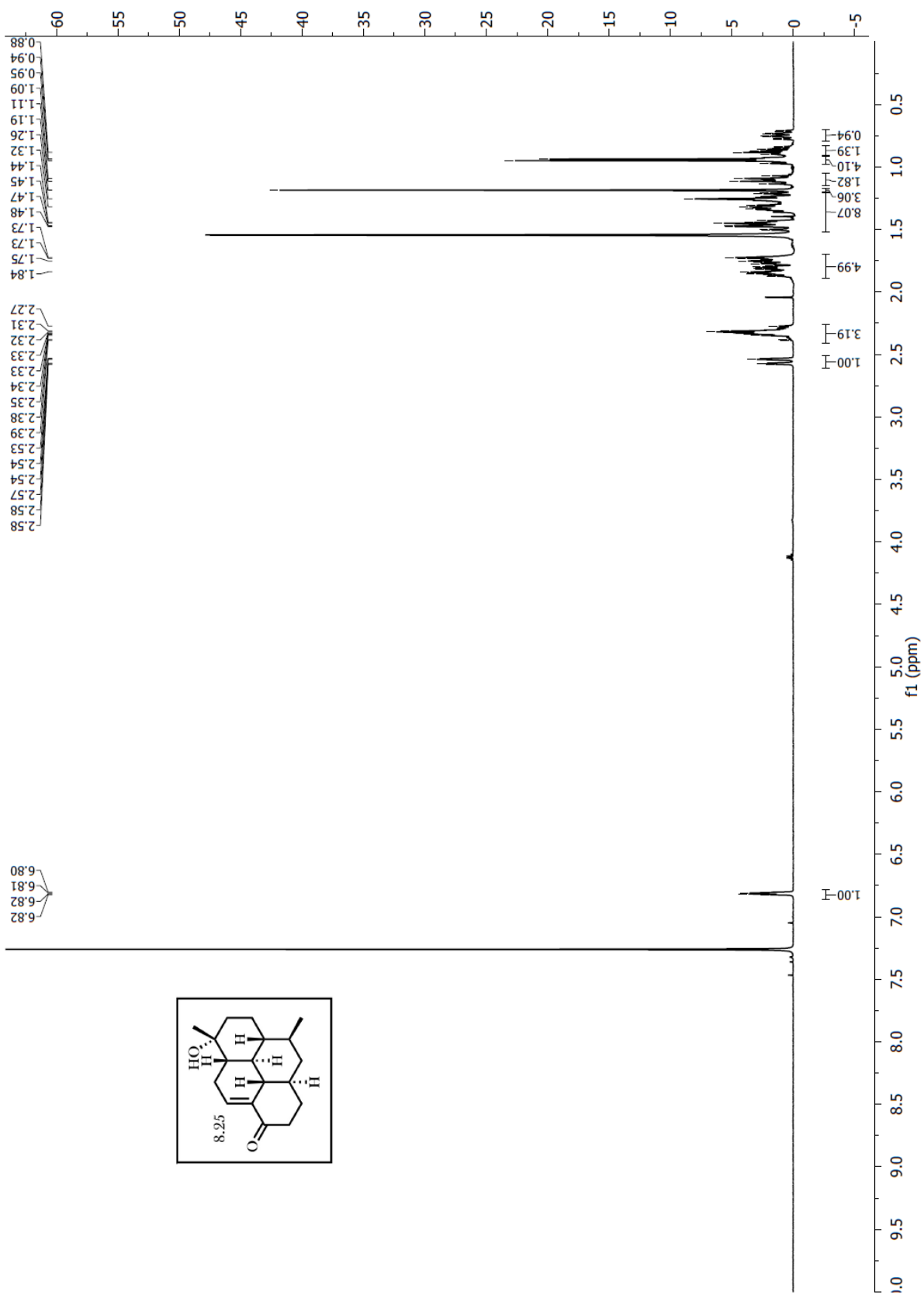


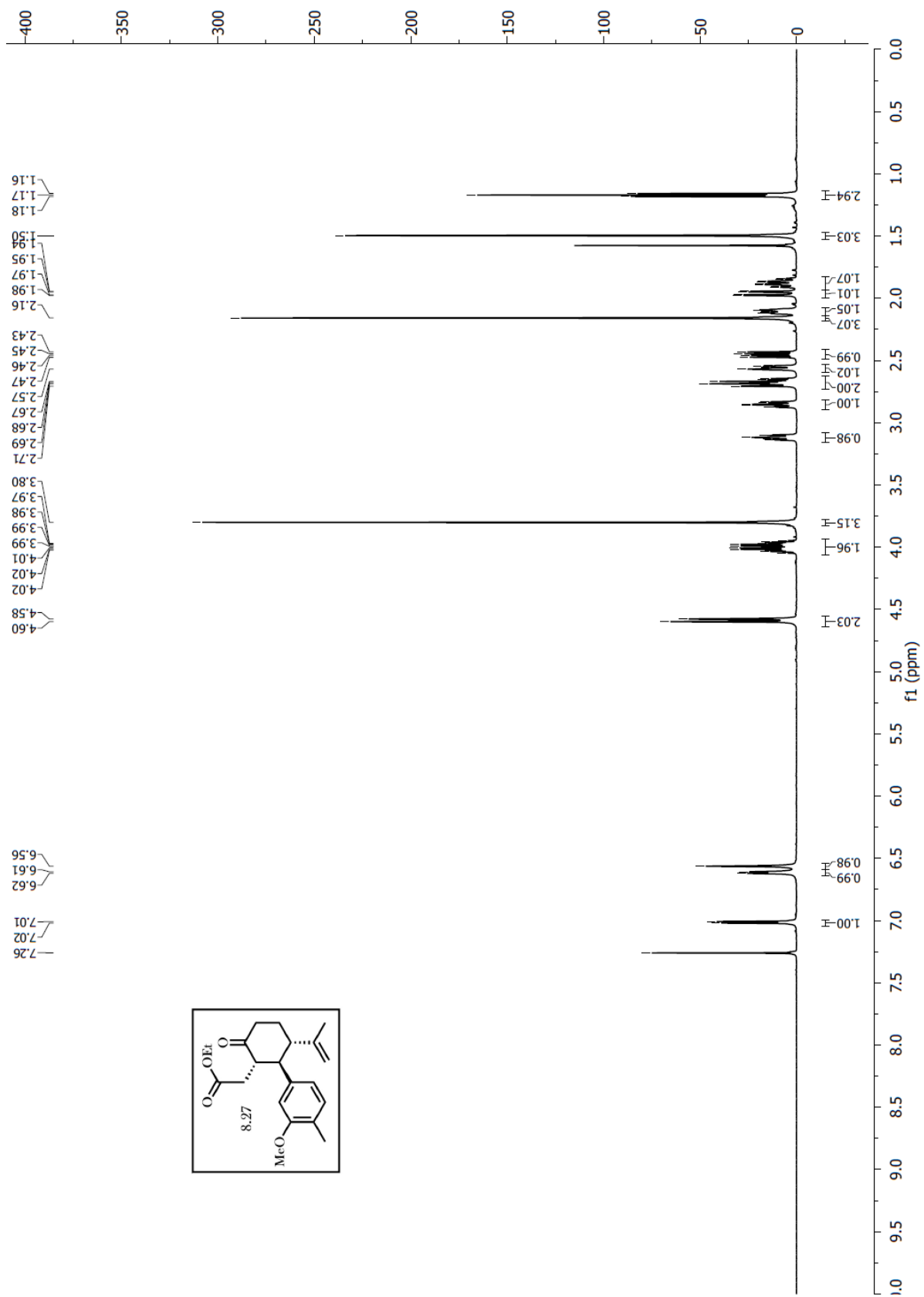


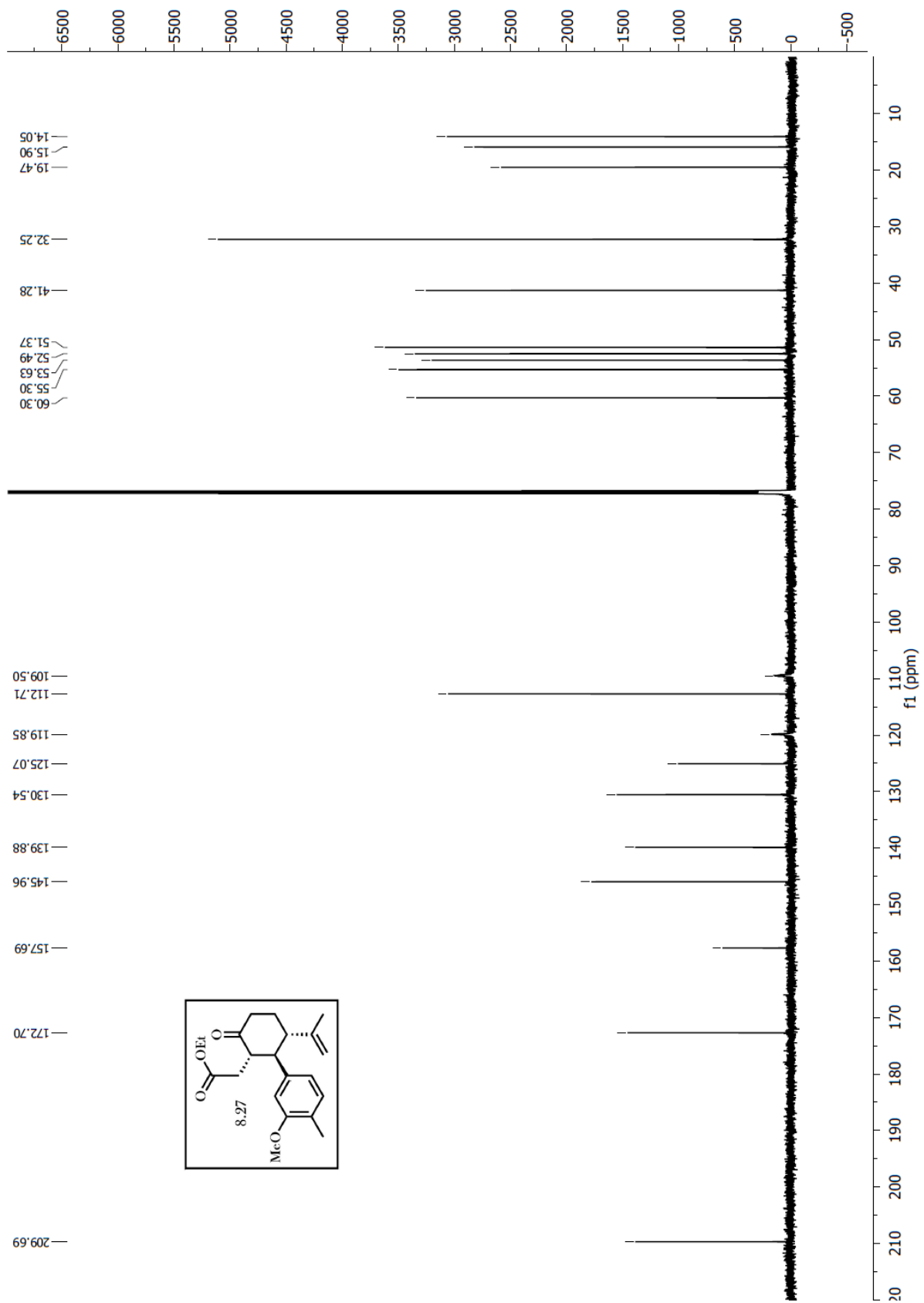


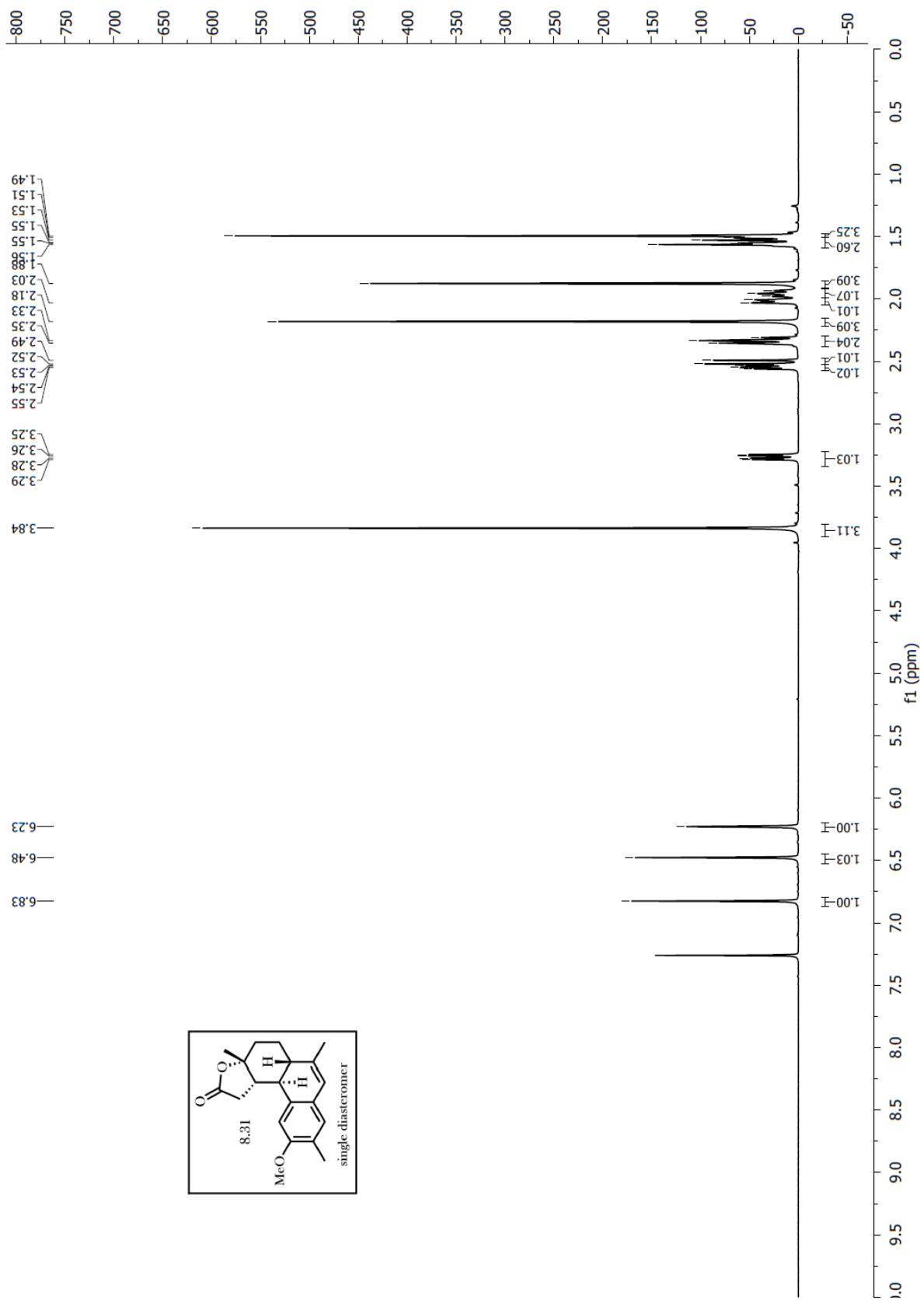


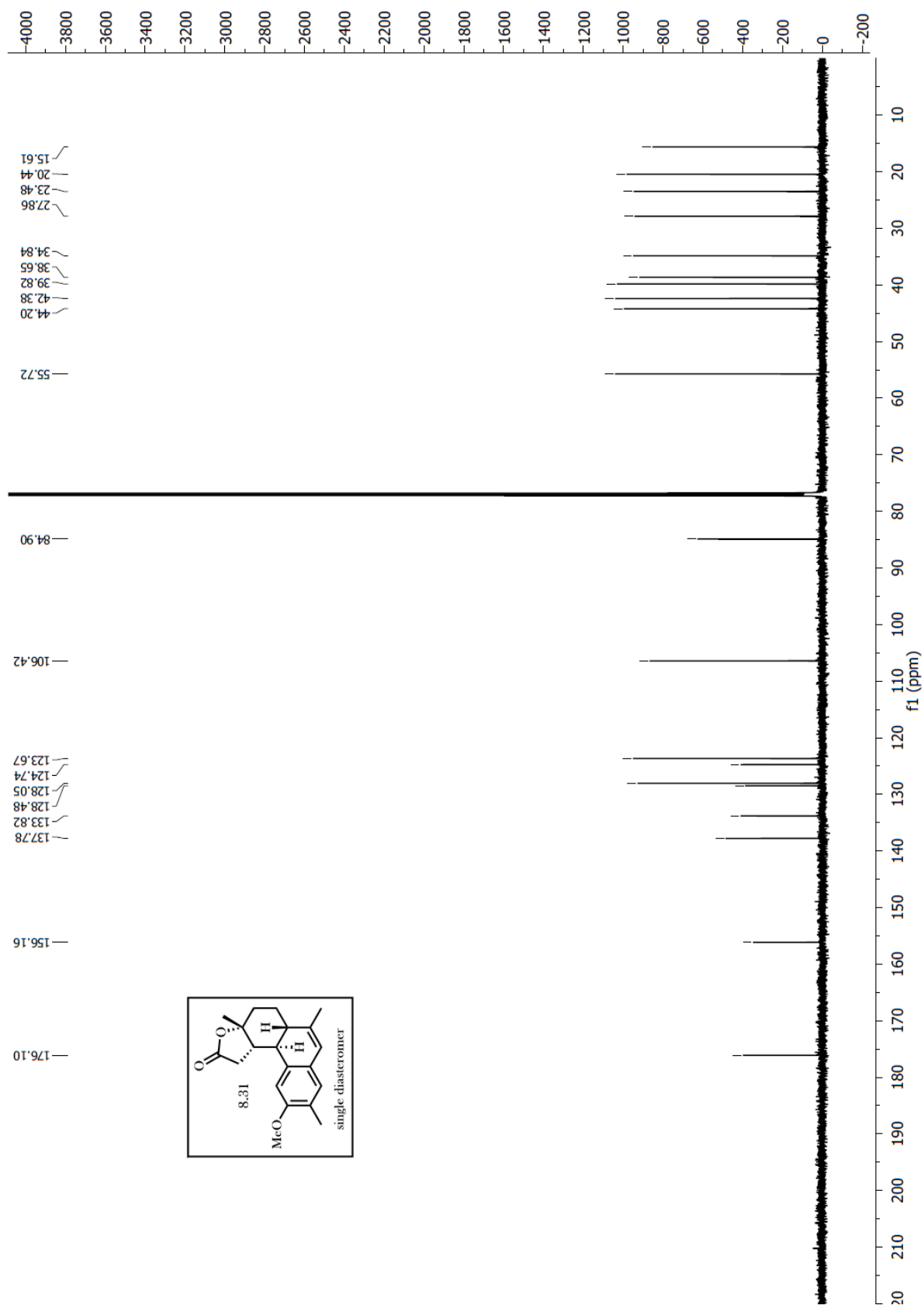


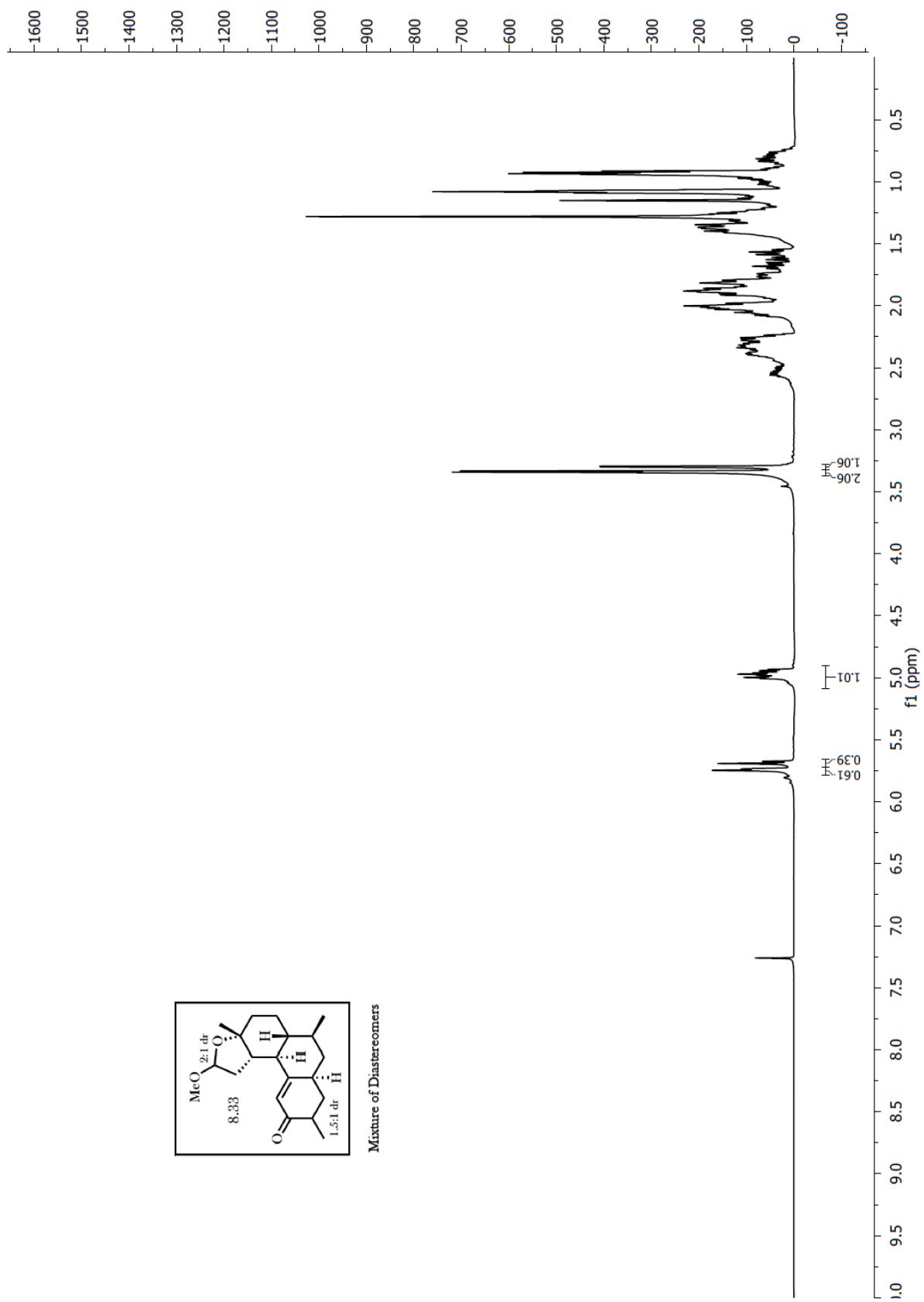


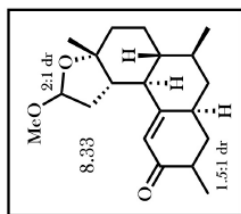




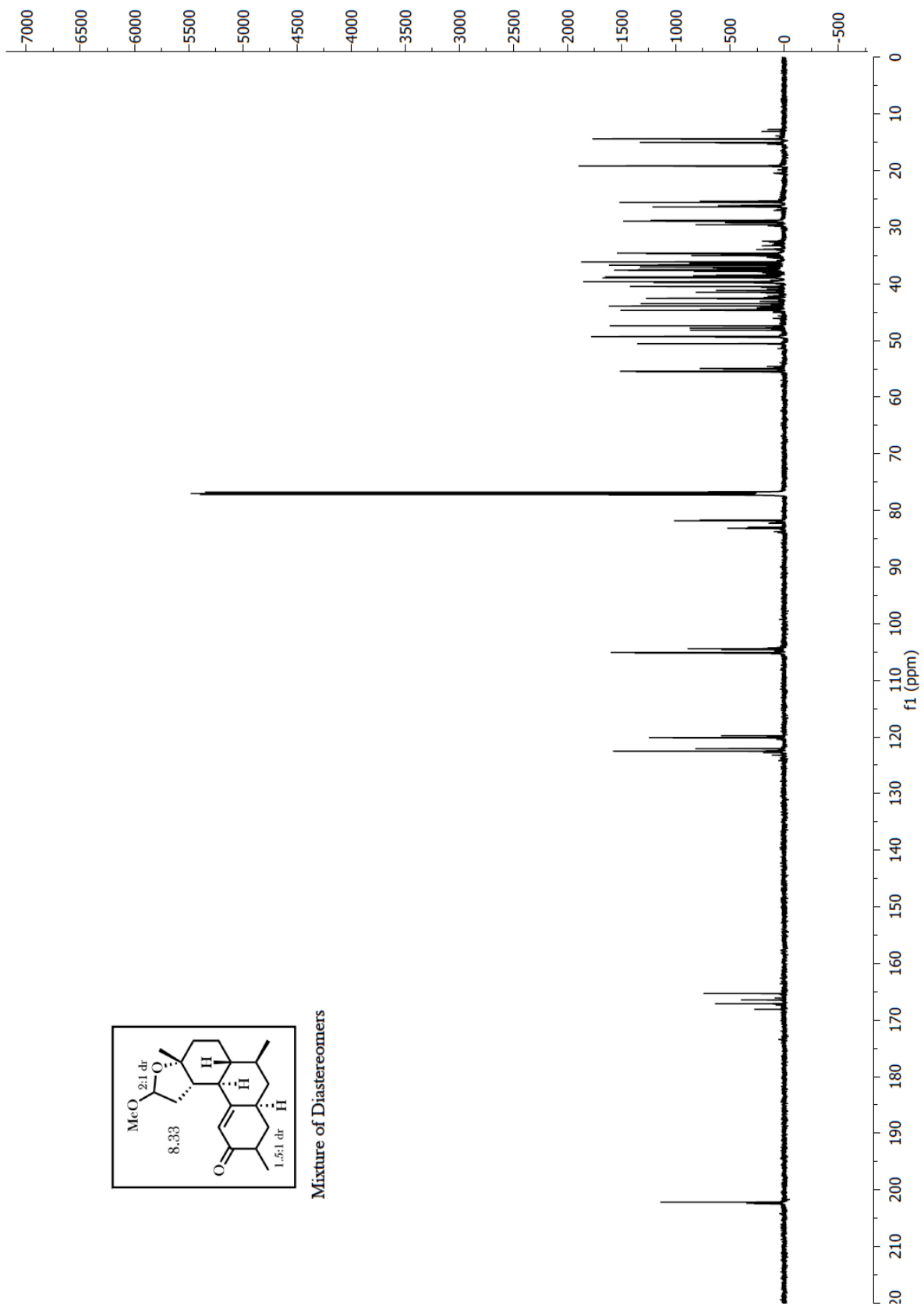


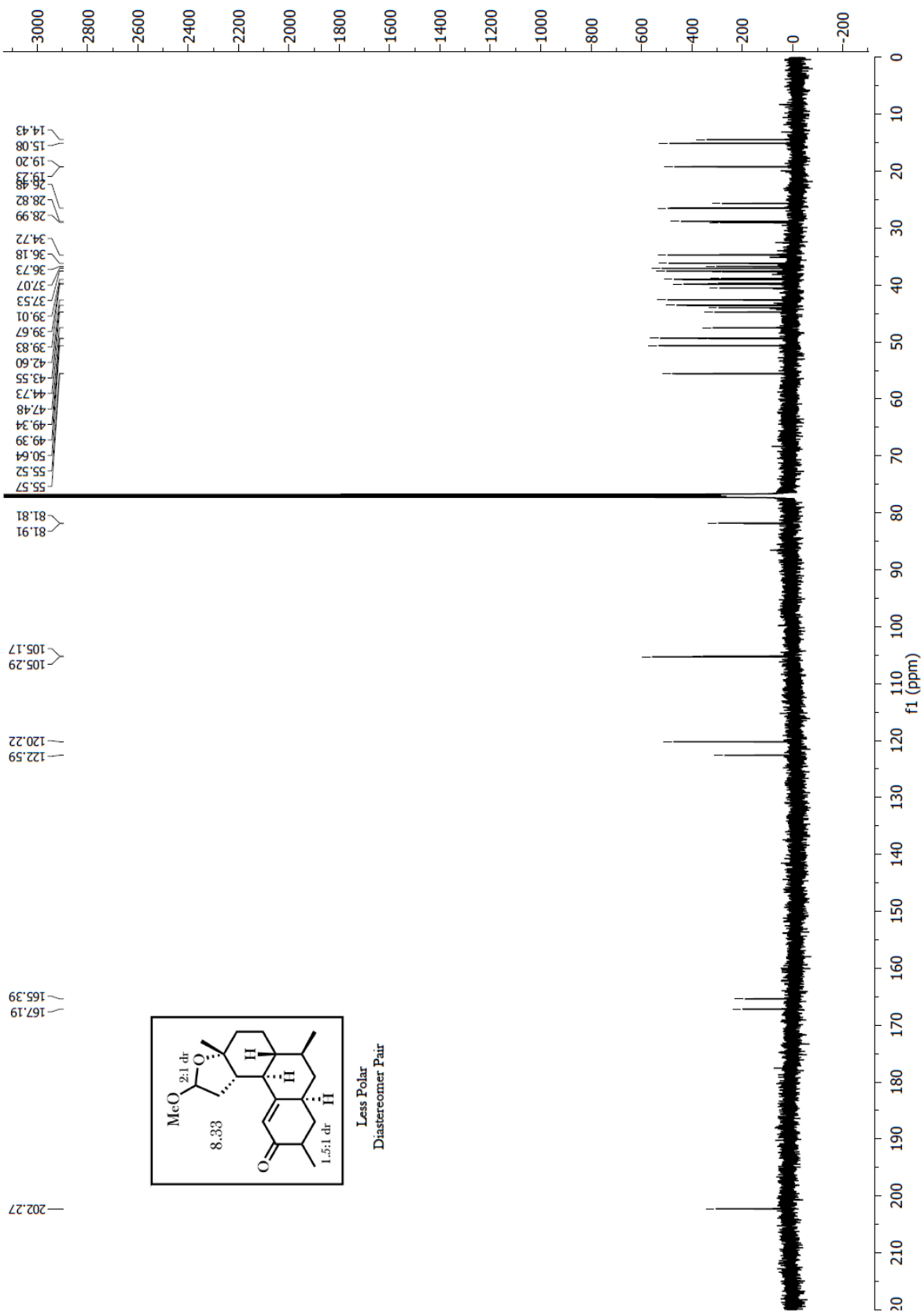


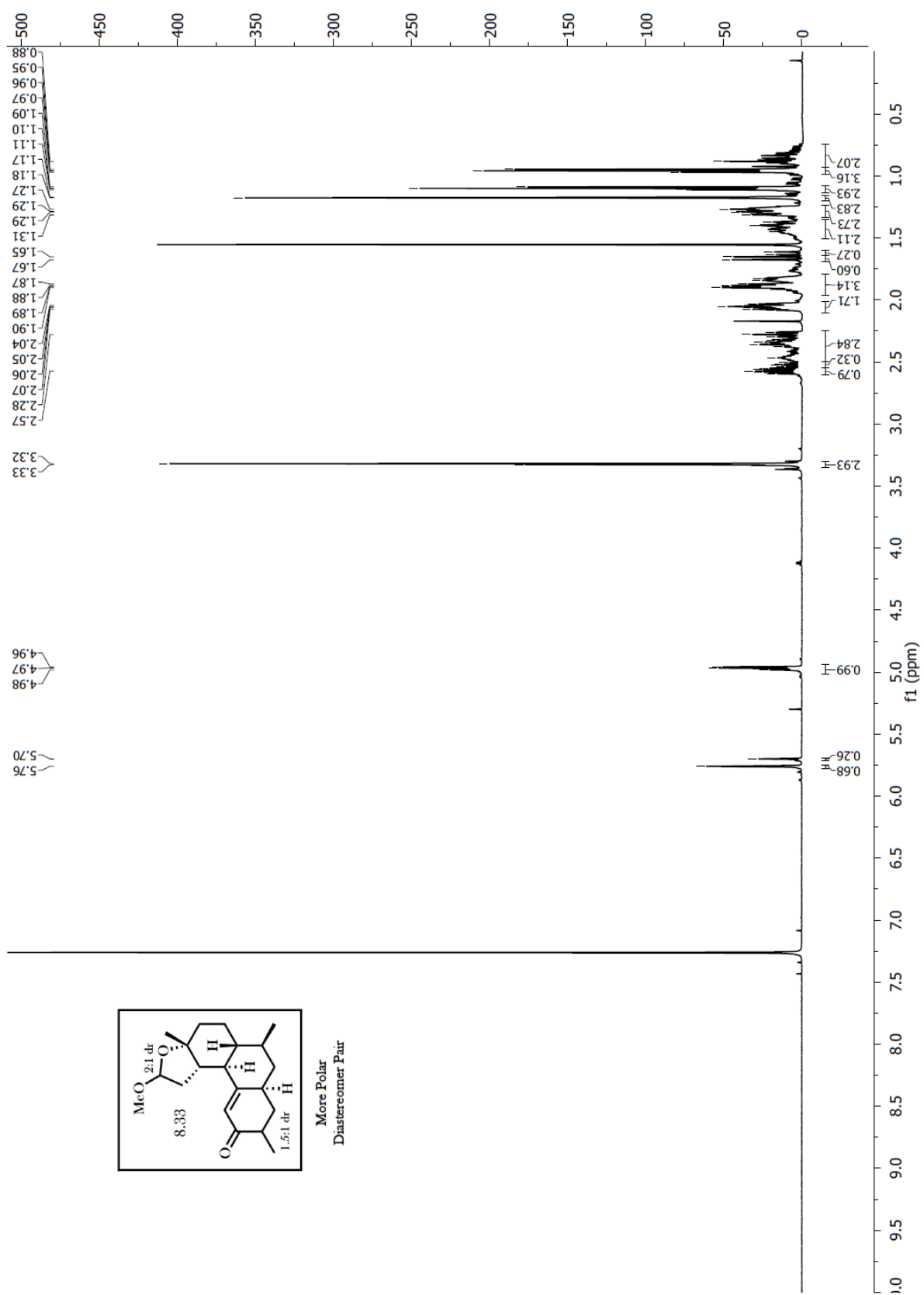


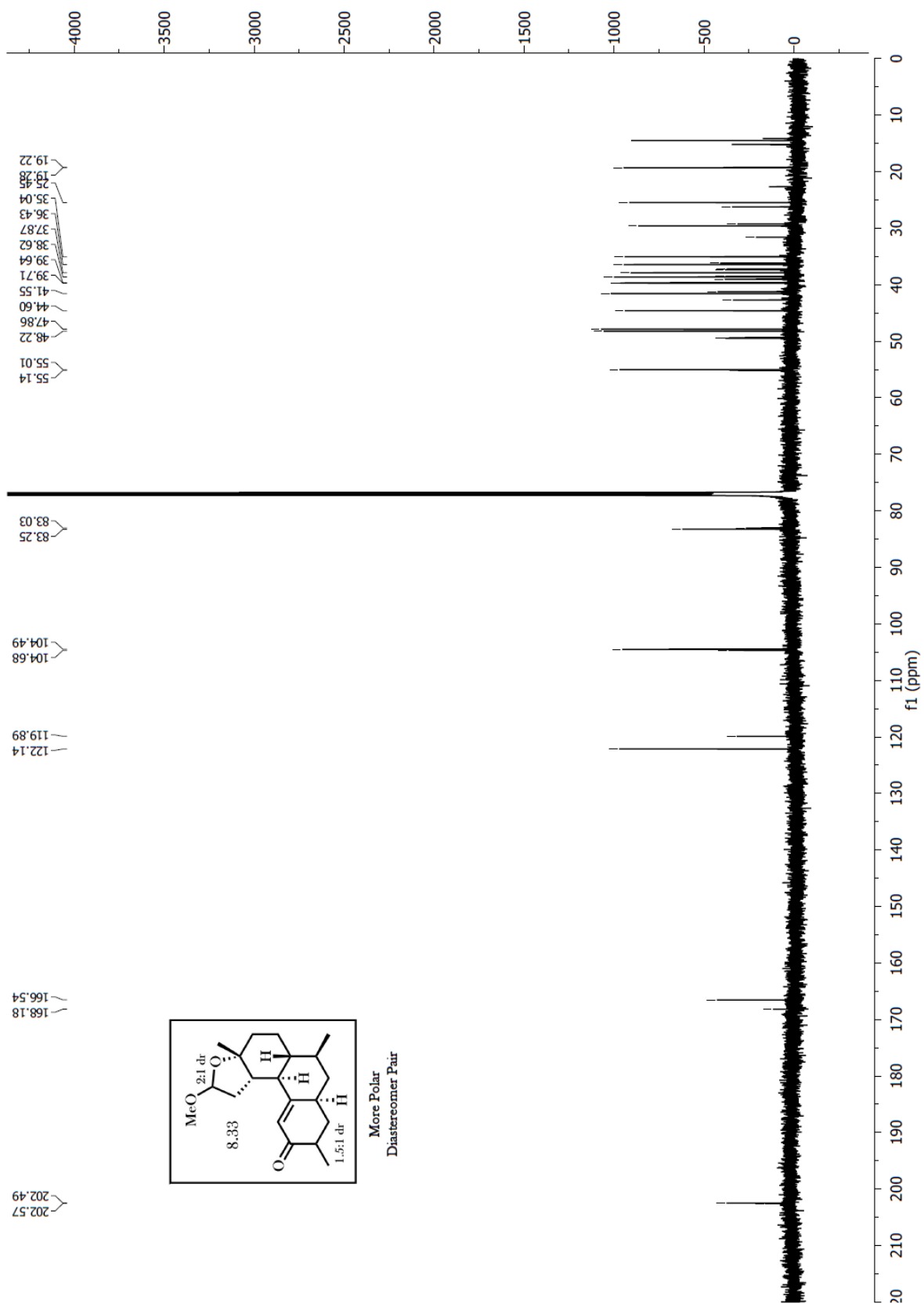


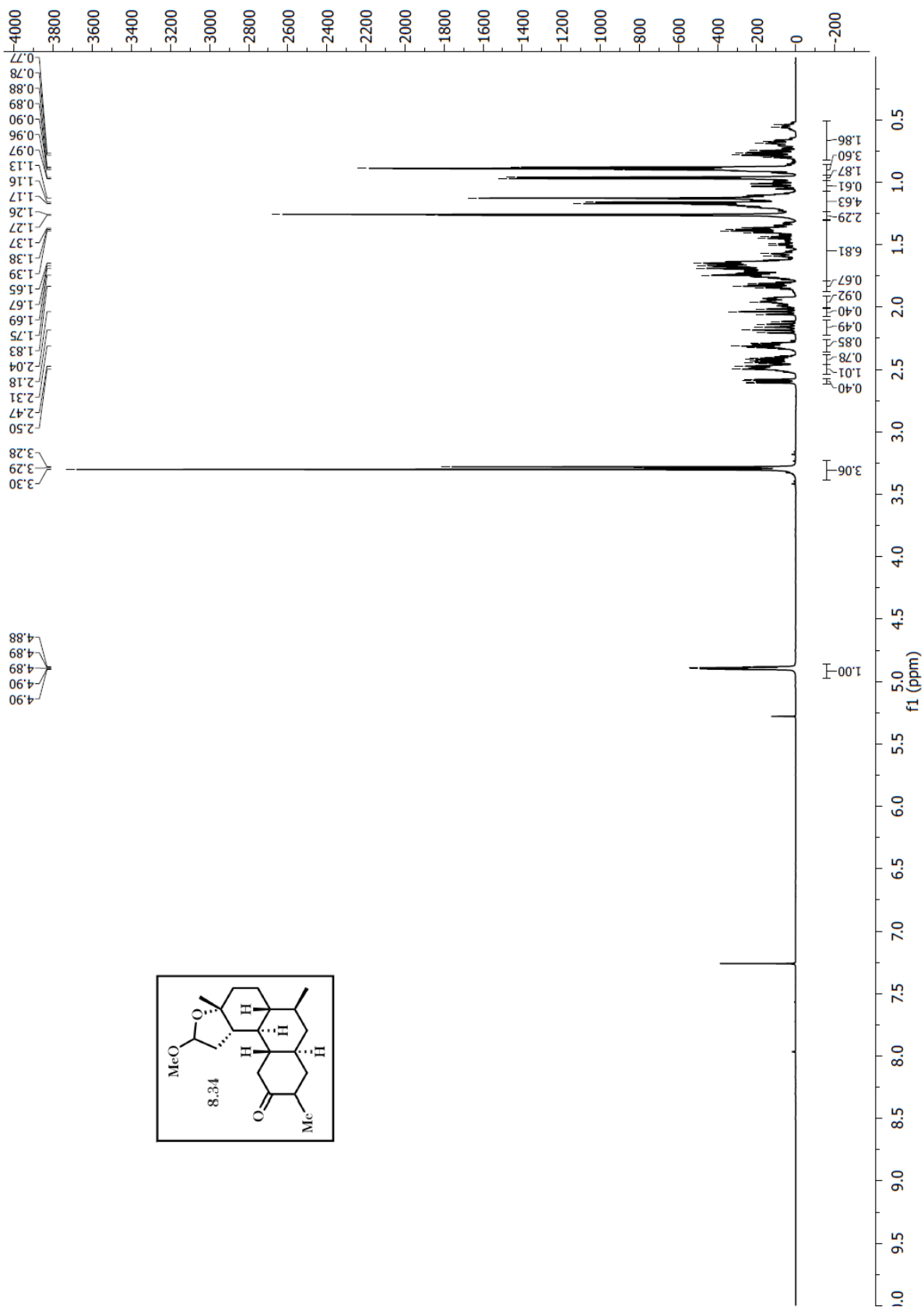
Mixture of Diastereomers

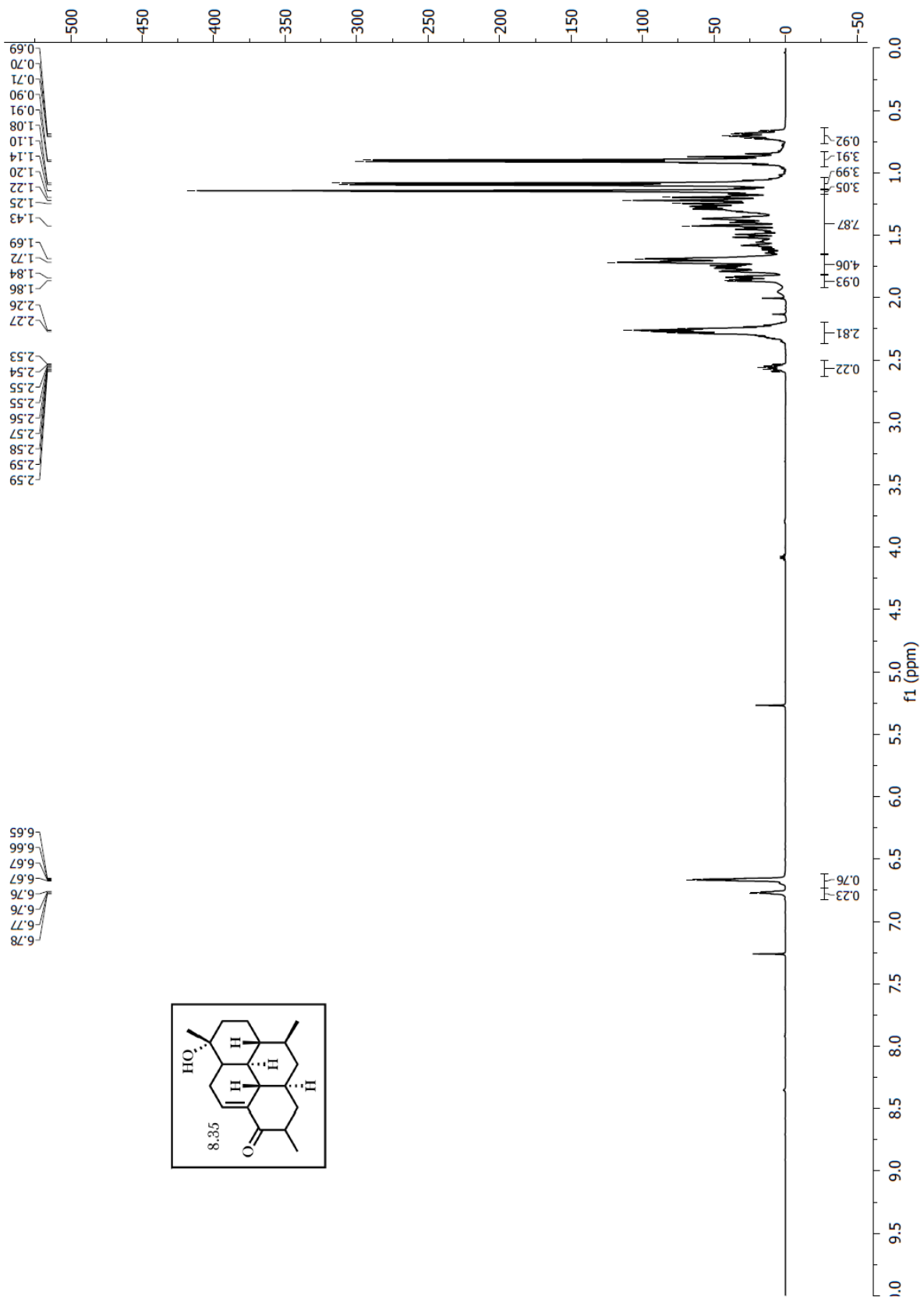


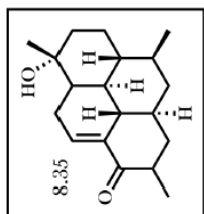
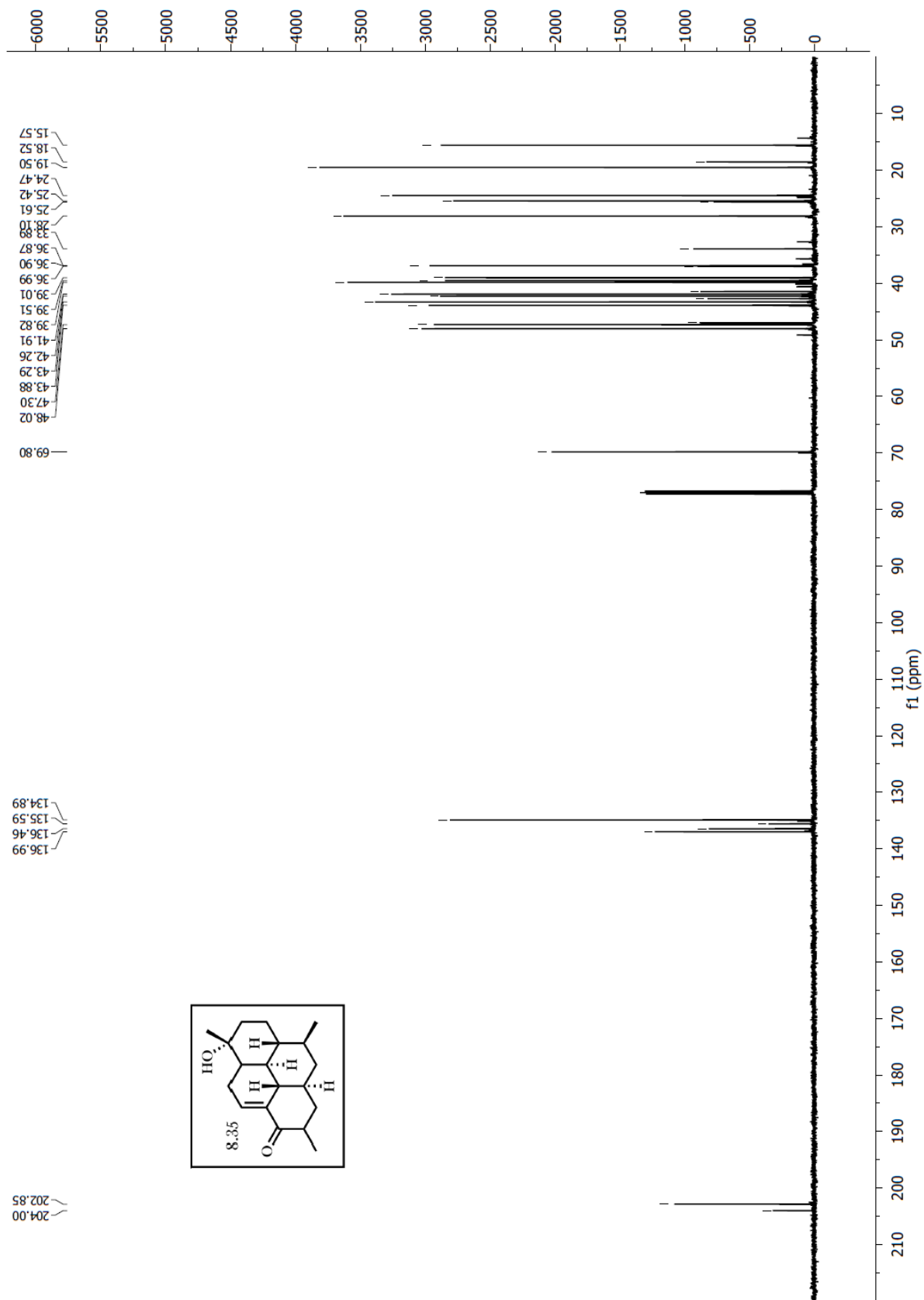


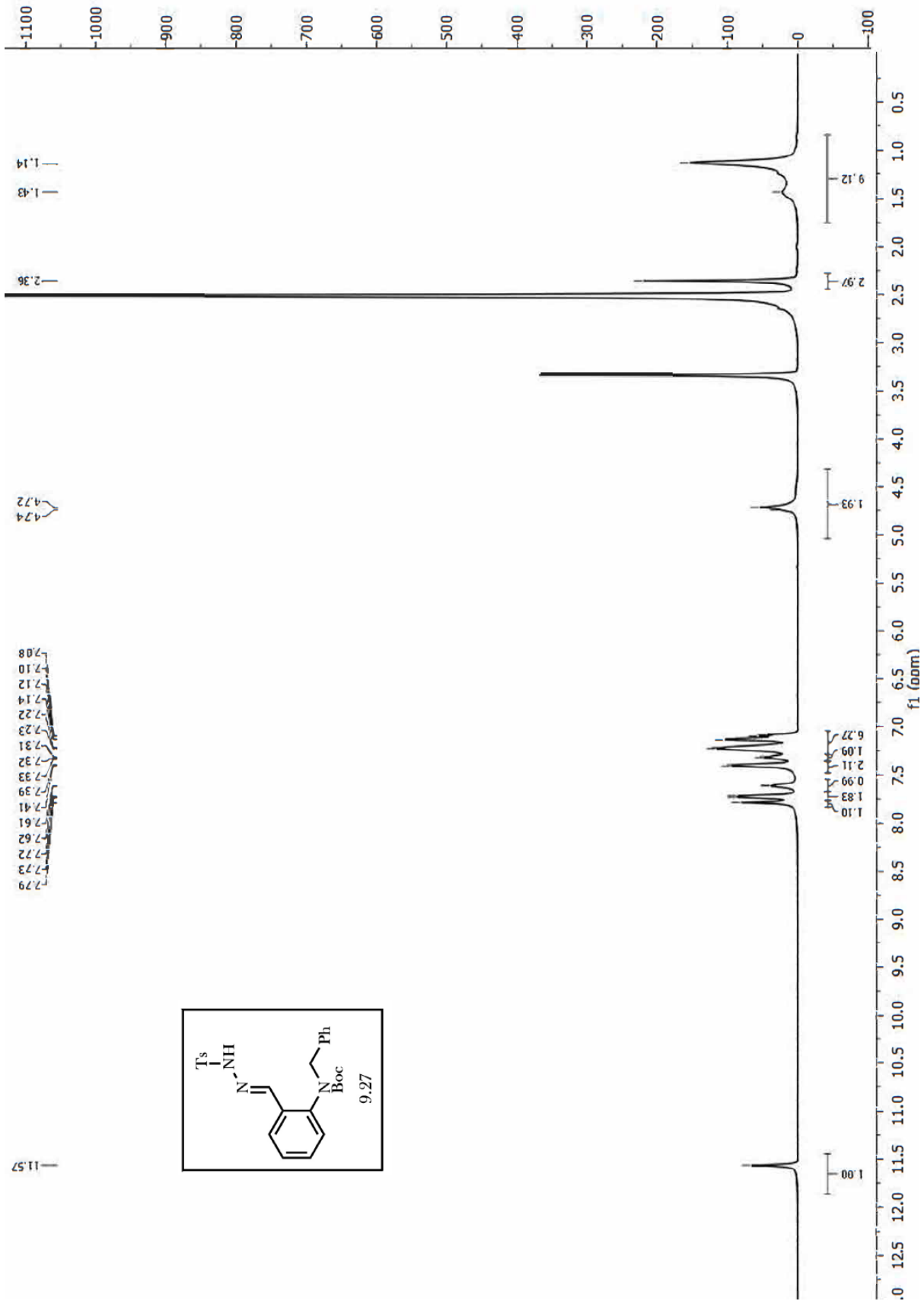


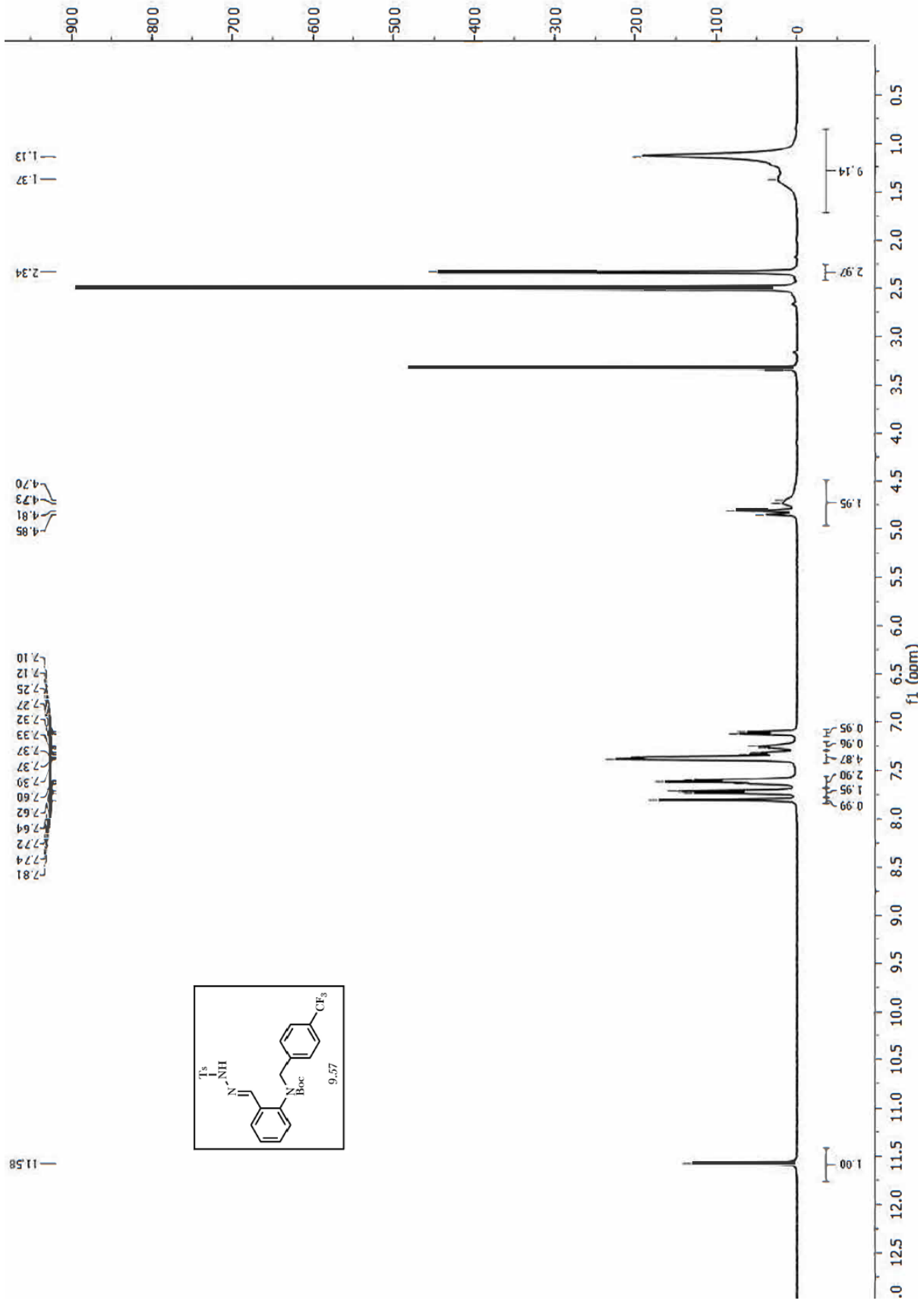


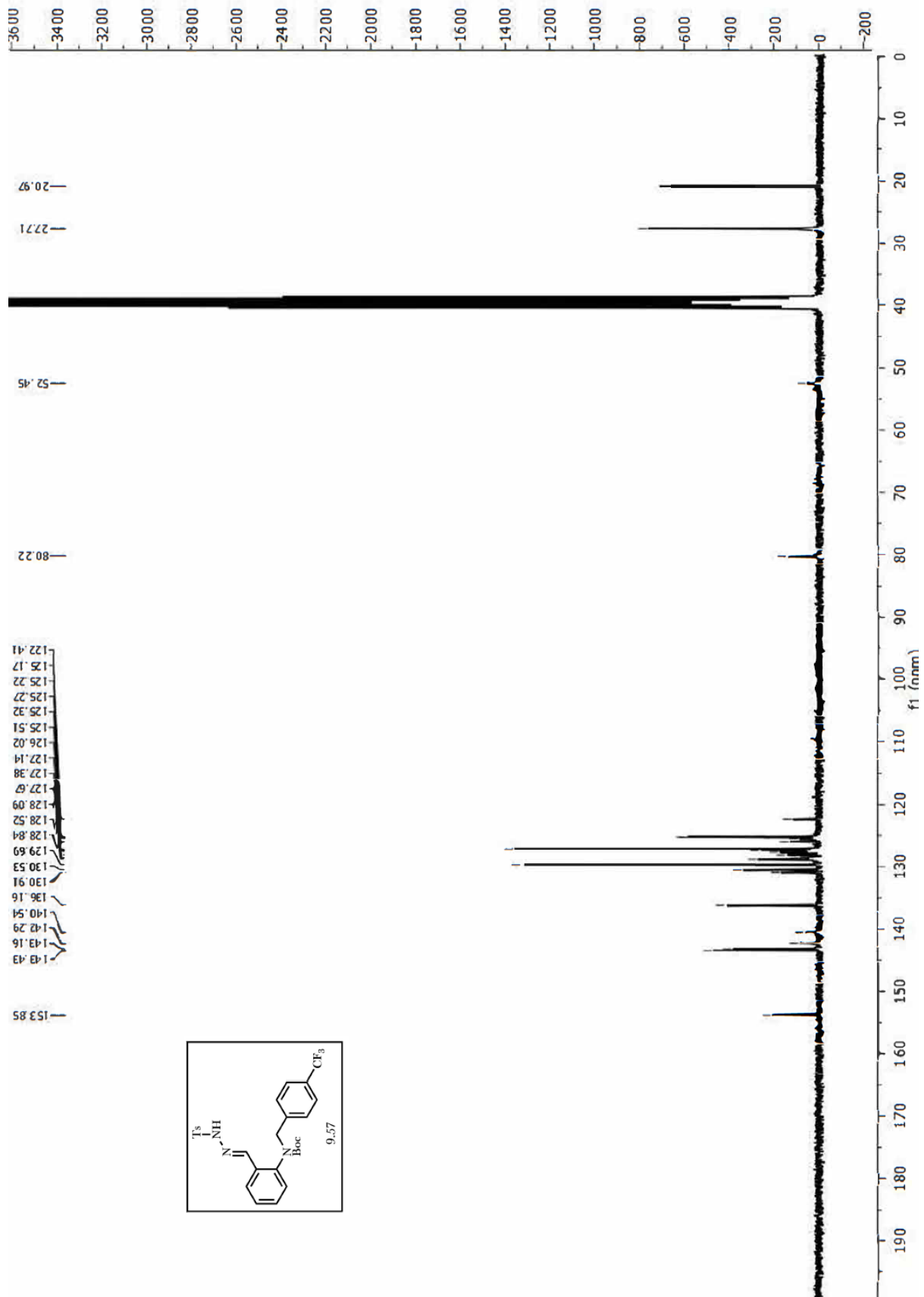


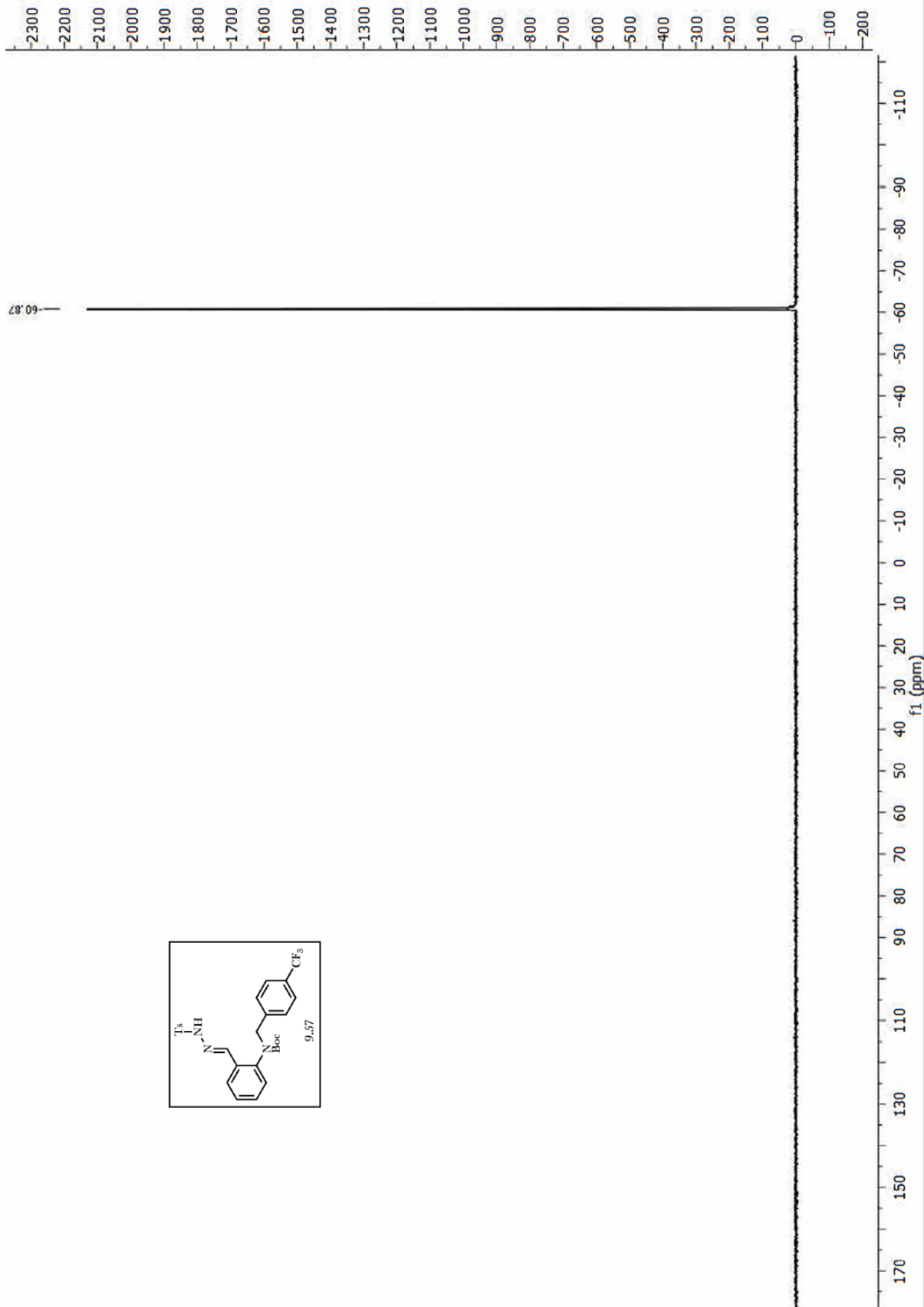


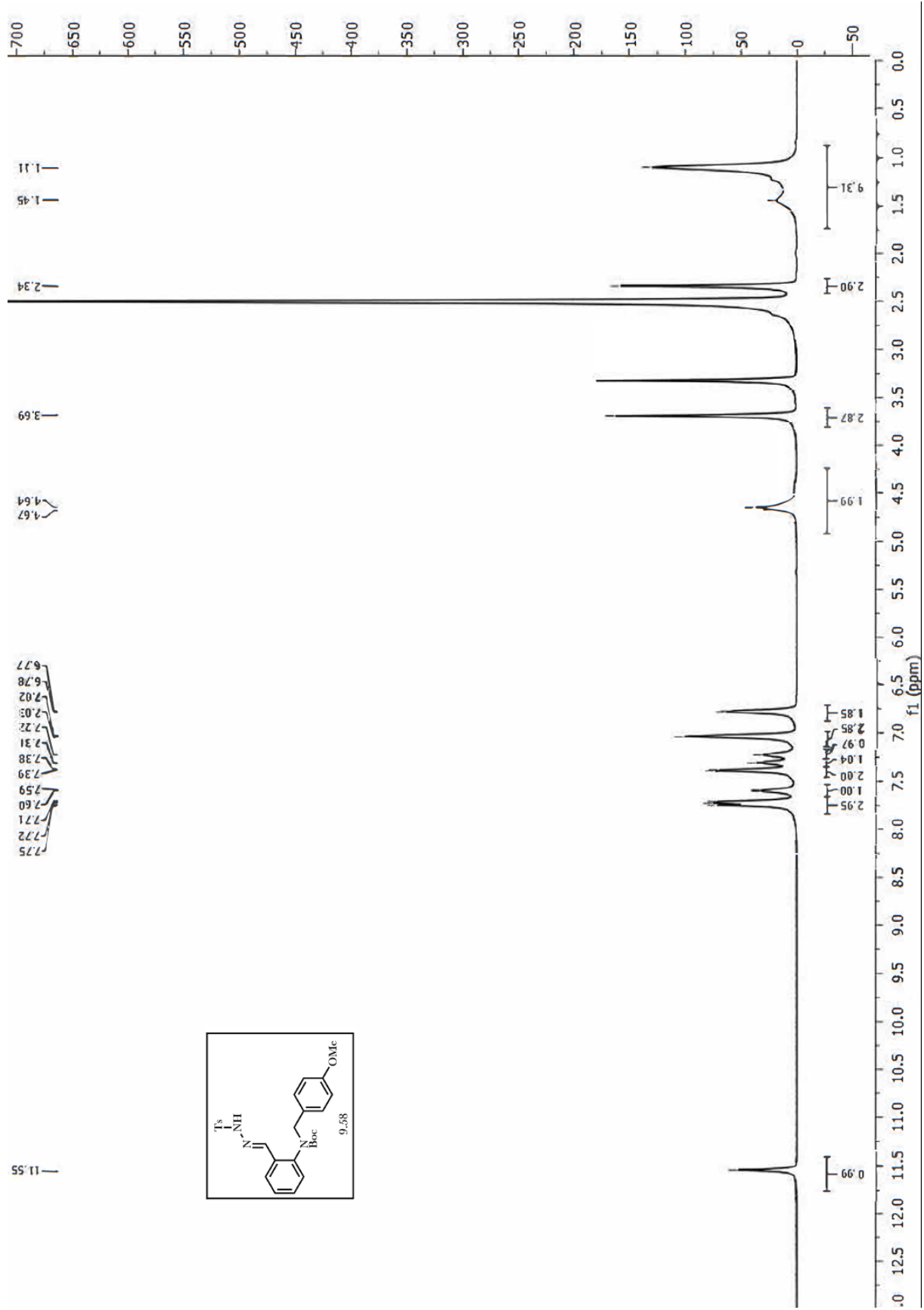


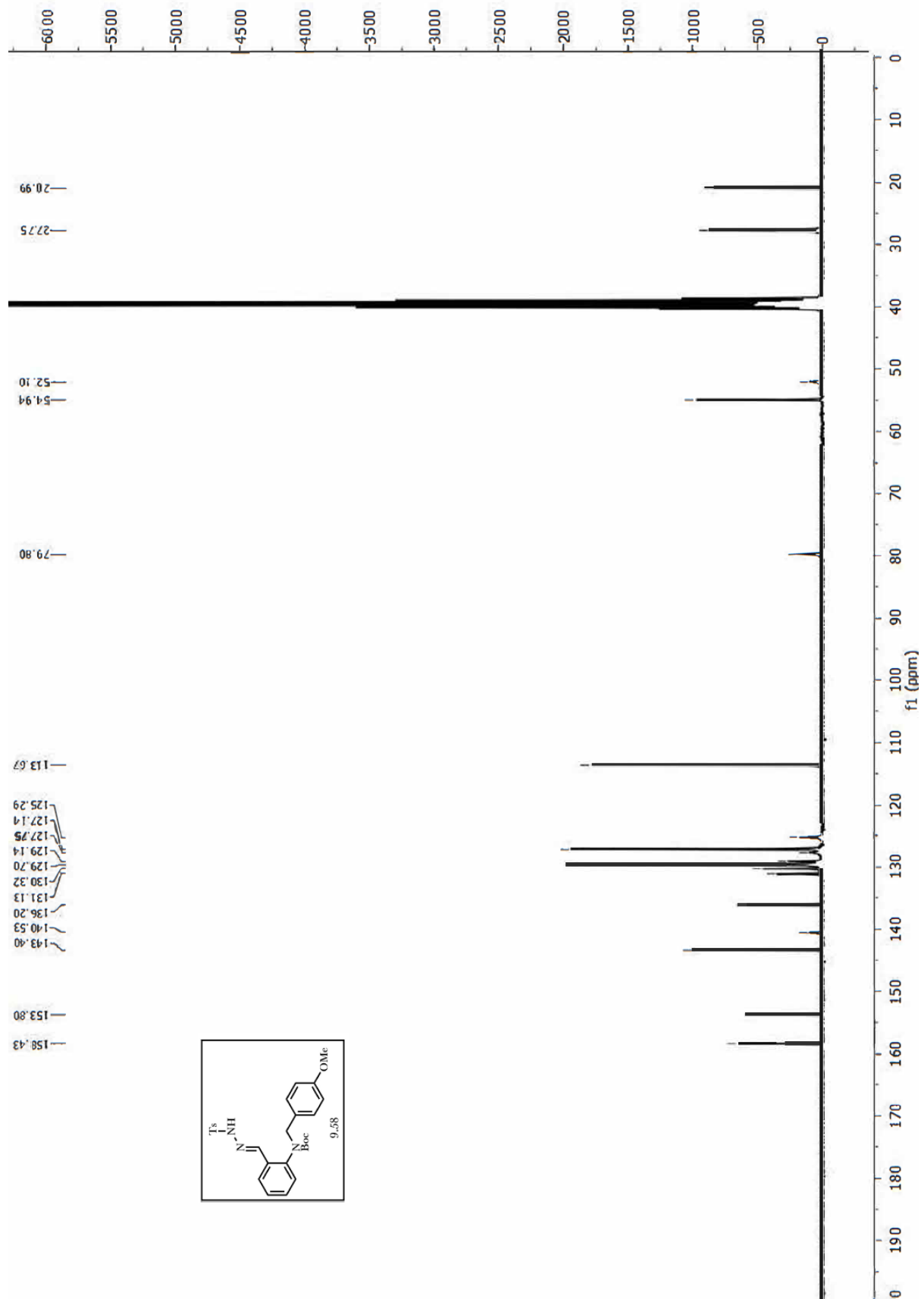


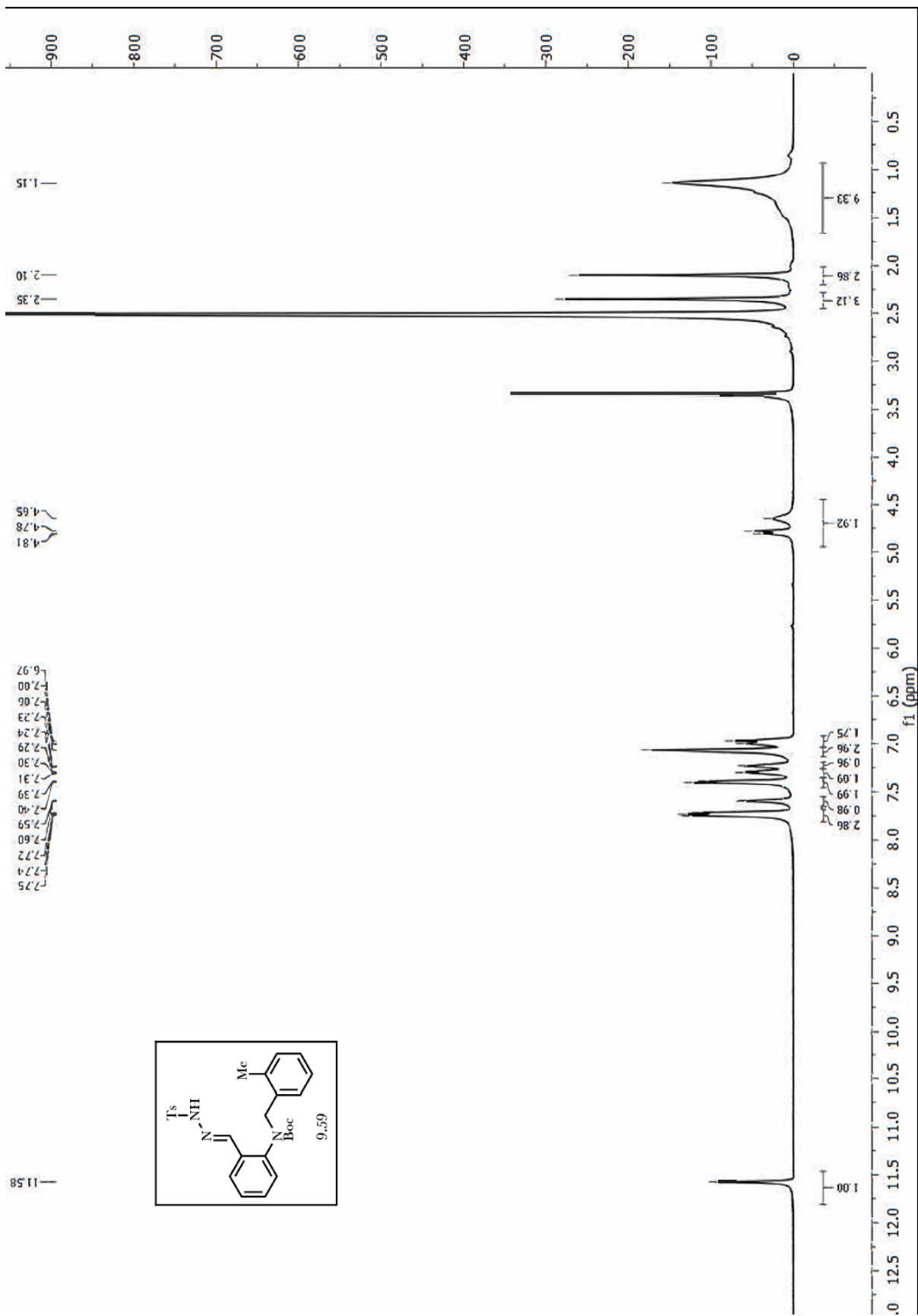


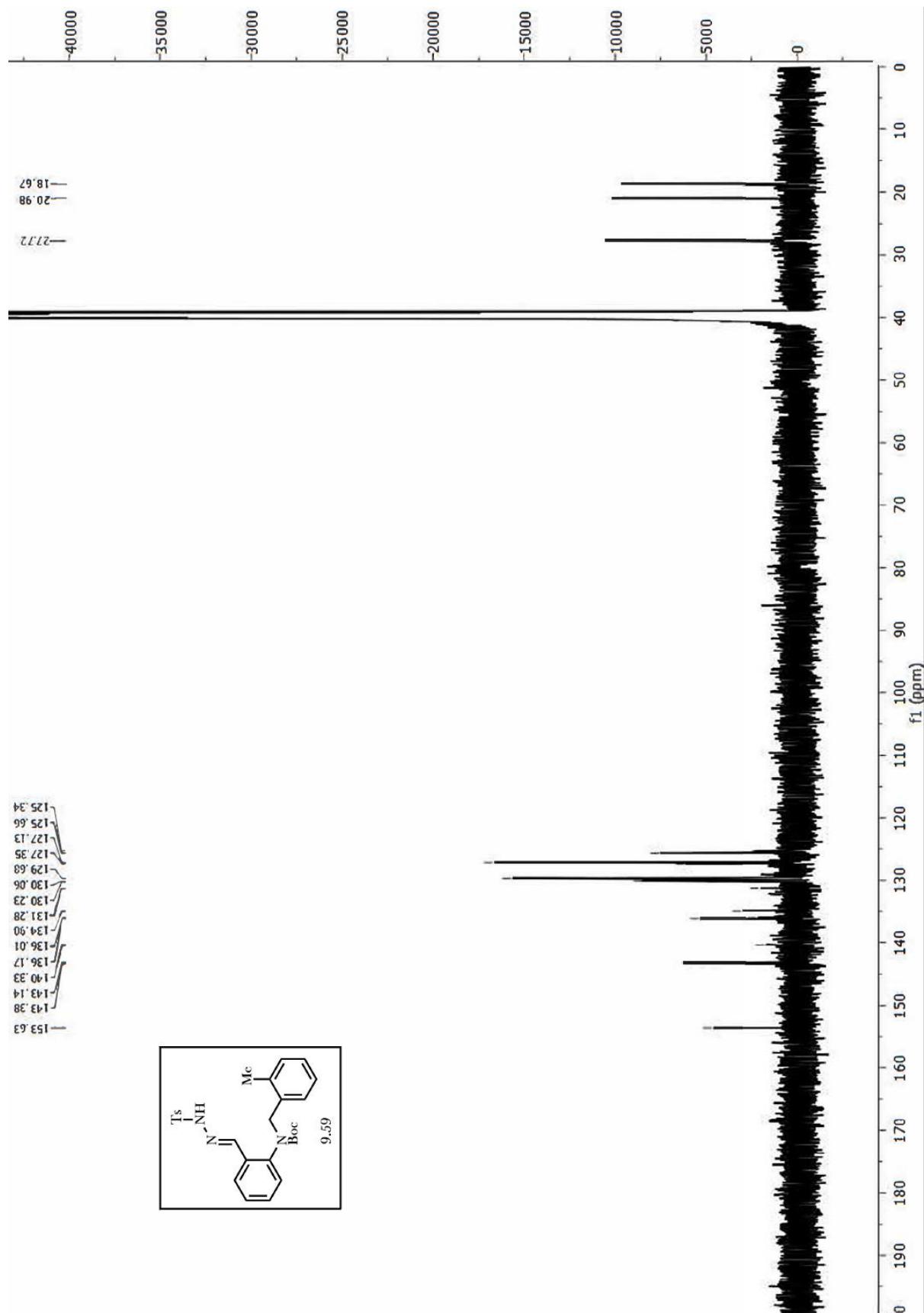


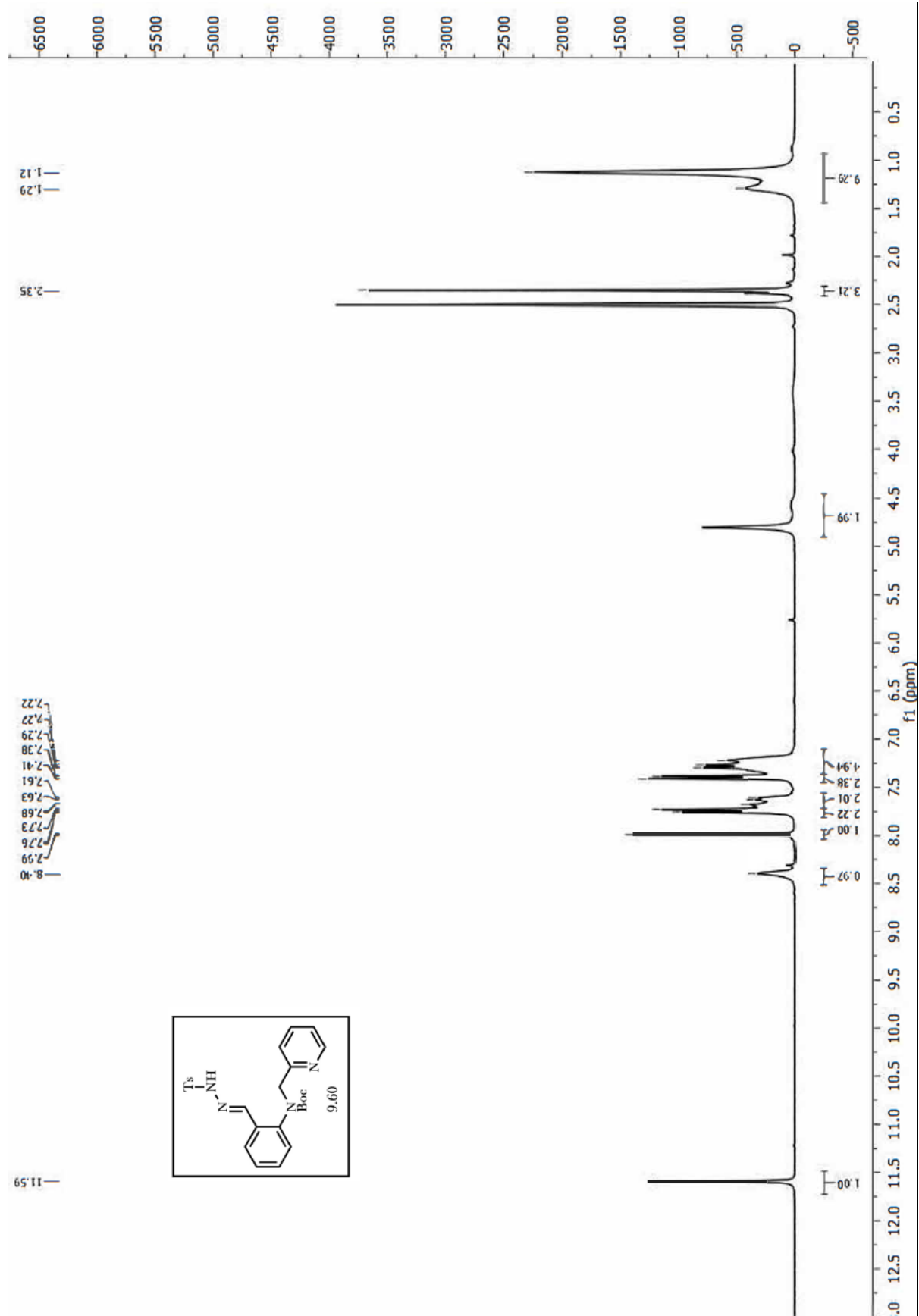


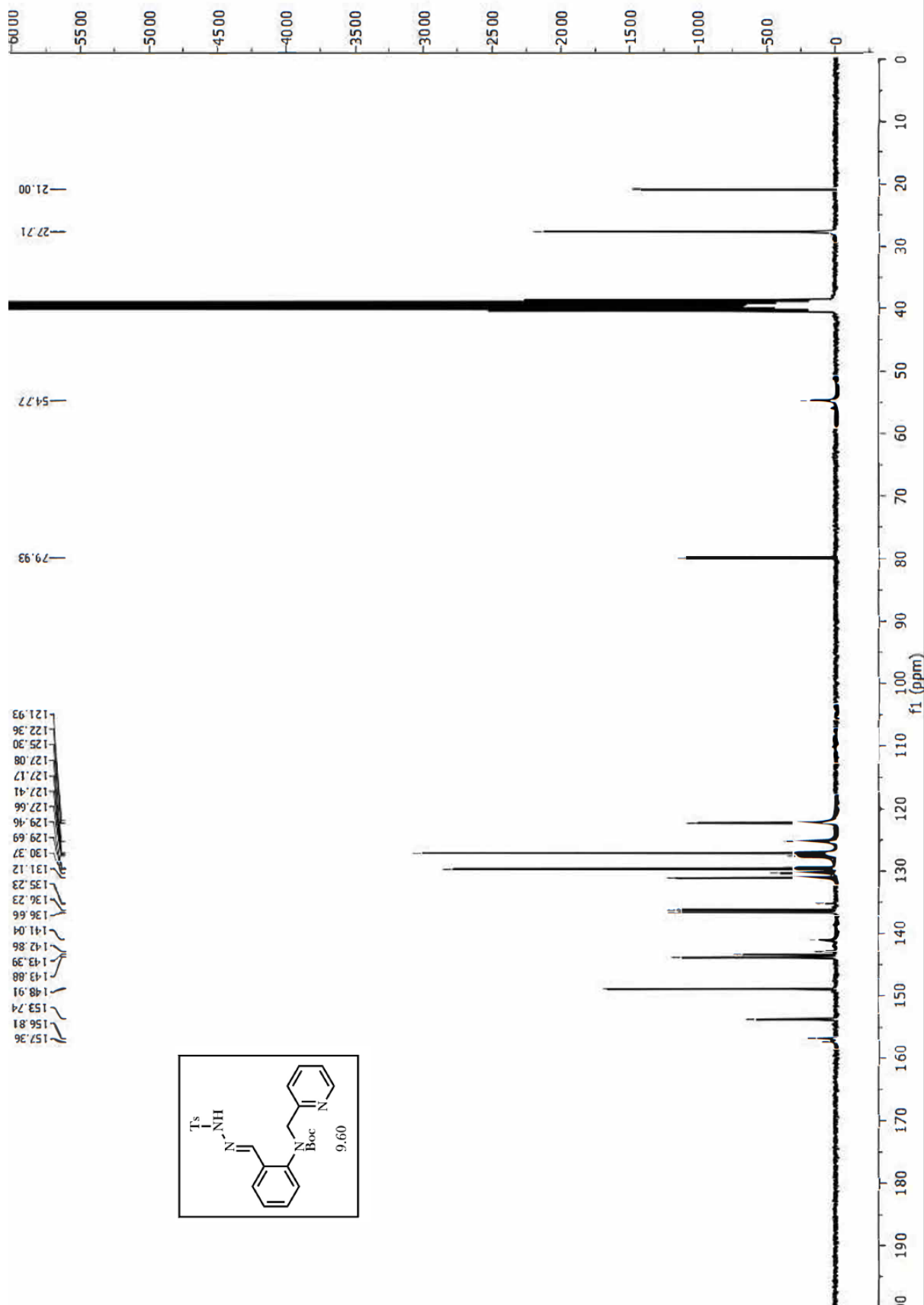


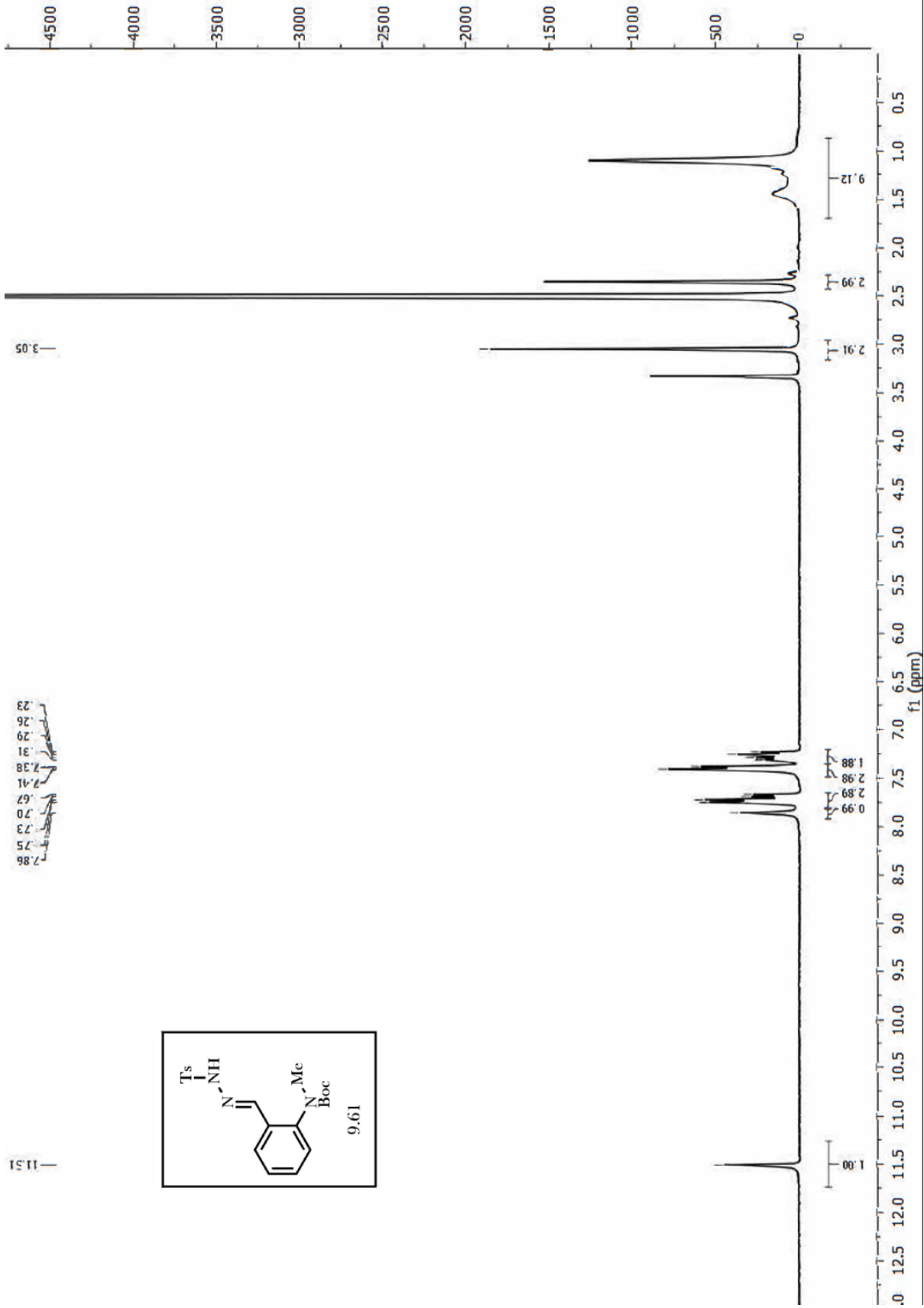


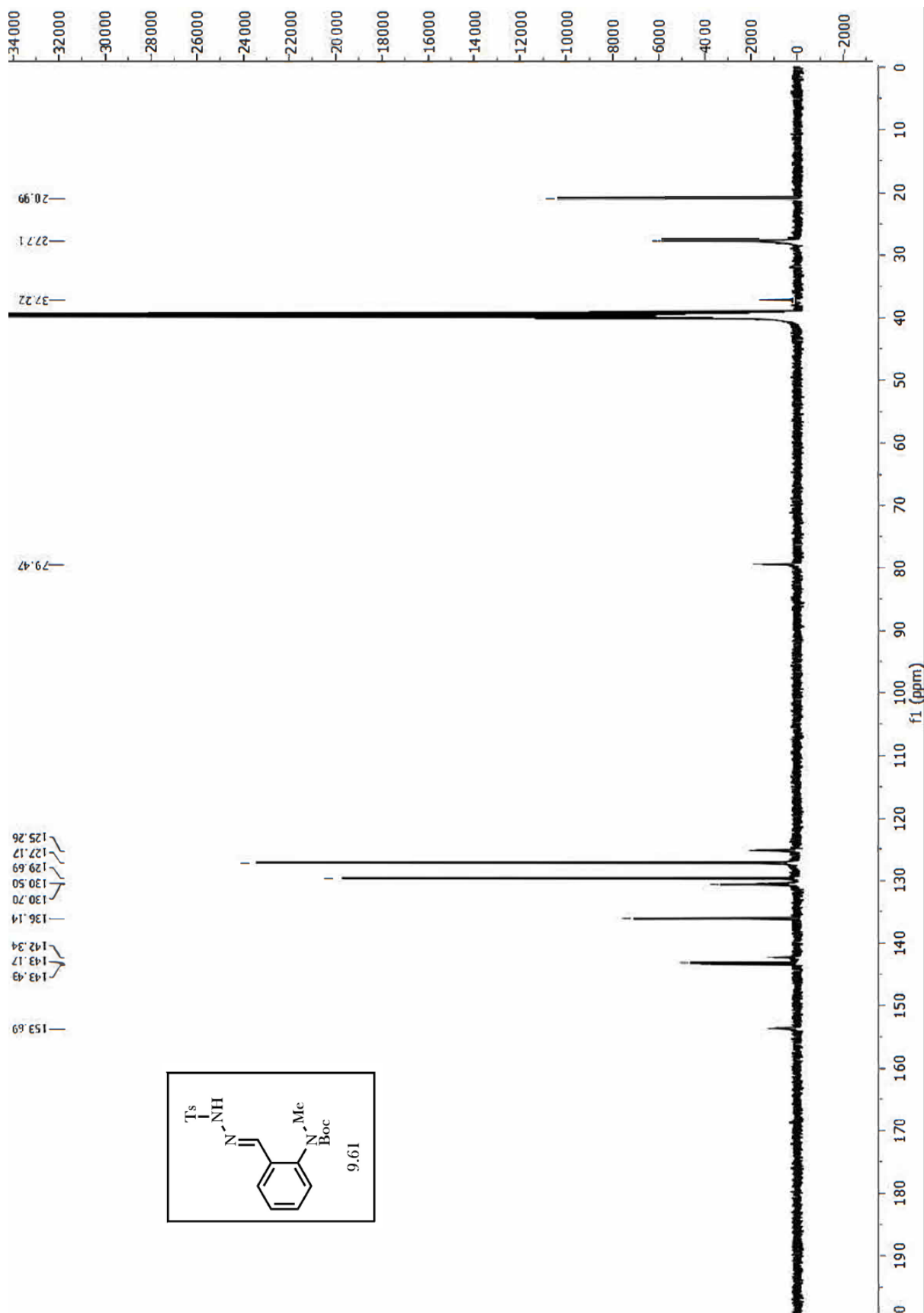


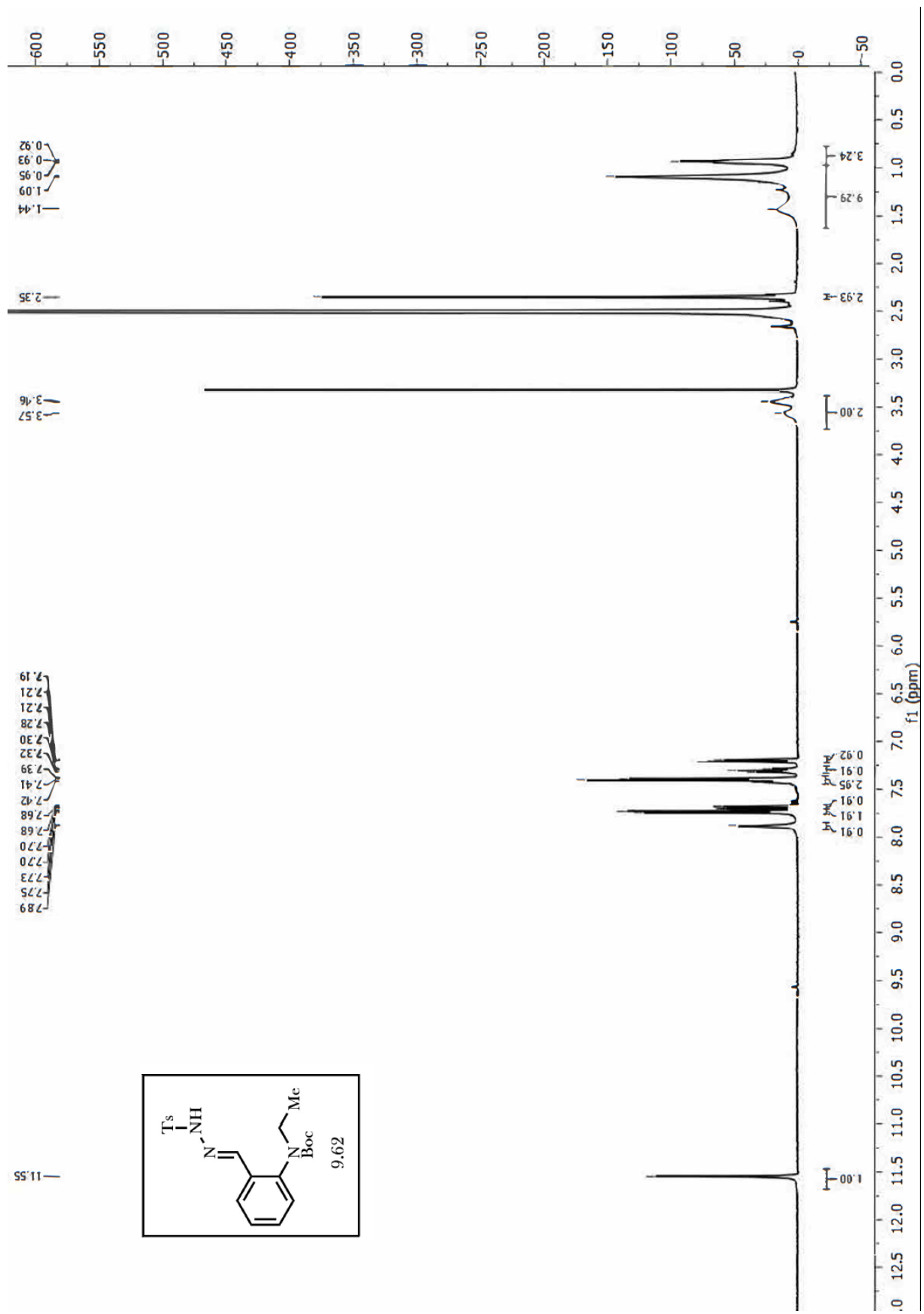


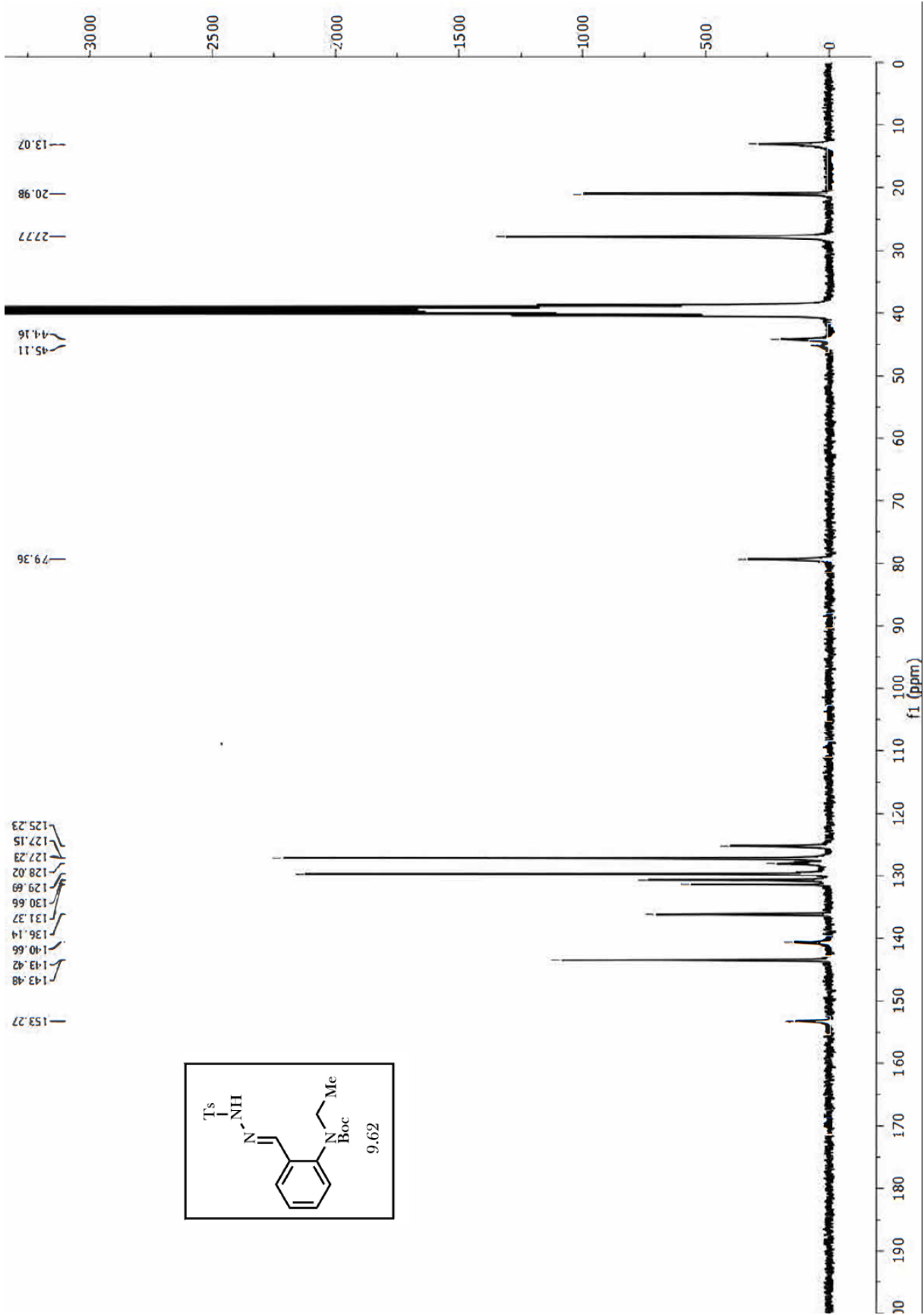


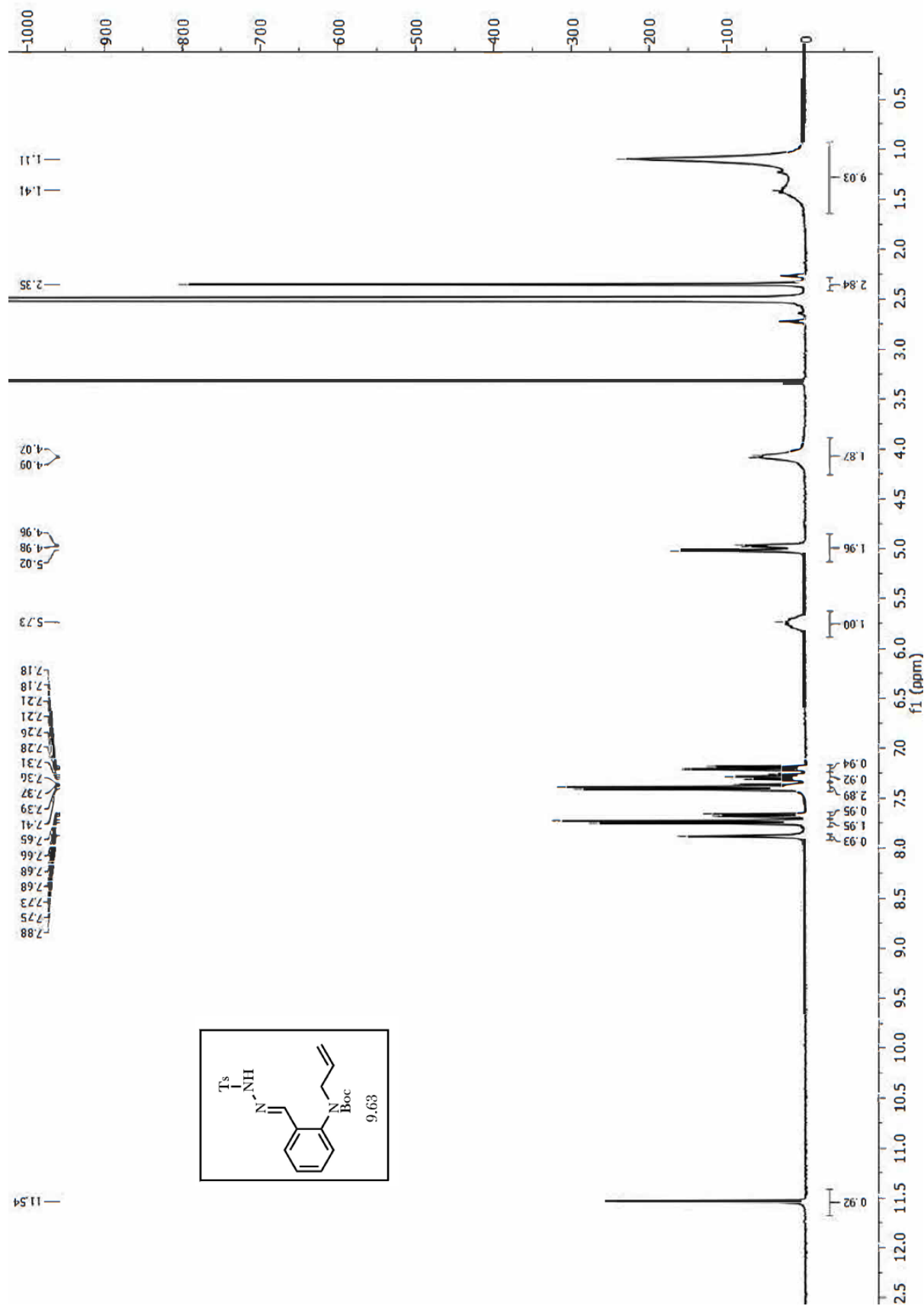


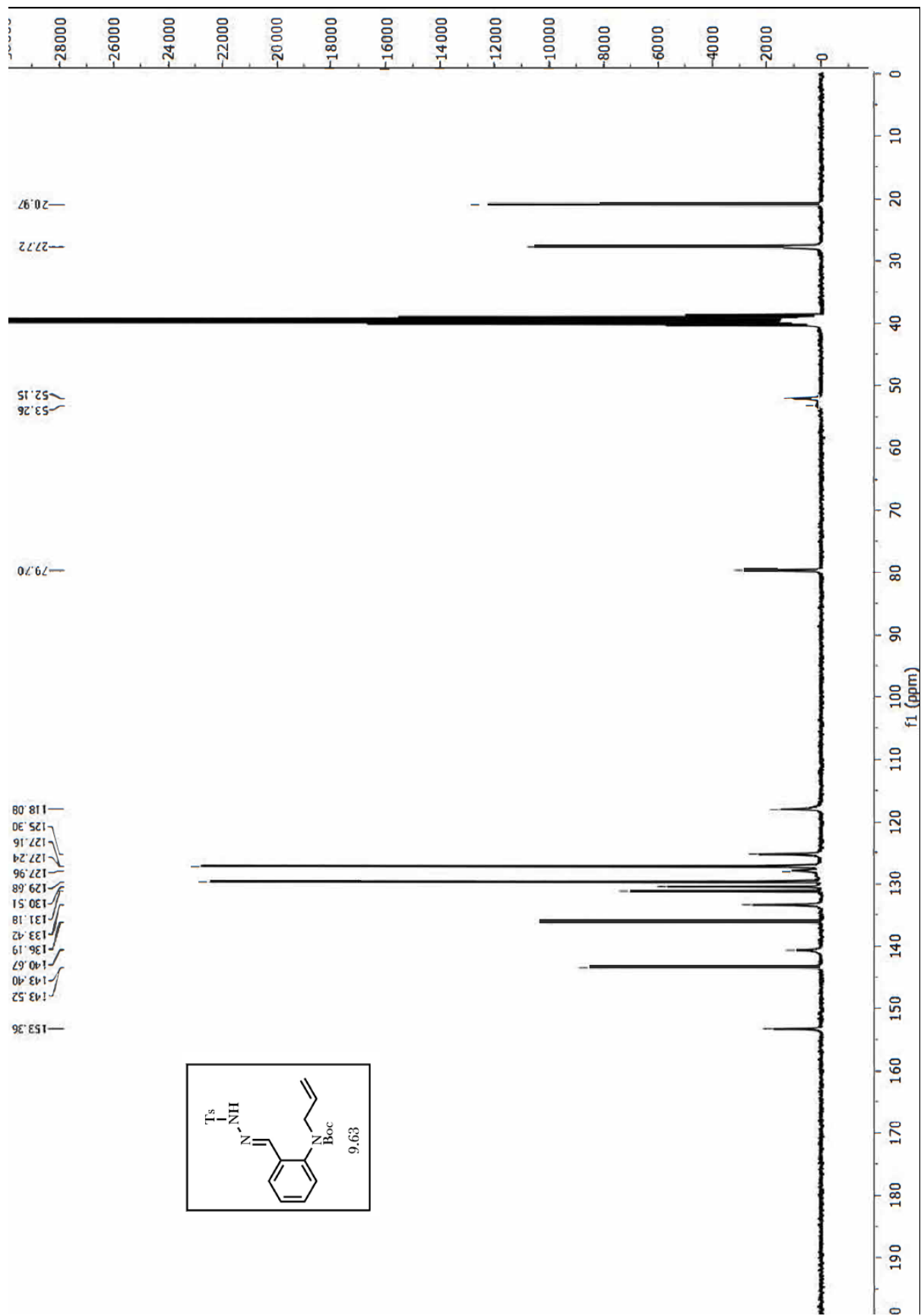


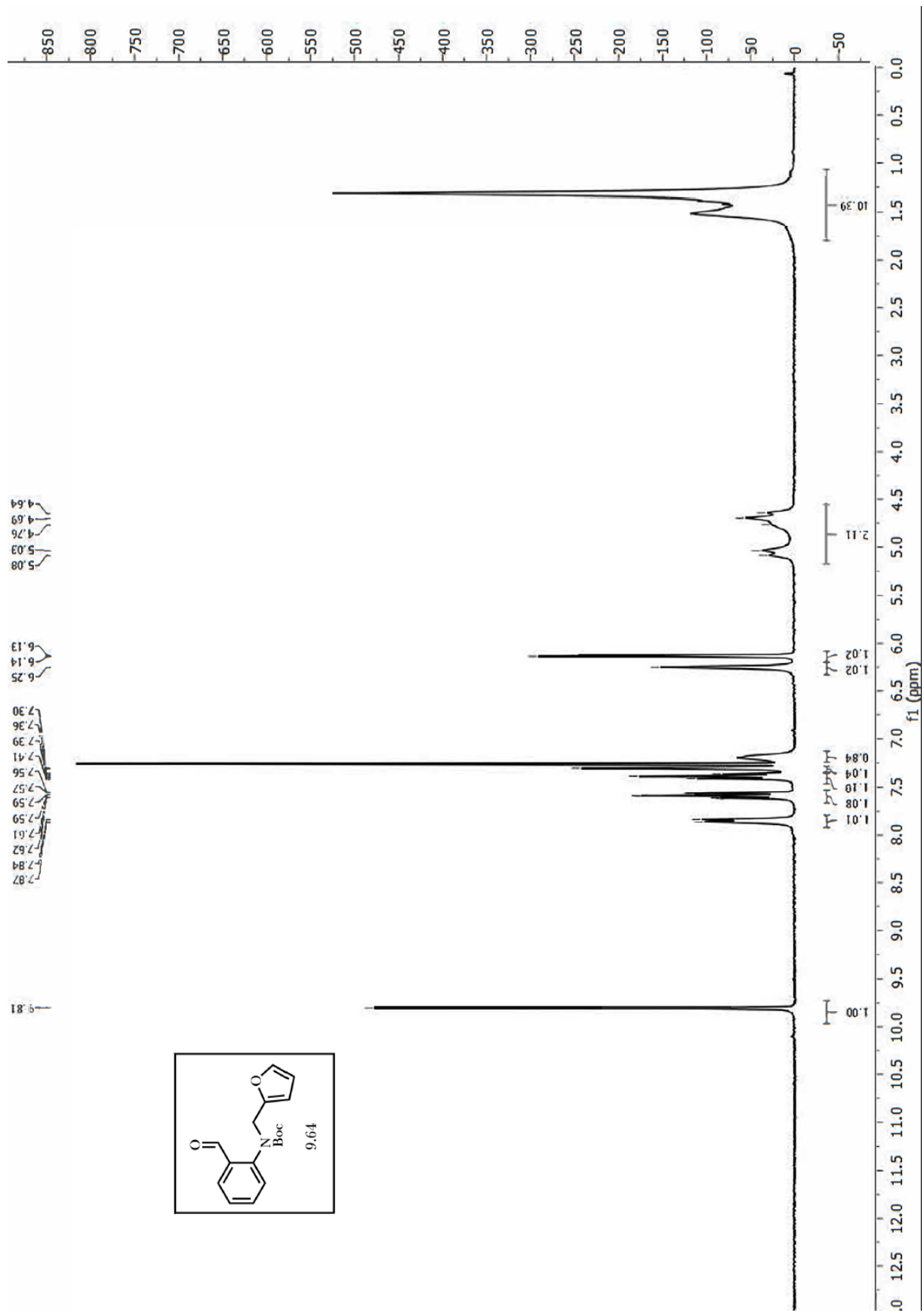


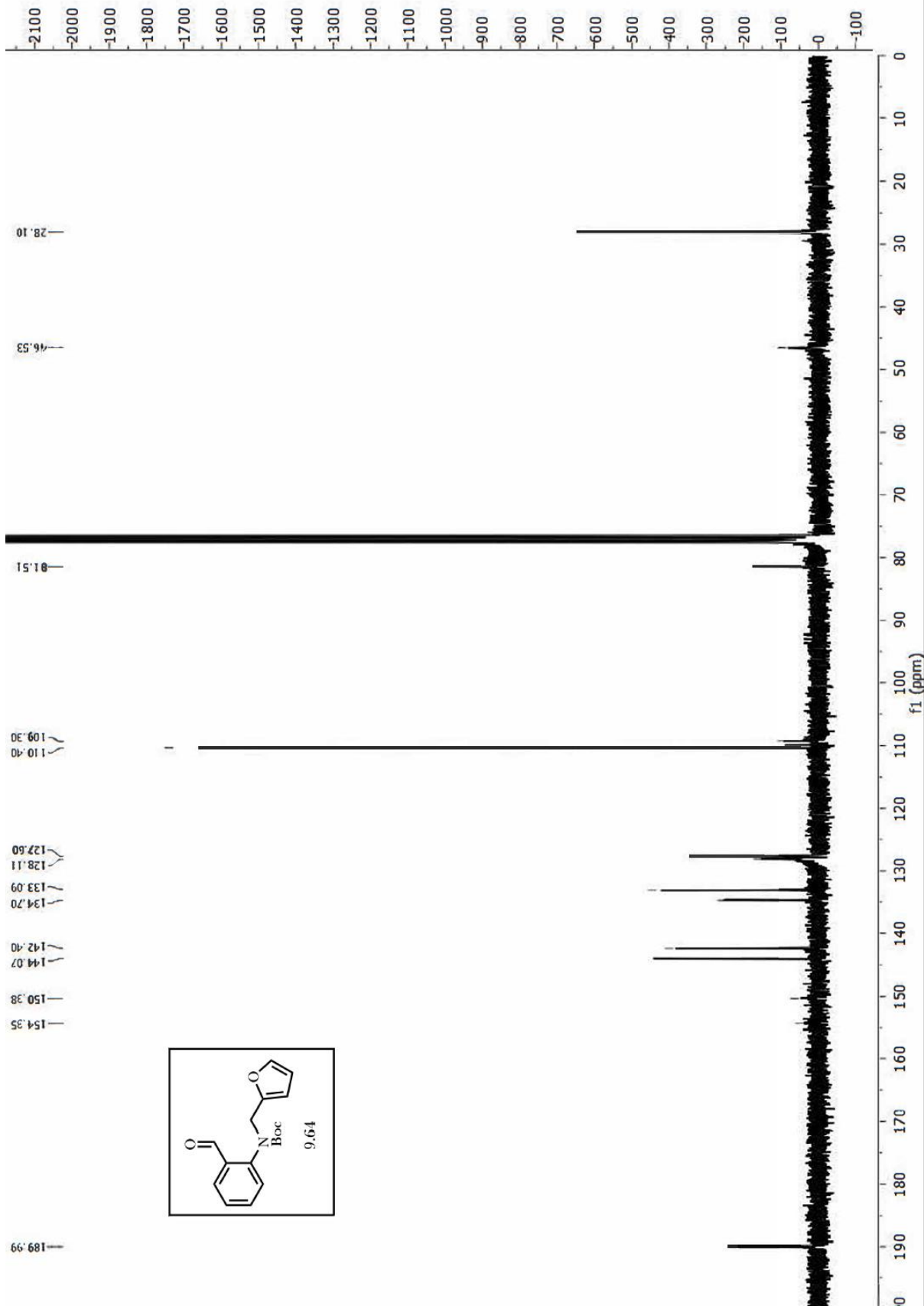


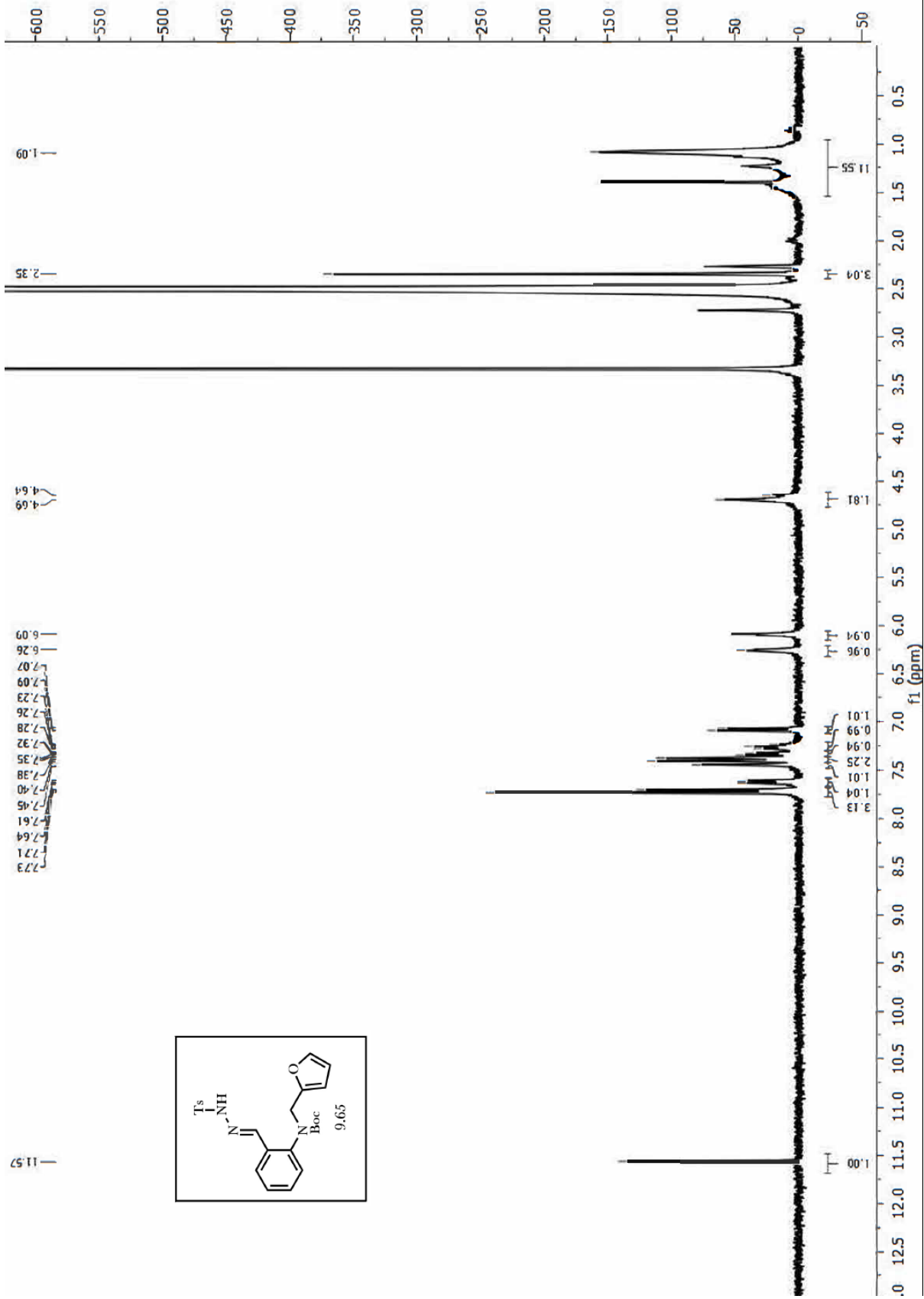


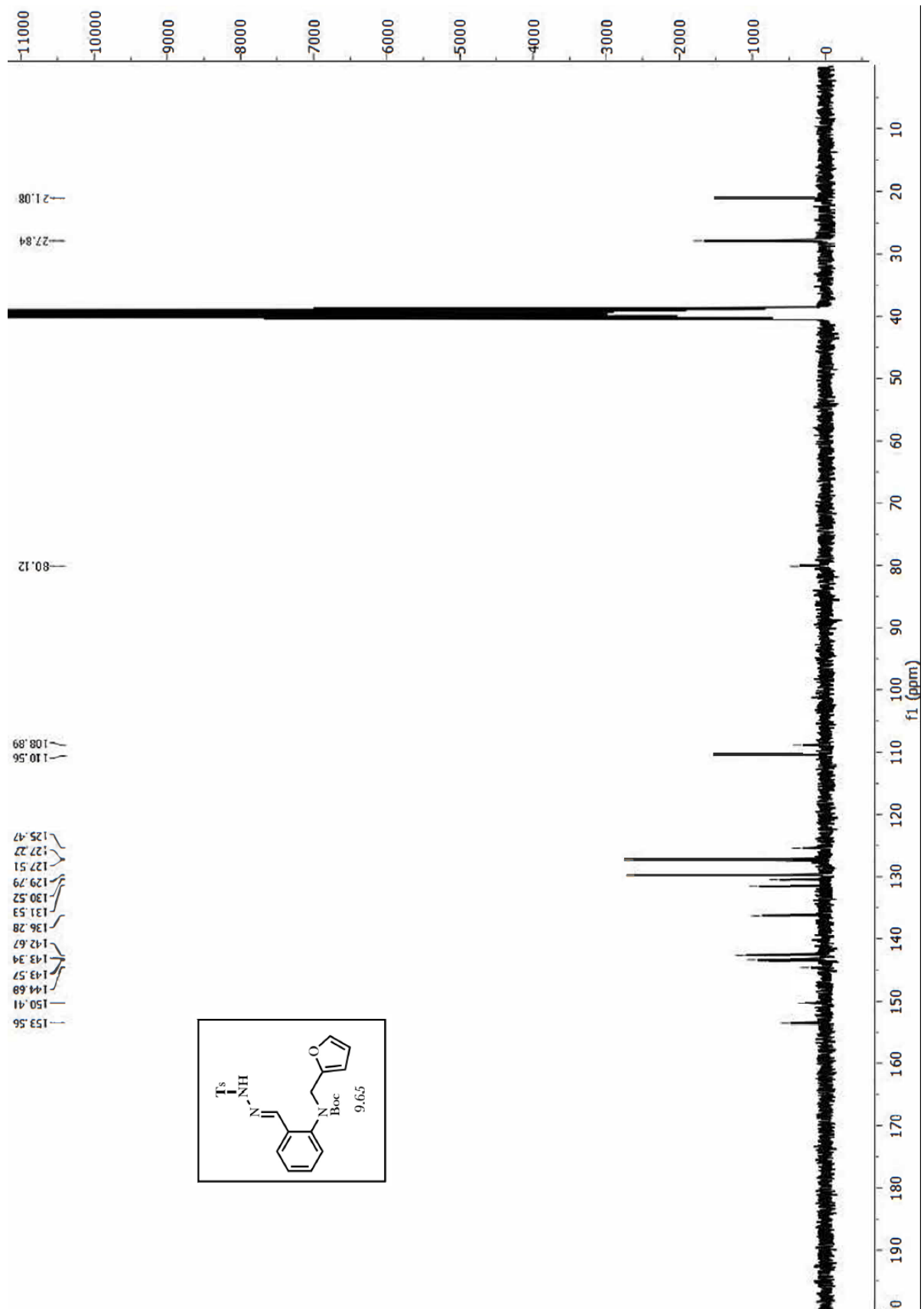


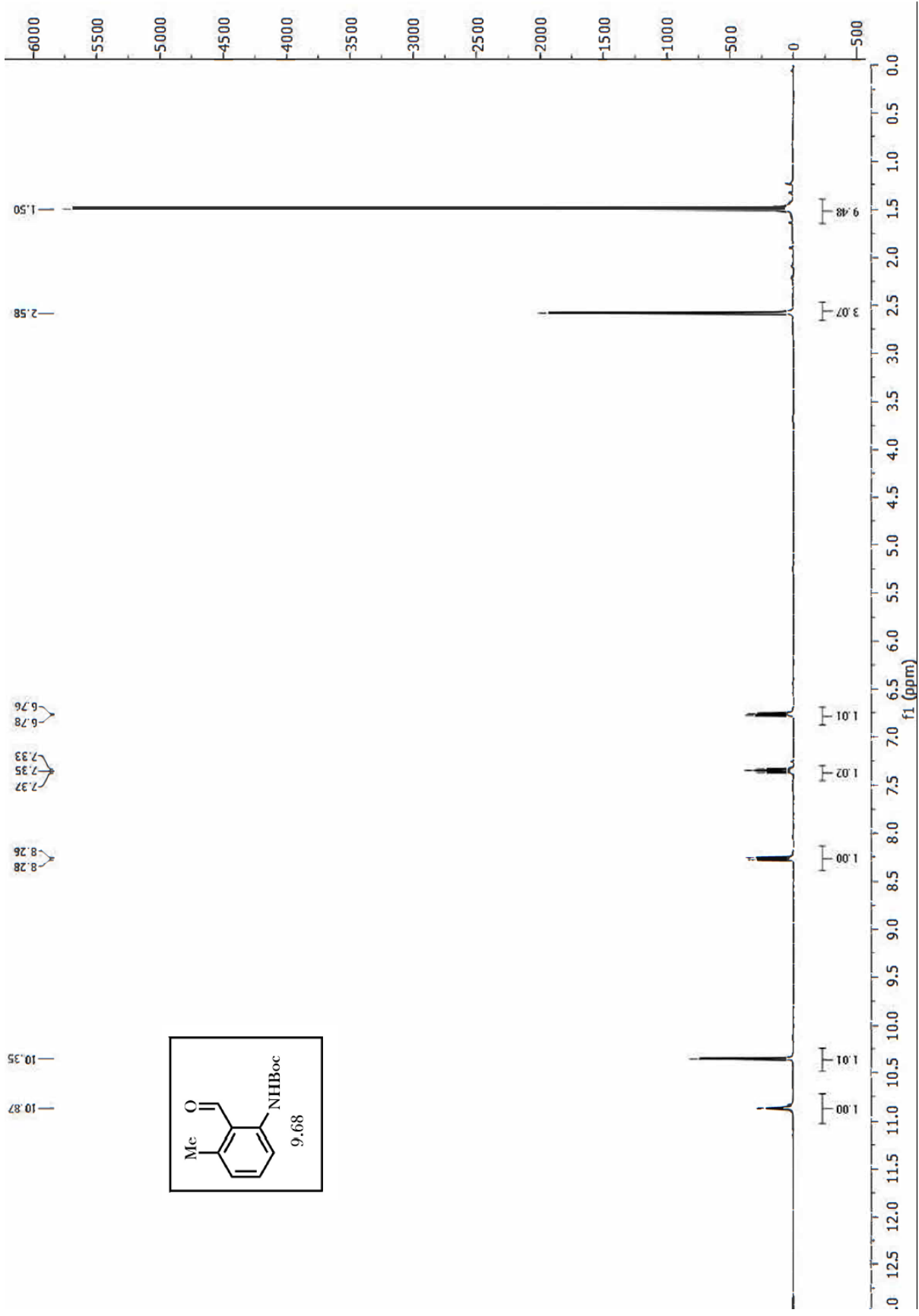


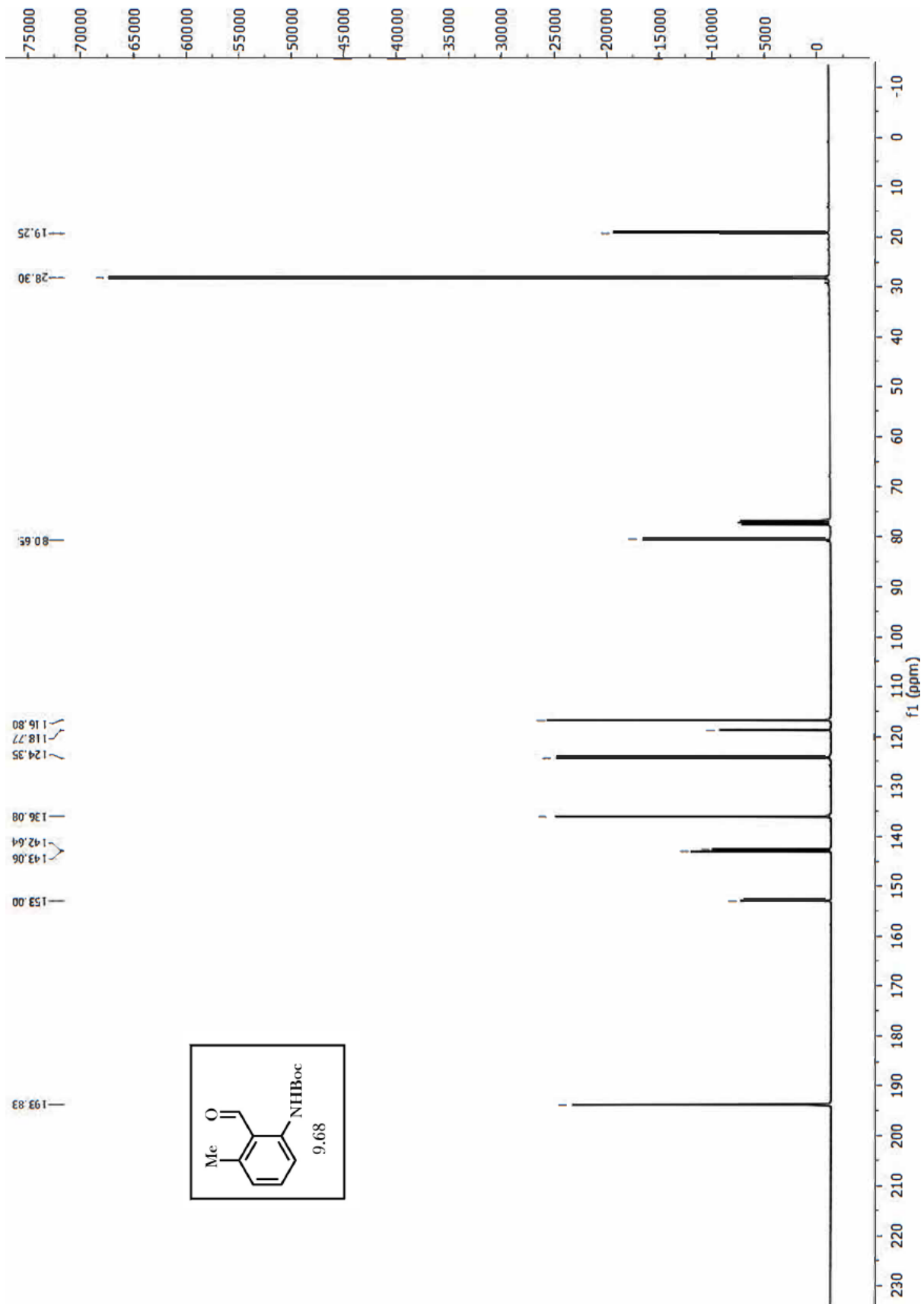


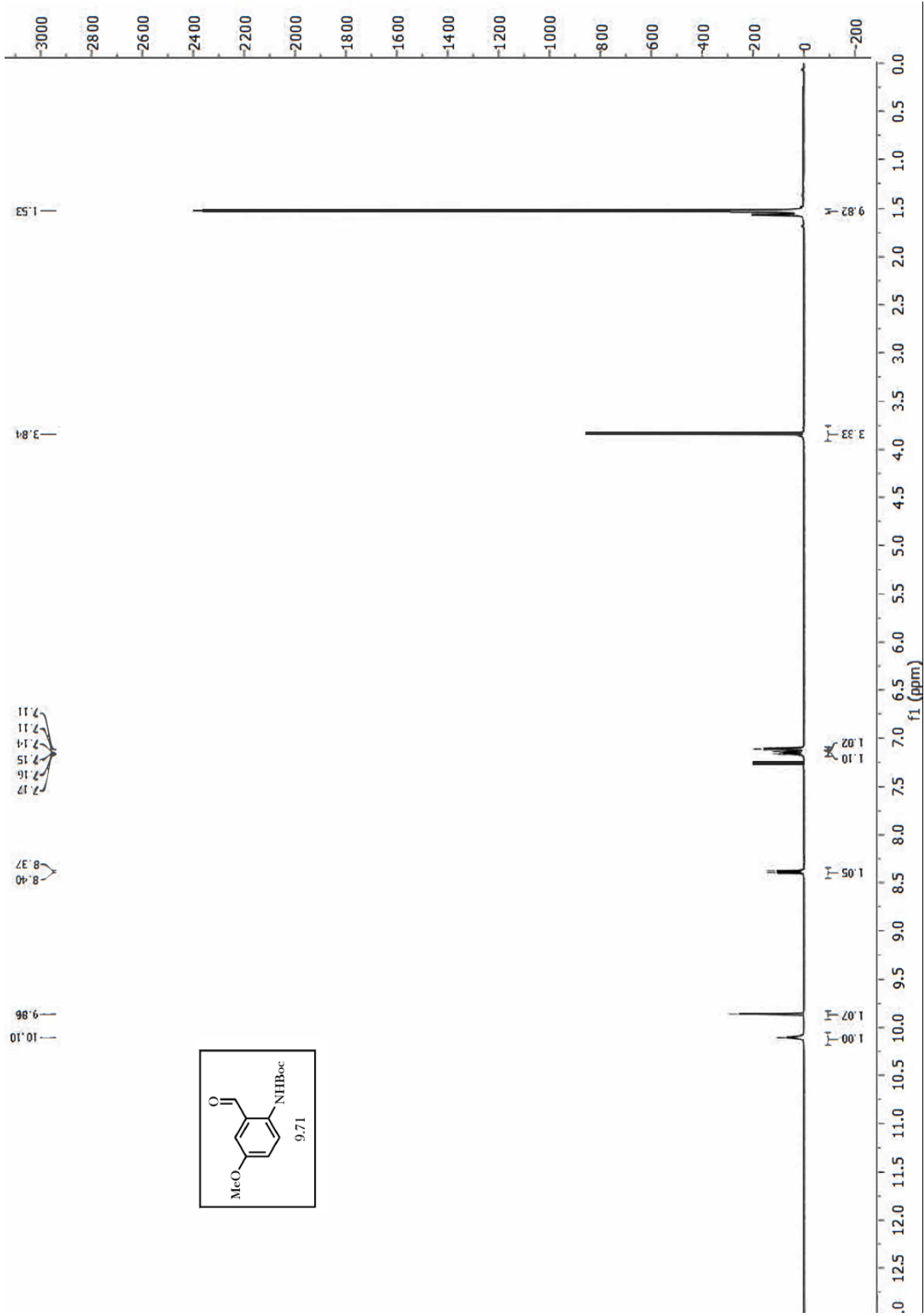


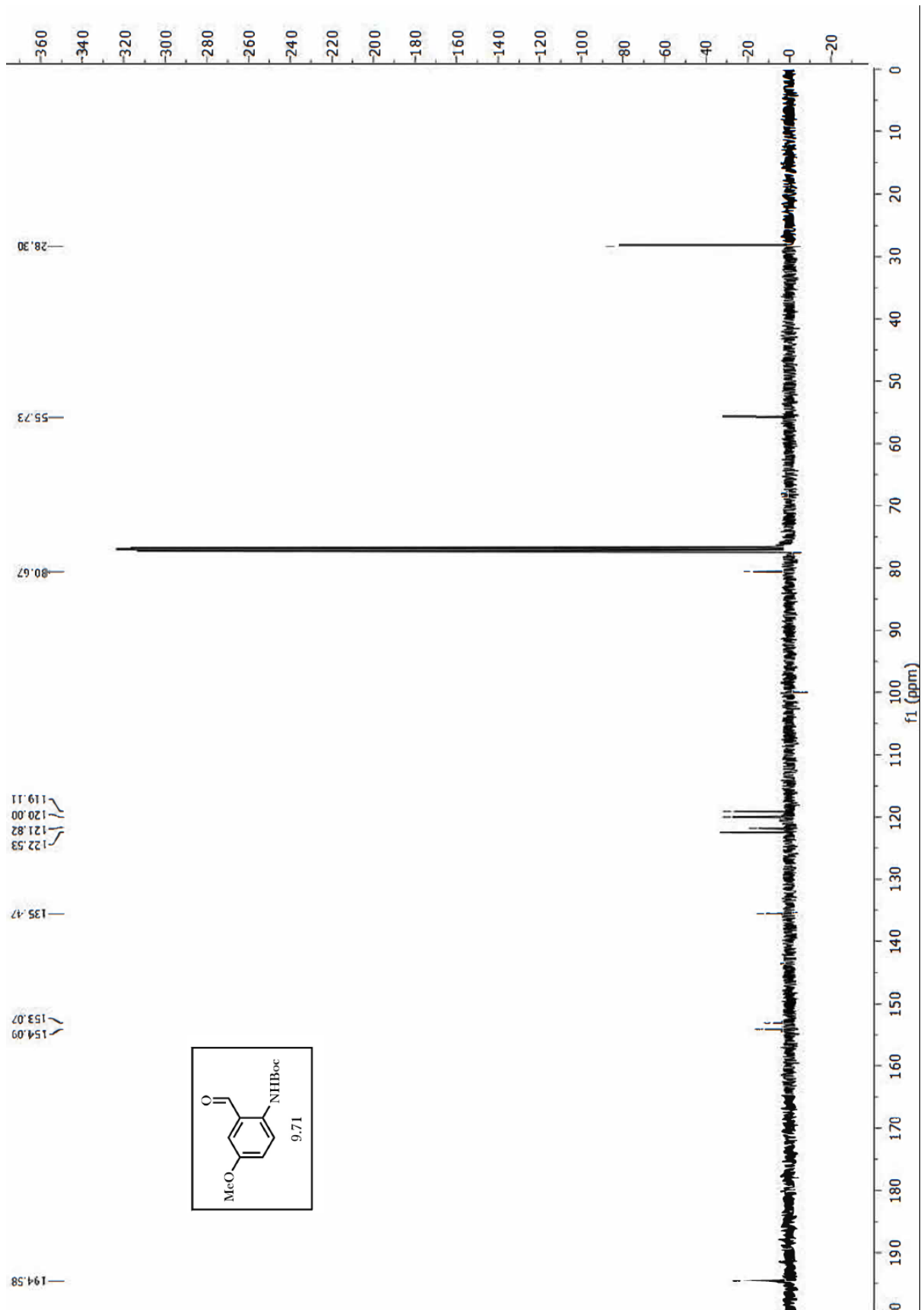


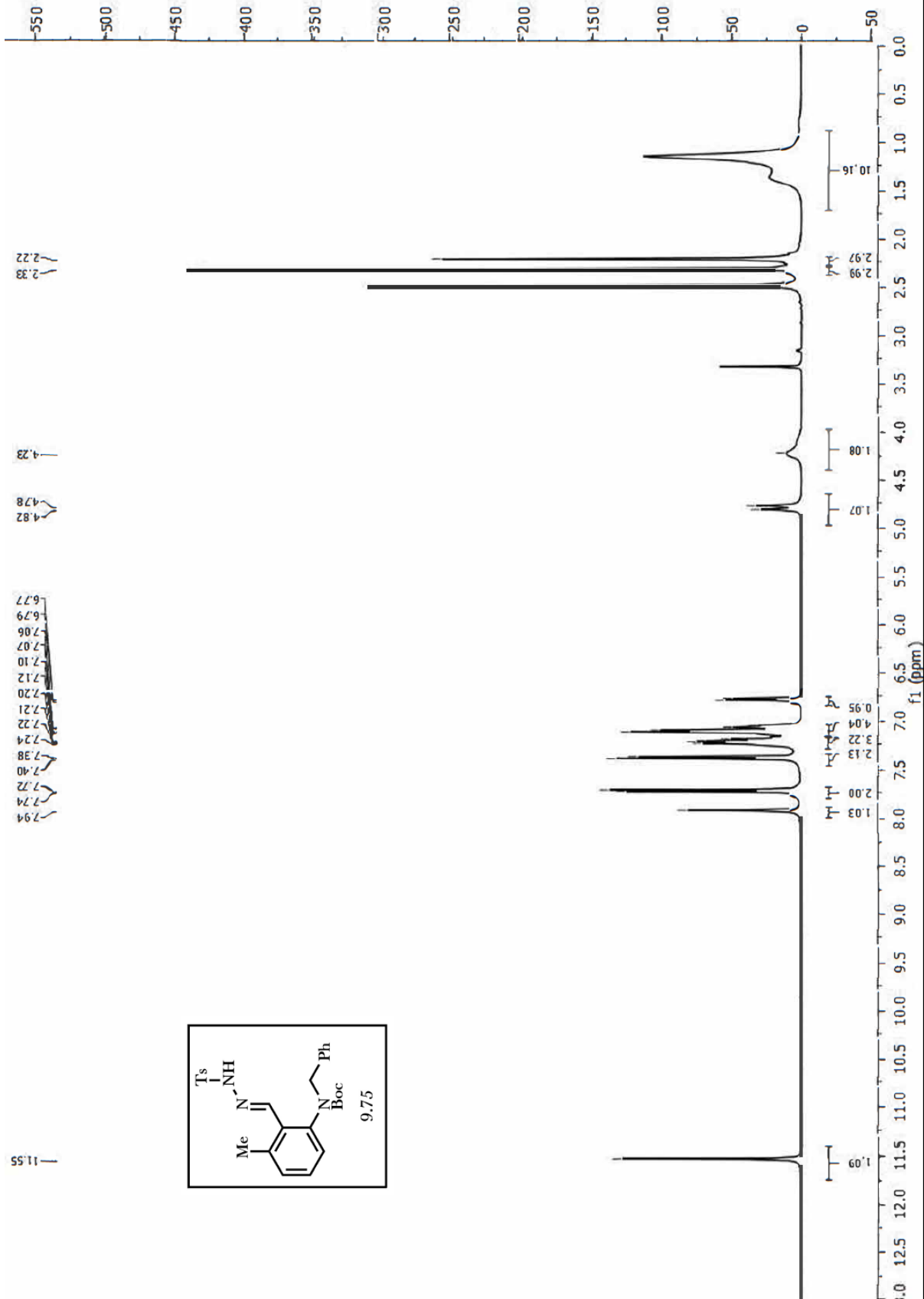


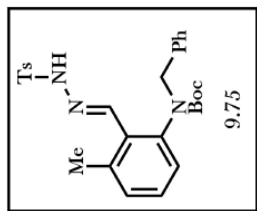
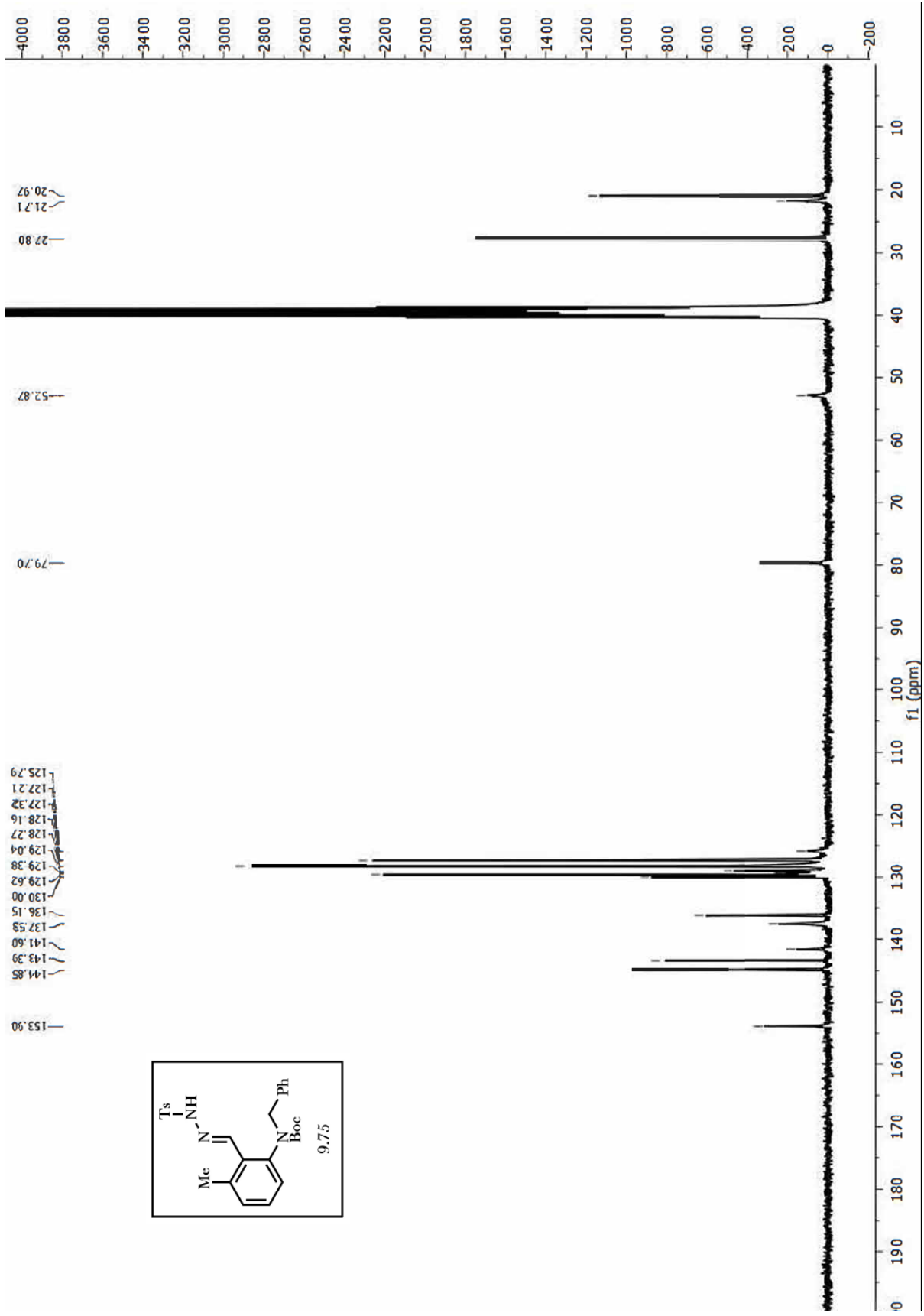


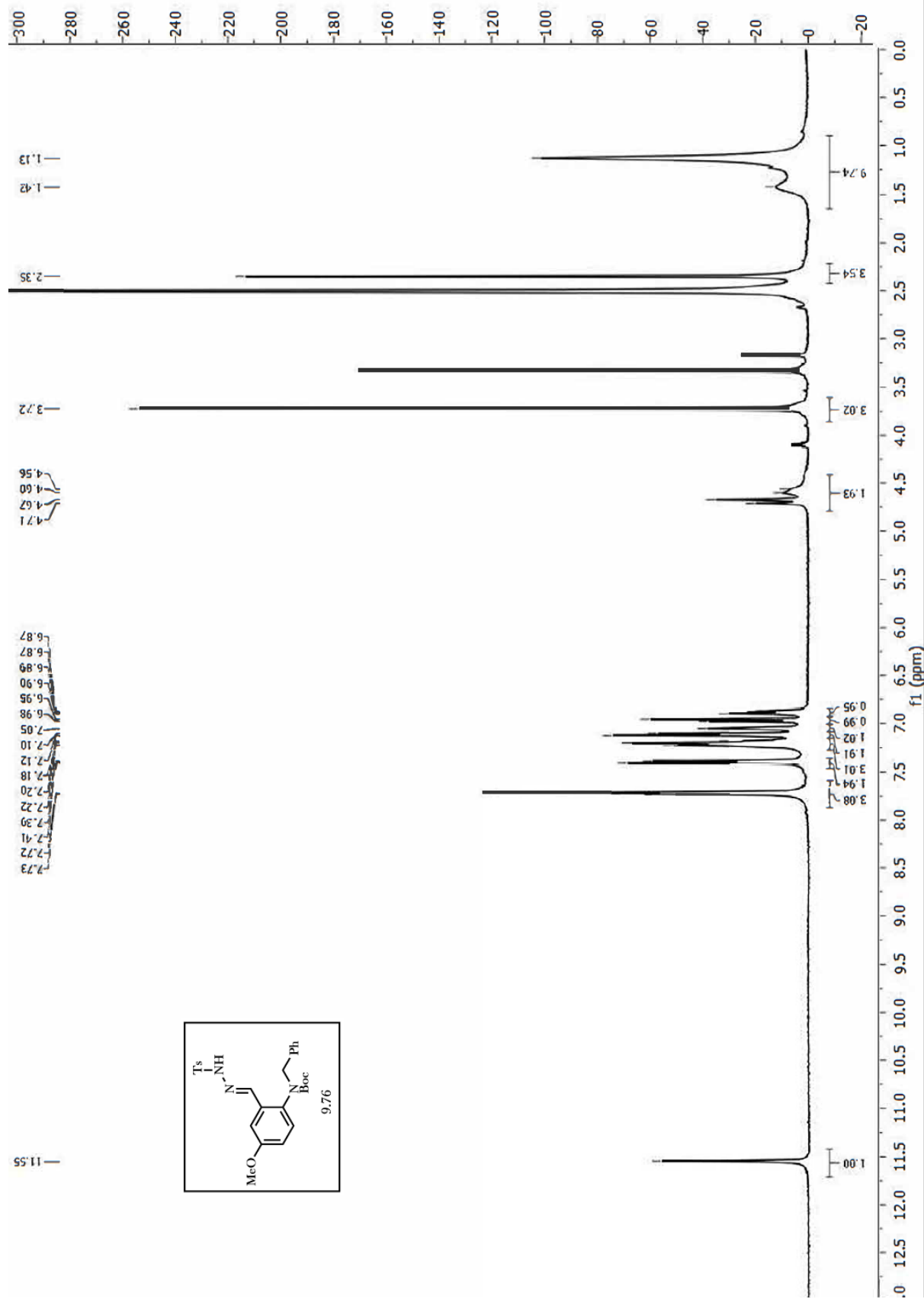


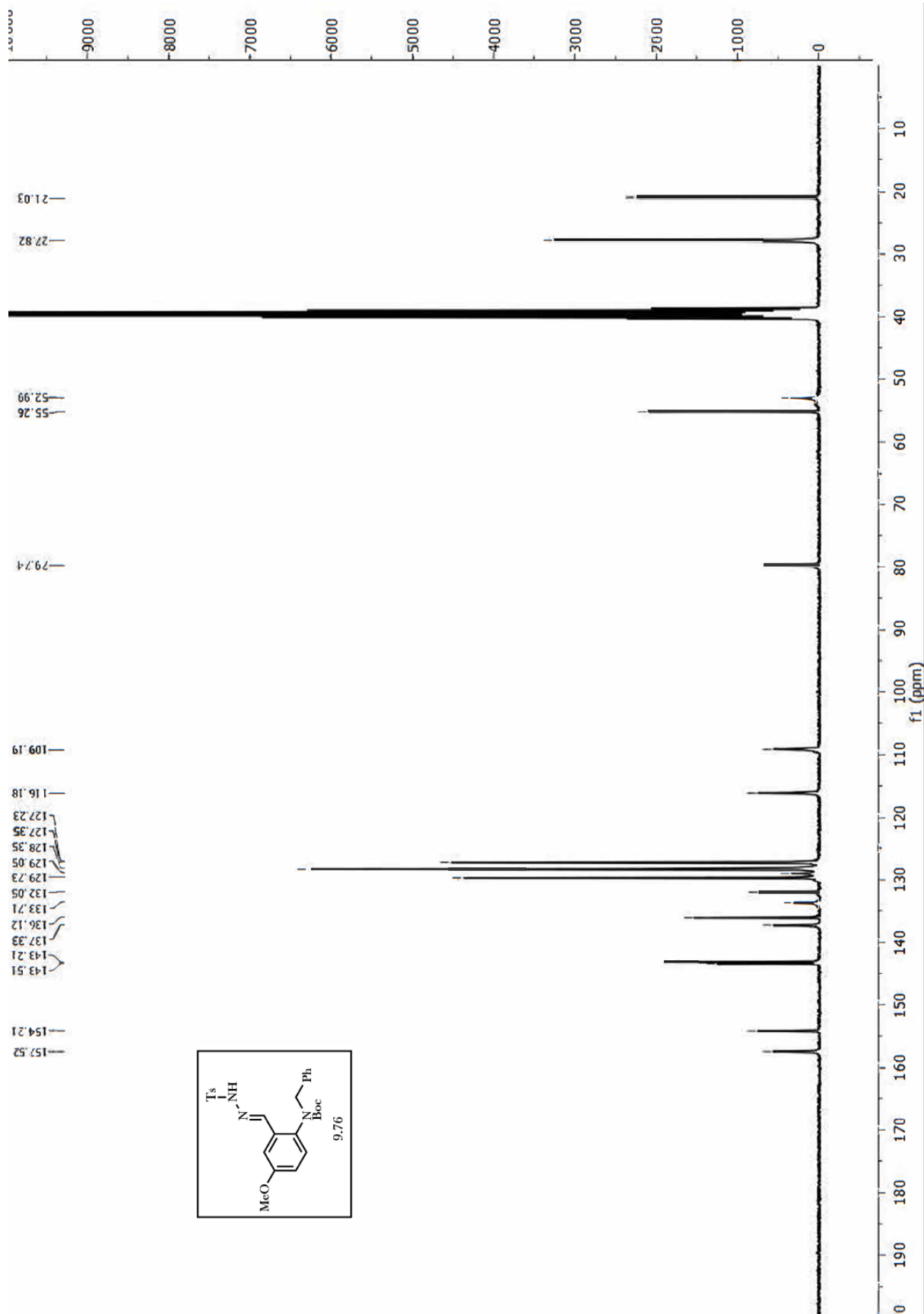


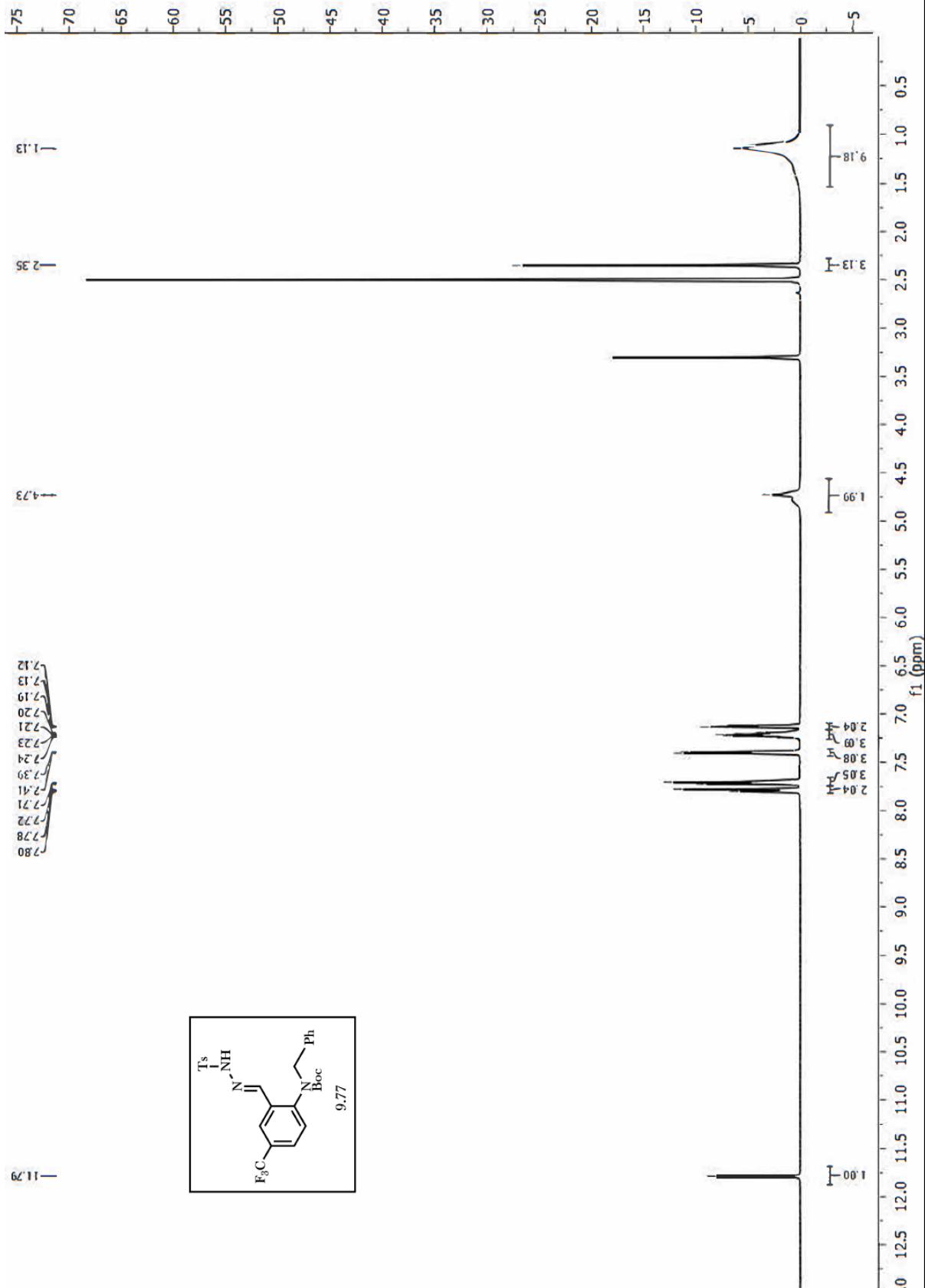


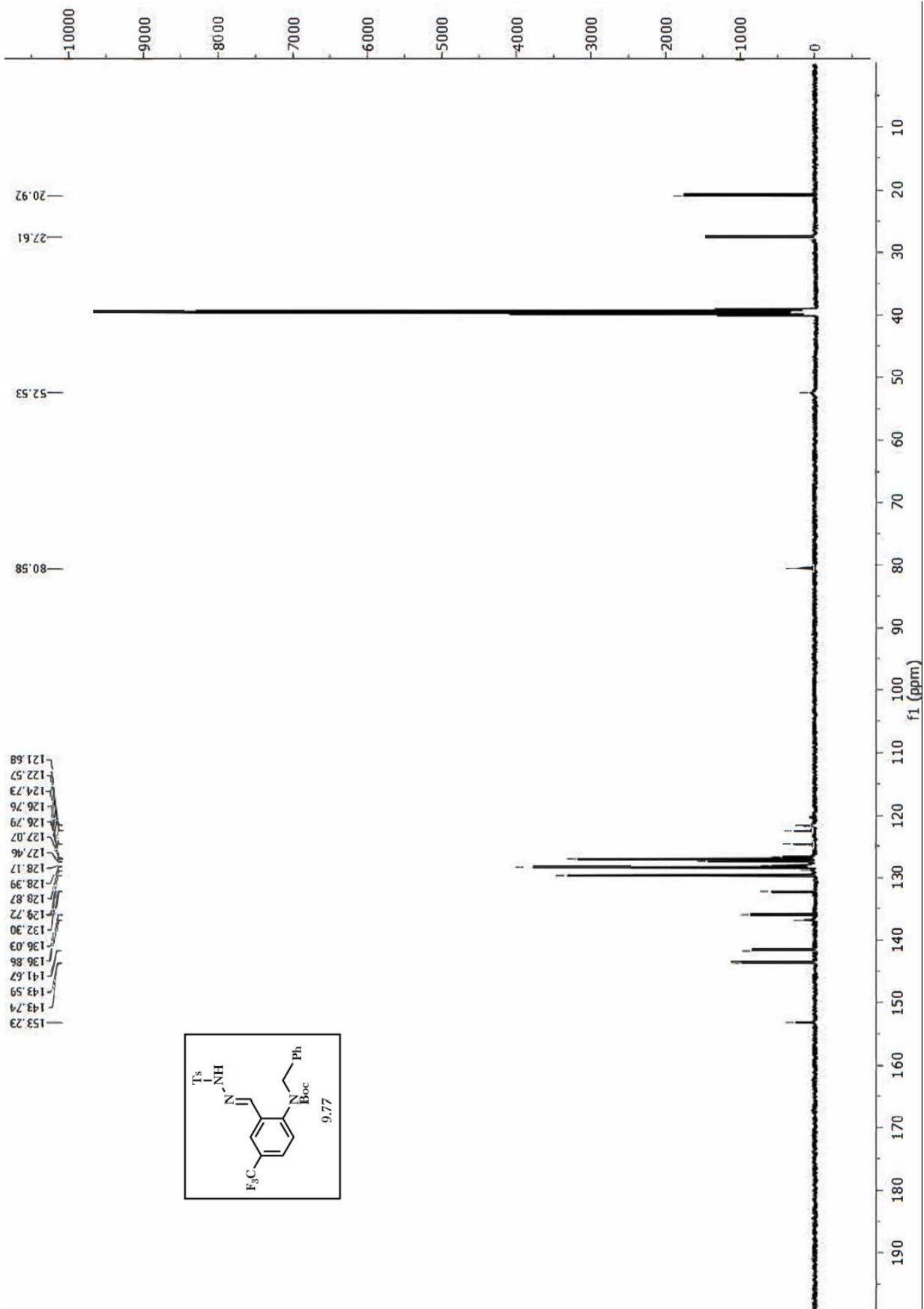












92.19

